CEPC-SPPC ACCELERATOR STATUS*

J. Gao†, IHEP, Beijing 100049, China

Abstract

In this paper we will give an introduction to Circular Electron Positron Collider (CEPC). The scientific background, physics goal, the collider design requirements and the conceptual design principle of CEPC are described. On CEPC accelerator, the optimization of parameter designs for CEPC with different energies, machine lengthes, single ring and crab-waist collision partial double ring options, etc. have been discussed systematically. The subsystems of CEPC, such as collider main ring, booster, electron positron injector, etc. have been introduced. The detector and MDI design have been briefly mentioned. Finally, the optimization design of Super Proton-Proton Collider (SPPC), its energy and luminosity potentials, in the same tunnel of CEPC are also discuss. It is decided that CEPC-SppC CDR baseline will be of 100km circumference, and the corresponding designs are underway.

INTRODUCTION

With the discovery of the Higgs particle at the Large Hadron Collider at CERN in July 2012, after more than 50 years of searching, particle physics has finally entered the era of the Higgs, and the door for human beings to understand the unknown part of the Universe is wide open! Thanks to the low energy of Higgs, it is possible to produce clean Higgs with circular electron positron colliders in addition of linear colliders, such as ILC and CLIC, with reasonable luminosity, technology, cost, and power consumption.

In September 2012, Chinese scientists proposed a Circular Electron Positron Collider (CEPC) in China at 240 GeV centre of mass for Higgs studies with two detectors situated in a very long tunnel more than twice the size of the LHC at CERN. It could later be used to host a Super Proton Proton Collider (SppC) well beyond LHC energy potential to reach a new energy frontier in the same channel.

After ICFA Higgs Factory Workshop held at Fermi Laboratory in Nov 2012, CERN proposed also a similar one, Future Circular Collider (FCC) with a much longer tunnel than that of LHC. From 12 to 14 June 2013, the 464th Fragrant Hill Meeting was held in Beijing on the strategy of Chinese high energy physics development after Higgs discovery, and the following consensuses were reached: 1) support ILC and participate to ILC construction with in kind contributions, and request R&D fund from Chinese government; 2) as the next collider after BEPCII in China, a circular electron positron Higgs factory (CEPC) and a Super proton-proton Collier (SppC) afterwards in the same tunnel is an important option as a historical opportunity, and corresponding R&D is needed. ICFA has given two successive statements in Feb. and July of 2014, respectively, that ICFA supports studies of energy frontier circular colliders and encourages global coordination; ICFA continues to encourage international studies of circular colliders, with an ultimate goal of proton-proton collisions at energies much higher than those of the LHC. During the AsiaHEP and ACFA meeting in Kyoto in April 2016, a positive statement of AsiaHEP/ACFA Statement on ILC+CEPC/SppC has been made with strong endorsement of the ILC and encouraging the effort led by China on CEPC/SppC. On Sept 12, 2016, during the meeting of the Chinese High Energy Physics of Chinese Physics Society, a statement on the future Chinese high energy physics based on accelerator has been made that CEPC is the first option for future high energy accelerator project in China as a strategic action with the aim of making CEPC as a large international scientific project proposed by China. The 572th Fragrant Hill Meeting dedicated to CEPC has been held from Oct. 18-19, 2016, and it is concluded that CEPC has a solid physics reason to be built with big physics potential in SppC. The optimization design, relevant technologies and industry preparation could be ready after a five years dedicated R&D period before CEPC starts to be constructed around 2022 and completed around 2030. CEPC will operate 10 ten years with two detectors to accumulate one million Higgs and 100 million of Z particle.

In the beginning of 2015, Pre-Conceptual Design Reports (Pre-CDR) of CEPC-SppC [1] have been completed with international review. The International Advisory Committee (IAC) of CEPC was also established in 2015. At the end of 2016 a CDR Status Report will be finished before finishing of the CDR at the end of 2017. In 2016, Chinese Ministry of Science and Technology has allocated several tens of million RMB on CEPC R&D to start with.

Finally, it is decided that CEPC-SppC CDR baseline will be of 100km circumference, and the corresponding designs are underway.

CEPC ACCELERATOR DESIGN

According to the physics goal of CEPC at Higgs and Z-pole energy, it is required that the CEPC provides e^+e^- collisions at the center-of-mass energy of 240 GeV and delivers a peak luminosity of 2×10^{34} cm$^{-2}s^{-1}$ at each interaction point. CEPC has two IPs for e^+e^- collisions. At Z-pole energy the luminosity is required to be larger than 1×10^{34} cm$^{-2}s^{-1}$ per IP. Its circumference is around 60 k-

* Work supported by National Key Programme for S&T Research and Development (Grant NO.: 2016YFA0400400) and National Natural Science Foundation of China (NO.11575218, 11505198, 11605211).

† gaoj@ihep.ac.cn

ISBN 978-3-95450-181-6

SEARCH FOR THE CHARGED PARTICLE ELECTRIC DIPOLE MOMENTS IN STORAGE RINGS

Y. Senichev#, IKP, Forschungszentrum Jülich, Germany
on behalf of the JEDI Collaboration

Abstract

The idea of searching for the electric dipole moment (EDM) of the proton and the deuteron using polarized beams in a storage ring was originally proposed at Brookhaven National Laboratory (BNL), USA. Currently, the "Jülich Electric Dipole Moment Investigations" (JEDI) collaboration is developing the conceptual design of such a ring specifically for the search of the deuteron electrical dipole moment (dEDM). The idea is that the oscillation of spin due to a possible finite electric dipole moment is separated from the influence of the magnetic dipole moment (MDM), and the behavior of spin indicates the existence of dEDM. In connection with this problem, two questions arise: (i) how to create conditions for maximum growth of the total EDM signal of all particles in the beam bunch, and (ii) how to differentiate the EDM signal from the induced MDM signal. For the design of such a ring, we need to address three major challenges:

- the ring lattice should meet the conditions of beam stability, and it has to have incorporated straight sections to accommodate the accelerating station, equipment for injection and extraction of the beam, a polarimeter, and sextupoles;
- the beam polarization lifetime must be around ~1000 seconds;
- systematic errors have to be minimized to eliminate the induced fake EDM signal.

In my contribution, I will present the current status of the project.

INTRODUCTION

One of the essential problems of modern physics is the baryon asymmetry of the Universe that represents the prevalence of matter over antimatter [1]. In addition, cosmic detectors, whose purpose is to search for antimatter, PAMELA and AMS haven't found any significant amount of it in the Universe yet [2]. The development of the new idea that claims one of the reasons for the baryon asymmetry is the breaking of CP invariance, has begun soon after its discovery. A. Sakharov established three necessary conditions for baryogenesis (initial creation of baryons) in 1967 [3]:

- Baryon number violation;
- C-symmetry and CP-symmetry violation;
- Interactions out of thermal equilibrium.

Many theories beyond the SM have been proposed and all of them of so-called "New Physics" are able to remove the difficulties that one meets in the Standard Model, but their experimental confirmation has yet to be found. One of the possible arguments for the breaking of CP-invariance is the existence of non-vanishing electric dipole moments (EDM) of elementary particles.

Currently, the "**J**ülich **E**lectric **D**ipole Moment **I**nvestigation" (JEDI) collaboration works in two directions: first on the existing accelerator COSY the precursor experiment is carried out to prove the feasibility of EDM measurement using the storage ring [4,5,6], and secondly the conceptual design of the ring specifically for search of the deuteron electrical dipole moment (dEDM) is being developed [7]. At present the RF flipper for installation on COSY ring is progressing successfully. Besides, we have already obtained very important experimental results with precise measurements of the spin precession frequency [4,5] which will allow calibrating the particle energy using the clock-wise and counter clock-wise procedure, and we have reached the longest spin coherence time ~1000 sec in horizontal plane [6].

This article is devoted mainly to the dEDM ring development. For the design of such a ring, we need to address three major challenges:

- the lattice should meet the conditions of stability of motion, minimization of beam loss, and it has to have incorporated straight sections to accommodate the accelerating station, equipment for injection and extraction of beam, a polarimeter, and sextupoles;
- using an RF cavity and a certain number of sextupole families, the beam polarization lifetime must be around ~1000 seconds;
- systematic errors have to be minimized to eliminate the induced fake EDM signal.

FROZEN AND QUASI-FROZEN SPIN CONCEPTS

In this paper, we will analyze two types of structures: the frozen spin (FS) and the quasi- frozen spin (QFS) lattices described in [7]. The concept of "frozen spin" lattice has been suggested by BNL [8], and it is based on the elements with incorporated electric and magnetic fields in one element, when the spin of the reference particle is always orientated along the momentum. Using this concept, a lot of lattice options for its implementation were proposed for protons and deuteron, in particular by R. Talman [9].

In the "frozen" spin method the main objective is to maximize the EDM signal growth, which is provided by the frozen orientation of spin along the momentum, i.e. by zero spin frequency $\vec{\omega}_G = 0$ relative to the momentum

#y.senichev@fz-juelich.de

ISBN 978-3-95450-181-6

THE EUROPEAN XFEL – STATUS AND COMMISSIONING*

H. Weise, Deutsches Elektronen-Synchrotron, Hamburg, Germany
on behalf of the European XFEL Accelerator Consortium

Abstract

The European XFEL under construction in Hamburg, Northern Germany, aims at producing X-rays in the range from 260 eV up to 24 keV out of three undulators that can be operated simultaneously with up to 27,000 pulses per second. The FEL is driven by a 17.5 GeV superconducting linac. Installation of this linac is now finished and commissioning is next. First lasing is expected for spring 2017. The paper summarizes the status of the project. First results of the injector commissioning are given.

INTRODUCTION

The accelerator complex of the European XFEL [1] is being constructed by an international consortium under the leadership of DESY. Seventeen European research institutes contribute to the accelerator complex and to the comprehensive infrastructure. Major contributions are coming from Russian institutes. DESY coordinates the European XFEL Accelerator Consortium but also contributes with many accelerator components, and the technical equipment of buildings, with its associated general infrastructure. With the finishing of the accelerator installation, the commissioning phase is now starting, with cool down of the main linac scheduled for end of November 2016.

LAYOUT OF THE EUROPEAN XFEL

In the following the overall layout of the European XFEL is given with emphasis on the different sections of the accelerator complex.

Introduction to the Accelerator

The European XFEL with its total facility length of 3.4 km follows the established layout of high performance single pass Self-Amplified Spontaneous Emission (SASE) FELs. A high bunch charge, low emittance electron gun is followed by some first acceleration to typically 100 MeV. In the following, magnetic chicanes help to compress the bunch and therefore increase the peak current. This happens at different energies to take care of beam dynamic effects which would deteriorate the bunch emittance in case of too early compression at too low energies. Thus the linac is separated by several of such chicanes. The European XFEL main linac accelerates the beam in three sections, following the first acceleration in the injector.

Injector

The injector design of the European XFEL is visibly affected by the need of long bunch trains which are required for the efficient use of superconducting linac technology. Like many other FELs it starts with a normal-conducting 1.6 cell radio frequency (RF) electron gun but here the source has to deliver 600 µs long trains i.e. the rf-on time is equivalently long, and not just some few µs. The produced 6 MeV electron beam is almost immediately injected into the first superconducting accelerator section which allows efficient acceleration of bunch trains. This first linac section consists of a standard eight cavity XFEL module, followed by a harmonic 3.9 GHz module. The latter is needed to manipulate the longitudinal beam profile together with the later bunch compression in magnetic chicanes. Beam diagnostics is used to verify the electron beam quality at energy of about 130 MeV. The in total 50 m long injector installation ends with a beam dump being able to take the full beam power.

The injector of the European XFEL was commissioned and operated during the installation period of the main linac sections. First beam was accelerated in 12/2015. At the end of the injector, 600 µs long electron bunch trains of typ. 500 pC bunches are available with measured projected emittances of 1 to 1.5 mm mrad. Most relevant for the FEL process is the slice emittance which was found to be of the order of 0.5 mm mrad for 500 pC.

The next section downstream of the injector is a warm beam line including a so-called dogleg and the first bunch compressor, for historical reasons named BC0. The dogleg takes care of the vertical offset between the injector tunnel and the main linac tunnel.

Compression in all bunch compressors is reached by creating different path lengths in a four dipole magnet chicane. Electrons with slightly lower beam energy are deflected stronger and thus pass the chicane on an 'outward curve'. The acceleration in the injector section is done slightly off-crest, i.e. the energy of the leading electrons in the bunch is intentionally lower. The above mentioned 3.9 GHz harmonic system helps to get the proper energy modulation along the bunch. Since all electrons have essentially the same speed, the leading ones travel slightly longer, and the bunch is compressed.

The XFEL bunch compressor BC0 does a first slight compression by roughly a factor 2. The bunches ready for further acceleration reach 1 mm length, approx. 100 A peak current, with an energy spread of 1.5% at 130 MeV beam energy.

At present the European XFEL uses the lower of two injector tunnels. The second one was originally built to install a copy of the first injector – availability depending on reliable injector operation was the issue. Meanwhile it seems to be more adequate to aim for a different injector favoring longer pulse or even continuous wave (CW) operation.

* Work supported by the respective funding agencies of the contributing institutes; for details please see http:www.xfel.eu

ISBN 978-3-95450-181-6

NOVOSIBIRSK FREE ELECTRON LASER: TERAHERTZ AND INFRARED COHERENT RADIATION SOURCE*

N.A. Vinokurov#, I.V. Davidyuk, Ya.V. Getmanov, Ya. I. Gorbachev, B.A. Knyazev, E.V. Kozyrev, S.S. Serednyakov, V.S. Arbuzov, K.N. Chernov, O.I. Deichuli, E.N. Dementyev, B.A. Dovzhenko, E.I. Kolobanov, A.A. Kondakov, V.R. Kozak, S.A. Krutikhin, V.V. Kubarev, G.N. Kulipanov, E.A. Kuper, I.V. Kuptsov, G.Ya. Kurkin, L.E. Medvedev, S.V. Motygin, V.N. Osipov, V.K. Ovchar, V.M. Petrov, A.M. Pilan, V.M. Popik, V.V. Repkov, T.V. Salikova, M.A. Scheglov, I.K. Sedlyarov, O.A.Shevchenko, A.N. Skrinsky, S.V. Tararyshkin, V.G. Tcheskidov, P.D. Vobly, V.N. Volkov, A.G. Tribendis, Budker INP SB RAS, Novosibirsk, Russia

Abstract

High-power free electron laser (FEL) facility NovoFEL has been created at Budker INP. Its wavelength can be tuned over a wide range in terahertz and infrared spectrum regions. As a source of electron bunches this FEL uses multi-turn energy recovery linac which has five straight sections. Three sections are used for three FELs which operate in different wavelength ranges (the first one - 90-240 microns, the second - 37-80 microns and the third - 5-20 microns). The first and the second FELs were commissioned in 2003 and 2009 respectively. They operate for users now. The third FEL is installed on forth accelerator track which is the last one and electron energy is maximal here. It comprises three undulator sections and 40 m optical cavity. The first lasing of this FEL was obtained in summer, 2015. The radiation wavelength was 9 microns and average power was about 100 watts. The designed power is 1 kilowatt at repetition rate 3.75 MHz. Radiation of third FEL has been delivered to user stations recently. The third FEL commissioning results as well as current status of the first and second FELs and future development prospects are presented.

OVERVIEW OF THE NOVOSIBIRSK FEL FACILITY

Accelerator and Two Old FELs

The Novosibirsk FEL facility [1] includes three FELs. All the FELs use the electron beam of the same electron accelerator. It is a multi-turn energy recovery linac (ERL). A simplified scheme of the four-turn ERL is shown in Fig. 1. Starting from low-energy injector 1, electrons pass four times through accelerating radiofrequency (RF) structure 2. After that they loose part of their energy in FEL undulator 4. The used electron beam is decelerated in the same RF structure, and low-energy electrons are absorbed in beam dump 5.

The Novosibirsk ERL has three modes, one mode for operation of one of the three FELs. The first FEL is installed under the accelerating (RF) structure (see Figs. 2 and 3). Therefore, after the first passage through the RF structure, the electron beam with an energy of 11 MeV is turned by 180 degrees in the vertical plane. After the use in the FEL, the beam returns to the RF structure in the decelerating phase. In this mode, the ERL operates as a single-orbit linac.

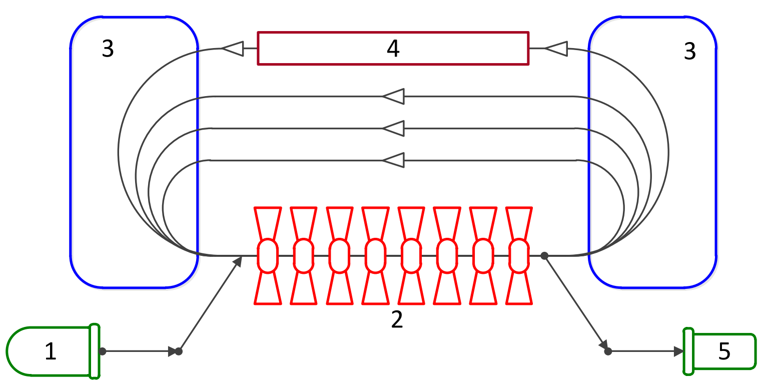

Figure 1: Simplest multi-turn ERL scheme: 1 – injector, 2 – linac, 3 – bending magnets, 4 – undulator, 5 – dump.

*Work supported by Russian Science Foundation project N 14-50-00080. #vinokurov@inp.nsk.su

PLANAR SUPERCONDUCTING UNDULATOR WITH NEUTRAL POLES

N.A. Mezentsev, S.V. Khruschev, V.A. Shkaruba, V.M. Syrovatin, V.M. Tsukanov,
Budker Insitute of Nuclear Physics, Novosibirsk, Russia

Abstract

Superconducting undulator with use of neutral poles was proposed in Budker INP. Period of the undulator is 15.6 mm. Pole gap and magnetic field are equal to 8 mm and 1.2 T correspondingly. A prototype of the undulator with 15 periods was fabricated and successfully tested. Calculations, design and test results of the prototype in the report are presented. The cryogenic and vacuum system of the undulator are discussed.

INTRODUCTION

The development and creation of new magnetic structures for bright synchrotron radiation sources, the emittance of which is close to the diffraction limit, makes high demands on the creation of an adequate generators radiation , such as short period undulators with minimal phase error. Creation of this type of an undulator with a short period, with undulator strength parameter K~2 and with phase error <3^{o} gives the opportunity to work on high harmonics. Widespread currently received undulators based on permanent magnets as radiation sources in the centers of synchrotron radiation. Despite the fact that there is progress in the production of new materials for permanent magnets the use of magnets based on superconductors has advantages in creating a higher field with less period, and less the value of the phase errors.

Several groups in the world [1-7] are busy the problem of a superconducting undulator with short period and with K~2. A variant of the arrangement of the windings in the vertical plane – the "vertical racetrack" is commonly under development.

In this paper we propose a variant of placing of the windings in the horizontal plane – "horizontal racetrack", which differs from the standard solutions used in the superconducting wigglers [8].

MAGNET DESIGN

The transverse electromagnetic field in the undulator, which are used for the generation of radiation, are created by transverse currents in coils near an electron beam orbit . The question of how these currents are closed is minor and relates more to technological solutions from the point of view of higher-quality fields with smaller phase errors. The most widely spread method of closing currents is the method of "vertical racetrack". In the article the method of close of the currents for the superconducting undulator is suggested as horizontal racetrack (Fig. 1). A key element of the undulator is a single magnetic pole (Fig. 2), consisting of a single section coil wound on an iron core.

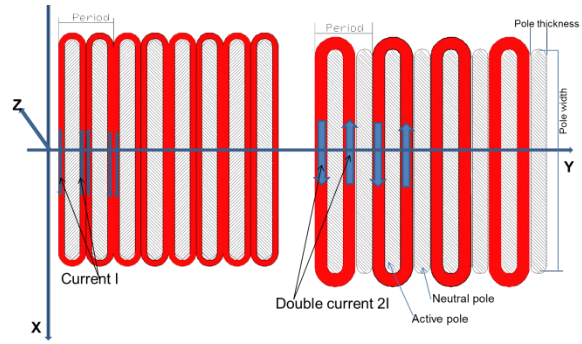

Figure 1: Schematic view of the location of poles and the currents in them for an undulator with horizontal racetrack coils: on the left the standard set of coils with standard of currents closing (coils type of a wiggler), right – set of coils with the neutral poles.

The period of the undulator is formed by magnetic pole with superconducting coil (active pole) and neutral pole, which is an iron core without windings. The undulator magnet consists of two identical halves which are located one above the other.

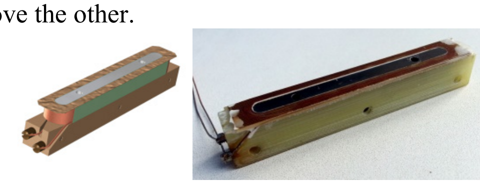

Figure 2: A separate pole is the basic element of the superconducting undulator

All the windings of the upper and lower parts of the magnet are connected in series with the same direction of the currents. The dimensions of the neutral poles and the active poles optimized with respect to the minimum of undesirable components of the magnetic field in the horizontal transverse region of ± 20 mm. When the currents are applied, the magnetic fields of each part of the magnet should be directed in opposite directions so that if you align the two halves in the longitudinal direction, in this case the transverse magnetic field should be zero on the median plane of the magnet. To create the transverse components of the magnetic field in the undulator, it is necessary to shift the top and bottom of the magnet on half period in the longitudinal direction (Fig. 3).

To check the possibility of the creation of this type of undulator, a prototype undulator was designed, manufactured and tested with 15 periods and period length of 15.45 mm. The prototype was performed as standard blocks containing five periods each, made of a soft magnetic iron (Fig. 4). Separate active poles were embedded in the grooves of these blocks. The role of the neutral poles played a rib of iron blocks.

ISBN 978-3-95450-181-6

CW 100 mA ELECTRON RF GUN FOR NOVOSIBIRSK ERL FEL

V. Volkov#, V. Arbuzov, E. Kenzhebulatov, E. Kolobanov, A. Kondakov, E. Kozyrev, S. Krutikhin, I. Kuptsov, G. Kurkin, S. Motygin, A. Murasev, V. Ovchar, V.M. Petrov, A. Pilan, V. Repkov, M. Scheglov, I. Sedlyarov, S. Serednyakov, O. Shevchenko, S. Tararyshkin, A. Tribendis, N. Vinokurov, BINP SB RAS, Novosibirsk, Russia

Abstract

Continuous wave (CW) 100 mA electron rf gun for injecting the high-quality 300-400 keV electron beam in Novosibirsk Energy Recovery Linac (ERL) and driving Free Electron Laser (FEL) was developed, built, and commissioned at BINP SB RAS. The RF gun consists of normal conducting 90 MHz rf cavity with a gridded thermionic cathode unit. Bench tests of rf gun is confirmed good results in strict accordance with our numerical calculations. The gun was tested up to the design specifications at a test bench that includes a diagnostics beam line. The rf gun stand testing showed reliable work, unpretentious for vacuum conditions and stable in long-term operation. The design features of different components of the rf gun are presented. Preparation and commissioning experience is discussed. The beam test results are summarized.

INTRODUCTION

Recent projects of advanced sources of electromagnetic radiation [1] are based on the new class of electron accelerators where the beam current is not limited by the power of rf system – energy recovery linacs (ERLs). Such accelerators require electron guns operating in continuous wave (cw) mode with high enough average current. The only solution is an rf gun, where the cathode is installed inside the rf cavity. The advantages of the rf guns are higher accelerating field, which is desirable to obtain low beam emittance. It has no problem with degradation of the cathode due to poor vacuum in the gun. The considered rf gun if it be used in the most power Novosibirsk FEL can increase it`s power by one order on magnitude more.

In this paper we describe the beam test results of our low-frequency rf gun (see [2-4]) built as the new electron source for ERL of the Novosibirsk FEL facility (see [5]). Measured rf gun characteristics are in Table 1.

Table 1: Measured rf Gun Characteristics

Name	Value
Average beam current, mA	0.003-100
Bunch energy, keV	100 ÷ 400
Bunch duration (FWHM), ns	0.2 ÷ 2.0
Bunch emittance, mm mrad	10
Bunch charge, nC	0.3 ÷ 3.8
Bunch repetition frequency, MHz	0.01 ÷ 90

#v.n.volkov@inp.nsk.su

RF GUN AND DIAGNOSTIC STAND

Here we shortly describe the rf gun and diagnostic stand presented by sketches of Figs. 1 and 2. Detailed information sees in [2-4]. Perfections of the stand are following: 30 kW water cooled beam dump, 5 cm lead radiation shield, wideband Wall Current Monitor (WCM2), new scheme of cathode-grid modulator with GaN rf transistor, Transition Radiation Sensor, and pair of standard WCM.

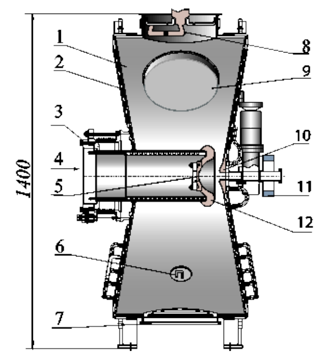

Figure 1: Rf gun sketch.

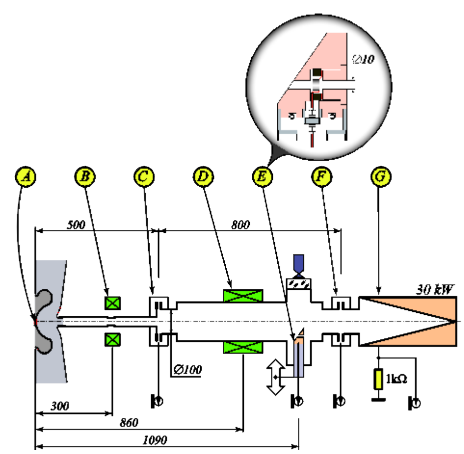

Figure 2: The stand layout.

In figures: 1- Cavity bi-metallic shell; 2-Cavity back wall; 3-Cathode Insert; 4-Cathode injection/extraction channel; 5-Thermionic cathode-grid unit (can be replaced by EIMAC); 6-Loop coupler; 7-Vacuum pumping port; 8-Power input coupler; 9-Sliding tuner; 10-Cone like nose; 11-Peripheral solenoid; 12-Concave focusing electrode.

A-Thermionic cathode-grid unit; B-Emittance compensation solenoid; C-First Wall Current Monitor (WCM1); D-Solenoid ; E-Wideband WCM and transition radiation sensor; F-third WCM; G-Faraday cup and Water-cooled beam dump.

ISBN 978-3-95450-181-6

STATUS OF THE KURCHATOV SYNCHROTRON LIGHT SOURCE

V. Korchuganov, A. Belkov, Y. Fomin, E. Kaportsev, Yu. Krylov, V. Moiseev, K. Moseev, N. Moseiko, D. Odintsov, S. Pesterev, A. Smygacheva, A. Stirin, V. Ushakov, V. Ushkov, A. Valentinov, A. Vernov,
NRC Kurchatov Institute, Akademika Kurchatova Sq., 1, Moscow, 123182 Russia

Abstract

The Kurchatov synchrotron light source operates in the range of synchrotron radiation from VUV up to hard X-ray. To improve facility capabilities in the last few years technical modernization of all facility systems is underway and new beam lines are constructed. In this report the present status and future plans of the Kurchatov synchrotron light source are presented.

INTRODUCTION

The Kurchatov synchrotron light source [1] includes 80 MeV electron linear accelerator, 450 MeV storage ring Siberia-1 with the horizontal emittance 800 nm·rad, the 2.5 GeV storage ring Siberia-2 with the horizontal emittance 78-100 nm·rad and two transport lines. Siberia-2 supplies users' experimental stations by synchrotron radiation in photon energy range 4-40 keV from its bending magnets. Siberia-1 is mostly used as a booster for Siberia-2 but also as an independent SR source.

KSRS OPERATION

The Siberia-2 operates nine months per year in around the clock mode. Within one week 9 working 12-hour shifts are provided. One more shift is dedicated to accelerator physics and machine tuning. As a rule there is one beam storing per day, typical electron current is 100 – 150 mA. Beam lifetime is equal 15 – 20 hours at 100 mA level and defined by vacuum conditions. Injection process at 450 MeV usually takes about 1 hour, energy ramping takes 3 minutes with 2-3% beam loss.

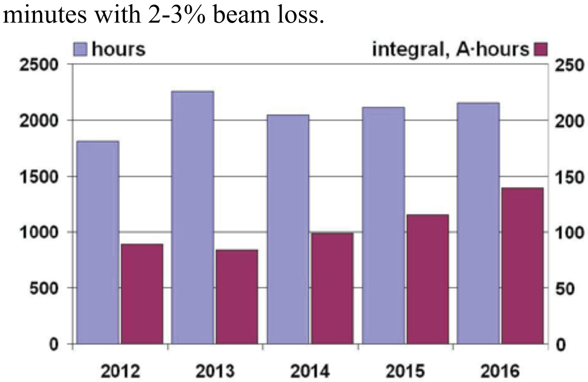

Figure 1: Total time used for experiments and beam current integral at 2.5 GeV for Siberia-2.

Fig. 1 demonstrates total time devoted for SR experimental work at Siberia-2 and electron current integral at 2.5 GeV during last 5 years.

A magnetic lattice of Siberia-2 provides horizontal emittance equal to 98 nm at 2.5 GeV. Betatron coupling is maintained at very small level of 0.001 so vertical beam size is determined by non-zero vertical dispersion function. At injection energy betatron coupling is artificially increased up to 10-15% in order to enhance beam lifetime.

There are 11 experimental stations using SR at Siberia-2 and 4 stations at Siberia-1. Three stations were put into operation during last year (Photoelectron spectroscopy, Phase-sensitive solid-state research, X-ray structure analysis). Two other stations will be commissioned next year (moved from DESY).

Siberia-2 Closed Orbit Distortions

Serious problem for users is slow drift of photon beam in vertical direction. It is caused by heating of machine basis from thick aluminum conducting bar of bending magnet power supply. This induces a progressive slope of magnets and vertical close orbit distortion as a result. We observe the slope with two time constants. First one is equal to approximately one hour and acts just after energy ramping. Second one is equal to one day and is observed during whole working week. As a result we must correct vertical orbit each time before beam storing and jus after energy ramping. As a rule we have RMS distortion of closed orbit about 40 microns in vertical plane and 500 microns in horizontal plane.

In order to stabilize photon beam position feedback system is used. Every beamline has luminophor sensor with TV camera for fixing beam image on luminofor strip. The feedback provides local orbit bump to stabilize photon beam with accuracy of 2-4 microns in sensor location. Plans for future are to improve cooling of power supply conductor by increasing of water flow using more powerful pumps.

DEVELOPMENT OF KSRS IN 2015-2016

The purpose of works in 2015-2016 was both modernization of the existing equipment and introduction of new diagnostics systems on Siberia-2 storage ring. Much attention was paid to developing of KSRS control system.

Siberia-2 New High Voltage Generators

Two new generators based on pseudo-spark switches (a thyrotron TPI1-10k/50) and RLC resonant circuits with a semi-sinusoidal form of currents were produced on "Pulse

ISBN 978-3-95450-181-6

NUMERICAL ANALYSIS OF THE EFFECTIVE WIDTH OF THE SPECTRUM OF SYNCHROTRON RADIATION

V. G. Bagrov, A. S. Loginov, A. D.Saprykin, Tomsk State University, Russia
D. M. Gitman, A. D. Levin, Institute of Physics, University of Sao Paulo, Brazil

Abstract

For an exact quantitative description of spectral properties in the theory of synchrotron radiation, the concept of effective spectral width is introduced. In the classical theory, numeric calculations of effective spectral width (using an effective width not exceeding 100 harmonics) for polarization components of synchrotron radiation are carried out. The dependence of the effective spectral width and initial harmonic on the energy of a radiating particle is established.

INTRODUCTION

As one of the major quantitative characteristics of spectral distributions for electromagnetic radiation, one commonly uses the concept of spectral half-width. For spectral distributions having a sharp maximum, spectral half-width is the most informative physical characteristic.

However, once a spectral distribution has no pronounced maximum, spectral half-width ceases to be an adequate quantitative characteristic. In particular, this is exactly the case of spectral distributions for synchrotron radiation (SR), and therefore SR spectral half-width has neither been calculated theoretically, nor measured experimentally.

Instead of spectral half-width, the present study proposes to introduce a new precise quantitative characteristic of SR spectral distributions: effective spectral width. It is shown how this quantity can be calculated theoretically, and which physically relevant information can be obtained using this quantity.

In order to set up the problem, we now present some well-known expressions of the classical SR theory for the physical characteristics of synchrotron radiation, which can be found in [1–7].

The spectral-angular distribution for radiation power of SR polarization components can be written as

$$W_s = W\sum_{\nu=1}^{\infty}\int_0^{\pi} f_s(\beta;\,\nu,\,\theta)\sin\theta d\theta. \qquad (1)$$

Here, the following notation is used: θ is the angle between the control magnetic field strength and the radiation field pulse; ν is the number of an emitted harmonic; the charge orbital motion rate is $v = c\beta$, where c is the speed of light; W is the total radiated power of unpolarized radiation, which can be reveled in [1–7]. The index s numbers the polarization components: $s = 2$ corresponds to the σ-component of linear polarization; $s = 3$ corresponds to the π-component of linear polarization; $s = 1$ corresponds to right-hand circular polarization; $s = -1$ corresponds to left-hand circular polarization; $s = 0$ corresponds to the power of unpolarized radiation. The form of functions $f_s(\beta;\,\nu,\,\theta)$ can be founded in [1–7].

SPECTRAL DISTRIBUTION FOR POLARIZATION COMPONENTS OF SYNCHROTRON RADIATION IN THE UPPER HALF-SPACE

It is well known [1–7] that the angle range $0 \leqslant \theta < \pi/2$ (this range will be called the upper half-space) is dominated by right-hand circular polarization, and the angle range $\pi/2 < \theta \leqslant \pi$ (this range will be called the lower half-space) is dominated by left-hand circular polarization (exact quantitative characteristics of SR properties were first obtained in [8–11]). To reveal these features, the expressions (1) can be represented as

$$W_s = W\left[\Phi_s^{(+)}(\beta) + \Phi_s^{(-)}(\beta)\right],$$

$$\Phi_s^{(\pm)}(\beta) = \sum_{\nu=1}^{\infty} F_s^{(\pm)}(\beta;\,\nu),$$

$$F_s^{(\pm)}(\beta;\,\nu) = \int_{0\mp\pi/2}^{\pi/2\mp\pi/2} f_s(\beta;\,\nu,\,\theta)\sin\theta d\theta, \qquad (2)$$

and it suffices to study the properties of functions $F_s^{(+)}(\beta;\,\nu)$ (respectively, the properties of functions $\Phi_s^{(+)}(\beta)$), due to the evident relations

$$F_s^{(-)}(\beta;\,\nu) = F_s^{(+)}(\beta;\,\nu)\,,\;\; \Phi_s^{(-)}(\beta) = \Phi_s^{(+)}(\beta)\;{}_{s=0,\,2,\,3};$$

$$F_{\pm1}^{(-)}(\beta;\,\nu) = F_{\mp1}^{(+)}(\beta;\,\nu)\,,\;\; \Phi_{\pm1}^{(-)}(\beta) = \Phi_{\mp1}^{(+)}(\beta)\,.$$

The exact form of the functions $F_s^{(\pm)}(\beta;\,\nu)$ and $\Phi_s^{(\pm)}(\beta)$ was revealed in [8–11].

EFFECTIVE SPECTRAL WIDTH FOR POLARIZATION COMPONENTS OF SYNCHROTRON RADIATION

As one of the quantitative characteristics of physical properties for spectral distributions of SR polarization components, it is proposed to introduce the concept of effective spectral width $\Lambda_s(\beta)$. Let us define $\Lambda_s(\beta)$ as follows.

For each fixed value of β, we examine the quantities of partial contributions $P_s(\beta;\nu)$ for individual spectral harmonics, introduced in [12].

ISBN 978-3-95450-181-6

STATUS OF THE FUTURE CIRCULAR COLLIDER STUDY*

M. Benedikt†, F. Zimmermann, CERN, Geneva, Switzerland

Abstract

Following the 2013 update of the European Strategy for Particle Physics, the international Future Circular Collider (FCC) Study has been launched by CERN as host institute. Its main purpose and long-term goal is to design an energy-frontier hadron collider (FCC-hh) with a centre-of-mass energy of about 100 TeV in a new 80–100 km tunnel. The FCC study also includes the design of a 90–350 GeV high-luminosity lepton collider (FCC-ee) installed in the same tunnel, serving as Higgs, top and Z factory, as a potential intermediate step, as well as an electron-proton collider option (FCC-he). The physics cases for such machines are being assessed and concepts for experiments will be developed by the end of 2018, in time for the next update of the European Strategy for Particle Physics.

This overview summarizes the status of machine designs and parameters, and it discusses the essential technical components being developed in the frame of the FCC study. Key elements are superconducting accelerator-dipole magnets with a field of 16 T for the hadron collider and high-power, high-efficiency RF systems for the lepton collider. In addition, the unprecedented beam power presents particular challenges for the hadron collider. First conclusions from geological investigations and implementation studies are available. We report the status of the FCC collaboration and outline the further planning.

INTRODUCTION

The Large Hadron Collider (LHC) presently in operation at CERN, and its high-luminosity upgrade, the HL-LHC, have an exciting physics program, which extends through the mid 2030's, i.e., covering the next 20 years. From the initial proposal in 1983, it has taken more than 30 years to design, build and fully commission the LHC. In view of such time scales, it is urgent for the community to start preparing the next accelerator for the post-LHC period.

European studies for a large post-LHC physics-frontier machine began in 2010–2013, for both lepton and hadron colliders (at the time called LEP3/TLEP and VHE-LHC, respectively). In response to the 2013 Update of the European Strategy for Particle Physics [1]. in early 2014 these efforts were combined and expanded as global Future Circular Collider (FCC) study [2, 3], hosted by CERN.

FCC STUDY SCOPE & TIME LINE

A large circular hadron collider seems to be the only approach to reach, during the coming decades, energy levels far beyond the range of the LHC. The long-term goal and focus of the FCC study [3], therefore, is a 100-TeV hadron collider (FCC-hh), which determines the infrastructure needs of the new facility. The energy reach of a high-energy hadron collider is simply proportional to the dipole magnetic field and to the bending radius: $E \propto B \times \rho$. Assuming a dipole field of 16 T, expected to be achievable with Nb_3Sn technology, the ring circumference must be about 100 km in order to reach the target value 100 TeV for the center-of-mass energy.

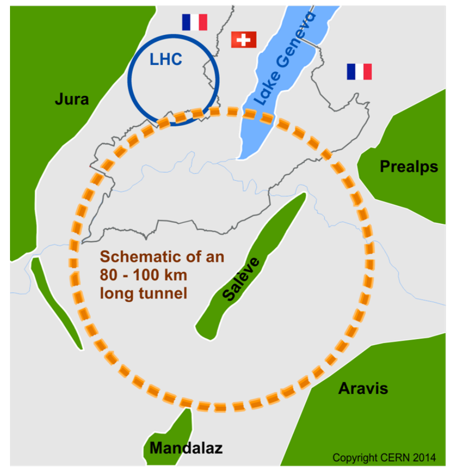

Figure 1: Schematic of a 100 km tunnel for a Future Circular Collider in the Lake Geneva basin.

Figure 1 presents a schematic of the FCC tunnel. Prior to FCC-hh installation, this new tunnel could host a high-luminosity circular e^+e^- collider (FCC-ee). Concurrent operation of hadron and lepton colliders is not foreseen, however. In addition, the FCC study considers aspects of *pe* collisions, as could be realized, e.g., by colliding the electron beam from an energy recovery linac with one of the two FCC-hh hadron beams. The FCC study also includes the design of a High-Energy LHC (HE-LHC) realized by installing 16 T magnets developed for FCC-hh in the existing 27 km LHC tunnel, so as to approximately double the energy of the LHC.

The FCC study has launched international R&D efforts on key enabling technologies through dedicated collaborative programmes, e.g. on high-field magnets, advanced cryogenics, superconducting radiofrequency systems (e.g. thin film coating) and highly efficient radiofrequency power sources. The FCC R&D includes the design of a 100 km tunnel infrastructure in the Geneva area, linked to the existing CERN accelerator complex, as requested by the European Strategy. The FCC study further explores the particle-physics opportunities and discovery potentials for the hadron, lepton and lepton-hadron colliders. The results of these physics studies drive the collider performance targets (e.g. luminosity, energy, lepton polarization). In addition, the FCC study is developing experiment concepts for the three types of colliders, addresses machine detector interface, and defines further R&D needs for detector technologies. Last not least,

* This work was supported in part by the European Commission under the HORIZON 2020 project EuroCirCol, grant agreement 654305.
† michael.benedikt@cern.ch

ISBN 978-3-95450-181-6

RECOMMISSIONING AND PERSPECTIVES OF VEPP-2000 COMPLEX

Yu. Rogovsky[#1], V. Anashin, D. Berkaev, A. Kasaev, I. Koop[1], A. Kenzhebulatov, A. Krasnov, G. Kurkin, A. Kyrpotin, A. Lysenko, S. Motygin, E. Perevedentsev[1], V. Prosvetov, A. Semenov, A. Senchenko[1], Yu. Shatunov, P. Shatunov, D. Shwartz[1], A. Skrinsky, I. Zemlyansky, Y. Zharinov,
Budker Institute of Nuclear Physics, Novosibirsk, Russia
[1]also at Novosibirsk State University, Novosibirsk, Russia

Abstract

VEPP-2000 is electron-positron collider exploiting the novel concept of round colliding beams. After three seasons of data taking in the whole energy range of 160-1000 MeV per beam it was stopped in 2013 for injection chain upgrade. The linking to the new BINP source of intensive beams together with booster synchrotron modernization provides the drastic luminosity gain at top energy of VEPP-2000. Recommissioning status, fist results and perspectives of the VEPP-2000 complex will be presented.

VEPP-2000 OVERVIEW

The VEPP-2000 collider [1] exploits the round beam concept (RBC) [2]. The idea of round-beam collisions was proposed more than 25 years ago for the Novosibirsk Phi-factory design [3]. This approach, in addition to the geometrical factor gain, should yield the beam-beam limit enhancement. An axial symmetry of the counter-beam force together with the *X*–*Y* symmetry of the transfer matrix between the two IPs provide an additional integral of motion, namely, the longitudinal component of angular momentum $M_z = x'y - xy'$. Although the particles' dynamics remain strongly nonlinear due to beam–beam interaction, it becomes effectively one-dimensional. The reduction of degrees of freedom thins out the resonance grid and suppress the diffusion rate resulting finally in a beam-beam limit enhancement [4].

The layout of the VEPP-2000 complex as it worked before shutdown for upgrade in 2013 is presented in Fig. 1.

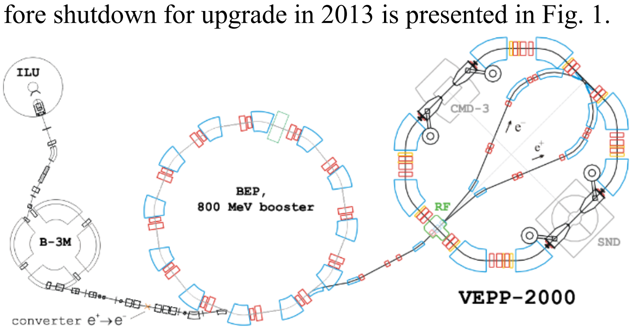

Figure 1: VEPP-2000 complex layout.

VEPP-2000 collider used the injection chain of it's predecessor VEPP-2M [5]. It consisted of the old beam production system and Booster of Electrons and Positrons (BEP) with an energy limit of 800 MeV. Collider itself hosts two particle detectors [6], Spherical Neutral Detector (SND) and Cryogenic Magnetic Detector (CMD-3), placed into dispersion-free low-beta straights. The final focusing (FF) is realized using superconducting 13 T solenoids. The main design collider parameters are listed in Table 1. In Fig. 2 one can find a photo of the collider ring.

#rogovsky@inp.nsk.su

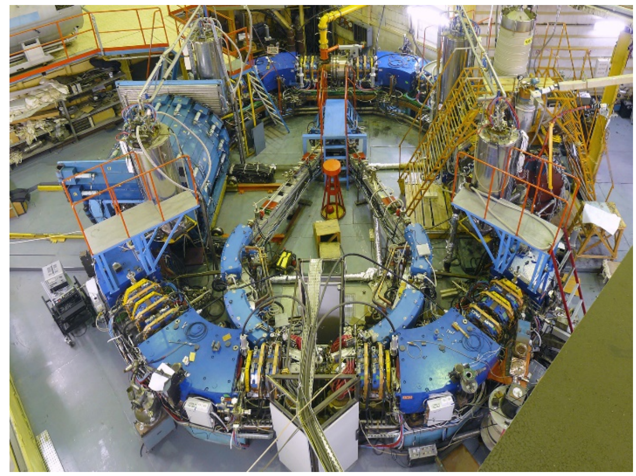

Figure 2: VEPP-2000 collider photo.

The density of magnet system and detectors components is so high that it is impossible to arrange a beam separation in the arcs. As a result, only a one-by-one bunch collision mode is allowed at VEPP-2000.

Table 1: VEPP-2000 Main Parameters (at E = 1 GeV)

Parameter	Value
Circumference, C	24.39 m
Energy range, E	150–1000 MeV
Number of bunches	1 × 1
Number of particles per bunch, N	1×10^{11}
Betatron functions at IP, $\beta^*_{x,y}$	8.5 cm
Betatron tunes, $\nu_{x,y}$	4.1, 2.1
Beam emittance, $\varepsilon_{x,y}$	1.4×10^{-7} m rad
Beam–beam parameters, $\xi_{x,z}$	0.1
Luminosity, L	1×10^{32} cm^{-2} s^{-1}

EXPERIMENTAL RUNS

VEPP-2000 started data-taking with both detectors installed in 2009 [7]. The first runs were dedicated to experiments in the high-energy range [8, 9], while during the last 2012 to 2013 experimental run the scan to the lowest energy limit [10, 11] was done (see Fig. 3). Apart from partial integrability in beam-beam interaction, the RBC gives a

ISBN 978-3-95450-181-6

STATUS OF U70

S. Ivanov, on behalf of the U70 staff#
Institute for High Energy Physics (IHEP) of NRC "Kurchatov Institute"
Protvino, Moscow Region, 142281, Russia

Abstract

The report overviews present status of the Accelerator Complex U70 at IHEP of NRC "Kurchatov Institute". The emphasis is put on the recent activity and upgrades implemented since the previous conference RuPAC-2014, in a run-by-run chronological ordering.

History of the foregoing activity and upgrades is recorded sequentially in Refs. [1].

GENERALITIES

Layout of the entire Accelerator Complex U70 is shown in Fig. 1. It comprises four machines — 2 linear (I100, URAL30) and 2 circular (U1.5, U70) accelerators. Proton mode (default) employs a cascade of URAL30–U1.5–U70, while the light-ion (carbon) one — that of I100–U1.5–U70.

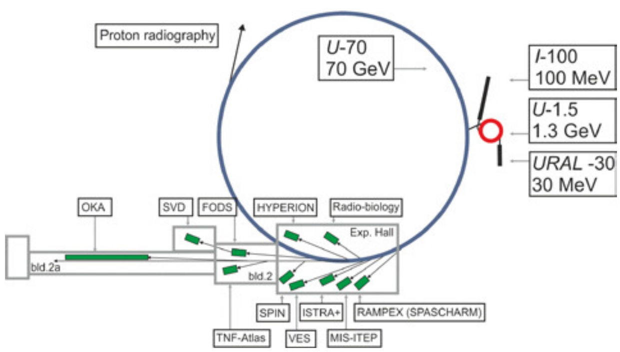

Figure 1: Accelerator Complex U70, beam transfer line network and fixed-target experimental facilities included.

Since the previous conference RuPAC-2014, the U70 complex operated for four runs in total. Table 1 lists their calendar data. The second run of 2016 was being launched during compiling this report.

Details of the routine operation and upgrades through 2014–2016 are reported in what follows run by run.

RUN 2014-3

It was the 3rd run per year of 2014 which has broken the long-term tradition of two annual (spring and autumn) runs of U70. The run had its specific features:

On the one hand, it was the 1st run of U70 for fixed-target physics when the machine was operated under the upgraded 1.5 km ring magnet main power supply plant equipped with the up-to-date static thyristor AC-DC convertors. The relevant upgrade activity took 1½ years.

The *B*-field ramping quality attained ensured safe acceleration (at least, in the single-particle limit) which is illustrated by Fig. 2.

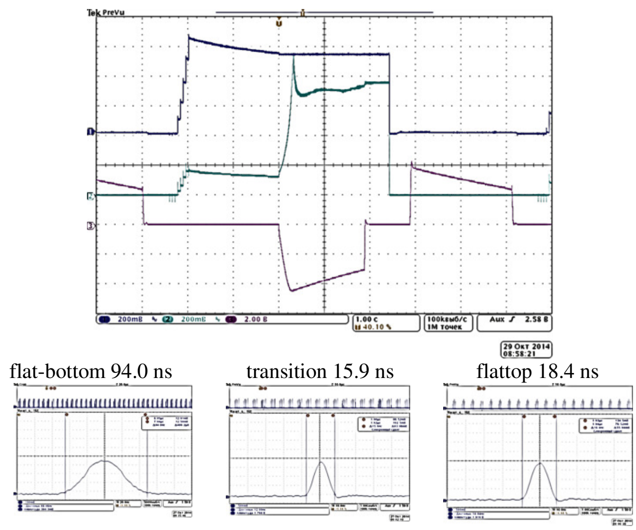

Figure 2: Acceleration in U70 with a new ring magnet power supply plant. Traces from top to bottom: beam DC current (5 bunches injected); bunch peak current (spike occurs at transition); *B*-field ramp rate (0.82 T/s max); bunch evolution through a cycle.

On the other hand, it was the 1st ever run when the 50 GeV proton beam was directed with the highest priority to the topical applied fixed-target research. It was ejected to the full-scale Proton-Radiographic Facility, named PRGK-100, operated jointly with RFNC–VNIIEF (Sarov, N. Novgorod Region).

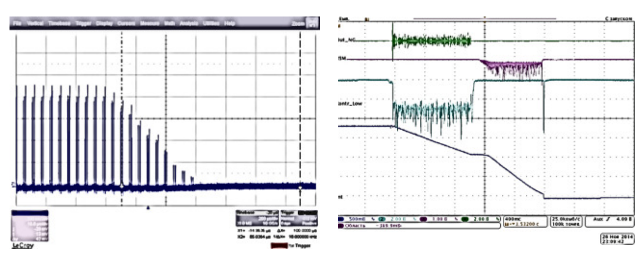

Figure 3: Beam extractions from U70. Left: 10-turm fast extraction of a short train of bunches. Right: Sequential beam sharing at flattop with slow extractions. Traces from top to bottom: AM-modulated feeding noise, spill to internal target IT35, stochastic slow spill, and waiting beam DC current decay (piecewise-linear).

To this end, the beam was extracted either with the conventional 1-turn fast (in 5 μs) or with the multi-turn (3–10 turns) fast extractions (refer to Fig. 3, left). The

N. Tyurin, A. Zaitsev, O. Lebedev, V. Kalinin, V. Lapygin, D. Demihovskiy, Yu. Milichenko, I. Tsygankov, I. Sulygin, N. Ignashin, S. Sytov, Yu. Fedotov, A. Minchenko, A. Maksimov, A. Afonin, Yu. Antipov, and D. Khmaruk.

ISBN 978-3-95450-181-6

INR HIGH INTENSITY PROTON LINAC. STATUS AND PROSPECTS.

A. Feschenko, L.V. Kravchuk, V.L. Serov,
Institute For Nuclear Research, Moscow 117312, Russia

Abstract

The status and the prospects of High Intensity INR Linac are presented. The routine beam intensity is equal to 130 μA. The annual accelerator run duration is about 1600 hours. The main beam user facilities are multipurpose complex for neutron science, isotope production facility and proton therapy facility. The primary activities are accelerator maintenance, modernization of accelerator systems and beam transportation channels, increasing of accelerator reliability, improvement of beam parameters.

INTRODUCTION

The detail information on INR Linac has been given previously [1, 2, 3]. The current report repeats some basic information about the accelerator and describes the current status, prospects and latest activities.

INR Accelerator Complex is located in science city Troitsk (Moscow) 20 kilometers to the south-west from Moscow circular road. It includes the high-intensity proton Linac, Experimental Area with three neutron sources and Beam Therapy Complex as well as Isotope Production Facility (IPF).

In nineties INR accelerator was the second large high intensity and medium energy linac after LANSCE (former LAMPF) at LANL, Los Alamos, USA. Since that time two new linacs of this type with improved parameters have been put in operation (SNS and J-PARC) and several more ones are being constructed or designed now. This activity shows the urgency of the researches made at the accelerators of this type and confirms extreme topicality of the INR research complex.

LINEAR ACCELERATOR

General Description and Parameters

The simplified diagram of the accelerator is shown in Fig. 1. The accelerator consists of proton and H-minus injectors, low energy beam transport lines, 750 keV booster RFQ, 100 MeV drift tube linac (DTL) and 600 MeV coupled cavity linac (CCL, Disk and Washer accelerating structure). There are seven 198.2 MHz RF channels for five DTL tanks and RFQ cavity (including one spare channel) as well as thirty two 991 MHz RF channels for 27 CCL accelerating cavities and one matching cavity (including three spare channels and one channel for equipment tests). Design, obtained and currently available operational Linac parameters are summarized in Table 1.

The accelerator is in regular operation since 1993. 123 accelerator runs with total duration of 45000 hours have been carried out so far including 55 runs of total duration of 16000 hours within the last decade. The availability of the beam for the users is 80÷90 % of the total beam time.

Table 1: Main Accelerator Parameters

Parameter	Design	Obtained	November 2016
Particles	p, H-minus	p, H-minus	p
Energy, MeV	600	502	247
Pulse current, mA	50	16	15
Repetition rate, Hz	100	50	50
Pulse duration, μs	100	200	0.3÷200
Average current, μA	500	150	130

Resent Modifications

The main isotope produced at INR IPF is Sr-82 used for positron emission tomography. The efficiency of isotope production depends on proton beam intensity at the target. The limitation of beam intensity is set taking into account several effects. One of the effects is heating of the target including that within the beam pulse. To decrease the pulse heating the fast raster system has been developed, built and implemented in the beam line to IPF [4]. The system provides a circular scan with adjustable amplitude and the frequency of 5 kHz thus providing one turn of the beam on the target within the 200 μs beam pulse. Due to implementation of this system the tolerable beam intensity for 143 MeV beam has been increased from 100 μA to 130 μA.

In order to increase the beam intensity twice the efforts to increase the beam pulse repetition rate from 50 Hz to 100 Hz have been undertaken. Doubling of the repetition rate will also give the possibility to effectively split the beam between the IPF and the experimental area with the help of the pulsed magnet installed several years ago in the intermediate beam extraction area (160 MeV) providing the 50 Hz beam to each facility pulse by pulse [5]. Though the whole problem has not yet been solved several intermediate results have been obtained:

- The proton injector beam pulse repetition rate has been doubled and reliable operation of the injector has been achieved at 100 Hz [6].
- Accelerating system and RF power supply systems have been tested at 100 Hz.

When testing the RF power supply systems the effect of bi-periodicity of the RF pulses has been found. The effect was due to mains supply and was observed in both accelerator parts. The problem has been investigated and

ISBN 978-3-95450-181-6

STATUS OF IFMIF-EVEDA RFQ

E. Fagotti, L. Antoniazzi, A. Baldo, A. Battistello, P. Bottin, L. Ferrari, M. Giacchini, F. Grespan, M. Montis, A. Pisent, F. Scantamburlo, D. Scarpa, INFN/LNL, Legnaro (PD), Italy
D. Agguiaro, A.G. Colombo, A. Pepato, l. Ramina, INFN/PD, Padova, Italy
F. Borotto Dalla Vecchia, G. Dughera, G. Giraudo, E.A. Macrì, P. Mereu, R. Panero, INFN/TO, Torino, Italy
T. Shinya, K. Kondo, QST, Rokkasho, Japan

Abstract

All IFMIF – EVEDA RFQ modules were completed in summer 2015. In the previous year the last three modules were RF tested at LNL at nominal power up to cw operation. At the beginning of this year all the modules were assembled in three 3.3 m long super-modules structures that were shipped to Japan. RFQ was then installed and tuned with provisional aluminum tuners and end plates to nominal frequency and field distribution. Replacement of movable aluminum components with copper fixed ones increased cavity quality value not affecting field flatness and frequency.

INTRODUCTION

The required acceleration in continuous wave (CW) of 125 mA of deuterons up to 5 MeV poses IFMIF RFQ at the forefront frontier of high intensity injectors [1].

This RFQ is indeed meant to be the injector of a 5 MW deuteron linac (40 MeV final energy) for fusion material irradiation tests. The International Fusion Materials Irradiation Facility (IFMIF) [2] project aims at producing an intense (about 10^{17} s^{-1}) neutron source facility, with spectrum up to about 14 MeV, in order to test the materials to be employed in the future fusion reactors. The facility will be based on two high power CW accelerator drivers, hitting a single liquid lithium target (10 MW power) to yield neutrons via nuclear stripping reactions.

The IFMIF-EVEDA project was funded at the time of the approval of ITER construction (2007); the task is to validate the IFMIF design by the realization of a number of prototypes, including a high-intensity CW deuteron accelerator (called LIPAc, Linear IFMIF Prototype Accelerator) for a beam power exceeding 1 MW.

LIPAc is being installed at the QST site in Rokkasho (Japan). Accelerating structures of the prototype linac, operating at 175 MHz, are the RFQ and the first Half Wave Resonator cryomodule (Fig. 1).

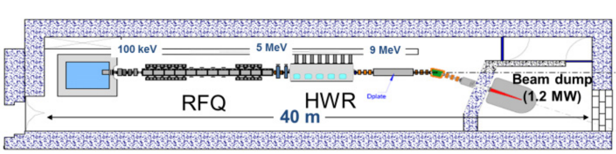

Figure 1: Schematic layout of the IFMIF-EVEDA prototype linac (125 mA, 9 MeV deuterons).

LIPAc realization is a strict collaboration between Japan and Europe. The detailed organization of such challenging project is discussed in [3].

Presently injector commissioning data are under evaluation, RFQ is assembled and tuned, MEBT and diagnostic plate are under set up and RF system is under completion [4]. The commissioning plane foresees four phases: Phase A that is the production of 140 mA deuteron current at 100 keV in CW; Phase B that is acceleration of 125 mA deuteron current at 5 MeV at 0.1% duty cycle; Phase C that is acceleration of 125 mA deuteron current at 9 MeV at 0.1% duty cycle; Phase D that is the ramping up of the duty cycle up to CW. In all phases it is planned to characterize and use, together with the deuteron beam, a proton beam with half energy, half current and similar space charge.

Phase A commissioning was concluded first week of November. Such phase was extremely important to establish the correct RFQ input conditions and guarantee the required LIPAc performances [5-7]. Unfortunately injectors didn't reach specifications at 100% DC. However, considering that a low duty cycle operation for the injector was demonstrated, it was decided to conclude phase A2, that is the characterization of injector parameters at the RFQ input location and move towards phase B. Possibility to have additional time for a phase A3, that is the characterization of injector parameters in the middle of the LEBT, was maintained.

During phase A2 commissioning, RFQ was installed 3.3 m downstream its nominal position for assembling and tuning allowing, in parallel, injector commissioning. At the beginning of November, RFQ was finally installed in its final position (Fig. 2) in view of RF conditioning and beam commissioning (phase B).

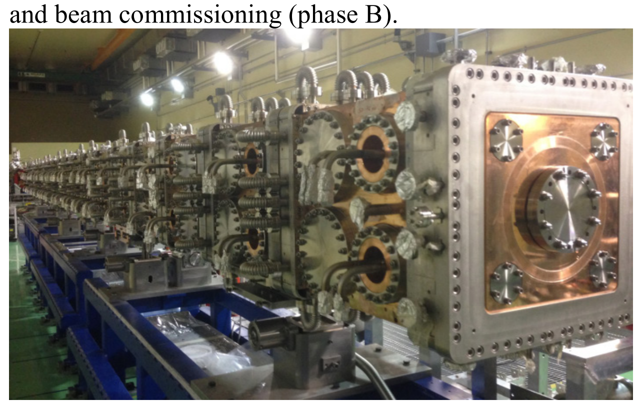

Figure 2: RFQ fully assembled and aligned in the final position.

ISBN 978-3-95450-181-6

FEEDING BINP COLLIDERS WITH THE NEW VEPP-5 INJECTION COMPLEX

F. Emanov*, A. Andrianov, K. Astrelina, V.V. Balakin, A. Barnyakov, O.V. Belikov, D.E. Berkaev, M. Blinov, Yu.M. Boimelshtain, D. Bolkhovityanov, A.G. Chupyra, N.S. Dikansky, A.R. Frolov, Ye.A. Gusev, G. Karpov, A. Kasaev, V. Kokoulin, A.A. Kondakov, I. Koop, I. Kuptsov, G.Ya. Kurkin, R. Lapik, N. Lebedev, A. Levichev, P. Logatchov, Yu. Maltseva, P. Martyshkin, A. Murasev, D. Nikiforov, A.V. Pavlenko, V. Pavlov, A. Petrenko, V. Podlevskih, V. Rashchenko, S. Samoylov, S. Shiyankov, A. Skrinsky, A. Starostenko, D.P. Sukhanov, A.G. Tribendis, A.S. Tsyganov, S. Vasiliev, V. Yudin, I. Zemlyansky, Yu. Rogovsky, A. Novohatsky, BINP, Novosibirsk, Russia
A.L. Romanov, Fermilab, USA

Abstract

VEPP-4 and VEPP-2000 e+e- colliders are switching to feed from VEPP-5 Injection Complex via newly constructed K-500 beam transfer line. Since first operation of K-500 at the end of 2015 injection complex delivered e+ and e- beams to VEPP-2000 facility and is getting ready to work with VEPP-4. Upgraded injection chain demonstrated ability to provide design luminosity to VEPP-2000 and techniques of reliable operation are now under development. The design and operation experience of Injection Complex and transfer lines will be presented.

INTRODUCTION

Injection complex was introduced in 1994 as e+/e- beam source of VEPP-5 project [1], which also included VEPP-3/4M electron-positron collider complex, charm-tau factory, phi-factory(abandoned collider project), linear accelerator (or synchrotron as alternative) for increasing injection complex beam energy to VEPP-4M and charm-tau factory experiments energy and beam transfer lines. It was later decided to build 250 m beam transfer line from injection complex to BEP in order to provide particles for VEPP-2000 [2].

First 2010-2013 run of VEPP-2000 showed 30 time lower luminosity than designed value $10^{32} cm^{-2} \cdot c^{-1}$, which was limited by insufficiency of positrons. Since injection complex had demonstrated acceptable performance by 2013/2014 season [3] upgrade of VEPP-2000 injection chain was performed in 2014-2015 [4]. VEPP-3 injection systems were switched to injection complex in summer 2016. The resulting layout of BINP colliders with injection complex is shown on Fig. 1

INJECTION COMPLEX

Injection complex is linear accelerator based e+/e- beams source with damping ring (see Fig. 2). It consists of electron gun, bunchers, 270 MeV electron linac, conversion system, 510 MeV positron linac, injection channels and dumping ring. Key designed parameters of VEPP-5 Injection Com-plex are presented in Table 1.

Table 1: VEPP-5 Injection Complex Design Parameters

parameter	value
Max. Beam Energy	510 MeV
Max. number of e- or e+ per bunch	$2 \cdot 10^{10}$
Energy spread in the bunch	0.07%
Longitudinal bunch sigma	4 mm
Horizontal emittance	0.023 mm mrad
Vertical emittance	0.005 mm mrad
beam transfers rate	1 Hz

Linear Accelerator

Linear accelerator is S-band and consists of four modules. Each module includes SLAC 5045 klystron, SLED-type [5] power compressor and 3 or 4 accelerating structures. Both linacs include 14 accelerating structures [6], which are round disk-loaded waveguide (see Fig. 3). The main design parameters of linear accelerators is presented in Table 2.

Table 2: Injection Complex Linear accelerators design parameters

parameter	value
Max. Beam Energy	280, 500 MeV
RF frequency	2855.5 MHz
Max. number of e- in beam	10^{11}
Max. number of e+ in beam	$6.3 \cdot 10^9$
Energy spread e+, e-	3%, 1%
repetition rate	50 Hz

Conversion System

In order to produce positrons we accelerate electron beam to 270 MeV and send it to tantalum conversion target.

* F.A.Emanov@inp.nsk.su

ISBN 978-3-95450-181-6

SOME PROBLEMS OF THE BEAM EXTRACTION FROM CIRCULAR ACCELERATORS

Serge N. Andrianov*, Nikolai Edamenko,
St. Petersburg State University, 7/9 Universitetskaya nab., St. Petersburg, 199034 Russia

Abstract

In this article some problems of optimizing the output beam of particles from the circular accelerator are discussed. In particular, we consider some problems of matching the booster, Nuclotron and collider in the NICA project. The main attention is paid to matching of the extraction beam systems. The proposed approach allows providing qualitative and quantitative analysis of the impact of various factors of the corresponding control systems.

INTRODUCTION

The problems of long time evolution of particles in cyclic accelerators arise not only in the implementation of the extraction of the particles. As an example, we should mention the problem of injection of particles into the accelerator, and also the problem of long time evolution (over millions of revolutions) of the particle beam in the storage rings and colliders. Let us look at the main types of problems that arise in similar types of tasks:

• construction of closed orbits in ideal and non-ideal machines;
• the problem of stability of the closed orbits in the framework of the linear and non-linear approximation of the control fields including possible deviations from the ideal parameters;
• problems of the beam injection and extraction from circular accelerators

It should be noted that when modeling of the long-time evolution (more than one billions revolutions) it is necessary to perform huge number of steps of integration and guarantee preserving both the energy of the particles and property of the symplecticity of corresponding mapping.

It is known that knowledge is information about control elements allows you to find the stable fixed points and areas (islands) with steady evolution in its neighborhoods. Knowing the location of these areas and their characteristics allows managing (using additional controls) during of extraction or injection processes using the information about topology of the corresponding closed orbits. Controlling by the corresponding classes of stable orbits can be carried out regardless. In particular, it allows not to use septum-magnets, which are traditionally used for extraction of the beam (see, eg, [**?**]). Note that the trend of development of modern circular accelerators leads to the need to include among the objects of control nonlinear control field with increasingly nonlinearity. The transition to an essentially nonlinear dynamics leads to the need for new and effective methods of mathematical modeling of long-term evolution of the beam in the accelerator channel. Increasing order nonlinear effects on the one hand allows you to "improve the quality of the beam" but to a significant complication of corresponding mathematical models and as a consequence corresponding algorithms and programs.

The purpose of this paper is to present the basic principles that not only form the basis of the proposed approach but and realized as special software and demonstrated effectiveness for a number of tasks [2]. The problems of extraction and injection of beam particles in cyclic accelerators included in the NICA complex, should be consider accurately enough, due to the peculiarity of the complex [3].

A study of the dynamic system in this case is carried out in terms of the map $\mathcal{M}_k$, generated by the control elements on the k-th step iteration $\mathbf{X}_{k+1} = \mathcal{M}_k \circ \mathbf{X}_k$, where $\mathbf{X}_k$ is the phase vector on k-th step of the iterative process, where $\mathbf{X}_k$ is phase vector on k-th step of the iterative process wich generated by the periodic dynamic system, where $\mathcal{M}_k$ is an operator of the evolution of a dynamical system corresponding to k-th period.

If $\mathcal{M}_k = \mathcal{M}$, then for any k we can talk about periodic mapping. In this case, the full map for k-th turns (for periodical channel) one can write

$$\mathcal{M}(s + kL|s) = \underbrace{\mathcal{M} \circ \ldots \circ \mathcal{M}}_{k \text{ times}} = \mathcal{M}^k,$$

where $\mathcal{M} = \mathcal{M}(s + L|s)$.

Before constructing the computational process for evolution of the beam, we should not only carefully examine the properties of the map $\mathcal{M}$, but also to ensure the fulfillment of these conditions in all stages of the computational experiment. Here we have in mind the preservation of the properties of symplecticity for the map $\mathcal{M}$ throughout interval solutions of the problem In particular, namely similar approach is implemented in a rather numerous modern works on the generation of symplectic difference schemes or integrators for Hamiltonian systems. In a number of previous works (see for example [4]) we considered the method of symplectification of block matrices included into the matrix solutions of Hamiltonian dynamical equations. Similar approach allows not only use unified mathematical tools, but create efficient algorithms and derive interpretable results.

* s.andrianov@spbu.ru

ISBN 978-3-95450-181-6

ANALYSIS OF THE PARTICLE DYNAMICS STABILITY IN THE PENNING-MALMBERG-SURKO TRAP

I.N. Meshkov, JINR, Dubna, Moscow Region; Saint Petersburg State University, Saint Petersburg
M.K. Eseev, NAFU, Arkhangelsk
A.D. Ovsyannikov*, D.A. Ovsyannikov, V.A. Ponomarev,
Saint Petersburg State University, Saint Petersburg

Abstract

Problem of stability of charged particle dynamics in the Penning-Malmberg-Surko trap is considered. It is shown that, magnetron motion is unstable for sufficiently small value of parameter a (which is the amplitude related parameter of the Rotating Wall (RW) electric dipole field). This contradicts the conclusion of the article [1] that there is a possibility of the compression of magnetron motions in the case of $\mid a \mid\to 0$. So it may indicate that the simplified model of the dynamics used by the author of the article is not accurately enough to describe the dynamics of the original system.

INTRODUCTION

Present report refers to the problem of the study of charged particle dynamics in the Penning-Malmberg-Surko trap. Various models of particle dynamics describing the magnetron and cyclotron motions are considered. The problems of the stability of the magnetron motion are investigated. In articles [1,2] the compression and expansion rates of the magnetron radius are discussed. Compression rates have been presented. The particle does not leave the area of the rotating field, and the bunch is compressed. These results are questionable.

PROBLEM STATEMENT

We consider a charged particle in the field of the potential

$$\Phi(z) = \frac{m}{q}\cdot\frac{\omega_z^2}{2}\cdot(z^2-\frac{r^2}{2})+ \\ +\frac{m}{q}a\cdot z\cdot r\cdot cos(\theta+\omega_r t), \quad (1)$$

and homogeneous longitudinal magnetic field $\vec{B}=\vec{e_z}B$. Here m and q are the mass and the charge of the particle, ω_z is the frequency of the particle longitudinal oscillations in the axially symmetric electric field of the trap electrodes, a and ω_r is amplitude related parameter and the frequency of the Rotating Wall (RW) electric dipole field asymmetric in the z-direction, z and r are the axial and radial coordinates with the axis coinciding with symmetry axis of the trap electrodes.

The magnitude of the parameter a can be estimated as

$$a=\frac{q}{m}\cdot\frac{U_r}{2RL}, \quad (2)$$

where U_r is the maximum of the potential difference between the segmented electrode plates, $2L$ is the length of the dipole RW field and R is the curvature radius of the cylindrical plates.

The charged particle motion in these fields is described by the following system of equations:

$$\ddot{x}=\frac{\omega_z^2}{2}\cdot x - a\cdot z\cdot cos(\omega_r t)+\Omega_c\dot{y}-k\dot{x}, \quad (3)$$

$$\ddot{y}=\frac{\omega_z^2}{2}\cdot y + a\cdot z\cdot sin(\omega_r t)-\Omega_c\dot{x}-k\dot{y}, \quad (4)$$

$$\ddot{z}=-\omega_z^2\cdot z-k\dot{z}-a(x\cdot cos(\omega_r t)-y\cdot sin(\omega_r t)). \quad (5)$$

Here $\Omega_c = qB/m$ is the particle cyclotron frequency, the parameter k presents the friction force related to the particle scattering by the trap buffer gas molecules.

Further, we transform the system (3-5) to the complex form. Multiplying the equation (4) by imaginary unit i and adding it with equation (3) we come to the equation for the complex function

$$\xi(t)=x+iy, \quad (6)$$

$$\ddot{\xi}+i\Omega_c\dot{\xi}+k\dot{\xi}-\frac{\omega_z^2}{2}\cdot\xi=-a\cdot z\exp(-i\omega_r t). \quad (7)$$

The equation (7) together with the equation (5) describes the particle motion in the trap.

FREE PARTICLE MOTION IN THE TRAP

The *general solution of the homogeneous differential equation* in (7) is the following

$$\xi(t)=A_1\cdot\exp(i\omega_+ t)+A_2\cdot exp(i\omega_- t), \quad (8)$$

where

$$\omega_\pm=-\frac{\Omega_c-ik}{2}\mp\frac{1}{2}\sqrt{(\Omega_c-ik)^2-2\omega_z^2}. \quad (9)$$

The constants A_1, A_2 should be found using the initial conditions.

* a.ovsyannikov@spbu.ru

ISBN 978-3-95450-181-6

RECENT EXPERIMENTS WITH HIGH ENERGY ELECTRON COOLER IN COSY

V. B. Reva, V.V. Parkhomchuk, BINP, Novosibirsk, Russia and Novosibirsk State University, Novosibirsk, Russia
M.I. Bryzgunov, BINP, Novosibirsk, Russia and FSBI "SSC RF ITEP" of NRC "Kurchatov Institute, Moscow, Russia
D.N. Skorobogatov, BINP, Novosibirsk, Russia
V. Kamerdzhiev, IKP FZJ, Jülich, Germany
I.N. Meshkov, JINR, Dubna, Russia

Abstract

The 2 MeV electron cooling system for COSY-Julich started operation in 2013 years. The cooling process was observed in the wide energy range of the electron beam from 100 keV to 1.256 MeV. Vertical, horizontal and longitudinal cooling was obtained at bunched and continuous proton beam. This report deals with electron cooling experiments at COSY with proton beam at energy 1.66 and 2.3 GeV. The proton beam was cooled at different regimes: RF on and off, barrier bucket RF, and cluster target on and off.

SETUP DESCRIPTION

The COSY cooler (see Table 1) may be used in experiments with polarized and unpolarized protons and deutrons with energies of up to 2880 MeV/u on the internal target or with extraction of the beam to the external target. In experiments with the internal target, the possibility of cooling the beam (i.e., of decreasing the spread of the particle momenta to suppress “warming effects”) is of great importance. Today, three cooling systems are already used in the COSY. Electron cooling to low electron energies (about 200 MeV) allows researchers to accumulate charged particles and raise the phase density of the beam prior to subsequent experiments. Stochastic cooling [1, 2] prevents the quality degradation of a beam interacting with a target at typical experimental energies. Unfortunately, stochastic cooling suffers from natural limitations, which hinder the operation of the synchrotron at a high intensity of the cooled beam and a small spread of the cooled particle momenta. Electron cooling at experimental energies can effectively prevent small angle scattering and ionization losses. Both factors are most probable when the energy of particles interacting with a material is high. When combined with stochastic cooling, electron cooling is expected to greatly enhance the luminosity in experiments with the internal target.

The schematic design of the high-voltage cooler is shown in Fig. 1. The design of the cooler and its main parameters are described in [3-5]. The electron beam is accelerated by an electrostatic generator that consists of 33 individual sections connected in series. Each section has two high-voltage power supplies with maximum voltage 30 kV and current 1 mA. The electron beam is generated in electron gun immersed into the longitudinal magnetic field. After that the electron beam is accelerated, moves in the transport line to the cooling section where it interacts with protons and deuterons of COSY storage ring. After interaction the electron beam returns to electrostatic generator where it is decelerated and absorbed in the collector.

Table 1: COSY Regime Parameters

Parametere	Value
Gamma transition	2.26/2.287
Proton numbers	10^8-10^9
Kinetic energy	1.66/2.3 GeV
Vacuum	10^{-9}-10^{-10} mbar
Qx	3.59-3.65
Qy	3.675-3.64
Slip-factor	-0.066/-0.1
Perimeter	183.5 m
Revolution frequency	1.524/1.564MHz
Electron energy	909/1265 kV
Electron current	0.5-0.8 A
Radius of electron beam in the cooling section	0.5 cm

EXPERIMENTS SETUP

The diagnostic of the proton beam was based on IPM (ionization profile monitor) and pickup of the stochastic cooling system. The proton current is measured by DCCT.

The transverse profiles of the beam were determined in real time with a profile monitor that measures the profiles of ions produced by electron beam ionization of residual gas. The momentum distribution was measured with pickup of the stochastic cooling system. The harmonic for Schotky noise detection was 1250.

The main parameters of COSY regime are listed in Table 1 for the regime with proton energy 1.66 and 2.3 GeV.

EXPERIMENTS WITH ENERGY 1.257 MEV

The most experiments in run 2014-2015 were carried out with electron energy 908 keV. The next step to high-voltage was done to energy 1.257 MeV. Before the cooling process the training of the high-voltage column was

ISBN 978-3-95450-181-6

OPTIMIZATION AND SIMULATIONS OF BEAM DYNAMICS IN APF ACCELERATORS

D. A. Ovsyannikov, V. V. Altsybeyev*,
Saint-Petersburg University, 7/9 Universitetskaya nab., St. Petersburg, 199034 Russia

Abstract

Design problem of APF accelerator for ensure enough high quality of output beam is considered. As we know, this problem is not easy because we have to achieve stability of longitudinal and transversal motions simultaneously. One of the first significant results in this subject were obtained by V. V. Kushin [1]. In the work [2] the problems of optimizations of ion beam are considered. The optimization approaches for some beam characteristics improving (acceleration and transmission ratios) are considered. Obtained results are confirmed by particle in cell simulations.

INTRODUCTION

Linacs with focusing by an accelerating field have long been part of the composition of any modern accelerating complex. In particular, the combination of radio frequency quadrupole (RFQ) [3–5] and APF linacs [1, 2, 6, 7] is a good decision for the initial part of the accelerating channel for high energies. In this case an ion beam is bunched in the RFQ and injected into a resonator with APF. A linac with APF has a high acceleration rate and no focusing magnetic elements. Therefore, the development of these linacs and the improvement of the beam quality remain important and current problems. When a linac is developed, parameters such as the linac length, beam current, current flow, effective emittance, etc. should be taken into account. These parameters can be improved using different optimization methods. Thus, the development of a linac based on the optimization approach can be of wide practical importance.

THE MAIN STAGES

Let us give a brief description of the main stages of accelerator modelling and optimization process.

1. Synchronous phase sequence calculation. At this stage we have to obtain a first approximation of a synchronous phase sequence. For example, application of a some analytical approximation (e. g. proposed be Jameson [8]) and swarm optimization methods may give a good enough results at this stage.

2. Cell lengths calculation and Drift tube structure generation. The lengths of accelerator cells are determined by the synchronous phase sequence. The diversity of cells lengths causes the deviation from the particular value of the resonant frequency. So the distribution of accelerating field may be non-uniform. This aberration can be eliminated by the adjustment of other geometry parameters period's length, gap ratio and drift tube diameter. For calculation of gaps lengths we use approach based on the tuning of resonant frequency of each cell on the operating frequency [9]. Follow this approach we calculate preliminary the set of dependences of resonant frequency of separate accelerator cell on the main parameters of this cell (cell length, gap length, drift tubes radii). These simulations are performed using COMSOL Multiphysics using Comsol API for Matlab in automatical mode. In following using these precalculated dependences one can choose a gap length and a drift tubes radii for a arbitrary cell length in order to tune a resonant frequency of each separate cell on the operating frequency.

3. PIC simulations. Then drift tube structure is generated one can compute the distribution of electric field and simulate particle dynamics with taking into account the space charge for the beam quality evaluation. Particle-in-cell simulations can give the most accurate result. At this stage we use the DAISI code [10–14].

4. Render decision on the optimization. If after simulations one detect that beam quality is not good enough (e. g. low transmission) we can render decision on the optimization of the synchronous phase sequence.

5. Optimization can be conducted using different approaches. In this report in follow we will consider optimization based on gradient descent method.

6. After optimization one have to regenerate the drift tubes structure and repeat the PIC simulation in order to estimate optimization process advances.

GRADIENT DESCENT OPTIMIZATION

Let us denoted $\tau = ct$, $\psi = \varphi - \varphi_s$, $p = \gamma_s - \gamma$, $\alpha_{tr} = eE_{max}/(2m_0c^2)$. Here c is the light velocity; φ and φ_s is the phases of synchronous particle and beam particle; γ and γ_s is the Lorentz factors of synchronous particle and beam particle; E_{max} is the accelerating wave amplitude. The approximation of accelerating field as an cos standing wave allows to accept the following mathematical model of beam dynamics in the an equivalent traveling wave:

$$\frac{d\beta_s}{d\tau} = \frac{\alpha_{tr}}{\gamma_s}\cos(\varphi_s(\tau)),$$
$$\frac{d\psi}{d\tau} = -2\pi\frac{\beta - \beta_s}{\lambda\beta_s},$$
$$\frac{dp}{d\tau} = \alpha_{tr}(\beta_s\cos(\varphi_s(\tau)) - \beta\cos(\varphi_s(\tau) + \psi)),$$

* v.altsybeev@spbu.ru

DEVELOPMENT OF MHF CONCEPTION AT ITEP

N.N. Alexeev, V.A. Andreev, M.M. Kats, A.A. Kolomiets, V.I. Nikolaev, Yu.A. Satov, A.V. Shumshurov, V.S. Stolbunov, A.B. Zarubin,
ITEP, B. Cheremushkinskaya 25, 117218, Moscow, Russia

Abstract

The conception of Multi-purpose Hadrons Facility (MHF) began to be discussed at ITEP in the late ~2010s [1] when ITEP-TWAC facility was intensively exploited for physical and applied research with the use of accelerated proton and ion beams varied in a wide range of operating parameters. Technological developments have continued to expand the scope of beams utilizing in diverse fields of science, medicine, industry and education. The ITEP-TWAC facility was decommissioned in 2012 and continues to remain in a state of waiting for reasonable decision on its recovery and upgrade, but conception of MHF is alive and aims at reviving in ITEP a technological base of particle accelerator technique intended for generation of proton and ion beams, covering the needs of many areas of fundamental, applied and technological research and industrial applications, represents a significant scientific and practical interest for modern and future engineering community. Created MHF environment should obviously be friendly and flexible for collaboration with industry, universities, and other national and foreign labs to provide continuous intelligent and technological progress. The key components of the MHF mission and vision are presented.

INTRODUCTION

The history of accelerator science and technology in our country, spanning more than seven decades, contains many glorious pages of the extraordinary contribution of national research institutions, scientists and engineers in the development and implementation of new ideas and the creation of unique installations.

ITEP is historically related to innovative accelerator center and it has been one of the basic institutions of the accelerator industry which specialized on the technological peculiarities of proton and ion beam accelerators. The ITEP School of accelerator science and technology has a long tradition and is focused on studying, invention, construction, creation, mastering and implementation to operation of equipment, systems and installations providing proton and ion beams for usage in physical experiments and applied research works.

Main accelerator facility of ITEP until 2012 was ITEP-TWAC which decommissioning not only significantly reduced the innovative ability of the Institute in the field of accelerator technology, but also virtually terminated all experimental work with usage of accelerated beams. The creation of MHF as a new generation of accelerator facilities would help to restore and significantly expand the accelerator technological base of the Institute and to bring the possibility of physical experiments and application works in usage of hadrons beams

TRENDS IN ACCELERATOR TECHNIQUE DEVELOPMENT

The project of MHF has to be elaborated on a base of world trends in accelerator development. The main motivation for the promotion of accelerator technologies remains still high energy physics which after the discovery of the Higgs boson has charted new frontiers of research on the accelerated beams in two main ways: the study of the properties of known and search for new particles at increasingly high both energies of interaction and luminosity; precision measurements of known processes to look for possible, tiny deviations from the SM expectations which require primarily high intensity beams [2]. At a time when accelerator projects at the high-energy frontier are experiencing difficulties in gaining financial support, projects at the high-intensity frontier are flourishing worldwide [3].

Super High Energy Colliders

There is international consensus that the priority for the short and medium term future is the full exploitation of LHC, including its luminosity upgrade (project HL-LHC). Two similar projects of colliders are currently being considered: SppC in China and FCC-hh in CERN [4]. The conceptual design for both projects foresees to 100 km ring equipped with 16-20 T magnets, to reach a pp centre-of-mass energy 100 TeV. Two projects of linear colliders being considered are: ILC [5], for which Japans has expressed interest as host country; and the CLIC [6], being developed at CERN. The needed RF gradients is 31 MV/m for 500 GeV ILC and 100 MV/m for 3 TeV CLIC.

High Intensity Proton Accelerators

Proton beam intensity is one of frontiers in advance of physics research including [7]: neutrino experiments (experimental studies of neutrino oscillations and neutrino interaction physics); kaon, muon, nucleon, and neutron precision experiments (studying ultra-rare kaon decays, searching for muon-to-electron conversion and nuclear electron dipole moments, exploring neutron properties at very high precision); material science and nuclear energy applications (critical input into the design of future energy systems, including next generation fission reactors, nuclear waste transmutation systems and future thorium fuel-cycle power systems).

During the past decades, accelerator-based neutron-generating facilities like SNS [8], J-PARC [9], PSI [10] and LANSCE [11] advanced the frontier of proton beam intensity to 1 MW power level. There are a number of different types of accelerators running at 100 kW or more today (TRIUMF, ISIS, FNAL MI, AGS, SPS). Many of these involve rapid cycling synchrotrons (RCS) as part of the acceleration chain. Many of these operate, or have

ISBN 978-3-95450-181-6

A RADIOACTIVE ION BEAM AND ISOTOPE PRODUCTION FACILITY FOR ITHEMBA LABS

J. L. Conradie, L. S. Anthony, F. Azaiez, S. Baard, R. A. Bark, A. H. Barnard, P. Beukes, J. I. Broodryk, J. C. Cornell, J. G. de Villiers, H. du Plessis, W. Duckitt, D. T. Fourie, P. Gardiner, I. H. Kohler, J. Lawrie, C. Lussi, N. R. Mantengu, R. H. McAlister, J. Mira, H. W. Mostert, C. Naidoo, F. Nemulodi, M. Sakildien, G. F. Steyn, R. W. Thomae, M. J. van Niekerk, P. A. van Schalkwyk, iThemba LABS, Somerset West, South Africa
A. Andrighetto, A. Monetti, G. Prete, M. Rossignoli, INFN, Laboratori Nazionali di Legnaro, Viale dell'Università, 2 - 35030 Legnaro, Padova, Italy

Abstract

iThemba LABS is a multidisciplinary research facility that provides accelerator-based facilities for physical, biomedical and material sciences, treatment of cancer patients with neutrons and protons and the production of radioisotopes and radiopharmaceuticals. The demand for beam time by the 3 main users, namely radioisotope production, nuclear physics research and medical applications, exceeds the available time by far.

During the past 3 years a feasibility study for a new radioactive ion beam and radioisotope production facility at iThemba LABS has been in progress. A dedicated isotope production facility is proposed which will free up the existing K=200 separated-sector cyclotron facility for nuclear physics research with stable beams. A facility for the production of low-energy radioactive ion beams is planned using the K=200 cyclotron as driver for the production of radioactive beams. A technical overview of the proposed isotope production and radioactive-ion beam facility will be given.

INTRODUCTION

iThemba LABS, located at Faure near Cape Town, operates a number of accelerators of which the Separated-Sector Cyclotron (SSC) is the largest. The SSC, a variable-energy machine, is extremely versatile and capable of producing high-intensity proton beams, a large variety of heavy ions and polarized protons at energies sufficient to probe the structure of sub-atomic matter. The SSC is primarily shared by three disciplines: nuclear physics research, proton/neutron therapy – along with radiation biology research – and radioisotope production. Over the past number of years it has become increasingly evident that the current beam allocation schedule is counterproductive and cannot satisfy the high demand for beam time from both research disciplines and radioisotope production.

The usual mode of operation is that nuclear physics research is conducted over weekends, while the rest of the week is scheduled for radiotherapy and the production of both short- and long-lived radioisotopes. iThemba LABS uses a 66 MeV proton beam from the SSC with currents of up to 250 µA to produce radioisotopes. The available beam time for radioisotope production is essentially fixed due to the current schedule and in order to expand the isotope production capacity, it became necessary to introduce a number of innovations. These include the installation of flat-topping systems for the injector cyclotron (SPC1) and the SSC, a new vertical-beam target station and beam-splitting. For operation with higher beam currents it also became essential to develop and implement non-destructive beam diagnostic equipment. Since, under present operating conditions, any further increase in the beam time for radioisotope production can only be achieved at the expense of one or more of the other programmes, it has now become essential to acquire a dedicated cyclotron for radioisotope production.

The long-term research strategy for the SSC includes the study of neutron-rich nuclei, which is rapidly becoming the focus of international research in order to understand how the elements were formed in astrophysical environments such as stars and supernovae. A forerunner to the long-term strategy is the already partially funded Low-Energy Rare Isotope Beam (LERIB) project, which aims at understanding the astrophysical processes that led to element formation. LERIB will make use of a high intensity 66 MeV proton beam from the SSC to produce different neutron-rich species. For the second phase it is envisaged that low-energy RIBs (<50 keV) will be accelerated to high energies, using a post accelerator.

The various projects will be carried out in phases. Phase 1 will involve the installation of a dedicated 70 MeV H-minus cyclotron for radioisotope production and the LERIB project. During Phase 2, a post-accelerator capable of accelerating radioactive beams from the LERIB project to an initial energy of ~ 5 MeV per nucleon will be installed.

RECENT INFRASTRUCTURE UPGRADE

Cooling Towers and Chillers Upgrade

The facility relies on a central cooling plant comprising four water-cooled chillers, seven cooling towers and associated pumps to supply chilled water at 6 °C with a cooling capacity of 4.4 MW. Chillers are operated in parallel and switched on demand as the heat load increases. During 2011 the cooling towers were replaced. Subsequently funds have been approved to replace the chillers and pumps this year. The new equipment will not only be more reliable, but will also offer a sustainable

ISBN 978-3-95450-181-6

FIRST COLD TESTS OF THE SUPERCONDUCTING CW DEMONSTRATOR AT GSI

F. Dziuba[1,*], M. Amberg[1,3,†], K. Aulenbacher[1,4], W. Barth[1,2,5], M. Basten[3], M. Busch[3], V. Gettmann[1], M. Heilmann[2], S. Mickat[2], M. Miski-Oglu[1], H. Podlech[3], M. Schwarz[3], S. Yaramyshev[2,5]

[1]HIM Helmholtz Institute Mainz, 55099 Mainz, Germany
[2]GSI Helmholtzzentrum für Schwerionenforschung GmbH, 64291 Darmstadt, Germany
[3]IAP Goethe University Frankfurt, 60438 Frankfurt am Main, Germany
[4]KPH Johannes Gutenberg University Mainz, 55128 Mainz, Germany
[5]MEPhI National Research Nuclear University, 115409 Moscow, Russia

Abstract

The future experimental program of super heavy element synthesis at GSI desires high intense heavy ion beams at or above the coulomb barrier, exceeding the capabilities of the GSI-UNILAC (Universal Linear Accelerator). Additionally, the existing GSI accelerator chain will be used as an injector for FAIR (Facility for Antiproton and Ion Research) primarily providing high power heavy ion beams at a low repetition rate. Due to this limitations a new dedicated superconducting (sc) continuous wave (cw) linac is proposed to keep the Super Heavy Element (SHE) research program at GSI competitive. The construction of the first linac section has been finished in the 3rd quarter of 2016. It serves as a prototype to demonstrate its reliable operability in a realistic accelerator environment. This demonstrator cryomodule comprises the sc 217 MHz crossbar-H-mode (CH) multigap cavity as the key component of the whole project and two sc 9.3 T solenoids. The performance of the cavity has been extensively tested at cryogenic temperatures. In this contribution the measurement results of initial cold tests will be presented.

INTRODUCTION

Regarding the future construction of a sc cw linac at GSI an R&D program has been initiated. It is intended to build and test the first linac section with beam [1]. In this context, a sc 217 MHz CH cavity [2] with 15 equidistant accelerating cells, $\beta = 0.059$ was built (see Table 1). The beam dynamics layout of the cavity is based on the special EQUUS (EQUidistant mUlti-gap Structure) [3]. Three dynamic bellow tuners inside the cavity adjust frequency changes during operation [4]. Furthermore, a helium vessel made from titanium provides a closed helium circulation around the cavity. Several flanges in each quadrant of the cavity allow an adequate surface processing. For future beam tests a 5 kW cw power coupler is available. After final surface preparation steps the new cavity has been extensively tested with low level rf power at 4.2 K.

Table 1: Main parameters of the cavity

β (v/c)		0.059
Frequency	MHz	216.816
Accelerating cells		15
Effective length ($\beta\lambda$)	mm	612
Diameter	mm	409
Tube aperture	mm	18 / 20
G	Ω	52
R_a/Q_0		3240
$R_a R_S$	kΩ^2	168
E_a (design)	MV/m	5.5
E_p/E_a		6.3
B_p/E_a	mT/(MV/m)	5.7

RF TESTS OF THE CAVITY

A first rf test of the sc 217 MHz CH cavity (without helium vessel) at the Institute of Applied Physics (IAP) of Goethe University Frankfurt has been performed beginning of 2016 [5]. At that time the performance of the cavity was limited by field emission caused by insufficient surface preparation. Regarding this, rinsing could be performed along the beam axis only. Due to a technical re-

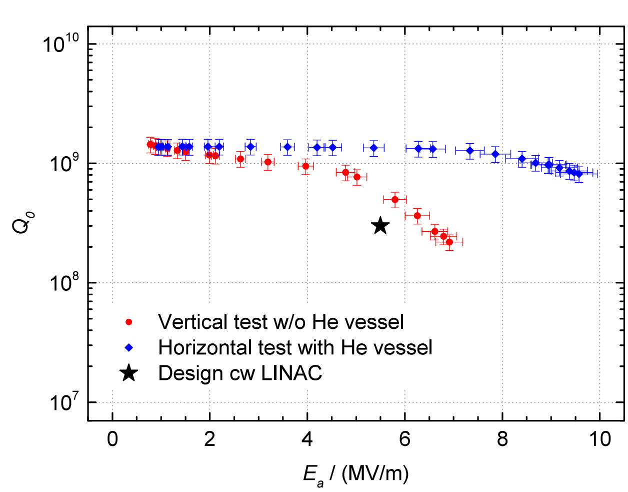

Figure 1: Q_0 vs. E_a curves at 4.2 K for two different rf tests.

[*] f.dziuba@gsi.de
[†] out of business

ISBN 978-3-95450-181-6

COLLECTOR RING PROJECT AT FAIR: PRESENT STATUS*

P. Shatunov, D. Berkaev, A. Kasaev, Yu. Rogovsky, D. Shwartz, Budker Institute of Nuclear Physics SB RAS, Novosibirsk, Russia and FSBI "SSC RF ITEP" of NRC "Kurchatov Institute", Moscow, Russia
V. Anashin, E. Bekhtenev, M. Bryzgunov, D. Gurov, V. Kolmogorov, I. Koop, A. Krasnov, O. Meshkov, T. Rybitskaya, A. Semenov, Yu. Shatunov, S. Shiyankov, A. Starostenko, A. Sukhanov, A. Tsyganov, A. Utkin, Budker Institute of Nuclear Physics SB RAS, Novosibirsk, Russia

Abstract

In November 2013, the FAIR management delegated the responsibility for the technical design, construction, installation, and commissioning of the whole Collector Ring and its components from GSI to Budker Institute of Nuclear Physics (BINP). Since that time a lot of modifications of the original design were made aiming to improve the beam parameters and the machine performance. This work shows the present status of the development.

INTRODUCTION

Collector Ring (CR) is one of the key installations of the FAIR project (Darmstadt, Germany). It is dedicated for stochastic cooling (SC) of incoming beams of antiprotons and rare ions. The cycle of the CR operation consists of injection, RF stretching, SC and finally extraction towards the HESR. Additionally there is a mode of operation for experiments with precise mass measurements of the particles in the ring. Main parameters of the storage ring for three main modes of operation are shown in Table 1. The sketch of the ring is presented in the Figure 1.

Table 1: The CR Main Parameters

	Antiprotons	Ions
Perimeter, Π	221.451 m	
Rigidity, Bρ	13 T·m	
Number of particles, N	10^8	10^9
Kinetic energy, K	3 GeV	740 MeV/u
Velocity, v	0.971c	0.830c
Relativistic factor , γ	4.20	1.79
Betatron tunes, ν_x, ν_y	4.39, 3.42	3.40, 3.44
Revolution frequency, ω_0	1.35 MHz	1.16 MHz

The work of BINP was based on the final version of the Technical Design Report (TDR) for the CR that was released by the GSI team in February 2014 [1]. Since that time a lot of modifications of the original design were made aiming to improve the beam parameters and the machine performance. All these changes were reported to the Machine Advisory Committee (MAC) in 2014 and 2015 and following its recommendations were published as a TDR Annex in 2016 [2]. These two Annexes to the TDR summarize all changes to the CR design made since February 2014. Here the part of the work done in BINP is presented.

*The work is carried out with the financial support of FAIR-Russia Research Center

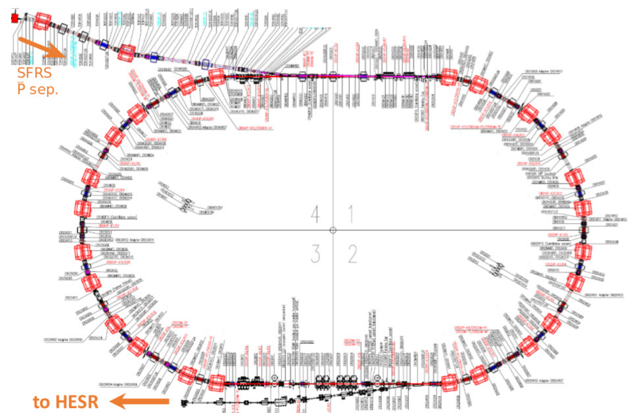

Figure 1: The Collector Ring overview.

LATTICE

The huge work was done to adopt the projects lattice to various demands coming from RF-system, SC-system, Injection/Extraction system and HESR team, taking into account all modes of operation. The apertures and lengths of magnets as well as conceptual design of all the correctors and beam diagnostic components were changed. Some magnetic elements were rearranged. Totally new concept for vacuum system was proposed.

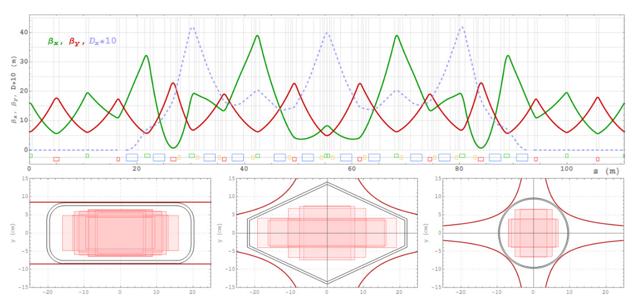

Figure 2: The lattice functions of the CR for the anitproton mode of operation and matching of the beam sizes to the aperture in the elements: the bending magnet, wide quadrupole and narrow quarupole (from left to right).

All these numerous changes were supported by adaptation of linear lattice with control of self-consistence of beam sizes, betatron phase advances between key azimuths, magnets apertures etc. Finally, in the end of 2015 the acceptable solution of overall CR conceptual design was found and the lattice (for all three operation modes) was frozen (see Fig. 2).

Since the momentum spread is very large in injected beam the natural betatron tunes chromaticity must be

ISBN 978-3-95450-181-6

SPALLATION NEUTRON SOURCE AT THE 1 GeV SYNCHROCYCLOTRON OF PNPI

O.A. Shcherbakov#, E.M. Ivanov, G.F. Mikheev, G.A. Petrov, G.A. Riabov, A.S. Vorobyev,
B.P. Konstantinov Petersburg Nuclear Physics Institute, NRC “Kurchatov Institute”, Gatchina, Leningrad district, 188300, Russia

Abstract

A description of the spallation pulsed neutron source and neutron TOF spectrometer GNEIS based on the 1 GeV proton synchrocyclotron of PNPI in Gatchina is presented. The main parameters of the GNEIS are given in comparison with the analogous world-class facilities. The experimental capabilities of the GNEIS are demonstrated by the examples of some nuclear physics and applied research experiments carried out during four decades of its operation.

DESCRIPTION OF NEUTRON SOURCE

The 1 GeV proton synchrocyclotron SC-1000 at the PNPI was commissioned in 1970 [1]. A few years later (1975), spallation neutron source and TOF spectrometer GNEIS have been developed at the accelerator and put into operation [2]. Since that time GNEIS was effectively used for neutron-nucleus interaction studies utilizing the time-of-flight technique over a wide range of neutron energies from thermal up to hundreds of MeV, both for basic nuclear physics and applied research.

The water-cooled lead target (40×20×5 cm^3) of the GNEIS neutron source is located inside the accelerator vacuum chamber (Fig. 1) below the median plane of the accelerator magnet magnetic field.

When the circulating proton bunch is deflected to strike the target, the short (~10 ns) pulses of fast neutrons are produced at a repetition rate of ≤50 Hz. At the average internal proton current of 3 μA and neutron yield of ~20 n/p for 1GeV protons, the average intensity of fast neutrons is equal to ~$3{\cdot}10^{14}$ n/s. Neutron source is supplied with a polyethylene moderator (30×10×5 cm^3) located above the target and median plane. The target and moderator are moved remotely in vertical and radial directions for optimum position during the accelerator and neutron source tuning. Five neutron beams are transported using evacuated flight tubes through the 6 m thick heavy concrete shielding wall of the accelerator main room into the experimental hall of the GNEIS. The beams are equipped with brass/steel collimators, steel shutters and concrete/steel beam dumps. Measurement stations for experimental installations are located in the GNEIS building (15×30 m^2) at the flight path distances of 35-50 m. Neutron beams #1- 4, whose axes pass through the moderator, are characterized by a $1/E^{\alpha}$ (α = 0.75-0.95) neutron spectrum shape (Fig. 2) being well suited for measurements at resonance energies (1 eV – 100 KeV). Neutron beam #5, whose axis “looks” at the surface of “bare” lead target, has a typical spectrum shape with spallation and cascade components in the neutron energy

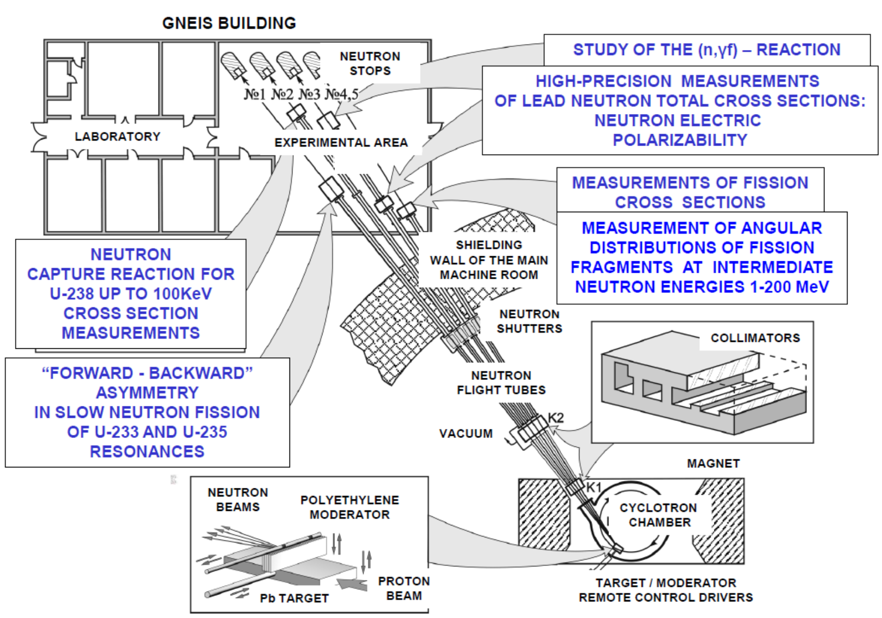

Figure 1: General layout of the GNEIS facility.

#shcherbakov_oa@pnpi.nrcki.ru

ISBN 978-3-95450-181-6

RADIOCARBON ANALYSIS OF DIFFEREENT SAMPLES AT BINP AMS

S.A. Rastigeev, V. V. Parkhomchuk, BINP SB RAS, Novosibirsk, Russia and NSU, Novosibirsk, Russia
A.R. Frolov, A.D. Goncharov, V. F. Klyuev, E.S. Konstantinov, N. A. Petrishchev, A. V. Petrozhitskii, BINP SB RAS, Novosibirsk, Russia,
L. A. Kutnykova, IAE SB RAS, Novosibirsk, Russia

Abstract

The accelerator mass spectrometer (AMS) created at BINP is used for biomedical, archaeological and other applications. Present status and experimental results are described.

INTRODUCTION

The accelerator mass spectrometry is an ultra-sensitive method of isotopic analysis for archaeology, geology, biomedical science and other fields. It's based on measurements of the ratio between isotopes. The ratio between isotopes in sample can be less than 10^{-15}. So, the counting methods are used for detection of such low radiocarbon concentration [1-5]. The AMS is based on the electrostatic tandem accelerator. The AMS system consists of the ion source, low energy channel, tandem accelerator and high-energy channel [6-8]. The low energy beam line is used for initial isotopes selection. The tandem accelerator is applied for rejection of the molecular ions and of course for obtaining necessary beam energy for radioisotopes detector. The high-energy beam line is used for the subsequent ions selection and for radioisotopes detection.

. The most distinguishing feature of our AMS machine is the use of additional electrostatic separator of ion beam, located inside the terminal. In this configuration of the AMS, the ions background is significantly reduced by the energy filter in the high voltage terminal. Interfering isobaric molecules are destroyed by collisions in the stripper into the terminal and are selected immediately after the stripping process. It is important to decrease the background from molecular fragments before the second stage of acceleration [9-10], because the energy of fragments is always less then the ion energy (at this moment). The next important distinguishing feature is magnesium vapours stripper [11] instead of the gas stripper. The gas flow into the accelerator tubes leads to big energy spread in the beam thus limiting the sensitivity and accuracy of spectrometer. The molecular destruction and ion recharging by magnesium are localized into the hot tube of the stripper. Moreover, the moment of time for ion detection can be registered with 16 µs channel width by TOF detector [12,13]. This data is used for calculation of number of detected ions per unit time, allowing filtering the background ions from electrical breakdowns.

AMS ANALYSIS ALGORITHM

During the measurements of user samples, the injection energy of radiocarbon beam was about 25 keV. The terminal voltage of tandem accelerator was 1 MV. The 180° electrostatic bend was set to transmit the ions with charge state 3+. The magnesium vapors stripper was heated for obtaining the equilibrium charge state distribution, but not more. The vacuum in the beam line was about 10^{-6} Torr.

The 20 graphitized samples are setted in the ion source sample wheel to measure the concentration of radiocarbon. Furthermore, the 3 control sample with a known concentration of radiocarbon is setted in ion source sample wheel for control and normalization of the measurement samples. Typically, this sample are two carbon wire with a carbon concentration on the natural content of modern plants and one sample of graphite MPG with radiocarbon concentration at $2*10^{-3}$ compared to modern plants. It should be noted that the control samples did not require the procedure of graphitization and setted in the sample wheel in natural form.

When measuring the concentration of radiocarbon in the samples, the switching algorithm is used. The isotope ^{14}C is detected by TOF telescope and ^{13}C currents are measured at the exit of AMS. For switching algorithm the high voltage of ion source is changed. The energy of the cesium ions remains constant. The electrostatic lens and correctors at the exit of the ion source are changed for each isotope. Thus, the passage of isotopes is carried out through a first dipole magnet, without changing the magnetic field. The magnetic field in high energy magnet is not changed to, because the radial aperture is wide enough for passing radiocarbon ions to TOF detector and ^{13}C ions to shifted FC.

The cycle of AMS-analysis of samples is represented as follows. For each sample, the ^{14}C ions are counted four times (10 seconds each) and twice the ^{13}C currents are measured for each 10 seconds counting. After that, the samples wheel is turned to the next sample for process repetition. Measuring of whole graphitized sample wheel (20 samples) takes about 15 minutes. For a set of statistics the wheel are moving to the second turn, third, etc. Typically, the measurement will take approximately 5 hours, with a statistical error of measurement for modern samples less than 1%. The process of isotope measuring and sample changing (wheel rotation) is fully automated.

ISBN 978-3-95450-181-6

COMMISSIONING OF HIGH EFFICIENCY STANDING WAVE LINAC FOR INDUSTRIAL APPLICATIONS

A.N. Ermakov*, V.V. Khankin, A.S. Alimov, L.Yu. Ovchinnikova, N.I. Pakhomov, N.V. Shvedunov, V.I. Shvedunov, Skobeltsyn Institute of Nuclear Physics, MSU, Moscow, Russia and Laboratory of Electron Accelerators MSU, Ltd., Moscow, Russia
V.V. Klementiev, Yu.N. Pavshenko, A.S. Simonov,
Laboratory of Electron Accelerators MSU, Ltd., Moscow, Russia

Abstract

We present the results of the commissioning of the pulsed linear electron accelerator with beam energy of 10 MeV, developed with the participation of scientists and engineers of the SINP MSU, LEA MSU Ltd. and JSC "RPE "Toriy". The source of RF power for accelerator is a multibeam klystron KIU-147A operating at 2856 MHz with pulse output power 6 MW and an average power of 25 kW. As a result of commissioning we received at the output of accelerator scanning system an electron beam with an energy of 10 MeV and an average power of more than 15 kW. Capture ratio and electronic efficiency of 1.24 m long accelerating structure are greater than 60% and 75%, respectively.

INTRODUCTION

Described in this paper a prototype of industrial electron linear accelerator for beam energy and average power of 10 MeV and 15 kW is based on our previous studies [1,2].

We describe the main accelerator systems: accelerating, RF, high-voltage power supply, beam scanning and diagnostic. Finally, a description of methods and results of measurements of the basic beam parameters is given.

ACCELERATING SYSTEM

Our linear accelerator is based on a standing wave bi-periodic on-axis coupled accelerating structure. In the process of the accelerating structure optimization we chose sufficiently large beam hole diameter and large webs thickness, thus increasing the vacuum conductivity, reducing the beam losses and increasing the limit of average RF losses in the walls. These features of accelerating structure are reason of a moderate value of the effective shunt impedance $Z_{eff} \approx$ 70 MOm/m. High overall efficiency of the accelerator is achieved by high value of accelerated pulse current.

The next relations provide rough estimation of accelerator parameters. Pulsed RF power required to get beam energy E = 10 MeV is:

$$P_w = \frac{E^2}{Z_{eff}L} \approx 1.14 \text{ MW} \quad (1)$$

for accelerating structure electrical length L = 1.25 m. With maximum klystron pulsed RF power $P_{kl} = 6$ MW, taking into account losses in the waveguide system, about $P_b =$ 4.5 MW pulsed beam power can be reached which corresponds to pulsed beam current $I_b = 450$ mA and average beam power 18 kW with maximum duty cycle of klystron KIU-147A D_{max} = 0.4 % [3].

Electronic efficiency of accelerating structure thus is:

$$\eta = \frac{P_b}{P_b+P_w} \cdot 100\% = 80\ \%, \quad (2)$$

which is obtained with optimal coupling coefficient of the accelerating structure with waveguide:

$$\beta = 1 + P_b/P_W = 4.94. \quad (3)$$

Detailed computer simulation of accelerating structure and beam dynamics was done in [4]. Parameters of the first three accelerating cells were optimized to provide high capture efficiency and proper beam focusing with space charge forces taken into account. The rest 21 accelerating cells are β = 1. With total electric length of the accelerating structure is L = 1.24 m, RF power losses in the walls necessary to reach 10 MeV are 1.5 MW.

About 60% of nominal 750 mA electron gun current is accelerated to final energy within energy spread of ±0.3%. Beam current losses take place mainly in the initial part of accelerating structure, so beam power losses in the structure do not exceed 1.4% of accelerated beam power.

Two more features of our accelerating structure should be mentioned. First, if a focusing coil is installed at the initial part of accelerating structure, then the beam energy can be changed in the range 5 – 10 MeV by regulation of accelerating field level within 70%, wherein the capture efficiency is varied in the range 45 – 60% (for energy spectrum width ±0.3 MeV).

Second, for pulsed RF power losses in the walls 1.5 MW and duty cycle 0.4%, average RF power losses per unit of accelerating structure length are 4.8 kW/m. Due to large webs thickness cooling channels can be drilled in them as described in [1]. In this case, the limit for RF power dissipation is about 200 kW/m [5] and maximum possible average beam power with appropriate RF source is above 700 kW.

Three electrodes electron gun operating at -50 kV cathode voltage is used as an injector. Injected beam current can be regulated between 200 – 900 mA by changing control electrode voltage in the range 2 – 15 kV with respect to cathode.

* a_ermak1978@mail.ru

ISBN 978-3-95450-181-6

A 5 TO 20 MEV ELECTRON LINEAR ACCELERATOR FOR METROLOGY

Yu.V. Zuev, Z.A. Andreeva, M.A. Kalinichenko, A.P. Klinov, A.S. Krestianinov,
O.L. Maslennikov, A.V. Tanchuk, V.V. Terentyev, NIIEFA, St. Petersburg, Russia
S.G. Trofimchuk, I.I. Tsvetkov, VNIIM, Saint-Petersburg, Russia

Abstract

The paper outlines design parameters and construction features of an electron linear accelerator to be operated in the Mendeleyev Institute for Metrology (VNIIM). The accelerator system is intended to form bremsstrahlung and electron radiation fields of variable intensity.

INTRODUCTION

A designed facility should be included into the National standard of units, which is used for metrological assurance of measurements in the nuclear-physical instrumentation, ship and aircraft building, rocket production, radiation processing and in the accelerating equipment for industry and medicine [1].

The accelerating facility consists of an electron source, accelerating structure, magnet–separator, and radiation head with an electrically-operated mechanism used for replacement of bremsstrahlung targets, foils and collimators. Table 1 presents the main design characteristics of the facility designated as follows: W_B is the energy of electrons in the spectrum maximum, ΔW is the energy spread, I_0 is the average electron current, D_B is the beam diameter in the plane of an extraction window. A required range of radiant flux is obtained by changing the pulse-repetition frequency and fine adjustment of the beam current in a pulse. This imparts a high spatial stability to radiation fields.

Table 1: Specification of the Facility

Radiation head input:	
W_B, MeV	5-20
$\Delta W/W_B$, %	±5
I_0, μA	0.1-10
D_B, mm(FWHM)	≤ 5
Electron radiation field at the 100 cm SSD:	
Area, cm^2	10x10
Flatness, %	≤ 2
Particle flux density (aver.), $c^{-1}\cdot cm^{-2}$	$6\cdot10^{11}$ - $6\cdot10^{13}$
Bremsstrahlung field at the 100 cm SSD:	
Area, cm^2	10x10
Flatness, %	≤ 2
Energy flux density (aver.), W/cm^2	0.5-200

ELECTRON SOURCE

The accelerator is equipped with a three-electrode electron source of a typical construction. Electrons are emitted from an oxide-nickel hot cathode 5 mm in diameter. The control electrode is closed with a grid of 0.1 mm-thick wires. The geometric transparency of the grid is 73 %. The grid voltage of 250-300 V provides 70-90 mA current at the gun output. Under these conditions, the electron beam has a minimum emittance well matched with the accelerator acceptance, Fig. 1. The energy of the beam injected into the accelerator is 50 keV. A separate gun modulator specifies the beam pulse duration of 5 μs; the pulses follow with a frequency from 2 up to 200 Hz.

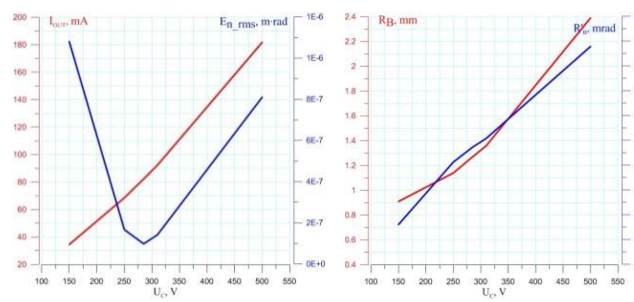

Figure 1: Calculated characteristics of the beam at the electron source output. I_{OUT} is the beam current, E_{n_rms} is the rms emittance (norm.), R_B, R'_B are the envelope size and slope, U_C is the grid voltage.

ACCELERATING STRUCTURE

A biperiodic electrodynamic structure with internal coupling cells is used for acceleration of electrons. The structure operates in the $\pi/2$ standing wave mode at 2856 MHz and comprises sixty one cells. The first ten bunching cells have cylindrical shape optimized for a minimum of high-energy particle losses over the whole beam line. The rest elements of the structure are standard Ω-shaped accelerating cells alternating with cylindrical coupling cells. The total length of the accelerating structure is 1.5 m.

The electric field of the structure is used both to accelerate particles and to confine transverse dimensions of the beam, consequently there are no external focusing elements. Energy of electrons is varied by changing the accelerating field amplitude (the field excitation power) and is accompanied with some degradation of the electron spectrum [2].

ISBN 978-3-95450-181-6

UNIVERSAL PROTON AND NEUTRON CENTRE FOR RADIATION RESISTANCE OF AVIONIC, SPACE ELECTRONICS AND OTHER APPLICATIONS AT THE 1 GEV SYNCHROCYCLOTRON IN PNPI

S.A. Artamonov#, D.A. Amerkanov, E.M. Ivanov, J.S. Lebedeva, G.F. Mikheev, G.A. Riabov, O.A. Shcherbakov, A.S. Vorobyev, B.P. Konstantinov Petersburg Nuclear Physics Institute, NRC "Kurchatov Institute", Gatchina, Leningrad district, 188300, Russia
V.S. Anashin, P.A. Chubunov, L.R. Bakirov, A.E Koziukov, Branch of the JSC "United Rocket and Space Corporation" – "Institute of Space Device Engineering", Moscow, 111250, Russia

Abstract

In PNPI RNC KI a universal center for testing electronic components for the needs of aviation and space and other applications is created on the synchrocyclotron SC-1000 with the proton energy of 1 GeV. The center consists of two protons and one neutron stands for test facilities developed at the PNPI in collaboration with the ROSCOSMOS Interagency Testing Center. The PNPI center is equipped with all necessary systems of diagnostics and monitoring of a beam, installation of targets on a beam. There is an opportunity to vary temperature of exemplars in the wide range. A unique conjunction of proton beams with variable energy 60-1000 MeV and atmospheric like neutron beam with broad energy range (1-1000 MeV) spectrum enable to perform complex testing of the semiconductor electronic devices at the SC-1000 within a single testing cycle.

INTRODUCTION

The proton synchrocyltrotron SC-1000 with the proton energy of 1 GeV and intensity of extracted proton beam of 1 μA [1] is one of the basic installations of the PNPI NRC "Kurchatov Institute". It was commissioned in 1970 and during exploitation it was significantly modernized. The experimental complex of the SC-1000 is used for investigations in fields of elementary particle physics, atomic nucleus structure and mechanisms of nuclear reactions, solid state physics and for the purposes of applied physics and nuclear medicine. Radiation resistances testing of electronics are conducted at the SC-1000 during more than two decades. Sharp growth of the needs in accelerated Single-Event-Effect (SEE)-testing of electronic components and systems intended for avionic/space and other applications has led to the development of new test facilities at the high-energy accelerators used as powerful sources of protons and neutrons.

In present report, a short description is presented of the proton (IS SC-1000 and IS OP-1000) and neutron (IS NP/GNEIS) test facilities developed at the PNPI in collaboration with the Branch of JSC "United Rocket and Space Corporation" - "Institute of Space Device Engineering", a Head Organization of the ROSCOSMOS Interagency Testing Center. A unique conjunction of proton beams with variable energy 60-1000 MeV and atmospheric like neutron beam with broad energy range (1-1000 MeV) spectrum enable to perform complex testing of the semiconductor electronic devices at the SC-1000 within a single testing cycle.

PROTON TEST FACILITIES

At present, 2 of 3 proton beam lines of the SC-1000 are used for radiation testing of electronics. The IS SC-1000 test facility has fixed proton energy of 1000 MeV and is located on the P2 beam line. At the IS OP-1000 facility located on the P3 beam line, proton energy can be varied from 1000 MeV down to 60 MeV by means of a system of copper degrader (absorber) of variable thickness from 73 mm (at 900 MeV) to 530 mm (at 60 MeV). A scheme of the proton beams and irradiation workstations placed in the experimental room, as well as a photo of the degrader system located in the SC-1000 main room are shown in Fig.1. The parameters of both proton test facilities are given in Table 1.

An adjustment of the proton beam profile is carried out roughly by means of quadrupole lenses whereas for final tuning a 2m-long steel collimator with 20 mm aperture is used. All irradiations are carried out at open air and room temperature. Both proton and neutron beam lines are equipped with a remotely controlled system intended for positioning the device under test (DUT) and heating in 20^o-125^oC temperature range.

Table 1: Parameters of the Proton Test Facilities

Parameter	IS SC -1000	IS OP - 1000
Irradiation conditions	Atmosphere	Atmosphere
Particle	Protons	Protons
Energy, MeV	1000	60 -1000
Flux, protons/cm^2 s	10^5 - 10^8	10^5 - 10^8
Irradiation area, mm	Ø ≥ 25	Ø ≥ 25
Uniformity, %	≤ 10	≤ 10
Status	In operation (1998)	In operation (2015)

#artamonov_sa@pnpi.nrcki.ru

ISBN 978-3-95450-181-6

ELECTRON ACCELERATORS SERIES ILU AND PROSPECTS OF THEIR APPLICATION IN THE FOOD INDUSTRY

A. A. Bryazgin, V.Bezuglov, B.L. Faktorovich, E.N. Kokin, M.V. Korobeynikov, A.N. Lukin, V. E. Nekhaev, A. D. Panfilov, V.M. Radchenko, A.V. Sidorov, E. Shtarklev V. O. Tkachenko, L.A. Voronin, A. Vlasov, BINP, Novosibirsk, Russia

Abstract

This report describes industrial accelerators type ILU as well as their basic parameters and characteristics. Their current applications in a cable industry, medicine and other fields are outlined. Recent experiments with food products irradiation are described, new features and ILU machines application in food industry are discussed. Some information about problems in the Russian legislation related tofoodstuff treatment by ionizing radiation is given.

INTRODUCTION

Research results in fields of radiation physics, chemistry and biology are a basis for the development of many industrial technologies. At present, the application of radiation technologies has been expanding in many developed and developing countries, such as USA, Japan, South Korea, China and others. Cost-effectiveness of the radiation technologies is attractive for industrial use.

Development of new technologies creates a demand for new industrial electron accelerators with improved parameters, namely increased energy and electron beam power, while maintaining operation ease and management.

Table 1: Basic Parameters of the ILU-type Accelerators

Parameters	ILU-6	ILU- 8	ILU-10	ILU-14
Energy of electrons, MeV	1.2-2.5	0.6-1.0	3.0-5.0	7.0-10.0
Average beam power (max), kW	20	25	50	100
Average beam current (max), mA	20	30	10	10
Power consumption, kW	100	80	150	450
Accelerator weight, tons	2.2	0.6	2.9	5
Weight of local protection, t	-	76	-	-

Budker Institute of Nuclera Physics (BINP) is one of the largest Russian research centers, it is widely known in Russia and abroad. BINP is known for fundamental works on problems of high energy physics, plasma physics and controlled thermonuclear fusion physics.

Applied works are also carried out in the BINP, namely creation and use of synchrotron radiation sources and powerful electron accelerators.

Powerful industrial electron accelerators type ILU are working round the clock operation in industrial lines for decades since 1970-s.

The ILU machines cover the energy range from 0.7 to 10 MeV at an accelerated beam power of up to 100 kW. The intrinsic features of these accelerators are simple design, ease in maintenance and a long term reliable operation under conditions of industrial production. Table 1 shows the basic parameters of the ILU-type accelerators produced by BINP [1-3].

GENERAL DESCRIPTION OF ILU MACHINES

A basic model of the ILU accelerators is the ILU-6 accelerator [1]. This machine has rather high parameters at modest dimensions and can be used for wide spectrum of technological processes. The protected hall with inner dimensions 3*4*5 m is big enough for its placement. The required volume of concrete for construction of such hall is about 180 m^3 (the required wall thickness is of about 1.5 m).

The model ILU-6 is widely used as in our country and abroad. A principle of high-voltage acceleration is used in majority of modern accelerators, i.e., the energy of electrons corresponds to the voltage generated by the rectifier. The industrial accelerators type ILU are an exception of this rule. A principle of acceleration of electrons in the gap of radio frequency (RF) resonator is used in the ILU machines. Such accelerator does not contain details, potentials of which in respect to the ground is comparable to accelerating voltage. So the complex high-voltage units (accelerating tubes, sections of rectifiers and etc.) which are damaged by the occasional discharges are not used in ILU machines. And so there is also no necessity to use insulating gas and high-pressure vessels.

RF acceleration has allowed us to create rather simple design of the machine having modest dimensions and weight. As a result the machine can be placed inside the hall of smaller dimensions comparing with the halls for high-voltage accelerators having the same parameters.

ISBN 978-3-95450-181-6

THE TARGET DEVELOPMENT FOR MEDICAL RADIONUCLIDES ^{67}CU AND ^{82}SR PRODUCTION

V. N. Panteleev, A. E. Barzakh, L. Kh. Batist, D. V. Fedorov, V. S. Ivanov, S .A. Krotov, F. V. Moroz, P. L. Molkanov, S. Yu. Orlov, and Yu. M. Volkov,
NRC "Kurchatov Institute" PNPI, 188300 Gatchina, Russia

Abstract

The RIC-80 (Radioactive Isotopes at cyclotron C-80) radioisotope complex which is constructed at the beam of cyclotron C-80 at the Petersburg Nuclear Physics Institute for the production of a wide spectrum of medical radionuclides for diagnostics and therapy has been discussed. The results of a new method utilization for the target development for the production of generator PET radioisotope ^{82}Sr and radionuclide ^{64}Cu are presented.

INTRODUCTION

The production of radionuclides that decay with emission of positrons, allowing their use for PET (Positron Emission Tomography), is very important for diagnostics of different diseases. The nuclear physics experimental methods, combined with very sensitive detectors of nuclear radiation, give a very good possibility for modern medicine in diagnostics and therapies.

In this paper the first results on the development of a new method of a high temperature separation of radioisotopes from different kind of target materials are presented, which has been worked out in the Petersburg Nuclear Physics Institute.

THE RIC-80 FACILITY

The proton beam energy of the C-80 [1] can be varied in the interval 40-80 MeV. The proton beam intensity will be up to 200 μA. This cyclotron is intended mainly for the production of a wide spectrum of medical radionuclides for diagnostics and therapy. A photograph of the C-80 cyclotron with three proton beam lines to the target stations is presented in fig.1. The RIC-80 radioisotope complex [2,3] is being constructed in the cellar of the experimental hall of the PNPI synchrocyclotron. The proton beam line is directed from the ground floor to the cellar where it can be deflected and focused to one of three target stations. The mass-separator with its target station [3] will allow for the production of separated medical radionuclides of a high purity, which will be implanted into corresponding collectors from which they can be easily extracted. The target stations will be equipped with special devices to transfer the highly radioactive targets into protection containers so that they can be transported safely to special storage places, or to hot cells for the after-treatment and corresponding preparations for pharmaceutics. The proton cyclotron C-80 gives a possibility to obtain sources of a high activity practically for the whole list of radionuclides produced at accelerators.

Figure 1: Cyclotron C-80 (ground floor) with three proton beam lines to the target stations (cellar).

These are ^{64,67}Cu, ^{68}Ge, ^{82}Sr, ^{111}In, ^{123,124}I, ^{223,224}Ra and others, which are at present under discussion in corresponding publications as perspectives for diagnostics and therapy. The mass-separator method [3] will give the possibility of the production of very pure beams of some radioisotopes. As the first steps they can be ^{81}Rb, ^{82}Sr, ^{111}In, ^{223,224}Ra, as radionuclides with respectively low ionization potentials, which can be produced by a mass-separator method with a high efficiency.

Experiment Description and Experimental Results of ^{82}sr Production and Extraction From RbCl Target Material

In the experimental tests for the production of ^{82}Sr the powder of RbCl was used as a target material. Radionuclide ^{82}Sr with a half-live $T_{1/2}$ = 25.55 days is a generator for its daughter isotope ^{82}Rb ($T_{1/2}$ = 1.25 min) which is widely used in PET diagnostics. For separation of the target material and produced strontium isotopes a new developed, high temperature method was utilized [4]. After irradiation by the 1 GeV proton beam at the PNPI synchrocyclotron RbCl powder was placed into a vessel manufactured from stainless steel which was put into Ta-

ISBN 978-3-95450-181-6

MCC-30/15 CYCLOTRON-BASED SYSTEM FOR PRODUCTION OF RADIONUCLIDES PROJECT

A.P. Strokach, Yu.N. Gavrish, S.V. Grigorenko, V.I. Grigoriev, M.L. Klopenkov, R.M. Klopenkov, V.G. Mudrolyubov, G.V. Muraviov, V.I. Nikishkin, V.I. Ponomarenko, JSC “NIIEFA”, St. Petersburg, Russia

Abstract

The projected MCC-30/15 cyclotron system is intended for operation in high-technology nuclear medicine centers. The system consists of a cyclotron, target systems for production of radionuclides in liquid, gaseous and solid states and a system for transport of accelerated ions to final units. The updated MCC-30/15 cyclotron with new systems for external injection, RF power supply and acceleration will ensure production of accelerated proton and deuteron beams in energy ranges of 18-30 and 9-15 MeV and currents not lower than 200 and 70 µA, respectively. Target systems are equipped with mechanisms for remote replacement of gaseous and liquid targets. Modular configuration of the beam transport system will allow the production of isotopes and carrying out of researches to be performed in separate experimental halls.

INTRODUCTION

The strategy for the development of nuclear medicine in RF is aimed at solving import substitution problems and providing international competitiveness of the equipment, which is one of the most high-technology products of industry. One of the main purposes of nuclear medicine is early diagnostics of diseases, which can significantly increase the efficiency of treatment and reduce the time needed. The most important tool for early diagnostics is functional diagnostics based on application of modern radiopharmaceuticals and apparatus for visualization of radionuclides’ distribution in a patient’ s body. Diagnostic studies in cardiology, oncology, neurology, etc. need a wide assortment of radiopharmaceuticals, for which purpose radioisotopes of high purity and a possibility for their production in close vicinity to a consumer must be provided. It is evident that organization of studies aimed at the development and application of new radiopharmaceuticals is possible only in research centers equipped with cyclotron equipment generating accelerated beams of hydrogen ions in a wide energy spectrum, which is proved by the world practice. The most expedient seems the use of a cyclotron with the energy of protons ranging from 18 to 30 MeV and that of deuterons varying from 9 to 15 MeV.

THE MAIN OBJECTIVES OF THE PROJECT

Prototype of the MCC-30/15 cyclotron has been designed and manufactured in the Efremov Institute (JSC “NIIEFA”). Put into operation in 2010 (see Fig. 1) [1-2].

Figure 1: General view of the MCC-30/15 cyclotron.

The experience gained in the process of the cyclotron operation has demonstrated the correctness of engineering solutions made at stages of its designing, development and manufacturing. However, more stringent current requirements for such facilities brought into being an urgent need for updating the cyclotron equipment while keeping unchanged its basic concept, namely, vertically located median plane, shielding-type magnet (which requires a radiation-shielded hall of a minimum size and offers easy maintenance/repair), combined functions of the magnet yoke and vacuum chamber, acceleration of H^- and D^- ions at one operating frequency (the 2nd and 4th harmonics).

The main purpose of the updating is attaining of higher intensity of accelerated ion beams and reliability of the system under long-term operation modes as well as designing of a new project of a system for beam transport to six remote targets. The main parameters and characteristics, which are supposed to be attained as a result of the updating are shown in Table 1.

Table 1: The main parameters of the cyclotron with updated systems.

Parameters	Values
Type of ions	
• Accelerated	H^-/D^-
• Extracted	H^+/D^+
Energy of accelerated ions, variable, MeV	
• Protons	18-30
• Deuterons	9-15
Number of devices for simultaneous beams extraction.	2
Total current of extracted beam, not less than, µA	
• Protons	200
• Deuterons	70
Power consumption, no more than, kW	
• Stand-by mode	30
• Operating mode	120

ISBN 978-3-95450-181-6

THE CC-18⁄9M CYCLOTRON SYSTEM FOR PRODUCTION OF ISOTOPES FOR PET

R.M. Klopenkov, O.L. Veresov, Yu.N. Gavrish, A.V. Galchuck, P.A. Gnutov, S.V. Grigorenko, V.I. Grigoriev, M.A. Emeljanov, M.L. Klopenkov, L.E. Korolev, A.N. Kuzhlev, A.G. Miroshnichenko,V.G. Mudroliubov, G.V. Muraviov, V.I. Nikishkin, V.I. Ponomarenko, K.E. Smirnov, Yu.I. Stogov, A.P. Strokach, S.S. Tsygankov, JSC "NIIEFA", St. Petersburg, Russia
A.S. Guchkin, I.A. Ashanin, I.P. Grigoryev, CHTD-Ltd, Moscow, Russia

Abstract

The CC-18/9M cyclotron system has been designed, manufactured and delivered to JSC "NIITFA", Moscow to be operated in a pilot PET center. Acceptance tests have been conducted. Design parameters of the updated cyclotron have been obtained: energy of accelerated proton and deuteron beams was varied within the ranges of 12-18 and 6-9 MeV with currents of 150 and 50μA, respectively. For the first time in NIIEFA practice the cyclotron is equipped with a target system intended for production of F-18 and C-11 radionuclides for PET. At present, the cyclotron system is put into commercial operation in the PETcenter.

INTRODUCTION

Successful treatment of a series of diseases in cardiology, oncology and neurology to a great extent depends on their early diagnostics, which provides a significantly higher efficiency and less time needed for treatment. Nuclear medicine is an undisputable leader in early detection of diseases, and wide application of nuclear medicine methods is proved by the fact that more than a half of radioactive isotopes produced in the world are intended for medicine. Absolute leaders in introduction of nuclear medicine into practice are the USA, Japan and some European countries. In particular, in the USA the nuclear medicine methods were used in 46% of the total diagnostic studies performed in cardiology, 34% in oncology and 10% in neurology.

Establishing of centers rendering high-tech medical assistance based on modern methods of nuclear medicine allowing us to make an early diagnosis of the most important socially significant diseases is highly urgent in the Russian Federation is highly urgent in the Russian Federation.

A pilot PET-center primarily intended for further development and optimization of the home-made equipment with the future aim of its serial production has been created in the JSC"NIITFA", Moscow. A CC-18⁄9M cyclotron system was designed and manufactured in JSC "The D.V. Efremov Scientific Research Institute of Electrophysical Apparatus" (NIIEFA) to be used in this PET-center. The machine was put into operation in 2014.

NEW ENGINEERING SOLUTIONS. COMPARATIVE CHARACTERISTICS

The cyclotron system is based on an updated CC-18⁄9M machine, which prototype is the CC-18/9 cyclotron [1, 2]. Three CC-18/9 cyclotrons have been previously manufactured and delivered to PET-centers of the Turky University, Finland (2005), the Russian research Center for Radiology and Surgical Technologies, Pesochny, St. Petersburg, Russia (2006) and Snezhinsk town, Chelyabinsk region, Russia (2010). In the updated cyclotron, the energy of accelerated proton and deuteron beams is varied in the ranges 12-18 and 6-9 MeV respectively, which widens fields of its application and raises its competitiveness. Simultaneously the design current of protons increased half as much compared to that of the basic model

It was for the first time in the NIIEFA practice that the cyclotron was delivered together with the target system providing the production of isotopes necessary for PET-diagnostics. The general view of the cyclotron [3] is shown in Fig. 1.

Figure 1: The CC-18⁄9M cyclotron system.

When designing the updated machine, the major engineering solutions proved by practice when operating CC-18⁄9 cyclotrons were kept unchanged:

- Shielding-type electromagnet with vertically located median plane to give an easy access to in-chamber devices by moving apart the movable part of the magnet along the guides (see Fig. 2). In addition, the radiation exposure of the operating personnel in the process of scheduled maintenance and repair works is significantly reduced.

ISBN 978-3-95450-181-6

GANTRY FREE TRANSPORT LINE FOR A PROTON/ION THERAPY

M.M. Kats#
FSBI SSC RF ITEP "Kurchatov Institute", Moscow

Abstract

For a long time a gantry was considered as a mandatory element for proton/ion therapy facility. However medics from MGH (Boston) suggested alternative concept which leads to decrease both cost and size of the facility [1]. The concept is based on the following provisions:

- immovable isocenter;
- active scanning of a target volume;
- different positions of patients at different fractions:
- using CT on the place of irradiation after each change of positions of the patient for improvement plan;
- using small change direction of the beam (like $\pm 10^0$).

The "Planar isocentric system" developed by author can be used to enlarge the flexibility of the concept [2]. It's relatively chip, small and can be realized for short time. It can be used for treatment for 90% of localizations. The system can replace gantry in centers of proton/ ion therapy providing significant decreasing of treatment price. The details of the system are presented and discussed.

INTRODUCTION

A therapy by beams of protons and ions is the technology of the twenty-first century. It is effective and necessary method to save human life. Its benefits in a cancer radiation therapy were known for a long time (see Figure 1). It is implemented in the radiation treatment for 20 years. But with the current technology today and in two years later the proportion of patients to whom it can be applied is about 1% of patients who are treated with beams of gamma rays [1-3].

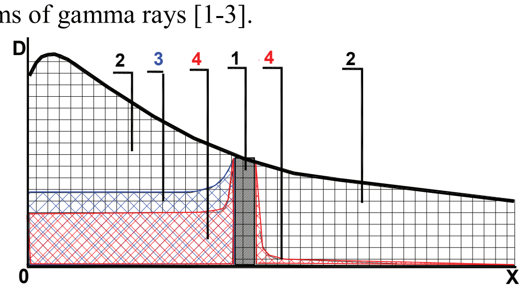

Figure 1: A scheme of energy distribution in the patient's body at irradiation by one direction at using different beams. 1 - target, 2 – gamma, 3 - protons, 4 - ions.

To generate beams of protons and ions useful for the treatment and for the further transportation of the beams to the patient it is necessary to use expensive and bulky equipment. Therefore, the treatment by proton and ion beams is significantly more expensive in a comparison with the treatment by gamma rays. In USA insurance companies pay now for the use of this treatment only for certain cancer locations, which need particularly important accuracy dose distribution (e.g., eyes), or for children treatment in order to prevent (on many years) reactions on small doses in healthy parts of the body.

In the world specialists are searching for more compact and less expensive equipment for proton and ion therapy. Compact and easy to use accelerators with superconducting magnets have been proposed. But beam transportation systems to the patient from different directions stay still bulky and expensive. Why a choice of directions of irradiation is necessary? In order not to irradiate those parts of body that must not be irradiated, and to spread the inevitable release of the energy in healthy parts of the body in a large volume, to different organs, in order to remain them at a relatively safe level.

Many years ago doctors formulated requirements for such equipment: the patient lies horizontally, motionless, the beam is transported from any direction of the plane perpendicular to the longitudinal axis of the patient. Systems that implement these requirements are generally called as a gantry. The gantry is expensive and bulky equipment because conventional electromagnets can rotate a beam of protons with a radius of about 1.5m and a beam of ions with a radius of about 4m. As a result, the standard gantry for proton's has a size of about $10m^3$ and the weight of the equipment rotated precisely in this volume is about 100t. Similar parameters of the HIT gantry for ion beam transport is 13m*13m* 18m and 660t. An optimal scheme for the proton's gantry is shown in Fig. 2.

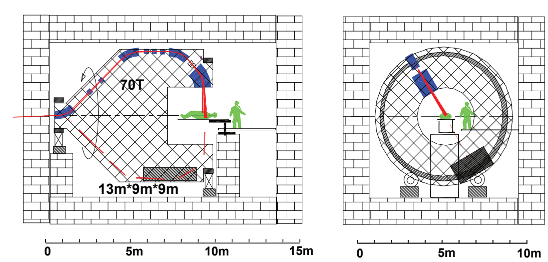

Figure 2: An optimal scheme of the gantry for a proton beam.

A significant part of the cost of a treatment is associated today with gantry systems (up to 70% for centers with four gantries). Attempts to develop a simple low-cost compact gantry based on superconductivity had not real success so far. A special conference of experts of this topic took place in the autumn of 2015 in Switzerland [4]. The problem is the necessity of fast enough distribution of the beam energy for the target volume ("scanning").

It were proposed in the form of compact "one room's" complexes by IBA, VARIAN, MEVION firms during recent years. But these complexes with one accelerator

#markmkats@gmail.com

HADRON THERAPY RESEARCH AND APPLICATIONS AT JINR

G. Shirkov†, G. Karamysheva, S. Gurskiy, O. Karamyshev, N. Morozov, D. Popov, E. Samsonov, S. Shirkov, G. Trubnikov, JINR, Dubna, Russia

Abstract

JINR has the unique experience in cancer treatment with proton beam during about 50 years. In 2005 the collaboration with IBA (Belgium) was established. During these years, the technical design of the first carbon superconducting cyclotron C400 was successfully created, the construction of serial proton cyclotron C235 was significantly improved and the fist modernized cyclotron C235 was assembled, debugged and put in the test operation in Dubna in 2011. This C235 will be used soon in the first Russian medical center with proton therapy in Dimitrovgrad. In 2015 the joint project with ASIPP (Hefei, China) on design and construction of superconducting proton cyclotron SC202 was started. Two copies of SC202 shall be produced, according to the Collaboration Agreement between JINR and ASIPP. One will be used for proton therapy in Hefei and the second one will replace the Phasotron to continue the proton therapy at JINR.

PROTON THERAPY IN JINR

The history of proton therapy in JINR began 50 years ago:

- 1967 – the beginning of the research on proton therapy;
- 1968 –1974 – first 84 patients treated with protons;
- 1975 –1986 – upgrading of accelerator and construction of a multi -room Medico -Technical Complex (MTC);
- 1987 -1996 – treating of 40 patients with protons;
- 1999– inauguration of a radiological department of the Dubna hospital;
- Since 2000 - regular treating of patients with tumors seated in the head, neck and thorax.

The modern technique of conformal three-dimensional proton therapy was realized firstly in the JINR Medical-technical accelerator complex which includes the Phasotron, the beam delivery systems and medical cabins.

Now JINR is the leading research centers of proton therapy in Russia. About 100 patients take a course of fractionated treatment in Dubna every year. During last 14 years from the startup of the Dubna radiological department more than 1000 patients were treated with proton beams [1].

The initial operation of the accelerator took place in 1949. In 1979-1984, the synchrocyclotron was converted into azimuthally varying field Phasotron. Now it is heavily depreciated and out of date, so it is important to replace it with the modern accelerator.

† email address: shirkov@jinr.ru

JINR (DUBNA) –IBA (BELGIUM) COLLABORATION

Superconducting C400 Cyclotron

IBA, the world's industrial leader in equipment of the proton therapy centers, in collaboration with JINR has designed the first superconducting carbon C400 cyclotron [2].

Most of the operating parameters (particle energy, magnetic field, RF frequency) of the C400 cyclotron are fixed. Small main field and RF frequency variation are necessary for the switching from one element to another. It is relatively small (6.6 m in diameter) and cost effective.

It offers very good beam intensity control for ultra-fast pencil beam scanning (PBS). But it requires an energy selection system (ESS) in order to vary the beam energy. The efficiency of the ESS for carbon is better than for protons due to lower scattering and straggling of carbon ions in the degrader.

The key parameters of the 400MeV/u superconducting cyclotron are listed in Table 1. The view of the cyclotron is presented in Fig.1.

Table 1. Main Parameters of the C400 Cyclotron

General properties	
accelerated particles	H_2^+, $^4He^{2+}$, $^6Li^{3+}$, $^{10}B^{5+}$, $^{12}C^{6+}$
injection energy	25keV/Z
final energy of ions, protons	400 MeV/u 265 MeV/u
number of turns	1700
Magnetic system	
total weight	700 t
outer diameter	6.6 m
bending limit	K = 1600
RF system	
number of cavities	2
operating frequency	75 MHz, 4th harmonic

ISBN 978-3-95450-181-6

SC AND HTS-RELATED ACTIVITY AT IHEP

S. Kozub, A. Ageyev, I. Bogdanov, E. Kashtanov, V. Pokrovsky, P. Shcherbakov, L. Shirshov, V. Shuvalov, P. Slabodchikov, M. Stolyarov, V. Sytnik, L. Tkachenko, O. Trusov, S. Zinchenko
State Research Center of Russian Federation - Institute for High Energy Physics (IHEP) of National Research Centre "Kurchatov Institute", Protvino, Moscow region, Russia

Abstract

The SC program at IHEP of NRC "Kurchatov Institute" has been developed intensively in the 1980s in the framework of the UNK project. More than a hundred of models of the SC magnets of various designs, and then the pilot batch consisting of 25 full-scale dipoles and 4 quadrupoles have been designed, manufactured and tested at IHEP. Two SC magnetic systems of Electron Lens for the Tevatron collider (USA) were developed, manufactured and successfully brought into operation. Development of fast-cycling SC magnets for SIS300 accelerator and wide-aperture high gradient quadrupole magnets for Plasma Experiments within the FAIR project (European Research Centre of Ions and Antiprotons, Germany) is discussed. Racetrack and annular coils from HTS-2G tape for electrical machines that were developed, manufactured and tested are reported. Test and trial results with HTS dipole magnets employing Bi2223 as well as second-generation HTS are also reviewed.

SC MAGNETS FOR UNK PROJECT

New generation of high energy proton accelerators is based on superconducting (SC) magnets. In the early eighties of the last century the special cryogenic and superconducting facilities have been created at IHEP in frame of UNK project. In collaboration with Bochvar's institute SC NbTi wire of 0.85 mm diameter with 8910 of 6 micron filaments was developed. More than 100 SC magnet models and pilot batch consisting of 25 full scale 6 m dipoles (Fig. 1) as well as four quadrupoles were developed, produced and tested at IHEP [1] - [2]. The main characteristics of the magnets are presented in Table 1.

Table 1: The Main Characteristics of UNK SC Magnets

Parameters	Dipole	Quad
Magnetic field, T	5.11	
Field gradient, T/m		97.4
Operating current, kA	5.25	5.25
Field ramp rate, T/s	0.11	
Rate of central gradient, T/m/s		2.1
Number of layers	2	2
Strand number in cable	19	19
AC losses, W	5.5	2
Stored energy, kJ	570	180
Inductance, mH	45	13
Coil inner diameter, mm	80	80
Length of the coil, mm	5800	3100
Length of the cryostat, mm	6420	4165
Mass of magnet, kg	6000	1600

Figure 1: UNK SC dipole magnet.

SC MAGNETIC SYSTEM OF TEVATRON ELECTRON LENS

In 1999 – 2003 two SC magnetic systems of Tevatron Electron Lens for Fermilab, USA were developed and produced. These systems were placed and operated at TEVATRON accelerator (Fig.2). The system consisted of seven SC and ten copper magnets [3]. Main SC solenoid had 6.5 T nominal magnetic field, 2.5m length, 152 mm coil inner diameter. The solenoid coil was wound by the Rutherford type cable from 10 SC wires of 0.85 mm diameter. Turn number of the solenoid is 7238 and nominal current – 1800 A. Six SC steering dipoles were placed over the solenoid. Two dipoles of 1840 mm length were arranged in the centre and four dipoles of 250 mm length in the end parts of the solenoid. The central dipole produced 0.2 T magnetic field at 50 A current and end dipole – 0.8 T at 200 A. All dipoles were wound by cable transposed from 8 SC wires of 0.3 mm diameter.

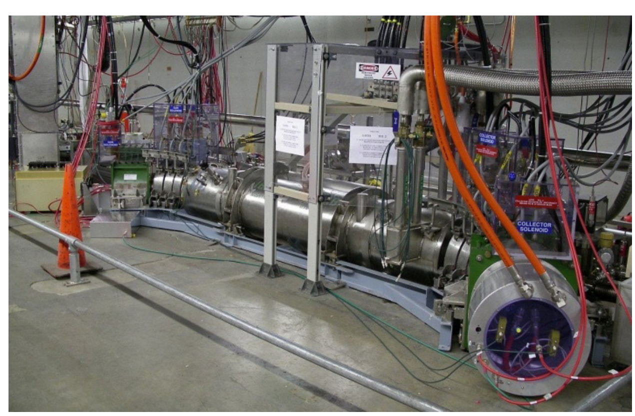

Figure 2: SC magnetic system of Tevatron Electron Lens.

ISBN 978-3-95450-181-6

STATUS OF SUPERCONDUCTING ISAC-II AND ELINAC ACCELERATORS, AND SRF ACTIVITIES AT TRIUMF

V. Zvyagintsev, Z. Ang, K. Fong, T. Junginger, J. Keir, A. Koveshnikov, C. Laforge, D. Lang, R.E. Laxdal, Y. Ma, N. Muller, R. Nagimov, D.W. Storey, E. Thoeng, B. Waraich, Z. Yao, Q. Zheng, TRIUMF, Vancouver, BC, V6T 2A3, Canada

Abstract

The development for superconducting accelerators has been started at TRIUMF in 2000. The main milestones and material implementations are: 2006 - commissioning of Phase-I of the heavy ion superconducting accelerator ISAC-II, 2010 - Phase-II, 2014 - commissioning of Phase-I of the superconducting electron linear accelerator eLinac. We are using the accumulated experience and resources for farther SRF development at TRIUMF and external projects VECC, RISP, FRIB and SLAC. TRIUMF is also running fundamental studies for SRF and educational program for universities. Status of Superconducting ISAC-II and eLinac accelerators and SRF development aspects, results and plans are discussed.

ISAC-II

SRF at TRIUMF began in 2000 with cavity and infrastructure development in support of the ISAC-II heavy ion linac as an extension of ISAC facility for ISOL based on radioactive ion beam production and acceleration. In 2006 Phase-I of ISAC-II with acceleration voltage of 20 MV was commissioned for operation [1]. In 2010 the design goal of ISAC-II for 40 MV of acceleration voltage was achieved with completion of Phase-II [2]. ISAC became a leading ISOL facility supporting a full physics program with both stable and radioactive beams being delivered: stable beams of 16O5+, 15N4+, 20Ne5+ and radioactive beams (and their stable pilot beams) of 26Na, 26Al6+, (26Mg6+), 6He1+, (12C2+), 24Na5+, (24Mg5+), 11Li2+, (22Ne4+) including 74Br14+ from the charge state booster.

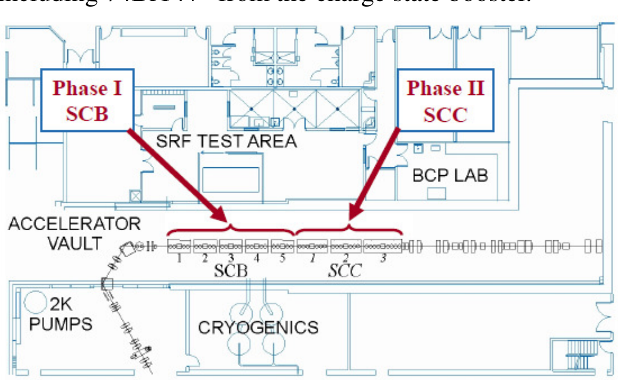

Figure 1: Layout of ISAC-II linac and SRF infrastructure.

*TRIUMF receives federal funding via a contribution agreement through the National Research Council of Canada

The Phase-I segment (SCB section of Fig. 1) consists of twenty 106 MHz quarter wave cavities housed in five cryomodules with four cavities per cryomodule.

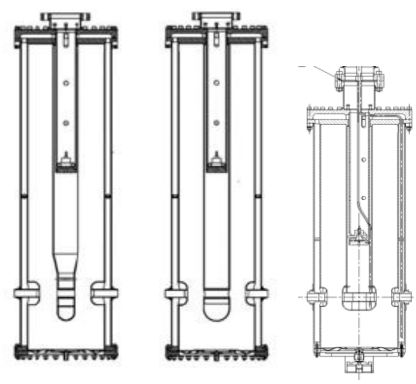

Figure 2: ISAC-II β=0.057, 0.071 and 0.11 cavities.

The Phase-II consists of twenty 141 MHz QWR cavities at β=0.11 in three cryomodules with six cavities in each of the first two modules and eight cavities in the third (SCC section in Fig. 1). Both Phase-I and Phase-II cryomodules have one 9T superconducting solenoid symmetrically placed in the cryomodule.

Cavities

The first eight of Phase-I cavities have a geometric β of 0.057 and the remainder a geometric β of 0.071 (Fig. 2). The cavity design was conducted in collaboration with INFN-LNL (Italy) with adoption of ALPI INFN-LNL coaxial bulk Nb cavities concept with vacuum volume open to cryomodule isolation vacuum; the cavities are specified to operate at 106MHz and to provide an effective acceleration of 1.1MV for a cavity power of 7W at 4.2K and corresponding peak surface fields of 30MV/m and 60mT [3]. 20 Phase-I cavities were fabricated at Zanon (Italy) and assembled in 5 cryomodules designed and fabricated at TRIUMF.

The Phase-II 141 MHz superconducting cavity with β of 0.11 is shown in Fig. 2. It was developed at TRIUMF and has a similar structure to the ISAC-II Phase-I linac cavity. The chief difference here besides the frequency is the inner conductor beamport region is outfitted with a donut style drift tube to improve the transit time factor. The Phase-II cavity has the same specification as the Phase-I cavities [4]. Twenty Phase-II cavities were produced by PAVAC Industries in Canada. Three cryomodules with high beta cavities were successfully commissioned in April 2010 [2]. An SRF infrastructure for SC development including SRF test area, clean room

ISBN 978-3-95450-181-6

CONCEPTUAL DESIGN OF SUPERCONDUCTING COMBINED-FUNCTION MAGNETS FOR THE NEXT GENERATION OF BEAM CANCER THERAPY GANTRY

S. Sanfilippo, C.Calzolaio, A.Anghel, A. Gerbershagen and J.M.Schippers,
Paul Scherrer Institut, Villigen PSI, Switzerland

Abstract

An increasing number of proton therapy facilities are being planned and built at hospital based centers. Many facilities use rotatable gantry beamlines to direct the proton or ion-beam at the patient from different angles. A key issue is the need to make future gantries lighter and more compact with the use of cryogen-free superconducting magnets, in particular for the final bending section which can be of large aperture. Benefits of using the superconducting technology are: (1) the possibility to have a large momentum acceptance, hence reducing the need to ramp the magnet and enabling new treatment techniques, (2) the size reduction due to a lower bend radius and (3) the weight reduction up to a factor ten. The latter will also significantly reduce the costs of the supporting structure. We present a conceptual design based on Nb_3Sn superconducting combined function magnets (dipole, quadrupole, sextupole). The geometry using racetracks, the superconducting strand and cable parameters and the results of the thermal and the mechanical studies are reported. These magnets will work at a temperature of about 4.2 K cooled with cryocoolers.

INTRODUCTION

The number of the centres offering proton therapy has grown significantly over the past years and the number of hospitals and research institutions delivering protons or carbon ions for tumour treatment is following also an increasing trend. For the next generation of these machines, the superconducting technology applied to magnet development will play a key role as it will enable developping compact and light gantries. A gantry is the final section of a proton therapy facility, which consists of beamline magnets, beam diagnostics elements and the mechanical support structure. The gantry rotates around the patient and irradiates the tumour from different directions. The increased field strengths using superconducting magnets will decrease the bending radius, decrease the overall weight of the system and reduce the demands on the mechanical structure. More-over superconducting magnets allow increasing the momentum acceptance, hence reducing the need to ramp the magnet and enabling new treatment techniques [1].

The present concept is based on an isocentric gantry design with the transverse scanning performed downstream of the final bending magnet (Fig.1). A transverse scanning field of 30 cm x 40 cm with a beam spot size of $2\sigma \approx 5$ mm at the isocenter is required. The gantry should also allow a beam energy modulation between 70 MeV and 230 MeV (corresponding to a magnetic rigidity $B\rho$ of 1.2 Tm and 2.3 Tm, respectively). In our gantry layout, the last bending section aims at deflecting the proton beam by 135°. An achromatic layout is chosen with a very large momentum acceptance ($\Delta p/p \sim \pm 12\%$). Energy change between two layers will be performed in less than 100 ms, within the momentum acceptance window, keeping a ramping speed of magnetic field between these windows below 0.1T/s.

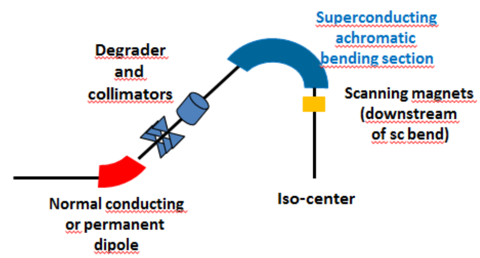

Figure 1: Gantry based on achromatic superconducting combined function magnets for the bending section.

The bending section consists of a series of superconducting combined function magnets described in this work, resulting from the conclusions of a preliminary study based on an upstream design [2]. The magnet geometry, the field maps, the conductor characteristics and the results of the thermo-mechanical calculations are discussed. Each dipole is cooled using two stage cryocoolers working at 4.2 K. To enable a sufficient temperature margin avoiding quenches after four consecutive current cycles (the treatment for the maximal target size), Nb_3Sn cables are used in the coils.

LAYOUT AND MAGNET DESIGN

Bending Section layout

The transport section is a curved, compact and locally achromatic, to minimize the proton beam dispersion. The section consists of three types of combined function magnets: (1) two superconducting combined dipoles-quadrupole and sextupole magnets (SDC1, SDC2), (2) a superconducting combined quadrupole-sextupole magnet (SCQ), (3) two tuneable normal conducting quadrupoles (Q1&2) at each side to meet with the beam optic conditions [1]. All the geometries are based on racetrack coils to keep the manufacturing as easy as possible. The design is optimized in different steps. From the magnets 3D field maps, the field harmonics are calculated and compared with the ones required by theoretical first order

ISBN 978-3-95450-181-6

RECENT OPTIMIZED DESIGN OF ILC CRYOMODULE WITH EXPLOSION WELDING TECHNOLOGY

B. Sabirov, J. Budagov, G. Shirkov, Yu.Taran, JINR, Dubna, Russia
A. Bryzgalin, S. Illarionov, E. Pekar, PWI, Kiiv, Ukraine
A. Basti, F. Bedeschi, P. Fabbricatore, INFN, Pisa/Genova, Italy

Abstract

The past few years, we have made a great deal of progress in developing and demonstrating the enabling technology needed for a linear collider for the modernization of the cryomodule for the International Linear Collider (ILC) in the frame of collaboration JINR (Dubna, Russia), INFN (Pisa/Genova, Italy) and PWI (Kiiv, Ukraine) [1-4].

INTRODUCTION

Based on our experience, the collaboration got down to creating a transition specimens between the steel shell of the cryomodule vessel and the niobium cavity (Fig. 1). Trimetallic Nb+Ti+SS specimens were produced using the explosion welding and successfully tested at liquid nitrogen and liquid helium temperatures. This version deserves special attention for its manufacturability, simpler design, guaranteed strength and reliability of the joint and above all for an appreciably lower cost. It is a promising new transition joint technology based on cladding side surfaces of a steel flange by titanium using explosion bonding and welding a Nb pipe to titanium by EBW.

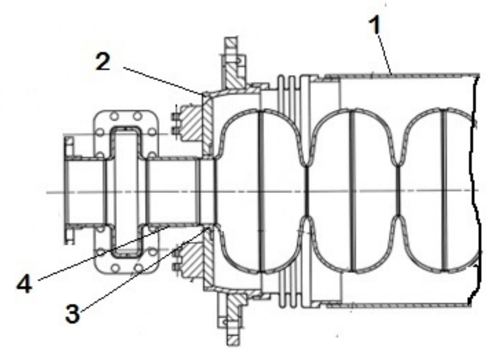

Figure 1: Scheme of combined adapter connection with a cryogenic module: 1 – steel shell; 2 - electron beam welding or argon arc welding connection of shell with steel flange of adapter; 3 - steel flange; 4 - niobium tube.

PROBLEM DEFINITION

It is known that welding of similar materials gives the best results. The adapter should consist of at least two metals, niobium and stainless steel. No fusion welding, including electron beam welding is suitable for joining niobium and stainless steel because it results in formation of intermetallic compounds like Nb_xFe_y, which do not allow the required adapter tightness to be obtained. In addition, this compound does not withstand the thermal load at cryogenic temperatures and fails.

Earlier experiments showed that electron beam welding of niobium and titanium did not result in formation of intermetallic compounds and ensured the required helium and vacuum tightness. In this connection the following adapter manufacture procedure was proposed [5]. First, the stainless steel disc is clad with titanium on both sided by explosion welding, the resulting trimetal is shaped as required (by planishing and turning to the size), and a hole is cut for the niobium pipe. The pipe is inserted in the hole and electron-beam welded to titanium (Fig. 2).

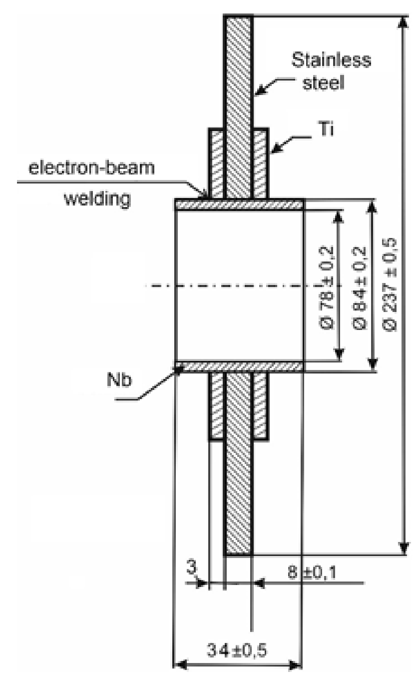

Figure 2: The design of the adapter, ensuring the absence of niobium intermetallic formations during welding.

Advantages of this adapter manufacture procedure are as follows:

- electron beam welding of niobium and titanium did not result in formation of intermetallic compounds and ensured the required helium and vacuum tightness;
- possible formation of intermetallic compounds in the explosion weld steel–titanium joint does not affect helium tightness;
- explosion welding of flat pieces is technologically much simpler than welding of pipes and allows joints with quality as much stable as possible;
- expenditure of steel and niobium decreases.

ISBN 978-3-95450-181-6

PROGRESS ON MANUFACTURING AND TESTING OF THE SC MAGNETS FOR THE NICA BOOSTER SYNCHROTRON

H.G. Khodzhibagiyan#, N.N. Agapov, P.G. Akishin, V.V. Borisov, A.V. Bychkov, A.R. Galimov, O.V. Golubitskiy, A.M. Donyagin, V.N. Karpinskiy, B.Yu. Kondratiev, S.A. Korovkin, S.A. Kostromin, A.V. Kudashkin, G.L. Kuznetsov, D.N. Nikiforov, A.V. Shemchuk, S.A. Smirnov, A.Yu. Starikov and G.V. Trubnikov, JINR, Dubna, Russia

Abstract

NICA is a new accelerator collider complex under construction at the Joint Institute for Nuclear Research in Dubna. The facility is aimed at providing collider experiments with heavy ions up to Gold in the centre of mass energy from 4 to 11 GeV/u and an average luminosity up to $1 \cdot 10^{27}$ cm^{-2} s^{-1} for Au^{79+}. The collisions of polarized deuterons are also foreseen. The facility includes two injector chains, a new superconducting booster synchrotron, the existing 6 AGeV superconducting synchrotron Nuclotron, and a new superconducting collider consisting of two rings, each 503 m in circumference. The booster synchrotron is based on an iron-dominated "window frame"- type magnet with a hollow superconductor winding analogous to the Nuclotron magnet. The design of superconducting magnets for the NICA booster synchrotron is described. The progress of work on the manufacturing and testing of the magnets is discussed. The calculated and measured values of the characteristics of the magnets are presented. The status of the facility for serial test of superconducting magnets for the NICA and FAIR projects is described.

INTRODUCTION

The NICA project [1], [2] started at the Joint Institute for Nuclear Research (JINR) in Dubna in 2007. The main goal of the project is to study hot and dense strongly interacting matter in heavy-ion (up to Au) collisions at the centre-of-mass energies up to 11 GeV/u. A study of spin physics is also foreseen with extracted and colliding beams of polarized deuterons and protons at the energies up to 27 GeV for protons. The NICA accelerator complex will consist of two injector chains, the new 600 MeV/u superconducting (SC) booster synchrotron, the upgraded SC synchrotron Nuclotron [3], and the new SC collider having two storage rings each about 503 m in circumference with luminosity up to $1 \cdot 10^{27}$ cm^{-2} s^{-1} for Au^{79+} and two interaction points. The Nuclotron-type design [4] – [6] based on a cold iron yoke and a saddle-shaped SC coil has been chosen for the booster and the collider magnet. The magnet includes a window frame yoke at 4.5 K and a SC coil made of a hollow Nb-Ti composite SC cable cooled with a two-phase helium flow. The yoke supports Lorentz forces in the coil.

DESIGN OF THE MAGNETS

The designs of the magnets for the NICA booster are given in [7] – [12]. The iron yoke of the magnet consists of two symmetric parts bolted together. The half-yokes are fabricated of the laminated isotropic 0.65 mm thick electrical steel M 530. The laminations are compressed with pressure of 5 MPa in the direction of the longitudinal axis of the magnet. The side plates 10 mm thick are welded with laminations and stainless steel end plates 20 mm thick. The magnet is 2.2 m long and has a radius of the curvature of about 14 m. Fig. 1 shows the dipole magnet for the NICA booster.

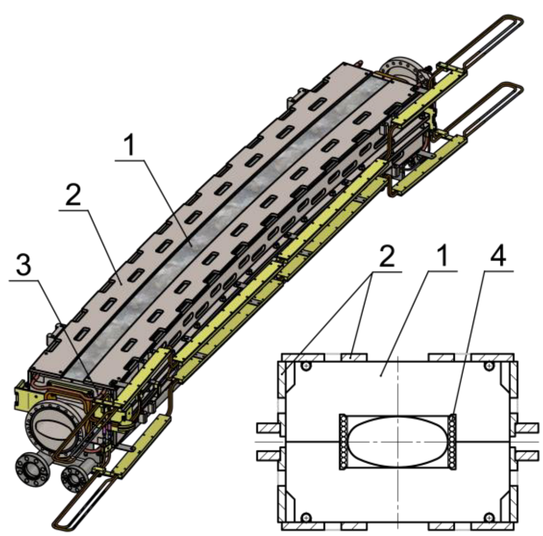

Figure 1: View of the dipole magnet. 1 – lamination, 2 - side plate, 3 - end plate, 4 – SC coil.

Each pair of lattice lenses is connected using the intermediate cylinder and form a doublet (see Fig. 2). The doublet of about 1.8 m length has a rigid mechanical design. It has a demountable construction that allows splitting the doublet into two horizontal parts to install the beam pipe. The doublet is fixed in a cryostat by means of eight suspension rods and adjusted in space as a unit.

Table 1: Main Characteristics of the Magnets

Characteristic	Dipole	Lens
Number of magnets	40	48
Max. magnetic field (gradient)	1.8 T	21.5 T/m
Effective magnetic length	2.2 m	0.47 m
Beam pipe aperture (h/v)	128 mm/ 65 mm	
Radius of curvature	14.09 m	-
Overall weight	1030 kg	110 kg

ISBN 978-3-95450-181-6

VACUUM INSULATION TANDEM ACCELERATOR: PROGRESS AND PROSPECTS*

S. Taskaev#, T. Bykov, A. Ivanov, D. Kasatov, Ya. Kolesnikov, A. Koshkarev, A. Makarov, Yu. Ostreinov, I. Shchudlo, E. Sokolova, I. Sorokin, T. Sycheva,
BINP and Novosibirsk State University, Novosibirsk, Russia

Abstract

A promising method of treatment of many malignant tumors is the boron neutron capture therapy (BNCT). It provides a selective destruction of tumor cells by prior accumulation of a stable boron-10 isotope inside them and subsequent irradiation with epithermal neutrons. It is expected that accelerator based neutron sources will be created for the clinical practice. One such source could be an original source of epithermal neutrons, created in BINP. To obtain proton beam a new type of particle accelerator is used – tandem accelerator with vacuum insulation. Generation of neutrons is carried out as a result of the threshold reaction $^{7}Li(p,n)^{7}Be$. Several changes were made in the construction of tandem accelerator with vacuum insulation during 2015-2016. This allowed us to suppress the unwanted flow of charged particles in the accelerator, to improve its high-voltage stability, and to increase the proton beam current from 1.6 to 5 mA. Such current value is sufficient for BNCT. The report describes in detail the modernization of the accelerator, presents and discusses the results of experiments on obtaining the proton beam and the formation of neutron flux using lithium target, and declares our prospective plans. The obtained neutron beam meets the requirements of BNCT: the irradiation of cell cultures provides the destruction of cells with boron and preservation of cells without boron. Irradiation of immunodeficient mice with grafted glioblastoma results in their recovery.

INTRODUCTION

Boron neutron capture therapy is currently considered as a promising technique for treatment of malignant tumors [1, 2]. For the widespread introduction of this technique in practice compact epithermal neutron sources based on charged particle accelerators are required. A new type of the accelerator – a tandem accelerator with vacuum insulation – was proposed [3] and constructed in BINP [4]. The accelerator is characterized by fast ion acceleration and a large distance between the ion beam and the insulator (on which electrodes are mounted). After the dark current was suppressed to an acceptable level [5], the injection of a negative hydrogen ion beam into the accelerator [6] and stripping in the gas target were optimized [7], the proton beam current was increased from the initial values of about 140 μA [8] to 1.6 mA [9], which was stable for more than one hour. In the elucidation of the reasons for the limitation of the current in the tube for accelerating negative hydrogen ions, a significant electron flow and a counter-flow of positive ions generated in the acceleration tube and in the stripping target were found and measured [10].

*Work supported by grant from the Russian Science Foundation (Project no. 14-32-00006), the Budker Institute of Nuclear Physics and the Novosibirsk State University
taskaev@inp.nsk.su

DESIGN OF THE ACCELERATOR

Figure 1 shows the accelerator. Coming from source *1* the low-energy negative hydrogen ion beam is defected in a magnetic dipole field by an angle of 15 degrees, focused by a pair of magnetic lenses *2*, injected into accelerator *3* and accelerated up to 1 MeV. In a gas (argon) stripper *7* which is installed inside a high-voltage electrode *6* negative hydrogen ions are converted into protons. Then protons are accelerated by the same 1 MV potential to an energy of 2 MeV. The potential for the high-voltage electrode *6* and five intermediate electrodes *5* of the accelerator is supplied by the sectioned rectifier *9* (most the source is not shown) through insulator *8*, wherein the resistive divider is set. Gas evacuation is performed by turbomolecular pumps *10* mounted on the ion source and at the accelerator exit and a cryogenic pump *4* via jalousies in the electrodes.

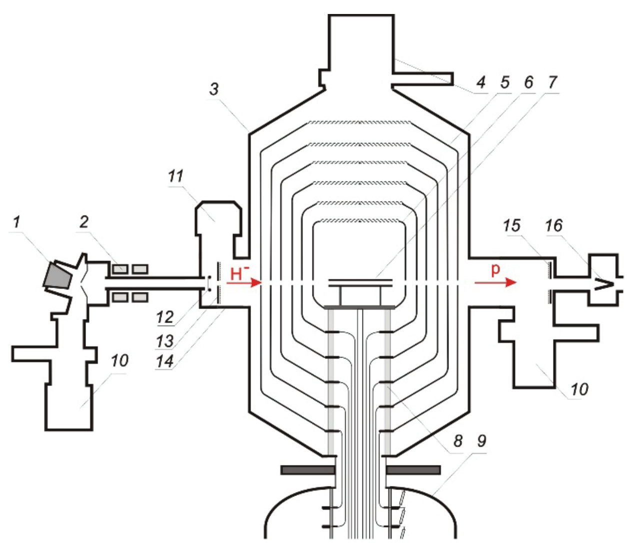

Figure 1: Modernized tandem accelerator with vacuum insulation: *1* – negative hydrogen ion source, *2* – magnetic lenses, *3* – accelerator, *4* – cryogenic pump, *5* –intermediate electrodes, *6* – high-voltage electrode, *7* – gas stripper, *8* – insulator, *9* – high-voltage sectioned rectifier, 10 – turbomolecular pumps, *11* – cryogenic pump, *12* – ring, *13* – cooled metallic diaphram and end detector with a grid, *14* – intake vacuum volume, *15* – detector with a grid, *16* – Faraday cup.

ISBN 978-3-95450-181-6

STATUS OF THE NUCLOTRON

A. Sidorin, N. Agapov, A. Alfeev, V. Andreev, V. Batin, O. Brovko, V. Bugaev, A. Butenko, D.E. Donets, A. Eliseev, V. Fimushkin, E. Gorbachev, I. Gorelyshev, A. Govorov, A. Grebentsov, E. Ivanov, V. Karpinsky, H. Khodzhibagiyan, A. Kirichenko, A. Kovalenko, O. Kozlov, K. Levterov, V. Mikhailov, V. Monchinsky, A. Nesterov, Yu. Nozhenko, A. Osipenkov, A. Philippov, S. Romanov, P. Rukoyatkin, A. Shurygin, I. Slepnev, V. Slepnev, A. Smirnov, E. Syresin, G. Trubnikov, A. Tuzikov, B. Vasilishin, V. Volkov, JINR, Dubna, Russia
A. Belov, INR RAS, Moscow

Abstract

Since last RuPAC two runs of the Nuclotron operation were performed: in January – March of 2015 and June 2016. Presently we are providing the run, which has been started at the end of October and will be continued up to the end of December. The facility development is aimed to the performance increase for current physical program realization and preparation to the NICA Booster construction and Baryonic Matter at Nuclotron experiment.

INTRODUCTION

The Nuclotron is the basic facility of the Veksler and Baldin laboratory for high energy physics (VBLHEP). Its scientific program includes experimental studies on relativistic nuclear physics, spin physics and physics of flavours. At the same time, the Nuclotron beams are used for research in radiobiology and applied research.

VBLHEP accelerator complex includes Alvarez-type linac LU-20, superconducting synchrotron Nuclotron equipped with an internal target station and slow extraction system and facilities for fixed target experiments located in experimental building of about 10000 m^2.

In future the Nuclotron will be main synchrotron of the NICA facility being constructed at JINR [1]. Presently the creation of the NICA general elements is realizing in the frame of three officially approved JINR projects: "Nuclotron-NICA" (accelerator part), MPD (the project oriented to creation of one of the collider detectors) and BM@N (Baryonic Matter at Nuclotron – the fixed target experiment with heavy ions, the detector is under construction).

Last two years general attention was paid to development of the injection complex, preparation for the NICA Booster construction and BM@N experiment. The Nuclotron operational time was optimized in accordance with the JINR topical plans with account the plan of the NICA construction. During this period two Nuclotron runs were performed and the spin physics run has been started 26 of October. In this report we are concentrated on the most important results of the machine development works. Results of the injection complex development are presented in dedicated talks [2, 3].

STATISTICS OF OPERATION

During the run #51, performed in the period from 26 January to 15 March 2015, the following machine development works were provided:
- development of Q-meter hardware and software,
- put into test operation of the system for precise current measurement of the Nuclotron magnetic system,
- the works for the current stabilization in magnets of the extracted beam lines,
- put into operation new thermometry system of the Nuclotron,
- methodical investigations of stochastic cooling and different modes of the beam adiabatic capture.

Total duration of the run was about 1150 hours, about 800 hours of the beam time was spent for experimental researches in accordance with JINR topical plan. For the first time all the subsystems of the BM@N detector were tested with the beam. During the run deuteron and carbon ions were accelerating. Maximum deuteron energy was about 5.3 GeV/u (magnetic field at the extraction plateau is 1.855 T).

General task of the technological run #52 was commissioning of new fore-injector, optimization of the source of polarized ions (SPI) and test of polarimetry. The run at total duration of about 650 hours was performed from 2 to 30 of June 2016. Its main result is successive operation of the new fore-injector and acceleration of deuteron beam from SPI at intensity of 10^9 at the experiment energy. During the run the polarimeters after linear accelerator LU-20, at Nuclotron internal target station and at extracted beam line have been tested. During the machine development shifts the prototypes of the Booster magnetic system power supplies were tested at superconducting load. During a few shifts the beam injection at the field plateau with adiabatic capture into acceleration were used in routine operation. Experimental fragment of White Rabbit Network was tested at BM@N detector systems.

The run #53 was started 26 October 2016 with the scheduled duration of about 1400 hours. Main task of the run is experimental investigations in spin physics in few body nuclear systems (with polarized deuterons). Development of the diagnostics, investigations of dynamic behaviors of the Booster power supply prototypes with the beam acceleration, test of new current source for optic elements in the extracted beam lines,

ISBN 978-3-95450-181-6

COMMISSIONING OF NEW LIGHT ION RFQ LINAC AND FIRST NUCLOTRON RUN WITH NEW INJECTOR

A.M. Bazanov, A.V. Butenko, A.I. Govorov, B.V. Golovenskiy,D.E. Donets, V.V. Fimushkin, V.V. Kobets, A.D. Kovalenko, K.A. Levterov, D.A. Lyuosev, A.A. Martynov, V.V. Mialkovsky, V.A. Monchinskiy, D.O. Ponkin, R.G. Pushkar, V.V. Seleznev, K.V. Shevchenko, A.O. Sidorin, I.V. Shirikov, A.V. Smirnov, G.V. Trubnikov, Joint Institute for Nuclear Research, Dubna, Moscow Region, Russia

S.V. Barabin, A.V. Kozlov, G.N. Kropachev, V.G. Kuzmichev, T.V. Kulevoy, Institute of Theoretical and Experimental Physics NRC "Kurchatov Institute", Moscow, Russia

A.S. Belov, Institute for Nuclear Research of the Russian Academy of Sciences, Moscow, Russia

S.M. Polozov, National Research Nuclear University – Moscow Engineering Physics Institute, Moscow, Russia

Abstract

The new accelerator complex Nuclotron-based Ion Collider fAcility (NICA) is under development and construction at JINR, Dubna now (Fig. 1). This complex is assumed to operate using two injectors: the Alvarez-type linac LU-20 as injector of light ions, polarized protons and deuterons and a new linac HILAc – injector of heavy ions beams. Old HV fore-injector of the LU-20, which operated from 1974, was replaced by the new RFQ accelerator, which was commissioned in spring 2016. The first Nuclotron technological run with new fore-injector was performed in June 2016 with beams of D^+ and H_2^+. The polarized deuterons beam were successfully injected and accelerated in the Nuclotron ring during the last run #53. Main results of the RFQ commissioning and the last Nuclotron run with new fore-injector are presented in this paper.

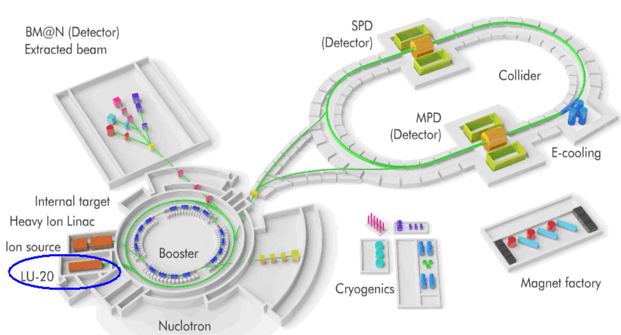

Figure 1: NICA complex. Proton, light and polarized ion linac LU-20 with new RFQ injector is marked.

INTRODUCTION

The injection system of the operating superconducting fast cycling synchrotron Nuclotron is under upgrade now.

Up to 2016 year, the charged particles for injecting into LU-20 linac were pre-accelerated with the electrostatic tube supplied by pulsed HV transformer with voltage up to 700 kV. The ion sources supply of up to 5 kW power placed at the HV "hot" platform was provided by feeding station consisting of motor and generator isolated one from the other with wood shaft. The new fore-injector of LU-20 based on the RFQ linac was constructed and put in to operation in 2016 (see Fig. 2). Pulsed HV supply up to 120 kV (based on HV pulsed transformer) was designed and assembled to provide necessary electric potential of the ion source terminal. The ion source systems supply is provided using isolation transformer on 160 kV, 35 kWA.

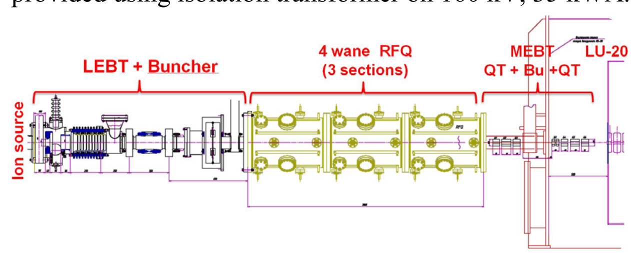

Figure 2: New fore-injector for LU-20 scheme.

New RFQ linac parameters are presented in Table 1, the project is performed in collaboration of JINR, MEPhI and ITEP. The beam dynamics simulation, the RFQ resonator simulation and design as well as RF system development were carried out in 2011-2013 [5]. The accelerator's resonator was manufactured in VNIITP (Snezhinsk).

Table 1: The LU-20 Fore-Injector Design Parameters

Z/*A*	0.5	0.3
RFQ input		
Injection energy, keV	61.8	103.0
Maximum current,mA	20	10
Normalized trans. emittance, π·cm·mrad	0.2	0.15
Operating frequency, MHz	145.2	
Output		
Output energy, MeV/u	0.156	0.156
Transmission RFQ, %	≥85	≥90
$\Delta p/p$, %	≤ 4	≤ 4
Normalized trans. emittance, π·cm·mrad	≤0.5	≤ 0.5
Resonator length, m	≤ 3	≤ 3
Voltage at electrodes, kV	84	140

ISBN 978-3-95450-181-6

COMMISSIONING OF THE NEW HEAVY ION LINAC AT THE NICA PROJECT

A.M. Bazanov, A.V. Butenko, B.V. Golovenskiy, D.E. Donets, V.V. Kobets, A.D. Kovalenko, K.A. Levterov, D.A. Lyuosev, A.A. Martynov, V.A. Monchinskiy, D.O. Ponkin, K.V. Shevchenko, A.O. Sidorin, I.V. Shirikov, A.V. Smirnov, G.V. Trubnikov, JINR, Dubna, Russia
D.A. Liakin, ITEP, Moscow, Russia
H.Höltermann*, U.Ratzinger, A.Schempp, H.Podlech, D. Mäder, BEVATECH GmbH, Frankfurt, Germany

Abstract

The new accelerator complex Nuclotron-based Ion Collider fAcility (NICA) is now under development and construction at JINR, Dubna. This complex is assumed to operate using two injectors: The modernized Alvarez-type linac LU-20 as injector of light polarized ions and a new Heavy Ion Linear Accelerator HILAc-injector for heavy ions beams. The new heavy ion linac, which accelerates ions with q/A-values above 0.16 to 3.2 MeV/u, is under commissioning. The main components are a 4-Rod-RFQ and two IH-drift tube cavities, operated at 100.625 MHz. Most recent results of the HILac commissioning with a carbon beam from a laser ion source are discussed.

INTRODUCTION

For the NICA collider ion beams from p to Au at energies from a few hundred MeV/u up to a few GeV/u. will be delivered by two superconducting synchrotrons- the Booster (magnetic rigidity is 25 Tm) and the Nuclotron (45 Tm) and 2 injector linacs [1]. The beams will be created by three new ion sources: SPP (Source of Polarized Particles), LIS (Laser Ion Source), Krion-6T (ESIS type heavy ion source). The ion sources will feed 2 linacs: The existing linac LU-20 with a new RFQ as front-end and the new heavy ion linac – HILac. The HILac design and development was performed by Bevatech GmbH [2] and described in detail in [3]. HILac commissioning with a C^{3+} beam from the laser ion source are presented. Parameters for HILac are given in table 1.

Table 1: HILac Parameters

Target Ion	Au^{32+}
A/q	6.25
Current	< 10 emA
Pulse length	10 µs – 30 µs
Rep. rate	< 10 Hz
LEBT energy	17 keV/u.
RFQ energy	300 keV/u.
LINAC output energy	3.2 MeV/u.

ION SOURCE & LEBT

The LIS is based on a commercially available Nd-YAG laser LPY 7864-2 The laser was tested at its operational regimes producing carbon ions at a test bench (Fig. 1).

The HILac LEBT with a length of about 2 m is split into 2 main parts. Part 1. is an electrostatic section the second part uses 2 magnetic solenoids. with a maximum magnetic field of 1.23 T. The whole LEBT has been simulated for investigating the beam matching into the RFQ acceptance (Fig 2).

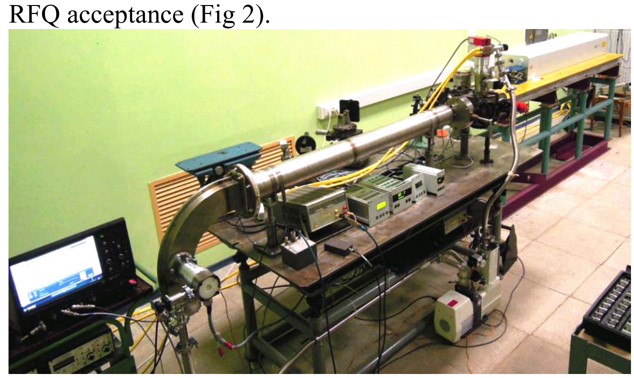

Figure 1: Nd-YAG laser at the test bench.

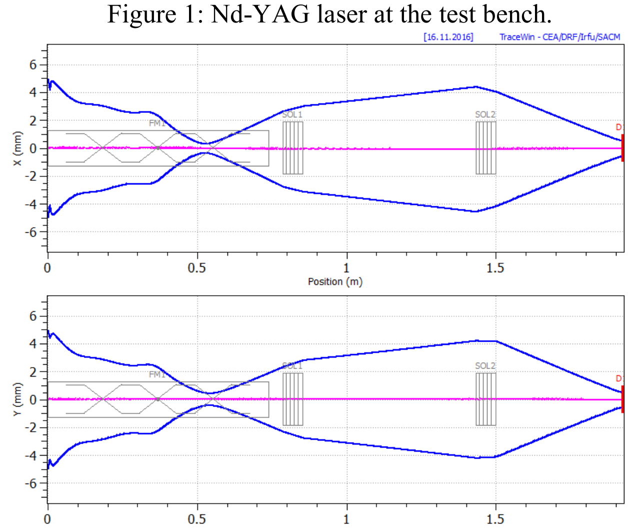

Figure 2: Matched case (rms envelope) for C^{3+} beam along the LEBT into the RFQ acceptance.

MEBT

The MEBT is equipped with two identical pulsed quadrupole-doubletts located in front and behind the

ISBN 978-3-95450-181-6

BOOSTER SYNCHROTRON AT NICA ACCELERATOR COMPLEX

A. Tuzikov, O. Brovko, A. Butenko, A. Eliseev, A. Fateev, V. Karpinsky, H. Khodzhibagiyan, S. Kostromin, I. Meshkov, V. Mikhaylov, A. Sidorin, A. Sidorov, A. Smirnov, E. Syresin, G. Trubnikov, V. Volkov, Joint Institute for Nuclear Research, Dubna, Russia
O. Anchugov, V. Kiselev, D. Shvedov, A. Zhuravlev,
Budker Institute of Nuclear Physics, Novosibirsk, Russia

Abstract

NICA is the new complex being constructed on the JINR aimed to provide collider experiments with ions up to Au at energy of 4.5x4.5 GeV/u. The NICA layout includes 600 MeV/u Booster synchrotron as a part of the heavy ion injection chain of the NICA Collider. The main goals of the Booster are the following: accumulation of $2\cdot10^9$ Au^{31+} ions; acceleration of the heavy ions up to energy required for effective stripping; forming of the required beam emittance with electron cooling system. The layout makes it possible to place the Booster having 210.96 m circumference and four fold symmetry lattice inside the yoke of the former Synchrophasotron. The features of the Booster, its main systems, their parameters and current status are presented in this paper.

INTRODUCTION

The Booster of the NICA accelerator complex [1] is a superconducting synchrotron which will be placed inside the yoke of the former Synchrophasotron (see Figure 1). Main goals of the Booster are accumulation of $2\cdot10^9$ Au^{31+} ions; acceleration of the heavy ions up to energy required for effective stripping; forming of the required beam emittance with electron cooling system. The Booster has four fold symmetry lattice with DFO periodic cells (see Figure 2). Each quadrant of the Booster has 10 dipole magnets, 6 focusing, 6 defocusing quadrupole lenses and multipole corrector magnets. Missing dipole cells of the lattice are used for installation of injection, extraction, RF and electron cooling systems.

Accumulation of ions is provided by means of multivariant injection of ion beams into the Booster [2]. Main methods of beam injection into the Booster are single-turn, multi-turn and multiple injections. Ions are accumulated on the horizontal phase plane of the Booster.

Fast (single-turn) extraction provides ion stripping and transfer from the Booster into the Nuclotron. Slow extraction is not designed for the current version of the Booster and is considered to be implemented during later modernizations of the accelerator.

The Booster has working cycle of 4.02 s duration (see Figure 3). In case of necessity a technological pause between the Booster cycles of 1 s duration is presumed. Beam injection energy is equal to 3.2 MeV/amu. Electron cooling of a beam is fulfilled in the energy range from 65 to 100 MeV/amu. Maximal magnetic field in the dipole magnets is 1.8 T that corresponds to energy of Au^{31+} ions equal to 578 MeV/amu.

The design working point of the Booster is $Q_x = 4.8$, $Q_y = 4.85$. Lattice functions of the Booster are presented on Figure 4.

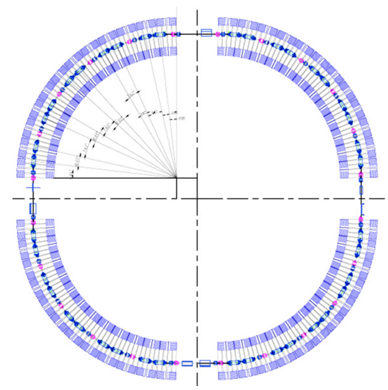

Figure 1: Layout of the Booster inside the former Synchrophasotron yoke.

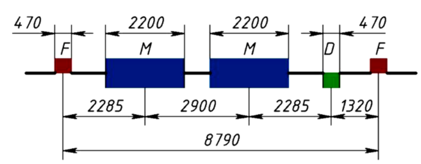

Figure 2: Regular DFO-cell of the Booster.

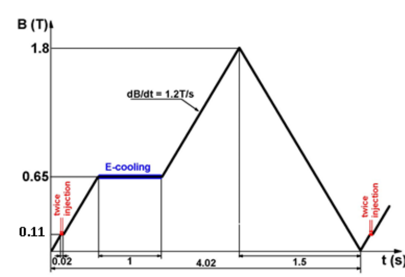

Figure 3: Working cycle of the Booster.

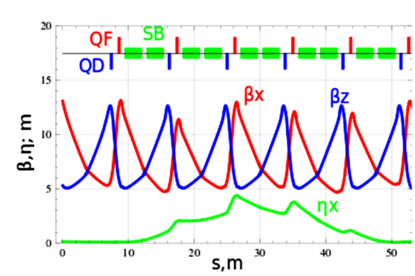

Figure 4: Lattice functions of the Booster synchrotron.

ISBN 978-3-95450-181-6

SIMULATION OF TWO-PLANE PAINTING MULTITURN INJECTION INTO BRING WITH SPACE CHARGE EFFECT

A.V.Smirnov#, JINR, Dubna, Russia
W.Chai, G.F.Qu, L.Yao, IMP, Lanzhou, China

Abstract

The new project HIAF is under design now in IMP (Lanzhou, China) [1]. One of the aim of the project is to accumulate up to 1×10^{11} ions U^{34+} in the booster ring (BRing) at the injection energy 17 MeV/u. Two-plan painting procedure in both horizontal and vertical spaces was proposed to fill out full acceptance of BRing. The space charge effect was estimated with the molecular dynamics technique which was effectively used for the crystalline beam simulation.

TWO-PLANE PAINTING

The aim of the two-plan painting at BRing is to reach the necessary beam intensity 1×10^{11} after an injection procedure (Table 1). The transverse emittance of the injected beam is 5 π mm mrad and the horizontal ring acceptance is about 200 π mm mrad. In this case, the maximum gain for one-plan injection is about 26 what is not enough to accumulate the necessary value of the particle number. In accordance with [2] the gain factor for two-plan painting procedure can be achieved a value up to 100.

Table 1: BRing parameters for Au^{34+}

Parameter	Value
Circumference, m	473
Rigidity, T m	1 – 34
Acceptance, hor/ver, π mm mrad	200 / 100
Longitudinal acceptance, Δp/p, %	±0.5
Injection energy, MeV/u	17
Injection intensity	1.5×10^{9}
Injection emittance, π mm mrad	5
Injected momentum spread, %	±0.5
Injection cycle number	90
Extraction energy, MeV/u	800
Extracted particle number	7×10^{10}

The two-plan painting can be realized with two groups of orbit bump for both horizontal and vertical, simultaneous injection in horizontal and vertical phase spaces using tilted septum (Figure 1). During injection procedure the septum position is coming to the reference orbit and the septum angle remains constant.

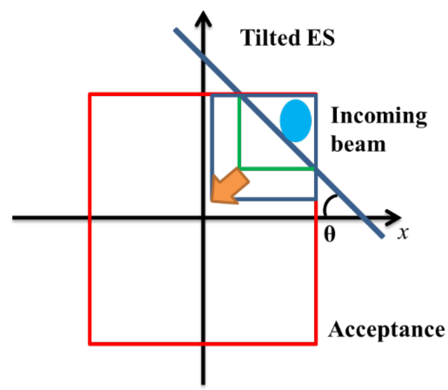

Figure 1: Scheme of injection in horizontal and vertical phase spaces using tilted septum.

The optimization of two-plan painting procedure was carried out with WinAgile [3], ORBIT [4] and BETACOOL [5] programs. The injection efficiency was optimized with the following input parameters: lattice functions at injection point, betatron values, septum angle, septum position, etc.

On Figure 2 is presented simulation results with BETACOOL for designed parameters (Table 1). Left picture is the particle distribution in the transverse plan, right picture is horizontal phase space after 90 cycles of the injection. The particle losses on the septum and transverse acceptance are taken into account. The dependence of the transverse emittances and particle number during injection procedure are presented on Figure 3.

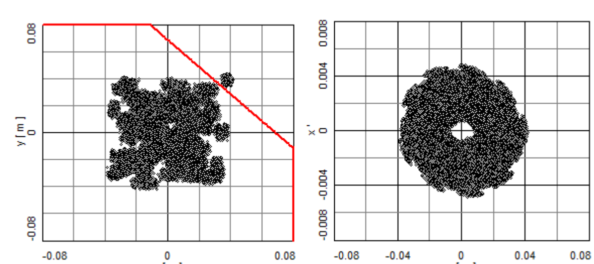

Figure 2: Particle distribution for transverse plan (left picture) and horizontal phase space (right picture) after 90 cycles of injection procedure.

Results of simulation with BETACOOL program have a good agreement with results of ORBIT program and show that without space charge effect the particle number can reach a necessary value 1×10^{11}.

#smirnov@jinr.ru

ISBN 978-3-95450-181-6

NICA COLLIDER LATTICE OPTIMIZATION

O. Kozlov, A. Butenko, H. Khodzhibagiyan, S. Kostromin, I. Meshkov, A. Sidorin, E. Syresin, G.Trubnikov, JINR, Dubna, Russia

Abstract

The Nuclotron-based Ion Collider fAcility (NICA) [1] is a new accelerator complex being constructed at JINR. It is aimed to collider experiments with ions and protons and has to provide the ion-ion (Au^{+79}) and ion-proton collision in the energy range of 1÷4.5 GeV/u and also polarized proton-proton (5÷12.6 GeV) and deuteron-deuteron (2÷5.8 GeV/u) collisions. Two collider rings are designed and optimized to achieve the required luminosity at two interaction points (IP). Taking into account space charge effects of the intense ion beam the application of electron beam or stochastic cooling methods were proposed to provide beam or luminosity lifetime. This paper is considering one of the most challenging problems of accelerator physics that is finding the dynamic aperture (DA) of the collider ring.

INTRODUCTION

NICA collider lattice development [2] has many necessary aspects of the design. The collider should operate in the energy range for Au-ions of 1÷4.5 GeV/u, with the average luminosity about $1\cdot10^{27}$ cm^{-2} s^{-1}. The ring should work with the different particle species (Au^{+79}, protons and deuterons). Collider has a certain circumference limitation. The collider lattice is based on the technology of super-ferric magnets developed in VBLHE, JINR [3]. The collider optics optimization includes the certain effects which set constraints on the lattice parameters: luminosity lifetime limitation by intrabeam scattering in a bunch (IBS), space charge tune shift, threshold of microwave instability, slippage factor optimization for efficient stochastic cooling, maximum required RF voltage amplitude. The maximum energy of the experiment is determined by the Nuclotron maximum magnetic rigidity of 45 T·m. This paper considers only the most developed heavy ion mode of facility operation and the $^{197}Au^{+79}$ ions as the reference particles.

LATTICE STRUCTURE

Technical constraints were taken into account in lattice optimization: ring circumference, a number of the dipole magnets in an arc, convenience of the beam injection into the ring. The FODO optics with 12 periods is a principal choice for arc structure. Two arcs and two long straight section form the collider racetrack shape and correspond exactly to two Nuclotron circumferences. The rings are vertically separated (32 cm between axes) and use two-aperture superconducting magnets (dipoles and quadrupoles) [3]. This lattice has a large efficiency of stochastic cooling at 4.5 GeV/u. The luminosity of 10^{27} cm^{-2} s^{-1} could be reached in the wide energy range.

Table 1: Collider Ring and Beam Parameters

Ring circumference, m	503.04		
Number of bunches	22		
Rms bunch length, m	0.6		
β-function in the IP, m	0.35		
Betatron tunes, Q_x/Q_y	9.44/9.44		
Chromaticity, $\xi_{x,0}/\xi_{y,0}$	-33/-28		
Ring acceptance	40 π·mm·mrad		
Long. acceptance, Δp/p	±0.010		
Gamma-transition, γ_{tr}	7.088		
Ion energy, GeV/u	1.0	3.0	4.5
Ion number per bunch	2.0e8	2.4e9	2.3e9
Rms Δp/p, 10^{-3}	0.55	1.15	1.50
Rms emittance, hor./vert. (unnorm.), π·mm·mrad	1.10/ 0.95	1.10/ 0.85	1.10/ 0.75
Luminosity, $cm^{-2}s^{-1}$	0.6e25	1e27	1e27
IBS growth time, s	170	470	1900

The convenient injection scheme could be realized through the arc dipole-empty cell.

FODO periodic cell (12 m length) consists of four rectangular dipole magnets per cell (80 magnets per ring), two quadrupoles [3], multipole correctors and BPMs. The maximum field in 1.94 m dipole of 1.8 T and gradient in 0.47 m quadrupoles of 23 T/m are chosen to avoid the saturation effects in iron yokes at higher energies. Multipole corrector includes the several types of windings – dipole (orbit correction), quadrupole (tuning), skew quadrupole (coupling correction), sextupole (chromaticity correction) and octupole.

Arc comprises 12 FODO cells (90^0 phase advance per cell). The last 1.5 cells realize the horizontal dispersion suppressor (the effective quadrupole gradient (3 families) tuned by the nearby quadrupole corrector).

Long straight sections are matched to the arcs, contain the insertion devices, produce the betatron tune variation and the vertical beam separation and final focusing in IPs.

Collider ring general parameters are given in Table 1 and Twiss-functions for the ring are shown in Fig. 1. Two rings are separated vertically. In this scheme, two-aperture quadrupoles should have the opposite connections for upper and bottom rings in arcs and long straights, but the final focus triplets should have the antisymmetric connections with respect to IPs providing the same horizontal and vertical betatron tunes for counter circulating beams.

ISBN 978-3-95450-181-6

DYNAMIC APERTURE OPTIMIZATION OF THE NICA COLLIDER*

S. A. Glukhov, E. B. Levichev, BINP, Novosibirsk, Russia

Abstract

NICA is a proton and heavy ion collider being built at JINR in Dubna, Russia. It was shown that nonlinear quadrupole fringe fields are among the main factors limiting dynamic aperture of the machine. In the present paper the following ways of dynamic aperture optimization were studied: betatron tunes optimization and placing octupole lenses to the lattice to compensate fringe fields' effect.

INTRODUCTION

Dynamic aperture (DA) optimization study for NICA lattice was started recently using the program codes MAD-X [1] and TrackKing [2]. At the moment the only nonlinearities taken into account are chromatic correction sextupoles, quadrupole nonlinear fringe fields in hard edge approximation [3] and octupoles added to compensate the latter effect. Figure 1 shows that DA is limited mainly by fringe fields of central lenses of final focus (FF) triplets (quads 2), contribution of the other triplet's lenses (quads 1, 3) is also significant. Additional DA reduction due to fringe fields of arc quadrupoles is negligible. Resulting

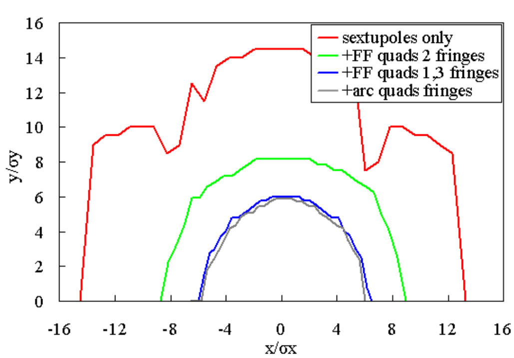

Figure 1: Effect of quadrupole nonlinear fringe fields on DA.

DA size is inacceptably small, therefore, optimization is necessary. In theoretical part of the present paper the relationship between quadrupole nonlinear fringe fields and octupole fields is shown. Then two steps of optimization are described. Firstly, we place two families of thin octupoles into the chromatic correction sextupoles and insert a "phase trombone" into the lattice (fictitious thin linear element which adjusts betatron tunes to the given values). Then we try to maximize DA with these octupoles and find the region of betatron working points where DA gain is the most significant. At the second stage we rematch the linear lattice using MAD-X to decrease influence of nonlinear fringe fields and bring working point to the previously defined region, then DA is optimized again with octupoles. Finally we make some estimations to prove that resulting increased DA is stable in the presence of magnetic field errors and misalignments.

* This work has been supported by Russian Science Foundation (project N14-50-00080).

NONLINEAR QUADRUPOLE FRINGE FIELDS AND OCTUPOLES

Hamiltonian for charged particle moving in a lattice with quadrupole and octupole fields can be written as follows

$$\begin{aligned} H = \frac{{p_x}^2+{p_y}^2}{2} + k_1(s)\frac{x^2-y^2}{2} + p_x k_1'(s)\frac{x^3+3xy^2}{12} - \\ - p_y k_1'(s)\frac{y^3+3yx^2}{12} + k_3(s)\frac{x^4-6x^2y^2+y^4}{24} \end{aligned} . \tag{1}$$

Here quadrupole gradient k_1' is introduced to take into account nonlinear quadrupole fringe fields.

If all octupoles are thin, then each of them causes the following coordinate transformation

$$\begin{aligned} (\bar{p}_x)_{\rm oct} &= p_x - (k_3 l)\frac{x^3-3xy^2}{6} \\ (\bar{p}_y)_{\rm oct} &= p_y - (k_3 l)\frac{y^3-3yx^2}{6} \end{aligned} , \tag{2}$$

where l is effective octupole length. If we also consider edges of each quadrupole as thin elements (so called "hard edge approximation" [3]), then the coordinate transformation for quadrupole fringe can be obtained

$$\begin{aligned} (\bar{x})_{\rm fringe} &= x + \Delta k_1 \frac{x^3+3xy^2}{12} \\ (\bar{y})_{\rm fringe} &= y - \Delta k_1 \frac{y^3+3yx^2}{12} \\ (\bar{p}_x)_{\rm fringe} &= \frac{p_x\left(1-\Delta k_1 \frac{x^2+y^2}{4}\right) + p_y \Delta k_1 \frac{xy}{2}}{1-(\Delta k_1)^2 \frac{(x^2-y^2)^2}{16}} \\ (\bar{p}_y)_{\rm fringe} &= \frac{p_y\left(1+\Delta k_1 \frac{x^2+y^2}{4}\right) - p_x \Delta k_1 \frac{xy}{2}}{1-(\Delta k_1)^2 \frac{(x^2-y^2)^2}{16}} \end{aligned} , \tag{3}$$

where Δk_1 is a variation of the quadrupole gradient, it has opposite signs at entrance and exit faces of the quadrupole. One can see that $\Delta(\bar{p}_{x,y})_{\rm oct}$ and $\Delta(\bar{x},\bar{y})_{\rm fringe}$ have similar structure but with different signs between terms. Therefore, nonlinear quadrupole fringe can be called "quasi-octupole".

ISBN 978-3-95450-181-6

COMMISSIONING AND FIRST TESTS OF THE NEW STANDING WAVE 10 MEV ELECTRON ACCELERATOR

D.S. Basyl, T.V. Bondarenko, M.A. Gusarova, Yu.D. Kliuchevskaia,
M.V. Lalayan, S.M. Polozov, V.I. Rashchikov, E.A. Savin
National Research Nuclear University – Moscow Engineering Physics Institute, Moscow, Russia
M.I. Demsky, A. Eliseev, V. Krotov, D. Trifonov
CORAD Ltd., Saint-Petersburg, Russia

Abstract

A new linear electron accelerator for industrial applications was developed by the joint team of CORAD and MEPhI. It is based on conventional biperiodical accelerating structure for energy range from 7.5 to 10 MeV and beam power up to 20 kW. The use of modern methods and codes for beam dynamics simulation, raised coupling coefficient and group velocity of SW biperiodic accelerating structure allowed to reach high pulse power utilization and obtain high efficiency. The first two accelerators with the new structure have been installed and tested.

INTRODUCTION

A number of commercial S-band 10 MeV linacs for industrial applications are nowadays available on the market. These linacs are developed and produced by MEVEX, GETINGE, NUCTECH and Wuxi El Pont companies and can provide 15-30 kW of beam power . New industrial linac for average beam power up to 20 kW and variable energy range from 7.5 to 10 MeV was developed in 2014-15 by the joint team of CORAD and MEPhI. New linac has high electrical efficiency, narrow beam energy spectrum, provide energy regulation and low accelerated beam loses.

We tried to realize the following statements in our new linac design: the accelerating structure should have high coupling coefficient for maximal RF pulse power usage efficiency; the gentle buncher should be used to provide high capturing coefficient and narrow energy spectrum for all output energies.

The first two new accelerators have been produced and installed at EB-Tech Company site in Daejeon, Republic of Korea, and for company ACCENTR in “Rodniki” Industrial Park, Ivanovo Region, Russia. In this article we will briefly report the main results of linac development, manufacturing and testing.

THE LINAC GENERAL LAYOUT AND BEAM DYNAMICS

The traditional three-electrode E-gun was used for injection. It should provide up to 400-450 mA of pulse beam current to reach 300-320 mA of accelerated beam. Injection energy is equal to 50 keV.

The conventional biperiodical accelerating structure (BAS) based on Disk Loaded Waveguide (DLW) was used in linac. It operates on standing wave with resonant frequency of 2856 MHz. Wide magnetic coupling windows were used to increase the coupling coefficient which leads to low RF transient time and high group velocity. Low (~200 ns) RF filling time was realized using such idea. It also leads to the beam loading effect decrease.

Beam dynamics simulation was done using BEAMDULAC-BL code developed at MEPhI for simulations with beam loading and Coulomb field effects taken into account self-consistently [1]. Beam dynamics optimization was directed to obtain effective beam bunching for all energy range of 7.5-10 MeV and to achieve low beam energy spread. It was proposed to use a gentle buncher for these aims. The phase velocities β_{ph} and RF field amplitudes are rising for effective beam bunching. The linac consists of 28 accelerating and 27 coupling cells, its total length is 143 cm. The bunching part consists of of 6 accelerating cell with variable length. The average field in the accelerating cells should be equal to 160 kV/cm for the effective beam bunching and acceleration up to 11 MeV. Maximal on-axis RF field amplitude will be equal to 210 kV/cm in this case. One of the middle cells is used as RF power coupler.

Four short ~20 cm focusing magnetic coils are used for beam focusing, three of the coils were installed before coupler and one after it. Magnetic field of 30 mT on the linac axis is necessary for effective beam focusing.

Some main beam dynamics simulation results are presented in Table 1: E_{RF} is averaged field into accelerating cells, kV/cm; I_{out} is output current, mA; K_T is current transmission coefficient, %; N_{main} is the part of electrons in the main beam energy distribution peak, %; $\delta\gamma/\gamma$ is the energy spread on the energy distribution peak base; η, % is RF efficiency. Experimental data was defined for the first linac, which was commissioned on Sep. 2015 at EB-Tech Company site. All experimental data are presented for the beam output current of 320 mA. It is clear that linac provides effective beam bunching and acceleration for wide bands of beam currents and energies. The current transmission coefficient is close to 65-70 % for all operating modes and output energy spectrum is limited by 10 % (full width on the distribution base). It is clear that RF efficiency η slowly decreases vs. E_{max} (or vs. W_{max}) for constant current. But it increases with the beam current growth for constant W_{max}. It should be noted that E-gun provide about 450 mA of injection current and results for higher beam currents are interesting for simulation only.

ISBN 978-3-95450-181-6

HIGH EFFICIENCY STRIPPING EXTRACTION ON 80 MEV H-MINUS ISOCHRONOUS CYCLOTRON IN PNPI

S.A. Artamonov#, A.N. Chernov, E.M. Ivanov, G.A. Riabov, V.A. Tonkikh, B.P. Konstantinov Petersburg Nuclear Physics Institute, NRC "Kurchatov Institute", Gatchina, Leningrad district, 188300, Russia

Abstract

H-minus cyclotron has the advantage that high intensity internal beam can be extracted from the acceleration chamber with practically 100% efficiency by transformation H-minus ions into H-plus ion by using thin foil. The extraction system is consists from the probe with stripping foil, extraction window in the vacuum chamber and two allaying magnets to match the extracted beam with beam transport line. The beam optics calculations in the measured magnetic field make it possible to find optimal relative position of the extraction system elements as well the parameters of the extracted beam with energy 40 - 80 MeV. At present time the beam is extracted from the chamber with efficiency about 100 % and there is good agreement with the optic calculations.

INTRODUCTION

The start up of a new high intensity isochronous cyclotron with the design beam energy from 40 up to 80 MeV and beam current of 100 microamperes was announced in November of 2016. The cyclotron is intended for production of high quality medicine isotopes, organization of eye melanoma treatment facility, treatment of surface forms of cancer and radiation resistance tests of the electronics for the aviation and space [1].

The external view of the cyclotron and the first part of the beam transport line is presented in Figure1.

Figure 1: The external view of the C-80 cyclotron and beginning part of the transport line.

Basic parameters of the cyclotron are summarized in the Table1.

Table 1: Parameters of C-80 Cyclotron

MAGNET	
Pole diameter	2.05 m
Valley gap	386 mm
Hill gap (min.)	163 mm
Number of sectors	4
Spiral angle (max.)	65°
Magnetic field in centre	1.352 Tl.
Flatter (max.)	0.025
Extraction radius	0.65-0.90 m
EXTRACTED BEAMS	
Energy	40 - 80 MeV
Method	stripping

Advantage of H – minus cyclotron is that high intensity internal beam can be extracted from the acceleration chamber with practically 100% efficiency by stripping H^- ions to H^+ ions using thin foils.

The 3D sketch of the cyclotron and extraction system is presented in Figure 2.

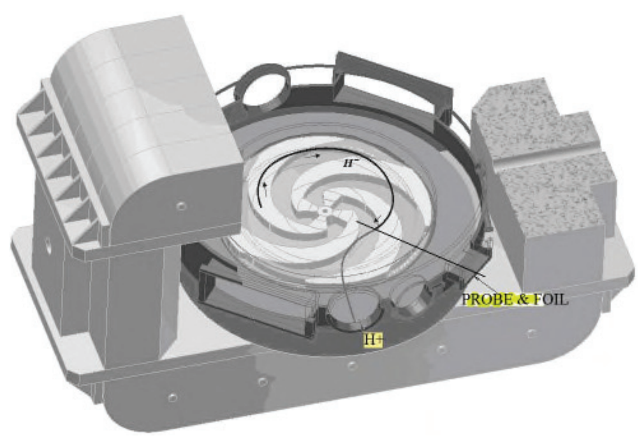

Figure 2: 3D sketch of C-80 cyclotron and the extraction system.

The extraction system consists of the probe with stripping foil, extraction window in the vacuum chamber and two correction magnets to divert the extracted beams of different energy into the transport line.

Schematic view of the extraction system is presented in Figure 3.

#artamonov_sa@pnpi.nrcki.ru

ISBN 978-3-95450-181-6

PHYSICAL START-UP OF THE C-80 ISOCHRONOUS CYCLOTRON

Yu.N. Gavrish, A.V. Galchuck, S.V. Grigorenko, A.N. Kuzhlev, V.G. Mudrolyubov,
JSC "NIIEFA", St. Petersburg, Russia
D.A. Amerkanov, S.A. Artamonov, E.M. Ivanov, G.F. Riabov, V.I. Yurchenko
PNPI, Gatchina, Leningrad region, Russia

Abstract

Works on the installation of a cyclotron system for the acceleration of H^- ions at energies ranging from 40 up to 80 MeV have been completed in the B.P. Konstantinov Petersburg Nuclear Physics Institute (PNPI), the National Research Centre "Kurchatov Institute". The cyclotron is intended for production of a wide assortment of radioisotopes including radiation generators (Sr-Rb, Ge-Ga) for medicine, proton therapy of ophthalmic diseases, tests of radioelectronic components for radiation resistance and studies in the field of nuclear physics and radiation material science.

In June, 2016 physical start-up of the cyclotron was realized in the pulsed mode. To date, the beam of ~38 μA was obtained at the inner probe of the cyclotron, the extracted beam at the first diagnostic device was ~28 μA. The beam transport to the final diagnostic device of the beamline (~35 m long) practically without losses was demonstrated. In the near future we plan to obtain the design intensity of 100 μA.

PURPOSE AND MAIN CHARACTERISTICS

The C-80 cyclotron system developed by specialists of PNPI and the D.V. Efremov Institute is intended for production of proton beams with energies ranging from 40 up to 80 MeV and current of up to 100 μA. The beams with such parameters will be used to finalize the development of the technology for production of a wide assortment of radioisotopes for medicine including radiation generators and for commercial production of these radioisotopes [1-3]. In the nearest future the following works are planned:

- Creation of a special line to form homogeneous proton beams of ultra-low intensity (10^7-10^9) for proton therapy of ophthalmic diseases.
- Creation of a test facility to carry out studies on the radiation resistance of radioelectronic equipment using intensive beams of protons and neutrons.

The cyclotron system equipment with the transport system of an accelerated proton beam to remote target stations is mounted in the experimental hall of building 2 and in its basement. The equipment of the cyclotron and that of the first section of the beam transport system is located on the first floor (see Fig. 1), the external injection system, the RF generator and the system for the beam transport to three targets are mounted in the basement. The main characteristics of the cyclotron are given in Table1.

The major unit of the cyclotron, an electromagnet, was designed using a model of the magnet of the synchrocyclotron operating in PNPI and further updated. Such a decision limited significantly the choice of engineering solutions when designing the cyclotron. In the process of commissioning works some structural deficiencies made at the design and manufacturing stages were detected and eliminated.

Figure 1: The C-80 cyclotron system.

Table 1: The main Characteristics of the Cyclotron

System, parameter	Characteristic, value
Type of accelerated particles	H^-
Type of extracted particles	H^+
Beam energy, variable, MeV	40-80
Beam current, μA.	100

TESTS AND RESALTS

In the process of preliminary tests of the cyclotron, appreciable losses of the beam intensity in the cyclotron central region were found out. Measurements of current performed with a three-electrode probe inside the cyclotron chamber demonstrated a noticeable beam shift relative to the median plane (see Fig. 2).

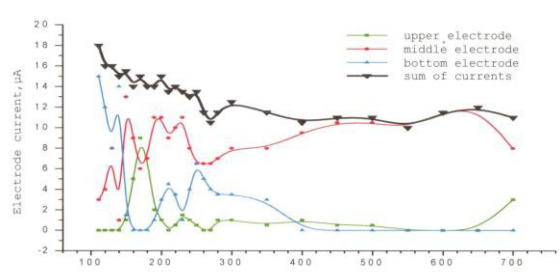

Figure 2: Results of current and beam position measurements in the process of acceleration.

ISBN 978-3-95450-181-6

THE CC1-3 CYCLOTRON SYSTEM. INSTALLATION AND TEST RESULTS

V.G. Mudrolyubov, A.V. Antonov, O.L. Veresov, Yu.N. Gavrish, A.V. Galchuck, S.V. Grigorenko, V.I. Grigoriev, M.A. Emeljanov, M.T. Kozienko, L.E. Korolev, A.N. Kuzhlev, A.G. Miroshnichenko, G.V. Muraviov, V.I. Nikishkin, V.I. Ponomarenko, K.E. Smirnov, Yu.I. Stogov, A.P. Strokach, S.S. Tsygankov, JSC “NIIEFA”, St. Petersburg, Russia

Abstract

Works on the installation and adjustment of a unique CC1-3 cyclotron system in the Vinca Institute of Nuclear Sciences, Belgrade, Serbia have been finished. The cyclotron system will be used in the laboratory of nuclear-physical methods of the elemental analysis. A compact cyclotron and a beam-forming system produce an accelerated proton beam in a wide range of energies from 1 to 3 MeV with a spectrum width not more than 0.1%. Tests of the cyclotron system have been carried out at proton energies of 1.0, 1.7 and 3 MeV with the beam transport to the final diagnostic device.

PURPOSE

The CC1-3 cyclotron system has been developed and manufactured in the D.V. Efremov Scientific Research Institute of Electrophysical Apparatus. Unique parameters of accelerated proton beams (energy ranging from 1 up to 3 MeV, energy spectrum width of not more than 0.1 %) allow the use of this system as an effective technological equipment for analytical studies on the basis of nuclear-physical methods [1]. A distinctive feature of these express methods is a high sensitivity and comprehensive analysis (detection of small concentrations up to 10^{-5}–10^{-7} g/g). Possibility for non-contactnon-destructive analysis of substances or objects is of special interest.

The following fields were defined as the main applications of this system:

- X-ray method for the elemental analysis with a possible extraction of the proton beam into the atmosphere to irradiate samples for a detailed study of their surface layer.
- The method of analysis based on the Rutherford backscattering (RBS) to study both the elemental composition and the concentration profile of elements implanted into a sample.
- Spectral (Y–ray) analysis, the method based on recording of γ–radiation produced by nuclear reactions (P, X, γ).
- In future, potentialities of the system can be extended by developing a new equipment, which will make possible the realization of the method for the target potential modulation to study the concentration profile of implanted elements by recording the secondary Y-radiation produced by nuclear reactions under irradiation with an accelerated proton beam.

BRIEF DESCRIPTION

The cyclotron system consists of a compact cyclotron and a system for the beam forming and transport to remote analytical chambers including the beam extraction into the atmosphere as well as systems for power supply, automated control, vacuum pumping and water cooling [2].

The compact cyclotron provides acceleration of negative hydrogen ions to the final energy in the range of 1-3 MeV and extraction of a proton beam to the beam transport system by stripping of two electrons on a thin carbon foil. The cyclotron comprises an electromagnet with a vacuum chamber, resonance system, diagnostic devices (probes) and stripping device, external injection system and RF generator.

The major part of the cyclotron is a four-sector shielding-type electromagnet 1400 mm in diameter with a horizontally located median plane (see Fig. 1). The pole diameter is 600 mm; the average induction of 0.98 T was chosen to provide an optimal separation of orbits to minimize the energy spread. To make easy maintenance/repair of the equipment located inside the vacuum chamber, the upper beam of the magnet can be moved upward up to 500 mm.

Figure 1: Electromagnet of the CC1-3 cyclotron.

The resonance accelerating system is located completely inside the vacuum chamber of the electromagnet (see Fig. 2) and is equipped with an inductive RF power in-feeding device, AFT trimmer and RF-probe. The operating frequency is 59.7 MHz and it corresponds to the 4th harmonic of the hydrogen ions revolution frequency.

PROGRESS IN CW MODE ELECTRON RESONANCE ACCELERATOR BETA-8 DEVELOPMENT

A.V. Telnov*, V.S. Gordeev, N.V. Zavialov, A.M. Opekunov, S.M. Pridchin, S.A. Putevskoy, M.L. Smetanin, I.V. Shorikov, RFNC-VNIIEF, Sarov, Russia
V.S. Arbuzov, V.N. Volkov, I.A. Zapryagaev, E.A. Kenzhebulatov, V.V. Kozlov, E.V. Kozyrev, E.I. Kolobanov, A.A. Kondakov, S.A. Krutikhin, G.Ya. Kurkin, S.V. Motygin, V.K. Ovchar, V.N. Osipov, V.V. Repkov, S.S. Serednyakov, S.V. Tararyshkin, A.G. Tribendis, V.V. Tarnetskiy, K.N. Chernov, BINP SB RAS, Novosibirsk, Russia
O.K. Belyaev, S.V. Ivanov, V.G. Kudryavtsev, A.I. Lepin, E.V. Mazurov, IHEP, Protvino, Russia

Abstract

The progress in mode high-power resonance accelerator BETA-8 is presented. The accelerator operates in the mode of electron beam continuous generation and is aimed at performing radiation researches. Basic parameters of the accelerator are as follows: electron beam variable output energy 1.5 – 7.5 MeV, beam average power up to 300 kW, operating resonance frequency ≈ 100 MHz.

There were developed, produced and tested basic components of the accelerator [1]. The HF characteristics of coaxial cavity assembled with a unit of HF power input (UPI) at a low RF power level were measured. Three modules of RF generator the output power of each of them being 180 kW and the device of their power summation were tested. HF injector with electron energy up to 100keV was tested. There was developed the pattern of accelerated electrons transport making it possible to fulfill up to five successive passes through the accelerating cavity. Operative embodiments of deflecting electromagnets were designed and produced.

INTRODUCTION

Electron accelerator BETA-8 is developed to implement radiation researches and radiation tests of large-size objects in a wide energy range of accelerated electrons. It will be possible to study and elaborate with its aid the technological processes requiring high power and high values of absorbed dose of electron radiation and bremsstrahlung.

The accelerator design parameters are as follows:

- Range of accelerated electron output energy – 1.5 ÷ 7.5 MeV;
- Maximum average power of the beam– 300 kW;
- Operating resonance frequency – 100 MHz;
- Modes of operation – continuous mode and pulse-periodic regime.

TESTING OF ACCELERATOR BETA-8 SYSTEMS OPERATION

At the first stage there were performed all preparative activities in testing the systems of the accelerator which is characterized by the accelerating cavity power supply from one of the three HF generator modules. Electrons acceleration is fulfilled in a half-wave coaxial cavity (Fig.1) similar to that described in paper [2].

To the cavity there are connected the required technological systems: vacuumization system, water- and air-cooling system that make it possible to train the standard mode of operation. The elements of the channel of HF power transfer – coaxial HF feeder and unit of HF power input (UPI) – are used to feed the cavity from one generator module with the average power up to 180kW. At this level of HF supply power there can be generated a beam of accelerated electrons with the average power up to 15 kW and energy up to 7.5 MeV what is enough for experimental verification of the possibility of achieving basic design objectives.

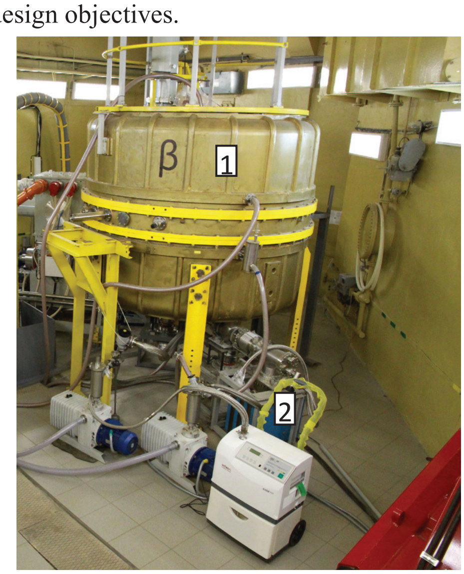

Figure 1: Accelerator BETA-8: 1 – accelerating cavity; 2 – exhaust cart.

*telnov@expd.vniief.ru

ISBN 978-3-95450-181-6

HF STRUCTURE OF BETA-8 ELECTRON RESONANCE ACCELERATOR

M.L. Smetanin, V.S. Gordeev, N.V. Zavyalov, S.A. Putevskoy, A.V. Tel'nov, I.V. Shorikov, A.N. Shein, RFNC-VNIIEF, Sarov, Russia
O.K. Belyaev, S.V. Ivanov, V.G. Kudryavtsev, A.N. Lepin, E.V.Mazurov, National Research Center "Kurchatov Institute" FSUE SSC RF – IHEP, Protvino, Moscow region, Russia

Abstract

RFNC-VNIIEF is developing a powerful resonance electron accelerator BETA-8, operating in the mode of continuous wave generation. The accelerator is developed on the basis of half-wave coaxial cavity, excited on the wave of T1 type.

The paper presents calculation results of accelerating cavity with operating frequency 100 MHz, as well as an inductive unit of HF power input (UPI) meant for transfer of continuous HF signal on the operating frequency with an average power level 600 kW. Calculation results are proved by measurements of HF characteristics of the cavity assembled together with UPI and a coupling wave guide.

The location of an indicator loop–pickup, mounted in a coupling wave guide is computed. The given loop–pickup is meant for operation in a frequency feedback circuit for the HF generator.

INTRODUCTION

Resonance electron accelerator BETA-8 (Figure 1) is being developed in RFNC-VNIIEF. Development of an accelerating facility with average electron beam power up to 300 kW with a control range of accelerated electron energies - from 1 up to 8 MeV and meant for study of radiation resistance and radiation tests of large-scale objects is based upon requirements, specified earlier [1, 2].

Figure 1: General accelerator view.

Below are reported results of three-dimensional electrodynamic calculation of basic components of accelerator HF structure as well as calculation methods of its radio-engineering tuning.

ACCELERATING CAVITY, UPI AND FEEDBACK WITH GENERATOR

A coaxial cavity, a transmitting feeder – coaxial wave guide and UPI are basic elements of BETA-8 accelerating HF structure. Estimated electric field distribution inside the cavity, in the electron acceleration region is given in fig. 2.

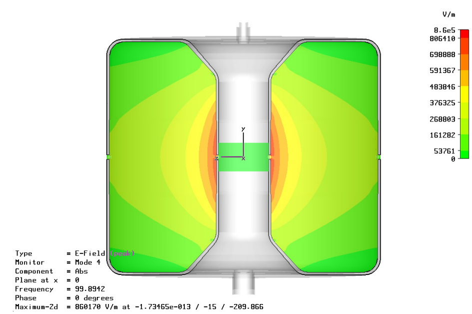

Figure 2: Waveform of electric field strength in the coaxial cavity median longitudinal plane.

The basic cavity's overall dimensions are: 1) inner conductor radius – 210 mm, 2) outer conductor radius – 1040 mm, 3) cavity height (longitudinal size) – 1626 mm. Electrons are accelerated in the cavity median transverse plane. The basic estimated electrodynamic characteristics (EDC) of the coaxial cavity comprise: resonance frequency f_0 = 99.9 MHz; kinetic energy gain per one pass We = 1.5 MeV; transit time factor T = 0.777; loss power within the cavity walls P_{loss} = 165.2 kW; resonator quality factor Q_0 = 56088; effective shunt impedance $Z_{sh.ef}$ = 15.25 MOhm.

At the first stage to supply the cavity, a single module of HF generator is used. At the matching mode it generates a signal with average power 180 kW and frequency ≈100 MHz [3].

UPI, developed in SSC RF IHEP (Protvino, Russia) is meant for operation as a connector, allowing connection of the transmitting feeder with accelerating coaxial cavity.

The main specification of UPI involves the following: coupling with the cavity – inductive; device input - coaxial, with wave resistance 50 Ohm; sizes of entrance air-filled coaxial feeder - Ø160/70 mm; UPI operates at any frequency in the range 98 - 102 MHz; operating frequency – 100 MHz; transmitting HF power in the mode of pulse and continuous generation – up to 600 kW; UPI provides an interface level of the feeder with a cavity with a voltage standing-wave ratio (VSWR) ≤ 1,2 in the frequency range 98-102 MHz.

ISBN 978-3-95450-181-6

DEVELOPMENT OF THE INR LINEAR ACCELERATOR DTL RF SYSTEM

A.V.Feschenko, A.I.Kvasha, V.L.Serov
Institute for Nuclear Research, RAS, Moscow

Abstract

Regular INR DTL RF system operation has started in 1992. By this point three new vacuum tubes, designed especially for INR linear accelerator, have been manufactured at "Svetlana" association in the amount sufficient for RF system operation for 20 years. Among them were two vacuum tubes for final and intermediate RF power amplifiers, GI-54A and GI-51A correspondingly, as well as one vacuum tube for powerful anode modulator – GMI-44A. In the late '80s the manufacture of these vacuum tubes was terminated and in 1990 development of new vacuum tube for RF output power amplifier instead of GI-54A has started. The new vacuum tube GI-71A with the output pulse RF power up to 3 MW, plate power dissipation up to 120 kW and power gain about 10 became simpler and less expensive in comparison with GI-54A. The transition to new vacuum tubes started in 1999 and completed in 2014. Successful test of GI-57A for preliminary RF amplifier was fulfilled in 2008 and opened the possibility to replace GI-51A. As for the modulator tube GMI-44A no vacuum tube with the required parameters produced in Russian Federation was found and a decision to use the RF power amplifier tube GI-71A instead of the modulator one has been done.

Below some problems connected with the vacuum tubes replacement and the main results of twenty years DTL RF system operation are described.

INTRODUCTION

Brief reference. *INR linear accelerator is in regular operation since 1993. The accelerator consists of two parts. The low energy part operates at the frequency of 198.2 MHz and includes RFQ, five Alvarez tanks and seven RF amplifier channels including a spare one. The second part operates at 991MHz and includes 28 disk and washer cavities. At present, the accelerator operates with beam pulse length up to 200 μs, repletion rate up to 50Hz and beam pulse current up to 15 mA.*

Each RF channel includes the following units:

- One solid state and four vacuum tube amplifiers;
- Vacuum tube plate modulator (AM) for the first and the second vacuum tube RF amplifiers;
- Powerful vacuum tube plate modulator (PAM) for the two last RF amplifiers;
- Coaxial line between the final RF power amplifier (FPA) and Alvarez tank with the switch enabling to connect any tank with the spare channel instead of a faulty one.
- High voltage power supply for powerful modulator including artificial forming line (AFL) with the impedance of 24 Ohm.

The simplified structure of RF channel is given in fig.1.

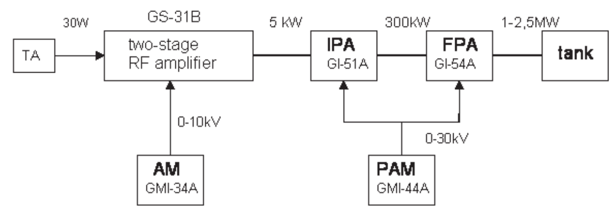

Figure1: Simplified structure of the DTL RF channel (TA – solid state RF amplifier, IPA - intermediate power RF amplifier, FPA - final RF power amplifier).

The pictures of vacuum tube RF amplifiers are shown in figures 2÷4.

Figure 2: Two-stage RF amplifier.

Except for the tubes GS-31B and GMI-34A developed earlier and being manufactured for a long time the following vacuum tubes have been specially developed for INR accelerator:

- Modulator triode GMI-44A with magnetic focusing. Due to the magnetic field the plate-grid characteristics are similar to those of tetrode with small grid current

ISBN 978-3-95450-181-6

THREE TRANSVERSE DEFLECTING SYSTEMS FOR ELECTRON BEAM DIAGNOSTICS IN THE EUROPEAN FREE-ELECTRON LASER XFEL*

A. A. Zavadtsev†
Institute for Nuclear Research of Russian Academy of Sciences, Moscow, Russia

Abstract

In frames of Russian in-kind contribution to European XFEL, INR in cooperation with DESY is responsible for Transverse Deflecting Systems (TDS) for special beam diagnostic in the XFEL linac. Three TDS have been developed: TDS INJ in the Injector, TDS BC1 in the Accelerator tunnel after Bunch Compressor 1 and TDS BC1 after Bunch Compressor 2. Each system includes S-band disk-loaded deflecting structure (DLS), waveguide system, klystron, pulse transformer, modulator and control system. TDS INJ has been built, assembled in the Injector building and tested. It is used to monitor the bunch length, longitudinal phase space and slice emittance now. Exceptionally small, exceeding expectations, slice emittance of electron bunch was measured using TDS INJ during the XFEL Injector commissioning. Three structures for TDS BC1 and TDS BC2 as well as the waveguide systems have been built, tested and TDS BC2 part installed in the XFEL tunnel.

INTRODUCTION

Tree Transverse Deflecting Systems operating at frequency 2998 MHz have been designed, built and installed (partially) for longitudinal electron beam diagnostics in the European XFEL at three locations: in the Injector, after BC1 and after BC2. The TDS location and corresponding electron energies are shown in the XFEL block-diagram (Figure 1).

The full scale prototype of the TDS INJ has been developed, designed, built and commissioned at DESY PITZ, Zeuthen facility [1]. It operates successfully now [2].

TRANSVERSE DEFLECTING STRUCTURE

Several travelling wave DLS operating at a hybrid mode have been considered for the XFEL TDS at the stage of development (Figure 2). These structures have been considered in details in [3] and [4]. Azimuthal inhomogeneity in these structures is used for stabilization of the azimuthal position of the deflecting field and for increasing frequency difference of two perpendicular polarizations of the hybrid mode.

All variants have very similar RF efficiency. The frequency separation of two perpendicular modes is about 40 MHz for variants A, B and D, 150 MHz for variant C and 900 MHz for variant E.

Basing on similar RF efficiency of these structures, taking into account the level of development and proven experience of high power operation at LOLA, the DLS of variant A was accepted for XFEL TDS.

The DLS of variant A has been developed in details. TDS systems include 16 cell structure for TDS INJ, 46 cell structure for TDS BC1 and two 46 cell structures for TDS BC2, so the lengths of these structures are 0.7 m and 1.7 m correspondingly. The same shape and the geometry dimensions have been chosen for all four structures to meet all requirements optimally. Therefore, the cells are the same and the couplers are the same for all structures. It simplifies the production and the tuning of the structures significantly [5].

The group velocity of the structure has been minimised to β_g=-0.018 choosing the shape of the cell. It allows us to use the TDS System for single bunch measurement.

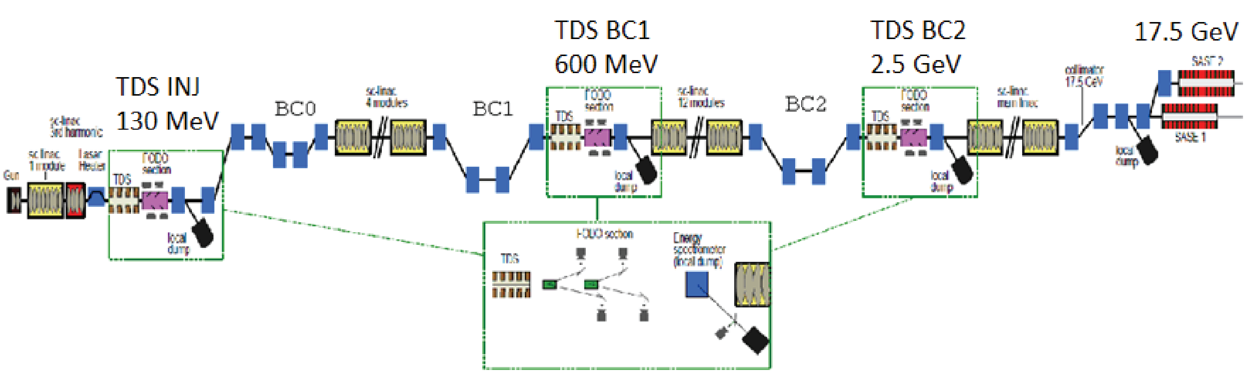

Figure 1: TDS Systems at the XFEL block-diagram.

The TDS Deflector INJ at the test stand is shown in Figure 3. The precision of the cell machining ensures the cell eigen frequency tolerance, which is equivalent to the cell

* Work supported by European XFEL GmbH and Ministry of Education and Science of Russia
† On behalf of the joint XFEL TDS team. azavadtsev@yandex.ru.

EFFECTIVE RF DEFLECTING STRUCTURES FOR BUNCH ROTATION AND DEFLECTION

V.V. Paramonov*, Institute for Nuclear Research of the RAS, Moscow, Russia

Abstract

The Deflecting RF Structures (DS's) find now applications for the bunch rotation with the purposes of diagnostic for the longitudinal distribution, the emittance exchange and the luminosity improvements in colliders. Results of development DS with minimized the level of aberrations in the distribution of deflecting field are described. Applied for bunch rotation along transverse axis, such DS's provide in orders smaller emittance growth, as compared to another options. In comparison with widely used deflectors, based on the Disk Loaded Waveguide, developed DS's have, depending on modification, in $2 \div 4$ times higher RF efficiency. Structures can operate both in Traveling Wave (TW) and in Standing Wave (SW) modes. To create longer RF cavities for SW operation, compensated DS's options are developed, adding field distribution stability and saving high RF efficiency. The main solutions are described and achieved parameters are reported.

INTRODUCTION

The periodical structures with transverse components of the electromagnetic field - DS's - were introduced for charged particle deflection and separation. The bunch cross DS synchronously with the Deflecting Field (DF) Ed, corresponding the phase $\phi = 0$ in the DS and all particles get the similar increment in the transverse momentum p_t. At present, for short and bright electron bunches DS found another applications in bunch rotation, for bunch special diagnostic, luminosity improvement and emittance exchange experiments. All directions are related to the Transformation of Particle Distribution (TPD) in the $6D$ phase space and DS operates in another mode - the Central Particle (CP) of the bunch center cross DS at zero E_d value, $\phi = 90^o$. Downstream and upstream particles get opposite increments in p_t.

The applications for TPD provide an additional requirement - a DS for TPD should provide the minimal, as possible, own distortions to the original distributions. The additional limitation to known DS's design naturally results in the reduction of the other parameters, RF efficiency and dispersion properties. Results of DS's development combining both field quality and saving another parameters are presented.

METHODICAL BASEMENT

The concept of DS's with the minimized level of own aberrations in the DF distributions was introduced in [1]. The DF distribution analysis was performed, [2], using the basis of hybrid waves HE and HM, [3]. The particles dynamic for the bunch rotation is studied and compared for different DS's in [4].

The equivalent DF is defined from the transverse component of the Lorenz force F^L, where the field components are expressed by using the basis of hybrid waves HE and HM, [3]:

$$\vec{F}^L = e(\vec{E} + [\vec{v}, \vec{B}]), F_x = eE_d = e(E_x - \beta Z_0 H_y), \quad (1)$$
$$\vec{E} = A\vec{E}_{HE} + B\vec{E}_{HM}, \vec{H} = A\vec{H}_{HE} + B\vec{H}_{HM},$$

and $Z_0 = \sqrt{\frac{\mu_0}{\epsilon_0}}$.

The reasons for the emittance growth during TPD are the aberrations - the non linear additions in the E_d distribution, which take place due to not relativistic energy of particles, $\beta < 1.0$, additions from higher sextupole modes, the higher spatial harmonics in the distribution of the deflecting field. The main attention should be paid to the higher spatial harmonics, see [2], [4] for details.

In any periodical structure each field component $E_j, H_j(x,y,z)$ in the beam aperture can be represented as the set over spatial harmonics:

$$E_j, H_j(x,y,z) = E_j, \widehat{H_j(x},y,z) e^{i\psi_j(z)} = \quad (2)$$
$$= \sum_{n \to -\infty}^{n \to +\infty} a_{jn}, b_{jn}(x,y) e^{\frac{-i(\Theta_0 + 2n\pi)z}{d}},$$

where $E, \widehat{H_j(x},y,z)$ and $\psi_j(z)$ are the amplitude and the phase distributions, d is the structure period and $a, b_{jn}(x,y)$ are the transverse distribution for the n-th spatial harmonics, Θ_0 is the operating phase advance. The same representation is valid for E_d also.

In the periodical slow wave structure each component of original fields $\vec{E}, \vec{H}$ can not exist without the higher spatial harmonics, $n \geq 1$ in (2). It is the law for slow wave structures. But DF is composed from two components of original fields, (1), and this law, generally, has no force for E_d. During DS design we can manage A and B relation in (1) in such way, that spatial E_x harmonics a_{jn} will compensate the H_y harmonics b_{jn}. To provide such compensation, the opposite phasing of hybrid waves $\vec{E}_{HE}$ and $\vec{E}_{HM}$ is required, $A \cdot B < 0$ in equation (1).

For harmonics estimations in values, the parameters $\delta\psi_j(z)$ and Ψ_j at the DS axis are introduced, [2]:

$$\delta\psi_d(z) = \psi_d(z) + \frac{\Theta_0 z}{d}, \quad \Psi_d = max(|\delta\psi_d(z)|), \quad (3)$$

with the physical sense as the deviation and the maximal phase deviation of the total E_d distribution from the main synchronous harmonic in E_d. During bunch rotation, $\phi = 90^o$, CP sees the effect of higher spatial harmonics, [2], as:

$$E_{rot} \approx E_{d0} sin(\Psi_d) \approx E_{d0}\Psi_d, \quad (4)$$

* paramono@inr.ru

ISBN 978-3-95450-181-6

INR RAS INSTRUMENTATION FOR BUNCH SHAPE AND BEAM CROSS-SECTION MONITORING

S. Gavrilov†, A. Feschenko, P. Reinhardt-Nickoulin
Institute for Nuclear Research of the Russian Academy of Sciences, Moscow, Russia

Abstract

Instruments for bunch shape and beam cross-section diagnostics at ion linacs are as important as complicated devices. Widespread Bunch Shape Monitors developed in INR RAS are used during a linac commissioning and optimization of beam dynamics. Beam Cross-Section Monitor implemented at INR RAS linac provide efficient non-destructive beam tuning and control. Features of both monitors investigated in simulations and beam tests are described. A variety of experimental results are presented.

INTRODUCTION

A bunch shape is defined usually as longitudinal distribution of particle intensity in bunches *I(z)* or *I(φ)*, which is one of the most difficult to observe characteristics of a beam at ion linear accelerators.

There are several methods for bunch shape measurements, however low energy secondary electrons are used most extensively because of weak dependence of their properties both on the type of primary particles and on their energy. The technique of a coherent transformation of a temporal bunch structure into a spatial charge distribution of low energy secondary electrons through RF-modulation was initially implemented by R. Witkover [1] for BNL linac. An energy (longitudinal) RF-modulation of secondary electrons was used.

In the Bunch Shape Monitor (BSM) [2], developed in INR RAS, a transverse RF-scanning is used. The general principle of BSM operation is clear from Fig. 1.

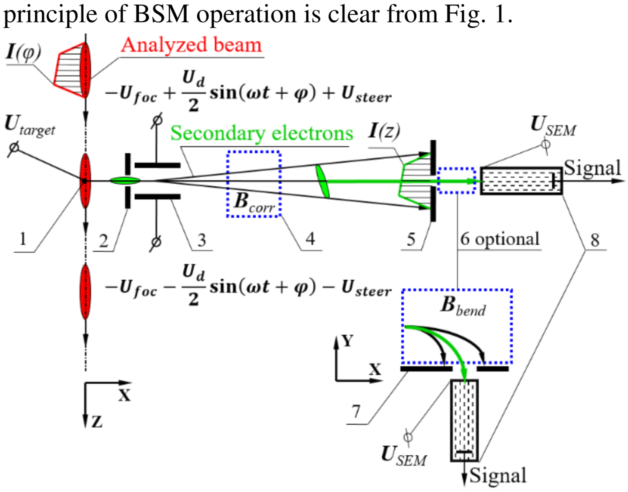

Figure 1: BSM scheme: 1 – tungsten wire target, 2 – inlet collimator, 3 – RF-deflector combined with electrostatic lens, 4 – correcting magnet, 5 – outlet collimator, 6 – optional bending magnet, 7 – registration collimator, 8 – secondary electron multiplier.

† s.gavrilov@gmail.com

Two-dimensional beam density distribution *I(x, y)* is one of the most informative beam parameters, enabling simultaneous measurements of beam position, profiles and emittance ellipses reconstructed from profiles data in combination with adjustable beam focusing elements for linear transformations in phase space. Luminescent screens, typical devices for 2D cross-section measurements, have all advantages and drawbacks of destructive diagnostics. More convenient, transparent technique of residual gas ionization, was initially proposed by V. Mihailov et al. [3] and used for both charged particle and synchrotron light beams [4].

The Beam Cross-Section Monitors (BCSMs) [5], based on ion component of the residual gas ionization, were implemented and upgraded at INR RAS linac for in-flight non-destructive diagnostics in the full range of beam parameters. The basic principle of operation is shown in Fig. 2. The energy of the ions at the slit linearly depends on their original coordinates X, hence their energy distribution downstream of the slit reproduces the transverse particle density distribution in the primary beam along X coordinate, while the distribution of the ions along Y coordinate keeps the same as that in the primary beam, similarly to 1D ionization profile monitors. In case of uniform fields the distances X_0 and X_1 are related as $X_1=2X_0(E_{ex}/E_a)$, that is independently of charge and mass of residual gas ions, and all types of ions contribute to formation of 2D image of particle density distribution in analyzing beam cross-section.

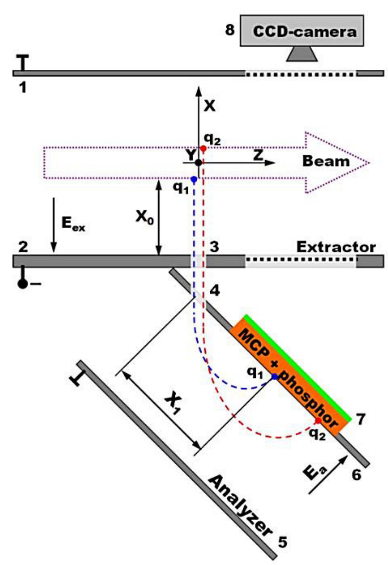

Figure 2: BCSM scheme: 1, 2 – electrodes of extractor, 3, 4 – double slit filter, 5, 6 – electrodes of analyzer, 7 – electro-optical converter, 8 – CCD-camera.

ISBN 978-3-95450-181-6

STRUCTURE AND HARDWARE OF LIA-20 CONTROL SYSTEM

G. Fatkin*, E. Bekhtenev, E. Kotov, A. Ottmar, A. Panov, A. Senchenko, S. Serednyakov,
M. Vasilyev, BINP and NSU, Novosibirsk, Russia
A. Batrakov, A. Chupyra, Ya. Macheret, V. Mamkin, A. Pavlenko,
A. Selivanov, P. Selivanov, K. Shtro, S. Singatulin, BINP, Novosibirsk, Russia

Abstract

The control system of a linear induction accelerator LIA-20 for radiography is presented in this paper. The accelerator is designed to provide a series of three consecutive electron pulses with energy up to 20 MeV, current 2 kA and lateral size less than 1 mm. To allow reliable operation of the whole complex, coordinated functioning of more than 700 devices must be guaranteed in time frames from milliseconds to several nanoseconds. Total number of control channels exceeds 6000. The control system structure is described and the hardware in VME and CAN standards is presented.

INTRODUCTION

Linear Induction Accelerator LIA-20 (see Fig. 1) is designed to pro-vide three consecutive electron beams with an energy up to 20 MeV, current up to 2 kA and the beam lateral size after focusing on the target less than 1 mm. It is planned to pro-vide three consecutive pulses, with one of them divided into 9 angles. The accelerator will be used for the flash X-Ray radiography. Successsfully commissioned LIA-2 accelera-tor (2 MeV, 2 kA) could be considered a prototype for the injector of the 20 MeV installation [1]. The control system of the LIA-2 is described in [2]. Both accelerators consist of a large number of complex electrophysical devices that require extensive control.

To attain the minimum possible beam size the structure with low acceleration rate was chosen. The upside of this approach is that common and cheap HV technology could be used (thyratrons, cabling). The downside is a large quantity of required devices. In case of LIA-20 we have more than 6000 control and measurement channels, this is approximately ten times more than LIA-2 and all known LIA flash radiography installations (DARHT, FXR, AIRIX, DRAGON)[3]. Therefore we had to introduce a lot of new approaches for design of our control system. Structure and hardware of the control system are the scope of this paper, while the software and the computational infrastructure are described in [4].

* G.A.Fatkin@inp.nsk.su

STRUCTURE OF THE ACCELERATOR

LIA-20 consists of the injector and a number of accelerating modules. The injector has 92 inductors and generates an electon beam with the current up to 2 kA and the energy 2 MeV. 30 “short” accelerating modules (SAM) are placed after the injector. Each of them consists of 16 inductors and adds an energy of 0.33 MeV to the beam. Then 12 “long” accelerating modules (LAM) are placed each of them consists of 32 inductors. Each LAM adds an energy of 0.66 MeV to the beam. The total length of the accelerator is about 75 meters, therefore controlling the positioning of optical system is critical. The injector has individual support, two SAM’s are placed on one support and each LAM is placed on a separate one. Two position control systems are provided to control the horisontal, vertical and angular offsets of the axis of supports.

Focusing solenoidal lenses and correctors are placed between accelerating modules. The lenses are powered by pulsed power supply that provides 0.5 kA, 2.05 ms sinusoidal pulse. Beam position monitors (BPM’s) are present between accelerating modules. Several other technological sub-systems including vacuum and insulating gas pressure require control.

Accelerating pulses on the inductors are formed by the

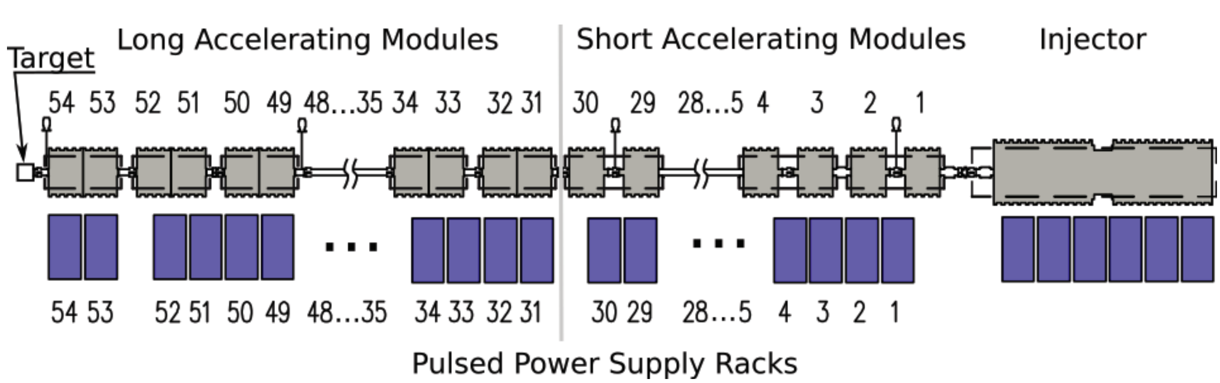

Figure 1: Scheme of LIA-20 Accelerator

ISBN 978-3-95450-181-6

THE MONITORING OF THE EFFECTS OF EARTH SURFACE INCLINATION WITH THE PRECISION LASER INCLINOMETER FOR HIGH LUMINOSITY COLLIDERS

B. Di Girolamo*, J.-Ch. Gayde, D. Mergelkuhl,
M. Schaumann, J. Wenninger, CERN, Geneva, Switzerland
N. Azaryan, J. Budagov, V. Glagolev, M. Lyablin,
G. Shirkov, G. Trubnikov, JINR, Dubna, Russia

Abstract

Earth surface movements, provoked for example by earthquakes or industrial noise, can induce a degradation of particle accelerators instantaneous luminosity or even sudden beam losses. This report presents the results from monitoring the effects of earthquakes on the present LHC beam orbit and luminosity, using a novel instrument, the Precision Laser Inclinometer (PLI). The aim is to characterize the response of accelerators to remote or nearby Earth surface movements and propose possible applications of the instrument for minimizing detrimental effects.

INTRODUCTION

The Precision Laser Inclinometer (PLI) is a novel type of instrument able to detect inclination of the Earth surface with high precision [1]. The instrument main characteristics have been studied in comparison with other known instruments and observing natural phenomena as a continuous source of calibrating events: the micro-seismic peak, the effects of the Moon attraction cycle and earthquakes. This report will briefly introduce the working principles of the PLI, the observations of relevant phenomena and finally discuss the possible applications to high luminosity colliders, which are notoriously very sensitive to Earth surface movements from natural and human (cultural noise) sources.

THE PRECISION LASER INCLINOMETER

The Precision Laser Inclinometer (PLI) is part of a large program of survey instrumentation developed at JINR - Dubna in the framework of research and developments for the ATLAS experiment in collaboration with the CERN Survey group. The deployment and the study of the results are being done in collaboration between JINR and CERN (the High Luminosity LHC Project and the Beam Operations).

A set of PLI prototypes have been installed at CERN, since 2015, in the TT1 tunnel, a former transfer tunnel of the Intersecting Storage Rings (ISR) and now used as stable environment for the development of surveyors instrumentation among other usage. The TT1 tunnel offers a suitable environment for the understanding of PLI characteristics.

The Experimental Setup and the First Measurements

The PLI setup is shown in Fig. 1. Schematically the setup is quite simple, a cuvette with liquid is placed on a very stable base plate (support S) and a Laser delivers a light ray, reflected by the surface of the liquid. The reflected light is detected by a quadrant photodiode (QPr).

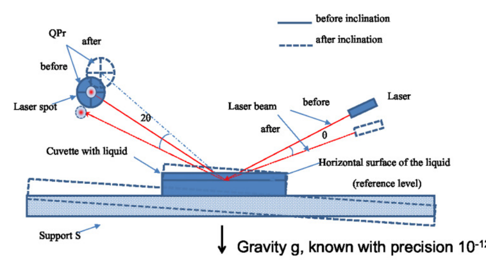

Figure 1: The PLI setup.

When the system is inclined by an angle θ, the surface of the liquid remains, by gravity, horizontal, while the Laser light is deflected by an angle $2\times\theta$ and this movement of the light spot is detected by the quadrant photodiode and recorded by the data acquisition system. The detection is in both planes and therefore it is easy to calculate the combined slope of the movement and its azimuth.

The very stable ground and temperature conditions in the TT1 transfer tunnel allowed to perform several studies of stability versus temperature, influence of industrial noise. Comparative measurements with known instruments [2, 3] allowed to to monitor, over a period of a month, a variety of phenomena inducing Earth inclinations, from industrial to natural kind, where the latter are dominated by the recording of the micro-seismic peak, the Moon attraction cycle and earthquakes. The precision of detection achieved was assessed to be better than $10^{-9}\ \mathrm{rad}/\mathrm{Hz}^{1/2}$ in the frequency range $[3\cdot 10^{-7}, 1]$ Hz, where $3\cdot 10^{-7}$ Hz corresponds to one month period. For daily measurements the precision achieved has been assessed to $10^{-10}\ \mathrm{rad}/\mathrm{Hz}^{1/2}$ in the frequency range $[10^{-3}, 1]$ Hz [2, 3]. Recently the working range of the PLI has been extended to 4 Hz via carefully selecting a liquid with lower viscosity.

*beniamino.di.girolamo@cern.ch

ISBN 978-3-95450-181-6

COMMISSIONING OF e^+/e^- TRANSFER LINE FROM BINP INJECTION COMPLEX TO VEPP-2000 FACILITY*

I.M. Zemlyansky#, Yu.S. Aktershev, V.V. Anashin, A.V. Andrianov, A.M. Batrakov, O.V. Belikov, D.E. Berkaev, M.F. Blinov, B.A. Dovzhenko, F.A. Emanov, V.V. Gambaryan, V.A. Kiselev, I.A. Koop, I.A. Mikheev, D.A. Nikiforov, A.V. Otboev, V.P. Prosvetov, V.V. Rashchenko, A.M. Semenov, P.Yu. Shatunov, Y.M. Shatunov, S.S. Vasichev, V.D. Yudin, Yu.M. Zharinov,
BINP SB RAS, Novosibirsk, Russia
A.A. Krasnov, A.V. Pavlenko, Y.A. Rogovsky, D.B. Shwartz, A.A. Starostenko,
BINP SB RAS, Novosibirsk; NSU, Novosibirsk, Russia

Abstract

VEPP-2000 e^+/e^- collider [1] was constructed in 2006 at BINP. The design luminosity of 1×10^{32} cm^{-2}s^{-1} may be achieved at filling rate of 1×10^8 e^+/e^- per second. Old VEPP-2M facility infrastructure provided only 1×10^7 e^+/e^- per second. We decided to use Injection Complex [2, 3]. The transfer line [4] connects Injection Complex and VEPP-2000 facility. Commissioning of e^+/e^- transfer line from Injection Complex to VEPP-2000 facility is done in 2016. Both electrons and positrons beams are injected to VEPP-2000 collider.

GEOMETRY AND OPTICS

We simulated the optics with the RING program [5]. Detailed geometry and optics are shown in Figures 1-9.

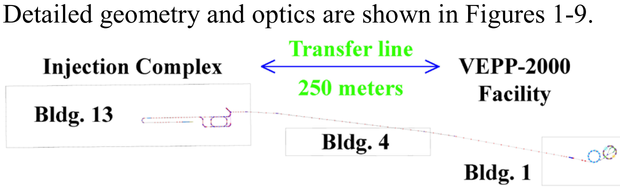

Figure 1: The transfer line location.

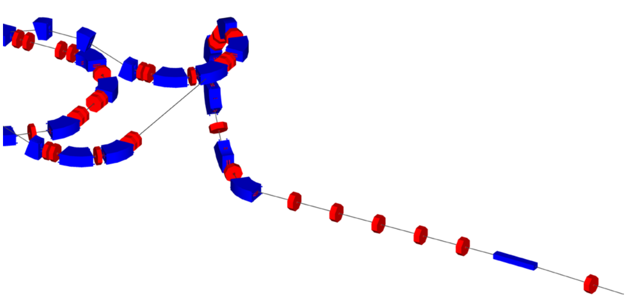

Figure 2: The descent from the storage ring.

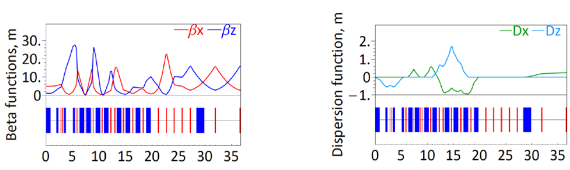

Figure 3: Lattice functions of the descent.

*The work is supported by the Ministry of Education and Science of the Russian Federation, NSh-10088.2016.2
#I.M.Zemlyansky@inp.nsk.su

Figure 4: First horizontal bend.

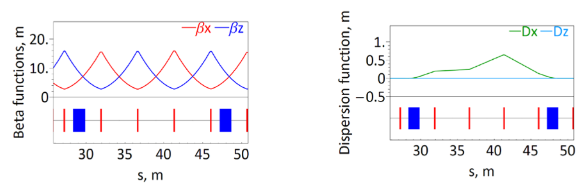

Figure 5: Lattice functions of first horizontal bend.

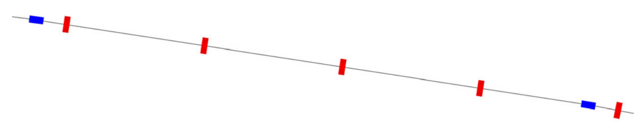

Figure 6: Second horizontal bend.

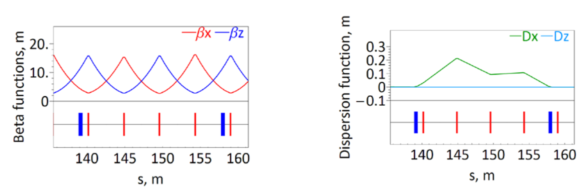

Figure 7: Lattice functions of second horizontal bend.

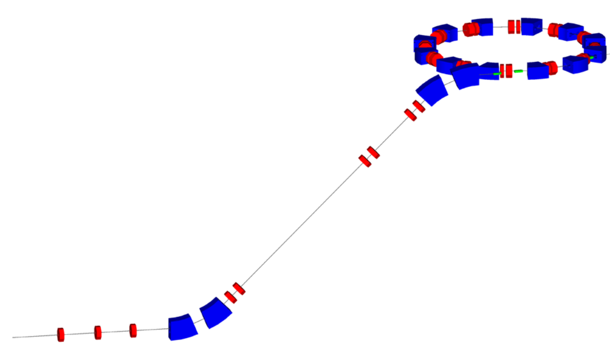

Figure 8: The ascent to booster BEP.

ISBN 978-3-95450-181-6

PROPOSAL OF THE ACCELERATING STRUCTURE FOR THE FIRST CAVITY OF THE MAIN PART OF INR LINAC

I.V. Rybakov†, Y.Z. Kalinin, V.N. Leontev, L.V. Kravchuk, A.N. Naboka, V.V. Paramonov, V.L. Serov, A.V. Feschenko, Institute for Nuclear Research of the RAS, Moscow, Russia

Abstract

For the improvement of beam power and operational stability of INR linac, replacement of the first four section cavity of the main linac part is required. The new cavity should not lose to the present one in beam dynamics and RF parameters with minimal modifications in the other linac systems. The results of more detailed study of possible accelerating structure are presented in this paper.

INTRODUCTION

The first cavity of the main part of INR linac works for proton acceleration in the range β=0.4313 – 0.4489 with acceleration gradient $E_0T\cos\varphi_s$ = 2.5 MV/m and the synchronous phase φ_s=-33°. The cavity has the aperture radius r_a= 17 mm, operating frequency f_a=991.0 MHz and the required operating regime is with RF pulse length τ=200 μs and Repetition Rate (RR) up to 100 Hz, Fig. 1.

Figure 1: The existing INR DAW cavity. 1 – accelerating sections, 2 – bridge coupling cavities, 3 – RF input, 4- focusing elements.

The main part of the INR linac is based on the Disks and Washers (DAW) structure [1], Fig. 1c. After a long time after linac construction, the direct repetition of the single DAW cavity in the industry is expensive and another options should be considered. Both proven in high intensity hadron linacs and promising new developments were considered preliminary for this purpose, [2], considering parameters of the existing DAW cavity as the reference points. From the total set of required parameters the INR development – Cut Disk Structure (CDS) - was pointed out as the most effective choice. This structure already is used for electron acceleration, β=1.0, with the accelerating gradient up to E_0T= 12 MV/m as the PITZ CDS booster cavity, [3], and operates in the regime with RF pulse length up to τ=800 μs, RR =10 Hz, hence, with the heavy heat load up to 25 kW/m. Application for low β~0.4313 case is not favorable for CDS parameters. We not can scale simply solutions for β=1.0 case, and additional development is required. Results of the more detailed CDS development for applications in the intense hadron linac with a moderate velocity of accelerating particles β=0.4313 – 0.4489 are presented below.

PARAMETERS OF THE STRUCTURES

Compared structures, DAW, CDS, Side Coupled Structure (SCS) [4] and Annular Coupled Structure (ACS) [5], are shown in Fig. 2 in a common scale for the same operating frequency.

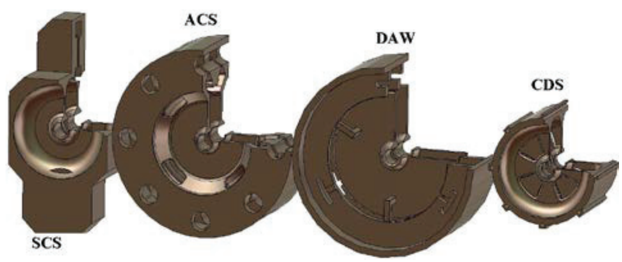

Figure 2: Considered accelerating structures: a) SCS, b) ACS, c) DAW, d) CDS.

For the proven structures DAW, SCS and ACS the key points of cavities design and parameters are known from references. Structures have a similar value of the effective shunt impedance Z_e, but strongly differ in value of coupling coefficient K_c. At the background of the known experience for DAW, there is no sense to consider structures SCS and ACS for the single cavity. But with two times smaller CDS transverse dimensions we can reduce costs of construction by less amount of raw OFE material and applying more usual Numerically Controlled (NC) equipment. Operating regime of the first cavity results in the heat load more than 7 kW/m. For such regime all considered structures require an internal cooling – cooling channels should be placed inside the structure closer to drift tube region to prevent a significant shift of operating frequency Δf_a and the temperature increase ΔT at the drift tube tip during cavity operation. In the proven structures it is realized by internal cooling channels inside web between accelerating cells and with necessity in the design there are brazed joints water-vacuum. In CDS for low β~0.44 the cooling problem is more severe.

CDS OPTIMIZATION

The schematic sketch of the CDS period is shown in Fig. 3. Internal channels should be placed in the web between coupling and accelerating cells only, see Fig. 3. It limits the web thickness to $t_w \geq$ 10 mm and the total distance d_w ~ 25 mm becomes comparable with the period length $d=\beta\lambda/2$ ~ 65 mm. In such conditions for all structures Z_e value decreases and we can not get directly required RF efficiency.

† rybakov@inr.ru

DEVELOPMENT OF RF ACCELERATOR ON PARALLEL-COUPLED STRUCTURE – TREND IN ACCELERATOR TECHNIQUE

Yu. D. Chernousov[†], Voevodsky Institute of Chemical Kinetics and Combustion SB RAS, Novosibirsk, Russia

Abstract

Development of parallel-coupled accelerating structure (PCS), creation of RF linier accelerator based on PCS is new and rapidly developing field of accelerator technology. Compared with conventional accelerating structures with serial communication - the standard traveling and standing waves structures, the PCS has a lot of features and advantages. There are many problems in the development of RF linear accelerators: breakdowns at high power levels, the destruction of the structure due to overheating, the excitation of higher-order mode, the decline of field strength along the structure, transients, beam loading, beam focusing, multipactor, radiation accelerator cleanliness, etc. PCS - the best accelerating structure for solving these problems.

INTRODUCTION

To construct RF accelerators, accelerating structures of traveling and standing waves [1] have been used and improved for a significant amount of time. By method of excitation, these are the structures with serial communication, where the microwave power is linked up with one of the structure's cavities and then it is subsequently circulated from one cavity to another. Both the accelerating structures with serial communication and the electron linear accelerators in these structures are characterized by a significant number of scientific and technical problems. Some of the problems and the challenges set accordingly are listed below:

- Cavity RF breakdown, and reduction of breakdown influence on the structure and the accelerating beam.
- Local pulsed overheating, input elements destruction, and heat reduction.
- Excitation of higher order modes, and "decimation" of the mode spectrum.
- Decline in strength of the accelerating field along the structure's axis, and challenge on developing the specified field.
- Accelerated particles focusing at considerable beam currents, and challenge on developing the effective system of beam focusing.
- Problems of injection current control, and challenge on developing the effective control systems.
- Transient processes in the structure, and stabilization of the microwave field amplitude.
- Load of the structure by the beam current, and stabilization of accelerating voltage.
- Radiation background, and provision with a high beam capture close to 100%.
- Excitation of secondary-emission resonant discharge, and its suppression.
- Forming the electron beams of considerable average power (at least 10-100 kW) at energy over 5 MeV.

The main solutions of these problems for standard accelerating structures intended for low-energy accelerators as well as for high-energy physics seemed to be found. For example, for structures with high accelerating gradient, these are an increase in the accelerating field frequency, reduction in the pulse duration, optimization of the cavity shape, selection of the work surface materials, preparation and training of accelerating structures [2]. For the standard structures, limit operations are defined, the optimal values are found.

Recently, an interest in parallel-coupled accelerating structures has been deepened. These structures are characterized not by the consistent, but by the parallel method to supply the microwave power to the accelerating cavities. Such a circuit design makes it possible to expect for higher limit values in comparison with the standard structures with serial communication - traveling and standing waves.

PARALLEL-COUPLED STRUCTURE FOR RF ACCELERATOR

Key Idea Development

An idea of the "Parallel Coupled Structure" (PCS) in the accelerator technology occurred upon the paper [3] published which describes the structure containing the accelerating cavities powered in parallel from the lead-in coaxial waveguide. The phase velocity of the wave in the coaxial line is equal to the light speed, thereby the wave and accelerated electrons synchronization is ensured. Currently, a new focus area in the accelerator technology is being developed, various schemes of accelerating structures are being offered, features and advantages of the PCS are being investigated [3-13].

A circuit scheme disadvantage [3] was a low level of microwave power supplied to the accelerating cavities through a coaxial line. Easy replacement of the coaxial line with the hollow waveguide is impossible, since the wave phase velocity in the waveguide is bigger than the light speed, the wave "runs away" from the accelerated particles, synchronism is impossible. While developing [3], we proposed a scheme with a counter-movement of waves and particles. The a concept of reverse power input is applied, the particles and accelerating field synchronization in the PCS can be achieved under usage of the rectangular waveguide as an exciting element operating in the traveling wave regime [4]. A structure schematic diagram is shown in Figure 1.

† email address: chern@catalysis.ru

ISBN 978-3-95450-181-6

NEW EXPERIMENTAL RESULTS ON RF ACCELERATOR WITH PARALLEL-COUPLED STRUCTURE AND RF CONTROLLED GUN

Yu. D. Chernousov†, I.V. Shebolaev, I.M. Ikryanov, Voevodsky Institute of Chemical Kinetics and Combustion SB RAS, Novosibirsk, Russia

Abstract

New data on the development and experimental investigation of the RF accelerator based on the 9-cavities parallel-coupled accelerating structure that is equipped with a high-frequency grid-controlled electron gun are presented. Accelerating structure, injection system and focusing system are improved. Previously observed second emission resonant discharge - multipactor is suppressed by increasing the field amplitude in the structure first cavity and using the protector. The parameters of the accelerated beam close to the design ones, i.e. electron energy up to 8 MeV, capture to the acceleration mode up to 100%, were received. Capture is provided by the RF electron focusing of the microwave field structure with usage of the magnetic focusing system based on permanent magnets and pulsed "π-injection" of the beam by the microwave grid control in the electron gun.

INTRODUCTION

A new type RF accelerator based on the accelerating structure with parallel connection (PCS) is being developed in ICKC and BINP SB RAS. In the paper [1], the first experimental results on investigation of the RF accelerator based on the PCS - 9-cavities accelerating structure prototype are presented. The results were discouraging. The secondary emission resonance discharge interfered with achieving the designed conditions of beam acceleration. At relatively small field amplitude values, the secondary emission resonance discharge was localized in the first and second cavity of the structure. The discharge stabilized the accelerating field amplitude at a low level, the first cavities didn't accelerate the beam and the electrons fell into the third cavity with energy shortfall. Although the rest structure cavities were operating in normal mode due to the PCS properties, the capture ratio was low; the estimated value of the beam output energy wasn't achieved. It was decided to improve the accelerating structure, increase the field amplitude in the first PCS cavities, and suppress the secondary emission resonance discharge. This was achieved by increasing the communication slots between the accelerating and exciting cavities. To eliminate the secondary emission resonance discharge, a method of suppressing was developed, i.e., a protector was found and conditions of its applying to the secondary emission centers on the cavity surface were selected. The protector application is carried out in the working installation without opening and subsequent contact with the external atmosphere.

Developed by us injection system [2] contains the electron gun with grid control and microwave signal control system supplied to the gun. Previously a circuit scheme was used where the microwave signal was branched off from the main microwave tract of the accelerating structure. There were problems of controlling the signal parameters - amplitude, duration, phase. At this stage, it was decided to upgrade the system, use an additional microwave power amplifier that enables fast electronic control of all the parameters of the microwave signal.

For additional beam grouping in the injection system, a grouping cavity was used previously [1,2], it made it possible to reduce the bunch phase length and increase the beam capture in acceleration mode. The field amplitude in such a cavity was relatively small, and it became an additional place of secondary emission resonance discharge occurrence. Calculations showed that in the acceleration mode high capture close to 100% is possible due to "π-injection", microwave and magnetic focusing and without additional grouping. It was decided to simplify the beam forming system, eliminate the grouping cavity from the electron gun tract. This led to simplification of the electro-optical and magnetic focusing system.

RF ACCELERATOR

Accelerator Bench

Figure 1 shows a bench to study properties of the developed RF accelerator based on the PCS. On the bench, there are installed an improved accelerating structure with integrated focusing system, a new injection system, the measurement elements. Microwave power is supplied through the feed waveguide 1 to the accelerating structure 3. To measure the current accelerated, the Faraday cup 2 mounted on the structure output is used. Focusing of the accelerated beam is made by the installed magnetic system 4. The magnetic system consists only of permanent magnets and shunts without additional focusing coils and tuning elements. Due to the radial input and reverse, a longitudinal focusing magnetic field is generated almost exclusively on the axis of the PCS accelerating cavities, in the area of the beam span, so the magnet mass is relatively small, and in this case, the total weight of the magnetic system is less than 2 kg. Usually in the accelerators in the initial acceleration stage, a solenoid which weight is comparable with the weight of the accelerating structure is used for focusing. Probes 5 are used for measuring the form of waving microwave signals from the first and second cavities of the structure. Microwave signal is supplied via high-voltage antenna lead-in 7 [3] to the electron gun 6. One of the antennas is grounded, and the other is under injection voltage. Among the antennas there is a ceramic insulator. The gun is equipped with an isolation

† email address: chern@catalysis.ru

ISBN 978-3-95450-181-6

GRADIENT LIMITATIONS FOR RF ACCELERATOR ON PARALLEL-COUPLED STRUCTURE

Yu. D. Chernousov†, I.V. Shebolaev, Voevodsky Institute of Chemical Kinetics and Combustion SB RAS, Novosibirsk, Russia

Abstract

RF breakdown is the main gradient limitation for RF accelerator [1,2]. It is believed that all the known ways to increase the accelerating gradient have been already investigated. These are increase in the frequency of the accelerating field, reduction in the pulse duration, the optimization of cavities form, selection of operating surface materials, preparation and training of accelerating structures. In this paper, we discuss the possibility of increasing the accelerating gradient due to the circuit design, i.e., the use of the parallel-coupled accelerating structure.

INTRODUCTION

To create RF accelerators, accelerating structures of traveling and standing waves are used and improved [1]. By method of excitation, these are the structure with the serial communication where the microwave energy is supplied to one of the structure cavities and then subsequently supplied from one cavity to another. For accelerating structures with serial communication and linear electron accelerators on these structures, there are a significant number of scientific and technical problems. One of them is the breakdown problem leading to a breach of the acceleration process in the structure as a whole, its destruction.

In recent years, an interest in accelerating structures with a parallel connection has been growing. The term "parallel coupled structure" (PCS) in accelerator technology came after the publication of [3] described the structure containing the accelerating cavities fed in parallel from the lead-in coaxial waveguide. Currently, a new focus area in accelerator technology is being developing rapidly, various circuit schemes of accelerating structures are offered, features and advantages of the PCS are investigated [3-11]. We have proposed a new type accelerating PCS containing successive accelerating cavities, microwave power supplied from a common passage excitation cavity through individual communication slots [7,8]. The structure accelerating cavities are excited individually; there is almost no communication along the electromagnetic field between them. While solving the problems in creating the RF accelerators, the use of these structures can produce better results than the use of conventional structures. In this paper, the features and advantages of the PCS under solving the problem of microwave breakdown are shown by calculations and experimentally on the model.

† email address: chern@catalysis.ru

PCS VS STANDARD STRUCTURES

Breakdown in Standard Structure

In the structures with the serial communication under the breakdown at any point of the structure due to a "serial communication", all the microwave energy stored in the structure is absorbed, apparently, mainly near breakdown places. The accelerating field disappears, vacuum is broken due to a discharge product and this pulse is lost. To restore the necessary vacuum conditions, a period of time is required: in the standard structure with serial communication (and consistent pumping) up to 10 seconds [2]. In the accelerators containing a significant number of accelerating structures, the structure with breakdown is disconnected from the microwave power generator and pumped to restore, and the energy shortage of the accelerated beam fills by the reserve system [2].

In the standard structure - with serial communication, α_{--} - breakdown probability during the pulse in the whole structure is N times bigger (N - number of accelerating cavities in the structure), than the β_{--} - breakdown probability in a certain cavity:

$$\alpha_{--} = N\beta_{--} \qquad (1)$$

For example, at N = 100, $\alpha_{--} = 10^{-2}$/pulse from (1), we can find $\beta_{--} = 10^{-4}$/pulse. This means that if the loss is allowed only of every hundredth impulse, at N = 100, one requires the breakdown probability in the certain cavity of such a standard structure no more than $\beta_{--} = 10^{-4}$/pulse. With the growth of the total number of cavities in the accelerator, the requirements to electrical durability of an individual cavity are increasing rapidly in accordance with the ratio (1).

Breakdown in PCS

The breakdown in the PCS occurs in a different way. We started to study the breakdown mods in the PCS in [11] on 5-cavities structure. Let us consider the results obtained in [11]. The PCS operation conditions are characterized by the pulses waveform and shown in Figure 1. Incident microwave power 1 reflected from the accelerating structure of microwave power 2 and a capacitance probe signal 3 proportional to the stored microwave power from the 5th cavity were detected (Fig.1, a - d).

The conditions without breakdown are shown in Figure 1, a. Under breakdown of the 5th cavity (Figure 1, b), all stored therein microwave energy is dissipated for 50 ns (curve 3), and is not restored till the end of the pulse.

ISBN 978-3-95450-181-6

ELECTRON BEAM DYNAMICS CALCULATION AND ACCELERATING STRUCTURE GEOMETRY DESIGN IN 10 MeV HYBRID ELECTRON LINAC

A.V. Bulanov, S.V. Matsievskiy, E.A. Savin, N.P. Sobenin,
National Research Nuclear University MEPhI, Moscow, Russia

Abstract

Electron linear accelerators with an energy of 10 MeV are widely used for industrial purposes. This article presents the electron dynamics calculations and the design of linac with a standing wave (SW) buncher based on the biperiodic accelerating structure and a constant impedance backward traveling wave (BTW) after it. In such accelerator, all unused RF power coming out from BTW section is used in SW section to improve the linac efficiency. Thus, no RF load is needed. Also, a beam is experiencing an RF focusing in the SW buncher. Solenoid focusing field influence on the beam dynamics in the TW section was studied.

INTRODUCTION

Electron linear accelerators to the fixed 10 MeV energy are in demand for the industrial purposes. For example, for the sterilization of medical supplies, food, cosmetics etc. [1]. One of the first choices the developer is faced – it is the choice between SW or TW operating regimes. Both options have their own advantages, disadvantages, and special issues. TW is suitable for the acceleration of high electron currents. In the meantime, SW buncher is much shorter than TW buncher and doesn't require additional focusing fields [2]. The way to combine advantages of both SW and TW structures is a hybrid linac [3], where the beam is bunching in the biperiodic accelerating SW structure (BPS) [4] and continuing to accelerate in TW structure based on the reliable diaphragm loaded structure technology.

ACCELERATOR SCHEME

We propose the hybrid structure (Fig.1), where the unused for the acceleration in BTW RF power goes not to the load but, via the rectangular waveguide, to the BPS buncher (Fig.2).

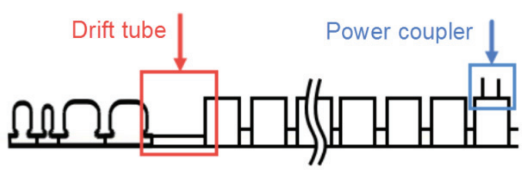

Figure 1: Hybrid linac scheme. Before the drift tube – BPS, after – BTW.

In the operating regime, power reflection from BPS, tuned to the optimal overcoupling [5], is equal to zero, thus accelerating section is operating in the TW regime. Accelerator operates at 2856 MHz frequency.

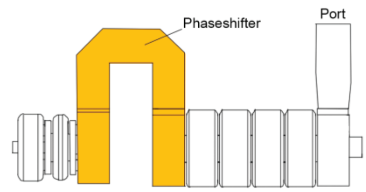

Figure 2: BTW and BPS connection.

ACCELERATOR GEOMETRY

Accelerating Section

Accelerating section for the relativistic particles is made from the disk-loaded waveguide (DLW) with an additional magnetic coupling. Magnetic coupling is designed to be higher than electric coupling, because for using BAS as a load, power flow in accelerating section should be in opposite direction to the beam propagation, i.e. negative group velocity. We studied dependencies of the main electrodynamics characteristics of BTW, such as shunt impedance r_{sh}, group velocity β_{gr}, Q-factor, attenuation coefficient α and normalized accelerating gradient $E\lambda/P^{1/2}$ as a function of phase shift per cell and normalized to the wavelength aperture radius a/λ. Shunt impedance is the highest at $2\pi/3$ mode and the optimum relative group velocity is ~1%. Table 1. shows, that shunt impedance rises with smaller aperture radius. We decided to choose $a/\lambda=0.08$ to both achieve high shunt impedance and avoid beam losses in accelerator walls.

Table 1: BTW electrodynamics parameters dependence from the normalized aperture radius at $2\pi/3$ mode, constant group velocity and 2856 MHz operating frequency.

a/λ	0.06	0.08	0.1
r_{sh}, MOhm/m	82.9	71.2	62.1
β_{gr}, %	1.3	1.2	1.2
Q	12500	12200	12000
α, m^{-1}	0.18	0.19	0.2
$E\lambda/P^{1/2}$	578	547	531

Phase Control Between Sections

Buncher and accelerating section are connected to each other by a rectangular waveguide with a fixed length and are separated by a drift tube. To ensure, that the accelerating mode phase difference between the last buncher cell and the first accelerating cell is suitable for the acceleration in resonance, i.e. $\Delta\varphi$=180+/-2π, we designed a waveguide phase shifter which allows tuning this phase difference in the whole 2π range (Fig.3). It consists of the

ISBN 978-3-95450-181-6

ELECTRON LINEAR ACCELERATOR WITH THE VARIABLE ENERGY FROM 6 TO 11 MeV

A.V. Bulanov, E.A. Savin, N.P. Sobenin
National Research Nuclear University MEPhI, Moscow, Russia
A.V. Gryzlov, Research and Production Enterprise TORIY, Moscow, Russia

Abstract

A standing wave electron linear accelerator with a variable energy of 6-11 MeV was designed. Electron energy is controlled by the injected current. A buncher was designed to provide capture above 70 % for the all injected currents range. The influence of using a permanent radially magnetized toroidal magnet

INTRODUCTION

Dual energy electron linacs with an energy range up to 11 MeV found their wide range of applications in cargo inspection systems [1] [2] and industrial applications such as sterilization systems [3].

Usually, a conventional particle accelerator system works in S or C-band frequency ranges, because the installation sizes allow designing one meter – scale accelerators for 10 MeV energy. X – band is required when the space of the installation is limited and low energy is required [4]. S-band linacs simplify the manufacturing process of the complicated geometry accelerating structures, also RPE TORIY [5] already in dispose of an S-band 2856 MHz klystron with 4-6 MW variable output power, thus 2856 MHz has been chosen as an operating frequency. For the conventional purposes of the linac, the beam power must be as high as possible with a limited input power, so we designed an efficient buncher and accelerating section to obtain the accelerator efficiency, which defines as P_{beam}/P_{in}, higher than 60% in 6-11 MeV energy range. Also, we studied the decreasing of the beam radius when permanent toroidal magnets are used as a focusing system.

BEAM DYNAMICS

Accelerator was designed to fit the requirements below:

- RF power: 5.5 MW klystron with 4-6 MW variable power at 2856 MHz;
- Injection: 30 kV with 0.3-0.8 A variable current;
- Length: less than 1.4 m;
- Beam energy: 6-11 MeV;
- Efficiency >60%;
- Beam radius to the drift tube radius ratio < 0.5

Electron beam emittances at the electron gun exit were calculated for the 0.3-0.8 A injected currents range and then used as input parameters to simulate beam dynamics in 3-cells buncher. Buncher cells lengths and accelerating fields amplitudes were optimized to obtain the capture coefficient > 70 %.

Gun

Electrons are injected into the accelerating section from the 3-electrode gun (Fig. 1) with the fixed 30 kV anode potential and variable controlling electrode potential (9.4-12 kV) [6]. By varying the controlling potential value one can change the injected current (Fig. 3a). For the different currents beam Twiss parameters [7] (Fig. 2) also are different (Fig. 3b).

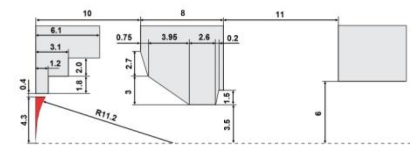

Figure 1: Electron trajectories in the gun at 0.5A current.

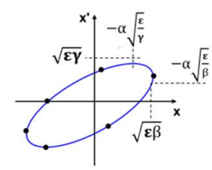

Figure 2: Twiss parameters to define a beam emittance.

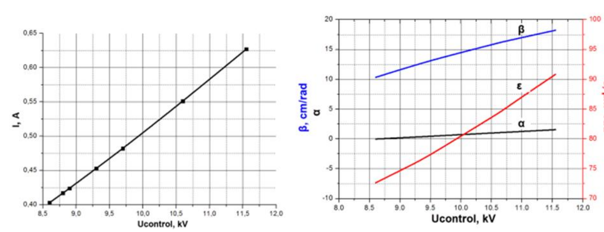

Figure 3: Electron current (a) and Twiss parameters (b) dependence in the gun from the control potential.

Buncher

Since the accelerator length is limited, standing wave is preferable because it allows getting higher energies than traveling wave structure on a shorter distance. We decided to use biperiodic structure (BPS) with inner coupling slots and nose cones [8] [9] because, even though the beam sees a π accelerating mode with a corresponding high shunt impedance (~80 MOhm/m), the RF structure itself operates at $\pi/2$ mode with a corresponding high coupling coefficient (~10%). Coupling coefficient basically describes the electric field distribution intolerance to the geometry change. Operating frequency is defined by the frequency of the klystron and is equal to 2856 MHz.

We optimized cells phase velocities and maximum electric field values on-axis (Table 1, Fig.4) both to obtain the capture >80% and energy spectrum less than 1 % after the 3rd cell with the 0.47 A injected current which corresponds

ISBN 978-3-95450-181-6

MATCHING THE PROTON BEAM BY MEANS OF INDEPENDENTLY PHASED BUNCHERS IN CYCLINAC CONCEPT

V.S. Dyubkov, S.M. Polozov, K.E. Pryanishnikov, National Research Nuclear University MEPhI, Moscow, Russia

Abstract

Nowadays a hadron therapy is one of the modern methods of a cancer treatment. For that purpose it is required that a proton beam, accelerated up to 250 MeV, penetrates on a depth about of 30 cm. It is known that linac, cyclotron and synchrotron can be used as a source of proton/ion beams. The main linac advantages are a high beam quality and a possibility of beam energy variation but, on the other hand, initial low-energy part of a linac is markedly expensive. Production of mentioned beams is possible on the base of a concept called CYCLINAC, when a commercial cyclotron is used as an injector, in which protons are accelerated up to 20-30MeV, for main linac. Matching the beam extracted from a cyclotron with a linac input is the main problem of this concept. It is caused by difference of operating frequencies of cyclotron and linear accelerator as well as a high phase size of a bunch from the cyclotron. It is proposed to use the system of independently phased bunchers for beam matching. The BEAMDULAC-CYCLINAC program is developed for simulation of the self-consistent dynamics of proton beams in a matching channel. Results of beam dynamics simulation for CYCLINAC will be presented and discussed.

INTRODUCTION

Due to the growth of cancer diseases it has recently become urgent task to develop effective methods of therapy with minimal side effects. Existing therapies such as surgery, chemotherapy, hyperthermia, radiotherapy is not completely effective in the treatment of deep-seated malignant tumours. With the development of technology accelerators, it became possible to create a complex proton and ion therapy. The expert community is actively discussing several options of implementing proton beam therapy systems. The main problem with these options is the choice of the initial part of such systems. In particular, in 1993, U. Amaldi proposed the concept of so-called CYCLINAC as the accelerator complex, in which the cyclotron used as injector in the linear accelerator [1]. Use of a PET-cyclotron for medical centres gives a significant economic effect. The most developed project concepts CYCLINAC are CABOTO [2], TULIP [3], ProTEC [4] and ProBE [5]. The main difficulty in the development of systems in accordance with the concept of CYCLINAC is the task of the transmission beam extracted from the cyclotron to the front-end of a linear accelerator, in view of the significant differences of operating frequencies of cyclotron and linac. In the present work it is compared two schemes of a beam transportation channel from the cyclotron on energy W to a linear proton accelerator energy of 250-300 MeV.

NUMERICAL SIMULATION RESULTS

At the beginning we consider a transportation channel based on three bunchers working at frequency 324 MHz that is in four times greater than cyclotron operation frequency. A schematic plot of the structure is shown in Fig. 1. It was assumed that particles continuously entered to transportation channel with average relative velocity equals to 0.248 and relative spread equals to 0.033. Beam current was presumed to be equal to 1 mA. The main transportation channel is presented in Table 1.

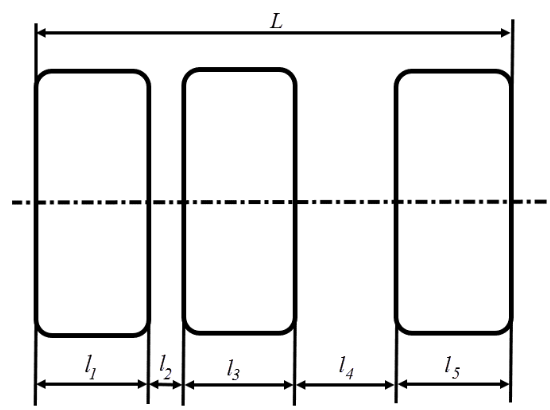

Figure 1: Layout of transportation channel.

Table 1: Main Channel Parameters

N	1	2	3	4	5
Length l, cm	34	1	16	31	16
E_{max}, kV/cm	170	–	175	–	170
Synchronous phase	π/2	–	π/5	–	π/5
Aperture, cm	5	5	5	5	5

It was obtained that the transmission coefficient was equal to 79.8% under bunch phase length equals to 2.43 (the physical length is about 6.5 cm). This bunch core conforms 70% of injected particles. Input (blue color) and output (red color) particle distributions in longitudinal phase space are presented in Fig. 2. Particle distributions in the transversal phase spaces are shown in Fig. 3 and Fig. 4. Particles spectra are shown in Fig. 5- 7. As one can see from Fig. 6 and Fig. 7 there is no significant beam envelope growth in channel without transversal focusing. In all mentioned figures blue objects are input and red are output. The above scheme allows one to decrease bunch phase width twice.

ISBN 978-3-95450-181-6

SUPERCONDUCTING STORED ENERGY RF LINAC AS FREE ELECTRON LASER DRIVER

V.G.Kurakin, P.V.Kurakin, Lebedev Physical Institute, Moscow, Russia

Abstract

Due to cavity losses in multi pass free electron laser (FEL), generation starts in it from definite threshold of driving electron beam current. Depending on generation wave range the threshold current strikes from fraction of ampere to dozens of amperes. In order to rich laser saturation, from hundreds to thousands electron bunches are required. Simple estimations give the value from units up to tens joules of bunches train energy in order to rich FEL saturation for infrared wave range (approximately 20 – 25 Mev of bunches energy and 3 A of pick current, bunch length being 1 cm). A beam with parameters mentioned might be obtained in rf superconducting linac operating in stored energy mode. The advantage of such approach is simplified linac power supply since dozens watts cw rf generator is required only to rich necessary accelerating voltage. At the same time the energy spread arising from beam loading may be compensated by additional cavities exited at shifted frequencies. In this paper Maxwell equations are used for beam-cavity interaction analysis. The bunch energy loss or the same the voltage induced by radiating bunch is expressed in terms of cavity external parameters. The detailed analysis of beam energy spread compensation is carried out followed by an example showing the reality of FEL schema suggested.

INTRODUCTION

Four decades of free electron lasers (FEL) development prove clearly their impressive and power status for human activity in scientific and other application. This is especially true for FELs in roentgen, ultraviolet and infrared range inaccessible for classical lasers. It is necessary to underline the main features of FELs – large power and tune ability – that are inherent to these devices due to physical mechanism of radiation generation. On the other hand FELs still are complicated and costly devises and for this reason not available for many research groups. There is no evident solution for accelerator scheme to match ridged parameters specification from light generation part and reduce simultaneously beam driver cost. Multi frequency superconducting linac that operates in stored energy mode [1] seems to be appropriate approach to drive FEL. This linac operation mode does not requires power rf source since dozens watts are necessary only in order to reach high gradient in multi cell superconducting cavity while the rf energy stored in the cavity (dozens joules) is quit sufficient to accelerate electron bunches train for laser excitation. It had been shown as well [1] that bunch train energy spread arising from beam loading might be compensated by additional cavities operating at slightly shifted frequencies.

Bunch energy and energy spread within individual bunches and in bunch train, bunch current and train length, undulator and laser cavity parameters – all these items are necessary to determine linac main parameters. For this reason we start from laser description, followed by appropriate formulae for linac parameters specification. Then appropriate formulae for bunch energy losses in cavity are derived based on solution of Maxwell equations and expressed over cavity external parameters. At last, multi frequency rf linac scheme with beam loading effect compensation is discussed followed by appropriate calculation.

FEL PARAMETERES SPECIFICATION

The processes in FEF are similar to those in traveling wave amplifier or rf linac. In latter devises electrons interact with longitudinal electric field of traveling electromagnetic wave and in the case of synchronism deliver part of their energy to field (amplifier) or take away it from a wave (accelerator). The difference is that in FEL electron interact with transverse electromagnetic wave with longitudinal electric field being equal to zero. The electrons must have transverse velocity in order to exchange their energy with the wave and for this reason a device that forces the beam to move in transverse direction – undulator - is necessary in beam environment. More over the synchronism and the energy exchange is effective when phase lag 2π between the electron and the wave takes place on one undulator period. Fig. 1 is a simple demonstration of the device just described.

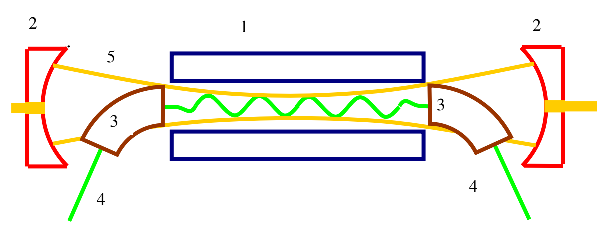

Figure 1: FEL layout. 1 – undulator, 2 – mirror, 3 – magnet, 4 – electron beam, 5 – optical mode envelope, 6 – laser radiation.

One pass of electron bunch in undulator area provides wave amplification. To transmit more energy to light train two mirror cavity is used. Twice reflected light bunch moves again in the same direction and acquires a portion of energy from new electron bunch entering the

ISBN 978-3-95450-181-6

INVESTIGATION OF A SECOND ORDER METHOD OF RFQ CHANNEL OPTIMIZATION

O.I. Drivotin*, D.A. Starikov,
St.-Petersburg State University, 7/9 Universitetskaya nab., St. Petersburg, 199034, Russia

Abstract

This report is devoted to a numerical method of solution of the RFQ structure optimization problem. The problem is considered as a control theory problem. Control functions representing geometry of the electrodes and a quality functional describing the beam are introduced. To solve the problem numerically these control functions are parametrized. The presented method is based on the computation of the derivatives of the first and the second order of the quality functional on the parameters. Results of investigation of efficiency of the method relatively to a method including computation of the derivatives only of the first order are presented.

INTRODUCTION

Methods of numerical optimization of accelerator structures were developed in the works of D.A. Ovsyannikov [1, 2, 3]. This theory was applied to the RFQ structure in the works [2, 4, 5, 6, 7, 8].

These methods have the first order, because the optimization process includes computation of derivatives of the first order of a functional describing beam quality over structure parameters. Application of these methods in practice requires a great amount of computations to achive acceptable results.

To reduce a number of computation, the method of the second order was proposed [9]. Here we present results of the second order method investigation, according to which number of computation during the process of optimization is reduced sufficiently.

FORMULATION OF THE PROBLEM

Consider a particles beam describing by the phase density [10, 11] $\varrho(x)$ defined on some surface S in the phase space $\Omega : x \in S \subset \Omega$. Coordinates on S can be taken as coordinates in the phase space. Let that at the initial instant t_0, the particle distribution density is given: $\varrho(t_0, x) = \varrho_{(0)}(x) = \varrho_{(0)\,1\ldots p}(x)\, dx^1 \wedge \ldots \wedge dx^p$, $x \in S_0 \subset \Omega$. At $t > t_0$, density $\varrho(x)$ can be found as the solution of the Vlasov equation [10, 11].

Let the trajectories of particles are described by the equation

$$\frac{dx}{dt} = f(t, x, u),$$

where $t \in T_0 = [t_0, T]$, $u \in U \subset R^r$ is a control function.

Also, introduce the following functional

$$\Phi(u) = \int\limits_S g(x_T)\varrho(T, x_T), \qquad (1)$$

where $g(x)$ is a piecewise continuous function. This functional characterizes quality of the beam at outlet of the accelerating channel. The problem of minimizing of functional (1) over control function $u \in U$ is called the terminal problem of charged particles beam control.

METHOD

Consider the equation for the first variation of x

$$\frac{d\delta x^i}{dt} = \frac{\partial f^i}{dx^j}\delta x^j + \delta_u f^i, \quad \delta x^i(t_0) = 0. \qquad (2)$$

Here and further, we apply the Einstein summation rule over repeated upper and low indices. The problem (2) has the following solution

$$\delta x^i(t) = \int\limits_{t_0}^{t} G^i_j(t, t')\delta_u f^j(t')dt',$$

where $G(t, t')$ is the Green matrix of the system (2), satisfying to the equation

$$\frac{dG^i_j(t, t')}{dt'} = G^i_k(t, t')\frac{\partial f^k}{\partial x^j},$$

and $G(t, t) = E$, where E is identity matrix.

Then variation of the functional (1) can be written as

$$\delta_u\Phi = \int\limits_{t_0}^{T}\int\limits_{\Omega} \frac{\partial g}{\partial x}G(T, t')\delta_u f(t, x)\varrho(t, x)\, dt. \qquad (3)$$

Consider the differential form

$$\psi(t, x) = -\left.\frac{\partial g}{\partial x}\right|_{x=x_T} G(T, t).$$

It satisfies the following equation and conditions

$$\frac{d\psi}{dt} = -\psi\frac{\partial f}{\partial x}, \qquad \psi(T) = -\left.\frac{\partial g}{\partial x}\right|_{x=x_T}.$$

Then expression (3) can be rewritten as follows

$$\delta_u\Phi = -\int\limits_{t_0}^{T}\int\limits_{\Omega}\psi(t, x)\delta_u f(t, x)\varrho(t, x)\, dt.$$

* o.drivotin@spbu.ru

ISBN 978-3-95450-181-6

A SIMPLE MODEL FOR ELECTROMAGNETIC FIELD IN RFQ CHANNEL

O.I. Drivotin*, I.T. Dulatov,
St.Petersburg State University, 7/9 Universitetskaya nab., St.Petersburg, 199034, Russia

Abstract

Numerical solution of the RFQ structure optimization problem requires a great amount of computation. Each consecutive step of the numerical optimization includes modification of geometry of the channel and computation of electromagnetic field for modified geometry. Therefore, a simple model describing the field in the channel is needed for the optimization. Such model is proposed in this report. It differs from the commonly used traditional model of the field, which can be applied when profiles of the vanes are described by the harmonic functions of the longitudinal coordinate. Our model is more general and can be applied for arbitrary profiles of the vanes.

INTRODUCTION

Professor D.A. Ovsyannikov proposed an approach which consists in the optimization of accelerator channel based on control theory methods [1-3]. During the optimization the functional characterizing the beam quality and the functional gradient of parameters describing the accelerator channel are computed. After that the parameters change according to the values of functional gradient components. Then iterations repeat until the appropriate structure is found.

Since the channel parameters are changing during the optimization process, the electromagnetic field in the accelerator channel is also changing. Optimization of the RFQ channel requires a great amount of computation [4-9]. Therefore, precise computation of electromagnetic field in the channel at each step of optimization means that optimization process is not executable for a real time. By this reason we should use simple models of electromagnetic field.

Most known model of the electromagnetic field in the RFQ channel was proposed by I.M. Kapchisky [10]. But it is applicable only for the case when the vane modulation is quasi-periodic. Within the framwork of this model the field is described by piecewise harmonic functions.

Here we propose a new simple model applicable in most general case. It allows to compute the electromagnetic field dynamically for each new channel configuration. This article presents the development and the investigation of this model.

* o.drivotin@spbu.ru

ELECTRIC FIELDS MODELS

Electric field potential u satisfies to the wave equation:

$$\frac{1}{c^2}\frac{\partial^2 u}{\partial t^2} - \Delta u = 0,$$

Here t is the time, c is the light velocity.

If electromagnetic oscillation frequency is not very great, the first term in this equation is small and can be neglected and we have quasi-stationary approximation:

$$\Delta u = 0. \tag{1}$$

Assume that on the vanes surfaces the following conditions holds:

$$u_\Gamma = \pm u_0 \cos \omega t. \tag{2}$$

Here $U_0 = V/2$, and V is amplitude of intervane voltage. Assume also that the vane surfaces are described by the equations

$$r^2 \cos 2\varphi = \mu(\pm 1 - \frac{4T}{\pi} I_0(kr) \sin \eta), \tag{3}$$

where $\eta(z) = \int\limits_{z_0}^{z} k(z')\,dz'$, $k(z)$ is function specifying dependency of the vane modulation along the longitudinal axis, I_0 is the modified Bessel function of the zeroth order. The interval where η is change from $(i-1)\pi$ to $i\pi$, $i = \overline{1, N}$, corresponds to one cell of the structure, and N is the total number of the cells.

Assume that $k(z)$ and $T(z)$ slowly change when z increases:

$$\frac{dk}{dz} \ll \frac{k(z_i)}{L_i} = \frac{k(z_i)^2}{\pi}.$$

Then length of the $i-$th cell is $L_i = \pi/k(z_i)$, where z_i can be any z inside the cell.

It is easy to see that the solution of the boundary problem (1), (2) is

$$u(r,\varphi,z) = -u_0(\frac{r^2 \cos 2\varphi}{\mu} + \frac{4T}{\pi} I_0(kr) \sin \eta) \cos \omega t.$$

Denote the channel aperture by a. It is minimal with respect to all cross-section of the cell distance from the axis to the nearest vane. From the equation (3) we have

$$a^2 = \mu(1 - \frac{4T}{\pi} I_0(ka)). \tag{4}$$

From (3) we have

$$a^2 = \mu(1 - \frac{4T}{\pi} I_0(ka)). \tag{5}$$

ISBN 978-3-95450-181-6

ACCELERATION OF DEUTERONS AND PROTONS IN SINGLE RFQ STRUCTURE

A.D .Ovsyannikov*, D.A. Ovsyannikov, Yu.A. Svistunov
Saint-Petersburg State University, Russia
A.P. Durkin, Moscow Radiotechnical Institute, Russia

Abstract

Some aspects of acceleration of protons and deuterons in single RFQ are considered. If effects of space charge are significantly hath nominal voltage for acceleration of deuterons can be too small to reach high efficiency of bunching and focusing of protons. It is shown that a raising of voltage up to nominal value for deuterons leads to increasing of capture and transmission for protons. Another problem is concerned with a choice of radial matching section parameters, which are optimal for both beams (proton and deuterons) simultaneously. Methods of optimization are discussed. Analysis of particles dynamics is illustrated by calculations results.

INTRODUCTION

Acceleration of ions with a different ratio of charge to mass e/m in a single channel is possible if two conditions are fulfilled:

1. longitudinal velocities at input of channel are equal for all beams,
2. for every type of ions voltage U is chosen to keep the relation eU/m is constant,
3. in case acceleration more then two types of ion with different A/Z in single RFQ one must have possibility to change intervene voltage in required diapason

$$\frac{eU}{m} = \frac{e_{nom}U_{nom}}{m_{nom}},$$

index "nom"means nominal parameters of ion, which were used in calculation of cell lengths.

So if a ratio e/m of some ion is more, than a nominal one we can use reduced voltage to copy beam dynamic when a space charge force is negligible. In our case we need to reduce voltage by one half.

However in opposite case when space charge influence is not negligible decreasing of voltage leads to weakening of external phasing and focusing forces which can compare with coulomb ones and decrease beam transmission and capture as result. On the other hand we have a reserve for doubling of voltage. So we need to estimate how we can use this reserve.

* E-mail: a.ovsyannikov@spbu.ru

CURRENT DEPENDENCE

Let consider transverse motion. Increasing voltage we move a working point on stability diagram up to its middle. Usually focusing factor is chosen as about half of value corresponding to a middle of stability interval.

In a longitudinal motion we have two opposing tendencies which counteract each other. On the one hand increasing of voltage leads to extension of separatrix for every accelerating period. On other hand a synchronization of acceleration is destroyed because we lose synchronous particle which gains given energy and phase passing the cell and which is a single center of longitudinal oscillations inside of beam. Now for every accelerating period there is its own particle, so we have additional coherent oscillation of beam inside separatrix.

As an example we used RFQ channel from the paper [1]. The main parameters of accelerator are shown in the table 1. The results are sufficient to allow conclusion: extension of separatrix is more significantly than additional coherent oscillation, transmission and capture are increased and particles does not leave separatrix. Nominal synchronous phase is changing as a smooth curve from -90 to -30 degrees. So, double voltage gives increasing of synchronous phase from -90 to -64 degrees only. As a result, current of accelerated beam depending of voltage and input current is illustrated on picture 1.

Results of these researches proves possibility of simultaneous acceleration of different types of ion with a wide spectrum of ratio e/m and with given input velocity.

Table 1: Example of RFQ Parameters

Parameters	Value
RFQ frequency (MHz)	432
Vane length (m)	6.5
Average channel radius(mm)	1.8
Vane voltage (kV)	50, 25
Injection energy of H-ions beam (KeV)	25
Injection energy of D-ions beam (KeV)	50
Initial dP/P	0
Final energy of H-ions beam (MeV)	2.5
Final energy of D-ions beam (MeV)	5
RMS emittance (cm · rad)	0.05

OPTIMIZATION PROBLEM

In general case when phase volumes of H and D beams have different orientation in phase planes xx'and yy'one

ISBN 978-3-95450-181-6

BEAM SIMULATION AND MEASUREMENTS AT BEAM LINE TO RADEX EXPERIMENTAL AREA OF INR LINAC

V.Aseev, S.Bragin, S.Gavrilov, P.Reinhardt-Nickoulin, O.Volodkevich

Institute for Nuclear Research of RAS, Moscow, Russia

Abstract

In 2015 the Experimental Complex beam lines of INR linac were upgraded. There is a need to study beam dynamics in these lines. The results of beam simulation at beam line to RADEX experimental area and comparison with beam measurements are presented.

INTRODUCTION

INR linear accelerator is a high-current proton beam source for researches on nuclear physics and applied researches. The Experimental Complex is the main experimental area of INR linac. The facility of Experimental Complex consists of the beam lines, the multipurpose Neutron Complex and complex of proton therapy. The Neutron Complex includes in turn: 1) the beam dump RADiation EXperiment (RADEX) facility, together with time-of-flight spectrometer; 2) the Pulsed neutron source; 3) the Lead slowing-down spectrometer.

RADEX INSTALLATION

RADEX installation makes it possible to generate high-intensity neutron fluxes in the target by high-current proton beams. It gives unique opportunities for nuclear materials testing under irradiation. For instance the radiation tests of fusion reactor candidate materials for first wall can be carried out in conditions close to the expected in reality. The installation has a vertical irradiation channel inside the beam stop for horizontally incident protons with energies up to 209 Mev. The researches in the field of neutron-nuclear interactions using the time-of-flight technique in special channels are also carried out at RADEX.

When working with a RADEX installation last time in April, 2016 the beam parameters were as follows: beam energy 209 MeV, pulse current 10 mA, pulse duration 0.3÷115 μs at pulse repetition rate 50 Hz.

The operation modes of Experimental Complex beam lines for different beam parameters are well studied [1]. But in 2015 beam lines were upgraded: re-aligning of beam line elements relative to beam axis was carried out and some new power supplies for quadrupoles were implemented. Therefore, there is a need to study beam dynamics in the new magnetic lattice of the channel to RADEX experimental area additionally.

BEAM MEASUREMENTS UPSTREAM THE EXPERIMENTAL COMPLEX

To study beam dynamics in the channel to RADEX installation it is necessary to determine correctly transverse beam parameters at its input. The measuring area at the linac exit (upstream the beam line to RADEX) is shown in Fig. 1. The following equipment is displayed at this area: 1) 8 quadrupole magnetic doublets D106÷D113 supplied from a common current source; 2) 4 quadrupole magnetic doublets D114÷D117 supplied from different current sources; 3) 3 wire scanners WS1÷WS3; 4) beam cross section monitor (BCSM).

BCSM is developed to provide non-intercepting measurements of beam parameters. Monitor operation is based on utilization of residual gas ionization. BCSM enables to observe proton distribution in beam cross section (Fig. 2) during adjustment and operation of the linac. The transverse beam profiles can be obtained from beam cross section too [2].

Wire scanners are used for transverse beam profile measurements [3]. The measurements by wire scanners may be carried out only at 1 Hz pulse repetition rate to avoid excessive equipment activation and damage of accelerator components due to their overheating in the point of significant beam losses.

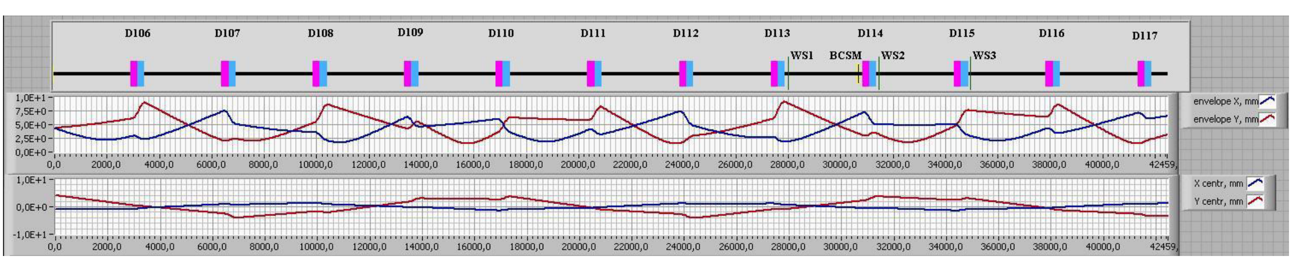

Figure 1: The accelerator area upstream the Experimental Complex beam line and beam tracing across it. D - quadrupole magnetic doublets; WS – wire scanners; BCSM – beam cross section monitor.

ISBN 978-3-95450-181-6

EXPERIMENTAL FACILITY FOR E-BEAM IRRADIATION TEST OF PROTOTYPE IF TARGET IN RISP

K.V. Gubin, ILP SB RAS, Novosibirsk, Russia
I.K. Chakin, S.N. Fadeev, M.G. Golkovskiy, Yu.I. Maltseva, P.V. Martyshkin, BINP, Novosibirsk, Russia
J.-W. Kim, J.Y. Kim, Y.-H. Park, IBS, Daejeon, Korea

Abstract

Nowadays project RISP is developed in IBS, Daejeon. One of the main project device is graphite target system for production of rare isotopes by means of the in-flight fragmentation (IF) technique. The power inside the target system deposited by the primary beam with energy of 200 MeV/u is estimated to be around 100 kW. The target represents rotating multi-slice graphite disc cooled by thermal radiation. Necessary step of the target development is integrated test of target prototype under high power electron beam modelling real energy deposit into target. This test is planned to be held in BINP, Novosibirsk, with the use of ELV-6 accelerator.

This paper presents the design of experimental facility as well as experimental program of test. Specifications of electron beam (energy close to 800 keV, size ~ 1mm, total power 30-40 kW) are discussed. Parameters and design of basic devices and systems of facility are described.

INTRODUCTION

At the present time in IBS (Institute of Basic Since, Daejeon, Korea) the RISP (Rare Isotope Science Project) is carried out [1,2]. Project purposes are production and investigation of new isotopes of chemical elements for fundamental research. In RISP, in particular, the In Flight (IF) fragmentation method of isotope production, wherein the heavy-ion beam energy is up to 200 MeV/u and diameter is ~1 mm cracks on the solid-state target (stripper), is realized [3]. IF target represented the rotating multi-layer thin graphite disk in vacuum with cooling by its own thermal radiation [4]. Its peculiarity is high working temperature (up to 1900 °C) and temperature gradient.

Presented paper describes planned testing of multi-layer target prototype under the high-power in vacuum.

EXPERIMENTAL PROGRAM

Goal of prototype testing is experimental check of general parts of IF target under conditions as close as possible to the operational ones. Test of prototype is envisaged to clarify a series of technical and physical problems which arise designing the target, including:

- to clear up the possibility of multi-layer target construction to dissipate the beam power, its resistance to thermal and mechanical stress;
- to test the cooling panels aimed to accept and remove the heat power, heat transfer balance;
- to check up the calculations of prototype operation conditions, in particular, the temperature fields of front and rear target layers;
- to test the control, measurement and protection methods proposed for the target subsystems design.

Heavy-ion beam will be modelled by the e^- beam of ELV-6 accelerator [5-6] with diameter down to ~1 mm, energy 800 keV (minimum possible) and power up to 40 kW. Maximum beam power will be limited by the graphite beam dump ability to utilize the e^- beam energy deposit [7].

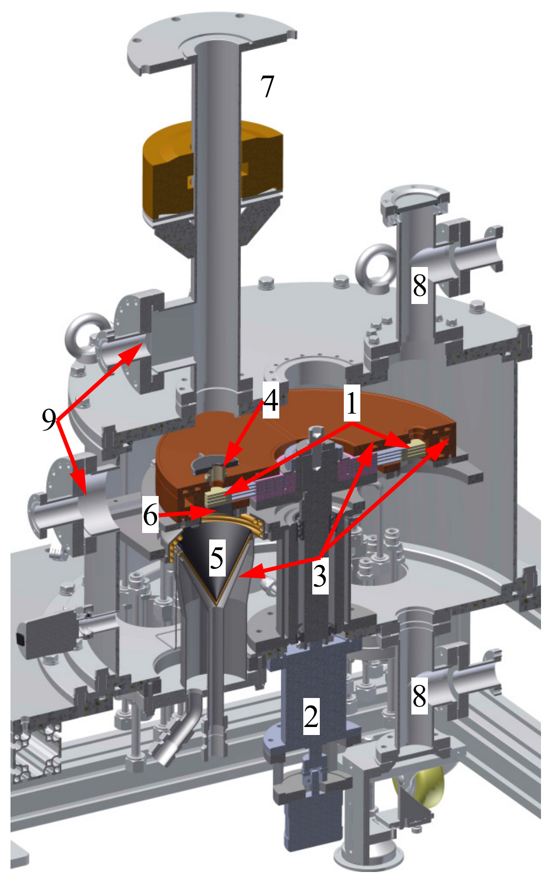

Figure 1: Experimental device. 1 – rotating target, 2 – rotary motion unit, 3 – cooling panels, 4 – protective diaphragm, 5 – graphite cone beam dump, 6 – protective graphite blanket, 7 – telescopic connecting tube to accelerator with beam control magnetic elements, 8 – optical ports, 9 – beam measurement plate ports.

ISBN 978-3-95450-181-6

UPGRADE OF THE RF SYSTEM ON THE LUE-200

K.I. Mihailov, E.A. Golubkov, V.V. Kobets, A.N. Repkin, A.P. Sumbaev, JINR, Dubna, Moscow region, Russia
V.N. Pavlov, BINP SB RAS, Novosibirsk

Abstract

In the report works on upgrade of RF system of the LUE-200 (IREN) electron linac are provided. The main attention is paid to system of preliminary excitement of klystrons. After work on installation of the second accelerating section RF system of Installation it was considerably remade that allowed to carry out start-up of the second stage of the IREN installation successfully. Methods, features and problems in case of a training of two accelerating sections are discussed. Influence of the temperature and frequency modes on joint operation of accelerating sections. Results of setup of the RF system and a training of sections, and also results of posting of a bunch are given.

INTRODUCTION

Created at the Laboratory of Neutron Physics, JINR linac LUE-200 electron on the particle energy of 200 MeV for resonance neutron source (IREN) [1,2] it is based on the best world achievements in the field of accelerator technology. The pace set energy of the particles in the LUE must be 35 MeV / m, the pulse repetition frequency - 150 Hz.

The project was implemented in two stages. First it was installed and launched the first stage of the accelerator, consisting of one section of the accelerating energy of 100 MeV. Currently it implemented the second stage of the accelerator - produced by the installation of the second accelerating section and the physical start-up of accelerator. The report presents the results of the physical start-up accelerator LUE-200 of IREN.

RF SYSTEM OF THE LUE-200

Scheme of the RF system of the accelerator LUE-200 is shown in Fig. 1. The main components of the system are: two-channel sets the high-frequency generator with the ability to shift the phase of the oscillation between the channels in the 360^0 revolution and the rapid phase of both channels simultaneously vibrations 180^0, two pulse amplifier RF power for driving high-power klystron, two multiplying power system supply waveguide path RF power to the accelerating section and grouper from the powerful klystron, a directional coupler, power regulator, shifter and measuring directional couplers.

Continuous RF signal power up to 10 mW and a frequency of 2856 MHz master oscillator to the input pulse pre-amplifier driving the first and second klystron over coaxial feeders. The required phase shift between the excitation signals is carried out phase shifter.

The output klystron RF oscillation power up to 50 MW in the first pulse klystron and up to 20 MW of output from the second klystron in a rectangular waveguide evacuated arrive at 3 dB bridges. The two arms of each bridge are located high-Q resonators cumulative power of multiplication (SLED), and the fourth arm of the bridge through the waveguide and the wave type transformer is connected to the input of the accelerating section. Increasing the pulse power supplied to accelerator sections is carried out by accumulating energy in the resonator with its subsequent reradiation in going to the waveguide section when turned phase signal supplied to the resonators 180^0. Required for this switching phase of the RF oscillations carries excitation system and synchronization of the klystron at a low level RF power.

Before entering the accelerating section of the waveguide directional couplers installed H01 and H02, which signals are used to control the incident and reflected waves. Signal attenuation in the taps is about 60 dB. The output of accelerating sections unused portion of the RF power supplied to the load. Between loads and output sections mounted directional couplers (similar H01 and H02). Waveguides made of rectangular cross-section waveguides evacuated 72X34 mm. Pumping waveguides made by ion pumps in the output window of klystron and 3 dB bridges.

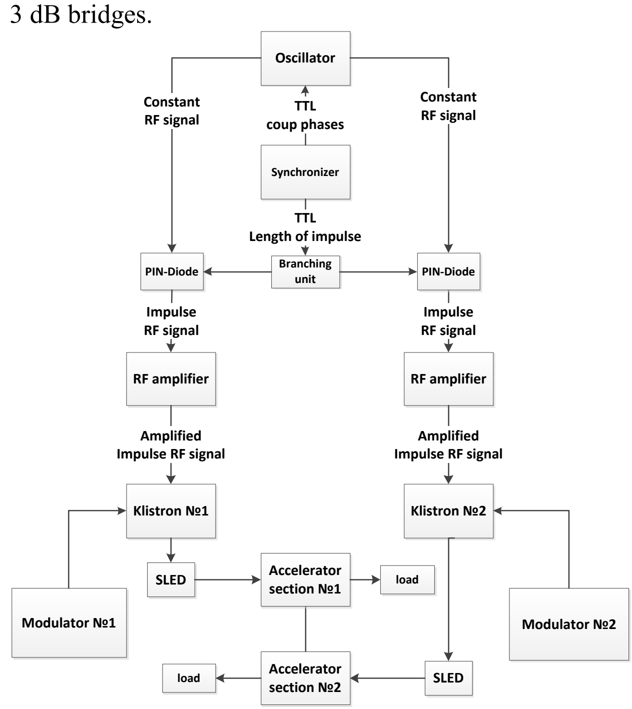

Figure 1: Scheme of the RF system of the IREN facility.

ISBN 978-3-95450-181-6

INSTALLATION FOR THE RESEARCH OF Z-PINCH PLASMA INITIATED BY THE ELECTRON BEAM

A. Drozdovsky, A. Bogdanov, S. Drozdovsky, R. Gavrilin, A. Kantsirev, V. Panyushkin, I. Roudskoy, P. Sasorov, S. Savin, V. Yanenko, SSC RF Institute of theoretical and experimental physics, Moscow, Russia

Abstract

For researches on plasma physics has been designed and constructed the electronic gun with the cold cathode on energy to 300 кэВ. The gun have the parameters: time width of pulses -100 ns, current amplitude - 100 A. The adiabatic plasma lens is developed for transportation and compression of the received electron beam. Results of researches are presented.

INTRODUCTION

At the present time, active works are underway for creating compact laser (electron and proton) accelerators [1]. For them, it is timely to solve problems of transportation and focusing of beams in discharges of the Z-pinch type, and it requires a thorough study of methods for forming such discharges. The goal of this work is to create a test installation for studying the dynamics of Z-pinch plasma with the discharge initiation by an electron beam. Typically, the discharge process begins after the high-voltage supply to the discharge tube, with the breakdown over the tube surface. It is also of interest to study the pinch development for the case when a breakdown is induced directly by an electron beam injected at the time of the application of high voltage.

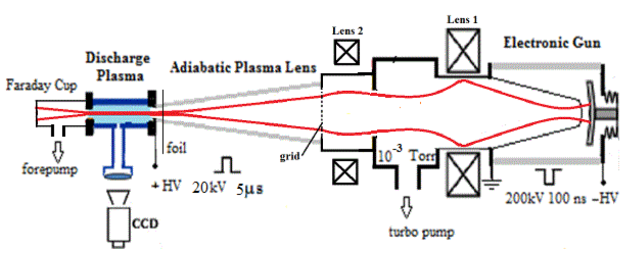

Figure 1: Installation for the research of z-pinch plasma initiated by the electron beam

THE INSTALLATION

The installation (fig. 1) consists of the electron gun [2] with magnetic lenses, experimental chamber with the scintillators located in it. Vacuum pumping of an electronic gun is conducted by the turbomolecular pump, and of plasma part of installation - the roughing-down pump. The electron beam is injected through the dividing foil into the experimental channel at a pressure of ~1 mbar. Inside the channel, the beam is compressed in the adiabatic plasma lens and then injected into the chamber of Z-pinch formation. For creation of the accelerating voltage was accepted the scheme of the generator on cable lines with use of the double forming line of Blumlein and the cable transformer of Lewis. Figure 2 shows oscillograms of the beam current and the voltage obtained on the Blumlein line with the 25 kV amplitude. The amplitude of beam current is 50 A and duration of the beam at the peak is 60 ns.

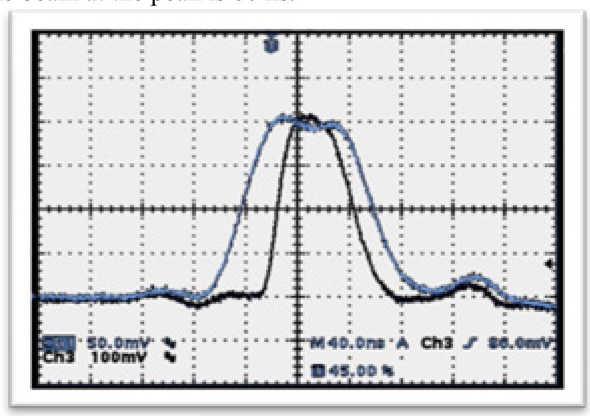

Figure 2: The electron beam current (black curve) and DFL voltage pulse signals.

Fig. 3 represents simulation results of the electron beam propagation from cathode to adiabatic plasma lens (APL). Emission current of 100 A and 50 mm cathode-anode gap under voltage of 250 kV were assumed during calculation. The simulation was performed using numerical code PICSIS-2D [3] based on use of Vlasov-Maxwell equations system with calculation of collisions of particles by Monte-Carlo method. The program enables to calculate a transportation of relativistic charged particles in arbitrary 2D electromagnetic fields taking into account its space charge and self-magnetic field.

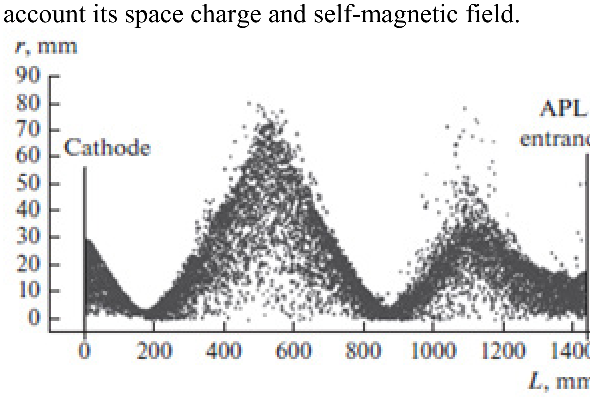

Figure 3. Calculation results of beam propagation. Concentration of dots is the product of the beam density n(r) and the coordinate r.

* Work supported by the Russian Foundation for Basic Research (grant № 16-02-01158/16)

ISBN 978-3-95450-181-6

ON STABILIZATION OF SYSTEMS OF LINEAR EQUATIONS WITH LINEAR INCREASING TIME DELAY BY OBSERVATION

O.N. Chizhova, A.P. Zhabko, Saint Petersburg State University, Saint Petersburg, Russia

Abstract

In this paper we investigate a possibility of the linear differential system stabilization with time proportional delay by the linear observation. Using the sufficient conditions of asymptotic stability for the linear systems with linearly increasing delay we obtain some conditions of the asymptotic evaluation system existence for the original system. Then we use the asymptotic evaluation system for the construction of the stabilizing control and derive the sufficient conditions for the existence of such control.

INTRODUCTION

Differential-difference equations with time delay are often used in mathematical models describing the dynamics of beams of the charged particles. For example linear equation of the second order with a constant time delay describes in the smoothed approach dynamics of a beam of the charged particles in synchrotrons with a feedback system [1]. However the time delay cannot always be considered constant. The time proportional delay can occur at acceleration of beams of the charged particles in the cyclotron. It should be noted that linear increasing time delay is unbounded and well known approaches are not applicable for stability analysis such systems.

The stabilizing control for the system of linear equations could be constructed by the information on a state vector of the system. Sometimes the state vector is unknown but we know some linear combinations of its components. Then there is a problem on construction of the stabilizing control with incomplete information.

Let us consider the following linear system

$$\dot{x} = A_0 x(t) + A_1 x(\alpha t) + Bu \qquad (1)$$

$$y = Kx(t). \qquad (2)$$

Here x is n-dimensional state vector; u is r-dimensional control vector; y is scalar output; A_0, A_1, B, K are given real matrices $n \times n$; $n \times r$ and $1 \times n$; $0 < \alpha < 1$. We must construct the control $u = u\big(x(t); x(\alpha t)\big)$ using output (2).

One of the basic methods of solving such problem is the construction of the asymptotic evaluation system [2]. Some sufficient conditions of existence of this system for n scalar outputs $y_i = Rx(t - ih); i = 1; \ldots; n$ are presented in [3].

The aim of this paper is to obtain the conditions for the matrices A_0, A_1, B, K under which the stabilizing control may be constructed by output (2). The main results of the paper are construction of the asymptotic evaluation system using the output (2) and construction of the stabilizing control for the system (1).

The paper is organized as follows. The next section contains the investigation of an auxiliary system of linear differential equations. The structure of the asymptotic evaluation system for system (1) is deduced in this section. The main result is presented in section 3. A theorem about the sufficient conditions for existence of the stabilizing control is proved here. Section 4 contains a numerical example on construction of the stabilizing control.

AUXILIARY RESULT

Definition [2]. A system

$$\dot{\hat{x}} = A\hat{x} + Bu + L(y - K\hat{x})$$

is known as asymptotic evaluation system of a system without time delay

$$\dot{x} = Ax + Bu$$
$$y = Kx$$

if matrix L can be chosen such that for any $x(0); \hat{x}(0)$ the following condition is satisfied:

$$\hat{x}(t) - x(t) \to 0 \quad \text{as} \quad t \to +\infty. \qquad (3)$$

We consider a time delay system of the form

$$\begin{aligned}\dot{\hat{x}} &= A_0\hat{x}(t) + A_1\hat{x}(\alpha t) + Bu + L_0\big(y - K\hat{x}(t)\big)\\ &+ L_1\big(y(\alpha t) - K\hat{x}(\alpha t)\big)\end{aligned} \qquad (4)$$

Here $L_0; L_1$ are unknown constant real vectors. Now we introduce two matrices:

$S_0 = \Big(K^T; A_0^T K^T; \ldots; \big(A_0^T\big)^{n-1} K^T\Big)$ and

$S_1 = \Big(K^T; A_1^T K^T; \ldots; \big(A_1^T\big)^{n-1} K^T\Big)$.

Theorem 1. If $rang S_0 = rang S_1 = n$ then vectors L_0 and L_1 of system (4) can be chosen so that condition (3) satisfied for any $x(0), \hat{x}(0)$.

Proof. Let $z(t) = \hat{x}(t) - x(t)$ where $x(t)$ is a solution of the system (1) and $\hat{x}(t)$ is a solution of the system (4). Then

ISBN 978-3-95450-181-6

FIRST RESULTS OF BEAM DYNAMICS SIMULATION IN ELECTRON INJECTOR LINAC FOR FCC-EE

S.M. Polozov, T.V. Bondarenko,
National Research Nuclear University - Moscow Engineering Physics Institute, Moscow, Russia

Abstract

New high-energy frontier project FCC is now under development at CERN. It is planed that all three modes as ee, hh and eh will be available for FCC. New injection system for FCC-ee is planned to consist of new ~ 2 GeV electron linac and electron-positron converter. Two possible layouts for further beam acceleration are discussed. The high-energy 14 GeV linac is the first layout and the booster synchrotron is the second one. Pre-injector linac design will have two regimes: ~250 pC bunches for injection and ~6 nC bunches for e^-/e^+ conversion. In the second case we will have extreme parameters: bunch charge up to 6 nC in 10 ps, up to 10 bunches per pulse and the pulse repetition rate up to 100 Hz. Such beam parameters lead to significant design difficulties caused by very high influence of Coulomb field in the near-cathode region and high peak beam loading. First results of beam dynamics simulation in FCC-ee injection linac and near-cathode dynamics problems are discussed in the report.

INTRODUCTION

New injection system for FCC-ee [1] is now under discussion by FCC collaboration [2-3]. A number of different injection schemes are discussed: linac (from 2 to 7 GeV) with booster synchrotron, high energy linac (up to 14 GeV) and reacceleration in main collider ring, top-up injection. It is obvious that linac should include the first stage (about 2 GeV) and the electron-positron converter with damping ring to generate the necessary positron flux. Beam intensities for two regimes (electron beam acceleration for injection and for e^-/e^+ conversion) will differ very significantly: it is necessary to have up to $1.65\cdot10^9$ e^-/bunch (~250 pC) for injection mode [2-3] and up to $4\cdot10^{10}$ e^-/bunch (~6 nC) for e^-/e^+ conversion mode; 10 ps bunch duration is the same for both cases. It is planned to have 10 bunches/pulse with distance between bunches of 25 or 50 ns. The pulse repetition rate will be up to 50 Hz. The separated bunches regime facilitates RF system design and operation because of low beam loading influence compared to the bucket of bunches mode. Note that 6 nC regime is very complex and limited number of linacs are operating with such currents.

The general scheme of the CLIC linac or the new SuperKEKB injector linac [4] could be proposed to use as the base of FCC injector. New SuperKEKB injector consists of the modern RF gun commissioned in 2013-14 and traveling wave regular sections. It is very interesting idea to combine thermionic RF gun for high-intensity high-emittance drive bunch for 5 nC mode and high-quality beam generated by photogun for injection into synchrotron.

The choice of operating frequency is very important too. It is proposed to use 2000 MHz structures which will have higher acceptance compared to conventional 3000 MHz band. Two notes should be done here: i) exactly 2000 or 3000 MHz structure can give 25 (or 50) ps of bunch separation (conventional 2856 MHz can not) and ii) there are no high-power RF sources for 2000 MHz (but they are available for 1816 and 1860 MHz and can be scaled). It is important because 10 bunches/pulse regime is planned. Current pulse duration will be 250 or 500 ns, SLED or other RF pulse compression scheme can be used to reduce necessary peak RF power and RF feeding system cost. Low average pulse current (but peak is very high) give us possibility to use a standing wave structure (biperiodic accelerating structure BAS, or side-coupled one), but it should have very high coupling coefficient (10-12 %) to realize low power filling time.

Two possible layouts of linac are presented in Fig. 1. Let us discuss first results of the beam dynamics simulation and RF gun and regular section electrodynamics study.

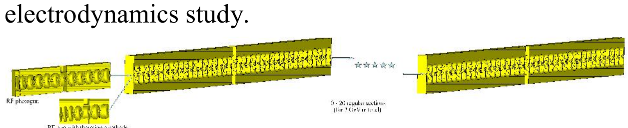

Figure 1: Two possible schemes of linac layout (RF gun with thermionic cathode is option for high intensity drive bunches production for e^-/e^+ conversion).

BEAM DYNAMICS IN PHOTOGUN

The beam dynamics simulation was done both for RF gun and regular section. The BEAMDULAC-BL code [5-7] was used for simulations. This code was developed in MEPhI for beam dynamics simulations in RF linacs and transport channels. It has modular structure and number of routines to solve different tasks: initial particles distribution (uniform, Gauss, KV, waterbag, etc.), motion equation integration (4^{th} order Runge-Kutta method), beam emittance calculation, post processing and other. The code package has versions that take into account own space charge effects: both Coulomb part and RF part (beam irradiation and beam loading) self-consistently. The excitation equation is solved to simulate RF part of own space charge field using the method of large particles. The Poisson equation is solved on grid by fast Fourier transform (FFT) method and well-known cloud-in-cell (CIC) algorithm is used to represent particles distribution on 3D grid. The BEAMDULAC-BL code

ISBN 978-3-95450-181-6

BEAM DYNAMICS STUDY FOR THE NEW CW RFQ

Sergey Polozov[1,2], Winfried Barth[1,3,4], Florian Dziuba[4],
Timur Kulevoy[1,2] , Stepan Yaramyshev[1,3], Yury Lozeev[1]
[1] National Research Nuclear University - Moscow Engineering Physics Institute, Moscow, Russia
[2] Institute for Theoretical and Experimental Physics of NRC Kurchatov Institute, Moscow, Russia
[3] GSI Helmholtzzentrum fur Schwerionenforschung, Darmstadt, Germany
[4] Helmholtz-Institut Mainz, Germany

Abstract

A compact "university scale" research CW proton accelerator, as well as driver linac with three branches of experimental beam lines, delivering beam energy of 2, 10 and 30 MeV for dedicated experiments, are recently under development in Russia. A proposed front-end system of both linacs comprises a 2 MeV CW RFQ, which is foreseen to bunch and accelerate up to 10 mA proton beam. The RFQ design is presented. The beam dynamics simulation results, obtained by means of different software, are discussed and compared.

INTRODUCTION

The development of a CW high-power proton linacs is a very actual aim of crucial accelerator technology. Such linac is useful for large scale research complexes as spallation neutron sources or accelerator driven systems. Low or medium-energy linacs can be used for several applications as boron-neutron capture therapy (BNCT), high productivity isotopes generation and material science. Also compact research facilities are the modern trend for high intensity CW proton and deuteron linac development [1,2].

The Russian accelerator-driver concept has been already developed by the collaboration of researchers from MEPhI and ITEP of NRC Kurchatov Institute [3-6]. The proposed linac layout is close to the conventional scheme: an RFQ and a normal conducting DTL with transverse focusing by integrated RF sections up to 30 MeV. The independently phased SC cavities are foreseen for medium and high beam energies. Three branches of experimental beam lines, delivering a beam energy of 2, 10 and 30 MeV for dedicated experiments, are foreseen as the main feature of the proposed facility concept [7,8].

Research and development of CW applications is an important step in RFQ design. A 2 MeV RFQ is under investigation for the compact CW research proton accelerator, as well as for the planned driver linac in Russia. The maximum beam current is fixed to 10 mA; the operating frequency has been set to 162 MHz; the RF potential should be limited by 1.3-1.5 of Kilpatrick criterion for the CW mode. The main RFQ parameters are shown in Tab.1.

The beam dynamics simulations for the new RFQ channel, as well as an analysis of the RFQ characteristics, have been performed with the codes BEAMDULAC [9] and DYNAMION [10], providing for a cross-check of the design features and the calculated results. The first results of the beam dynamics simulations have been briefly discussed in [12].

* SMPolozov@mephi.ru

Table 1. Main Parameters of the CW RFQ

Ions	protons
Input energy	46 keV
Output energy	2.0 MeV
Frequency	162 MHz
Voltage	90 kV
Length	345 cm
Average radius	0.530 cm
Vanes half-width	0.412 cm
Modulation	1.000 - 2.250
Synchr. phase	-90° - -33°
Max. input beam current	10 mA
Max. input beam emittance	6 cm·mrad (total)
Particle transmission	> 99%

A preliminary design of a CW RFQ linac has been already started at MEPhI and ITEP [11,12]. The recent detailed layout of the presented 2 MeV CW RFQ is based on a preliminary concept, exploiting long-term experience for proton and heavy ion linac development at MEPhI and ITEP [13,14], as well as decades of GSI expertise in construction, optimization and routine operation of ion linac facilities [15-21]. Most recently, the prototype for a heavy ion CW linac with a SC main part is under construction at GSI and HIM [22-26].

ANALYSIS OF RFQ CHARACTERISTICS

The maximum electrical field strength on the vane surface along the channel strongly influences on all RFQ parameters. For the presented CW RFQ design the field strength $\boldsymbol{E_{max}}$ has been limited by the 1.5 Kilpatrick criterion.

The average radius $\boldsymbol{R_0}$ = 0.530 cm and the vanes half-width/rounding $\boldsymbol{R_e}$ = 0.412 cm have been defined together with the RFQ voltage of 90 kV. The Kilpatrick criterion $\boldsymbol{E_{kp}}$ = 148 kV/cm for the given operating frequency of 162 MHz has been calculated using modified Kilpatrick equation:

$$R_0 E_{kp}^3 \cdot \left(1 - \exp\left(-\frac{48.6 E_{kp}}{R_0 f^2}\right)\right) = 1.8 \cdot 10^5 \cdot \exp\left(\frac{170}{E_{kp}}\right)$$

with average radius $\boldsymbol{R_0}$ given in cm, frequency $\boldsymbol{f}$ in MHz and the Kilpatrick criterion $\boldsymbol{E_{\kappa p}}$ in kV/cm [27].

ISBN 978-3-95450-181-6

THE STUDY OF THE HELICAL RF RESONATOR FOR THE 300 keV NITROGEN ION CW IMPLANTER

N.V. Avreline, TRIUMF, Vancouver, B.C., Canada
S.M. Polozov, A.G. Ponomarenko, National Research Nuclear University -Moscow Engineering Physics Institute, Moscow, Russia

Abstract

The helical RF resonator for the single charged 300 keV nitrogen ion CW implanter was designed, simulated in CST Microwave Studio and the results were experimentally verified. The current setup of the implanter is described as well as possible modifications to accelerate ions of other types. The results of the field distribution's RF measurements and the results of the high-power test are also presented.

INTRODUCTION

The implanter RF system consists of the helical type accelerating resonator that is loaded by the channel of drift tubes, the Duoplasmatron source of nitrogen single charged ions with 25 keV of energy, the mechanical backing pump, the turbomolecular vacuum pump TMN-500, the ion pump Nord-250, 3 kW CW RF amplifier, the control cabinet with power supplies and the turning magnet that is used to analyze the resulting beam (Fig. 1). This implanter was primarily designed to accelerate CW beam up to 100 μA. It could accelerate ions with other charge-to-mass ratio after changing the helical inductor.

Figure 1: The 300 keV Implanter of single charged nitrogen ions.

THE DESIGN OF THE RF RESONATOR

Given a rather low operating frequency of 13.56 MHz, in the efforts to reduce the size of an accelerating structure, the resonator of a helical type loaded by an accelerating channel was selected in the design. The accelerating channel is composed of 10 drift tubes and is operating in π mode. These tubes are connected to the two longitudinal bars that are connected respectively to the ends of the half-wave length helical elements of the resonator. The main advantage of using this accelerating resonator in this implanter is that just the accelerating channel is in the vacuum chamber, but not helical inductor. This kind of a design allows to change the inductance by just replacing the helical part without opening the vacuum chamber. Specifically, the frequency of the resonator could be modified and the implanter could be used to accelerate different kinds of ions. The photo of the open resonator is presented in Fig. 2. To tune the resonance frequency of this resonator, two plates were used to shorten the windings.

Figure 2: The opened resonator with the replaceable helical part that is connected to the accelerating channel via a feedthrough.

ISBN 978-3-95450-181-6

QWR RESONATOR CAVITIES ELECTRODYNAMICS SIMULATIONS FOR NEW NUCLOTRON-NICA INJECTOR

A.V. Butenko, Joint Institute for Nuclear Research, Dubna, Moscow Region, Russia
M.A. Gusarova, M.V. Lalayan, N.P. Sobenin, D.V. Surkov, S.A. Terekhov, S.E. Toporkov, National Research Nuclear University – Moscow Engineering Physics Institute, Moscow, Russia
T.V. Kulevoy, S.M. Polozov, National Research Nuclear University – Moscow Engineering Physics Institute, Moscow, Russia and Institute of Theoretical and Experimental Physics of NRC "Kurchatov Institute", Moscow, Russia
A.O. Sidorin, G.V. Trubnikov, Joint Institute for Nuclear Research, Dubna, Moscow Region, Russia and Saint-Petersburg State University, Saint-Petersburg, Russia
V.L. Zvyagintsev, National Research Nuclear University – Moscow Engineering Physics Institute, Moscow, Russia and TRIUMF, Vancouver, Canada

Abstract

New linac-injector for Nuclotron-NICA is planned to consist of quarter-wave coaxial cavities (QWR) having velocities of ~0.07c and ~0.12c (beam energy from 5 to 17 MeV). These cavities are to be superconducting and operating at 162 MHz. Current results of the QWR cavities electrodynamics simulations and geometry optimizations are presented.

INTRODUCTION

The joint collaboration of JINR, NRNU MEPhI, INP BSU, PTI NASB, BSUIR and SPMRC NASB started a new project on superconducting cavities design, production and test technologies development and new linac-injector design in 2015. This linac intend for protons acceleration to 25 MeV (up to 50 MeV after upgrade) and light ions acceleration up to ~7.5 MeV/u for Nuclotron-NICA injection [1-4]. The operating frequency of the linac medium energ part after RFQ is 162 MHz being further doubled to 324 MHz. Geometry choices for first group of resonators considered in this research.

The first design of the linac-injector for Nuclotron-NICA considers quarter-wave coaxial cavities (QWR) operated at 162 MHz as the best choice for velocities range of ~0.07*c* to ~0.14*c* [5-6]. QWRs are effective for frequency up to 200 MHz and velocity below 0.2*c*. At high velocities exceeding about 0.14*c*-0.15*c* half-wave coaxial cavities (HWR) are preferable due to many disadvantages and limitations QWRs have.

Calculations showed that for velocity 0.141*c* and frequency 162 MHz structure chosen as initial version, the steering effect is significant and the displacement of the beam axis is not enough to compensate it. It leads to drift tubes design modifications making cavity production more complicated.

Comparative analysis of the QWR and HWR along with beam dynamics simulation showed that there is a possibility to decrease the geometrical velocity β_G for the second group of resonators to 0.12*c*. It makes the cavity cheaper because less niobium is needed and also it moves the cavity design to a lower steering effect area.

The next step was to consider 162 MHz QWR for velocities 0.07c and 0.12*c*. Choice of optimal geometry and overall dimensions, performance, operation and maintenance issues were considered.

GEOMETRY CHOICE

Cavity basic dimensions optimization allowed us to use identical cryomodules, flanges, tuning devices etc. and minimize the number of unique parts.

Modern elliptical and conical shapes of QWR allow performance improvements, including rise in shunt impedance and decrease losses [5]. Initially simple models of cylindrical QWR based on the primary technology requirements were considered. Change of acceleration and drift sections in cavities for different β_G force us to optimize central conductor length for overall dimensions and frequency kept unchanged.

At the first stage accelerating gaps simulation for both constructions was done. Figure 1. presents acceleration path of two gap cavity, where L is resonator diameter.

According to ratio $d=\beta\cdot\lambda/2$, optimal distance between accelerating gaps was found for 0.07*c* and 0.12*c* cavities. Results presented in Table 1. According to relation $g/d = 1/3$ [6] optimal *g* was founded.

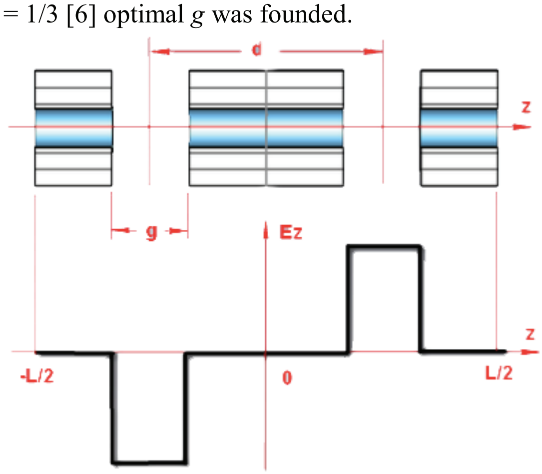

Figure 1: Acceleration path of 2-gap resonator.

ISBN 978-3-95450-181-6

HIGH POWER SOLID STATE RF GENERATOR FOR NEUTRAL BEAM INJECTOR

E.I. Shubin, V.V. Kolmogorov, BINP SB RAS, Novosibirsk, Russia
A.S. Styuf, Novosibirsk State University, Novosibirsk, Russia

Abstract

Neutral Beam Heating Injector of 1 MW beam power for the TCV tokamak (Lausanne, Switzerland) was developed in BINP. The plasma is formed in a plasma box with inductively coupled RF power at frequency about 4MHz. Required RF power in the plasma box is up to 40kW during the period of 2 seconds with 5 minutes intervals [2]. Solid state RF generator with such capability has been developed in BINP. Description of the RF generator design, main features and the test results are presented in the report.

INTRODUCTION

The TCV tokamak (literally "variable configuration tokamak") is a research fusion reactor of the Federal Institute of Technology in Lausanne (EPFL). The upgrade program that is underway on TCV extends the power range of existing Electron Cyclotron Resonance Heating (ECRH) and adds direct ion auxiliary heating using Neutral Beam Injection [1]. At this time Neutral Beam Injector (NBI) is installed and the first 1 MW neutral beam is being commissioned. Plasma emitter of the NBI is powered with RF energy up to 40 kW from the solid state RF Generator.

GENERATOR LAYOUT

The Solid State RF generator is a modular system, it consists of 16 identical RF modules (placed in 2 racks), control modules, combiners, DC power supply – RFG DC PS. Output signal through coaxial feeder, matching network and decoupling HV transformer is applied to plasma emitter. Plasma emitter inductance with additional capacities form a resonant circuit tuned to the operating frequency of 4 MHz. "Matching network" converts subsequent circuit impedance to the characteristic impedance of the feeder at this frequency.

Generator's block diagram is shown in Fig. 1. Output signal is formed by summing the voltages of two identical generators RFG20 in "Final combiner". Both generators are working in-phase. The only difference is that one of them operates in "Master" mode while another one in "Slave" mode. Mode of operation is defined by operation mode of RF Control modules.

Block diagram of one of generators RFG20 is shown in Fig. 2. Generator is placed in one electronic rack and consists of 8 identical units "RF Module", output signals of which are summed in two stages of summation: first stage is Combiner1 and second is Combiner2. Both stage's combiners are implemented by identical scheme of 4-inputs combiner with 50 ohm input and output impedances. Each 4-inputs combiner of the first stage is supplied by in-phase signals from two "RF Modules" with two identical power cells inside. Similarly, the second stage's Combiner2 is supplied by signals from two combiner modules of the first stage.

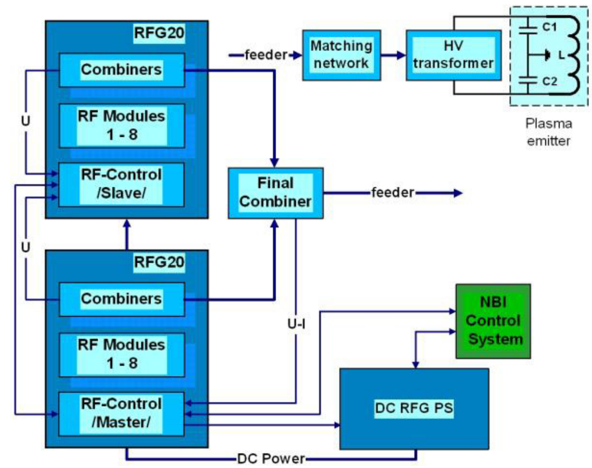

Figure 1: Generator layout.

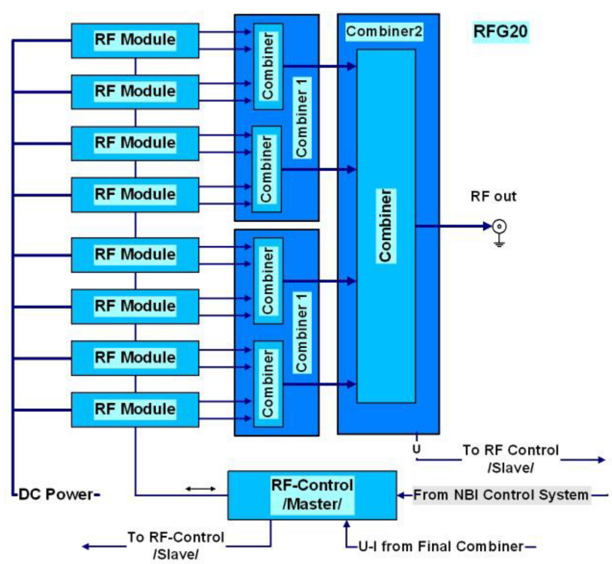

Figure 2: Block diagram of RFG20 generator.

DC power supply unit provides power cells of RF modules with adjustable power voltage. Output RF voltage of 4 MHz in the load is proportional to DC power supply voltage. The NBI system must be able to on/off modulate the beam with a minimum on/off-time of a few ms and to gradually vary the power injected into the tokamak in the range of 30-100% of full nominal power. Beam current from Injector is modulated by changing RF

ISBN 978-3-95450-181-6

REGULATION OF THE WAVEGUIDE COUPLING FACTOR OF STANDING WAVE LINEAR ACCELERATOR

D.S. Yurov, V.I. Shvedunov, Lomonosov Moscow State University, 119992 Moscow, Russia
also at Laboratory of Electron Accelerators MSU Ltd., Moscow, Russia

Abstract

Regulation of the waveguide coupling factor of standing wave linear accelerator allows to adjust the value of accelerated current, keeping the reflected RF power close to zero. This ensures the most efficient use of RF energy and absence of overvoltage in the waveguide elements. The paper presents studies results for various methods of coupling factors regulation with continuous wave (CW) normal conducting linear accelerator used as an example. The results of calculations and measurements on the mock-up of the accelerating structure are presented.

INTRODUCTION

Matching of the RF source and the accelerating structure (AS) of standing wave linear accelerators in traditional designs of the waveguide power coupler is ensured through selecting dimensions of the coupling iris. Iris dimensions as a rule are selected for fixed beam current loading, at that, optimum waveguide-to-AS coupling factor is determined in accordance with the following formula: $\beta = 1 + \frac{P_b}{P_w} = 1 + \frac{I_b E_b}{P_w}$, where P_w is RF power loss in the walls of the AS, I_b and E_b are current and energy of the accelerated beam. If value of the current deviates from the optimum value, a reflected wave appears, which results in lowering of the accelerator efficiency and appearance of overvoltage in the waveguide.

Industrial CW linear RF accelerators have another aspect of the matching problem. The simplest arrangement of the RF system for such accelerators is self-oscillating arrangement with AS in the feedback loop of the klystron excitation circuit [1]. In such arrangement, if the level of the reflected wave is low, klystron can operate without ferrite isolator, which simplifies the accelerator design and makes it cheaper. However, to minimize the reflected wave that adversely affects the RF source, it is necessary to be able to change the coupling factor in accordance with changes in the beam current. Possible design of the 2,856 MHz MIT storage ring cavity adjustable coupler is described in [2]. In this paper we discuss other arrangements of the coupler with coupling factor regulated over a wide range.

COMPUTER SIMULATION

We studied regulation of the coupling factor through insertion of cylindrical plungers (6 mm in diameter) to different depths into the 72x34 mm feeding waveguide perpendicular to its wide wall. Several configurations of plunger positioning were considered.

- 4 plungers near the coupling iris (Fig. 1a).
- 2 plungers opposite each other at the center of wide wall of the waveguide at some distance from the iris (Fig. 1b).
- 1 plunger at the center of wide wall.

Calculations were performed using CST Studio Suite software package [3] on the coupler model consisting of the power input cell without coupling slots in the frequency range of 2,450-2,490 MHz, which is similar to the 1 MeV CW accelerator power coupler [4].

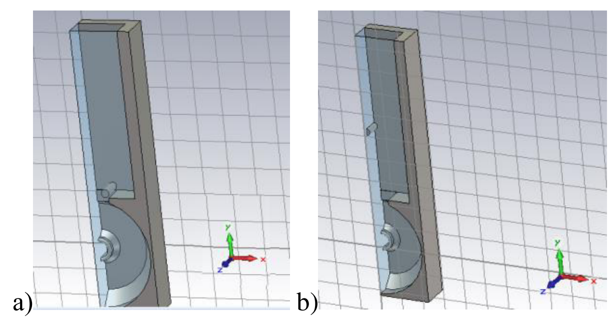

Figure 1: Models for calculating RF power coupler with adjustable coupling factor.

Feeding waveguide input port was excited by the Gaussian envelope signal. Resonance frequency f_{res} was determined by the minimum of the S_{11} parameter, and coupling factor - by the time constant τ_E of the cavity stored energy decay after the end of excitation signal: $\beta = 2\pi f_{res} \tau_E$.

One of the main criteria for evaluating calculation results was minimum shift of the resonance frequency of the power input cell and maximum range of coupling factor regulation. Resonance frequency shift results in appearance of the fields in the coupling cells located near the power input cell of the bi-periodic standing wave AS.

Calculations of the Coupler with 4 Plungers Near the Iris

Idea behind of this arrangement was regulation of the effective width of the iris by changing plunger's position. Due to symmetry a quarter of the power input cell was used in calculations (Fig. 1a). Depth of the plunger insertion L_{pl} was changed in the range of 0-17 mm (17 mm depth corresponds to closure of the opposite plungers). Fig. 2 shows the graphs of the coupling factor and resonance frequency change vs. plunger insertion depth. Without the plungers, the power coupler coupling factor was $\beta_0 = 32$, and resonance frequency was $f_0 = 2{,}486.9$ MHz.

ISBN 978-3-95450-181-6

THE CASCADE INTERFERENCE SWITCH COMPRISING A TRANSMISSION RESONATOR*

S. Artemenko, S. Gorev, V. Igumnov, Institute of Physics and Technology, Tomsk Polytechnic University, Tomsk, Russia

Abstract

The new concept of microwave interference switches is reported. Interference switch is based on series of H-plane T-junctions (cascade switch) in the view of decreasing switched power at Off state and comprises irises in both its own input and output arms. At On state the irises act as a transmission resonator localizing the nodes of the standing wave at the junctions. Such distribution is expected to decrease the plasma losses. It was shown with a simulation that the cascade switch with additional irises increases the efficiency of the active microwave compressors. The simulation was made with CST studio and COMSOL.

INTRODUCTION

The most effective way to boost microwave power feeding linear particle accelerator is usage of microwave resonant compressors. The compressor accumulates microwave energy into its cavity and rapidly discharges accumulated energy towards the load.

There are two types of resonant compressors. Passive compressors keep resonant characteristics of their resonant cavities. Passive SLED system increases an input power in factor of 4 or 9 under a condition of synchronous phase shift of a supplying generator. An active resonant compressor changes Q-factor of its resonant cavity while emitting stored energy. The ratio of Q-factors at accumulating regime and discharging regime determines amplification factor of active compressors.

The level of accumulated energy is comparable for both active and passive compressors. Active compressors have an operating power less though. The reason of it is a switching element having limited dialectical strength. Moreover, the switch has significant losses up to 3 dB.

The most frequent type of the switch is a microwave interference switch. Such switch is based on H-plane T-junction which has one direct arm coupled with a cavity and other arm short circuited. The last arm is connected to the load. A discharge gap is placed at quarter wavelength from a shorting plane. When plasma is broken down running waves from the cavity and the shorted arm add constructively and the microwave power leaves towards the load. The interference switch is simple and effective. Though, power handling capability is limited by cross-section of a waveguide. Moreover, a gas-discharger and its inner elements such as a quartz tube decrease the handling power.

To enhance the operating power a cascade interference switch was suggested [1, 2, 3]. The cascade switch divides the switching power among discharge gaps. This method allows decreasing the switching power as much as $1/2^N$, where N is number of H-tees. However, interaction between the switching wave and gas plasma discharge keeps large amount of losses.

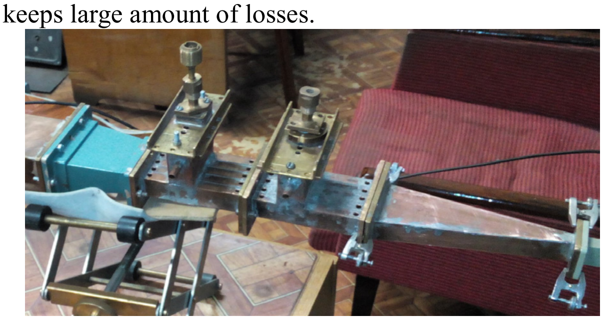

Figure 1: Overmoded cascade interference switch.

The work [4, 5, 6] proposed an overmoded microwave interference switch (Fig. 1) having enhanced handling power. Such switch has two variants of implementation an overmoded waveguide and a package of regular waveguides with a mutual side arm (Fig. 2). The cascade switch based on overmoded T-junctions brought about further enhancement of the operating power. However, interaction between plasma and the switching waves had still stood the same.

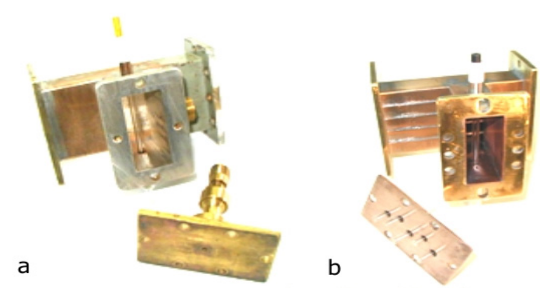

Figure 2: Overmoded interference switches (a – a switch based on overmoded waveguide; b – a package of singlemoded waveguides with a mutual side arm).

This paper concerns a method to increase the operating efficiency of the gas-discharge switches.

RESULTS OF SIMULATION AND ANALYSIS

Overmoded Cascade Switch

The singlemoded cascade switch has an interesting regularity in its act [3]. As one can see from a simulation a behavior of the overmoded cascade switch is quiet similar to the singlemoded cascade switch. Nodes of the

*The work was supported by the Program on Competitiveness Enhancement of the National Research Tomsk Polytechnic University and by Russian Foundation for Basic Research (Grant №15-08-01853).

520 MEV TRIUMF CYCLOTRON RF SYSTEM: MAINTENANCE, TUNING AND PROTECTION*

N.V. Avreline, V.L. Zvyagintsev, I.V. Bylinskii, C. Bartlett, B. Jakovljevic, T. Au
TRIUMF, Vancouver, B.C., Canada

Abstract

1 MW CW 23 MHz RF system of the TRIUMF's 520 MeV Cyclotron has been in operation for over 40 years. Continuous development of the RF power amplifiers, the waveguide system and the measurement and protection devices provides reliable operation and improves the performance of the RF System. In this article, operation and maintenance procedures of this RF system are analysed and recent as well as future upgrades are being analysed and discussed. In particular, we discuss the improvements of the transmission line's VSWR monitor and its effect on the protection of the RF system against RF breakdowns and sparks. We discuss the new version of the input circuit that was installed, tested and is currently used in the final stage of RF power amplifier. We analyse various schematics and configurations of the Intermediate Power Amplifier (IPA) to be deployed in the future.

INTRODUCTION

TRIUMF 520 MeV Cyclotron's high power RF system consists of three main parts – the 1.8 MW CW RF amplifier, the transmission line (TL) and the resonator [1]. The TL itself is composed of two coaxial lines with wave impedances of 50 and 30 ohm. The second part of the TL has three capacitor stations that match 50 ohm impedance of the TL's first part with the coupling loop port of the resonator that is at TL's terminus.

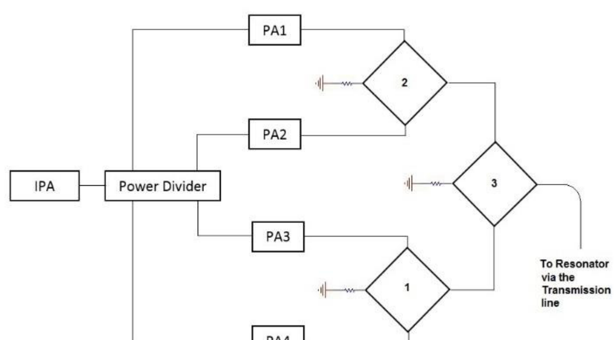

Figure 1: RF System of the 520 MeV Cyclotron.

TRANSMISSION LINE RESONATOR OPERATION AND SPARK PROTECTION

Instability in the RF system's operation appears when there are sparks, electrical breakdowns, multipactor discharge in the resonator and a presence of an essential screen current in the vacuum tubes. The VSWR monitor is used to protect the RF system. This monitor turns off the RF system, if the reflected power in one of the 12 channels exceeds a specified threshold value. The RF control system analyses the rate of the Dee voltage drop, classifies the events and then tries to recover the system. The follow up analysis of where sparks and electrical breakdowns took place is done using an oscilloscope. The oscilloscope operates in stand-by mode otherwise. An example of a typical signal pattern that illustrates a spark inside the resonator is presented in Fig. 2.

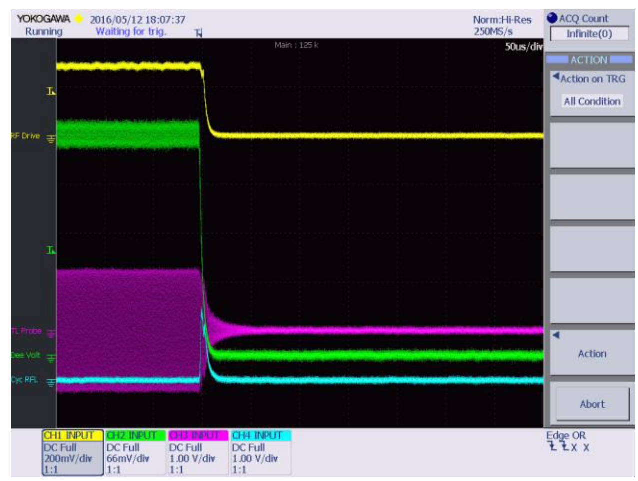

Figure 2: Resonator RF signals following a spark, when the drive is OFF (yellow – drive amplitude, green – Dee voltage, pink – RF signal, blue – rectified voltage of the reflected signal).

The rate of the Dee voltage drop allows to determine whether this spark happened inside the resonator or inside the TL and how large the spark was. The RF control system has sensors to determine the Dee voltage drop and if zero Dee voltage is detected. If either case is detected, the RF control system generates the signal to turn OFF the RF drive and to determine the time when RF system's recovery should be attempted.

However, if these sensors didn't respond properly or responded with some delay, the standing beat wave in the TL could reach double amplitude of the original signal (Fig. 3). As a result, some parts of the TL, such as matching capacitors, the water feedthrough or the TL conductors and insulators could be damaged.

To protect cyclotron's equipment in such an event, the RF switch was built into the VSWR monitor to disconnect the RF drive from the RF amplifiers (Fig. 4).

*TRIUMF receives federal funding via a contribution agreement through the National Research Council of Canada.

ISBN 978-3-95450-181-6

ESTIMATION OF MULTIPACTING IN CDS STRUCTURE

I.V. Rybakov†, Institute for Nuclear Research of the RAS, Moscow, Russia
I.I. Isaev[1], DESY, Zeuthen, Germany

Abstract

Within the framework of the INR's linac upgrade the Cut Disk Structure (CDS) was recommended for the linac's main part first cavity replacement [1]. The stable cavity work in operation regime requires absence of multipactor discharge. The multipactor phenomenon in a CDS structure studies are presented in this paper.

INTRODUCTION

CDS structure was first applied as a booster cavity in DESY PITZ test facility in Zeuthen [2]. For this cavity according to our analytical estimation multipaction should appear at the operating power level in coupling cells, but it was not confirmed by the numerical simulation with both accelerating and coupling modes excitation for RF energy transfer along the cavity. The multipactor appears only with the Secondary Emission Yield (SEY) growth which could happen if the inner surface of the cavity is polluted. The results of multipactor investigation in CDS PITZ were used as the reference for the CDS structure in the first cavity of the main part of INR linac. The analytical estimation and numerical simulation of multipactor in CDS INR structure shows the appearance of the discharge in coupling cells with the OFC copper SEY for the operating regime of the cavity. An option for the multipactor damping with the forced excitation of oscillations in coupling cell with voltage higher than upper multipactor limit was considered.

METHODICS OF ESTIMATION

The multipactor discharge in CDS cavity could appear in the coupling cell, which is geometrically like a flat capacitor (see Fig. 1).

The field level in the coupling cell depends on the accelerating field rate and position of the cell relative to the RF coupler.

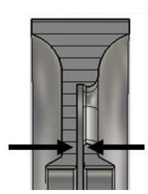

Figure 1: The design of CDS cavity.

For the power transfer through the cavity the coupling mode should be excited additionally [3]. This is the operating regime of compensated structure. The coupling mode is excited with the attenuation coefficient per period *d*:

$$\alpha d = (1 + \frac{I_b U_a}{P_a}) \frac{\pi\beta}{2\beta_g Q_a} , \quad (1)$$

$$\frac{\beta_g}{\beta} = \frac{\pi k_c}{4} , \quad (2)$$

where I_b is the beam current, β_g is the group velocity, β is relative phase velocity, U_a, P_a and Q_a are the accelerating voltage, power and quality factor, k_c is the coupling coefficient. For each cavity cell the αd value multiplies by coefficient N, which depends on the cell position relative to feeding waveguide.

Analytical Estimation

For the coupling cell of the CDS structure the analytical estimation of multipactor voltage level could be obtained using the flat gap approximation [4]:

$$U=4\pi^2 (fs)^2 \frac{m}{e} (\frac{1+K_v}{1-K_v} \pi n \cos\psi + 2\sin\psi)^{-1} \quad (3)$$

Where f is the cavity operating frequency, s is the gap length, K_v is the relation between secondary and primary electrons velocity, ψ is the secondary electron yield phase and n is the multipactor order. The multipactor voltage levels for different f*s parameters and discharge orders could be represented by a diagram (see Fig. 2).

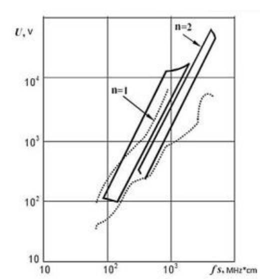

Figure 2: Multipactor voltage levels.

The analytical estimation shows the voltage levels in the gap when the multipaction is possible. We considered only 1st order discharge in case of low current in high order multipactor.

Numerical Simulations

For the numerical simulation of multipacting, the CDS structure was tuned to the secondary electron emission parameters corresponding to pure OFC copper [5]. The secondary emission yield (SEY) graph is shown at Fig. 3. All the simulations were made using the CST studio software [6], the simulation procedure is presented in [7].

† irybakov@inr.ru
[1] on leave from NRNU MEPhI, Moscow, Russia

ISBN 978-3-95450-181-6

MANUFACTURING TOLERANCES ESTIMATION FOR PROTON LINAC CAVITIES

I.V. Rybakov†, V.V. Paramonov, A.K. Skasyrskaya, Institute for Nuclear Research of the RAS, Moscow, Russia

Abstract

The definition of tolerances for mechanical treatment of the cells in accelerating structures is the step in the total procedure of accelerating structures development and construction. The method of tolerances estimations for mechanical treatment is presented in this paper with examples of application for single periodic and bi-periodic structures.

INTRODUCTION

The natural deviations of the cells dimensions after manufacturing with respect to design values lead to deviations in the structure parameters. From parameters of accelerator should be limitations, which restrict possible deviations in the parameters of accelerating structure. In the case of high intensity proton linacs with long multi-cells structures a critical parameter is the homogeneity of accelerating field distribution, which defines the beam dynamic quality of accelerated beam. Field deviations from the designed distribution is described be standard deviation σ_E and for high intensity high energy proton linacs, [1], a typical limitation is of field $\sigma_E < 1\%$. From the theory of periodical structures are know relations between field deviations and deviations in frequencies $\sigma_{fa,c}$ and coupling coefficient σ_{kc} of cells in the accelerating structure. A method to reduce the efforts by avoiding separate simulations for each geometrical parameter of the structure cell is extended and presented. The required values could be obtained by numerical simulations only for a few the characteristic modes in the cell. After that the theory of perturbations is applied.

BASEMENT AND REALIZATION

The standard deviation of accelerating field distribution σ_E is defined as:

$$\sigma_E^2 = \frac{\sum_{i=1}^{N_p} (E_i - \bar{E})^2}{N_p}, \tag{1}$$

where N_p is the number of accelerating gaps, E_i is the filed amplitude in each gap. According to the theory, the contributions of cells deviations in frequency and in coupling coefficient contribute into field deviation independently:

$$\sigma_E^2 = \sigma_{E_f}^2 + \sigma_{E_k}^2 , \tag{2}$$

where σ_{Ef}^2 is the dispersion caused by frequencies spread of accelerating and coupling modes, σ_{Ek}^2 is the dispersion caused by coupling coefficient spread [1].

Bi-periodic (Compensated) Structures

For the π/2 mode (or bi-periodic) accelerating structures the values of σ_{Ef}^2 and σ_{Ek}^2 can be obtained with expressions [2]:

$$\sigma_{E_f}^2 \approx \frac{16\sigma_{f_a}^2}{k_c^4}\left(\sigma_{f_c}^2 \frac{N_p^2+3N_p}{12} + \left(\frac{\delta f}{f_a}\right)^2 \frac{N_p^3+4N_p^2+6N_p}{3}\right) \tag{3}$$

$$\sigma_{E_k}^2 = \sigma_{k_c}^2 \frac{N_p+2}{3}, \tag{4}$$

where $\sigma_{fa,c}$ are the dispersions of frequencies for accelerating and coupling modes, $\delta_f = f_c - f_a$ is the stop band width, N_p is the number of structure periods in the cavity and k_c is the coupling coefficient. The values of $\sigma_{fa,c}$ and σ_{kc} are related with deviations in geometrical parameters of cells x_i as:

$$\sigma_{f_{a,c}} = \frac{\sqrt{\sum_i \left(\frac{\partial f_{a,c}}{\partial x_i}\right)^2 \sigma_{x_i}^2}}{f_{a,c}} \tag{5}$$

$$\sigma_{k_c} = \frac{\sqrt{\sum_i \left(\frac{\partial k_c}{\partial x_i}\right)^2 \sigma_{x_i}^2}}{k_c}, \tag{6}$$

where σ_{xi} is the dispersion of geometrical parameter x_i spread which corresponds to the tolerance value $dx_i = \pm 3\sigma_{xi}$, $\delta f_{a,c}/\delta x_i$ and $\delta k_c/\delta x_i$ are the sensitivities of frequencies and coupling coefficient to deviations in geometrical parameter x_i. In the cell geometry each parameter x_i, as a rule, defines a surface S_i, and the change in parameter δx_i means this surface displacement. The sensitivity of frequencies to the surface displacement we can define by using Slatter perturbation theorem:

† irybakov@inr.ru

ISBN 978-3-95450-181-6

POWERFUL RF TRIODE AS ANODE MODULATOR VACUUM TUBE

A.I. Kvasha, V.L. Serov, Institute for Nuclear Research, RAS, Moscow, Russia

Abstract

For 20 years modulator vacuum tube GMI-44A successfully operated in DTL RF system of INR Linac. The vacuum tube had been designed and manufactured at OKB "Swetlana" (now joint stock company SED-SPb) in the 70-ies - 80-ies of the last century. A quantity of manufactured tubes had achieved nearly 80 and allowed the accelerator operating up to date. In the middle of 80-th manufacture of the tubes was stopped. Attempts of the GMI-44A manufacture restoration or repair were unsuccessful ones.

As it is turned out, the only decision in the circumstances is use of vacuum tube GI-71A (the former name "Katran" [1]) as modulator tube. The tube GI-71A operates for the last ten years in all final RF power amplifiers (FPA) of INR Linac instead of GI-54A.

Use of RF triode GI-27A in anode modulator as control valve was considered in [2], but a creation of the HV modulator pulse was realized by means of the "soft" discharger.

ITRODUCTION

The powerful anode modulator simplified scheme is shown at fig.1, where AFL – artificial forming line (storage device), TRPM – transistor pre-modulator, TR-thyristor regulator of GI-71A filament voltage.

To simplify the subsequent discussion the modulator vacuum tube will be marked as GI-71AM though in the modulator and the FPA the same vacuum tube GI-71A sets in.

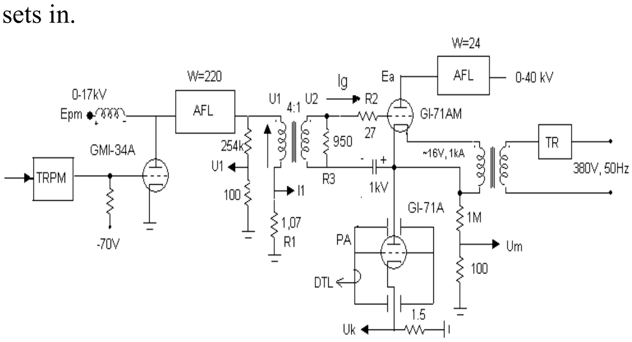

Figure1: Simplified scheme of anode modulator.

At fig.1 pre-modulator devices are additionally represented at the scheme: pulse transformer between output stage of the pre-modulator (at vacuum tube GMI-34A) and GI-71AM input, a source of negative grid bias relatively cathode, resistive dividers, which allows to measure voltages in the main point of scheme, final RF power amplifier (FPA), connected in series with modulator vacuum tube GI-71AM. Resistor R2 limits the grid current value in a case of emergency situation (short circuit of GI-71AM grid-cathode gap) and brings down oscillations in the circuit consisted from pulse transformer secondary winding inductance and capacity grid-cathode *Cgc* of the modulator vacuum tube.

It should be noted that modulator vacuum tube performs several functions such as:

- Creation of PA plate pulse voltage up to 35-40 kV with current 150-200A;
- Control of plate voltage by a signal of negative feedback from the tank;
- Interruption of pulse modulator in the case of breakdowns in PA vacuum tube [3]
- Aging of PA vacuum tube because of series crowbar operation particularities [3] - due to delay between signals from current transformer in the modulator vacuum tube plate network and at the GI-71AM input a part of energy, accumulated in AFL, is delivered in a point of break-down, destroying non uniformity at electrode surface of the FPA vacuum tube.

Before estimate problems, which are appeared after replacement of GMI-44A at GI-71A it follows to compare both vacuum tubes options (see table 1).

Table 1: Tubes Options

	GMI-44A	GI-71AM
Cag, pF	300	80
Cgc, pF	1000	200
Cac, pF	20	3
- Eg, kV	2	1.5
Ea, kV	60	45
Iem, A	500	900
Iao, A*)	140	100
Igo, A*)	1	25
Pa, kW	150	140
Pg, kW	1.5	2
Filament voltage	6V, 50Hz	16V, 50Hz
Filament current	2kA	1kA

*) At voltages Ugk = 500 V and Uak = 6kV

As can be seen from table 1 the vacuum tubes options noticeably differ in values of inter-electrode capacities and grid currents. The last one means, that pre-modulator pulse power needs to be increased 20-30 times. That can be achieved by two ways: increasing of transistor pre-modulator gain and optimization of GMI-34A mode of operation, particularly by means of plate voltage increasing.

Moreover, as follows from table 1 GI-71AM filament options demand changes of the high-voltage filament transformer. It should be noted that GI-71A modes of operation in modulator and in RF final power amplifier are significantly different ones. In FPA there is pulse plate voltage 25-30 kV and automatic pulse grid bias due small resistor in cathode circuit. Value of pulse grid bias doesn't exceed 400V. During setting GI-71A in anode modulator there are dc plate voltage up to 40kV and dc

ISBN 978-3-95450-181-6

THE RF POWER SYSTEM FOR RFQ-INJECTOR OF LINAC-20

V. Kuzmichev, A. Kozlov, Yu. Stasevich, D. Seleznev, Institute for Theoretical and Experimental Physics, Moscow, Russia
A. Butenko, Joint Institute for Nuclear Reseach, Dubna, Russia
C. Polozov, National Research Nuclear University MEPhI, Moscow, Russia
T. Kulevoy, Institute for Theoretical and Experimental Physics, Moscow, Russia and National Research Nuclear University MEPhI, Moscow, Russia

Abstract

In the frame of the NICA project the electrostatic injector of LU-20 is replaced by a RFQ accelerator, which has been developed in ITEP. The construction of 400 kW 145 MHz RF power system for RFQ-injector are described. Parameters and test results of the RF power system operated on the resistive load and on RFQ during ion beam acceleration are presented.

INTRODUCTION

In the framework of the NICA project the modernization of injection line is realized. As a result of upgrading the 700 kV electrostatic injector of the DTL LU-20 was replaced by an RFQ. It enables to decrease the potential at the ion source high voltage platform to 150 kV and as result to deliver on it the 35 kW electric power needed for the polarized ion sources operation [1].

The RFQ accelerator, RF power system and low-level RF system were developed in ITEP. The oscillating tube specially developed for application in accelerator technology is used in the RF amplification system [2].

The RF system of the existing linear accelerator LU-20 operates in self-exciting oscillation mode. This requires the dynamic phase synchronization between RFQ and DTL cavities. The RFQ cavity works at the same frequency as DTL and the stability of phase difference between the oscillations in these two cavities has to be kept within tolerance of one degree. The synchronization is provided by a high performance FPGA-based digital Low-level RF system (LLRF).

DESCRIPTION OF RF SYSTEM

RFQ is driven by an RF power system consisting of a solid-state amplifier (SSA), four-stage preamplifier and the final stage based on the high-power water-cooled GI-27AM tube. Block diagram of the RF system is presented in Figure 1.

The RF signal is generated by master oscillator. The SSA amplifies the 10 mW output signal from the master oscillator to a level of 150 W. To protect the SSA, the ferrite circulator with low insertion losses is used at its output. The preamplifier consists of four units with GI-39B triodes, RF power splitter and combiner. It provides the RF power up to 50 kW at the input of the last stage.

The resonator uses two identical RF coupling loops (Figure 2) installed symmetrically in the middle section of the RFQ. The area of loops is about 870mm^2. The non-compensated inductance of couplers leads to a resonant frequency decrease by 33kHz. Fine adjustment of the coupler input impedance is carried out by loop rotation against its axis.

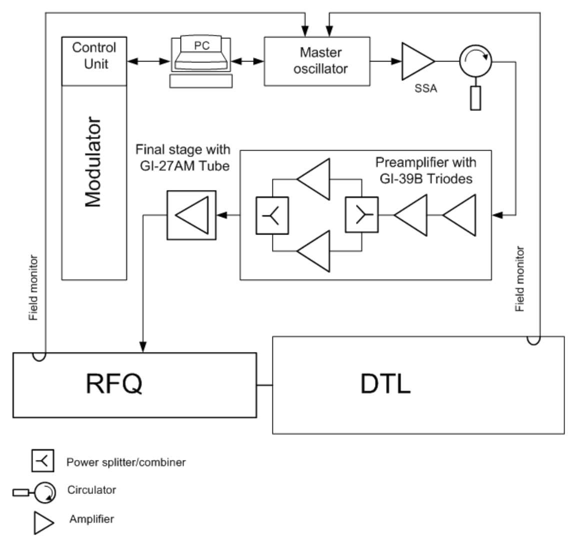

Figure 1: Block-diagram of RF system. PC-computer, SSA–solid state amplifier, RFQ- accelerator, DTL- linear accelerator LU-20.

In the final stage of RF amplifier a powerful generator tube GI- 27AM is used. To obtain the required output power, the tube the power of about 50 kW is needed at the input circuit of. The single unit with GI-39B was tested to define the output power achievable at the DTL frequency 145.2 MHz with pulse length of 150 µs. It was demonstrated that the single lamp can produce power up to 30-35 kW for routine operation.

Also it was found that the output power of two GI-39B connected in parallel get 50 kW which can be transmitted to the input circuit of GI-27AM tube.

A lay-out of the final unit based on the GI-27AM triode is shown in Figure 3. Detailed design of the generator is described in [3].

ISBN 978-3-95450-181-6

S-BAND CHOKE MODE CAVITY FOR LOW ENERGY STORAGE RING

L.Yu. Ovchinnikova, V.I. Shvedunov, Skobeltsyn Institute of Nuclear Physics, Lomonosov Moscow State University, Laboratory of Electron Accelerators MSU, Moscow, Russia
A.D. Ryabov, Institute of High Energy Physics, Protvino, Russia

Abstract
Several variants of a low-energy storage ring for Thomson scattering X-ray source were considered in [1]. The most promising variant "C" of the ring with small dimensions and large dynamic aperture has also large momentum compaction factor, which would lead to too long bunches with RF cavity operating at 714 MHz, so shorter wavelength must be used. In this paper we present results of optimization of S-band double-cells cavity with parasitic mode damping by chokes similar to [2]. Interaction of the bunch circulating in the ring with cavity parasitic modes is simulated.

INTRODUCTION

Thomson scattering of laser photons on relativistic electrons enables generating monochromatic X-radiation with adjustable energy. High average intensity of radiation can be achieved through higher collision frequency of photon and electron bunches with small cross-sectional dimensions at the interaction point. High collision frequency is achieved through circulation of electron bunches in compact storage ring. Four variants of Thomson generator ring with electron energy of ~50 MeV and bunch charge of ~1 nC are presented in publication [1]. For further consideration, we selected option C with the largest dynamic aperture and smallest dimensions. A modified variant of the ring is given in Fig. 1, and its characteristics are given in Table 1.

Distinct feature of this variant is large value of the momentum compaction factor, which along with other parameters determines RMS length of the bunch circulating in the ring:

$$\Delta l_{rms} = \frac{\Delta p_{rms}}{p_s}\sqrt{\frac{cL\alpha\, E_s}{2\pi f_{RF} eV_{RF}\cos\varphi_s}}, \quad (1)$$

where Δp_{rms} is the RMS momentum spread, and other designations are given in Table 1. To ensure acceptable length of the bunch, we increased operating frequency of the RF cavity from 714 MHz [3] to the frequency of the injector of 2,856 MHz [4]. For the ring parameters given in Table 1, such modification results in the following ratio of the bunch length and momentum spread: $\Delta l_{rms} \approx 1.75\frac{\Delta p_{rms}}{p_s}$ (m). It should be noted that such high operating frequency of the cavity was also used in the MIT-Bates storage ring [5].

In the process of the RF cavity optimization and choice of its design, a number of problems must be solved, the most significant ones being suppression of the higher order modes (HOM) and increasing of the cavity efficiency. To solve the above problems, we analyze two variants of the RF cavity: cavity with removal of the HOMs into the beam pipe which walls are covered by RF absorbing material (see e.g. [5]); and cavity with a choke suggested in [2] that has little impact on the operating mode, but ensures absorption of the HOMs.

Table 1: Storage Ring Parameters

Parameter	Value
Operating frequency of the RF cavity, $\boldsymbol{f_{RF}}$	2856 MHz
Frequency of bunch circulation, $\boldsymbol{f_0}$	35.7 MHz
Orbit length, $\boldsymbol{L}$	8.397 m
Momentum compaction factor, $\boldsymbol{\alpha}$	0.13
RF voltage, $\boldsymbol{V_{RF}}$	300 kV
Synchronous particle momentum, $\boldsymbol{p_s}$	50.5 MeV/s
Synchronous phase, $\boldsymbol{\varphi_s}$	0^0
Bunch charge, $\boldsymbol{q_B}$	1 nC
Number of bunches at orbit, $\boldsymbol{M}$	1
Bunch replacement period, $\boldsymbol{\tau_{ch}}$	20 ms
Average beam current, $\boldsymbol{I_b}$	35.7 mA
Synchrotron tune, $\boldsymbol{Q_s}$	0.05
$\boldsymbol{\beta}$ –function at cavity position,	2/2 m
Betatron tunes, $\boldsymbol{Q_x}$ / $\boldsymbol{Q_y}$	2.7 / 1.8

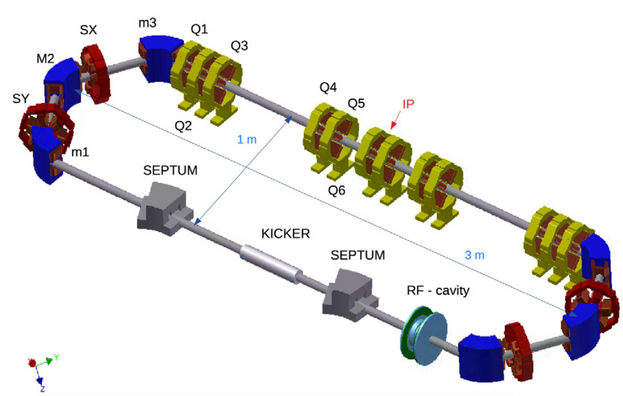

Figure 1: Storage ring layout.

HOMS SUPPRESSION CRITERION

Electron bunches circulating in the ring excite HOMs of the cavity, subsequent interaction with which at certain values of the beam current can result in two types of instability, longitudinal and transversal. In case of Thomson generator with low energy of the circulating beam (35 – 50 MeV), emittance growth due to intrabeam scattering effect stipulates the need to replace bunches in the ring with the period of τ_{ch} ≈20 ms, which is much shorter than the dumping time due to synchrotron radiation, the value of which at such low energy is > 1 s. As such, stable motion of bunches in the ring is determined by the condition that

ISBN 978-3-95450-181-6

HIGH-ENERGY MICRO-BUNCHER BASED ON THE MM-WAVELENGTH DIELECTRIC STRUCTURE

I. Sheinman*, Saint Petersburg Electrotechnical University
A. Petrenko, CERN, Geneva, Switzerland

Abstract

The proton-driven plasma wakefield acceleration is a recently proposed technique promising a GeV/m rate of acceleration to a TeV-scale energy in a single plasma stage. In order to excite high-amplitude plasma wakefields a long proton bunch from a synchrotron should be broken into a sequence of sub-mm long micro-bunches which can drive the plasma oscillations resonantly. We suggest a novel approach to produce the required train of micro-bunches using collinear wakefield acceleration in a dielectric-loaded structures. First the energy modulation is introduced into the proton beam with the help of the mm-wavelength dielectric accelerating structure. Then the energy modulation is transformed into the longitudinal micro-bunching using proton beamline with magnetic dipoles. Beam dynamics simulations were used to find the appropriate parameters of the dielectric accelerating structure, driving electron bunch and the beam focusing system.

INTRODUCTION

Hadron beams in high-energy synchrotrons provide the highest-energy particles available in laboratories today. Synchrotrons also hold the record for the maximum total energy stored in the beam. For example, both rings of the Large Hadron Collider currently operate at 6.5 TeV with 2200 bunches of $1.1 \cdot 10^{11}$ protons each. This beam has the total energy of 250 MJ which is equivalent to the kinetic energy of a typical fully-loaded airliner (80 t) at the take-off speed of 300 km/h (280 MJ). Even the single bunch ($3 \cdot 10^{11}$ protons at 400 GeV) in the 40 year old Super Proton Synchrotron (SPS) at CERN carries an order of magnitude more energy than the single bunch in the proposed International Linear Collider ($2 \cdot 10^{10}$ electrons or positrons at 250 GeV). Several techniques have been suggested to transfer a fraction of the proton beam energy to other particles which cannot be accelerated in a circular machine either because of the prohibitively high energy loss due to the synchrotron radiation (electrons/positrons) or because of the short life-time of the unstable particles (muons, pions) [1–3]. Such accelerated particles can be used for instance in the collider experiments which do not require high luminosity [4]. The proton-driven plasma wakefield acceleration [3] is the recently proposed method promising a GeV/m rate of acceleration to a TeV-scale energy in a single plasma stage. GV/m plasma wakefields correspond to the plasma wavelength of around 1 mm, while proton bunch in a typical synchrotron is several tens of cm long. In order to excite high-amplitude plasma wakefields the proton bunch should be either compressed longitudinally by a large factor [2, 3] (which is technically very challenging) or the single proton bunch should be broken into the sequence of sub-mm long micro-bunches which can drive the plasma oscillations resonantly. The Self-Modulation Instability (SMI) of a long proton beam in plasma has been suggested as a convenient way to create such a resonant sequence of micro-bunches [5]. The feasibility of this technique will be tested in the forthcoming AWAKE experiment at CERN [6]. However the efficiency of the SMI is low since the majority of protons are lost from the beam during the development of this instability. In this article we propose a more efficient alternative approach to create the sequence of sub-mm long proton micro-bunches via the longitudinal bunching process first described in the "proton klystron" proposal [1]. We rescale it down to the mm-wavelength using the collinear wakefield acceleration in the dielectric-loaded structures. A resulting train of sub-mm proton micro-bunches could be useful not only for the plasma wakefield acceleration but also as a powerful source of mm-wavelength radiation or as a driver for the similar dielectric accelerator.

* ishejnman@yandex.ru

GENERAL DESCRIPTION OF THE METHOD

The basic idea of the proposed scheme is shown in Figure 1 [7]. First the energy modulation is introduced into the proton beam with the help of a mm-wavelength accelerating structure. Then the energy modulation is transformed into the longitudinal micro-bunching using the beamline with magnetic dipoles. Proton path length inside the dipoles linearly depends on the proton momentum therefore the energy modulation is transformed into the longitudinal micro-bunching. The 400 GeV SPS proton beam used here as an example has the energy spread $\sigma_{\Delta E}$ = 120 MeV (the relative value $\sigma_{\Delta E/E}$ = 0.03%). In order to produce micro-bunching suitable for the plasma wakefield acceleration the energy modulation introduced by the mm-wavelength accelerating structure should be several times larger than the uncorrelated energy spread of the incoming proton beam, – we take ±500 MeV as a typical value. The dielectric wakefield acceleration is based on excitation of electromagnetic wave with a longitudinal component of electric field by a high-current electron bunch in the vacuum channel of a dielectric wave guide. The proton beam will pass the dielectric channel behind the electron bunch. At a typical field of 100—150 MV/m the required ±500 MeV energy modulation can be obtained in 3—5 m. Since the length of the proton beam is much larger than the wavelength the wakefield should be excited in a single mode. It's important to note that the

ISBN 978-3-95450-181-6

SOFTWARE COMPLEX "DYNPART" FOR THE CALCULATION OF SELF-CONSISTENT BEAM DYNAMICS IN DIELECTRIC WAKEFIELD ACCELERATING STRUCTURES

I. L. Sheinman*, A. E. Yakushkin,
Saint-Petersburg Electro-Technical University «LETI», Saint-Petersburg, Russia

Abstract

Dielectric waveguide structures are a basis for development of new generation of accelerators on the basis of a wakefield method of the charged particle acceleration, beam manipulation, and also free electron lasers. A self-coordinated dynamics of relativistic particle beams in a single layer cylindrical waveguide with dielectric filling is investigated. The computer code is developed based on mathematical expressions for the analysis of the radial dynamics. The possibility of modelling interaction of different types of particles in a bunch is realized. Influence of both own wake fields and external fields of focusing and deflection systems on bunch dynamics is analyzed.

INTRODUCTION

Wakefield acceleration principle is based on a generation by high-current charged particles bunch in the waveguide structure of an electromagnetic wave with a longitudinal component of the electric field up to 100 MV/m. This wake field is used to accelerate a following low-current bunch of high energy. In free electron lasers electromagnetic wave generated by high-current electron bunch is extracted from the waveguide and structure is used as an electromagnetic radiation source.

Dielectric wakefield accelerating structures are single or multilayer dielectric cylindrical waveguides with outer metal covering and vacuum channel along the axis. Along with the longitudinal fields there are transverse fields, leading to bunch deflection from the axis of the waveguide and subsidence of particles on its wall.

Development of new methods of acceleration based on principle of wakefield acceleration, requires a detailed analysis of the self-consistent beam dynamics taking into account both own and external focusing and deflecting fields.

Nowadays, wakefield accelerators often use light particles, electrons, as driving bunch, to generate the wakefield for acceleration of another electron bunch (which is usually called “witness”) like it is organized at AWA/APS accelerator complex in Argonne National Laboratory (USA) [1]. Wakefield acceleration of heavier particles, like protons, is not used because of traditional cyclic accelerators like synchrotrons are more effective for acceleration of heavy particles. Nevertheless wake field generated by driving electron bunch in the wakefield structure can be used for energy modulation of long proton bunch [2].

*isheinman@yandex.ru

At the same time wakefield acceleration with its high acceleration gradient would be promising in case of muons acceleration which can live in their self-reference system only 2.2 μs.

Effectiveness of wakefield acceleration is limited by “Wakefield’s theorem”. In accordance with "Wakefield's theorem" in the accelerator, where the electron bunches move along the same line, in the case of symmetric driving electron bunch accelerated bunch cannot increase its energy more than twice the value of electron energy of the driving bunch. This limit can be overcome by using a proton beam accelerated in synchrotron as a driver and electron or muon bunch as a witness.

SPECIALIZED SOFTWARE

For the analysis of the radial beam dynamics in the accelerating structure, methods of computational experiment are used. Specialized software, like CST Particle Studio [3], has been developed to aid in accelerator modelling; however, these codes based on particle-in-cell solver being universal are rather slow. Some special codes like BBU-3000 developed for self-consistent beam dynamics in wake fields uses numerical methods for differential equation solving. We decided to take a different approach and develop a software complex that uses strict analytic solutions to dynamics equations to calculate particle coordinates [4, 5].

DYNPART SOFTWARE COMPLEX

Analysis of the beam dynamics in the developed software is based on the method of macroparticles. In this method charge distribution function is realized by generating an array of particles with a given distribution in space, and field calculation is organized by summation of field generating of each macroparticle over the array. In case of high-current relativistic beams electrostatic approximation inapplicable to determine the Cherenkov wake field. Our algorithm for calculating wake fields is based on dot charge field expansion in series on waveguide eigenfunctions. That requires for the self-consistent beam dynamics calculation using the "particle – particle" method. The number of operations in this method increases with the square of the number of macroparticles that increases the calculation time and thus imposes restrictions on their accuracy. For accelerating of calculations an analytical solutions of the equations of relativistic dynamics and optimized for calculation speed algorithm for finding wake fields based on expansion on waveguide eigenfunctions were used (Fig. 1).

ISBN 978-3-95450-181-6

WAKE FIELD COMPONENTS IN A RECTANGULAR ACCELERATING STRUCTURE WITH DIELECTRIC ANISOTROPIC LOADING

I. L. Sheinman*, Yu. S. Sheinman,
Saint-Petersburg Electro-Technical University «LETI», Saint-Petersburg, Russia

Abstract

Dielectric lined waveguides are under extensive study as accelerating structures that can be excited by electron beams. Rectangular dielectric structures are used both in proof of principle experiments for new accelerating schemes and for studying the electronic properties of the structure loading material. Some of the materials used for the waveguide loading of accelerating structures possess significant anisotropic properties. General solutions for the fields generated by a relativistic electron beam propagating in a rectangular dielectric waveguide have been derived using the mode expansion method for the transverse operators of the Helmholtz equation. An expression for the combined Cherenkov and Coulomb fields obtained in terms of a superposition of LSM and LSE-modes of rectangular waveguide with anisotropic dielectric loading has been obtained. Numerical modeling of the longitudinal and transverse (deflecting) wake fields has been carried out. It is shown that the dielectric anisotropy influences to excitation parameters of the dielectric-lined waveguide with the anisotropic loading.

INTRODUCTION

Physics of particle accelerator now is on the edge of traditional and new accelerating methods. One of the promising directions is development of linear colliders with high acceleration rate on the base of wakefield accelerating structures. Wakefield waveguide structures can contain plasma or dielectric loading excited by laser, RF source or high current charged beam. Unlike plasma structures, dielectric filled waveguides with vacuum channel provide collisionless transport of the beam [1,2]. The cherenkov accelerating structure is a dielectric waveguide with an axial vacuum channel for beam passing covered by conductive sleeve.

Dielectric wakefield structures provide both high acceleration rate and ensure the control over the frequency spectrum of the structure by introducing additional ferroelectric layers [3] as well as a possibility using of perspective materials with unique properties like diamond and sapphire [4].

The high current short generating bunch (usually called driver) with low energy excites Vavilov-Cherenkov wake field. Generated longitudinal field accelerates a low intensive but higher energy bunch (witness). The witness is placed to a distance behind the driving bunch corresponds to an accelerating phase of the wake field.

As usual, the cylindrical geometry for structures with dielectric filling is proposed. Nevertheless, structures with a rectangular cross section and dielectric filling in some cases are also used [5–14]. Advantage in usage of this geometry is simplification of manufacturing techniques. Such structures (along with cylindrical structures) for generating electromagnetic radiation and producing wakefield acceleration in the frequency range 0.5–1.0 THz are considered [4]. In THz range, the planar geometry can be preferable because of difficulties of precise cylindrical structure manufacture. Rectangular structures can be used for test experiments in analysis of new accelerating systems [14] and for studying the properties of materials effective for producing high acceleration rates and pulsed heating of the structure (diamond, sapphire) [4].

THEORETICAL ANALYSES OF RECTANGULAR WAVEGUIDE EXCITATION

Let us consider a rectangular waveguide with a symmetric filling in the form of dielectric transversal isotropic layers (2) parallel to the x axis and with a vacuum channel (1) at the centre (Fig. 1).

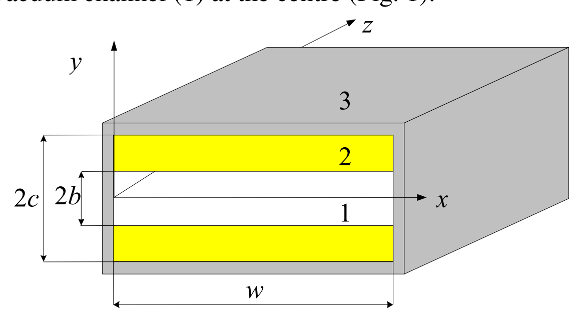

Figure 1: Rectangular waveguide.

In this case, the filling in the direction of the y axis is inhomogeneous, and the permittivity and permeability tensors are functions of y: $\hat{\varepsilon} = \hat{\varepsilon}(y)$ and $\mu = \mu(y)$.

$$\hat{\varepsilon} = \begin{pmatrix} \varepsilon_\parallel(y) & 0 & 0 \\ 0 & \varepsilon_\perp(y) & 0 \\ 0 & 0 & \varepsilon_\parallel(y) \end{pmatrix}, \quad \mu = \begin{pmatrix} \mu_\parallel(y) & 0 & 0 \\ 0 & \mu_\perp(y) & 0 \\ 0 & 0 & \mu_\parallel(y) \end{pmatrix}.$$

Let us transform initial Maxwell equations combined with material relations for this case. Equations give biorthogonality of the eigenfunctions and similarity of the operator to a self adjoint operator [15-16].

Maxwell equations can be transformed to equations for normal to dielectric layer electric and magnetic field components in isotropic [15-16] and anisotropic [17] cases.

*isheinman@yandex.ru

EXPERIMENTAL ANALYSIS OF DIPOLE MODES IN ELLIPTICAL CAVITY*

M. Lalayan, A. Orlov, Ya. Shashkov, N. Sobenin,
National Research Nuclear University MEPhI, Moscow, Russia

Abstract

The experimental measurements of transverse shunt impedance for higher order modes TM_{110} and TE_{111} for S-band elliptical cavity were carried out. The experiments using dielectric and metallic spheres as perturbing objects and with ring probe were done.

INTRODUCTION

While studying the accelerating structures besides the calculation of electrodynamic characteristics (EDCs) at operating mode and higher order modes (HOMs) it is important to determine these parameters experimentally.

Today a considerable number of universally acknowledged numerical simulation codes used for EDCs calculation is known. Possibilities of an experimental study are modest compared to the ones of simulation approach and depend on the availability of modern measuring equipment and methods.

The most well-known field measurement method is the small perturbation technique using dielectric and/or metal perturbing bodies of different shapes. This article presents the results of measurements of the transverse shunt impedance using this method. In addition to the known approaches [1-2] application of ring-type perturbing bead is considered [3].

CAVITY MODEL

All simulations were done using software to model of elliptical harmonic cavity without drift tubes [4]. Figure 1 shows the cavity cell geometry together with basic dimensions and illustrates principle of cavity design.

We considered two dipole modes TM_{110} and TE_{111}, as they are the most dangerous for beam dynamics.

There are two methods of calculating linear transverse shunt impedance $r_{sh\perp}$ [5]:

1. By using Panofsky–Wenzel (PW) theorem one could derive the following equation:

$$r_{sh\perp} = \frac{\int_0^l \frac{1}{k_z}\frac{\partial E_z}{\partial r} \exp(ik_z z)dz}{P_{loss}*l} \quad (1)$$

where k_z - longitudinal wave number, E_z – longitudinal component of the electric field, P_{loss} – power loss in the structure, r – transverse coordinate offset in the plane of the dipole polarization of the wave off the cavity axis, l – length of the structure.

2. The direct integration (DI) method based on the transverse components of the electric $E_y(z)$ and magnetic $H_x(z)$ fields calculation.

*Work supported by Ministry of Education and Science grant 3.245.2014/r

$$r_{sh\perp} = \frac{\left| ic*\mu_0*\int_0^l H_z(z)\exp(ik_z z)dz - \int_0^l E_y(z)\exp(ik_z z)dz \right|}{P_{loss}*l} \quad (2)$$

where c – speed of light , μ_0 – magnetic constant.

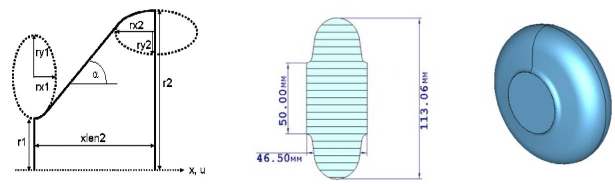

Figure 1: Geometry of elliptical harmonic cavity cell.

PERTURBING BODIES

Dielectric (DS), metallic (MS) spheres and metal wire loop probe as perturbing bodies were used for our research.

Table 1. Characteristics of Ceramic and Metallic Spheres

Parameter	simulation	experiment
Diameter, mm	1,8	1,8
DS form-factor k^E*10^{-20}, $(m^2\times s)$/Ohm	1,50	1,32
Electric constant	9,4	
MS form-factor k^E*10^{-20}, $(m^2\times s)$/Ohm	2,03	1,87
MS form-factor k^H*10^{-15}, $m^2\times s\times$Ohm	1,44	1,19

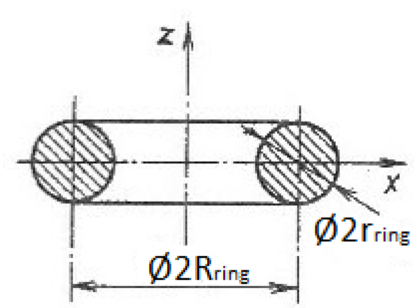

Figure 2: Geometry of ring probe.

Ring probe as bead for magnetic field and axially symmetric electric fields measurements is considered in [3]. Ring probe shape and dimensions are illustrated by

ISBN 978-3-95450-181-6

ELECTROMAGNETIC FIELD IN DIELECTRIC CONCENTRATOR FOR CHERENKOV RADIATION*

S.N. Galyamin†, A.V. Tyukhtin, V.V. Vorobev, A.A. Grigoreva, Saint Petersburg State University, St. Petersburg, Russia
E.S. Belonogaya, Saint Petersburg Electrotechnical University "LETI", St. Petersburg, Russia

Abstract

Recently we have reported on axisymmetric dielectric concentrator for Cherenkov radiation that focuses almost the whole radiation in the vicinity of the given point (focus) located on the trajectory of the charge [1]. Particularly, we have shown that this structure can increase the field up to two orders of magnitude. In this report we continue investigation of this concentrating target and analyse in more detail the field near the focal point depending on parameters of the target.

INTRODUCTION

Various dielectric targets are considered as candidates for development of modern non-invasive system of bunch diagnostics [2]. However, rigorous theory describing radiation processes for most of targets' geometries cannot be developed. Therefore, various approximate approaches are considered [3-6]. We have applied our original approach to calculate the shape of axisymmetric dielectric target concentrating most of generated Cherenkov radiation (CR) in a small vicinity of a focus point. We call this target "dielectric concentrator for CR" [1]. Here we proceed with investigation of this structure and perform analysis of the field components near the focal point.

THEORY

Figure 1 shows $x-z$ cut of the axisymmetric dielectric target with cylindrical channel (where a charge q passes) and specific form of the outer boundary. In the coordinate system shown in Fig. 1, this hyperbolic surface x_0, y_0, z_0 is determined as

$$\begin{aligned} x_0 &= \rho_0 \cos\varphi, \quad y_0 = \rho_0 \sin\varphi, \\ \rho_0 &= r(\theta)\sin\theta, \quad z_0 = z_f + r(\theta)\cos\theta, \end{aligned} \tag{1}$$

$$r(\theta) = f(1-n)\left[1+n\sin(\alpha+\theta)\right]^{-1}, \tag{2}$$

where r is a distance from $z = z_f$ to the surface, $n=\sqrt{\varepsilon\mu}>0$, $\sin\alpha=(n\beta)^{-1}$, $\beta = Vc^{-1}$ (V is a charge velocity and c is a speed of light in vacuum), f is a focal parameter, i.e. minimal distance from the focus to the surface, $f = r(3\pi/2-\alpha)$. For θ satisfying $\sin(\alpha+\theta) = -1/n$ we obtain $r\to\infty$, and this angle corresponds to the asymptote of hyperbola. In order to

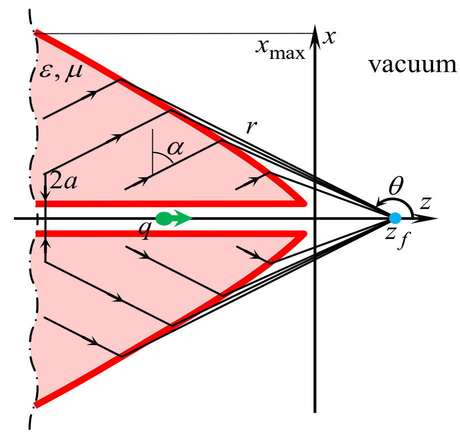

Figure 1: Geometry of concentrator ($x-z$ cut).

obtain the outer surface of the final target, we should take a piece of (2) for $\theta\in[\theta_{\min}, \theta_{\max}]$, where $\rho_0(\theta_{\max}) = a$ (a is a channel radius), $\rho_0(\theta_{\min}) = x_{\max}$, and rotate this piece over z axis. Length of the target $z_{\max}$ is

$$z_{\max} = z_0(\theta_{\max}) - z_0(\theta_{\min}) \,. \tag{3}$$

Consideration of the refracted rays shows that they converge exactly to the focus point, while ray optics formulas give divergent field magnitude [1]:

$$H_{\varphi\omega} \approx H^*_{\varphi\omega} T_{\|} \left|\frac{1}{1-l/r(\theta)}\right| \exp\left(\frac{i\omega}{c} l\right), \tag{4}$$

where l is a distance from the surface to the observation point along the ray, $T_{\|}$ is a Fresnel transmission coefficient,

$$T_{\|} = 2\cos\theta_i \left[\cos\theta_i + n\cos\theta_t\right]^{-1}, \tag{5}$$

and $H^*_{\varphi\omega}$ is the field at the inner side of the surface [7]:

$$H^*_{\varphi\omega} = \frac{iq}{2c}\eta s H_1^{(1)}\left(s\rho^*\right)\exp\left(i\frac{\omega}{\beta c}z^*\right), \tag{6}$$

$s=\omega(\beta c)^{-1}\sqrt{\varepsilon\mu\beta^2-1}$, $\operatorname{Im} s \ge 0$, $k = |\omega|(\beta c)^{-1}\sqrt{1-\beta^2}$,

$$\eta = \frac{-2i/(\pi a)}{\dfrac{(1-\varepsilon\mu\beta^2)}{(1-\beta^2)\varepsilon} I_1(ka) H_0^{(1)}(sa) + s I_0(ka) H_1^{(1)}(sa)}, \tag{7}$$

ρ^* and z^* are cylindrical coordinates of the ray start point at the surface. Since for the focus point there is an equality $l = r(\theta)$, we obtain divergence in (4).

*Work supported by the Grant of the President of Russian Federation (No. 6765.2015.2) and the Grant from Russian Foundation for Basic Research (No. 15-32-20985).
† s.galyamin@spbu.ru

ISBN 978-3-95450-181-6

ELECTRON BEAM STABILITY IN THE ENERGY RECOVERY LINAC FOR THE LITHOGRAPHIC FREE ELECTRON LASER*

Ya.V.Getmanov#, N.A. Vinokurov, O.A. Shevchenko, Budker INP, Novosibirsk, Russia

Abstract

According to microelectronic production leaders the lithography based on the free electron laser (FEL) could become the main technology for the elements mass production with scale to 5 nm in the nearest future. One of the main problem is the absence of the working FEL with required parameters. The feasibility study of those FEL based on superconducting energy-recovery linac (ERL) was made in Budker INP. The ERL average current is limited by longitudinal and transverse instabilities, caused by interaction between electron beam and its induced fields in the superconducting cavities. The estimations of the threshold currents and ERL parameters were made.

INTRODUCTION

The feasibility study of high power radiation source for the lithographic applications has been discussed the last decade [1-2]. Using Free Electron Laser (FEL) based on multiturn Energy Recovery Linac (ERL) looks promising for this challenge due to high power radiation and energy efficiency in comparison to another machine types. For the industry application it is necessary to have high power laser radiation and therefore high average electron current and energy in the ERL. For the high energy of the electron beam is the most suitable to use the superconducting radio-frequency system (SRF).

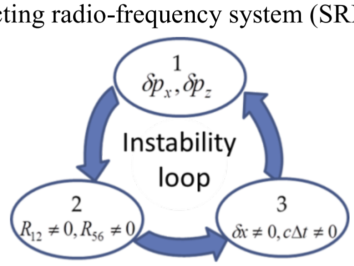

Figure 1: The threshold instability loop.

One of the main problems of the accelerator based on superconducting RF-cavities is the interaction between electron beam and long-living RF-field modes. This phenomenon could cause the degradation of the beam quality and moreover could limit the maximum achievable electron average current. Cavity modes could be spatially divided on transverse and longitudinal by the additional electron momentum obtaining. There is no fundamental difference in mechanics of the instabilities growth between them (Fig. 1): 1 – electron bunch passes through the cavity and gains additional momentum deviation from exited dipole or fundamental RF field modes; 2 – at the magnetic structure momentum deviation transforms to the coordinate, if the appropriate transport matrix elements are nonzero; 3 – electron bunch returns to the cavity and closes the instability loop enhancing dipole and deflecting fundamental RF modes.

ACCELERATOR SCHEME

The using of multiturn ERL scheme reduces the total cost of the facility. The experience with Novosibirsk multiturn ERL (NovoFEL) [3] shows one of the disadvantages the scheme with one accelerating structure. The adjusting of the electron-optical system is complicated by simultaneously pass of accelerating and decelerating beams with different energy spread due to FEL lasing. Therefore it was considered to use the scheme with separated acceleration structure (Fig. 2) [2, 4-5]. The main advantage of such structure is the possibility to independently adjust the arcs optic system for two types of beam. Principle of operation is the following: electrons from injector 1 pass to the pre-linac 2, are accelerated two times in linacs 3, are used in undulator 5, then in decelerating phase follow to the linacs, return energy to thee RF fields and drop to the dump 7. The wavelength of the first harmonic undulator radiation determines the maximum electron energy 800 MeV. For increasing the threshold value and more effective focusing it was considered to have different energy gain at main linacs 100 MeV and 275 MeV while the preliminary linac energy is 40 MeV.

TRANSVERSE STABILITY

All along of unbound arcs optical system main linacs can be considered independently. Therefore due to lower electron energy the lower threshold current is expected in the first main linac. The RF system of the first linac consists of 10 nine cell cavities with accordingly nine horizontal dipole modes. Consequently there are 90 horizontal dipole modes determine the threshold current. To determine the lowest values of the quality it was used the same parameters for the all modes $Q=5\cdot 10^4$, $\rho=100$ *Ohm*.

The threshold current can be estimated using the ultra-relativistic approximation for non-overlapped modes of the accelerating structure. For the multiturn ERL it is given by

$$I_{th} = -2\frac{m_0 c^3}{e}\frac{1}{\omega_m\left(\frac{R_{sh}}{Q}\right)_m Q_m \sum_{k=1}^{2N-1}\sum_{n=k+1}^{2N} M_{12}^{kn}\sin\left(\omega_m\left(T_n - T_k\right)\right)}, \tag{1}$$

where c, m_0, e – speed of light, mass and charge of the electron, ω_m, $R_{sh,m}$, Q_m – frequency, shunt impedance and quality of the cavity dipole mode with number m, T_n is the time of the n-th pass through the cavity.

* Work supported by Russian Science Foundation project N 14-50-00080.
#y_getmanov@mail.ru

ISBN 978-3-95450-181-6

FORM-FACTOR DETERMINATION OF AN ARBITRARY BUNCH SEQUENCE FOR THE COHERENT RADIATION CALCULATION*

D. A. Shkitov#, A. E. Harisova, Tomsk Polytechnic University, Tomsk, Russia

Abstract

The approach how to calculate the form factor of an arbitrary bunch sequence is developed and described in this report. The form factors for different beam parameters of LUCX facility (KEK, Japan) are calculated and discussed.

INTRODUCTION

It is well known that the coherent effect occur when charged particles in a bunch radiate in phase [1]. This is accompanied by a quadratic increase in the radiation intensity and significantly influences the radiation spectrum. The coherent radiation is characterized by a form factor, which is the coefficient mainly depending on the ratio of bunch dimensions to the observed radiation wave length. The form factors will be different for the synchrotron and transition radiation because of their different nature of radiation. Now electron accelerators that produced beams with a sub-picosecond bunch length and a picosecond distance between them already exist [2]. Through the appearance of interference between radiation from such a sequence of bunches, the total intensity is no longer equal to the sum of radiation from each bunches [3, 4]. For this reason, it is essential to determine the form factor of an arbitrary electron bunch sequence. Herein the uniform bunch distribution will be the special case. One of the examples, how such a radiation from sequence can be used, is represented in [5, 6]. In this report we describe an approach to obtaining the form factor of arbitrary bunch sequence.

COHERENT RADIATION

The total radiation from a bunch of charged particles is generally considered consisting of incoherent and coherent part. Following to Ref. [7], these parts may be derived by way which described below. Assuming that electromagnetic field does not depend on the coordinates of individual particles in the bunch, we may write an expression of total bunch field as:

$$E_R = \sum_{i=1}^{N} E_i = \sum_{i=1}^{N} E_0\, e^{i\Delta\varphi_i} = E_0 \sum_{i=1}^{N} e^{i\Delta\varphi_i}$$

Where E is an electric component of radiation field and $\Delta\varphi$ is a radiation phase shift. Throughout this report all of E and $\Delta\varphi$ are the functions of $E(r,\omega)$ and $\Delta\varphi(r,\omega)$ respectively. Further the radiation intensity from the single bunch is written as:

$$\frac{d^2W}{d\omega d\Omega} = cR^2 E_R E_R^* = cR^2 |E_R|^2 \sum_{i=1}^{N} e^{i\Delta\varphi_i} \sum_{j=1}^{N} e^{-i\Delta\varphi_j} = \frac{d^2W_0}{d\omega d\Omega} \cdot \Sigma$$

Where R is the distance to an observation point, $\frac{d^2W_0}{d\omega d\Omega}$ is the radiation intensity from single particle and sign (*) is a complex conjugate. Let's divide the sum term Σ into two parts. First part Σ_{inc}, when $j = i$, is responsible for the incoherent radiation:

$$\Sigma_{inc} = \sum_{i=1}^{N} 1 = N$$

Second part Σ_{coh}, when $j \neq i$, is responsible for the coherent radiation:

$$\begin{aligned}\Sigma_{coh} &= \sum_{i=1}^{N} e^{i\Delta\varphi_i} \sum_{\substack{j=i \\ j\neq i}}^{N} e^{-i\Delta\varphi_j} \\ &= \sum_{i=1}^{N} \int e^{i\Delta\varphi_i}\, \delta(r - r_i) dV \\ &\cdot \sum_{\substack{j=1 \\ j\neq i}}^{N} \int e^{-i\Delta\varphi_j}\, \delta(r' - r_j) dV' \\ &= \int e^{i\Delta\varphi_i} \sum_{i=1}^{N} \delta(r - r_i) dV \\ &\cdot \int e^{-i\Delta\varphi_j} \sum_{\substack{j=1 \\ j\neq i}}^{N} \delta(r' - r_j) dV'\end{aligned}$$

Where δ is the Dirac function. In the transformations we employ the integral property of Dirac function. We have also introduced the notation: $\sum_{i=1}^{N} \delta(r - r_i) = N\rho(r)$ and $\sum_{\substack{j=1 \\ j\neq i}}^{N} \delta(r' - r_j) = (N-1)\rho(r')$, here ρ is spatial distribution of the particles in the bunch. When $N \gg 1$ we have $\rho(r) \approx \rho(r')$, then:

$$\Sigma_{coh} = N(N-1) \int e^{i\Delta\varphi}\, \rho(r) dV \cdot \int e^{-i\Delta\varphi}\, \rho(r') dV' = N(N-1) f(\omega) \cdot f^*(\omega)$$

Where $f(\omega) = \int e^{i\Delta\varphi}\, \rho(r) dV$ is the geometric form factor of the bunch. After all transformations we will obtain a general expression for the radiation intensity in the following form:

$$\frac{d^2W}{d\omega d\Omega} = [N + N(N-1) \cdot |f(\omega)|^2] \frac{d^2W_0}{d\omega d\Omega}$$

RADIATION FROM BUNCH SEQUENCE

Further we consider the radiation from the irregular sequence of identical electron bunches which moving along

* Work was partially supported by the grant of the President of Russian Federation No SP-261.2015.2.
#shkitovda@tpu.ru

ISBN 978-3-95450-181-6

FIRST ORDER PERTURBATION THEORY EVALUATION OF INITIAL STAGE OF SELF AMPLIFIED CRYSTAL-BASED X-RAY EMISSION

A. Benediktovitch, Belarusian State University, Minsk, Belarus *

Abstract

Mechanisms of x-ray generation by relativistic electrons in the energy range below 100 MeV by interaction with crystals are discussed in view of possibility to obtain self amplification of spontaneous emission. To investigate the initial stage of self amplified spontaneous emission process the first-order perturbation theory that enables to describe the collective beam response as effective susceptibility is used. Based on this approach Cherenkov radiation in the anomalous dispersion frequency range, parametric x-ray radiation and axial channeling radiation mechanisms are considered. The axial channeling mechanism in the case of grazing incidence electrons was shown to be most promising one.

INTRODUCTION

X-ray Free Electron Lasers (XFELs) open new revolutionary opportunities for investigations in materials science, chemistry, biology and other areas. However, due to high cost of construction and maintain, the access to these facilities for wide scientific community is quite limited. This motivates search for schemes of compact bright x-ray sources. The size of X-ray Free Electron Lasers is dictated by basic properties of undulator radiation: to produce x-rays with Angstrom wavelength from cm period undulator one needs electrons with energy in GeV range. If one considers the radiation mechanisms accompanying the propagation of electron beam through a crystal structure (channeling radiation, parametric x-ray radiation, Cherenkov radiation near K-edge), one can see that to get photons in x-ray range one needs electrons with energy of tens to hundreds MeV. The dramatic 10 orders of magnitude increase of brightness of XFELs compared to III generation synchrotron became possible due to phenomenon of self amplified spontaneous emission (SASE). In the case of XFELs the spontaneous emission which is amplified is the undulator radiation, the SASE process being developed due to high charge, short duration and small emittance of the bunch as well as long undulator length. In the present paper we will investigate the possibility of SASE process for which as a spontaneous radiation mechanisms serve x-ray radiation mechanisms in crystals. The development of rigorous SASE theory in this case is extremely difficult task due to large number of phenomena accompanying electron propagation in crystals and complexity of SASE phenomena itself, however, one can use the first order perturbation theory to describe the first stage of SASE process [1] and determine the most promising radiation mechanism and experiment geometry.

* andrei.benediktovitch@atomicus.by

RADIATION MECHANISMS

One of the ways to find at which conditions x-ray radiation of electrons in crystal will take place is to find phase match between the electromagnetic field that can exist in the crystal and current of electron in the crystal. In the Fourier space this condition can be expressed as intersection of dispersion surface of electromagnetic radiation

$$k^2 - \frac{\omega^2}{c^2}(1+\chi(\omega)) = 0 \tag{1}$$

here $\chi(\omega)$ is the susceptibility of the crystal; and condition that should be satisfied for Fourier components of a single electron current

$$\omega - \vec{k}\cdot\vec{v} = 0 \tag{2}$$

here $\vec{v}$ is the velocity of electron. In order to organize intersection of (1) and (2) one can act in two ways: either modify properties of the medium to bring (1) in intersection with (2), or modify the movement of the electron and correspondingly (2) to bring it in intersection with (1). Let us name the first scenario as case I and the second as case II.

In the x-ray domain for electrons in crystals case I can be realized if Re$\chi(\omega) > 0$ that leads to Cherenkov radiation, or under the Bragg diffraction conditions under which dispersion equation (1) is modified to

$$\left[k^2 - \frac{\omega^2}{c^2}(1+\chi_0)\right]\left[(\vec{k}+\vec{H})^2 - \frac{\omega^2}{c^2}(1+\chi_0)\right] - \chi_{\vec{H}}\chi_{-\vec{H}}\frac{\omega^4}{c^4} = 0 \tag{3}$$

here $\vec{H}$ is the reciprocal lattice vector for which the Bragg condition $(\vec{k}+\vec{H})^2 = k^2$ is satisfied, $\chi_{\vec{H}}$ is the spatially periodic part of the susceptibility corresponding to crystallographic planes with reciprocal lattice vector $\vec{H}$, the polarization in the plane orthogonal to vectors $\vec{k}$, $\vec{H}$ is considered for simplicity. Under the conditions of intersection of (3) with (2) parametric x-ray radiation takes place.

The case II can be realized if one introduce oscillatory component in the electron current. In the case of relativistic electrons in the crystal, the oscillatory component can appear if the electron goes into the channeling regime, in this case (2) is modified to

ISBN 978-3-95450-181-6

PRODUCTION OF INTENSE BEAMS OF IRON IONS FROM ECR ION SOURCES BY MIVOC METHOD AT THE CYCLOTRON DC-60

A.E. Bondarchenko, K.I. Kuzmenkov, V.N. Loginov, Joint Institute for Nuclear Research, FLNR, Dubna, Russia
V.V. Alexandrenko, A.A. Amirova, M.V. Zdorovets, Astana branch of Institute of Nuclear Physics, Astana, Kasakhstan
I.A. Ivanov, E.K. Sambayev, A.E. Kurahmadov, S.G. Kozin, D.B. Kadyrzhanov, Astana branch of Institute of Nuclear Physics, Astana, Kasakhstan and Eurasian National University named after L.N. Gumilyov, Kazakhstan
A.E. Ryskulov, Eurasian National University named after L.N. Gumilyov, Kazakhstan

Abstract

The article describes the experiments carried out in 2015 at the accelerator complex DC-60 of Astana branch of the INP (Alma-Ata, Kazakhstan Republic), to develop methods for production of intense beams of multi charged ions of iron with the use of volatile compounds (Metal Ions from Volatile Compounds) – MIVOC [1]. As a result of performed work for the first time at DC-60 cyclotron a beam of iron ions was obtained, acceleration mode of $^{56}Fe^{10+}$ ions to the energy of 1.75 MeV/n was optimized

PRODUCTION OF IONS $^{56}Fe^{10+}$ USING VOLATILE COMPOUNDS MIVOC

For production of the iron ions from the ECR ion source DECRIS-3 [2] the ferrocene compound $Fe(C_5H_5)_2$ was used as a working substance. The working substance was put into the metallic container, which was connected to the ECR source via piezoelectric leak valve SNA-2.

The smoothly opening of the piezoelectric leak valve allows the injection of molecular flow of substance into the source. If the substance flow is not sufficient for stable source operation, helium can be used as a support gas. After optimization of the ECR ion source settings the following results were obtained: 50 eμa of Fe^{9+} ions, and 15.6 eμa of Fe^{10+} ions.

Figure 1 shows charge state distribution of iron ion beam, obtained after the bending magnet of the axial injection system of the DC-60 cyclotron, source settings being optimized for the production of Fe^{10+}.

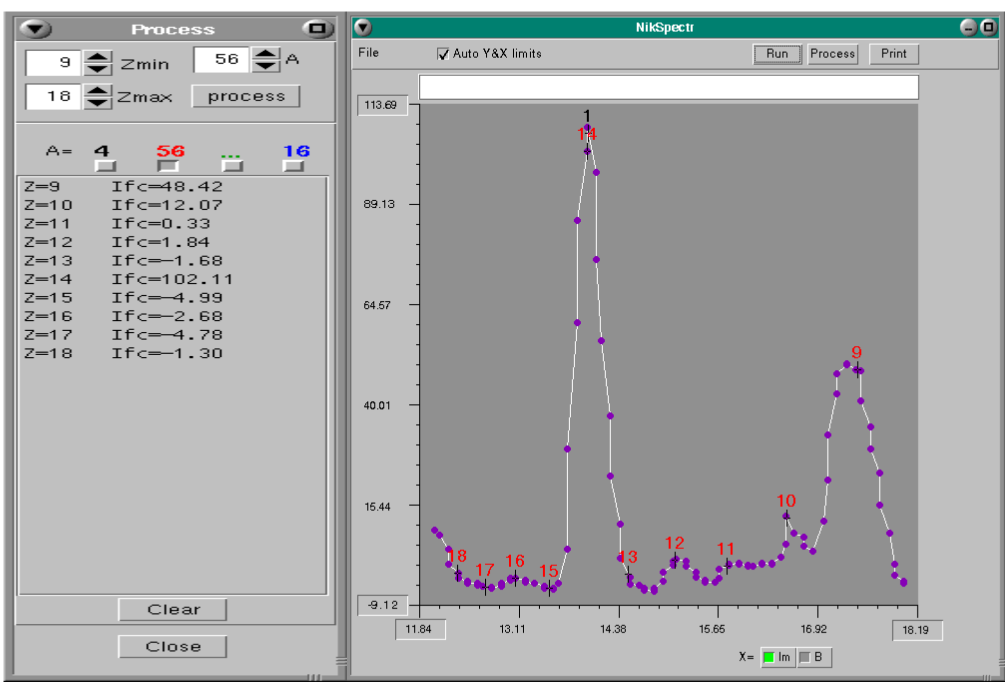

Figure 1: Charge spectrum of iron ions produced by the DECRIS-3 ion source. The position of Fe^{14+} ions coincides with the position of C^{3+} ions.

ISBN 978-3-95450-181-6

PRODUCTION OF INTENSE METAL ION BEAMS FROM ECR ION SOURCES USING THE MIVOC METHOD

A. E. Bondarchenko, S. L. Bogomolov, K.I. Kuzmenkov, V.N. Loginov, V.Ya. Lebedev, JINR, Dubna, Moscow Region, Russia
Z. Asfari, B. JP. Gall, IPHC, Strasbourg Cedex 2, France

Abstract

The production of metal ion beams by electron cyclotron resonance (ECR) ion sources using the MIVOC (Metal Ions from Volatile Compounds) method [1] is described. The method is based on the use of metal compounds which have high vapor pressure at room temperature, e.g., $C_2B_{10}H_{12}$, $Fe(C_5H_5)_2$, etc. Intense ion beams of B and Fe were produced using this method at the FLNR JINR cyclotrons. Experiments on the production of cobalt, chromium, vanadium, germanium, and hafnium ion beams were performed at the test bench of ECR ion sources.

Main efforts were put into production and acceleration of ^{50}Ti ion beams at the U-400 cyclotron. The experiments on the production of Ti ion beams were performed at the test bench using natural and enriched compounds of titanium $(CH_3)_5C_5Ti(CH_3)_3$. All these efforts allowed the production of accelerated titanium and chromium ion beams at the U-400 cyclotron.

PRODUCTION OF METAL IONS USING THE MIVOC METHOD

The experiments on the production of chromium, cobalt, vanadium, nickel, and hafnium ion beams were performed using the DECRIS-2m (Dubna ECR ion source) source [2] installed at the test bench. Natural compounds $Cr(C_5H_5)_2$, $Co(C_5H_5)_2$, $V(C_5H_5)_2$, $Ni(C_5H_5)_2$, and $(C_5H_5)_2Hf(CH_3)_2$ were used as working substances. For the production of germanium ions, two compounds were tested, i.e., tetraethylgermane $Ge(CH_2CH_3)_4$ and tetramethylgermanium $Ge(CH_3)_4$. Experiments with tetramethylgermanium yielded better results. The results obtained at the test bench are presented in Table 1.

Table 1. The intensity (eμA) of metal ion beams produced at the test bench using the MIVOC method (* - intensity optimisation)

Z	5+	6+	7+	8+	9+	10+	11+	12+	13+
Fe		43	93	125	172	145*	114	73	45
Co		57	80	86	98		82*	25	
Cr	50	70*	60	37	17	7			
V	75*	54	41	54	55.5*	43	34	19.5	
Ni		45*	43	48	53*		30	10	
Ge			43*	54		47*			
Z	**13+**	**14+**	**16+**	**17+**	**18+**	**19+**	**20+**		
Hf	31	45	50*	45*	36	27	17		

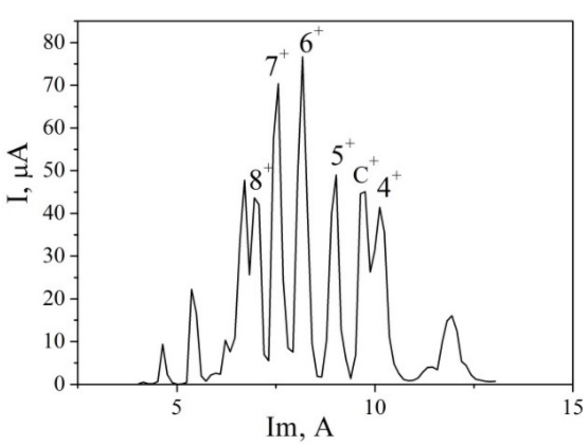

Figure 1. Charge spectrum of chromium ions produced by the ECR4M source.

After the tests ^{48}ti and ^{52}cr ions were accelerated at the u-400 cyclotron for the experiments on fission physics using the $c_5(ch_3)_5ti(ch_3)_3$ and $cr(c_5h_5)_2$ compounds as a working substances. the stable beams of ti^{5+} and cr^{6+} were produced during three weeks experiments.

Figure 1 shows charge state distribution of chromium ion beam, obtained after the bending magnet of the axial injection system of the u-400 cyclotron, source settings being optimized for the production of cr^{6+}.

ISBN 978-3-95450-181-6

COMPARATIVE RESEARCH OF LOW ENERGY BEAM TRANSPORT SYSTEMS FOR H-MINUS ION BEAM

B.A.Frolov, National Research Centre "Kurchatov Institute" State Research Center of Russian Federation – Institute for High Energy Physics, Protvino, Moscow Region, Russia
V.S.Klenov, Institute for Nuclear Research, Russian Academy of Science, Moscow, Russia

Abstract

The source of H-minus ions for the injection in LU-30 accelerator is constructed in IHEP. A three-dimensional simulation code IBSimu (Ion Beam Simulation) has been utilized for modeling of the transport and matching system of beam from the H-minus ion source into RFQ. A magnetic low energy beam transport (LEBT) line consisting of two solenoids and LEBT consisting of six magnetic quadrupole lenses were analyzed. The particle data from the 50 mA 100 keV ion beam extraction system simulations were taken as the starting data for the LEBT simulations. The final aim of calculations was to achieve the required Twiss parameters and to minimize emittance growth of beam at RFQ entrance. LEBT consisting of two solenoids is more convenient in adjustment and as simulation results have shown this system offers more acceptable beam characteristics at the match point in comparison with LEBT composed of quadrupole lenses.

INTRODUCTION

The collaboration of IHEP and INR is developing the source of H-minus ions for injection in the linear accelerator LU-30. The implementation of the negative ion source as the linear accelerator injector and the organization of multi-turn charge-exchange injection at the circular accelerator exit U-1.5 (buster) will allow to several times raise the intense of the IHEP acceleration complex. This will provide new possibilities for fundamental research and applied studies. For charge-exchange injection implementation the source generating H-minus ion beams with the following parameters: current ≥ 50 mA, pulse duration – 25 μs, repetition rate - 25 Hz, energy of ions -100 keV, normalized rms emittance ≤ 0.25 π mm·mrad, e/H^- ratio < 5 is being developed. The surface-plasma source with the Penning gas-discharge chamber with axially symmetric emission aperture at the ion source exit was chosen as a source of H-minus ions. The three-electrode ion-optical system (IOS) was simulated with 3D code IBSimu [1] to extract H-minus ions from plasma, form beam and accelerate it up to the energy of 100 keV in [2].

At the LU-30 accelerator entrance the ion beam with the energy of 100 keV should have the following parameters: normalized 4•rms emittance (for the 50 mA beam current) $\varepsilon \leq 1\pi$ mm·mrad and Twiss parameters of phase ellipse α=2.3, β=0.14. In [2] as a first approximation the beam transportation through the two solenoid matching channel to the RFQ entrance was simulated with by code TRACE-2D. Matching channel calculations done with the help of TRACE-2D do not take into consideration the fields distribution and space charge and do not allow to evaluate the beam emittance growth at its transportation to RFQ. In the current work the 3D modelling of the whole system including three-electrode IOS and two-solenoid LEBT with consideration of real field distribution for the 50 mA beam current was done with the help of code IBSimu. The matching channel consisting of the magnetic quadrupole lenses was examined. For the quadrupole lenses channel it resulted hard to provide the beam matching with the accelerator entrance because of considerable angle divergence which the beam acquires at the drift length before the channel entrance. IOS consisting of five electrodes was projected to reduce the radius and the beam divergence angle at the matching channel entrance.

IOS OF BEAM EXTRACTION AND ACCELERATION TO 100 KEV

The three-electrode IOS of H-minus ions extraction is formed by plasma, extraction and acceleration electrodes. Plasma electrode works as gas discharge anode and is at the impulse potential of 100 kV. The extraction electrode potential is +20 kV relative to the plasma electrode, acceleration electrode is ground. Emission aperture with 3 mm diameter was selected upon analog of the version of the penning source developed in BINP SB RAS [3]. The selection of the three-electrode IOS optimal geometry (radii of extraction (2 mm) and acceleration (2 mm) electrodes and lengths of extracting (3.3 mm) and accelerating (7.5 mm) gaps) was done [1] basing on a series of detailed calculation under the condition of getting minimal emittance at the matching channel entrance. 3D modeling and IOS optimization was carried out with the help of code IBSimu taking into account scattered transverse magnetic field of penning discharge for the H-minus beam current of 50 mA with the co-extracted electrons current of 150 mA.

IOS variants with additional electrodes with accelerating or decelerating potential were investigated to reduce the radius and divergence angle of the beam at matching channel entrance and to extend IOS focusing capacities. The optimal variant which ensured minimal emittance growth in such a system consisting of five electrodes with the potential of 0 kV - 20 kV - 100 kV - 50 kV – 100 kV (in the line of beam) is demonstrated in fig.1. The first three electrodes have the same geometry (diameters and gaps) as those in the 3-electrode IOS. The radius of the forth electrode is 2.5 mm and the distance from it to the third and fifth electrodes is 4 mm. The ion source magnetic field with the induction of around 0.1-

ISBN 978-3-95450-181-6

MODELING OF TRIODE SOURCE OF INTENSE RADIAL CONVERGING ELECTRON BEAM

V. Altsybeyev *, V. Engelko, A. Ovsyannikov, D. Ovsyannikov, V. Ponomarev
Saint-Petersburg State University, 7/9 Universitetskaya nab., St. Petersburg, 199034 Russia
R. Fetzer, G. Mueller
Karlsruhe Institute of Technology, Institute for Pulsed Power and Microwave Technology,
PO Box 3640, 76021 Karlsruhe, Germany

Abstract

The considered source of triode type produces intense radial converging electron beam for irradiation of cylindrical targets. As an electron emitter an explosive plasma cathode is used. The role of initial transverse velocities of electrons, defocusing effect of the controlling grid, the beam self-magnetic field, electron and ion emission from the controlling grid, backscattering of electrons and ion flow from the target is analyzed. Conditions for achieving required electron beam parameters (the electron kinetic energy - 120 keV, the beam energy density on the target 40 J/cm^2 on a maximum possible length of the target surface) were determined.

INTRODUCTION

In ref.[1] the design of the electron source of triode type producing an intense radial converging electron beam employed for modification of the outer surface of cylindrical targets (such, for example, as fuel element claddings) is described. In this paper we performed the set of numerical simulations and try to analyze the following physical effects arising in the considered source: the role of the initial transverse velocity of electrons, defocusing effect of the controlling grid, the beam self-magnetic field, backscatter of electrons, ion flow from the target. Using obtained results one can can determine the source parameters that ensures stable operation mode and conditions for achieving the required beam energy density on the target ~ 40 J/cm^2 per 40-60 μs impulse. For numerical particle-in-cell simulations [2] the DAISI code will use [3–8].

SCHEME OF THE SOURCE

The electron source consists of the outer cylindrical cathode, anode and controlling grid [1]. The values of the main parameters are presented in Table l.

Table 1: Parameters of the Source

Cathode length, m	$L = 0.98$ m
Cathode radius, m	$r_c = 0.15$ m
Grid radius, m	$r_g = 0.1$ m
Anode/Target radius, m	$r_a = 0.005$ m
Cathode-grid voltage, V	$U_{cg} = 20 - 40$ kV
Cathode-anode voltage, V	$U_{ca} = 80 - 140$ kV

* v.altsybeev@spbu.ru

In the new source design a multi-arc plasma cathode is applied. At such a cathode plasma is produced by a vacuum arc discharge provided by a large number of discharge gaps equally spaced on the cathode area. The space occupied by the plasma is separated from an external electric field by a separating grid. Such cathode design allows to control the value of the emission current density and to reduce the initial angular spread of electrons.

STABLE AND UNSABLE OPERATION MODES

We performed a set of simulations for different cathode–grid and cathode–anode voltages, for monopolar electron flow and bipolar electron and ion flows, for different grid electrode radius. Main results are the following. For each grid radius and cathode–anode voltage there is a critical value of the cathode-grid voltage U_{cr} dividing the mode of the source operation for stable and unstable regime (Fig. 1. As an example, $U_{cr} = 25$ kV for the grid radius $r_g = 0.1$ m and $U_{ca} = 120$ kV. If U_{cg} is less than or equal to the critical value the source operates stably, electron and ion trajectories are laminar, currents reach their stable magnitudes within several tens of nanoseconds, and the distribution of the power density on the target length 0.75 m is sufficiently homogeneous, as it is seen from.

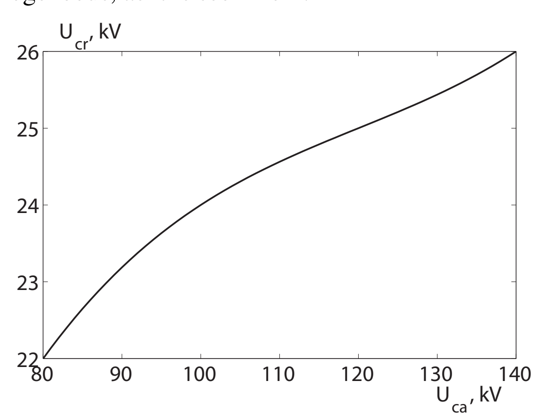

Figure 1: Dependence of U_{cr} on U_{ca} for $r_g = 0.1$ m.

When the cathode–grid voltage exceeds the critical value the source operation is unstable, electron and ion currents do not reach stable magnitudes, particle flows are not laminar. Under the influence of the beam self magnetic field electrons move from the edges of the source to its central part, which leads to inhomogeneity of the power density

ISBN 978-3-95450-181-6

THE ELECTRON TRAJECTORIES CONSTRUCTION IN THE SYSTEM WITH A "REAL" GEOMETRY OF THE FIELD CATHODE

A. Yu. Antonov*, Saint Petersburg State University, Saint Petersburg, Russia
M. I. Varayun†, Saint Petersburg Electrotechnical University "LETI", Saint Petersburg, Russia

Abstract

The problems of the trajectories constructing for field electrons and emission images simulation are considered. As an approximation of the emitter shape an explicitly and implicitly defined surfaces are selected. Hyperboloidal, ellipsoidal and paraboloidal models are studied. Also an equipotential surface of the charged sphere-on-orthogonal-cone system is used. A simple solution of the field distribution problem is allowed to formulate the Cauchy problem for the motion equations. The shape of the anode (the projector microscope screen) can be selected in any desired form. Achieving a screen by electrons is performed with dense output technique in numerical approach to the solution. The distribution of the work function on the cathode surface is obtained. The trajectories for the projection of the field emission activity as the image are used.

INTRODUCTION

The phenomenon of field electron emission is a recognized tool for the analysis of electron sources. These sources are necessary for accelerating technology and for high-precision microscopes. Surface shape, distribution of the force field in the interelectrode space and the cathode material affect emission main characteristics. Advanced emitters search will be more relevant for a long time [1].

In this paper the number of the tasks required to build emission images are considered. Emission images show the current density distribution on the surface of the cathode. The source itself and the work function maps modeling, and the construction of electron trajectories in diode systems with elements of a statistical approach are performed.

PHYSICAL AND MATHEMATICAL MODELS

To initiate a field electron emission at low voltages V, sources are often made in the form of tips (figure 1).

Figure 1: Shapes of the real cathodes ([2], [3] and [4]).

* a.antonov@spbu.ru
† m.varayuan@spbu.ru

As the approximation of the emitter surface the part of the two-sheeted hyperboloid, prolate ellipsoid of revolution, paraboloid of revolution and sphere-on-orthogonal-cone system are utilized.

As emission control parameters of the system the radius of curvature r_0 at the top of the cathode, the distance d from the top of the cathode to the anode (screen), the voltage V between the electrodes are considered. As the example the following values were used: $r_0 = 1.00$ μm, $d = 2.00$ cm, $V = 20.0$ kV.

RESULTS AND DISCUSSION

The potential distribution is found by solving the Laplace equation. It exists in an analytical form for all of the systems in question [3], [5]. It leads us to the determination of the force field structure in the gap between the electrodes. For the example the picture of the field in the system with the paraboloidal tip is presented (figure 2).

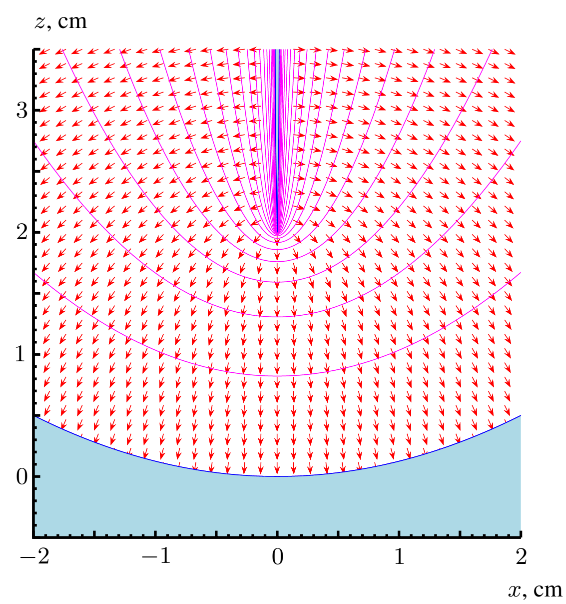

Figure 2: Equipotentials and force field.

For a single crystal cathode it is important to have an idea of the work function Φ distribution of on its surface. In the metal samples case the semi-empirical model proposed in [6] is well established:

$$\Phi = A + B\Delta t.$$

Here A and B must be found by linear regression method with the experimental data. Parameter Δt depends on the type of crystal lattice and Miller indices. The model has

ISBN 978-3-95450-181-6

THE INFINITELY THIN FIELD EMITTER MATHEMATICAL MODELING

E.M. Vinogradova*, N.V. Egorov, E.V. Kalaturskaja,
Saint Petersburg State University,
7/9 Universitetskaya nab., St. Petersburg, 199034 Russia

Abstract

In this work an axisymmetric diode electron-optical system based on a field emitter is simulated. The field emitter in the form of a thin filament of finite length is located on the flat substrate with the dielectric layer. The anode is a plane. The electrostatic potential distribution was found in an analytical form — in the form of Fourier-Bessel series in the whole area of the system under investigation. The coefficients of Fourier-Bessel series are the solution of the system of linear equations with constant coefficients.

INTRODUCTION

The field emitters as a nanostructured materials with nanometer-scale sharp tips are extensively applied in the various domains of nano-scale electronic devices [1]– [3].

This article is devoted to the modeling of the axially symmetric emission diode system on the field emitter basis [4]. The field emitter is a thin filament of finite length on the flat substrate [5]. The cathode substrate is coated with a dielectric layer. The anode is a plane. Fig. 1 shows a schematic representation of the diode system. The potentials of the emitter and substrate are zeros.

To find the distribution of the electrostatic potential $U(r,z)$ the variable separation method in the cylindrical coordinates (r,z) for the axially symmetric system is used [6].

The problem parameters:

$r = R_1$ — the radius of the system region,

$z = 0$ $(0 \le r \le R_1)$ — the surface of the emitter substrate,

$z = Z_1$ $(0 \le r \le R_1)$ — the boundary between two dielectrics,

Z_2 — the emitter length,

$z = Z_3$ $(0 \le r \le R_1)$ — the anode surface,

$U(r,0) = 0$ $(0 \le r \le R_1)$ — the boundary condition at the substrate,

$U(0,z) = 0$ $(0 \le z \le Z_2)$ — the boundary condition at the emitter,

$U(R_1,z) = f_1(z)$ $(0 \le z \le Z_3)$ — the boundary condition at the surface $r = R_1$,

$U(r,Z_3) = f_2(r)$ $(0 \le r \le R_1)$ — the boundary condition at the anode.

* e.m.vinogradova@spbu.ru

MATHEMATICAL MODEL

The electrostatic potential distribution $U(r,z)$ is the solution of the boundary value problem for the Laplace equation

$$\begin{aligned}
&\triangle U(r,z) = 0;\\
&U(r,0) = 0, \quad 0 \le r \le R_1;\\
&U(0,z) = 0, \quad 0 \le z \le Z_2;\\
&U(R_1,z) = f_1(z), \quad 0 \le z \le Z_3;\\
&U(r,Z_3) = f_2(r), \quad 0 \le r \le R_1.
\end{aligned} \tag{1}$$

The conditions on the the boundary $z = Z_1$ between two dielectrics with the the dielectric constants ε_1 and ε_0 can be written as:
— continuity conditions of the potential distribution

$$U(r,z)\Big|_{Z_1-0} = U(r,z)\Big|_{Z_1+0}, \tag{2}$$

— the normal derivative of the electric displacement vector continuity conditions

$$\varepsilon_1 \frac{\partial U(r,z)}{\partial z}\Big|_{Z_1-0} = \varepsilon_0 \frac{\partial U(r,z)}{\partial z}\Big|_{Z_1+0}. \tag{3}$$

SOLUTION OF THE BOUNDARY – VALUE PROBLEM

To solve the boundary value problem (1)–(3) the interior of the diode system can be divided into three subdomains:

1 — $(0 \le r \le R_1,\ 0 \le z \le Z_1)$ with dielectric constants ε_1,

2 — $(0 \le r \le R_1,\ Z_1 \le z \le Z_2)$ with dielectric constants ε_0,

3 — $(0 \le r \le R_1,\ Z_2 \le z \le Z_3)$ with dielectric constants ε_0.

Then the potential distribution $U(r,z)$ for $0 \le r \le R_1$ can be represented as:

$$U(r,z) = \begin{cases} U_1(r,z), & 0 \le z \le Z_1,\\ U_2(r,z), & Z_1 \le z \le Z_2,\\ U_3(r,z), & Z_2 \le z \le Z_3. \end{cases} \tag{4}$$

ISBN 978-3-95450-181-6

SIMULATION OF S-BAND RF GUN WITH RF BEAM CONTROL

A. Barnyakov, A. Levichev, D. Nikiforov, BINP SB RAS, Novosibirsk, Russia
M. Maltseva, NSU, Novosibirsk, Russia

Abstract

The RF gun with RF control is discussed. It is based on the RF triode and two kinds of the cavities. The first cavity is a coaxial cavity with a cathode-grid assembly, where beam bunches are formed, the second cavity is required for the beam acceleration. The features of the gun are the following: bunched and relativistic beams in the output of the injector, absence of the back bombarding electrons, low energy spread and short length of the bunches. The scheme of the injector is shown. The electromagnetic field simulation and beam dynamics are presented.

INTRODUCTION

The RF gun with a thermionic cathode can be used as the injector. It is based on the cavity joint with the cathode-grid assembly [1, 2]. Emitted by the cathode electrons are accelerated by the cavity electric field. The main advantages of this system are the following. Firstly, the beam is immediately formed to the bunches that follow with the cavity frequency. Secondly, the particles can become relativistic at the output of the injector. This beam can be directly injected to the linear accelerator regular accelerating structures operating with a frequency of the injector cavities. But if the thermionic cathode without an additional control of the beam current is used, the electrons are emitted continuously. In this case some negative effects occur: wide energy spread of the particles at the injector output, back bombardment of the cathode and the cavity walls by the electrons, additional heating of the cathode. Besides that, output bunches have significant “tails”. Then, during the acceleration, these “tails” are usually lost. If they are of a high energy, an additional radiation background can occur when “tails” hit the inner walls of the accelerator channel.

To avoid disadvantages of the conventional RF gun the additional control cavity can be used. This cavity is coaxial type cavity with capacitance, which is based on the RF triode [3, 4]. Generating the necessary phase shift between the controlling RF signal (which is applied to the cathode-grid gap) and the electric field in the accelerating cavities, one can reduce the output bunch duration and decrease the particle spread. In case of a sufficient RF power in the accelerating cavities, particles at the injector output have ultrarelativistic velocities.

In this paper a principle scheme of the injector with a frequency of 2856 MHz is discussed. The control system of the beam current is described. Results of the output beam dynamics simulations with an emission current of 10 A are presented. The most attention is paid to the longitudinal beam dynamics. The beam emittance is unconsidered in the paper.

SCHEME OF THE INJECTOR

General scheme of the controlled RF gun is presented in Figure 1. RF power from the klystron which can also be used to feed the regular accelerating structures is transmitted to the gun accelerating cavities along the waveguide section through the isolator and the vacuum window. Part of the klystron power is derived to the coaxial cavity which is a part of the RF triode. The triode grid is the continuation of the accelerating cavity end wall. To tune the voltage amplitude on the cathode-grid gap and the phase delay relative to the accelerating cavities in the RF section of the coaxial cavity, an adjustable attenuator and a phase shifter are used. Cathode heating is realized by the power source through the inner conductor of the coaxial cavity. To compensate the accelerating cavity field which penetrates to the cathode-grid gap due to the grid transparency, an additional bias voltage can be applied.

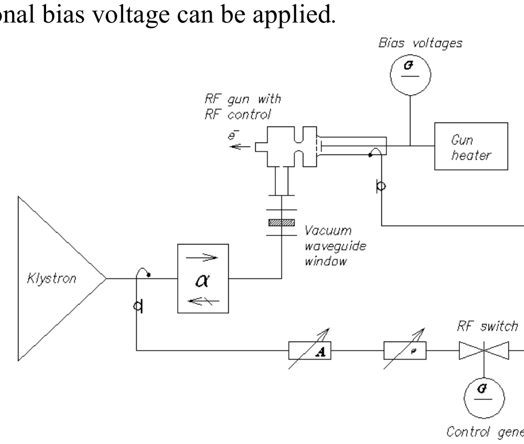

Figure 1: Scheme of the RF gun with RF control.

In the scheme of the RF gun with RF control presented in Figure 1, the common RF power generator is used to feed the accelerating cavities and the control coaxial one. In this case the beginning of the beam current pulse and its duration are always connected with the common RF pulse of the generator. For the independent control of the beam current duration without using an additional RF power source, it is proposed to use the coaxial RF switch at PIN diodes developed before [5-6]. By means of the control voltage on the diodes, one can let pass a RF signal through the coaxial line or provide its full reflection. The RF pulse edges have the duration of about 50 ns, so one can form the current with a pulse base duration of 100 ns. Also the independent RF power source for the control cavity can be

ISBN 978-3-95450-181-6

OPTIMIZATION OF AN RF PROBE VICINITY FOR RF GUN CAVITIES

V.V. Paramonov*, Institute for Nuclear Research of the RAS, Moscow, Russia

Abstract

To provide electron bunches with exceptionally high brightness, RF gun cavity should operate with the extreme electric and magnetic fields. The RF probe is required for the mostly reliable and precise measurements of the RF field phase and amplitude directly from the cavity. The implementation of an RF probe in the cavity design generates a set of coupled problems, which is analyzed and compared for different operating frequencies and different RF pulse length. Both general dependencies and particularities are considered. Some recommendations for practical choice of the RF probe are presented.

INTRODUCTION

RF gun cavities are intended for generation of high brightness electron bunches for Free Electron Lasers (FELs), based on linear accelerators. The normal conducting Fel's linacs operate in the S band frequency range with a relatively short length of RF pulse τ. For FEL's based on superconducting technology the L band range is adopted with much more long RF pulse. Instead of a large variety particular technical solutions, The major part of existing gun cavities is based on BNL concept, [1], which is shown in Fig. 1 with modern solutions. A gun cavity consists of two cells, surrounded by cooling circuit in cavity walls. The length of cells is optimized to have a small emittance of the bunch. A photo cathode is placed in the first short cell

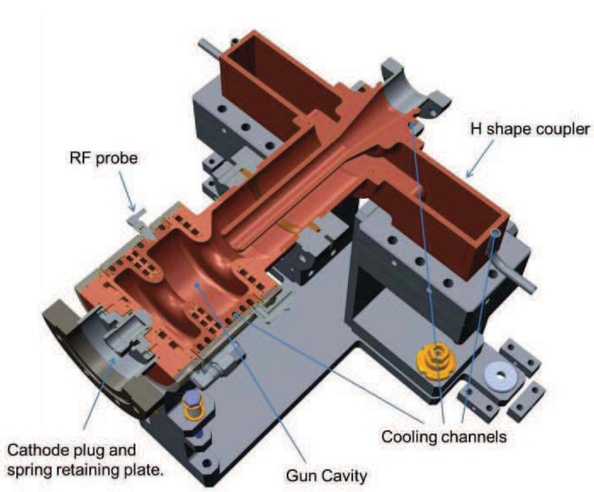

Figure 1: The modern design of RF gun cavity, [2].

of the cavity. For RF power input in Fig. 1 is shown the coaxial RF coupler to avoid an azimuthal nonhomogenuity of the cavity field. To provide electron bunches with an exceptionally high peak bunch current as well as a small transverse emittance, RF gun cavities should operate with an extreme electric field at the photo cathode E_c and, hence, in the total cavity. To provide the required performance of the FEL facility, the phase of the RF field in the gun cavity should be controlled with a maximal possible precision for synchronization with the main linac RF system. An RF probe in the cavity cell provides perturbation in the gun cavity surface resulting in perturbation of the field distribution both in the nearest probe vicinity and in the total cavity volume. It leads to a set of coupled effects, which are estimated below. To point out particularities of the cavity operating regime we will the S mode as operation with frequency $f_0 \approx 3\,GHz, E_c \approx 115\,\frac{MV}{m}, \tau \approx 3\,\mu s$ and L mode with parameters $f_0 \approx 1.3\,GHz, E_c \approx 60\,\frac{MV}{m}, \tau \approx 1000\,\mu s$.

EQUIVALENT CAVITY

For the analysis we have to know with the high precision the field distributions in a small region, compared in dimensions with a probe hole. This case the details of the total cavity design are not so important. To have the dense mesh and the high precision in numerical simulations the equivalent sector cavity was considered together with the probe hole vicinity, Fig. 2a. Simulations were performed by using ANSYS software, [3].

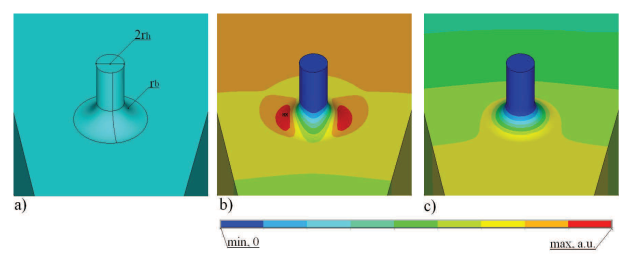

Figure 2: The equivalent cavity in with the RF probe hole, (a), and distributions of magnetic, (b), and electric, (c), fields intensity near the probe hole.

VICINITY OF THE PROBE HOLE

The set of coupled effects is estimated below.

Perturbation of the field distribution

Essential dimensions of the probe hole, the hole radius r_h and the radius of edge rounding r_b are shown in Fig. 2a. In the nearest vicinity the probe hole provides different perturbations in the distributions of electric and magnetic fields. For magnetic field the perturbation is like dipole addition, Fig. 2b, while for for electric field the perturbation is like monopole, Fig. 2c. Because the maximum values are interesting, let us consider the field enhancement, $\frac{H_{max}}{H_0}, \frac{E_{max}}{E_0}$, where H_{max}, E_{max} are the maximal values of field intensities in the probe vicinity and H_0, E_0 are the values of field

* paramono@inr.ru

ISBN 978-3-95450-181-6

FIRST EXPERIMENTAL DEMONSTRATION OF THE EXTRACTION OF LOW ENERGY BEAMS FROM THE ESR TO THE CRYRING@ESR

S. Litvinov, Z. Andelkovic, D. Beck, A. Braeuning-Demian, S. Fedotova, W. Geithner, R. Hess, F. Herfurth, C. Kleffner, I. Kraus, M. Lestinsky, F. Nolden, M. Steck, G. Vorobyev
GSI, Darmstadt, Germany

Abstract

The CRYRING@ESR facility [1] will provide the unique possibility for studying properties of highly charged cooled stable and short-lived ions stored at low energy for atomic and nuclear research within the FAIR project [2]. Heavy ion beams will be stored, cooled and decelerated to energies between 10 and 4 MeV/u in the ESR [3] and then delivered to the CRYRING@ESR. There is no dedicated kicker magnet for the fast extraction in this direction. However, a specially developed distorted closed orbit of the beam stored in the ESR in combination with the injection kicker has been suggested for the extraction and experimentally verified in 2014. In the first experiment the ion beam was extracted and transported over a distance of 20 m towards the CRYRING@ESR [4]. In the 2016 machine development run the heavy ion beam was successfully extracted from the ESR and delivered to the first fluorescent screen inside CRYRING@ESR for the first time. Detailed ion-optical simulations as well as the experimental results will be discussed.

CRYRING@ESR FACILITY

The Experimental Storage Ring (ESR) is a symmetric ring with two arcs and two straight sections and a circumference of 108.36 meters. The ESR consists of six 60° dipole magnets, 20 quadrupole and 8 sextupole magnets. The ESR can be operated at a magnetic rigidity in the range of 0.5 – 10 Tm. For reducing transverse and longitudinal emittances of the stored ion beams, the ESR is equipped with an electron cooler which is installed in one of the straight sections of the ring. Another straight section is foreseen for the experiments [3].

The CRYRING@ESR is a magnetic heavy ion storage ring with a circumference of 54.17 m, which corresponds to half of ESR perimeter. The CRYRING@ESR consists of twelve 30° dipole magnets connected by twelve straight sections, each of which is about 3.3 meters long. Every second section is occupied by a quadrupole triplet for the first-order focusing (18 quadrupoles in total) and 2 sextupoles (12 magnets in total) for the second-order corrections. The other straight sections are foreseen for the injection/extraction, electron-cooler, RF cavity, Schottky diagnostic and experiments. The ring will operate at a magnetic rigidity in the range between 0.054 and 1.44 Tm. Highly charged ions decelerated in the ESR to the lowest possible energy of 4 MeV/u then can be stored and decelerated in the CRYRING@ESR down to few 100 keV/u and delivered to the experiments [1].

The CRYRING@ESR is located behind the ESR and they are connected via a transfer line, which has a length of about 90 meters. The layout of the CRYRING@ESR facility is illustrated in Fig. 2.

CALCULATION

High energy ion beams are usually injected from the synchrotron SIS18 [5] into the ESR on the orbit of $\Delta p/p \approx +1\%$, and then stored and cooled with the electron cooler (solid black curve in Fig. 1). In order to keep the beam parallel to the electron beam in the cooler section, 4 horizontal correctors in 2 neighboring main dipole magnets are used. The ESR is equipped with one injection and two extraction septum magnets as can be seen in Fig. 2. The horizontal width of the beam pipe around the septa is 104 mm and in addition, there is the narrow knife of 17 mm width of each septum (see Fig. 1). The injection kicker magnet is placed after the first dipole downstream (see Fig. 2). The stored beam goes after the kick either to the northern extraction septum (towards HITRAP) or to the wall (dotted black curve in Fig. 1). In order to extract the beam properly to the CRYRING@ESR, it is necessary to change the trajectory of the kicked beam, such that it avoids the north extraction septum and the injection septum but reaches the southern extraction septum. This orbit distortion has been performed with a special bumped closed orbit, which has been calculated using 8 horizontal correctors in the 4 main dipoles, which are marked by brown boxes in Fig. 2. The corresponding trajectory is shown by the dashed black curve in Fig. 1. Applying the kick on the distorted orbit the beam can freely be extracted to the CRYRING@ESR (dotted-dashed red curve in Fig. 1).

EXPERIMENT

In August 2014, the calculations has been tested in an experiment at the ESR. Firstly, the proposed extraction scheme was verified with 100 and 400 MeV/u proton and $^{58}Ni^{26+}$ beams. The extracted beam was observed directly after the extraction septum using the TT1DF0 fluorescent screen (see Fig. 2). Later, a $^{14}N^{7+}$ beam at 30 MeV/u was injected, stored and stepwise decelerated to the final energy of 4 MeV/u ($B\rho = 0.58$ Tm), the lowest possible magnetic rigidity usable at the ESR. At each energy, the beam was successfully extracted, changing only the kick angle of the injection kicker by several tenths of a milliradian. The distortion orbit was unchanged.

ISBN 978-3-95450-181-6

DESIGN RELATIVISTIC CHARGED PARTICLE BEAM TRANSPORTATION CHANNELS

G. P. Averyanov, V. A. Budkin, I.O.Osadchuk, MEPhI, Moscow, Russia

Abstract

This paper contains results of development new version (2016) of program for channels design high-energy beams of charged particles. The program includes application package modeling the dynamics of charged particles in the channel, operational tools to change the channel parameters, channel optimization tools and processing output beam parameters with graphic and digital presentation of its key features. The MATLAB (Scilab) was used as programming tools, allows to make the source code modular, compact and scalable. New object-oriented graphical user interface provides an interactive assembly of new or modernization of previously developed channel - selection and arrangement of its elements, as well as the installation and the variation of their parameters. The relational database, which is part of the new version of program, providing additional functionality to the designer. It is intended for storage of the current development, and to preserve the previously completed projects, as well as other useful designer related information. A multi-output of all the main parameters of the beam at the output, as well as anywhere in the channel. In this case, the developer has the ability to interactively search and setting the optimum mode of operation channel.

INTRODUCTION

The effectiveness of the design on the stage of computer simulation is largely determined by the convenience of the user interface of the used software package and the time of adaptation of the user to that application [1-4].

This paper presents a new approach in the implementation of interface software package KATRAN, designed for the design of channels of transportation of a relativistic charged particle beams.

THE PACKAGE STRUCTURE AND ALGORITHM DESIGN

The package contains four main modules:

- graphical interface, consisting of the Builder module of the channel and the processing module results of the calculation;
- calculation module;
- database module.

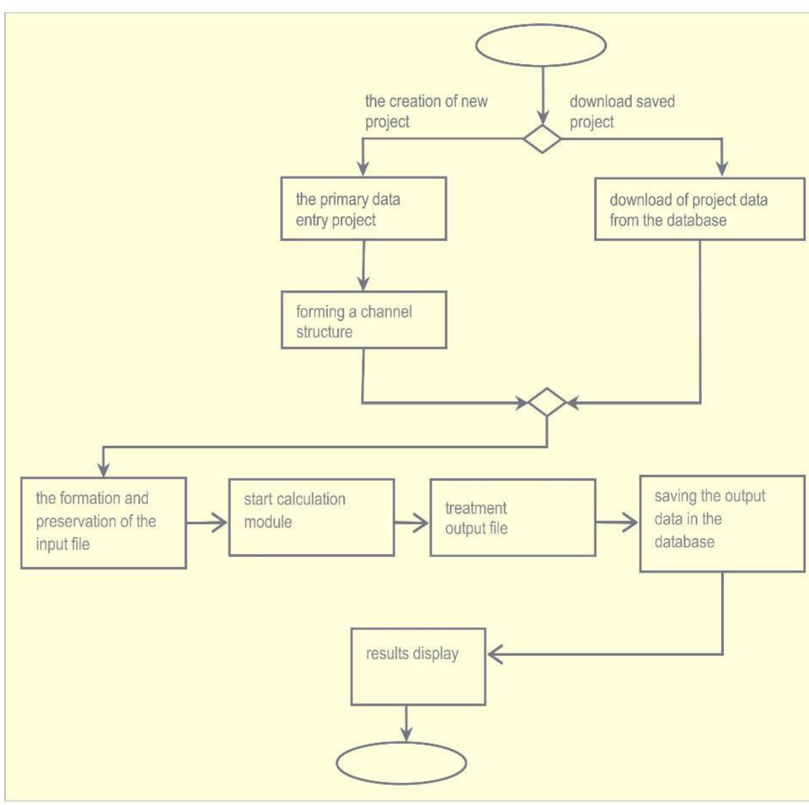

Figure 1: The package structure and algorithm design.

ISBN 978-3-95450-181-6

THE INTELLIGENT OBJECT-ORIENTED INTERFACE IN THE DESIGN ENVIRONMENT OF THE CHARGED PARTICLES RELATIVISTIC BEAMS TRANSPORT CHANNELS

G.P. Averyanov, V.A. Budkin, A.V. Kobylyatskiy, I.O. Osadchuk, MEPhI, Moscow, Russia

Abstract

The effectiveness of the design during the computer modeling is significantly determined by the user interface convenience of the application package and the time adaptation of the user to that application. This paper presents a new approach in the implementation of KATRAN software interface for the transport channels design of the charged particles relativistic beams. The interface is a sequence of operations for the designer during the virtual channel creation setting beam parameters at the channel input, the choice of the displayed elements of the channel, the channel assembly, setting the calculation algorithm with the parameters optimization. Thus the immersion of the designer into the details of the computing environment, the features of the software and channel modeling mathematical methods is not needed. The data objects are the typical elements of the transport channels (quadrupole lenses, magnets, open intervals, etc.). The work is carried out in interactive mode. After the "build and run" of the channel is finished, the full-screen multi-factor analysis of all major parameters of the beam and channel transparency is provided.

INTRODUCTION

The channel configuration is determined by the dimensions of the accelerator hall and the experimental hall, as well as the requirements to the beam parameters and intensity [1-4]. Numerical modeling allows to identify the causes of loss of particles along the channel length and the "contribution" of each feed item in the total loss.

Adaptive modular approach to the design of channels is to pre-select separate focusing systems (modules). Preliminary optimization of the parameters of the modules based on the requirements as to the channel as a whole, and to individual modules. It defines the alignment of elements along the length of the module and the orientation of the lens (focusing-defocusing). Then, a parameter optimization of the whole channel in general. The channel calculation is performed using the software package "KATRAN" in MATLAB and Scilab.

The graphical tool environment allow you to display trajectories of individual particles, the envelopes and phase portraits of beam in horizontal and vertical plane. This information is enough to prompt the channel of the desired operation mode and adaptation of the entire focusing system to the requirements of the focusing of the beam.

The transport channel parameters

Particle dynamics in the transport channel is described by the transformation matrix in the quadrupoles, the magnets and the drifts in the horizontal m_{ij} and vertical n_{ij} plane. The relationship of the beam parameters (linear dimensions – x, z and divergence – x', z') at the output of channel (or individual element) with the input parameters is written as:

$$\begin{bmatrix} x_{out} \\ x'_{out} \end{bmatrix} = \begin{bmatrix} m_{11} & m_{12} \\ m_{21} & m_{22} \end{bmatrix} \begin{bmatrix} x_{in} \\ x'_{in} \end{bmatrix} \cdots, \cdots \begin{bmatrix} z_{out} \\ z'_{out} \end{bmatrix} =$$

$$= \begin{bmatrix} n_{11} & n_{12} \\ n_{21} & n_{22} \end{bmatrix} \begin{bmatrix} z_{in} \\ z'_{in} \end{bmatrix} \qquad (1)$$

The elements of the matrices are functions of the geometric parameters of the channel and the values of the magnetic field in the quadrupole lenses and magnets. Thus, based on the values of matrix elements it is possible to form the target function Ft, which reflects the degree of achievement of the desired parameters of the beam in the plane of the experimental setup.

As an example, consider the modernization of the existing channel electron synchrotron (Fig. 1).

THE OPTIMIZATION OF CHANNEL PARAMETERS

The optimization of transportation channels includes next basic premises:

- The length of the channel and location of the bending magnets remains unchanged (determined by existing premises).
- Only the values of the magnetic fields in the lenses and doublets and their location along the channel varied.

The channel is formed from three types of focusing systems.

There are three focus system types:

- Two single quadrupole lenses
- A doublet of quadrupole lenses
- A doublet of quadrupole lenses in combination with a rotary magnet

Requirements for the beam parameters from the experiment – may be a little linear and angular dimensions of the beam at the exit of the channel.

These two requirements are competing, using methods of extreme search allows you to obtain a compromise solution. Minimum linear size of the beam in both planes at the exit of the channel is ensured by the conditions stigmatically image $m_{12} \to 0$, $n_{12} \to 0$ and about a single transformation $m_{11} \to 1$, $n_{11} \to 1$. The minimum divergence of the beam of electrons is mainly determined by the condition $m_{21} \to 0$, $n_{21} \to 0$.

ISBN 978-3-95450-181-6

ON THE MINIMAX PROBLEM OF BEAM DYNAMICS OPTIMIZATION

M. Mizintseva*, D. Ovsyannikov
Saint Petersburg State University, Universitetskaya nab. 7/9, St. Petersburg, Russia

Abstract

The problem of simultaneous optimization of the ensemble of trajectories and some selected trajectory arises in the research of the charged particle beam dynamics [1–8].
The present work suggests the use of a smooth functional for the evaluation of the selected trajectories and a minimax functional for the evaluation of the dynamics of the beam of trajectories. A combination of those functionals is considered.

INTRODUCTION

In the present work a new approach to the beam dynamics optimization, based on the use of smooth and non-smooth functionals for the evaluation of the dynamics of the charged particles, is developed. The problem of simultaneous optimization of the program motion and the ensemble of trajectories is formulated. The dynamics of the program motion is evaluated using a smooth integral functional and the dynamics of the ensemble of disturbed motions is evaluated using a non-smooth functional.
In this paper the analytical form of the variation for the combination of a smooth and non-smooth functionals is presented, allowing to develop various methods of optimization. Those methods can be implemented, for instance, to the optimization of particle dynamics in a RFQ structure. It should be noted that the problems of analysis and optimization of the particle dynamics in RFQ accelerators in an equivalent running wave were explored in numerous works [9–14], but those did not utilize non-smooth functionals.

MATHEMATICAL MODEL

Let us consider the following system of differential equations

$$\frac{dx}{dt} = f(t,x,u), \qquad x(0) = x_0. \tag{1}$$

Here $t \in [0,T]$ — independent variable, $T > 0$ is a fixed moment of time; x — n–dimensional phase-vector; $u = u(t)$ — r–dimentional piecewise continuous control vector-function from a class D; $f(t,x,u)$ — n–dimentional reasonably smooth vector-function . Let us call the solution of system (1) a program motion.
At the same time we consider the so-called disturbed motions, which are the solutions of the following system of equations [1]

$$\frac{dy}{dt} = F(t,x,y,u), \qquad y(0) = y_0 \in M_0. \tag{2}$$

Here y — n–dimensional phase-vector; $F(t,x,y,u)$ — n-dimensional reasonably smooth vector-function; M_0 — a compact set.
The trajectories of system (2) are vector-functions $y = y(t, x(t,x_0,u), y_0, u)$, continuously dependent on the program motion $x(t,x_0,u)$ and initial conditions $y_0 \in M_0$.
Let us introduce the set of terminal positions of the system (2)

$$Y = \{y(T,x_0,y_0,u) \mid u \in D, x(0) = x_0, y_0 \in M_0\}.$$

On the solutions of system (1) let us introduce a functional

$$I_1(u) = \int_0^T \varphi_1(x(t,x_0,u))dt + g(x(T))$$

and on the trajectories of system (2) the following functional

$$I_2(u) = \max_{y_T \in Y} \varphi_2(Y).$$

Here φ_1 and φ_2 are non-negative smooth functions.
In the present paper the following functional is studied

$$I(u) = I_1(u) + I_2(u).$$

VARIATION OF THE FUNCTIONAL

Let us consider a variation of the control function $\Delta u(t)$, so that $\tilde{u}(t) = u(t) + \Delta u(t) \in D$.
Let us introduce a set $R_T(u)$, dependent on the control $u = u(t)$ and defined by expression

$$\begin{aligned} R_T(u) = \{\bar{y}_0 : \bar{y}_0 \in M_0, \varphi_2(y(T,x_0,\bar{y}_0,u)) = \\ = \max_{y_0 \in M_0} \varphi_2(y(T,x_0,y_0,u))\}. \end{aligned} \tag{3}$$

Following the logic of [10] lemma can be proved.
Lemma *Let us consider sets $R_T(u)$ and $R_T(\tilde{u})$, defined by the relations (3), corresponding to the allowed controls $u(t)$ and $\tilde{u}(t)$, then*

$$\max_{y_0'' \in R_T(\tilde{u})} \min_{y_0' \in R_T(u)} \|y_0'' - y_0'\| \to 0 \quad \text{when} \quad \|\Delta u\|_L \to 0.$$

The variations equations correspoding to the systems (1 –2) are as follows

$$\begin{aligned} &\frac{d\delta x}{dt} = \frac{\partial f(t,x,u)}{\partial x}\delta x + \Delta_u f(t,x,u), \\ &\delta x(0) = 0; \\ &\frac{d\delta y}{dt} = \frac{\partial F(t,x,y,u)}{\partial x}\delta x + \frac{\partial F(t,x,y,u)}{\partial y}\delta y + \\ &\qquad + \Delta_u F(t,x,y,u), \\ &\delta y(0) = 0. \end{aligned}$$

* m.mizintseva@spbu.ru

ISBN 978-3-95450-181-6

ON MODELING AND OPTIMIZATION OF INTENSE QUASIPERIODIC BEAM DYNAMICS

I. Rubtsova#, SPbSU, Saint-Petersburg, Russia

Abstract

The paper is devoted to quasiperiodic beam dynamics investigation. Particle density is modeled by trigonometric polynomial. Space charge field is represented in the similar form. This approach is applied to beam dynamics investigation in klystron-type buncher. Numerical algorithm of polynomial coefficients calculation from the positions and impulses of model particles is formalized. As a result Coulomb field intensity is expressed in the form of integral over the set of particle phase states. Integro-differential beam evolution model is presented. Analytical expression of the variation of beam dynamics quality criterion is obtained. It makes possible directed methods using for beam dynamics optimization.

BEAM DYNAMICS EQUATIONS

Consider quasiperiodic beam dynamics in accelerator or some beam forming system. Let us take klystron buncher as an example (the bunching process is supposed to be adiabatic). The channel is supposed to be cylindrical tube of radius a. Let us introduce the cylindrical coordinates r, θ, z with Oz axis coincided the channel axis.

Beam evolution is simulated on the basis of particle-in-cell method. Model particles are supposed to be "thick" disks with radius R. Dynamics equations are as follows:

$$\frac{dz_i}{d\tau} = \frac{p_i}{\sqrt{1+p_i^2}}, \quad \frac{dp_i}{d\tau} = -\frac{e}{m_0 c^2}\left(E_i^{(RF)} - E_i^{(int)}\right). \quad (1)$$

Here $\tau = ct \in [0,T]$, t is the time, c is the velocity of light; z_i and p_i are longitudinal coordinate and reduced impulse of i-th particle; e and m_0 are absolute charge value and rest mass of electron; $E_i^{(RF)}$ and $E_i^{(int)}$ are the intensity functions characterizing the action on model particle of RF and Coulomb fields correspondingly.

PARTICLE INTERACTION ACCOUNT

Assume that independent variable value τ is fixed. We suppose beam spatial quasiperiod to be cylinder $[0,R]\times[0,2\pi)\times[z_c - H, z_c + H)$ where z_c is center coordinate; the cylinder is charged uniformly across the radius. We presume the beam to be periodic when calculate space charge forces. Coulomb field calculation algorithm is as follows.

1. Introduction of longitudinal coordinate grid $\left\{\xi_j = z_c - H + 2jh,\ j = \overline{0,2M}\right\}$, where $2h = H/M$.

2. Calculation of grid cell charges q_j, $j = \overline{0,2M-1}$ with the use of clouds-in-cells method. It is supposed that $q_{2M} = q_0$ due to beam spatial periodicity. Approximation of bunch charge density by piecewise constant function $\left\{\tilde{S}(z,z_c) = q_j/(2h\pi R^2), z \in [\xi_j - h, \xi_j + h), j = \overline{0,2M-1}\right\}$.

3. Approximation of the function $\tilde{S}(z,z_c)$ by trigonometric polynomial $S(z - z_c)$ taking the values $S_j = q_j/(2h\pi R^2)$, $j = \overline{0,2M-1}$ at grid points [1-3]:

$$S(\varsigma) = \sum_{m=0}^{M}\left[A_m \cos(m\pi\varsigma/H) + B_m \sin(m\pi\varsigma/H)\right]. \quad (2)$$

The coefficients A_m, B_m, $m = \overline{0,M}$ are expressed by trigonometric interpolation formulae:

$$A_m = \frac{(-1)^m}{M\nu_m}\sum_{j=0}^{2M-1} S_j \cos(m\,j\,\pi/M),\ m = \overline{1,M},$$
$$B_m = \frac{(-1)^m}{M}\sum_{j=0}^{2M-1} S_j \sin(m\,j\,\pi/M),\ m = \overline{0,M}, \quad (3)$$
$$A_0 = Q/(2H\pi R^2),\ \nu_m = [1 + m/M],$$

where Q is bunch charge value, ν_m is the integer part of the value $1 + m/M$.

4. Calculation of potential field intensity characterizing the periodic beam action on the model particle. The intensity expression is derived on the basis of potential function obtained by Poisson equation solving with right-hand part proportional the polynomial $S(z - z_c)$ [2-4]. The intensity calculation formula is as follows:

$$E_i^{(int)} = C\sum_{k=1}^{\infty} D_k \sum_{m=1}^{M} C_{km}(p_c)\times$$
$$\times\left[A_m\Gamma_{sm}(z_i, z_c, p_c) - B_m\Gamma_{cm}(z_i, z_c, p_c)\right], \quad (4)$$

where

$$C = \frac{(2\pi Ra)^2 H}{\varepsilon_0};\ D_k = \frac{J_1^2(\mu_k R/a)}{\mu_k^2 J_1^2(\mu_k)};$$
$$C_{km}(p) = \frac{m}{(m\pi a)^2 + \mu_k^2 H^2(1+p^2)};$$

#rubtsova05@mail.ru

ISBN 978-3-95450-181-6

ON APPLICATION OF MONTE CARLO METHOD FOR POISSON PROBLEM SOLVING

L.V. Vladimirova[#], I. Rubtsova, SPbSU, Saint-Petersburg, Russia

Abstract

The paper presents the application of random grid walk for Dirichlet problem solving for Poisson equation. Boundary value problem is discretized and reduced to the system of linear algebraic equations. The matrix of this system is used for stochastic matrix constructing. Thus, there is a possibility of Markov chains obtaining. The special random value is defined on Markov chain trajectories; this value is used for approximation of the desired solution. The advantages of this method are discussed in the paper.

The algorithm is applied for electric potential calculation in the cell of support lattice of exit window in large-aperture electron accelerator.

DIRICHLET PROBLEM FOR POISSON EQUATION

Consider the Dirichlet problem for electric potential. Poisson equation for unknown potential $u(x,y)$ has the form

$$\frac{\partial^2 u}{\partial x^2}+\frac{\partial^2 u}{\partial y^2}=\tilde{f}(x,y), \quad (x,y)\in G \tag{1}$$

with boundary conditions

$$u\big|_{\Gamma}=\varphi(x,y)\,. \tag{2}$$

Here $G\subset R^2$ is some domain, Γ is the boundary of the domain G, $\tilde{f}(x,y)$ and $\varphi(x,y)$ are given functions.

Let us consider problem (1)-(2) discretization algorithm for the rectangle domain. The modification of this algorithm for the domain of any other form is given in the book [1].

For numerical solution of Dirichlet problem (1)-(2) we introduce sufficiently fine grid S with the step l: $S=\left\{s_{i,j}=(x_i,y_j):\ x_i=il,\ \ y_j=jl,\ \ i=\overline{0,L_x},\ \ j=\overline{0,L_y}\right\}$. We distinguish the set of boundary grid points $S_\Gamma=\left\{s_{i,j}=(x_i,y_j)\in S:\ \ i=0,L_x,\ j=0,L_y\right\}$. The internal grid points set is $S_G=S\setminus S_\Gamma$.

After that we introduce the following grid functions: $\left\{u_{i,j}=u(s_{i,j}):\ \ s_{i,j}\in S\right\}$, $\left\{\tilde{f}_{i,j}=\tilde{f}(s_{i,j}):\ \ s_{i,j}\in S_G\right\}$, $\left\{\varphi_{i,j}=\varphi(s_{i,j}):\ \ s_{i,j}\in S_\Gamma\right\}$.

Let us replace the equation (1) at internal grid points by the difference equation

$$u_{i,j}=(1/4)(u_{i-1,j}+u_{i+1,j}+u_{i,j-1}+u_{i,j+1}-l^2\tilde{f}_{i,j})\,. \tag{3}$$

At boundary grid points we assume

$$u_{i,j}=\varphi(x_i,y_j)\,. \tag{4}$$

The solution of algebraic system (3)-(4) converges to the solution of Dirichlet problem (1)-(2) as $l\to 0$ [2,3].

Let us number all the grid points in any order (using one index) and rewrite the equations (3)-(4) in the same order. Now the grid S is described as follows: $S=\left\{(x_k,y_k),k=\overline{1,L}\right\}$, where $L=(L_x+1)(L_y+1)$. Let I_G and I_Γ be the sets of numbers of internal and boundary grid points correspondingly.

After that we introduce the grid functions $u=(u_1,\ldots,u_L)$, $\tilde{f}=(\tilde{f}_1,\ldots,\tilde{f}_L)$ and $\varphi=(\varphi_1,\ldots,\varphi_L)$ representing the grid values of potential, right-hand part of equation (1) and boundary function correspondingly.

Now the system (3)-(4) takes the form

$$u=Au+f, \tag{5}$$

where A is $L\times L$ matrix of coefficients; L-vector f is determined as follows:

$$f_i=\begin{cases}(-1/4)\,l^2\tilde{f}_i, & i\in I_G\\ \varphi_i, & i\in I_\Gamma\end{cases}. \tag{6}$$

As for matrix A, when $i\in I_G$, the line $A_i=(a_{i,1},\ldots,a_{i,L})$ contains four elements equal $1/4$ and other elements zero; if $i\in I_\Gamma$ the line A_i is zero.

"WALK-ON-GRID" METHOD

Stochastic Matrix

To obtain the solution of the system (5) we apply "walk-on-grid" algorithm.

Let us construct stochastic matrix P by the rule:

$$i\in I_G \Rightarrow \begin{Bmatrix}p_{i,j}>0 \ \ if\ \ a_{i,j}>0\\ p_{i,j}=0\ \ if\ \ a_{i,j}=0\end{Bmatrix},\ j=\overline{1,L};\ \sum_{j=1}^{L}p_{i,j}=1;$$

$$i\in I_\Gamma \Rightarrow p_{i,j}=\delta_{i,j},\ \ j=\overline{1,L},$$

#sergvlad@sp.ru

ISBN 978-3-95450-181-6

ABOUT BEHAVIOR OF ELECTRONS AND IONS IN THE ACCELERATING INTERVAL

A.S.Chikhachev, SSC VEI, Moscow, Russia
H.Y.Barminova, NRNI MePhI, Moscow, Russia

Abstract

The behavior of the electron-ion ensemble in accelerating gap. Hot electrons are described by the distribution function, which is a solution of the collisionless kinetic equation, which depends not only on the integrals of motion. For a description of cold ions used hydrodynamic equations. The possibility of excess ions ion-acoustic velocity. The equation that determines the relative density of the ions in the case of closed phase trajectories characterizing the dependence of the field on the coordinate

INTRODUCTION

To study the actual recovery process of heavy ions from the plasma carried out a large number of studies on the review of the process models. In [1] it was shown that the plasma leaving the ions at velocities exceeding the ion-sound velocity. Because in the real world, the electron temperature substantially greater than the temperature of the ion number of accelerated ions is exponentially small. Note, however, the work [2], to study the acceleration of a thin ion beam. In this paper we show that the ion velocity can exceed the speed of ion-sound when changing the beam radius .. In [3] studied the state of the accelerated flow of cold ions in resting, in general, the hot-electron cloud. In particular, in [3], the transition layer system "plasma-vacuum" is infinitely large. In all these works the electron current is zero. In [4] studied the equilibrium state of the system in the presence of a nonzero electron current by using hydrodynamic description of electrons. The paper [5] examines the state of the ion flux in the layer of electrons moving in a direction perpendicular to the flow of electrons. In this work, the maximum energy which can acquire ions in a layer equal to the temperature of electrons, whereas in the conditions of [4], the energy can exceed the electron temperature. problems are also considered in [6] studied in the present work.

FORMULATION OF THE PROBLEM

We shall describe the ensemble of collisionless kinetic equation for electrons and ions to describe the hydrodynamic equations, assuming for the sake of simplicity, one-dimensional problem. For electrons, the kinetic equation is:

$$\frac{p}{m}\frac{\partial f}{\partial x}+e\frac{d\Phi}{dx}\frac{\partial f}{\partial p}=0, \qquad (1)$$

where m - the mass of the electron, $-e$ the charge, Φ - the potential, x - coordinate, p - momentum, $f(x,p)$- particle distribution function.

Let us put

$$f=\sigma\left(p-\sqrt{2m\left(C_0+e\Phi\right)}\right)\Psi(H). \qquad (2)$$

Here $\sigma(x)$- Heaviside function., $C_0>-e\Phi(x)$ for any x. Expression (2) determines non-zero fluid of electrons: $\Gamma_e=\int\limits_{\sqrt{2m(C_0+e\Phi)}}^{\infty}\frac{p}{m}\Psi(H)dp=\int\limits_{C_0}^{\infty}dH\Psi(H)$. In the case of exponential distribution $\Gamma_e=\kappa_0 T\exp\left(-\frac{C_0}{T}\right)$. The electron density in this case is expressed as follows:

$$n_e=\kappa_0\sqrt{\frac{\pi mT}{2}}\exp\left(\frac{e\Phi}{T}\right)\left(1-erf\left(\sqrt{\frac{C_0+e\Phi}{T}}\right)\right) \qquad (3)$$

Here $erf(x)=\frac{2}{\sqrt{\pi}}\int\limits_0^x\exp(-y^2)dy$ - error integral.

The role of the factor $\sigma\left(p-\sqrt{2m(C_0+e\Phi)}\right)$ in the expression (2) is significant - the one hand, the particle density varies view, on the other - particle current is not zero. Using the hydrodynamic description of one-dimensional flow of cold ions, it is easy to obtain $n_i=\frac{\Gamma_i}{\upsilon_i}=\frac{n_{i0}\upsilon_0}{\sqrt{\frac{M\upsilon_0^2}{2}+e\Phi}}$

Here M - ion mass.

Put the fluid density as: $\Gamma_i=n_{0i}\upsilon_0$, n_{0i} - initial ion density, υ_0- initial ion velocity. If we introduce the dimensionless potential $u=\frac{e\Phi}{T}$ and to identify the ion-sound velocity $\upsilon_s=\sqrt{\frac{2T}{M}}$, the ion density becomes:

$$n_i=\frac{n_{i0}\upsilon_0}{\upsilon_s\sqrt{\frac{\upsilon_0^2}{\upsilon_s^2}-u}}$$

Let $n_{0e}=\kappa_0\sqrt{\frac{\pi mT}{2}}$

We introduce the dimensionless variables: $t=\frac{x}{l_0}$, $l_0=\sqrt{\frac{T}{4\pi e^2 n_{0e}}}$, $\frac{C_0}{T}=\zeta_0$. Then the Poisson equation becomes:

$$\frac{d^2u}{dt^2}=\exp(u(t))\left(1-erf\sqrt{\zeta_0+u}\right)-\frac{\nu_i}{\sqrt{\frac{\upsilon_0^2}{\upsilon_s^2}-u(t)}} \qquad (4)$$

Here $\nu_i=\frac{n_{0i}}{n_{0e}}\frac{\upsilon_0}{\upsilon_s}$.

ISBN 978-3-95450-181-6

THE BEHAVIOR OF POWERFUL RELATIVISTIC ELECTRON BEAM WITH ELLIPTICAL CROSS-SECTION IN LONGITUDINAL MAGNETIC FIELD

A.S. Chikhachev , SSC VEI, Moscow, Russia
H.Y. Barminova, NRNU MEPhI, Moscow, Russia

Abstract

The behavior of relativistic intense electron beam with elliptical cross-section moving in a longitudinal magnetic field is investigated with the help of self-consistent model. The solutions for the beam envelopes are obtained in the case of the beam current differed from Alfven limit and the beam charge neutralized. The conditions of stationary beam propagation are determined, however it is discovered that for the case of non-zero self-consistent magnetic field the stationary beam propagation is violated, the partial emittance oscillations being observed. The found time- dependence of the partial emittances and the beam envelopes illustrates the effect of emittance transfer caused by the coupled particle motion in magnetic field.

INTRODUCTION

In [1,2,3] studied the behavior of the electron beam in a quadrupole system, the aim of this study was the possibility of compression - reducing the area of the cross-section of the beam when changing quadrupole forces. If the [1] to the transverse emittance were considered equal, in [2], these values are considered to be different, but continuing when the beam moves. In this paper we study the distribution of the electron beam decompensated with an elliptical cross-section in the absence of external quadrupole system and in the presence of a longitudinal magnetic field. The presence of the longitudinal magnetic field greatly complicates the situation - there are not two independent integrals of motion. Emittance can be converted (pumped). It is not a conserved quantity as the product of these values.

EQUATIONS

Consider a beam whose charge is compensated by the secondary particles. Lateral movement can be separated from the lengthwise when the current satisfies the following condition:

$J << J_A$, where $J_A = mc^3\gamma_0\beta_0/e$. The distribution function can be written as: $F = \delta(\beta_z - \beta_0) f(\vec{r}_\perp, z, \vec{v}_\perp)$. In this paraxial approximation the longitudinal velocity of the particles can be considered constant and equal for all particles. The stationary problem instead of the time you can use a coordinate z. In accordance with the invariant that defines the movement, should depend on $x(z), y(z), x' = \frac{dx}{dz}, y' = \frac{dy}{dz}, z$. We derive the equations of motion of particles in the laboratory frame. Consider that in the system connected to the main beam axes(x_1, y_1) have their own self-compression force directed to the beam axis: $F_{x_1} = -\frac{2ix_1}{R_x(R_x+R_y)}, F_{y_1} = -\frac{2iy_1}{R_y(R_x+R_y)}$. Here $i = J/J_A$ beam current related to Alfven,, $R_x(z), R_y(z)$ - the value of the semi-axes of the elliptic beam cross section). Calculating further, $F_x = F_{x_1}\cos\theta - F_{y_1}\sin\theta, F_y = F_{x_1}\sin\theta + F_{y_1}\cos\theta$, which should be considered $x_1 = x\cos\theta + y\sin\theta, y_1 = -x\sin\theta + y\cos\theta$, and $\theta(z)$ - angle of rotation of the principal axes of the ellipse relative to fixed axes, the equation can be obtained:

$$x'' = \omega_H y' - \alpha(z)x + \beta(z)y,\; y'' = -\omega_H x' + \beta(z)x - \gamma(z)y, \tag{1}$$

where

$$\alpha = \frac{i}{R_xR_y}\left(1 - \frac{R_x - R_y}{R_x + R_y}\cos 2\theta\right)$$

$$\beta = \frac{-i}{R_xR_y}\frac{R_x - R_y}{R_x + R_y}\sin 2\theta$$

$$\gamma == \frac{i}{R_xR_y}\left(1 + \frac{R_x - R_y}{R_x + R_y}\cos 2\theta\right)$$

In equations (1) are also taken into account the presence of an external longitudinal magnetic field, and $\omega_H = \frac{eH}{mc^2\gamma_0\beta_0}$, the dimension of this magnitude - the inverse length.Invariant system (1) can be represented as:

$$\begin{aligned} I = A_1(z)x'^2 + 2A_2(z)x'x + A_3(z)x^2 + B_1(z)y'^2 + \\ 2B_2(z)y'y + B_3(z)y^2 + C_1(z)x'y' + \\ C_2(z)x'y + C_3(z)xy' + C_4(z)xy \end{aligned} \tag{2}$$

From condition $\frac{dI}{dz} \equiv 0$ using (1) we obtain:

$$\begin{aligned} A_1' &= -2A_2 + \omega_H C_1, \\ A_2' &= -A_3 + A_1\alpha(z) + 0.5\omega_H C_3 - 0.5C_1\beta(z), \\ A_3' &= 2A_2\alpha(z) - C_3\beta(z), \\ B_1' &= -2B_2 - \omega_H C_1 \\ B_2' &= -B_3 + B_1\gamma(z) - 0.5\omega_H C_2 - 0.5C_1\beta(z), \\ B_3' &= 2B_2\gamma(z) - C_2\beta(z), \\ C_1' &= -C_2 - C_3 + 2\omega_H(B_1 - A_1), \\ C_2' &= -C_4 + C_1\gamma(z) - 2A_1\beta(z) + 2\omega_H B_2, \\ C_3' &= -C_4 + C_1\alpha(z) - 2A_2\omega_H - 2B_1\beta(z), \\ C_4' &= C_2\alpha(z) + C_3\gamma(z) - 2B_2\beta(z) - 2A_2\beta(z). \end{aligned} \tag{3}$$

Converting, furter, I. Instead x', y' introduce variables ξ, η.

$$x' = \xi\cos\alpha + \eta\sin\alpha, \quad y' = -\xi\sin\alpha + \eta\cos\alpha \tag{4}$$

ISBN 978-3-95450-181-6

THE USE OF MULTI-OBJECTIVE GENETIC ALGORITHMS FOR ACCELERATOR AND LIGHT SOURCE OPTIMIZATION*

Ye. Fomin#, V. Korchuganov, A. Smygacheva, NRC «Kurchatov Institute», Moscow, Russia

Abstract

The nonlinear effects are very important in development of new accelerators and synchrotron light sources. Nowadays they are one of the main factors limiting the achievement of the required facility parameters. In many cases in development of new accelerators the analytical estimations give very rough results and in some cases they don't apply at all. Therefore, the best way to research and design accelerators is to use numerical simulation. Nevertheless, very often during complex physical process simulation (taking into account many nonlinear effects) the use of classical optimization methods is difficult and does not give the desired results.

The article deals with the application of multi-objective optimization using genetic algorithms for accelerators and light sources. These algorithms allow both simple linear and complex nonlinear accelerator structures to be optimized with the same effectiveness when obtaining the required facility parameters.

INTRODUCTION

There are many methods of optimization. All of them can be divided into three groups: determinate, random (stochastic) and combined.

Most accelerator and light source optimization problems can be attributed to combinatorial problems with many different quality solutions. An exhaustive search of all solutions or only subset of solutions is the main feature of combinatorial algorithms. To find the best solution directed, random and combined an exhaustive search of all possible problem variables is used. Therefore, the search of proper solutions often becomes the art. After all, very often if you want to optimize nonlinear multi-objective problem (for example – beam emittance minimization and dynamic aperture maximization) with many variable parameters and restrictions you will face serious difficulties (most rapid and effective optimization methods can't be used, there are many local minima solutions, solving time is directly related to the number of variable parameters, etc.).

One of the effective way to solve combinatorial problems within a reasonable time is the use of genetic algorithms. Genetic algorithms are heuristic search algorithms used to solve optimization problems by random selection, combining and modification of desired parameters using process like the biological evolution.

Genetic algorithms as any other optimization algorithms have their own advantages and disadvantages. Their most important advantages may be said to be:

- Any information about the fitness function behavior is not required.
- Discontinuities of the fitness function don't have a significant effect on optimization.
- Methods are relatively stable to fall into local minima.

Their most important disadvantages may be said to be:

- Methods are inefficient for optimizing fitness functions which have a long calculation time.
- A large number of parameters often turns «work with genetic algorithm» to «play with genetic algorithms».
- In the case of simple fitness functions, genetic algorithms are slower than specialized optimization algorithms.

Nowadays, genetic algorithms are powerful computing tool to solve different multidimensional multi-objective optimization problems. The use of genetic algorithms for accelerator and light source optimization allows to simplify and speed up the search of proper solutions.

The common block diagram for optimization process using genetic algorithms is shown in Fig. 1.

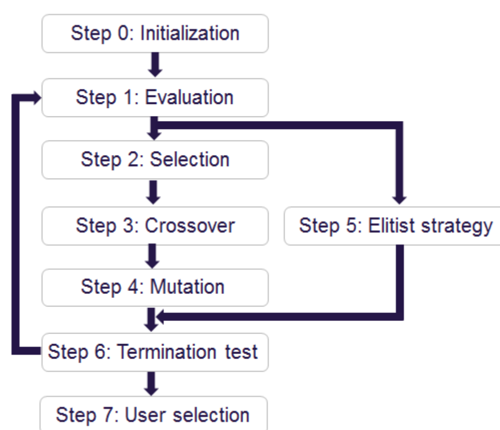

Figure 1: The block diagram of the optimization process using a genetic algorithm.

DESCRIPTION OF OPTIMIZATION METHOD

In general, all optimization problems can be divided into two groups. The first group contains only one fitness function optimization problems, the second one – at the same time two or more fitness function optimization problems. To solve the problems of each group it is advantageous to use a little different algorithms.

One fitness function optimization problem is the simplest situation with easy-to-analyse results. These kinds of problems can be efficiently solved with the help of the differential evolution method [1] is well suited.

*The reported study was funded by RFBR according to the research project No. 16-32-00336 мол_а.
#yafomin@gmail.com

ABOUT DEVELOPMENT SYSTEM FOR THE ANALYSIS OF CHARGED PARTICLE BEAM DYNAMICS

M. Balabanov*, Saint-Peterburg State University, Saint-Peterburg, Russia

Abstract

Modern research process of scientific problems often requires large computational resources. To solve them we have to use distributed computing systems. Researcher groups need to use them simultanieously and mostly remotely. The paper describes build of the distributed system for collaborative research process. As example was chosen a problem of the optimization dynamics charged particle beams using high-performance computing systems. The solution of many topical tasks leads to nonlinear optimization problems for example the controlling beams of charged particles [1-10].

Optimization is performed by minimizing some quality functional the choice of which is a corollary fact that the control functions which provides a functional minimum should determine the accelerating structure with the desired characteristics. The problem is usually formulated as finding the control functions for which the controlled system satisfies the given constraints. There is a necessity of the quality functional choice which ensures the problem solution. Research objectives: the development of a distributed information-computational system for the analysis of charged particle beam dynamics.

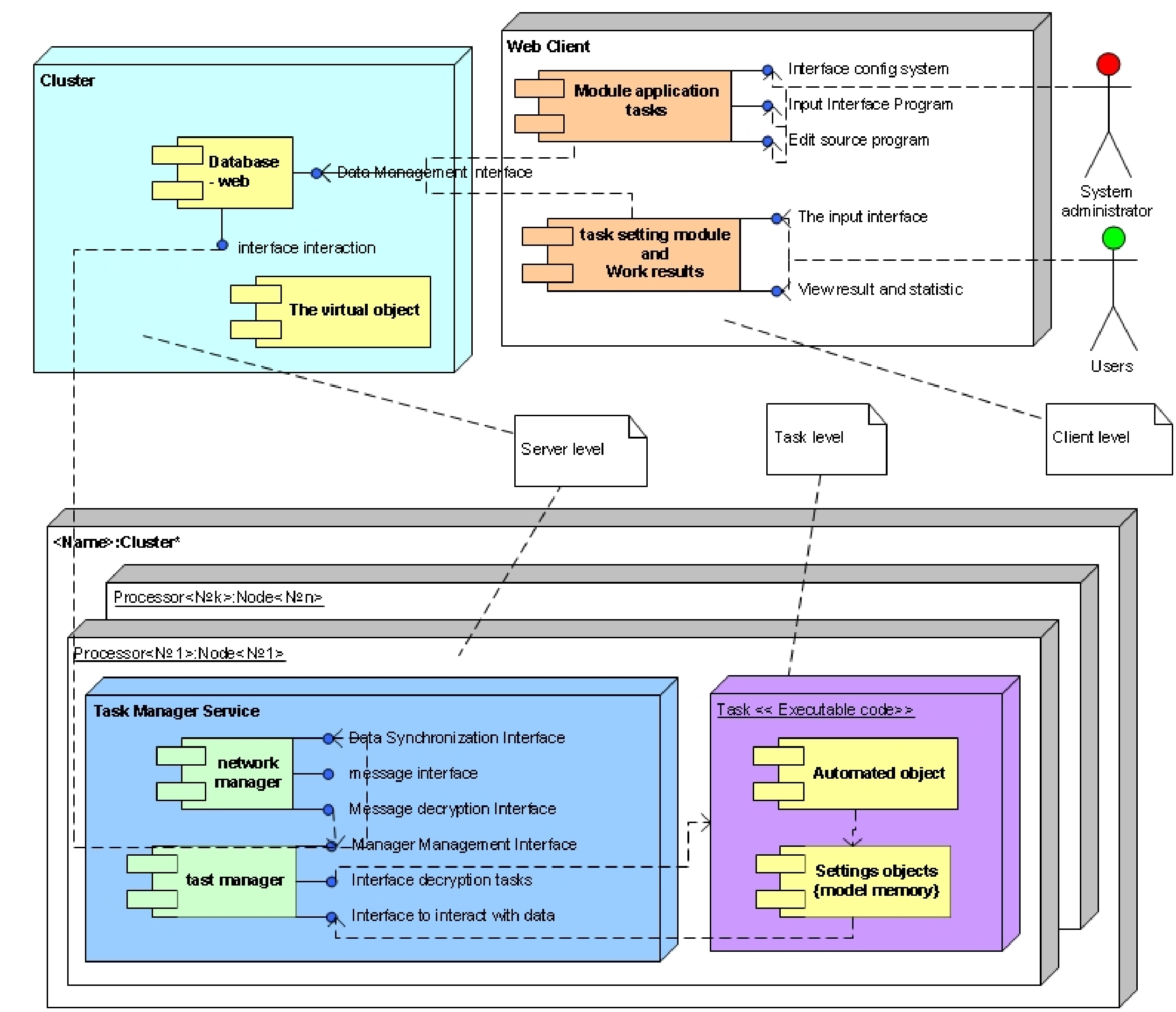

Figure 1: System architecture.

* BalabanovMYu@gmail.com

ISBN 978-3-95450-181-6

ON THE BEAM DYNAMICS SIMULATION IN THE INJECTION SYSTEM

A. D. Ovsyannikov[1], S. A. Kozynchenko, V. A. Kozynchenko
Saint-Petersburg State University, Saint-Petersburg, Russia

Abstract

When developing a particle accelerator for generating the high-precision beams, the injection system design is of importance, because it largely determines the output characteristics of the beam. At the present paper we consider the injection systems consisting of electrodes with given potentials. The design of such systems requires carrying out simulation of beam dynamics in the electrostatic fields. For external field simulation we use the new approach, proposed by A.D. Ovsyannikov, which is based on analytical approximations, or finite difference method, taking into account the real geometry of the injection system. The software designed for solving the problems of beam dynamics simulation and optimization in the injection system for non-relativistic beams has been developed. Both beam dynamics and electric field simulations in the injection system which use analytical approach and finite difference method have been made and the results presented in this paper.

INTRODUCTION

The paper mostly focuses on exploring the ways of algorithmic and software realization of the optimal design methodology in the beam dynamics area, which is proposed in [1-3] and intended to be applied in the injection systems producing the high-precision beams. The development of the optimal design methodology for beam dynamics is considered to be rather complex and laborious problem. It has given rise to a large and growing body of research [4-12].

The main issue in the optimal design techniques that we try to address in the paper consists in finding an analytical representation of both the field U_ξ inside the working domain and the control function $\phi(\eta)$ defined over the domain contour which to be used in further optimization.

$$F(\xi,\phi) \equiv \frac{1}{2\pi i}\int_L f(z)dz = \frac{1}{2\pi i}\left[\int_L u(x,y)dx - v(x,y)dy + i\int_L v(x,y)dx + u(x,y)dy\right], \quad (1)$$

where $f(z) = u(x,y) + i\cdot v(x,y)$ is a function of a complex variable $z = x + i\cdot y$. Therefore, the potential function U can be defined as a real line integral.

[1] a.ovsyannikov@spbu.ru

The paper starts with some algorithmic study relating to the numerical solution of the integral of Cauchy type that is applied in the given problem to calculate the electrostatic field. Then we consider a case study model of the axial symmetrical field in an injection system. Some numerical data obtained in the C++ computer simulation are presented.

A POSSIBLE BASIC ALGORITHM OF FINDING THE INTEGRAL OF CAUCHY TYPE

Let us consider a three-dimensional simply connected bounded domain having the axial symmetry and let G be its diametric cross section. This two-dimensional domain is bounded by a contour L that is supposed to be a smooth closed curve. Hereinafter the real plane R^2 containing the domain G will be identified with the complex plane C. Let a continuous complex function $\phi(\eta)$ be defined over the contour L. The complex potential of the external electrostatic field inside the domain G can be evaluated with the use of an integral of Cauchy type

$$F(\xi,\phi) = \frac{1}{2\pi i}\int_L \frac{\phi(\eta)}{\eta-\xi}d\eta, \quad \xi \notin L, \quad (2)$$

where $\xi = z_G + i\cdot r_G \in G,\ \eta = x_L + i\cdot y_L \in L$. Then the complex potential of the three-dimensional external field can be represented as follows (see [3], p. 97):

$$H(z,r,\phi) = \frac{1}{2\pi}\int_0^{2\pi} F(z + i\cdot r\cos\alpha, \phi)d\alpha \ .$$

The real part of H, i.e. the function $U = \mathrm{Re}\,H$, will be considered as a function determining the electrostatic field in the three-dimensional domain. The complex contour integral (1) can be written as

$$U(x,y) = \frac{1}{2\pi}\int_L v(x,y)dx + u(x,y)dy$$

taken over the same contour L as the complex integral. Let us consider the simplest case when the function $\phi \equiv \phi_0$ is a constant. Then the following expressions can be written

$$f(z) = \frac{\phi_0}{z},\ u(x,y) = \frac{x}{x^2+y^2},\ v(x,y) = -\frac{y}{x^2+y^2},$$

and the real part of the integral (1) is evaluated as follows

$$U \equiv \mathrm{Re}\,F(\xi,\phi_0) = \frac{\phi_0}{2\pi}\left[\int_L -\frac{ydx}{x^2+y^2} + \int_L \frac{xdy}{x^2+y^2}\right], \quad (3)$$

where $x = x_L - z_G,\ y = y_L - r_G$.

ISBN 978-3-95450-181-6

ON APPROACH FOR RESONANT FREQUENCY TUNING IN DRIFT TUBE STRUCTURES ON THE DESIGNING STAGE

I. S. Skudnova, V. V. Altsybeyev*,
Saint-Petersburg University, 7/9 Universitetskaya nab., St. Petersburg, 199034 Russia

Abstract

Current research considers the crossbar H-mode linear resonant accelerator with drift tubes mounted inside the cavity. The focus of the study has been on the dependence of resonant frequency on the parameters of the geometry. Since Alternating-Phase-Focusing (APF) type of accelerator is investigated, the efficiency of the operation depends on the synchronization of the charged particle velocity and accelerating field oscillations. Researchers can control it by the variation of longitudinal size of the cells of the structure (periods). On the other hand, the effective performance of this resonant system requires the equality of resonant frequencies of its cells, because it affects the uniformity of accelerating field distribution along the axis. The diversity of cells longitudinal sizes causes the deviation from the particular value of the resonant frequency. This aberration can be eliminated by the adjustment of other geometry parameters period's length, gap length and drift tube radii. We have conducted the study to analyze the relation between resonant frequency and these values. Using the this dependency we can tune the geometry parameters of each period in the structure. We first create the computer-aided design (CAD) geometry model of the accelerator cavity. Then, using Comsol Multiphysics, the platform for physics-based modeling and simulation, we conduct the calculation of resonant frequencies.

INTRODUCTION

On the first steps of linear accelerator production many parameters of the structure should be considered. One of the main parameters - period's lengths L is determined by the synchronous phase sequence. It is quite difficult for analytic field approximation model to embody many other structure parameters such as drift tube inner and outer radii and holder position and thickness. Of course, one can do a numerical simulation with any given geometry. Accelerator structure usually consists of dozens of periods, each one characterized by 5-6 parameters. The field computation of all acceptable combinations of parameters is severely time-consuming. Therefore, in the study we investigate the dependencies between electric field and some particular geometry parameters.

FREQUENCY CALCULATION

The resonant frequencies of the periods can be significantly different because length of periods are not equal. In this case the amplitude distribution of the electric field in the cavity is non-uniform, which requires considerable additional tuning. However, the resonant frequency of each period can be adjusted by means of gap length, drift tube radii and holder design [1]. With the appropriate choice of this parameters period frequency of some estimated value can be obtained. If we fix values of some basic parameters like cavity radius and holder design we can calculate the dependencies of resonant frequency from period's length, gap length, drift tube radii.

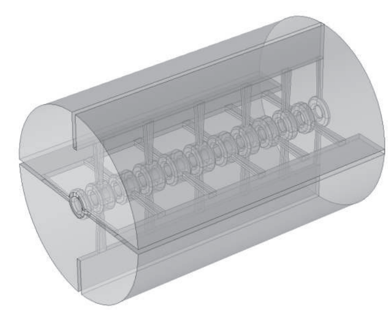

Figure 1: CAD model of the cavity with 11 periods.

In order to calculate the dependency we have created a computer-aided-design (CAD) geometry model of the cavity (figure 1). We are using COMSOL Multiphysics together with MATLAB. COMSOL Multiphysics is a general-purpose software platform, based on advanced numerical methods, for modeling and simulating physics-based problems. Its toolbox LiveLink for MATLAB allows us to utilize the full power of MATLAB as well as use COMSOL Multiphysics functions in the MATLAB script file (.m).

The volume of the cavity ω has a boundary surface S. The electric field E inside the volume satisfy the Helmholtz equation (1).

$$\nabla^2 \mathbf{E} - \left(\frac{\omega}{c}\right)^2 \varepsilon_r \mu_r \mathbf{E} = 0. \quad (1)$$

ε_r and μ_r are relative permittivity and relative permeability respectively. As for the boundary condition, we assume the perfectly conducting surface (2).

$$\mathbf{n} \times \mathbf{E}|_S = 0. \quad (2)$$

To solve the problem (1)-(2) we use the finite-element solver of COMSOL Multiphysics - Radio Frequency, Electromagnetic Waves.

* v.altsybeev@spbu.ru

ISBN 978-3-95450-181-6

SYMMETRICAL PARAMETERIZATION FOR 6D FULLY COUPLED ONE-TURN TRANSPORT MATRIX*

S. A. Glukhov, BINP, Novosibirsk, Russia

Abstract

Symmetry properties of 6D and 4D one-turn symplectic transport matrices were studied. A new parameterization was proposed for 6D matrix, which is an extension of the Lebedev—Bogacz parameterization for 4D case. The parameterization is fully symmetric relative to radial, vertical and longitudinal motion. It can be useful for lattices with strong coupling between all degrees of freedom.

INTRODUCTION

For the case of a 2×2 transport matrix a well-known Twiss parameterization exists [1]. It can be used also in the case of 4×4 and 6×6 matrices if there is no coupling between different degrees of freedom. The usual case is when transversal modes are uncoupled but there is a small interaction between either of them (or both) and longitudinal one. But if longitudinal tune is much smaller than transversal ones, then longitudinal Twiss functions are assumed to be constant. So, longitudinal motion is eliminated and taken into account only in terms of the dispersion functions.

If there is an interaction between transversal modes, then different parameterizations for coupled motion can be used [2], [3], [4]. These parameterizations make use of the fact that horizontal and vertical degrees of freedom are identical mathematically. But this is also the case for the longitudinal one. In this paper we will derive some symmetry properties of a 6×6 transport matrix and build up a totally symmetrical parameterization for it. This parameterization can be used for lattices with strong coupling between all degrees of freedom. Then using the same approach we will reduce the dimensionality to 4×4 and derive Lebedev—Bogacz parameterization [4].

BASIC DEFINITIONS

Let us define a *block-diagonal matrix* as matrix having non-zero elements only within its 2×2 diagonal blocks. Then we introduce the following notation

$$\mathbf{I} = \begin{pmatrix} 1 & 0 \\ 0 & 1 \end{pmatrix}, \ \mathbf{S} = \begin{pmatrix} 0 & 1 \\ -1 & 0 \end{pmatrix}, \ \begin{matrix} \mathbf{I}_6 = \mathrm{diag}\,(\,\mathbf{I} \quad \mathbf{I} \quad \mathbf{I}\,) \\ \mathbf{S}_6 = \mathrm{diag}\,(\,\mathbf{S} \quad \mathbf{S} \quad \mathbf{S}\,) \end{matrix} .$$

Let $\mathbf{M}$ be a 6×6 symplectic one-turn transport matrix, i.e. $\mathbf{M}^T \mathbf{S}_6 \mathbf{M} = \mathbf{S}_6$. Then all the eigenvalues of $\mathbf{M}$ can be grouped into mutually inverse pairs [1]. Let λ_1 and λ_2 form such a pair, $\mathbf{v}_1$ and $\mathbf{v}_2$ be their eigenvectors, then

$$\overset{\leftrightarrow}{\mathbf{M}}\,\mathbf{v}_{1,2} = \hat{\lambda}\mathbf{v}_{1,2}\,, \tag{1}$$

where $\overset{\leftrightarrow}{\mathbf{M}} = \mathbf{M} + \mathbf{M}^{-1}$ is *recurrent matrix*, and $\hat{\lambda} = \lambda_1 + \lambda_2$. This means that $\overset{\leftrightarrow}{\mathbf{M}}$ has at most 3 different eigenvalues, each of them is degenerated at least twice. $\mathbf{M}$ describes stable motion if and only if all $|\lambda_j| = 1$ [1], so $\hat{\lambda} = 2\,\mathrm{Re}\,\lambda_{1,2}$.

For any 2×2 matrix $\mathbf{A}$ a *pseudoinversed matrix* $\hat{\mathbf{A}}$ can be defined (this operation was introduced in [1] as "symplectic conjugate")

$$\hat{\mathbf{A}} = -\mathbf{S}\mathbf{A}^T\mathbf{S}$$

with the following properties

$$\mathbf{A} + \hat{\mathbf{A}} = (\mathrm{Tr}\,\mathbf{A})\mathbf{I}\,, \quad \mathbf{A}\hat{\mathbf{A}} = |\mathbf{A}|\mathbf{I}\,.$$

Now one can write down the 6×6 transport matrix, its inverse and recurrent matrix in a blockwise form

$$\mathbf{M} = \begin{pmatrix} \mathbf{M}_{11} & \mathbf{M}_{12} & \mathbf{M}_{13} \\ \mathbf{M}_{21} & \mathbf{M}_{22} & \mathbf{M}_{23} \\ \mathbf{M}_{31} & \mathbf{M}_{32} & \mathbf{M}_{33} \end{pmatrix}, \ \overset{\leftrightarrow}{\mathbf{M}} = \begin{pmatrix} b_1\mathbf{I} & \mathbf{R}_3 & \hat{\mathbf{R}}_2 \\ \hat{\mathbf{R}}_3 & b_2\mathbf{I} & \mathbf{R}_1 \\ \mathbf{R}_2 & \hat{\mathbf{R}}_1 & b_3\mathbf{I} \end{pmatrix},$$
$$\mathbf{M}^{-1} = \begin{pmatrix} \hat{\mathbf{M}}_{11} & \hat{\mathbf{M}}_{21} & \hat{\mathbf{M}}_{31} \\ \hat{\mathbf{M}}_{12} & \hat{\mathbf{M}}_{22} & \hat{\mathbf{M}}_{32} \\ \hat{\mathbf{M}}_{13} & \hat{\mathbf{M}}_{23} & \hat{\mathbf{M}}_{33} \end{pmatrix},$$

where $\mathbf{R}_i = \mathbf{M}_{\vec{i}\,\overleftarrow{i}} + \hat{\mathbf{M}}_{\overleftarrow{i}\,\vec{i}}$, $b_i = \mathrm{Tr}\,\mathbf{M}_{ii}$ and $|\mathbf{R}_i| = d_i$. From now on we will assume that indices $i, j \in \{1, 2, 3\}$, also $\overleftarrow{i}$ and $\vec{i}$ mean cyclic permutation of these values (e.g. $1 = \overleftarrow{2} = \vec{3}$).

EIGENVALUES OF RECURRENT MATRIX

Our method for eigenvalues calculation is similar to the one proposed in [2]. Let $\overset{\leftrightarrow}{\mathbf{v}}$ be 6-component eigenvector of $\overset{\leftrightarrow}{\mathbf{M}}$, i.e. $\overset{\leftrightarrow}{\mathbf{M}}\overset{\leftrightarrow}{\mathbf{v}} = \hat{\lambda}\ \overset{\leftrightarrow}{\mathbf{v}}$. We split $\overset{\leftrightarrow}{\mathbf{v}}$ into 3 two-component subvectors, so as $\overset{\leftrightarrow}{\mathbf{v}}^T = (\,\mathbf{X}_1^T \quad \mathbf{X}_2^T \quad \mathbf{X}_3^T\,)^T$. Then

$$a_{ij}\mathbf{X}_i + \mathbf{R}_{\overleftarrow{i}}\mathbf{X}_{\vec{i}} + \hat{\mathbf{R}}_{\vec{i}}\mathbf{X}_{\overleftarrow{i}} = \bar{\mathbf{0}}\,, \tag{2}$$

where $\bar{\mathbf{0}}$ is a zero two-component vector, $a_{ij} = b_i - \hat{\lambda}_j$. Eliminating 2 of 3 $\mathbf{X}_i$ one can obtain

$$a_{1j}d_1 + a_{2j}d_2 + a_{3j}d_3 - a_{1j}a_{2j}a_{3j} = t\,, \tag{3}$$

where $t = \mathrm{Tr}\,(\mathbf{R}_1\mathbf{R}_2\mathbf{R}_3)$.

As we proved earlier, each eigenvalue of $\overset{\leftrightarrow}{\mathbf{M}}$ is degenerated at least twice, so its characteristic polynomial is a perfect square of some $\hat{P}(\hat{\lambda})$ with real coefficients. So, (3) can be regarded as characteristic equation of $\overset{\leftrightarrow}{\mathbf{M}}$, i.e.

$$\hat{P}(\hat{\lambda}) = \sqrt{|\overset{\leftrightarrow}{\mathbf{M}} - \hat{\lambda}\mathbf{I}|} = \hat{\lambda}^3 - (b_1 + b_2 + b_3)\hat{\lambda}^2 + \\ +(b_1b_2 + b_2b_3 + b_1b_3 - d_1 - d_2 - d_3)\hat{\lambda} + \\ +(b_1d_1 + b_2d_2 + b_3d_3 - b_1b_2b_3 - t)$$

* This work has been supported by Russian Science Foundation (project N14-50-00080).

ISBN 978-3-95450-181-6

ON THE INTEGRO-DIFFERENTIAL EQUATIONS FOR DYNAMICS OF INTERACTING CHARGED PARTICLES MODELING

D.A. Ovsyannikov*, N. Edamenko,
St. Petersburg State University, 7/9 Universitetskaya nab., St. Petersburg, 199034 Russia

Abstract

In this paper we consider some integral-differential model of the dynamics of charged particles with smoothed interaction. This model is used in solving various problems of optimization of the dynamics of intense beams. Using the proposed model in optimization problems allows you to find analytical expressions for the functional variation that characterize the dynamics of the particles, and then consruct methods of directed search of extremum.

INTRODUCTION

Problems of the analysis of charged particles dynamics in view of their interaction have long been the focus of many researchers. One of the basic mathematical models describing the dynamics of the interaction of particles is the mathematical model proposed by A.A.Vlasov [1]. Vlasov equation widely used to solve a variety of application problems. Of particular interest is the finding of the self-consistent distributions to a beam of charged particles in an electromagnetic field [2-4,15]. The problems of existence and uniqueness of solutions of the Vlasov equation considered in [5,6]. It should be noted that in the numerical simulation of the dynamics of intense beams mainly smoothed interaction of charged particles is used [7-10]. In this paper we consider some integral-differential model of the dynamics of charged particles with smoothed interaction. This model is used in solving various problems of optimization of the dynamics of intense beams. Using the proposed model in optimization problems allows you to find analytical expressions for the functional variation that characterize the dynamics of the particles, and then construct methods of directed search of extremum [11-14]. The paper describes an example of the construction of such integral-differential model for the dynamics of charged particles.

INTEGRO-DIFFERENTIAL MODEL

Suppose that the dynamics of the beam of interacting charged particles is described by the system of integro-differential equations

$$\frac{dx}{dt} = f(t,x), \tag{1}$$

$$\frac{\partial\rho}{\partial t} + \frac{\partial\rho}{\partial x} f(t,x) + \rho \, div_x f(t,x) = 0, \tag{2}$$

$$f(t,x) = f_1(t,x) + \int_{M_t} \rho(t,y) f_2(t,x,y)\, dy \tag{3}$$

* d.ovsyannikov@spbu.ru

with initial conditions

$$x(t_0,x_0) = x_0 \in \overline{M}_0, \quad \rho(t_0,x) = \rho_0(x). \tag{4}$$

Here the nonempty open bounded set $M_0 \subset R^n$; the real-valued nonnegative continuous function $\rho_0(x)$ in $\overline{M}_0$ specifies a density of particle distribution in the phase space at the initial time t_0; the vector-function $f_1(t,x)$ is determined by the external electromagnetic fields acting on particles; the vector-function $f_2(t,x,y)$ is determined by considering the particle interaction. Solution of (1)-(4) represent a set of vector-functions $x(t,x_0)$ that determine the bundle of trajectories emanating from the set M_0. Note that $M_t = \{x(t,x_0) : x_0 \in M_0\})$ and $\rho(t,x(t,x_0))$ is the density of particle distribution along these trajectories. Equality (2) means that

$$\int_{M_t} \rho(t,y) f_2(t,x,y)\, dy = \int_{M_0} \rho_0(y_0) f_2(t,x,x(t,y_0))\, dy_0,$$

that is, we consider the system of integro-differential equations

$$\frac{dx(t,x_0)}{dt} = f(t,x(t,x_0)) = f_1(t,x(t,x_0)) + \int_{M_0} \rho_0(y_0) f_2(t,x(t,x_0),x(t,y_0)) dy_0 \tag{5}$$

with initial conditions

$$x(t_0,x_0) = x_0 \in \overline{M}_0. \tag{6}$$

Suppose that the vector real functions $f_1(t,x)$ and $f_2(t,x,y)$ are defined and continuous on the sets $(\alpha,\beta)\times\Omega$ and $(\alpha,\beta)\times\Omega\times\Omega$ respectively, where $(\alpha,\beta) \in R^1$, and Ω is a region in R^n.

Denote $R_a = \{t : |t-t_0| \le a\}$, $\overline{M}_b = \{x : ||x-x_0|| \le b,\ x_0 \in \overline{M}_0\}$, $R_1 = R_a \times \overline{M}_b$, $R_2 = R_a \times \overline{M}_b \times \overline{M}_b$.

We have the following theorem of existence and uniqueness.

Theorem Suppose the following conditions are satisfied:
1) the nonnegative function $\rho_0(x) \in C(\overline{M}_0)$ is given: $\rho_0(x) \neq 0$ for $x \in M_0$, and $\int_{M_0} \rho_0(x)dx = \rho < +\infty$;
2) numbers $a > 0$ and $b > 0$ are given, such that $R_a \subset (\alpha,\beta)$, $\overline{M}_b \subset \Omega$;
3) $M_1 = \sup_{(t,x)\in R_1} ||f_1(t,x)||$, $M_2 = \sup_{(t,x,y)\in R_2} ||f_2(t,x,y)||$;
4) the vector-functions $f_1((t,x)$ and $f_2((t,x,y)$ satisfy the Lipschitz condition in the variables x and x,y with constant L_1 and L_2 on the sets R_1 and R_2, respectively.

ISBN 978-3-95450-181-6

COUPLED BUNCH INSTABILITIES IN THE STORAGE RINGS*

A.S. Smygacheva#, V.N. Korchuganov, Y.A. Fomin
NRC «Kurchatov Institute», Moscow, Russia

Abstract

Coherent instabilities of the bunched beam are one of the reasons that limit a total beam current in the storage rings. Although there are solutions of this problem, the estimation and reduction of the wake-fields influence on the longitudinal beam dynamics remain important things. In the article we return to the subject of coherent instabilities of the unevenly-filled bunches in the storage rings.

INTRODUCTION

The interaction of the bunched beam with its wake-fields in the vacuum chamber of the storage ring causes the coherent single-bunch and coupled-bunch instabilities. The growth of the coherent instabilities contributes to an increase of the longitudinal and transverse emittances and the energy spread of the single bunch. Also it leads to the partial losses and to complete losses of the bunch particles in some cases. The result of this process is the limitation of the maximum synchrotron radiation brightness of a facility.

Since most of the modern storage rings operate in a multi-bunch mode, a primary task is to cure the coupled-bunch instabilities. To dump the coherent oscillations of a bunch sequence the feedback systems are used [1]. But it's not a single way to solve the problem. To increase the instability threshold and the total beam current in the storage ring, it requires the reducing the wake-fields influence. In view of this fact the RF cavities with the HOM dumping or with a good HOM frequency control and stabilization, the smoothing of a vacuum chamber structure and the using the harmonic RF cavities for Landau damping have place at the accelerators [2].

The review of bunched beam coherent instabilities can be found in [3, 4, 5, 6, 7]. In most cases authors considered the interaction of the symmetrically disposed point charge bunches with wake-fields. Whereas the operation with the non-symmetrical beam and unevenly-filled bunches allows to increase the instability threshold and the total beam current. The attempts to determine the wake-field contribution to the longitudinal dynamics and the bunch sequence have led to the development of the several calculation schemes [8, 9, 10]. But these are special cases of a symmetrically-filled ring, and in some of them estimation results not always agreed to the experiment data.

The coherent frequencies of the non-symmetrical bunched beam were found following a basic approach that uses a notion of the beam spectrum and an impedance function to describe the beam-chamber interaction. This analytical solution allows to estimate the influence of each field mode on the coherent oscillations of bunches with known mode parameters (the resonant frequency, the shunt impedance, the quality factor), the given bunch sequence and the Gauss distribution of particles in the phase plane.

*The reported study was funded by RFBR according to the research project No. 16-32-00335 мол_а.
#sasmyga@mail.ru

COUPLED BUNCH INSTABILITIES

The longitudinal dynamics of the bunched beam under the influence of the external RF fields and its own wake-fields is presented in this article.

The M electron bunches circulate in the accelerator with an angular revolution frequency ω_o. Bunches fill the orbit in the arbitrary order. Maximum number of bunches corresponds with the separatrix number of the ring, which is equal to the ratio of the RF frequency to the revolution frequency.

The appearance of the coherent oscillations adds to stationary distribution the components of the density perturbation. Then the electron distribution function can be written as:

$$\begin{cases} \Psi(\hat{\tau},\varphi,t) = \Psi_o(\hat{\tau}) + \sum_{m\neq 0}\Psi_m(\hat{\tau})e^{jm\varphi}e^{j\omega_{sm}t} \\ \tau = \hat{\tau}\cos\varphi\,,\ \frac{\dot{\tau}}{\omega_s} = \hat{\tau}\sin\varphi \\ \varphi = \omega_s t + \varphi_o \end{cases}, \quad (1)$$

where $\Psi_o(\hat{\tau})$ – the stationary distribution function of particles in the bunch, $\Psi_m(\hat{\tau})$ – the amplitude of the density perturbation component for the *m*-mode of oscillations, ω_{sm} – the coherent angular frequency of the *m*-mode of oscillations, τ – the time deviation of the particle from the reference particle place, $\hat{\tau}$ и φ – the amplitude and phase of oscillations in polar coordinates, ω_s – the incoherent synchrotron frequency taking into account the potential well distortion effect [11], φ_o – the initial phase of oscillations.

The longitudinal dynamics of electrons in the *k*-bunch is described by a synchrotron motion equation of the single particle and the Vlasov equation for the distribution function of particles in the bunch [3]. For small oscillations the linearized equations are:

$$\ddot{\tau} + \omega_{so}^2\tau = -2\pi\frac{e\eta}{\beta^2 T_o E}\sum_{p,m,i} j^{-m}\cdot I_b^i\cdot Z(p\omega_o+\omega_{sm})\cdot F_{pm}^i\cdot e^{-jp\omega_o(i-k)\frac{T_o}{h}}\cdot e^{jp\omega_o\tau}\cdot e^{j\omega_{sm}t}, \quad (2)$$

$$\left(\frac{\partial}{\partial t} - \omega_s\frac{\partial}{\partial\varphi}\right)\sum_m \Psi_m^k(\hat{\tau})e^{jm\varphi}e^{j\omega_{sm}t} = -(\ddot{\tau}+\omega_s^2\tau)\cdot\frac{\sin\varphi}{\omega_s}\cdot\frac{\partial\Psi_o^k(\hat{\tau})}{\partial\hat{\tau}}, \quad (3)$$

where

ISBN 978-3-95450-181-6

CHROMATIC AND NONLINEAR DYNAMICS OF ANTIPROTONS INJECTED TO COLLECTOR RING AT FAIR*

D. Shwartz[#,1], I. Koop[1], P. Shatunov, BINP, Novosibirsk, 630090, Russia
[1] also at Novosibirsk State University, Novosibirsk, 630090, Russia

Abstract

Collector Ring (CR) is the storage ring for capturing and stochastic cooling of secondary beams of antiprotons or secondary ions. It is a part of a FAIR project being presently at the early start of a construction phase. Due to the proposed large acceptance in both transverse and longitudinal phase spaces, the chromatic aberrations and their correction with sextupoles are very important for capture efficiency. Calculations results for beam transfer from Pbar target to the ring are presented.

INTRODUCTION

The concept for the production of antiproton ($\bar{p}$, pbar) beams at FAIR is determined by the luminosity requirements for experiments with cooled $\bar{p}$ beams colliding with an internal H_2-target in the kinetic energy range from 0.8 GeV to 15 GeV at the High Energy Storage Ring (HESR) with $\bar{\text{P}}$ANDA [1].

Antiprotons are produced in inelastic collisions of high-energy protons with nucleons of a target. In the present accelerator layout for FAIR (see Fig.1) the SIS100 synchrotron accelerates protons to a kinetic energy of 29 GeV. Every 10 seconds the target will be hit with 2×10^{13} protons in a bunch of about 50 ns duration. The maximum yield (production and collection with reasonable emittance and momentum spread) is achieved for $\bar{p}$ kinetic energy of around 3 GeV that corresponds to 13 Tm of magnetic rigidity.

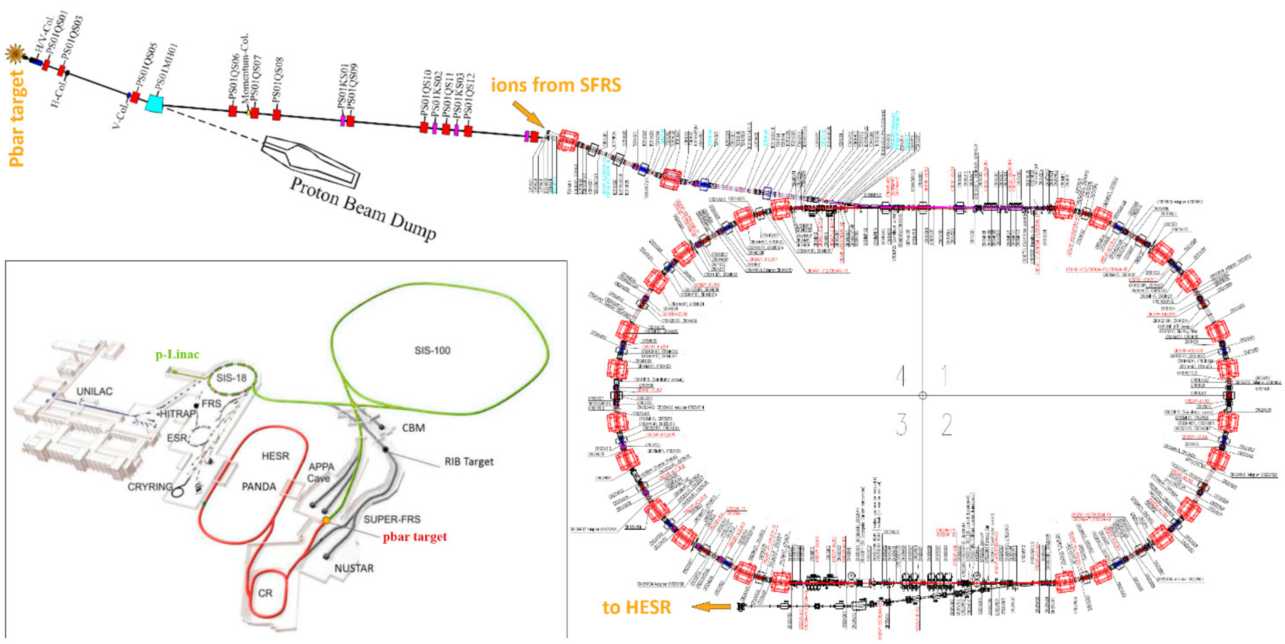

Figure 1: The overall antiproton program scheme at FAIR (left-down), and layout of AS-TCR1 beamline and Collector Ring.

TRANSPORT CHANNEL

The antiproton beam coming from target is focused by magnetic horn and passed through Antiproton Separator (AS) beamline with 4 consecutive collimators [2]. The calculated distribution of $\bar{p}$ in transverse phase space is shown in Fig.2 [3]. Only particles within aperture of first H/V collimator are shown.

The beamline following junction with path of ion beam from SFRS is called TCR1. The aim of the whole transfer line is to separate and to pass antiprotons with transverse emittance of $\varepsilon_{x,y}$ = 240 mm·mrad and momentum spread of $\Delta p/p = \pm3\%$ that corresponds to CR acceptance.

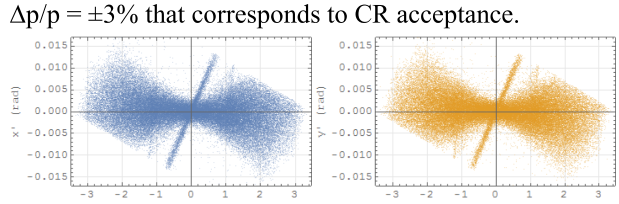

Figure 2: Transverse phase space after horn.

The lattice functions of whole transfer channel including straight section of CR ending with kickers are presented in

*Work supported by FAIR-Russia Research Center (FRRC)
#d.b.shwartz@inp.nsk.su

ISBN 978-3-95450-181-6

BEAM DYNAMICS CALCULATION OF ELECTRON BUNCH SEQUENCE PASSING THROUGH DIELECTRIC *

A.Altmark, Saint-Petersburg Electrotechnical University "LETI" ,Russia,
A.Kanareykin, EuclidTechLabs LLC, Gaithersburg MD, US

Abstract

The present work involves modelling the electron beams dynamics for development of new THz source based on cylindrical dielectric waveguide. The sequence of relativistic electron bunch generates Cherenkov radiation, which is a superposition of the TM and HEM-modes. The distances between bunches is selected for creating of monochromatic THz radiation. We made calculation of beam dynamics considering the Space Charge and focusing field with help of original BBU 3000 code. The main parameter of radiation was investigated: length of wave pocket, monochromaticity and frequency.

INTRODUCTION

This work was initiated by the experimental works [1-4] aimed at exploring new sources THz sources based on dielectric waveguide. Numerical calculations of the sources are made in previous works [5].

The THz Cherenkov radiation is generated in dielectric waveguide by electron beam. Spectrum of radiation is defined by parameters of waveguide (outer and inner radius, dielectric constant). Charge profile of electron beam can be used for selecting and damping of TM-modes in Cherenkov radiation. We are considering a new method of frequency selecting based on using of bunch sequence as source of radiation, figure 1. Variation of distances between bunches allow to select radiation frequency. The main disadvantage of this method is inability of frequency variation.

The main point of present work is beam dynamics which limits way passed by bunches. This parameter limits wave pocket of radiation.

Transverse dynamics caused by influence of asymmetric HEM–modes and focusing system. The value of transverse field grows with offset increasing from the axis of waveguide. In this paper, we study the dynamics of bunch sequence and influence of the focusing system to control of the transverse instability.

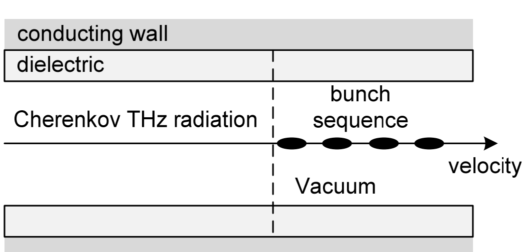

Figure 1: Longitudinal section of cylindrical dielectric waveguide with sequence of bunches.

The radiation (wakefield) with strong Ez component behind single bunch consist principally set of TM modes. One mode regime with frequency of TM_{01} mode can be realized by increasing of bunch length. The sequence of bunches permits to excite one mode radiation based on high order TM modes. This monochromatic radiation can be realized by fine tuning of distances between bunches. The sequence with founded distances allow to damp all TM mode except selected one.

INITIAL PARAMETERS

The dielectric waveguide presented in this work (Table 1) can be used as THz source for next frequencies: 142 GHz (TM_{01}-mode), 439 GHz (TM_{02}-mode), 765 GHz (TM_{03}-mode).

Parameters of bunch sequence are presented in Table 2. All bunches have same radial offset, which caused strong transverse instability particularly for low energy (15 MeV).

It is very important to consider the attenuation of the wakefield (loss tangent of dielectric and conductivity of metal wall in Table1), as well as the effect of group velocity. The group velocity grows with order of TM modes. It is means the wave pocket for high frequency will be shortest.

Table 1: Dielectric Waveguide Parameters

Waveguide	**Value**
Inner radius (um)	600
Outer radius (um)	850
Epsilon	3.8
Length (cm)	10
Loss tangent	0.001
Wall conductivity (S/m)	5.7E+07

Table 2: The Bunch Sequence Parameters

Bunch sequence	**Value**
Transverse beam size (um)	120
Longitudinal bunch length (um)	~ 100
Beam energy (MeV)	~ 15
Offset (um)	~ 100
Number of bunches	6-8
First frequency (GHz)	439
Second frequency (GHz)	765

ISBN 978-3-95450-181-6

ORBITAL MOTION IN MULTIPOLE FIELDS VIA MULTISCALE DECOMPOSITION

A.N. Fedorova, M.G. Zeitlin*, IPME RAS, St. Peterburg, Russia

Abstract

We present applications of methods of nonlinear local harmonic analysis in the variational set-up for a description of multiresolution representations in polynomial approximations for nonlinear motions in arbitrary n-pole fields. Our approach is based on the methods allowed to consider the best possible dynamical beam/particle localization in phase space and provided exact multiscale represention via nonlinear high-localized eigenmodes for all observables with exact control of contributions to motion from each underlying hidden scale.

INTRODUCTION

In this paper, we consider the applications of a numerical-analytical technique based on the methods of local nonlinear harmonic analysis [1] (in the particular case of underlying affine group a.k.a. wavelet analysis) to the calculations of orbital motion in arbitrary n-pole fields. Our main generic examples here are orbits in transverse plane for a single particle in a circular magnetic lattice in case when we take into account multipolar expansion up to an arbitrary finite number, and particle/beam motion in storage rings [2]. We reduce the complicated initial dynamical problem to a finite number of algebraical problems and represent all dynamical variables via multiscale expansions in the bases of modes maximally localized in the phase space. Our methods here are based on our general universal variational-wavelet approaches considered in papers [3]. Starting in next section from Hamiltonian of orbital motion in magnetic lattice and rational approximation of classical motion in storage rings, in the subsequent part we consider very flexible variational-biorthogonal formulation for a dynamical system with rational nonlinearities and construct the explicit representations for all dynamical variables as expansions in the bases/frames of proper nonlinear high-localized eigenmodes.

MOTION IN MULTIPOLAR FIELDS

The magnetic vector potential of a magnet with $2n$ poles in Cartesian coordinates is

$$A = \sum_n K_n f_n(x, y), \tag{1}$$

where f_n is a homogeneous function of x and y of order n. The cases from $n = 2$ to $n = 5$ correspond to low-order multipoles: quadrupole, sextupole, octupole, decapole. The corresponding Hamiltonian is (ref. [2] for designation):

$$\begin{aligned} H(x, p_x, y, p_y, s) &= \frac{p_x^2 + p_y^2}{2} + \\ &\left(\frac{1}{\rho^2(s)} - k_1(s)\right) \cdot \frac{x^2}{2} + k_1(s)\frac{y^2}{2} \\ &-\mathcal{R}e\left[\sum_{n\geq 2} \frac{k_n(s) + i j_n(s)}{(n+1)!} \cdot (x+iy)^{(n+1)}\right]. \end{aligned} \tag{2}$$

* zeitlin@math.ipme.ru

Then we may take into account an arbitrary but finite number of terms in expansion of RHS of Hamiltonian (2) and from our point of view the corresponding Hamiltonian equations of motions are not more than nonlinear ordinary differential equations with polynomial nonlinearities and possibly variable coefficients. As the second generic example, we consider the beam motion in storage rings [2]. Starting from Hamiltonian described classical dynamics in storage rings, and using Serret–Frenet parametrization, we have, after standard manipulations with the truncation of power series expansion of square root, the following approximated (up to octupoles) Hamiltonian for orbital motion in machine coordinates:

$$\begin{aligned} \mathcal{H} &= \frac{1}{2} \cdot \frac{[p_x + H \cdot z]^2 + [p_z - H \cdot x]^2}{[1 + f(p_\sigma)]} \\ &+p_\sigma - [1 + K_x \cdot x + K_z \cdot z] \cdot f(p_\sigma) \\ &+\frac{1}{2} \cdot [K_x^2 + g] \cdot x^2 + \frac{1}{2} \cdot [K_z^2 - g] \cdot z^2 - N \cdot xz \\ &+\frac{\lambda}{6} \cdot (x^3 - 3xz^2) + \frac{\mu}{24} \cdot (z^4 - 6x^2z^2 + x^4) \\ &+\frac{1}{\beta_0^2} \cdot \frac{L}{2\pi \cdot h} \cdot \frac{eV(s)}{E_0} \cdot \cos\left[h \cdot \frac{2\pi}{L} \cdot \sigma + \varphi\right] \end{aligned} \tag{3}$$

and the corresponding polynomial series expansion for function $f(p_\sigma)$. We consider here only arbitrary polynomial/rational (in terms of dynamical variables) expressions.

BIORTHOGONAL VARIATIONAL APPROACH VIA LOCALIZED MODES

The first main part of our consideration is some variational approach to these problems, which reduces the initial problem to the problem of solution of functional equations at the first stage and some algebraical problems at the second stage. Multiresolution representation [1] is the second main part of our construction. As a result, the solution is parameterized by solutions of two reduced algebraical problems, one is nonlinear and others are linear problems obtained from proper multiresolution/multiscale constructions. Finally, we obtain the exact (fast convergent numerically) multiscale decomposition via high-localized modes, like compactly supported wavelets or wavelet packets. Because the integrand of our (invariant) variational functional is represented by the bilinear form, it seems more reasonable to consider the constructions which take into account

ISBN 978-3-95450-181-6

ON A NEW APPROACH FOR DESCRIPTION OF SELF-CONSISTENT DISTRIBUTIONS FOR A CHARGED PARTICLE BEAM

O.I. Drivotin*, D.A. Ovsyannikov,
St.Petersburg State University, 7/9 Universitetskaya nab., St. Petersburg, 199034, Russia

Abstract

The present report is concerned with the problem of particle phase space distributions for a charged particle beam. A new approach is presented. It provides the possibility to specify various coordinates in the phase space. The main attention has been focused on the case where motion integrals are taken as phase coordinates. Using such coordinates, one can obtain a lot of self-consistent distributions. Some distributions for a breathing beam are considered as examples: generalized Brillouin flow, generalized KV distribution, and others. Besides, this approach allows simple graphical representation of various self-consistent distributions.

PHASE DENSITY

Main feature of the presented approach is covariant description of the particle distribution density in the phase space. The phase space particle distribution is described by a tensor density instead of the scalar distribution function. It allows specifying various coordinates in the phase space. This concept was previously formulated in the works [1, 2].

Let us consider a charged particle beam as a continuous media that occupies an open set in the phase space M. Such distribution are nondegenrate, and this cases can be regarded as most general. According to this model, particle number in an open subregion G, $G \subset M$, is a real number. Call the differential form $n(t,q)$ of degree $m = \dim M$ such that integration of the form over each open set G gives particle number in G the particle distribution density in the phase space, or the phase density:

$$\int_G n = N_G.$$

Here q and t denote position in the phase space and the time correspondingly. The boundaries of G and the form n are assumed sufficiently smooth for integration being possible. Such tensor density has the following physical sense. If we take a cell in the phase space defined by m displacement vector, the density as a polylinear form acting on these displacement vectors gives us a number of particles in this cell.

Consider another case when particle are distributed on an oriented surface S in the phase space that can move, $\dim S = p$, $0 < p < m$. Call the differential form $n(t,q)$ of degree p defined on the surface S such that for any open set G, $G \subset M$,

$$\int_{G\cap S} n = N_G$$

the particle distribution density for this case. This form depends on orientation of the surface. The orientation is defined by an ordered set of $m-p$ vectors. For example, orientation of a two-dimensional surface in the three dimensional space is defined by a vector, and in the four-dimensional and orientation of A change of the orientation can result in change of sign of the form components [3]. Assume that form n and the surface S are also sufficiently smooth for integration being possible.

At last, consider the case of a collection of dicrete particles. Define the scalar function

$$\delta_{q'}(q) = \begin{cases} 1, & q = q', \\ 0, & q \neq q'. \end{cases} \tag{1}$$

If q' depends on t, then this function is also function of t. All functions which values are nonzero only in finite set of points can be represented as linear combination of the functions of form (1). Restrict ourselves only to combinations with all coefficients equal to 1:

$$n(t,q) = \sum_{i=1}^{N} \delta_{q_{(i)}}(q), \qquad q_{(i)} \neq q_{(j)}, \quad \text{if} \quad i \neq j. \tag{2}$$

In this class of functions, define an operation of taking sum of function values in all points $q_{(i)}$, where the function value is nonzero:

$$\sum_{q\in G} n(t,q) \equiv \sum_{i:\, q_{(i)}\in G} n(t, q_{(i)}). \tag{3}$$

Operation defined by equation (3) is analogous to integration of the form of higher degree over G. A scalar function can be regarded as the differential form of degree 0. Therefore, equation (3) set a rule of integration of a form of degree 0 over open set G. As previously, call function of form (2) the phase density for system of pointlike particles if

$$\sum_{q\in G} n(t,q) = N_G.$$

It is easy to understand that the phase density is given by equality (2), where $q_{(i)}$ are positions of the particles in the phase space, $i = \overline{1,N}$, N is the total number of particles in the ensemble.

* o.drivotin@spbu.ru

ISBN 978-3-95450-181-6

FORMATION OF A GIVEN DISTRIBUTION OF THE BEAM IN THE PERIODIC CHANNEL

Serge N. Andrianov*, Nikolai Edamenko,
St. Petersburg State University, 7/9 Universitetskaya nab., St. Petersburg, 199034 Russia

Abstract

Accelerators and beam transport systems are the most widely used in various fields of fundamental and applied science. This leads to the need for construction of correct models of the corresponding objects and processes. In this paper we consider the problem of forming a beam with a given distribution. Note that similar requirement to the beam occurs in circular accelerators, and in the beam transport systems for various fields of physics, chemistry, biology and so on. Special attention is paid to the development of effective mathematical methods and computer programs to modeling of control systems to ensure the necessary requirements to the beam.

INTRODUCTION

At the moment, we have a long experience in the study of the dynamics of the distribution of particles in the beam in a periodic channel (see, eg, [1], [2], [3]). It is well known that variety of self-consistent density distributions can be built in a uniform focusing channel, see [4], [5]. However, the question of purposeful formation of the desired particle distribution (for example, in the configuration space) in our opinion was not sufficiently developed in theory and practice of accelerator systems, despite the relatively high demand for similar tasks. Requirements for particle beams in modern accelerators, are constantly increasing. First of all, it concerns aspects of modeling optimal systems. Secondly, the inclusion of non-linear control elements for targeted management to produce beams with the specified parameters.

In this direction there are some "basic" approaches. The first type (direct) is based on a careful study of the influence of various factors on the beam dynamics. The second method uses optimization techniques, in which there essentially are solved the inverse problems. Indeed, in this case, we can formalize the requirements for the beam parameters and to implement the search process of optimal solutions for ensuring specified requirements with a given accuracy. It should be noted that inverse problems are a class of ill-posed problems requiring the construction of special methods of solution. However, in both methods there are some common features. In the following we briefly describe the formalism in which the beam itself and the control system of the accelerator are described. This formalism is based on an approach based on the matrix representation for evolution operators [5] on the one hand and different forms of descriptions of the beam as a collective object.

* s.andrianov@spbu.ru

CONCEPT OF MATRIX FORMALISM

Let us briefly describe the essential features of the mathematical formalism of the matrix formalism and its features that allow realizing for effective computational experiments. Following [5] for the nonlinear ordinary differential equations describing the evolution of the particles in the accelerator we can write

$$\frac{d\mathbf{X}}{ds} = \mathbf{F}^{\mathrm{ext}}(\mathbf{B}^{\mathrm{ext}}(\mathbf{X}, s, \mathbf{E}^{\mathrm{ext}}(\mathbf{X}, s), \mathbf{X}, s)+ \mathbf{F}^{\mathrm{self}}(\langle f(\mathbf{X}, s)\rangle_{\mathfrak{M}}, \mathbf{X}, s), \quad (1)$$

where $\langle f(\mathbf{X}, s)\rangle_{\mathfrak{M}}$ means that the distribution function is included in the $\mathbf{F}$ via integral and the integration is over volume occupied by particles $\mathfrak{M} = \mathfrak{M}(s)$, where s is the length measured along the reference orbit. According to [5] one can introduce the evolution operator $\mathcal{M}(t\,|\,t_0; \mathbf{F})\colon \mathbf{X}_0 \to \mathbf{X}(t)$ in by equation (1). Given the property of the evolution operator one can write

$$\mathbf{F}^{\mathrm{self}}(\langle f(\mathbf{X}, t)\rangle_{\mathfrak{M}}, \mathbf{X}, t) = \mathbf{F}^{\mathrm{self}}(\langle f_0(\mathcal{M}^{-1}(t\,|\,t_0, \mathbf{F}) \circ \mathbf{X}_0)\rangle_{\mathfrak{M}_0}, \mathbf{X}, t). \quad (2)$$

In accordance with the equations (1) and (2) one can write the following integral operator equation

$$\mathcal{M}\left(t\,|\,t_0; \mathcal{V}^{\mathrm{ext}} + \mathcal{V}^{\mathrm{self}}\right) = \mathcal{I}d + \int\limits_{t_0}^{t} \left(\mathcal{V}^{\mathrm{ext}}(\tau)+ \mathcal{V}^{\mathrm{self}}(\tau)\right) \circ \mathcal{M}\left(\tau\,|\,t_0; \mathcal{V}^{\mathrm{ext}}(\tau) + \mathcal{V}^{\mathrm{self}}(\tau)\right) d\tau. \quad (3)$$

We note that equation (3) is an integral equation of Volterra–Urysohn of type II (see, eg, [6]), as in fact the control system (the transportation system) – the control object (beam) is covered by the feedback. It proves that the sequence $\mathcal{M}^k$ converges (in some sense) to some element $\mathcal{M}^{\mathrm{fin}}$, and one can install the identity $\mathcal{M}^{\mathrm{fin}} = \mathcal{A} \circ \mathcal{M}^{\mathrm{fin}}$. We should note that similar approach not only allows us to use different forms describe the beam dynamics, taking into account the impact of its own charge but and allows us to build different methods of description of the beam dynamics, taking into account the impact of their own charge. The similar approach allows us to build different forms describe the beam dynamics, taking into account the impact

ISBN 978-3-95450-181-6

PROGRAM COMPLEX FOR MODELING OF THE BEAM TRANSVERSE DYNAMICS AND ORBIT CORRECTION IN NUCLOTRON, LHEP JINR

I.V. Antropov, V.A. Kozynchenko*, V.O. Khomutova, D.A. Ovsyannikov,
Saint-Petersburg State University, Saint-Petersburg, Russia
I.L. Avvakumova, O.S. Kozlov, V.A. Mikhaylov, A.O. Sidorin, G.V. Trubnikov,
JINR, Dubna, Moscow Region, Russia

Abstract

Program complex for modelling of transverse dynamic of particle beams and orbit correction at Nuclotron synchrotron (LHEP JINR) is considered in current work. The program complex provides calculation of transverse dynamic of charged particle beams in Nuclotron and its axis, based on linear model with transport matrix of lattice elements, calculation of Nuclotron Twiss parameters, acceptance and emittance of the beam. A possibility to optimize the location of beam position monitors (pick-up) and multipole correctors is foreseen as well as calculation of the orbit with measuring data of pick-up stations of Nuclotron. Program complex includes realizations of orbit correction algorithms with response matrix and provides correction of the orbit in Nuclotron. User's graphic interface provides interaction of user with program complex, including performance on demand of the user of separate functions of the program complex, providing input and maintenance of parameters, download from file and record into the file of parameters and calculation results, graphical view of the calculations results in program complex. Program software environment is integrated with MAD-X program (upload, processing of data to and from, visualization). Format of input and output data is compatible with relevant MAD-X format.

INTRODUCTION

At present, in the Joint Institute for Nuclear Research (Dubna, Russia) successfully operates the Nuclotron – a synchrotron for accelerating beams of multicharged ions, protons and deuterons [1]. To reduce losses in the Nuclotron, various orbit correction methods are used [2]. When studying the problem of orbit correction, the necessity has arisen for creating a package of programs that would allow making cooperative use of both the accumulated experience and new developments. The program comlex considered in the paper includes an extensive graphical interface and a variety of tool kits, methods and algorithms that allows the researcher mostly to be focusing on the model development. The package also includes the BDO Nuclotron laboratory, a general description of which is the subject of this article.

*v.kozynchenko@spbu.ru

DESCRIPTION OF THE PROGRAM COMPLEX

The program complex consists of a control program, laboratories and libraries.

BDO Shell [3],[4] – a control program having the rich graphical user interface, a library of model parameters, and system functions. One may refer to the specific features of this product the following:

- the possibility of dividing the calculation process into stages with specifying the groups of input and output data files;
- the ability to automate the simulation process for a given parameter ranges;
- using various case studies with pre-described sets of parameters, input and output data files, settings of calculation stages.

BDO Nuclotron - laboratory for modeling and optimization of particle beams dynamics in the Nuclotron. The laboratory consists of several models allowing computation of the linear transverse dynamics of the beam center of gravity, the beam transverse dynamics, and the structural features of the Nuclotron. There is also a library of initial distributions, and a library of the correction methods for a closed orbit.

MODULES

The Module for Calculating the Lateral Dynamics of the Center of Gravity of the Beam in the Nuclotron Based on a Linear Model

The module for calculating a transverse beam dynamics in the Nuclotron provides computing the lateral dynamics of the center of gravity of the beam at the Nuclotron that is based on a linear model and uses the transport matrices of structural elements of the Nuclotron (dipole bending magnets, focusing and defocusing quadrupole lenses, drift gaps, and multipole magnetic correctors). When calculating the dynamics, the structural elements intended for the slowed-down beam extraction from the Nuclotron channel are not considered. One can add other structural elements of the Nuclotron, as well as change the location of pick-up displays and multipole correctors. When calculating the dynamics, the own beam field is ignored. It is possible to take into account the errors of the magnetic field in the elements of the transport matrix. The module provides for the formation of the response matrix being made on the base of computing the transverse

ISBN 978-3-95450-181-6

APPLICATION OF GPGPUs AND MULTICORE CPUs IN OPTIMIZATION OF SOME OF THE MPDROOT CODES*

A. Fatkina#, O. Iakushkin, N. Tikhonov, St. Petersburg State University, St. Petersburg, Russia

Abstract

We analyzed the ways to optimize MPDRoot algorithms using existing solutions from external libraries. We also examined the libraries designed to work with graphics accelerators and multi-core CPUs, such as cuRAND, cuFFT and OpenCL FFT.

The paper describes the ways to expedite a portion of Kalman filter by transferring it to GPUs or multi-core CPUs using the implementation included into the MPDRoot package.

INTRODUCTION

MPD (Multi Purpose Detector) is a part of NICA (Nuclotron-based Ion Collider fAcility) [1]. MPDRoot is a framework based on ROOT and FairRoot technologies. It is designed to simulate experiments conducted on MPD and to analyze the resulting data. According to the MPD documentation, collected data can be huge. Fast data processing is necessary to cope with extreme data sets. Thus it is a task of crucial importance that algorithms work well in parallel and distributed environments [2-6]

In this paper, we look into how Graphic Processing Units (GPUs) and multicore CPUs may be applied in MPDRoot project optimization.

PERFORMANCE ANALYSIS OF MPDROOT FRAMEWORK TESTS

The following methods were used to analyze MPDRoot framework:

- Doxygen utility was used to generate classes and functions dependency graphs. It was also used to code navigation.
- ValgrindCallgrind tool was used to profile the package. By using this we got callgraphs for MPDRoot tests.

We selected some algorithms that can be ported on coprocessor architectures and seems to be optimizable.

PROPOSED OPTIMIZATIONS

The following algorithms were considered:

- Fast Fourier Transform;
- Random number generation;
- Kalman Filter.

Figure 1 shows calls of the Rndm() function in the ROOT framework. It is called over 32 million times in the runMC test. The function employs MT (Mersenne Twister) algorithm described in [7].

Random Number Generation

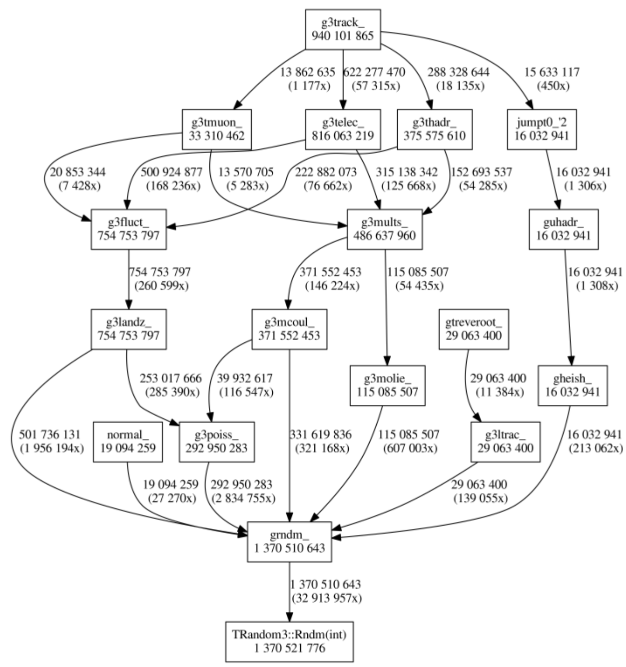

Figure 1: Profiling data - Random number generation.

There is a modified version of this algorithm — SFMT (SIMD-oriented Fast Mersenne Twister) [8], which is twice as fast owing to the SIMD (Single Instruction Multiple Data) principle. It should be noted that the version of MT described in that paper can only be executed on a CPU with a vector processing unit (VPU).

CuRAND library may be used as an alternative to ROOT-based MT. It makes it possible to generate random numbers on GPGPU (general-purpose computing for graphics processing units) using CUDA architecture. The library provides a wide range of generators including MT and MTGP (Mersenne Twister for Graphic Processors) [9].

The use of the cuRAND library to generate random numbers in the GEANT4 framework was proposed at the Annual Science Meeting in 2013 [10]. This approach can either be integrated into the MPD Root project directly with the cuRAND library or indirectly by using GEANT4.

Kalman Filter

MPD Root reconstructs the particles' tracks using Kalman filter. This algorithm is sequential and uses matrixes.

* supported by SPbU (Saint Petersburg State University) grants 9.37.157.2014, 0.37.155.2014 and Russian Foundation for Basic Research grant (project no. 16-07-01113 and no. 16-07-01111).
# st035020@student.spbu.ru

ISBN 978-3-95450-181-6

DYNAMICAL APERTURE BEYOND PERTURBATIONS: FROM QUALITATIVE ANALYSIS TO MAPS

A.N. Fedorova, M.G. Zeitlin*, IPME RAS, St. Peterburg, Russia

Abstract

We start with a qualitative approach based on the detailed analysis of smoothness classes of the underlying functional spaces provided possible evaluation of the dynamical aperture in general nonlinear/polynomial models of particle/beam motion in accelerators. We present the applications of discrete multiresolution analysis technique to the maps which arise as the invariant discretization of continuous nonlinear polynomial problems. It provides a generalization of the machinery of local nonlinear harmonic analysis, which can be applied for both discrete and continuous cases and allows to construct the explicit multiresolution decomposition for solutions of discrete problems which are the correct discretizations of the corresponding continuous cases.

INTRODUCTION

The estimation of the dynamic aperture of accelerators is an important, complicated and long standing problem. From the formal point of view the aperture is some border between two types of dynamics: relative regular and predictable motion along of acceptable orbits or fluxes of orbits corresponding to KAM tori and stochastic motion with particle losses blown away by the Arnold diffusion and/or chaotic motions. According to the standard point of view this transition is being done by some analogues with map technique [1]. Consideration for aperture of n-pole Hamiltonians with kicks

$$H = \frac{p_x^2}{2} + \frac{K_x(s)}{2}x^2 + \frac{p_y^2}{2} + \frac{K_y(s)}{2}y^2 + \frac{1}{3!B\rho}\frac{\partial^2 B_z}{\partial x^2}(x^3 - 3xy^2)L\sum_{k=-\infty}^{\infty}\delta(s-kL) + \dots \quad (1)$$

is done by linearisation and discretization of canonical transformation and the result resembles (pure formally) standard mapping. This leads, by using the Chirikov criterion of resonance overlapping, to the evaluation of aperture via amplitude of the following global harmonic representation:

$$x^{(n)}(s) = \sqrt{2J_{(n)}\beta_x(s)}\cdot \cos\left(\psi_1 - \frac{2\pi\nu}{L}s + \int_0^s \frac{\mathrm{d}s'}{\beta_x(s')}\right). \quad (2)$$

The goal of this paper is two-fold and presents a sketch of alternative approaches located beyond any linearization or perturbation approaches. In the next part, we consider some qualitative criterion which is based on the attempts of more realistic understanding of the existing difference between motion in KAM region and stochastic regions: motion in KAM regions may be described by regular functions only (without the influence of complicated internal structures leading to nonuniform hyperbolicity generating chaos) while motion in stochastic regions/layers may be described by functions with internal (self-similar, e.g.) structures (definitely, created by actions of symmetry generated groups, like discrete groups, or by actions of hidden symmetries of background functional space, like affine group in the most simple case) i.e. fractal type functions which realized the proper orbits [2]. In the subsequent section according to the invariant Marsden-Veselov approach, we consider symplectic and Lagrangian background for the case of discretization of flows by the corresponding maps [3]. Affter that, in the next section, we present the construction of the corresponding solutions by applications of the multiscale approach of A. Harten [4] based on generalization of multiresolution analysis for the case of maps. Such approaches provide the principles and the possibilities for the control of aperture behaviour in the space of machine parameters. All details, constructions, and results can be found in [5].

QUALITATIVE ANALYSIS

The fractal or chaotic image is a function (distribution) which has structure at all underlying scales. Such objects have additional nontrivial details on any level of resolution. But they cannot be represented by smooth functions, because they resemble constants at small scales [2]. We need to find self-similarity behaviour during movement to small scales for the functions describing non-regular motion. So, if we look on a “fractal” function f (e.g. the Weierstrass function) near an arbitrary point at different scales, we find the same function up to the scaling factor. Consider the fluctuations of such function f near some point x_0

$$f_{loc}(x) = f(x_0 + x) - f(x_0), \quad (3)$$

then we have the renormalization (group)–like behaviour/transformation

$$f_{x_0}(\lambda x) \sim \lambda^{\alpha(x_0)} f_{x_0}(x), \quad (4)$$

where $\alpha(x_0)$ is the so-called local scaling exponent or Hölder exponent of the function f at x_0. According to [2] general functional spaces and scales of spaces can be characterized through wavelet coefficients or wavelet transforms. Let us consider continuous wavelet transform

$$W_g f(b,a) = \int_{R^n} \mathrm{d}x \frac{1}{a^n}\bar{g}\left(\frac{x-b}{a}\right) f(x),$$

* zeitlin@math.ipme.ru

ISBN 978-3-95450-181-6

COMPUTER SIMULATION OF THE SLOW BEAM EXTRACTION FROM NUCLOTRON

I. Avvakumova, V. Emelianenko, A. Kovalenko, V. Mikhaylov, VBLHEP, JINR, Dubna, Russia

Abstract

The results of modelling of particles motion during slow beam extraction from Nuclotron at the energy of 6 GeV/u are analyzed. Influence of the measured sextupole component of dipole magnets and fringe fields of the Lambertson magnets on the characteristics of extracted beam is presented. The calculations have been done using the MadX package.

INTRODUCTION

The Nuclotron, superconducting heavy ion synchrotron with iron shaped magnets, has been under operation since 1993. Physics experiments were carried out only in internal circulating beams before March, 2000. Preparation of the extraction system elements [1], their final bench tests and installation in the ring were performed in 1999. In 2000 the works were completed, and the equipment was installed into the ring and put into operation that made it possible to carry out further experiments at the extracted beams as well [2], [3].

EXTRACTION SYSTEM

System of slow beam extraction from Nuclotron includes electrostatic septum (ES), pair of Lambertson magnets (LM), 4 sextupole lenses and 4 special quadrupole lenses. The sextupoles produce 22-th harmonic of sextupole nonlinearity to excite the resonance $Q_x = 22/3$. The first pair of the lenses is located in second and sixth octants of the Nuclotron lattice whereas the second pair in fourth and eighth octants respectively. Special quadrupole lenses are used to shift the horizontal tune to the resonance vicinity. The lenses are located in the first, third, fifth and seventh octants respectively. The ES and LM are located within the fifth octant. These elements provide two-stage particle deflecting system, namely: ES in horizontal plane and LM in vertical plane to the level of existing beam-transport channels in experimental halls. The LM is superferric magnet consisting of two sections 1.5 m long each. Composition of the lattice is shown in Fig. 1.

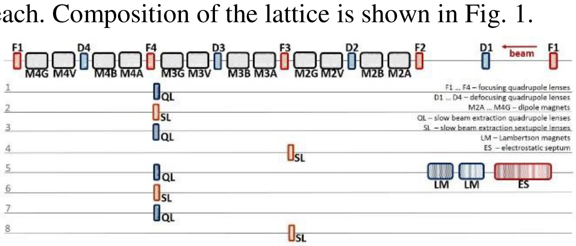

Figure 1: Composition of the Nuclotron elements.

The main task of this work is to consider how sextupole nonlinearity of dipole magnets and fringe fields of the LM disturb beam dynamics and to estimate possibility to extract the beam with high efficiency at the maximum energy. All the calculations were done for the betatron tunes $Q_x \sim 22/3$ and $Q_y = 7.4$. The gap between 3 cm and 5 cm on horizontal plane (XX' plane) is marked at each plot to show the gap of the ES. The possibility of entering this gap for the particle means its extraction.

SIMULATION AND RESULTS

At first, the case with zero nonlinearities of the structural dipoles and the other elements was considered. In this situation, there is no reason for the resonances exciting and for the extraction of the beam. Horizontal and vertical plane of the beam phase portrait at the entrance in ES are shown on Fig. 2a and Fig. 2b.

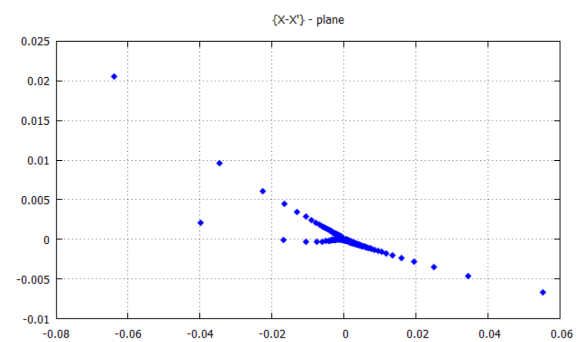

Figure 2a: XX' plane without nonlinearities

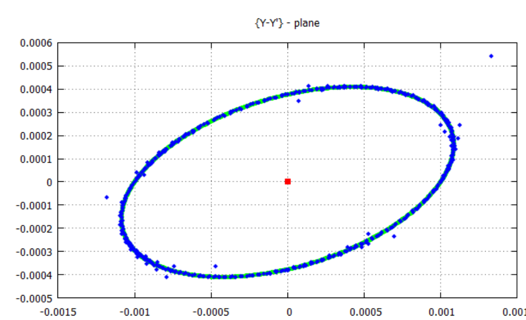

Figure 2b: YY' plane without nonlinearities.

At the next stage the sextupole nonlinearity of the dipoles was taken into account. The appearance of additional areas of stability (see Fig. 3) is observed even without switching the sextupole lenses of slow beam extraction.

ISBN 978-3-95450-181-6

PARALLELIZATION OF ENVELOPE DYNAMICS OF HIGH INTENSIVE BEAMS*

N. Kulabukhova†, Faculty of Applied Mathematics and Control Processes,
Saint-Petersburg State University, St. Petersburg, Russia

Abstract

In this work the survey of methods for high intensive beam dynamics is given. As an alternative to them the approach based on envelope dynamics was used. This method is focusing on the use of the matrix form for Lie algebraic methods for calculating the beam dynamics in the presence of self-field of the beam. In particular, the corresponding calculations are based on the predictor-corrector method. Pros and cons of using described approach on hybrid systems are discussed.

INTRODUCTION

The number of methods and software for modeling beam dynamics is out of counting. The most popular software packages are MAD, COSY Infinity, TRANSPORT, BEAMBEAM3D, IMPACT-Z, IMPACT-T and some others [1]. But the problem of gathering different packages under one software product (figure 1) is not yet solved [2, 3]. Software for modeling beam dynamics with the

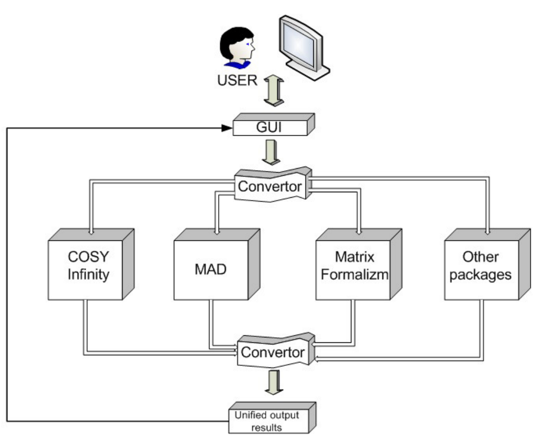

Figure 1: Unified user access.

space charge forces in the concept of matrix forms is the part of project of making a unified user interface "Virtual Accelerator Laboratory"(VAL) [4]. The main use of the VAL is simulation of beam dynamics by different packages with the opportunity to match the results (in case of using different solution methods for the same problem) and the possibility to create pipelines of tasks when the results of one processing step based on a particular software package can be sent to the input of another processing step.

However, in all these packages methods of tracking particle by particle through the whole system. The most commonly used is Particle-in-Cell method (PIC)[5, 6]. The Fortran-based environment COSY INFINITY is based on computations of perturbation expansions of Poincare maps to high orders. MARYLIE [7] is a FORTRAN program for beam transport and tracking based on a Lie algebraic formulation of charged particle trajectory calculations.

And in case of intensive beams, which can lead to the so called the filamentation effect or to the Halo, the number of particles is bigger then 1 billion. Though, the computer resources allow us to calculate large amount of data, the practice shows that it is better to have a parallel algorithm than a good and powerful machine. That was the goal: to make the algorithm that can be parallelized easily.

ENVELOPE DYNAMICS IN MATRIX FORM

It is well known that the envelope equations for continuous beam with uniform charge density and elliptical cross-section were first derived by Kapchinsky and Vladimirsky (KV). This very useful result has been put into different approaches to charged beams description with any charge distribution with elliptical symmetry. More over this is also true in practice for three dimensional bunched beams with ellipsoidal symmetry.

Matrix formalism is a high-performance mapping approach for Ordinary Differential Equation solving. It allows to present solution of the system in the following form

$$X = \sum_{i=0}^{k} R^{1i}(t) X_0^{[i]}$$

where R^{1i} are numerical matrices. As it was said above, there are different ways of modeling beam dynamics:

- Trajectory analysis. In this case the beam is presented as a particles assemble and can be written using the following matrix $X^N = \{\vec{X}^1, \ldots, \vec{X}^N\}$, where $\vec{X}^k$ is a phase vector of k-th particle and N is a number of particles.
- Beam envelope dynamics. In this case the beam is described in the terms of envelope matrices [8]. We will speak about them later.
- Distribution function dynamics. In this case one present the beam in the terms of a distribution function, which satisfies to the Maxwell-Vlasov equations system.

In this paper, we describe an approach to construct analytical expressions for the electric field produced by the

* Work supported by SPbSU 0.37.155.2014 and RFBR 16-07-01113A
† n.kulabukhova@spbu.ru

ISBN 978-3-95450-181-6

NUMERICAL ANALYSIS OF CAVITY MODE OPERATION AND ELECTRON BEAM DYNAMICS IN LEBEDEV INSTITUTE MICROTRON

V.S. Dyubkov, Yu.Yu. Lozeev, National Research Nuclear University MEPhI, Moscow, Russia
Yu.A. Bashmakov, National Research Nuclear University MEPhI and P.N. Lebedev Physical Institute of the Russian Academy of Sciences, Moscow, Russia

Abstract

Dynamics of electrons in classic microtron is studied. 3D cavity model is developed and electromagnetic field distribution is simulated. Dependence of output beam parameters on microtron operation mode is investigated and discussed.

INTRODUCTION

The microtron is a circular resonance electron accelerator that was first proposed by V.I. Veksler in 1944 [1]. Electrons are accelerated in RF cavity located inside the magnet that forms a uniform time-constant field. Electrons, captured in synchronous acceleration mode, move in circles with stepwise increasing radii. Note all these circles theoretically have a common point that located inside the cavity. The main advantages of the microtron are extremely narrow energy spectrum and small sizes of accelerated beams [2,3]. Additionally, the microtron has relatively simple design and low cost of operation. Classical microtrons are used in variety application of science, industry and medicine. Thus, microtron is used as injector for electron synchrotrons with average energy is equal to (0.250 – 1.5) GeV [4,5]. It can be an effective source of high energy photon radiation in photon and neutron activation analysis. Microtrons can be used for photonuclear reaction production [6], as well as for neutron production for pulsed fast neutron reactor [7]. Today, one of the actual problems is a design of THz FEL based on microtron [8-10], one of the first realization attempts could date to the sixties of the last century.

NUMERICAL SIMULATION RESULTS

Electron dynamics simulation in 7 MeV Lebedev Physical Institute (LPI) microtron was carried out in present paper. This accelerator is an injector for 1.3 GeV "Pakhra" electron synchrotron (LPI). This microtron is also used to study bremsstrahlung characteristics of relativistic electrons in complex structures.

Circular cylindrical cavity based on the operating mode of E_{010} (TM_{010}) type at frequency of 2856 MHz is used as an accelerating element in LPI microtron. Electron source is a thermionic cathode mounted in a wall of the resonator (the so-called intracavity injection). LPI microtron is operated with the first type of acceleration [2,11,12]. The cavity cross section in microtron median plane is shown in Fig. 1. There are the basic geometric dimensions of the cavity in Fig. 1: radius (R), cavity length (d), distance between center of thermal emitter and the resonator axis (r_{emit}). Resonator geometry has a deviation from axially symmetric because of electron dynamics feature at the first turns. We consider that cavity length d was equal to 19 mm. Note that $R = 0.383\lambda_{010}$, λ_{010} – wavelength for E_{010} mode.

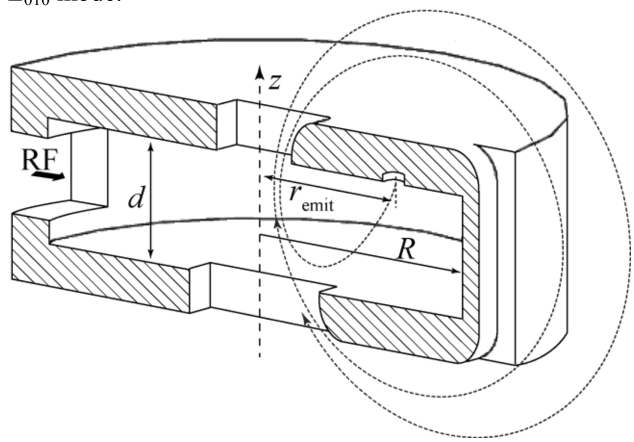

Figure 1: Cross-sectional view of RF cavity.

In the beginning 3D distribution of RF electromagnetic field (both electric and magnetic components) in microtron cavity was calculated by means of specialized code [13]. Typical spatial distribution of electric field absolute value in median plane is shown in Fig. 2. There are accelerating component of the cavity field as a function of longitudinal and transversal coordinates in Fig. 3 and Fig. 4 correspondingly.

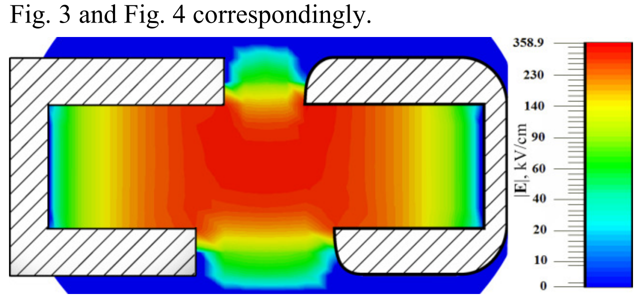

Figure 2: Typical spatial electric field distribution in median plane.

Further, dependence of output beam parameters on microtron operation mode, namely on amplitude of accelerating voltage, was investigated. In the first step it was written a special MICRO code that allowed us to carry out a two-dimensional one particle electron dynamics simulation in the field, calculated above, in microtron median plane. The energy of the emitted electrons was equal to 5 eV and r_{emit} was equal to 27 mm (shifted-emitter microtron). On simulating the electron dynamics we found that uniform magnetic field for circular motion is 0.12 T. Energy gain for one period is defined as follows

ISBN 978-3-95450-181-6

FOCUSING OF CHARGED PARTICLES BY MAGNETIC DIPOLES

G.V. Dolbilov, Joint Institute for Nuclear Research, Dubna, 141980, Russia

Abstract

The possibility of using magnetic dipoles for tight focusing of charged particles is discussed. Plane-parallel geometry of the magnetic poles of the dipoles greatly simplifies lens design and reduces the cost of creating a focusing system. Focusing is performed using gradient pulses of force of the magnetic dipoles.

INTRODUCTION

The strong focusing of linear beams of charged particles is performed quadrupole lenses. The magnetic fields of the quadrupole lenses can be created by the magnetic poles, the surface of which is isosceles hyperbolic cylinders. In practice, using simpler forms of poles, but this reduces the working area of the lens, and decrease the maximum value of the induction in the working area. The focusing action of the quadrupole lenses is associated with alternate deviation of the particle to the axis and off-axis focusing system. As a result of this action carried out "hard" beam focusing.

The use of dipoles with the gradient of the force impulse allows you to create lenses that strongly focus the beam in one of the mutually perpendicular direction reject particles only to the axis of the focusing system. In such lenses particles get two of the equal magnitude, but oppositely direction of the momentum force, if they are on the axis of the focusing system. As a result, the total moment of force is zero. All particles which are offset from the axis is always deflected to the axis of the focusing system. In the other direction the particles are defocused by edge fields on the boundary dipoles with opposite polarity field.

DYNAMICS OF PARTICLES IN THE BIPOLAR SYSTEM OF DIPOLES

Particle motion in a uniform field dipole is described by the equations

$\frac{dP_y}{dt} = qv_xB_z, \quad dP_y = qB_zdx, \quad dv_y = \frac{v}{R}dx,$

$$v_{n,y} = v_{(n-1),y} + \frac{v}{R}x_n\,, dx = \frac{R}{v}dv_y \qquad (1)$$

were $R = M\gamma v/qB_z = P/qB_z -$ circular radius of the particle in the field B_z; $q, M, v, P -$ charge, mass, speed and momentum of the particle, respectively, $\gamma -$ the relativistic factor of the particle, $x -$ the projection length of the trajectory of a particle on the x-axis.

$$\frac{dy}{dt} = v_x\frac{dy}{dx} = v_y\,, \quad \frac{dy}{dx} = \frac{v_y}{v_x} = \frac{v_y}{\sqrt{v^2 - v_y^2}}\,,$$

$$dy = \frac{v_y}{\sqrt{v^2 - v_y^2}}dx = \frac{R}{v}\frac{v_y dv_y}{\sqrt{v^2 - v_y^2}}\,,$$

$$y_n = y_{(n-1)} + \frac{R}{v}\int_{v_{(n-1),y}}^{v_{n,y}} \frac{v_y dv_y}{\sqrt{v^2 - v_y^2}} =$$

$$= y_{(n-1)} + \frac{R}{v}\left(\sqrt{v^2 - v_{n,y}^2} - \sqrt{v^2 - v_{(n-1),y}^2}\right)$$

In focusing systems, transverse speed of the particles is much less than the longitudinal velocity

$$\frac{v_y}{v} = \delta \ll 1,$$

Therefore, in the first approximation, ignoring the parameter of the second order of smallness δ^2 compared to unit, have

$$y_n = y_{(n-1)}\,, \qquad v_{n,y} = v_{(n-1),y} + \frac{v}{R}x_n$$

In the second approximation, when $\sqrt{v^2 - v_y^2} \cong v\left(1 - v_y^2/2v^2\right)$

$$y_n = y_{(n-1)} + \frac{R}{2}\left(\frac{v_{n,y}^2}{v^2} - \frac{v_{(n-1),y}^2}{v^2}\right),$$

$$v_{n,y} = v_{(n-1),y} + \frac{v}{R}x_n$$

FOCUSING LENS WITH TWO DIFFERENT POLARITY DIPOLES

Changing the parameters of a particle - displacement Δy and the relative velocity $\Delta\, v_y/v$, , a focusing lens consisting of two dipoles with uniform, equal in magnitude, but different polarity of the magnetic field and form of magnetic poles, as shown in Fig.1, will be as follows:

In the case where the first dipole deflects particles in the of positive $y -$ direction, on the output of the first dipole change of the transverse velocity and coordinate are equal

$$\Delta v_1 = v_1 - v_0 = v\frac{x_1}{R}$$

$$\Delta y_1 = y_1 - y_0 = \frac{R}{2}\left(\frac{v_{1,y}^2}{v^2} - \frac{v_{0,y}^2}{v^2}\right)$$

If the second dipole deflects particles in the negative $y -$direction on the output of the second dipole Δv_2 *and* Δy_2 will be equal

$$\Delta v_2 = v_2 - v_0 = v\frac{x_1 - x_2}{R}\,,$$

$$\Delta y_2 = y_2 - y_1 = \frac{R}{2}\left(\frac{v_{2,y}^2}{v^2} - \frac{v_{1,y}^2}{v^2}\right) \qquad (2)$$

where x_1 и $x_2 -$ projection of the particle trajectories in the first and second dipoles, respectively.

Particles injected into the lens parallel to the axis of the lens, $v_0 = 0$, are rejected by the lens on the angle $\Delta\varphi$ (Fig.1) .

$$tg\Delta\varphi = \frac{v_{2,y}}{v_x} \cong \frac{v_{2,y}}{v} = \frac{x_1 - x_2}{R} = -\frac{2\Delta x}{R}$$

Since (Fig.1)

$$tg\Delta\varphi = \frac{v_y}{v_x} \cong \frac{v_{3y}}{v} = \frac{1}{R}(2x_1 - x_2)$$

$$x_1 = x_0 - \Delta x, \quad x_2 = x_0 + \Delta x, \quad \Delta x = y \cdot tg\alpha$$

ISBN 978-3-95450-181-6

THE ELECTROMAGNETIC FIELD STRUCTURE IN THE CIRCULAR WAVEGUIDE WITH TRANSVERSE BOUNDARY*

A.A. Grigoreva†, A.V. Tyukhtin, V.V. Vorobev, S.N. Galyamin
St. Petersburg State University, 7/9 Universitetskaya nab., St. Petersburg, 199034 Russia

Abstract

We consider the electromagnetic field structure in a circular partially regular waveguide. One semi-infinite part of the waveguide is empty and the other consists of a cylindrical dielectric layer and a vacuum channel. It is assumed that the incident field is the transverse symmetrical magnetic mode launching either from the vacuum part or from the dielectric one. The analytical investigation is performed by use the technique of mode decomposition for reflected and transmitted fields. Typical dependencies of the field excitation coefficients on the channel radius are presented and discussed. Also the comparison of analytical results with numerical simulations is adduced.

INTRODUCTION

The work is devoted to the study of the electromagnetic field in the circular infinite waveguide which has a transverse boundary between vacuum area and the dielectric area containing axisymmetric vacuum channel. Earlier the problems in sectionally regular waveguides were solved for planar waveguide [1] or for cylindrical in the absence of the coaxial channel [2, 3]. Underline that the presence of the channel leads to emergence of mode transformation effect on the transverse boundary, which in turn causes an infinite sets on eigenmodes in the reflected and transmitted fields.

The considered problem is of interests, for instance, for the wakefield acceleration technique [4], namely for the analysis of formation process of the wave field by bunch moving in a dielectric waveguide structure. Therefore it is important to consider the field excited by bunch entering into the dielectric area.

Another example relates to the problem of the terahertz radiation generation by an electron bunch in a dielectric loaded waveguide structure [5]. In this case the question of the wave field which is excited by a bunch entering into the vacuum area of the waveguide becomes critical.

Here we consider the problem where the incident field is a symmetrical TM mode. In this paper the waveguide characteristics are chosen so that the incident mode can be both propagating or evanescent.

ANALYTICAL INVESTIGATION

We consider the problem with harmonic $(exp(-i\omega t))$ axially symmetrical TM_{0i} mode undergoing transformation on the transverse boundary of the waveguide. It is assumed that the left part of the waveguide $(z<0)$ is loaded with medium having characteristics ε_c, μ_c and the right part $(z>0)$ contains the cylindrical dielectric layer and a coaxial channel with characteristics ε_d, μ_d and ε_c, μ_c respectively (Fig. 1). Initially it is assumed that the mediums are dissipative, that is, $Im(\varepsilon_{c,d})>0$ for positive frequencies. Note that the dissipation is negligible quantity and the values ε_c, μ_c are set to 1 (vacuum) for further numerical calculations. Both mediums are isotropic, homogeneous and nondispersive.

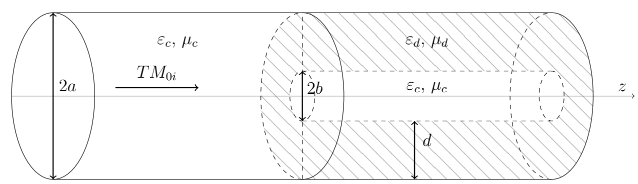

Figure 1: The case of the mode launching from the vacuum part of the waveguide

The incident field can be written by using the single-component vector-potential (the cylindrical coordinates (r,φ,z) are used):

$$A_z^{(i)} = J_0\left(\eta_i r/a\right)\exp\left(ih^{(i)}z\right), \tag{1}$$

where η_i is the zero of Bessel function $J_0(\eta)$, $h_i = \sqrt{k_c^2-\eta_i^2/a^2}$ is the longitudinal wavenumber and $k_c = \omega\sqrt{\varepsilon_c\mu_c}/c$. Note that the attenuation condition results in the inequality $Im\left(h^{(i)}\right)>0$.

Analytical study is performed by using the well-known cross-linking method. According to this method the reflected and transmitted fields are written in a form of the infinite series of eigenmodes for the empty part of the waveguide and partially dielectric part respectively:

$$A_z^{(r)} = \sum_{n=1}^{\infty} R_n \frac{\eta_i}{\eta_n} J_0\left(\eta_n\rho\right)\exp\left(-ih_n^{(r)}z\right),$$
$$h_n^{(r)} = \sqrt{k_c^2-\eta_n^2/a^2}, \quad \mathrm{Im}\left(h_n^{(r)}\right)>0, \tag{2}$$

$$A_z^{(t)} = \sum_{n=1}^{\infty} T_n \frac{\eta_i}{\chi_{cn}} \left\{ \begin{array}{l} J_0\left(\chi_{cn}\rho\right) \quad \text{for } \rho<b/a \\ C_{1n}H_0^{(1)}\left(\chi_{dn}\rho\right)+C_{2n}J_0\left(\chi_{dn}\rho\right) \\ \text{for } b/a<\rho<1 \end{array} \right\}$$
$$\times\exp\left(ih_n^{(t)}z\right),$$
$$h_n^{(t)} = \sqrt{k_c^2-\chi_{cn}^2/a^2}, \ \mathrm{Im}\left(h_n^{(t)}\right)>0. \tag{3}$$

* Work supported by Russian Foundation for Basic Research (No. 15-02-03913) and Grant of the President of Russian Federation (No. 6765.2015.2).
† aleksandra.a.grigoreva@gmail.com

ISBN 978-3-95450-181-6

MODEL OF THE OPTIMAL PARAMETERS CHOICE FOR THE CHARGED PARTICLES BEAM

O.A.Malafeyev, S.A.Nemnyugin * SPbSU, Saint-Petersburg, Russian Federation

Abstract

Problem of the optimal parameters choice for the charged particles beam is considered. It is supposed that the beam is characterized by the set of quality characteristics and may be controlled by multiple parameters. It is assumed that in general case choice of the control parameters that is optimal for all criteria is not possible. In the article the optimization problem is formulated as the conflict control problem. The case is considered when parameters that should be optimized form the vector. Two cases are under consideration. In the first one fully optimal solution may be found. In the second case finding of the compromise solution is considered. Computing algorithms are proposed.

INTRODUCTION

The charged particles beams are used in different areas of technics, science, medicine etc. Accurate adjustment of the beam characteristics often plays crucial role in producing final results of a target irradiation. There are different approaches to the optimization of the beam parameters adjustment [1], [2], [3]. In many cases there are multiple criteria of the beam quality which should be taken into account. Some of these characteristics should be considered in tight connection with the target properties. For example in the hadron therapy among possible characteristics of the particles beam following ones may be mentioned: energy, intensity, biological efficiency, depth of the Bragg peak localization, influence of the fragmentation products and so on. Importance of the problem is confirmed by projects in hadron therapy [4], new facilities in high energy physics [5].

In the article [6] problem of the focusing system optimization was considered with the only one beam characteristic - beam divergence. The only control device was the accelerator's focusing system. In more general situations few beam characteristics may be important and few control channels may be used. For example, in stereotactic radiosurgery a set of up to few hundreds of irradiation channels are used which should be adjusted for more efficient action on tumor. In these case all optimization parameters may be considered as independent. On the other hand multiple quality characteristics may be dependent. In the hadron radiotherapy energy of the therapeutic beam is connected with its biological efficiency. But change of the beam energy influences depth and width of the Bragg peak localization. Shift of the depth-dose distribution maximum and its broadening will affect treatment effect. Also increasing of the beam energy will increase effects of fragmentation also affecting results of the hadron therapy. So some criteria of optimization may be contradictory. In this case choice of optimal parameters should be considered from the point of view of finding of a compromise of all characteristics of the particles beam.

At the present paper the problem of the beam optimization with multiple quality characteristics is considered as the problem of conflict control. Both cases of independent and conflicting characteristics are considered. Formalization of the problem and algorithms of its solution are proposed.

FORMALIZATION OF THE CONFLICT CONTROL PROBLEM

It is supposed that dynamic of the beam characteristics may be described by the system of differential equations:

$$\dot{\mathbf{X}} = \mathbf{f}(\mathbf{X}, \mathbf{u}, \mathbf{v}), \tag{1}$$

with initial condition

$$\mathbf{X}(t = 0) = \mathbf{X}_0, t \in [0, T] \tag{2}$$

Here $\mathbf{X} \in \mathrm{R}^m$ is state vector, $\mathbf{u} \in U \subset \mathrm{R}^p$ are control parameters which should be adjusted to improve the beam's quality, and $\mathbf{v} \in V \subset \mathrm{R}^q$ are control parameters, associated with uncontrollable external actions. U and V are compact sets in Euclidean spaces R^p and R^q. It is supposed that vector function $\mathbf{f}(\mathbf{X}, \mathbf{u}, \mathbf{v})$ in (1) satisfies following conditions:

1. $\mathbf{f}$ is continuous on $(\mathbf{X}, \mathbf{u}, \mathbf{v}) \in R^m \times U \times V$;
2. $\mathbf{f}$ satisfies Lipschitz condition for $\mathbf{X}$ with constant A, i.e. for any $\mathbf{u} \in U$, $\mathbf{v} \in V$ and $\mathbf{X}, \overline{\mathbf{X}} \in R^m$ the following inequality holds:
$$\left|\mathbf{f}(\mathbf{X}, \mathbf{u}, \mathbf{v}) - \mathbf{f}(\overline{\mathbf{X}}, \mathbf{u}, \mathbf{v})\right| \leq A \left|\mathbf{X} - \overline{\mathbf{X}}\right|, \tag{3}$$
3. $\mathbf{f}$ is bounded, i.e. for any $\mathbf{u} \in U$, $\mathbf{v} \in V$, $\mathbf{X} \in R^m$:
$$|\mathbf{f}(\mathbf{X}, \mathbf{u}, \mathbf{v})| \leq B, \ \ (B > 0); \tag{4}$$
4. for any $\mathbf{X} \in R^m$ set
$$\{\mathbf{f}(\mathbf{X}, \mathbf{u}, \mathbf{v}) \mid \ \mathbf{u} \in U, \ \mathbf{v} \in V\}$$
is convex.

We assume that these conditions hold for a wide range of physical situations under consideration.

Definition. Measurable on the interval $[0, T]$ vector functions $\mathbf{u} = \mathbf{u}(t)$ $(\mathbf{v} = \mathbf{v}(t))$ which satisfies conditions

* s.nemnyugin@spbu.ru

ISBN 978-3-95450-181-6

GOLD IONS BEAM LOSSES AT THE NUCLOTRON BOOSTER

A. V. Philippov†, A. V. Tuzikov
Veksler and Baldin Laboratory of High Energy Physics,
Joint Institute for Nuclear Research, Dubna, Russia

Abstract

The calculation results of the gold ions beam losses along the Nuclotron Booster perimeter are given. The presented results take the ion stimulated desorption from the cold surface of the vacuum chamber and collimation of charge-exchanged gold ions into account.

INTRODUCTION

The main goals of the Booster as the intermediate machine in NICA accelerator complex are the following [1]: to accumulate of $2{\cdot}10^9$ gold $^{197}\mathrm{Au}^{31+}$ ions and to accelerate them from 3.2 MeV/u up to 578 MeV/u which is sufficient for their effective stripping to the bare gold nuclei state in the Booster-Nuclotron beam transport channel; forming of the required beam emittance with electron cooling system at energy 65 MeV/u; providing a fast extraction of the accelerated beam for its injection into the Nuclotron.

The Booster acceleration ramp is divided into four stages (see Figure 1): adiabatic ion capture into the separatrix during 0.02 s at the magnetic field plateau at injection energy of 3.2 MeV/u, ion acceleration up to 65 MeV/u during 0.4 s, electron cooling of $^{197}\mathrm{Au}^{31+}$ ions during 1 s and ion acceleration up to energy 578 MeV/u during 1.3 s.

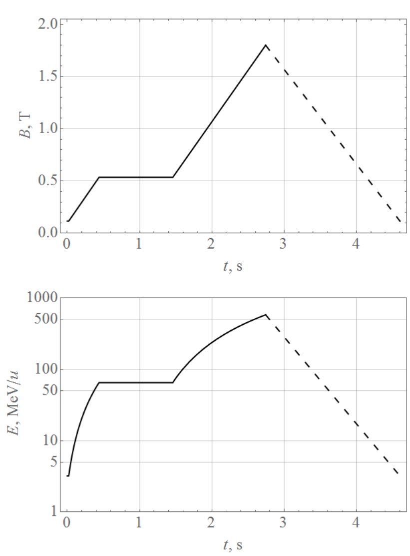

Figure 1: Booster time diagrams: magnetic field ramp (top) and acceleration ramp (bottom) of $^{197}\mathrm{Au}^{31+}$ ions.

The vacuum system of the Booster divided into cold and warm parts. The surface of the cold part of the vacuum beam chamber has a temperature about 10 K, while the surface temperature of the warm part is close to room temperature 300 K. The cold part occupies most of the length of the Booster (circumference of the Booster is 210.96 m). Four warm straight part with a length about 7 m are present: injection (section 1); RF stations (section 2); extraction (section 3) and electron cooling system (section 4).

BEAM LOSSES MECHANISMS AND PROBLEM STATEMENT

Beam losses mechanisms are well known and studied in several number papers ([2] and references therein). The charge-exchange of accelerated ions with molecules of the residual gas and the ionization of these molecules are the primary processes that result in the loss of multicharged ions in circular accelerators and affect the vacuum pressure. In the first case, recharged ions of a beam are deflected by the lattice dipoles and hit the walls of the accelerator chamber with a higher energy at a small angle. In the second case, the residual gas ions are accelerated by the beam potential and hit the walls with a low energy (about 30 eV for the Booster case) under nearly perpendicular angle to their surface. In both cases a large amount of desorbed molecules from the chamber walls go back the chamber, however, the first process is the dominant one [3].

The charge particles beam losses are characterized by the set of differential equations based on the results presented in [2]:

$$\begin{cases} \dfrac{dN_q}{dt} = -N_q \sum\limits_{\alpha} \left\langle \Gamma_{\alpha,q\to q-1} + \Gamma_{\alpha,q\to q+1} + \Gamma^{\text{Bethe}}_{\alpha,q\to q+1} \right\rangle, \\ N_q\big|_{t=0} = N_{q,0}, \\ V\dfrac{\partial n_\alpha}{\partial t} = \dfrac{\partial}{\partial z}\left(C_\alpha \dfrac{\partial n_\alpha}{\partial z}\right) - n_\alpha S_\alpha + \dfrac{Q_\alpha A}{k_B T} + \\ \qquad + N_q \left(\sum\limits_{\alpha} \left\langle \Gamma_{\alpha,q\to q-1} + \Gamma_{\alpha,q\to q+1} \right\rangle \eta_{\angle,\alpha} (1-\theta) + \right. \\ \qquad \left. + \sum\limits_{\alpha'} \left\langle \Gamma^{\text{Bethe}}_{\alpha',q\to q+1} \right\rangle \eta_{\perp,\alpha'/\alpha} \right), \\ n_\alpha\big|_{t=0} = n_{\alpha,0}, \quad n_\alpha\big|_{z=0} = n_\alpha\big|_{z=L}, \quad \left.\dfrac{\partial n_\alpha}{\partial z}\right|_{z=0} = \left.\dfrac{\partial n_\alpha}{\partial z}\right|_{z=L}. \end{cases} \tag{1}$$

Here N_q — beam intensity that depends on time t only; n_α — concentration *of* α-kind of residual gas that depends on the longitudinal coordinate z and time t; V — accelerator volume; $\eta_{\angle,\alpha}$ and $\eta_{\perp,\alpha/\alpha'}$ — desorption coefficients; θ — collimation efficiency; A — the Booster vacuum chamber surface area; Q_α — outgassing rate; S_α — pumping speed; k_B — Boltzmann constant; T — temperature; $\Gamma_{\alpha,q\to q+1}$ and $\Gamma_{\alpha,q\to q-1}$ — charge-exchange rate for one electron loss and one electron capture by beam ions due to interaction with residual gas atoms or molecules; $\Gamma^{\text{Bethe}}_{\alpha,q\to q+1}$ — ionization rate of residual gas atoms or molecules by beam ions; C_α — specific conductivity of the Booster vacuum chamber; L — the Booster circumference. The values V, A and S_α are

† philippov@jinr.ru

ISBN 978-3-95450-181-6

BEAM TRANSFER FROM HEAVY-ION LINEAR ACCELERATOR HILAC INTO BOOSTER OF NICA ACCELERATOR COMPLEX

A. Tuzikov†, A. Butenko, A. Fateev, S. Kolesnikov, I. Meshkov, V. Mikhaylov, V. Shvetsov, A. Sidorin, A. Sidorov, G. Trubnikov, V. Volkov,
Joint Institute for Nuclear Research, Dubna, Russia

Abstract

Designs of systems of ion beam transfer from the linear accelerator HILAC into the Booster of the NICA accelerator complex (JINR, Dubna) [1] including the transport beam line HILAC-Booster and the beam injection system of the Booster are considered in the report. The proposed systems provide multi-variant injection for accumulation of beams in the Booster with required intensity. Special attention is paid to various aspects of beam dynamics during its transfer. Main methods of beam injection into the Booster are described. These are single-turn, multi-turn and multiple injection ones. Results of beam dynamics simulations are presented. Status of technical design and manufacturing of the systems' equipment is also highlighted.

INTRODUCTION

The systems of beam transfer from the HILAC linear accelerator to the Booster include the HILAC-Booster beam transport channel and the system of beam injection into the Booster (see Figure 1).

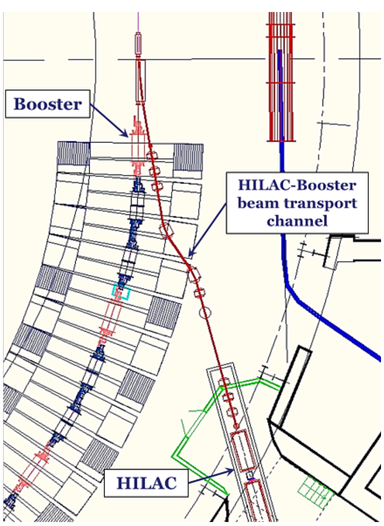

Figure 1: Layout of the HILAC linear accelerator, the Booster synchrotron and the HILAC-Booster beam transport channel.

The beam transfer in the HILAC-Booster transport channel involves beam debunching, betatron matching of ion beam of the target charge state with the Booster, separation and collimation of neighbor parasitic charge states of ions. The ion-optical system of the transport channel and the beam injection system of the Booster provide multi-variant injection for accumulation of beams in the Booster with required intensity [2]. Main methods of beam injection into the Booster are single-turn, multi-turn and multiple injections. Ions (see Table 1) are accumulated on the horizontal phase plane of the Booster.

Table 1: Main Beam Parameters

Ions	Au^{30+}, Au^{31+}, Au^{32+} (from HILAC); Au^{31+} (inside Booster)
Intensity	up to $2.5\cdot10^9$ (Au^{31+}); up to $6\cdot10^9$ (total)
Current, mA	4
Energy, MeV/amu	3.2
Repetition rate of beam injection into Booster, Hz	0.25
Repetition rate of stages of multiple injection, Hz	10 (3 injection stages per 4 s)
Transition, %	90
Transverse 95% emittance, $\pi\cdot$mm$\cdot$mrad:	
at the exit of HILAC;	10
at the entry of Booster;	15
after filamentation in Booster.	$15 \div 135$ (hor.) / 15 (vert.)

BEAM INJECTION INTO BOOSTER

Concept of multi-variant injection into the Booster synchrotron implies possibility of beam injection by means of several schemes of single-turn, multi-turn and multiple injection methods. The beam injection system of the Booster is designed to create a local closed orbit bump and also has useful feature: ability of rapid change of fields inside the system's kickers that allows ions to fill the horizontal phase plane of the Booster more compact.

Single-turn injection is a conventional method providing minimal transverse beam emittances after filamentation of phase space distribution of ions in the Booster. The beam duration in case of single-turn injection is less than 8.5 μs. Horizontal emittance of the injected beam is equal to 15 $\pi\cdot$mm$\cdot$mrad. Vertical emittance does not depend on beam injection method used and is 15 $\pi\cdot$mm$\cdot$mrad.

Multi-turn injection method involves accumulation of ions on the horizontal phase plane during 2-3 periods of the beam revolution so the beam duration is 17 or 25.5 μs. Two schemes of multi-turn injection are considered: with single-plateau (ordinary) pulses of the injection system's kickers and with double-plateau pulses formed by rapid change of fields in the kickers. Horizontal emittances of

† tuzikov@jinr.ru

ISBN 978-3-95450-181-6

MULTIGAP AND POLYHARMONIC BUNCHING SYSTEMS AT FLNR CYCLOTRONS

I.V. Kalagin†, G.G. Gulbekian, B.N. Gikal, S.V.Prokhorov, N.N. Pchelkin,
Joint Institute for Nuclear Research, FLNR, Dubna, Moscow region, Russia

Abstract

Since 1997, different variants of bunching systems have been used at the axial injections of FLNR cyclotrons to increase ions capture into acceleration efficiency. Combination of two single gap Sine and Line bunchers are used at the axial injections of U400 and DC110 cyclotrons. Since 2015, a single gap double RF harmonic buncher has been installed into the upper part of the U400M injection in addition to the lower sine buncher, the experimental results is being presented. For the HV axial injection of the new DC280 cyclotron, two variants of polyharmonic bunchers will be used: a multigap buncher and a single gap one.

INTRODUCTION

At present time, axial injection systems with ECR ion sources are integral components of heavy ion cyclotrons at the Flerov Laboratory of Nuclear Reaction of the Joint Institute for Nuclear Research (FLNR, JINR). The axial injections allowed us to use bunchers for matching the longitudinal ion beam emittance with the cyclotron phase acceptance, as for linacs. The typical voltage of ion extraction from our ECR sources is U_{inj}=15÷20 kV. The typical phase acceptance (CPA) of our cyclotrons is 20°÷30°. The typical capture into acceleration efficiency (CIAE) without beam bunching is 5÷8%.

The best type of bunchers from the point of view CIAE increasing is the buncher with saw-tooth voltage in the gap (linear buncher) [1]. The calculated CIAE with the bunchers is 80÷90%, but their using is restricted by technical difficulties. The simplier type of bunchers is the buncher with sinusoidal voltage in the gap (sine buncher). The simulated CIAE for the sine buncher is about 50% [2].

Unlike linacs, the design of the sine buncher for the FLNR cyclotrons cannot been made in form of a single gap λ/4 resonant cavity because our cyclotrons use relatively low accelerating frequencies: 5.4-22 MHz (λ/4= 3.5÷14 m). Therefore, we have utilised bunchers with two grids that are fed with a special resonant system. The resonant system consists of two extended coaxial resonators (or cables), matching inductors and variable capacitors for resonance turning. The system allows us to form sinusoidal voltages at both buncher grids in anti-phases to prevent additional acceleration of ions in central phases and for decreasing influence RF fringing fields on CIAE before and after the buncher gap. The buncher can be installed into the vertical part of an axial injection at various distances from a cyclotron median plane (CMP). We received the best CIAE at the U400 cyclotron when the buncher was situated at 0.8 m above the CMP. The voltage amplitude at the gap was about 700 V (optimized by maximal CIAE). The CIAE was 15÷29% depending on ion current (the parameter decreases with ion current increasing) [3].

Experimental values of CIAE with our bunchers are typically lower than calculated ones. The reasons of it can be influence of space-charge effects. The effects become significant in vicinity of the CMP where the bunch pulse current is in one order higher than the DC ion current at the ECR exit. In addition, there are other factors such as: path difference of ions into longitudinal magnetic field of the axial channel and into the helical inflector; losses of ions at the buncher grids and at residual gas.

For further improvement of the FLNR cyclotrons CIAE we have made multigap and polyharmonic bunching systems.

One more way of the CIAE improvement is to increase energy of injected ions, we are planning to apply the method for our new DC280 cyclotron [4].

MULTIGAP BUNCHING SYSTEMS

Multigap Buncher for the U400

As a variant of a multigap system we have unilized two single gap bunchers. The bunchers have been situated at different distances from the U400 CMP. We use combination of linear buncher and existing sine buncher (Fig. 1). The linear buncher has been situated at 4.4 m from the CMP [5]. The system has been developed for RF frequency range of 5.4÷12 MГц and U_{inj}=13÷15 kV (βλ=80 mm). The voltage amplitudes at grids were about 180 V (linear) and 650 V (sine). The U400 CIAE without bunchers is over 5%. The system allowed us to reach 23÷38% of CIAE, depending on ion current [6]. The contribution of the linear buncher to the CIAE was about 1.4.

Multigap Buncher for the DC110

The similar system has been installed at the D110 cyclotron injection [7]. The system was developed for RF frequency of $7.65^{\pm 0.16}$ MГц and U_{inj}=20 kV (βλ=98 mm). The bunchers have been situated at 0.8 m (sine) and 2.45 m (linear) above the CMP. The calculated phase distribution after bunched beam drifting for 2.45 m and corresponding distribution of the particle density in the bunch of $_{132}Xe^{20+}$ ions at the DC110 CMP are shown in Fig. 2. The calculations have been carried out with the use of the large particle method without account for the space charge effects and other effects mentioned above. The voltage amplitudes was 700 V for linear buncher (with ideal saw tooth voltage) and 300 V for sine one. The calculated CIAE was about 61% for the CPA value of 30°.

† kalagin@jinr.ru

ISBN 978-3-95450-181-6

NEW TECHNIQUES FOR OPERATION AND DIAGNOSTICS OF RELATIVISTIC ELECTRON COOLERS

M. W. Bruker, A. Hofmann, E. Riehn, T. Weilbach, K. Aulenbacher, J. Dietrich
Helmholtz Institute Mainz, Germany

W. Klag
Institute for Nuclear Physics Mainz, Germany

M. I. Bryzgunov, V. Parkhomchuk, V. B. Reva
BINP SB RAS, Novosibirsk, Russia

Abstract

The Helmholtz Institute Mainz (HIM) performs experiments related to possible improvements of high-energy d.c. electron coolers. Results and activities concerning non-invasive beam diagnostics and beam control at large operating currents will be shown. Furthermore, progress of our project to use turbo generators as a means for potential-free power generation in high-energy electron coolers is presented.

INTRODUCTION

High-intensity electron beams are getting more and more popular (e.g. in planned electron cooling devices) but make high demands on diagnostics and power supplies. With an energy of several MeV and a current of amperes, the use of conventional destructive diagnostic tools is very limited just as the use of conventional power supplies is. In this paper we present three experimental set-ups connected to high-energy electron coolers: non-invasive beam diagnostics, the impact of secondary electron emission in energy recovery machines and turbine-driven power supplies for focusing magnets. All experiments have been performed at the Institute of Nuclear Physics and the Helmholtz Institute in Mainz.

EXPERIMENTAL SET-UP FOR MEASUREMENT OF SECONDARY CURRENT

The energy recovery method used in electron coolers results in secondary electrons emitted from the collector surface being re-accelerated, possibly harming operational stability. Research done by BINP indicates that a Wien filter as part of the collector optics is a suitable means to suppress electron backflow, increasing the total recuperation efficiency by a factor of 100 [1]. However, stopping these particles in turn creates new secondaries with a different energy and angle distribution. This gives rise to a cascade that depends heavily on the geometry of the electrodes and the vacuum chamber.

HIM operates a test set-up capable of providing a magnetized 17 keV, 0.5 A electron beam and measuring the currents flowing onto the relevant aperture plates independently. A sketch of the device including the distribution of electric potentials is shown in Fig. 1.

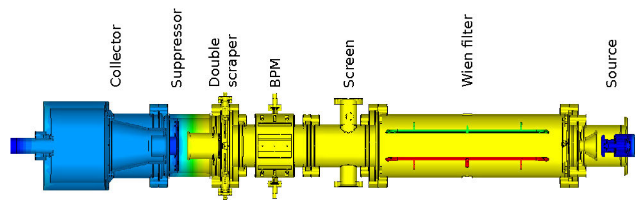

Figure 1: Schematic view of the vacuum chamber. Blue: $U < 0$. Yellow: $U = 0$.

The potential minimum inside the suppressor electrode results in secondary electrons with an energy $E_{\mathrm{kin}} < e\left|U_{\mathrm{col}} - U_{\mathrm{sup}}\right|$ being reflected to the collector. By varying this potential, secondary losses can be distinguished from primary losses. In the absence of primary losses, the integrated energy spectrum of secondary electrons exiting the collector can be obtained except for the elastic peak. Figure 2 shows that while the shape of the spectrum is what can be expected [2], several surfaces contribute to the total losses because of higher generations of secondary electrons emitted from the deceleration aperture plate and the Wien filter collector plate.

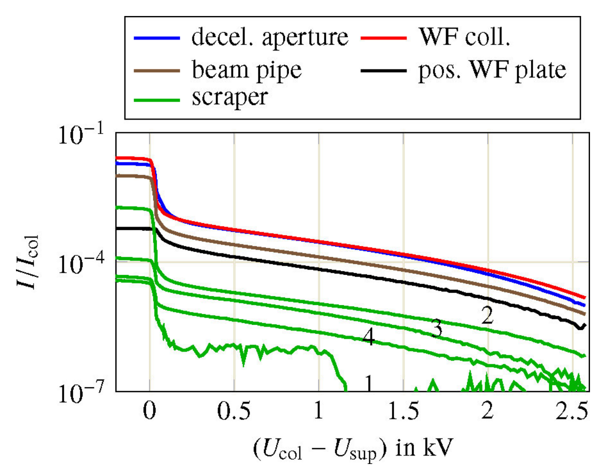

Figure 2: Secondary currents vs. suppressor voltage. $I_{\mathrm{col}} = 20\,\mathrm{mA}$.

These losses are irrelevant to the cooler as long as the particles cannot enter the high-energy section. To determine the possible trajectories of higher-generation secondary elec-

ISBN 978-3-95450-181-6

COMMISSIONING OF THE 60 KEV ELECTRON COOLER FOR THE NICA BOOSTER

A. Bubley, M. Bryzgunov, A. Denisov, A. Goncharov, V. Panasyuk, V. Parkhomchuk, V. Reva, BINP SB RAS, Novosibirsk, Russia

Abstract

The 60 keV electron cooler for the NICA booster was designed and constructed at BINP SB RAS. The article describes results of various measurements obtained during its commissioning. Also some details of design and construction of the cooler are discussed.

INTRODUCTION

NICA collider contains a big number of complicated systems and subsystems. One of them is gold ion booster, which is located at the existing hall of former synchrophasotron, and new superconductive magnets sit inside old giant iron yokes [1]. Low energy cooler is one of the elements of the booster those provides sufficient improvement of the ion beam quality.

Main specifications of the cooler are listed below:

ions type	p+ up to $^{197}Au^{31+}$
electron energy, *E*	1,5 ÷ 50 keV
electron beam current, *I*	0,2 ÷ 1,0 Amp.
energy stability, *ΔE/E*	$\leq 1\cdot 10^{-5}$
electron current stability, *ΔI/I*	$\leq 1\cdot 10^{-4}$
electron current losses, *δI/I*	less than $3\cdot 10^{-5}$
longitudinal magnetic field	0,1 ÷ 0,2 T
inhomogeneity of the field, *ΔB/B*	$\leq 3\cdot 10^{-5}$
transverse electron temperature	≤ 0,3 eV
ion orbit correction:	
displacement	≤ 1,0 mm
angular deviation	≤ 1,0 mrad

The requirement for vacuum condition is usual for heavy ion accelerators $\leq 1\times 10^{-11}$ mbar [1].

MEASUREMENTS OF THE ELECTRON GUN PERVEANCE

After long term training of the electron gun cathode, efficiency of the cathode increased and behavior of the perveance became similar to that of the electron gun being used in the electron cooler for COSY (Fig.1).

The main source of the current losses in the electron cooler is the secondary emission of electrons from the collector. In order to reduce losses, the suppressor placed before the collector creates a potential barrier that constrains the secondary emission. However, the magnitude of this barrier depends on the distance from the vacuum pipe axis and reaches its minimum at the center of the beam electron. The space charge of the electron beam produces the potential, which behaves the opposite way – the farther from the beam's axis, the lower the potential created by beam's space. With growth of the electron beam current the resulted potential barrier can lock the secondary emission and decrease the current losses (Fig.2). However, further increase of the beam current is limited as the beam's space charge can form an electrostatic mirror and lead to the breakdown.

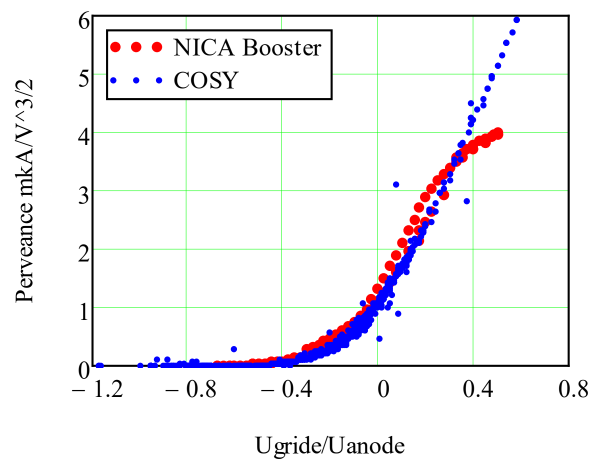

Figure 1: Electron gun perveance.

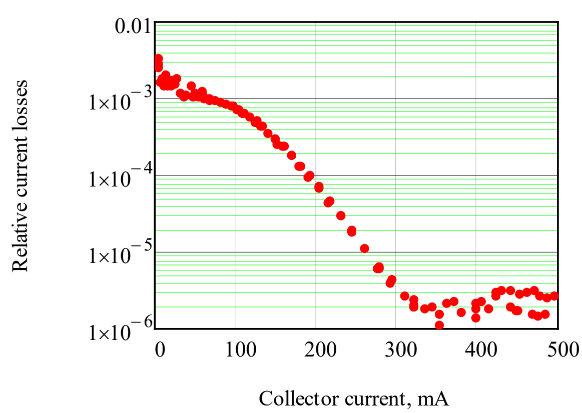

Figure 2: Electron current losses at collector.

VACUUM GENERATION

The vacuum system of the cooler has a volume approximately 0.2m^3 .On the other hand the internal surface of the vacuum chamber is very advanced as it contains bending plates and other various electrodes. That leads to rather high outgassing rate. The scheme of the vacuum system is shown in Fig.3.

ISBN 978-3-95450-181-6

STOCHASTIC COOLING SYSTEM AT NICA PROJECT

I. Gorelyshev#, N. Shurkhno, A. Sidorin, G. Trubnikov, VBLHEP, JINR, Dubna, Russia

Abstract

Stochastic cooling system is one of the crucial elements for luminosity preservation at NICA accelerator-collider complex. The foundation of main parameters of the stochastic cooling system is provided. The preparatory experimental work for longitudinal stochastic cooling was performed at Nuclotron accelerator. The description of Nuclotron system components, adjustment algorithms and remote control is given.

INTRODUCTION

NICA accelerator-collider complex is under construction in JINR [1]. One of the challenging technologies of the collider project is the stochastic cooling. It is required for beam accumulation and luminosity preservation. Stochastic cooling is developed in Russia for the first time and operational regimes differ from those used before in the world. So before the run of NICA a test channel was put into operation at Nuclotron.

GENERAL SCHEME

Stochastic cooling is a microwave broadband system with feedback via the beam. The working principle is the following: pickup electrodes detect noise from the beam, signal propagates through the system and applies on the kicker. For effective operation signal has to be properly amplified and delayed. If delay and amplification are correctly adjusted one has the reduction of betatron amplitudes in case of transverse cooling or momentum spread in case of longitudinal cooling. General scheme of Nuclotron stochastic cooling system is presented at the figure 1. This system has bandwidth 2-4 GHz and 60 W maximum output power. It consists of pickup with preamplifiers, notch filter, block of switches, variable delay and attenuation and diagnostic devices to maintain different modes of operation, main amplifier and kicker.

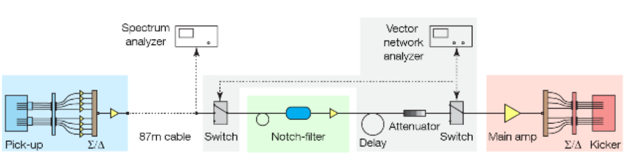

Figure 1: General scheme of the Nuclotron stochastic cooling system.

Pickup and Kicker

Pickup and kicker are HESR type ring-slot couplers which were designed and constructed in FZ Jülich [2]. Pickup is installed in vacuum chamber and has 8 outputs from 8 azimuthal positions around the beam (fig. 2a). Signals from outputs are amplified and can be combined into transverse horizontal, transverse vertical and longitudinal common signals (figure 2b).

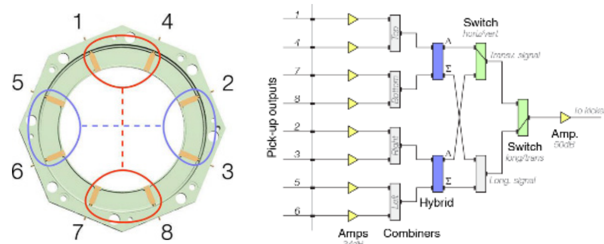

Figure 2: Pickup transverse cross section (left) and commutation scheme (right).

Kicker is the same device as pickup. It has identical commutation scheme with no amplifiers. The difference is that common signal splits to 8 signals at kicker.

Notch Filter

Notch filter (figure 3) receives RF signal from pickup. The signal is modulated by infrared laser and is divided into two lines.

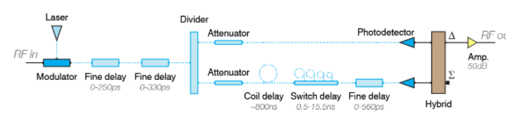

Figure 3: Scheme of optical notch filter.

Part of the signal from the short line passes directly to the output, another part from the long line passes through coil delay, switch delay and fine delay. Each line has photodetector demodulating optical signals to RF at its end. Signals from two lines are combined with 180° phase shift and outgoing signal is enlarged by 50 dB amplifier. To realize time-of-flight method the long line of the filter has to be switched off.

Variable Delay and Attenuation

These simple devices are manipulated by a set of switches. Each switch contacts either short line or modified (delay or attenuation) line (figure 4).

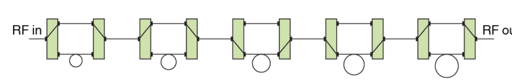

Figure 4: Scheme of variable delay.

Variable delay has 0.5, 1, 2, 4, 8 ns modified lines and range of manipulation 0-16 ns. Variable attenuation has 1, 2, 4, 8, 16, 24 dB lines and range of manipulation 0-55 dB.

ivan_v_gorelyshev@mail.ru

ISBN 978-3-95450-181-6

COMMISSIONING OF ELECTRON COOLING DEVICES AT HIRFL-CSR*

X. D. Yang†, L. J. Mao, J. Li, X. M. Ma, T. L. Yan, G. H. Li, M. T. Tang, Institute of Modern Physics, CAS, Lanzhou, 730000，China

Abstract

Electron cooling plays an important role in the Heavy Ion Research Facility of Lanzhou cooler storage ring (HIRFL-CSR). Two electron coolers were equipped in main ring (CSRm) and experimental ring (CSRe) in HIRFL-CSR respectively.

Two electron cooling devices have commissioned for twelve years since they were installed and completed in 2004.

The function and operation procedure of electron cooler were presented in this report. Their performance and the highlights of experiments results were described. Their commission and optimization were summarized here. The issues and troubles during the commission were enumerated and collected in this presentation. The future upgrade and improvement were suggested, and the new operation scenario and requirement were proposed.

INTRODUCTION OF HIRFL-CSR

HIRFL-CSR (Heavy Ion Research Facility at Lanzhou--Cooling Storage Ring) is multi-purpose accelerator complex [1], it is consisted two storage ring, the heavy ion beam with energy range 8-50 MeV/u from HIRFL—composed two existing cyclotron SFC(K=69) and SSC (K=450) is used as injector, will be accumulated, cooled and accelerated to the high energy range of 100—400 MeV/u in the main ring (CSRm), then extracted fast to produce RIB or highly charged heavy ions. The secondary beams will be accepted and stored by experimental ring (CSRe) for many internal target experiments or high precision spectroscopy with beam cooling, On the other hand, the beam with energy range of 100-900 MeV/u will also be extracted from CSRm with slow and fast extraction.

Accelerated ion beam from the CSRm through the radioactive beam separator line with the length of 100m was injected into the CSRe. Generally the CSRe operated with the DC mode. A gas jet internal target was installed in the opposite side of electron cooler.

ELECTRON COOLING FOR CSR

In CSRm, the electron cooling device [2, 3, 4, 5, 6] plays an important role in the heavy ion beam accumulation at injection energy. The new state-of-the-art electron cooling device was designed and manufactured in the collaboration between BINP and IMP, it has three distinctive characteristics, namely high magnetic field parallelism in cooling section, variable electron beam profile and electrostatic bending in toroids.

Each ring was equipped an electron cooling device, the electron energy in the main ring is 35 keV and 300 keV for the experimental ring.

The electron cooling device plays an important role in HIRFL-CSR experimental ring for the heavy ion beam. Continuous electron cooling is applied to the stored ion beam for the compensation of the heating by various scattering. The most important is the ability to cool ion beams to highest quality for physics experiments with stored highly charged ions.

STATUS OF HIRFL-CSR

In the past several years, more than 7000 operational hours was scheduled yearly for HIRFL-CSR, half of them were provided by the storage ring. Most beamtime was dedicated to the mass measurement experiments, recombination of ion with the free electron of cooler and the internal target experiments. The other beamtime was devoted to the cancer therapy and related experiments. More than 100 patients were treated in CSRm with the carbon beam. However, the extremely heavy ion beam like Bi and U were successfully cooled and accumulated with very low injection energy and weak intensity. A few times commission for accumulation of proton with the help of electron cooling were performed in CSRm, including instead of proton with H_2^+, these commission were not successfully completed carried out up to now due to the mismatching parameters between injector and storage ring.

COMMISSIONING AND OPERATION OF ELECTRON COOLING IN CSR

About kind of ion beam was accumulated with the help of electron cooling in CSRm. The ion species from H to Uranium, and the energy range from to 1.2MeV/u to 21.7MeV/u. The experiments and operation results were reported in the workshop on the beam cooling and related topics from 2005 to 2013 [7, 8, 9, 10, 11] and RuPAC 2010 [12], RuPAC 2012 [13]. One can find the related papers in the references. Some investigation and optimization experiments [14, 15] were completed in CSR. Some accumulation experiments in CSRm, cooling force measurement, optimization of electron cooling and bunch length measurement in CSRe were implemented.

WHAT WE HAVE DONE

Temperature Stabilization System

During the operation, we found the tunnel temperature have the influence on the stability of high voltage output of cooler system, it presented a sine wave in the day and

* Work supported by The National Natural Science Foundation of China, NSFC (Grant No. 11375245, 11475235, 11575264)
† yangxd@impcas.ac.cn

ISBN 978-3-95450-181-6

DESIGN AND CALCULATION OF CYLINDRICAL ELECTROSTATIC DEFLECTOR FOR THE TRANSPORT CHANNEL OF THE HEAVY ION BEAM

N.Kazarinov#, I.Kalagin, S.Zemlyanoy, JINR, Dubna, Russia

Abstract

The cylindrical electrostatic deflector is used in the beam transport channel of GALS spectrometer that is created at U400M cyclotron in Flerov Laboratory of Nuclear Reaction of Joint Institute for Nuclear research. The design and calculation of the deflector are presented in this report. The angular length of the electrodes and gap between potential electrode and screen are found by using of the minimization procedure.

INTRODUCTION

GALS is the experimental setup for selective laser ionization with gas cell [1] that will be created at U400M cyclotron in FLNR JINR [2]. The cylindrical electrostatic deflector is the optical element of the part of the channel intended for transportation of the secondary ion beam. The deflector rotates the researched ion beam from the focal plane of the spectrometric magnet onto the particle detector.

The design of the deflector is proposed in this report. In accordance with results of works [3,4] the deviation of the trajectory of the beam center of mass from the designed orbit have been minimized by appropriate choice of angular length of the deflector electrodes. The influence of the nonlinearities of the transverse electric field on the dynamics of the particles have been reduced by means of variation of angular distance between electrodes and grounded screen.

The beam dynamics simulations were performed by using the MCIB04 program code [5]. 2D field map of the deflector electric field calculated with the help of POISSON program code [6] was used in the simulations.

2D MODEL OF THE DEFLECTOR

The scheme of the deflector is shown in Fig.1.

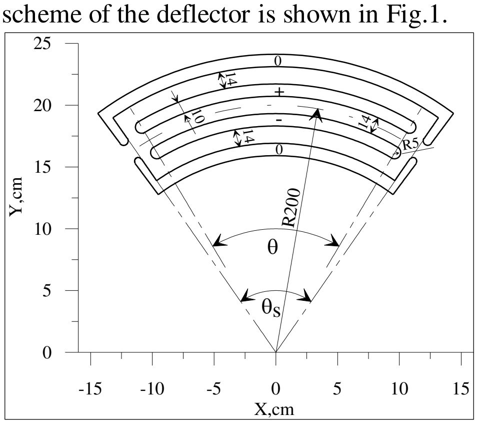

Figure 1: Scheme of deflector GALS

The deflector consists of two electrodes under potentials U_1 (-), U_2 (+) and two grounded screens (0). The design bending radius R = 20 cm, design bending angle φ = 67 degrees and the gap between the electrodes d = 14 mm. The optimal value of the angular size of the electrodes θ is equal to 62.6 degrees. The optimal angular distance between the inner end face of the screens is equal to $\theta_s = \theta + 8^0$. The vertical size of the electrodes (in the Z axis direction) is 80 mm.

2D computational models of the GALS deflector are shown in Fig.2. The first one (Fig.2a) corresponding to cylindrical system of coordinates (r,z≥0) has been used for evaluation of the electric field inhomogeneity inside the deflector aperture. The second one (Fig.2b) corresponding to Cartesian frame (X≥0,Y≥0) was used during determination of the optimum angular dimensions of the electrodes.

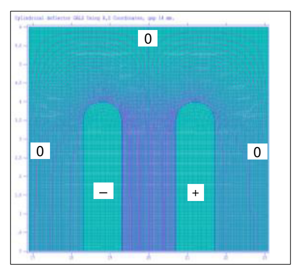

Figure 2a: 2D model in cylindrical frame

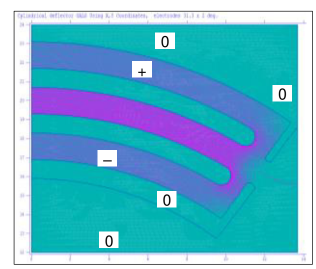

Figure 2b: 2D model in Cartesian frame

Two independent distributions of the electric field of the deflector were found for each of the potential electrodes. The electric field strength of the deflector for arbitrary voltages at the electrodes was calculated as a superposition of these distributions.

The inhomogeneity of the bending electric field within the working aperture of the deflector is shown in Fig.3,4.

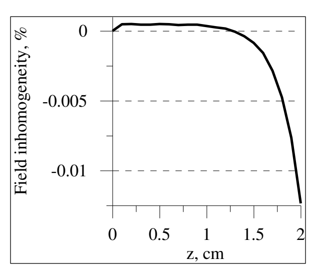

Figure 3: Inhomogeneity of bending electric field in Z-direction

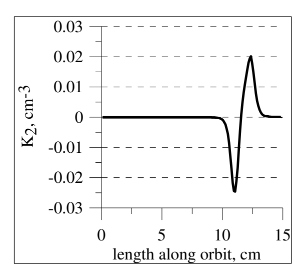

Figure 4: Sextupole coefficient K_2 of bending electric field

#nyk@jinr.ru

ISBN 978-3-95450-181-6

THE WAY TO IMPROVE CONFORMITY OF PROTON THERAPY

I.A. Yakovlev, S.V. Akulinichev, Yu.K. Gavrilov, INR RAS, Moscow
R. D. Ilić, VINCA, Belgrade

Abstract

In the case of small tumors, the pencil beam width may be comparable with the target size. In these cases, the application of classic method of passive beam scattering with a one-stage formation of dose distribution may be reasonable. However, the last method in its standard implementation fails to provide the dose conformity: either the maximal dose exceeds the tumor volume on its proximate site or the dose deviates too much within the tumor. In order to overcome this shortcoming of the passive scattering method, we suggest a new construction of a two-component ridge filter (the corresponding patent is pending). We have performed a series of calculations with the Monte-Carlo code SRNA in order to find the optimal construction from the point of view of dose delivery accuracy and of the device manufacturability. With that ridge filter the 95% isodose does not notably leave the tumor volume. The usual "wings" of isodoses on proximate side are now absent and the volume of irradiated healthy tissue is significantly reduced. The experimental tests with proton beams are now in progress.

PROTON THERAPY AND DOSE FORMATION METHODS

Proton therapy has remarkable advantages over conventional photon radiation therapy. The depth dose distribution shows the increase with penetration depth leading to a maximum energy deposition near the end of range in matter (Bragg peak). This feature allows to spare healthy tissue while delivering maximal dose to the tumor [1].

Today proton therapy is represented by two techniques of dose formation: methods of passive spreading, mostly known as passive scattering and of active spreading or scanning. The first one implies installation of various beam-forming devices on the beam path. These devices alter the width of the beam by scattering and modify its energy spectrum. This method also implies the use of custom-made collimators and compensators for conforming the dose to the target volume. The active scanning technique uses magnets for deflecting and steering the proton beam. The depth of penetration can be varied by adjusting the beam energy. Thus, voxel by voxel, target volume can be covered by maximum dose.

Both methods of formation have their pros and cons. The letter one is considered as more advantageous as it provides the conformance of dose delivery to a tumor of any size with no significant radiation damage to healthy surrounding tissues. Also, due to absence of scattering materials fewer amount of stray radiation is generated. However, this method has the risk of target voxel misses because of organ motion. Small targets with the size comparable to the beam's width can be an additional difficulty for this technique. In these cases, the "old" method of proton scattering may be more effective as it allows to irradiate the whole target volume simultaneously. But in this case, distal edge formation by compensators of standard type inevitably leads to the emergence of hot lesions in the proximal region, beyond the borders of the target volume. Thereby, for better conformity the target has to be irradiated from multiple directions which themselves demand additional forming devices (i.e. custom-made collimators and compensators).

OUR PREVIOUS EXPERIMENTS

In our earlier study the technique of passive spreading was tested on proton beams of INR linac. The system of double scattering for the beam widening and a ridge filter for spread-out Bragg peak (SOPB) formation was used (see Fig. 1).

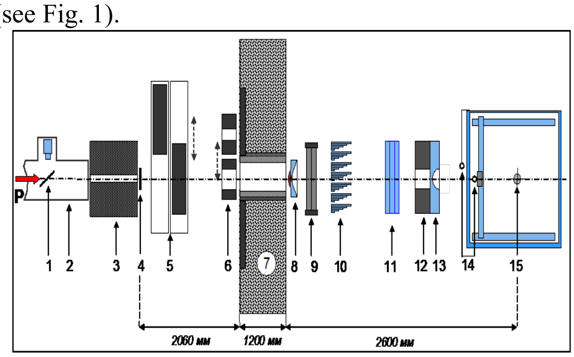

Figure 1: Formation system of INR medical proton beam. 1 – luminophor with TV-camera, 2 - beam channel; 3 - graphite collimator, 4 - the primary scatterer (S1), 5 – beam stop, 6 – beam aperture collimators of 40 and 70 mm, 7 - shielding, 8 – secondary scatterer (S2), 9 - ion chamber, 10 - ridge filter, 11 - energy degrader, 12 – individual collimator, 13 – bolus, 14 - ion chambers in a water phantom, 15 – target isocenter.

A number of measurements with the beams of 160 and 209 MeV was carried out, some results are presented in figs. 2-4.

In order to form a wider beam, we used scatterers S1 and S2 which are represented by copper foils and contoured scatterer with Lucite compensator. This formation system was calculated with the program NEU [2].

ISBN 978-3-95450-181-6

A CYCLOTRON COMPLEX FOR ACCELERATION OF CARBON IONS

V. Smirnov* and S. Vorozhtsov, Joint Institute for Nuclear Research, Dubna, Russia

Abstract

An accelerating complex for hadron therapy is proposed. Facility consists of two superconducting cyclotrons and is aimed to produce beams of $^{12}C^{6+}$ ions with energy of 400 MeV/nucleon. Accelerator-injector is a compact 70 MeV/nucleon cyclotron. Main machine is separated sector cyclotron consisting of six magnets. Basic features of the main cyclotron are high magnetic field, compact size, and feasible design of a magnetic system. The advantages of the dual cyclotron design are typical of cyclotron-based solutions. The first design studies of the sector magnet of the main cyclotron show that the beam dynamics is acceptable with the obtained magnetic field. Due to its relatively compact size (outer diameter of 12 m) the complex can be an alternative to synchrotrons. Design study of the main cyclotron is described here.

INTRODUCTION

Development of accelerators for producing carbon beams with the energy of 400–450 MeV/nucleon for hadron therapy appears to be an increasingly important issue today. The existing facilities for producing these beams are mainly based on synchrotrons. It seems interesting to use isochronous cyclotrons instead, as is the case in proton therapy. However, the developed designs of compact superconducting cyclotrons have some disadvantages in addition to their advantages [1]. An alternative solution can be a facility based on a superconducting sector cyclotron justified in detail in [2]. The design of this facility should comply with a number of conditions. First, the size and weight of the accelerator must be as small as possible, which makes it expedient to use the maximum high magnetic field. Second, the injection energy should be low enough for the injector to be of tolerable size. Third, the magnetic system design should be feasible, that is, the parameters of the superconducting coil (engineering current density, acting forces) should be adequate and the space between the sectors should be large enough to accommodate accelerating elements, inject a beam, etc. [3]. A separate task is to develop a system such that both maintains isochronism of the magnetic field and allows beam acceleration with a minimum number of resonance crossings.

INJECTION SYSTEM

The injection energy is chosen to be 70 MeV/nucleon because the accelerator with this final energy can be also used to accelerate H_2^+ ions. Their subsequent stripping allows obtaining protons of the appropriate energy suitable for medical applications. This cyclotron can be used for treating eye melanomas and also for producing radioisotopes.

A compact superconducting cyclotron seems to be the most optimal option. The optimum solution is a cyclotron with a central field of 2.4 T operating at the fourth harmonic of the accelerating field. The magnetic field is formed by four spiral sector shims (Fig. 1). With an acceptable spiral angle of 50°, the external diameter of the accelerator will be no larger than 3 m and the weight will be about 100 t.

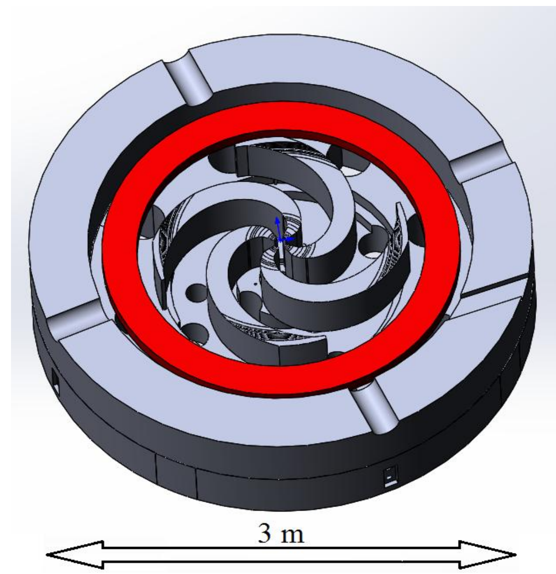

Figure 1: Cyclotron-injector.

The magnetic rigidity of 70-MeV/nucleon C^{6+} ions is about that of 250-MeV protons in the Varian cyclotron [4]. So, some technical solutions of the Varian machine can be applicable to the injector.

The system for injection in the main cyclotron consists of four magnetic channels and an electrostatic deflector (Fig. 2, Fig. 3).

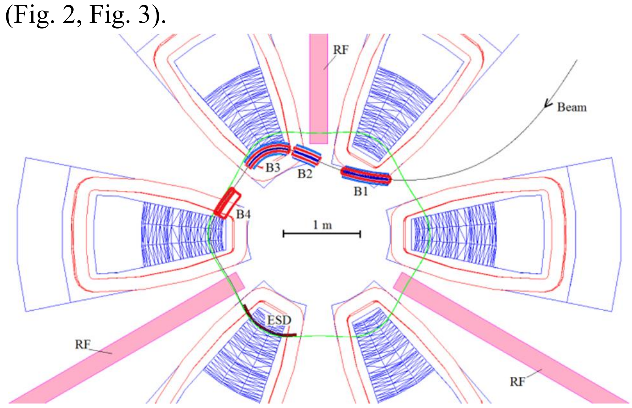

Figure 2: Injection system.

*vsmirnov@jinr.ru

ISBN 978-3-95450-181-6

BEAM SHAPING ASSEMBLY OPTIMIZATION FOR BORON NEUTRON CAPTURE THERAPY*

T. Sycheva#, S. Frolov, S. Lezhnin, S. Taskaev,
Nuclear Safety Institute, RAS, Moscow, Russia,
Novosibirsk State University, Novosibirsk, Russia,
BINP SB RAS, Novosibirsk, Russia

Abstract

Epithermal neutron source based on vacuum insulation tandem accelerator and lithium target has been developed and is now in use in the Budker Institute of Nuclear Physics. Neutrons are generated by $^7Li(p,n)^7Be$ reaction with proton beam energies from 2 to 2.5 MeV. A beam shaping assembly (BSA) for therapeutic neutron beam forming is used. It includes moderator, reflector, and absorber. In this work the simulation results of the depth dose rate distribution in modified Snyder head phantom for a range of neutron energies are presented and discussed. Variants of BSA optimization depending on tumor depth are proposed. The calculations were carried out by Monte-Carlo neutron and photon transport code NMC that was developed in NSI RAS. Our research reveal that high quality neutron beam generation may be obtained with proton energy of 2.3 MeV. Discovered optimal schemes of BSA including sizes and materials are presented and discussed.

INTRODUCTION

The main requirements to neutron source for BNCT is to generate epithermal neutron beam with neutron flux density more than 10^9n/cm^{2}s for treatment time less than 1 hour. Neutrons with energies from 0.5 eV to 10 keV are considered to be epithermal. The results of recent research clarified the requirements to the neutron spectrum and the range of neutron energies of 1 to 30 keV was established as the most suitable for BNCT [1].

For the therapy and determination of optimal treatment conditions such parameters as dose rate in healthy tissue and tumor, advantage ratio (AR, the ratio of maximum dose in tumor and healthy tissue), advantage depth (AD, the distance from the surface of the tissue in which the dose in tumor equals the dose in healthy tissue) are principal.

Minimum required values of these parameters are the following [1]:

- tumor dose rate 1 Gy/min;
- AD is 8 cm;
- AR is 4.

*The work supported by Russian Science Foundation (project N 14-32-00006), Budker Institute of Nuclear Physics and Novosibirsk State University

sychevatatyanav@gmail.com

DETERMINATION OF THE OPTIMAL RANGE OF NEUTRON ENERGIES

To determine the range of neutron energies that are optimal for BNCT we performed the simulations of the depth dose rate distribution in the healthy tissue and in the tumor in modified Snyder head phantom for monodirectional, monoenergetic from 0.025 eV to 100 keV neutron beams with the diameter of 10 cm.

All calculations were carried out by Monte-Carlo neutron and photon transport code NMC that was developed in NSI RAS using cross sections from the ENDF-VII.0 nuclear database [2].

Code validation was performed using benchmarks of the thermal, intermediate and fast spectral regions as well as shielding experiments from the International Criticality Safety Benchmark Evaluation Project (ICSBEP) [3].

The simulation results of the dose rates in tumor and healthy tissue and therapeutic ratio are shown in Fig. 1 and 2. The results are given for neutron and photon flux 10^{10}particles/cm^{2}s. In the calculations ^{10}B concentrations in tumor and in healthy tissue were set to 52.5 ppm and 15 ppm, respectively. It can be seen that the values of dose rate, depth and therapeutic ratio most suitable for therapy are achieved with neutron energies from 1 eV to 10 keV.

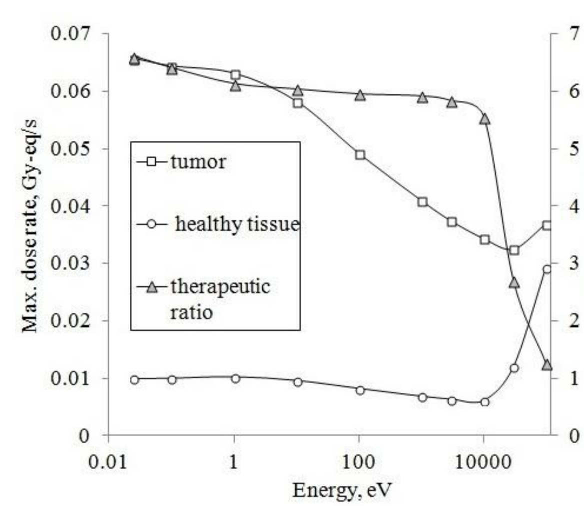

Figure 1: The dose rates in tumor and healthy tissue and therapeutic ratio for neutron beams with different energies.

ISBN 978-3-95450-181-6

TEMPERATURE CONTROL SYSTEM FOR THERMORADIOTHERAPY FACILITIES

A.M. Fadeev, S.M. Ivanov[1], S.M. Polozov
National Research Nuclear University - Moscow Engineering Physics Institute, Moscow, Russia
[1] and N.N. Blokhin Russian Oncological Research Center, Moscow, Russia
E.A. Perelstein, Joint Institute for Nuclear Research, Dubna, Russia

Abstract

As known, thermoradiotherapy and hyperthermia are widely used to improve the efficiency of cancer treatment.

Whole-body hyperthermia is used to treat metastatic cancer that has spread throughout the body, regional is used to treat part of the body (for instance leg or abdominal cavity). Local hyperthermia permits to heat tumour without overheating of healthy tiisues. It was proposed to use an array of eight independently phased dipoles operating on 100-150 MHz to focus the RF energy in deep-situated volume of 30-50 mm size. But the problem of non-invasive temperature measurement should to be solved for correct operation of the local thermoradiotherapy system. Conventional invasive thermometry devices as thermocouples, thermistors or Bragg optical sensors can not be widely used because of serious risk of the cancer cells transport to healthy tissues. Radiothermometry or acoustic thermometry can not be used for tissues located deeper than 5-7 cm. As known electrodynamics characteristics of tissues are sufficiently depends on temperature. It was proposed to use this effect for active radiothermometry in local hyperthermia. Two opposite RF dipoles can be used as generator and receiver of pick-up signal. It was shown by simulations that such method can be used for thermometry of deep-situated tissues and this method produces high resolution. Results of simulation will present in report.

INTRODUCTION

Hyperthermia is an adjuvant methods of cancer treatment in which tumour temperature is increased to high values (40-44 °C). It is usually used in combination with radiotherapy (thermoradiotherapy, TRT). The most evident approach is using an RF applicator(-s) situated around the patient body. RORC clinical studies demonstrate improving results of treatment by combined using of hyperthermia and radiation for the several tumour localizations. But only applicators for superficial hyperthermia were used in RORC. Common RORC-MEPhI-JINR project is pointed to expand the range of utilizing devices, i.e. using of devices for the regional hyperthermia gives more advantages for an oncological diseases treatment [1-6].

It was shown by many sets of simulations and experiments that such termoradiotherapy facility can provide the effective RF power focusing by means of amplitude and phase control for each applicator and effective local hyperthermia can be provided. As one example, the array of dipoles operating on 150 MHz with aperture diameter of 60 cm can provide RF power focusing wherever of patient body with spot diameter about 30 mm. A 450 MHz system can be used for hyperthermia of head and neck tissues with heated volume size of 15-20 mm.

Thermometry into heating volume is one of the major hyperthermia tasks. It is more difficult for deep-situated tissues. It is possible to use invasive or contact thermometry systems as thermistors and thermo-couples for deep-situated tissues and tumours. Russian hyperthermia protocol permits installation of thermocouples inside the patient body. But this causes pain and temperature probe can transport tumor cells to the healthy region of the patient body. European hyperthermia protocol forbids installation any temperature probes inside the patient body. They prefer to simulate any radiation process with phantoms. Moreover noninvasive thermometry of human tissues is important for other cases. It is suggested to determine tissues temperature by means of measurements effects that could be observed during heating. Optical fiber sensors based on Bregg grids became more popular last years. The measured parameter as temperature or mechanical displacement is coverts to the length of the light shift. But all of such sensors (thermo-couples, thermistors or optical fiber sensors) provide only invasive temperature measurement. Noninvasive control is possible by using of the magnetic resonance imaging (MRI) as it is proposed and realized by BSD Medical Systems (now Pyrexar Medical). But such way has serious difficulties and the price of MRI system is higher than the same of the hyperthermia system. Acoustic thermometry is one of new technologies. 2D and 3D temperature distributions were successfully imaged by means of acoustic thermometry experiments. But such technique can be used only for tissues located not deeper than 3-5 cm (for mammography as an example). Well-known radiothermometry (RTM) also can be used for deep-situated tissues. As known, the specific heat release of tumour is directly proportional to its growth velocity. More fast growth tumours will be “hotter” and will be brighter on the thermograph. The possibility to find the fast growth tumours is an unique advantage of the RTM. Main sufficient disadvantage is inherent as for acoustic thermometry: RTM can not be used for the deep suited tissues. The depth of temperature anomaly localization will not be greater than 3-7 cm depending of the tissues humidity.

ISBN 978-3-95450-181-6

LABORATORY MODEL OF THERMORADIOTHERAPY FACILITY: EXPERIMENTAL RESULTS

A.M. Fadeev, S.M. Ivanov[1], S.M. Polozov
National Research Nuclear University - Moscow Engineering Physics Institute, Moscow, Russia
[1] and N.N. Blokhin Russian Oncological Research Center, Moscow, Russia
E.A. Perelstein, Joint Institute for Nuclear Research, Dubna, Russia

Abstract

Hyperthermia and its combination with radiotherapy (thermoradiotherapy) or with chemotherapy is one of promising ways to improve cancer treatment efficiency. The treatment of deep-situated tumors is sufficient problem which can not be solved by means of traditional facilities developed for whole-body or regional hyperthermia because of overheating of healthy tissues and blood. A cylindrical array of independently phased dipoles was proposed to focus electromagnetic energy in deep-situated tumors. Early it was shown by simulations that array of eight independently phased dipoles operating on 100-150 MHz is able to focus energy in an ellipsoid of 30-50 mm in size. Later the laboratory model of thermoradiotherapy facility was developed and constructed and a series of experiments were carried out. Experimental results and its comparison with simulation will discussed in report.

INTRODUCTION

Hyperthermia is an adjuvant method of cancer treatment in which tumor temperature is increased to high values (40-44 °C). Many researches have shown that high temperature can damage and kill tumor cells, thus reduces tumor size. However the main advantage is that hyperthermia is a promising approach to increase efficiency of chemotherapy or radiation therapy. Under hyperthermia some tumor cells become more sensitive to the radiation and anticancer drugs. The effect on surviving fraction depends both on the temperature increase and on the duration of the expose. The main mechanism for cell death is probably protein denaturation at temperatures above 40 °C, which leads to changes in molecular structures such as cytoskeleton and membranes, and changes in enzyme complex for DNA synthesis and repair [1]. Heat also enhances the cytotoxicity of X-rays. Increased cytotoxicity is maximized when radiation and hyperthermia are given simultaneously. The combined effect decreases with time when the treatments are separated by more than one hour [2]. When cells are exposed to increased temperatures to anticancer drugs, their response is often different from the one at normal temperature. Drugs whose rate-limiting reaction is primarily chemical are expected to be more efficient at higher temperatures. Thus the combination of chemotherapy with hyperthermia has high potential in clinical practice [3].

The thermal therapy combined with the radiation (thermoradiotherapy, TRT) has been successfully applied in N.N. Blokhin Russian Oncological Research Center (RORC) since 1980th [4]. More than 1000 patients have been treated to date. Such program allows to sufficient and authoritative reduce of the regional cancer recrudescence and metastases comparatively to the surgery or independently radiotherapy (RT) [5].

One of the major problems of the devices mentioned above is the limited depth of penetration due to the principle of skin-effect. Only tumors located 2-3 cm (7-8 cm for the contact flexible microstrip applicator) from the surface can be heated by these applicators. To increase sufficient specific absorption rate (SAR) value in the tumors situated deeper than 10 cm relative to the surface SAR value it is necessary to focus energy of electric fields produced by an array of applicators. It consists of several antennae surrounding the patient and emitting radio-waves. Single antenna or groups of antennae are fed separately. Thus by proper selection of amplitudes and phases the interference patterns of the produced fields can be focused to create desirable temperature distribution [5]. Significant research successes have been obtained for the deep hyperthermia with the phased array. Simulation and measurements results are presented in [6].

FACILITY FOR TRT BASED ON ANTENNAE ARRAY

The most evident approach is using an antennae array of applicator situated around the patient body. Top view of this structure is shown in Figure 1. Arrays of applicators with variations in frequency, phase, amplitude and orientation in space give more possibilities to control heating pattern during hyperthermia treatment [6]. RF power feeding scheme is presented in [7]. Thus the phased array provides deeper tissue penetration of electromagnetic waves in comparison with single applicator, reduces undesirable heating of healthy tissues situated between applicator and tumour and improve local control for heating area. Also using array of applicators gives ability to control and to plan heating process without changing of patient position. Suggested phased array consists of eight copper dipoles, attached on the inner side of the dielectric cylinder, and surrounds a patient body. The aperture radius is up to 60 cm which can be applied in more cases. Dipoles are fed independently; this approach permits to control wave's phases and amplitudes. Space between dipoles and the patient body is filled by deionised water (conductivity $\sigma \approx 0.001$ S/m and $\varepsilon \approx 80$). Thus applicators are squeezed from the inner side by lossy medium with high permittivity (deionised water), and from the outer side by

ISBN 978-3-95450-181-6

MATHEMATICAL AND COMPUTER METHODS OF DATA PROCESSING IN NUCLEAR MEDICINE STUDIES

E.D. Kotina, A.V. Babin, P.V. Bazhanov, D.A. Ovsyannikov, V.A. Ploskikh, A.Yu. Shirokolobov, St. Petersburg State University, 7/9 Universitetskaya nab., St. Petersburg, 199034 Russia

Abstract

Currently nuclear medicine is a high-tech field. Its development requires solutions of problems related both to the improvement of hardware and computer processing of the information obtained in the course of study. The basic types of hardware of nuclear medicine are gamma cameras and single photon emission computed tomography (SPECT) [1], positron emission tomography (PET) and hybrid scanners (SPECT/CT, PET/CT).

The methods of SPECT data processing include analysis of static, dynamic, tomographic and ECG-gated images [2-9].

The PET data reconstruction software restores the three-dimensional distribution of the radiopharmaceutical in the body. Performance of iterative methods increases with the use of modern graphics processors [10]. Three-dimensional imaging allows a detailed analysis of the study area. The software also implements a fusion imaging of SPECT/CT, PET/CT scans performed in the same coordinate system.

An application of data flow model in medical software development is considered. Web-based imaging front-end of storage and processing system is presented.

DATA PROCESSING

The flexible platform with batch execution support and imaging elements is required during the process of development and testing new processing algorithms.

Mathematical modelling software such as MatLab is usually used for this purpose. But it makes harder to integrate the solutions into data processing applications as it often require redevelopment for application native platform.

Dataflow Programming

An approach to efficient development of data processing algorithms on .NET Framework is considered: program is represented as dataflow graph.

Dataflow consists of set of simple processing units called activities and connections. Activities represent simple operations such as data acquisition, reconstruction, volume transformations, ROI extraction, dynamic curves computation and analysis, etc. Each activity define a list of Inputs (or Attributes), a list of Outputs (or Results) and the Execution method, which supports cancellation and progress reporting. Dataflow connections bind activities outputs to inputs. Unbound inputs' data can be set from UI or file.

Dataflow are presented as an XML files. Activities are classes implementing interface *IActivity* and marked with *Activity* attribute. Its writable public properties define list of inputs, and read-only properties of generic type *ActivityResult* represent list of outputs. Sample dataflow graph is presented on fig. 1.

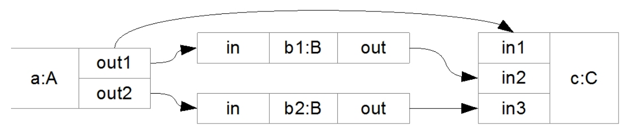

Figure 1: Example of dataflow application.

Basic dataflow execution environment (DEE) is developed. It supports running dataflow programs in interactive and batch modes. In interactive mode DEE dynamically loads user interface from a XAML file and binds UI components to inputs and outputs. Batch mode allows running dataflow with different input values provided from text files.

Reconstruction

Using dataflow approach we conducted series of experiments in tomographic reconstruction of PET data. Its goal was determination of correction parameters which adjust reconstructed values to physical units (Bq/ml).

Mathematical modeling of PET acquisition was performed. Cylindrical phantom (radius – 100 mm, length – 190 mm) with variable activity (10^5, 10^6 and 10^7 Bq) was used as positron source. Time of acquisition was selected in inverse ratio to activity (1000, 100 and 10 sec).

Ring detector configuration (radius – 410 mm) with different axial field of view (FOV) (50, 100, 150 and 200 mm) and number of detectors (720, 360, 240 and 144) was used.

The above experiments were repeated with photon attenuation in phantom volume.

Total of 96 sinograms were calculated.

Tomographic reconstruction of the sinograms was performed using 15 iterations of MLEM [10]. The iterative process is described by formula

$$x_j^{k+1} = \frac{x^k}{\sum_i m_i A_{ij}} \sum_i \frac{A_{ij} p_i}{\sum_l A_{il} x_l^k}, \quad (1)$$

where x – reconstructed image in vector form, p – sinogram in vector form, A – system matrix, m – correction vector.

Images were reconstructed with three different resolutions: 32x32 (pixel size – 10 mm), 64x64 (5 mm) and 128x128 (2.5 mm).

ISBN 978-3-95450-181-6

THE USE OF GRAPHENE AS STRIPPER FOILS IN SIEMENS ECLIPSE CYCLOTRONS

S. Korenev, R. Dishman, Siemens Healthineers, Knoxville, TN 37932, USA
A.M. Yerba, Siemens PETNET Solutions, Denver, CO 80210, USA
N. Mesheriakov, Siemens LLC, Moscow, Russia
I. Smirnov, Siemens LLC, Ekaterinburg, Russia
I. Pavlovsky, R.L. Fink, Applied Nanotech Inc., Austin, TX 78758, USA

Abstract

This paper presents the results of an experimental study for the use of graphene foils as an extractor (stripper) foil in the 11-MeV Siemens Eclipse Cyclotron. The main advantage of graphene foils compared with carbon is very high thermal conductivity. The graphene also has significant mechanical strength for atomically thin carbon layers. The life time of these foils is more than 16,000 μA*H. The graphene foils showed a significant increase in the transmission factor (the ratio of the beam current on the stripper foil to the current on the target), which was approximately more 90%. The technology in fabricating these graphene foils is shown. The pros and cons of using the graphene material as a stripper foil in cyclotrons are analysed.

INTRODUCTION

The use of stripper foils in the cyclotrons with negative hydrogen ions allows for easy output of the proton beam from the cyclotron into the target [1]. The 11-MeV Eclipse Cyclotron [2] uses this approach for the production of medical isotopes. The standard stripper foils based on carbon materials are widely used for these goals. The discovery of graphene [3] and the unique properties of graphene have created a large interest in this material as a stripper foil compared to the standard graphite and carbon foils. The main difference is the thermal conductivity of graphene which is up to 20 times higher than that of polycrystalline graphite. This gave interest for the application of graphene as a stripper foil in accelerators of charged particles and especially in commercial cyclotrons, such as the Eclipse cyclotron. The preliminary application of graphene foils from Applied Nanotech [4] as a stripper foil shows the main advantages of this material in comparison with the standard carbon and graphite foils. The main focus of this study was to determine the lifetime of stripper foils and to understand any cyclotron operating performance improvements. One the main questions was to characterize the radiation damage of graphene under irradiation by negative hydrogen ions with a kinetic energy of 11 MeV and current up to 100μA.

THE TECHNOLOGY OF FABRICATION FOR GRAPHENE FOILS

The technology for the fabrication of graphene foils is described in more detail in [5]. The foil fabrication method is based on the controlled reduction of graphene oxide by hydrazine with addition of ammonia in an aqueous dispersion. The dispersion of graphene oxide with loading of 0.5% wt. in water was obtained from Angstron Materials. The dispersion was reduced for 4 hours at 95°C and then cooled down to room temperature. The thickness of graphene foils was controlled by using a calculated volume of graphene dispersion knowing the loading of graphene. A commercially available stainless steel filter holder was used to make graphene foils by pressure filtration. The diameter of the fabricated foils was 13 cm. The filter holder allowed increasing the differential pressure across the filter. A compressed air line with a pressure regulator was connected to the filter holder to pressurize the air space above the graphene dispersion. Pressure up to 300 kPa was used to filter the dispersion. Commercially available polymer filter membranes with a diameter of 142 mm were used for the filtration. After filtration, graphene foils still on the filter membrane were removed from the filter holder and peeled off the filter membrane to obtain free-standing graphene foils. The described process can be adapted to fabricate foils with a wide range of foil thickness and using different isotopes of carbon.

EXPERIMENT

The experiments with graphene foils with a thickness of about 3μm (0.5mg/cm^2) were conducted on four Siemens Eclipse cyclotrons. The graphene foils were installed on the carousels of the Eclipse cyclotron. The general picture of the graphene material is shown in Figure 1.

a) b)

Figure 1: General view of graphene foils: a) fabricated foil; b) graphene cross section.

ISBN 978-3-95450-181-6

THE PROBLEMS OF ACCELERATOR-DRIVER DESIGN FOR ADS

A. G. Golovkina*, I. V. Kudinovich[1], D. A. Ovsyannikov, Yu. A. Svistunov[2]
Saint Petersburg State University, St. Petersburg, Russia
[1]also at Krylov State Research Center, St. Petersburg, Russia
[2]also at JSC "NIIEFA", St. Petersburg, Russia

Abstract

Main problems of accelerator-driver design for ADS are considered. Accelerator-driver should meet additional requirements in comparison with accelerators for other purposes: - high neutron production rate; - higher reliability; - continuous operation for more than 5000 hours; - possibility of accelerator parameters adjustment to regulate ADS power level. Different types of accelerators were analyzed taking into account the mentioned features and the fact that the most prospective way of ADS application nowadays is transmutation. It's shown that the most preferable accelerator type is proton linac. Also it's marked that for demonstration facilities accelerators with lower requirements and correspondingly cost can be used.

INTRODUCTION

In contrast to traditional critical reactors, where the control on reactor power rate is fulfilled with neutron absorbing rods, in ADS subcritical reactor is controlled by charged particle accelerator [1]. Reactivity coefficient decreases as a result of nuclear fuel burning and fission products and actinide accumulation during reactor operation. So to maintain fixed ADS power-level dynamics of subcritical reactor driven by accelerator should be investigated [2].

ADS is most perspective for effective actinide transmutation, because it allows safely load large amount of transuranic elements to the reactor core in contrast to traditional critical reactors. However, it should be noted that construction of high power ADS will require to use accelerators also with high beam power not less than 10 MW. It is obvious, that such facilities are very expensive and the necessity of their construction as the alternative to fast reactors requires serious justification.

Nowadays R&D activities on ADS are focused on demonstration and experimental low-power facilities construction and also design of industrial ADS conceptual projects. In this paper the possibility of low-power ADS construction based on the proton linac is considered. The choice of such accelerator type as an ADS driver is justified. Also the problem of subcritical reactor control via accelerator is discussed.

THE CHOICE OF ACCELERATOR-DRIVER TYPE FOR ADS

There are three main accelerator types that are considered as drivers for ADS: proton [3] and electron linac [4] and cyclotrons [5]. In the majority of works devoted to the transmutation of nuclear waste using ADS RF proton accelerator is considered as a driver. It can be explained by the fact that neutron production per watt of beam power for heavy elements targets (Pb, W, U etc) reaches a plateau just above energy 1 GeV (Fig. 1) [3]. That allows achieve necessary for transmutation neutron fluxes $10^{17} \div 10^{18}$ n/s with the beam power 10 MW. At energy 1 GeV, it corresponds to a relatively low average current of 10 mA. For electron beam, neutron yield growth as a result of photo-nuclear reaction practically stops at energy of 50-60 MeV (Fig. 2) [6], and even at the average current of 200 mA neutron flux does not exceed 10^{16} n/s.

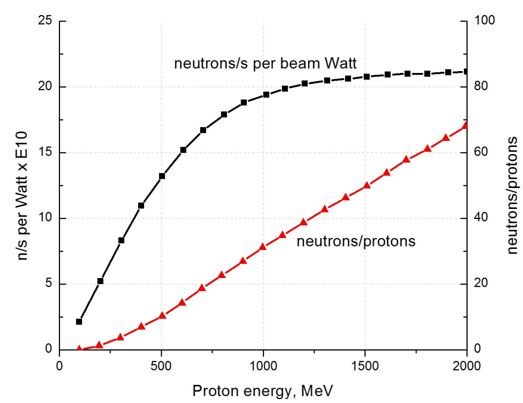

Figure 1: Neutrons/s per beam Watt, neutrons per proton, for a beam incident on axis of cylindrical W target 50-cm diam. x 100-cm long.

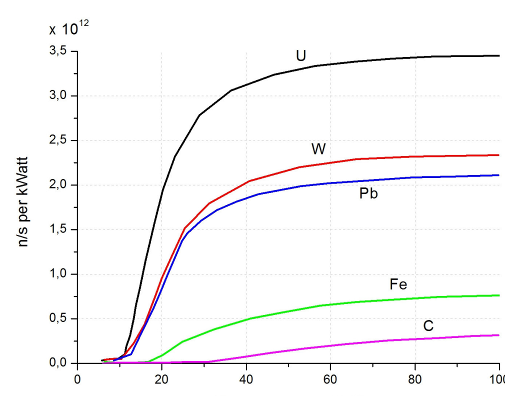

Figure 2: Neutrons/s per beam kWatt in photonuclear and photo fission reactions from Bremsstrahlung photons for an electron beam.

* a.golovkina@spbu.ru

ISBN 978-3-95450-181-6

STUDY OF OIL WELLS WITH THE USE OF ACCELERATOR TUBES, TIME AND ENERGY SPECTROMETERS OF NEUTRONS AND GAMMA RAYS IN A SINGLE GEOPHYSICAL COMPLEX

B.Yu. Bogdanovich, E.D. Vovchenko, A.V. Ilinskij, K.I. Kozlovskij, A.A. Isaev, A.V. Nesterovich, A.E. Shikanov, National Research Nuclear University "MEPhI" (Moscow Engineering Physics Institute), Moscow, Russia

Abstract

The report discusses the finding of the coefficient of oil saturation of the reservoir by of nuclear methods. For this purpose, the data about pulse and the activation neutron logging and spectral logging of natural gamma activity are used in a single geophysical complex. As sources of neutron radiation can been applied accelerating tube (AT) based on different ion sources, such as plasma discharge with oscillating electrons (gas AT), vacuum arc and laser-plasma (vacuum AT). For investigation of the oil reservoir, in particular with heavy oil, we discuss the prospects of using vacuum accelerating tube based on a laser-plasma source of deuterons with coaxial acceleration geometry and pulsed magnetic isolation of electrons.

INTRODUCTION

The coefficient of oil saturation $k_н$ (i.e. the relative volume of the pores in oil collector occupied with a productive fluid) is the most important criterion that shows a technical condition of a working oil well. It is determined by the properties of the reservoir, which can also contain water and clay. Between k_n, volumetric content of the solid phase (skeleton) – k_{sk}, relative water content in the pores (water saturation coefficient) – k_w and the relative content of clay in the pores (coefficient of clay content) – k_c installed connection [1]: $k_{sk} + k_c + k_w + k_n \approx 1$.The sum of k_w and k_n is the porosity coefficient: $k_p = k_w + k_n$. The information for the evaluation of k_n can be obtained by using combinations of different nuclear-geophysical methods, such as pulsed neutron lodding (PNL), activation logging, wells logging of natural γ-activity (JCC), laboratory nuclear techniques, well as the classical methods of petrophysics [1].

Method PNL gives information about the state of the forwation developed in the presence of the casing of the well, creating inconvenience for other "opaque" geophysical methods [2 – 3]. In the process of implementing a temporary field, analysis PNL thermal neutrons or γ-quanta of radiation capture (RC) generated in the borehole accelerator (AT). Their temporary structure is determined by the sum of the exponentials:

$$n(t,z) = A_п(z)\exp(-\lambda_п t) + A_c(z)\exp(-\lambda_c t),$$

$n(t,z)$ – spatial density of neutrons or γ-quanta; z – coordinate, set along the wellbore; λ_n и λ_c – decrements recession of density radiation field in the reservoir and wellbore respectively as a result of the RC.

The mathematical apparatus of separation exhibitor at wireline signal received as a result of the interim analysis [4] makes it possible to determine the parameter λ_n, as well as amplitude $A_n(z)$. In Fig. 1 is shown a typical example of computer processing logging signal.

Using the additivity rule, you can set up a relationship between the λ_n and radiation capture sections based on its individual components using the ratio:

$$\lambda = (\Sigma_{ск}k_{ск} + \Sigma_н k_н + \Sigma_в k_в + \Sigma_{гл}k_{гл})(1+\varepsilon),$$

$\Sigma_{с,н,в,гл}$ – macroscopic cross-section of RC in the skeleton, in reproductive fluid, in water and clay, respectively; $\varepsilon \approx 0.1$ – dimensionless correction option, resulting in model experiments.

This formula allows to judge quality of reservoir fluid saturation and determine the position of the boundary water-productive fluid because of the cross-section of RC in water significantly more than the hydrocarbons due to the presence of salt, and, hence, chlorine whose nuclei are abnormally high micro-cross RC.

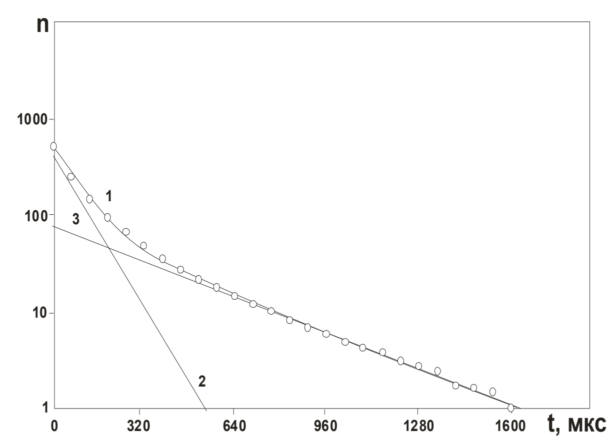

Figure 1: An example of splitting the Exhibitor in a logging signal. Slopes define by the direct signal λ_n (3) and λ_c (2).

The ratio $A_п(z_1)/A_п(z_2)$ carries information about slowing down and diffusive properties of formation, which are determined by the content of hydrogen there [2]. The relative content of hydrogen in water and hydrocarbons are close enough, so one could argue that this attitude will clearly depend on porosity ratio and will serve as a device for its definition.

ISBN 978-3-95450-181-6

BEAM DYNAMICS IN NEW 10 MEV HIGH-POWER ELECTRON LINAC FOR INDUSTRIAL APPLICATION

S.M. Polozov, V.I. Rashchikov National Research Nuclear University – Moscow Engineering Physics Institute, Moscow, Russia
M.I. Demsky, CORAD Ltd., Saint-Petersburg, Russia

Abstract

Beam dynamics simulation in electron gun, bunching and accelerating cells of new 10 MeV high-power electron linac was fulfilled with the help of developed at MEPhI SUMA [1] and BEAMDULAC-BL [2] codes. Three-electrode electron gun was used to obtain up to 400-450 mA of pulse beam current which is necessary to produce 300 mA of the accelerated beam. Precise gun simulation was conducted to satisfy all necessary output beams characteristics, such as profile, energy spectrum, phase space size etc. Some additional calculation was conducted to provide wide range of gun output beam parameters which will be used for subsequent accelerator modification. The conventional biperiodical accelerating structure (BAS) based on disk loaded waveguide (DLW) was used in linac. Beam dynamics optimization was pointed to obtain effective beam bunching for all energy range and to achieve narrow energy spectrum. Simulation results shows that linac provides effective beam bunching and acceleration for wide bands of beam currents and energies.

ELECTRON GUN SIMULATION

PIC code SUMA was used for beam dynamics simulation in the electron gun. The traditional three-electrode gun with cathode-grid voltage 1-1.3 kV, emission current 0.5-0.7 A, cathode-anode voltage 50 kV was investigated. Fig. 1 shows computer simulation result for cathode-grid voltage 1 kV and emission current 0.7 A.

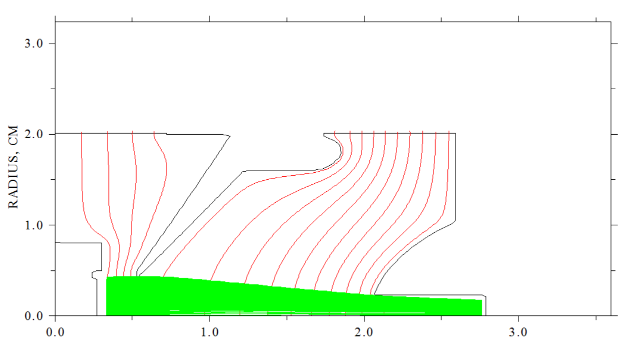

Figure 1: Electron trajectories (green lines), electric field equipotential lines (red lines) and boundary (black lines).

Output energy spread is 1.2% and transverse emittance 2.5 cm·mrad.

For code testing some experiments were conducted. Beam envelope was measured by collimated diaphragm current collector on different distance from gun anode. Fig.2 shows beam envelope dependence on anode distance for different gun currents and cathode – anode voltage is 20 kV, greed - anode microperveance is 0.078. SUMA simulation results for this case are presented in Fig. 3.

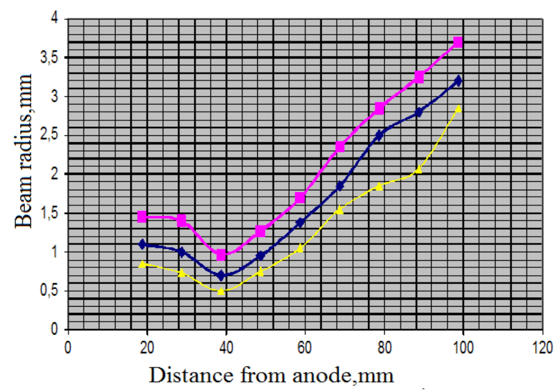

Figure 2: Beam envelope for different current values: red-0.222 A, blue-0.19 A, yellow-0.16 A, cathode-anode voltage 20 kV.

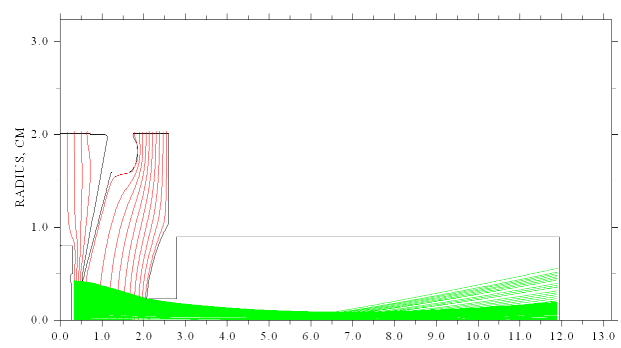

Figure 3: Electron trajectories (green lines), electric field equipotential lines (red lines) and boundary (black lines). Current value -0.222 A.

We obtain a good experimental and calculated results agreement for the beam emittance equals 2.42 cm·mrad and taking into account that distance between cathode and anode equals 25 mm.

For further accelerator modification program it might be necessary to increase output beam diameter from 2 to 3.5 – 4.0 mm or even more. For this purpose some new gun modifications were fulfilled. The main aim was to obtain necessary result with a few changes as possible. First step in this way is to increase the anode hole. Output beam radius rises due to potential sage on the anode hole. Fig. 4 shows beam profile for anode hole radius equals 3 mm (initial value 2.25 mm).

ISBN 978-3-95450-181-6

REALIZATION OF POSITRON ANNIHILATION SPECTROSCOPY AT LEPTA FACILITY

K. Siemek, E.V. Ahmanova, M.K. Eseev, V.I. Hilinov, P. Horodek, A.G. Kobets, I.N. Meshkov, O.S. Orlov, A.A. Sidorin, JINR, Dubna, Russia

Abstract

The Positron Annihilation Spectroscopy (PAS) unit was created as a part of LEPTA project at JINR in Dubna. Currently works performed in PAS laboratory focus on studies of defects in solid state, especially on studying radiation damages in novel materials and semiconductors as a part of the international project “Novel Semiconductor for Fundamental and Applied Research”. This report aims to present a current status of realization and progress in PAS methods at LEPTA facility at JINR.

INTRODUCTION

Positrons are used in materials science to study open volume defects such as vacancies, vacancy clusters and dislocations. Several positron annihilation spectroscopy (PAS) techniques exist. These methods are based on detection of the 511 keV gamma quantum. The first method is the analysis of the Doppler broadening of annihilation line and provides information about defect concentration. Both annihilation quanta can be observed. Coincidence observation of two quanta gives additional information about the environment around defect. The second method is based on lifetime concept, which allows us to distinguish type of defects. Nowadays, positron beams are of great interest for materials science. Using a low energy, monoenergetic beam it is possible to control the positron penetration depth, see Fig. 1, from the sample surface to a depth of several microns. Thus, the beam can be used to characterize thin films, analysis of surface modification, studying influence of ions on matter etc.

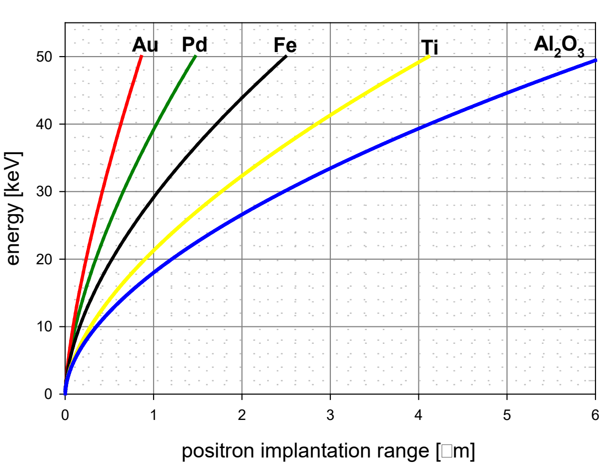

Figure 1: Dependency of positron energy on mean positron implantation depth [1].

THE DOPPLER BROADENING OF ANNIHILATION GAMMA LINE

The basics of method rely on registration energies of annihilation quanta. Due to Doppler’s phenomenon quantum energies are changed according to the formula:

$$E_\gamma \cong mc^2 + E_B \pm \frac{p_{\|}c}{2}, \qquad (1)$$

where E_b is the energy of positron-electron pair coupling and $p_{\|}$ is a component longitudinal to annihilation quanta direction of the pair’s momentum. It is worth emphasising that positron’s momentum is negligibly small in relation to electron’s momentum, therefore it is usually omitted in deliberations.

The heart of Doppler broadening spectroscopy is a detector which requires a high energetic resolution. Typical available germanium detectors allow us to take measurements with resolution equal to 1-2 keV around 511 keV energy. The scheme of Doppler broadening spectrometer unit working in PAS laboratory at JINR is shown in Fig. 2. The important parameters of high purity germanium Detector (HPGe) made by Baltic Scientific Instruments working at LEPTA facility is gathered in Table 1. Next year also the second detector should appear in PAS laboratory, which will allow to perform coincidence measurements.

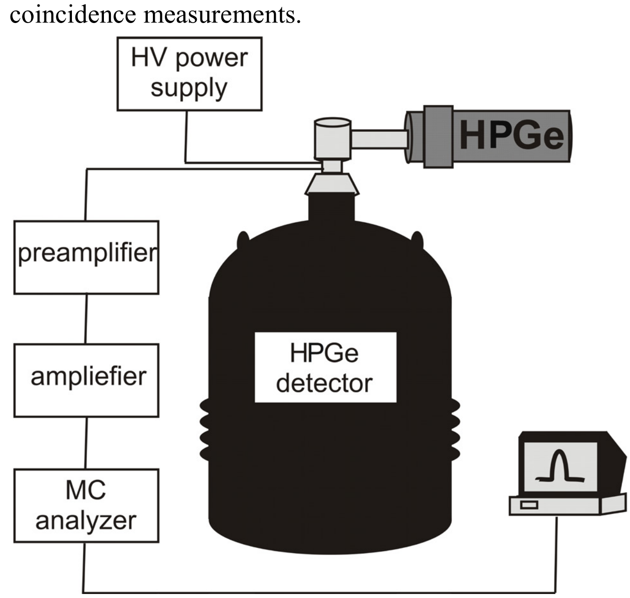

Figure 2: The scheme of Doppler broadening of annihilation gamma line 511 keV spectrometer.

ISBN 978-3-95450-181-6

DEVELOPMENT OF POSITRON ANNIHILATION SPECTROSCOPY AT THE LEPTA FACILITY

I.N. Meshkov[#,1], E.V. Ahmanova, V.I. Hilinov, O.S. Orlov, A.A. Sidorin, Joint Institute for Nuclear Research, Dubna, Moscow region, Russian Federation
M.K. Eseev, Joint Institute for Nuclear Research, Dubna, Moscow region, Russian Federation and Northern (Arctic) Federal University, Arkhangelsk, Russian Federation
P. Horodek, K. Siemek, Joint Institute for Nuclear Research, Dubna, Moscow region, Russian Federation and Institute of Nuclear Physics of the Polish Academy of Sciences, Cracow, Poland
A.G. Kobets, Joint Institute for Nuclear Research, Dubna, Moscow region, Russian Federation and Institute of Electrophysics and Radiation Technologies NAS of Ukraine, Kharkov, Ukraine
[1]also at Saint Peterburg University, Saint Petersburg, Russian Federation

Abstract

The report aims to present the status of the development of the LEPTA facility for further enhancement of the positron annihilation spectroscopy (PAS) method application at the LEPTA facility. The research in solid state physics performed currently is based on slow monochromatic positron flux from the injector and Doppler PAS.

The new positron transfer channel being under construction at the LEPTA allows us to develop more advanced PAS method – so called “Positron Annihilation life-time spectroscopy” (PALS). It will enrich significantly the research program at the LEPTA. PAS method is sensitive to microdefects in solids. A pair of gamma quanta, born as a result of positron-electron annihilation carries information about the density of the defects that have the size less than 10 nm and are located at the depth from the surface of the material depending on the positron energy.

New monochromatic positron source construction supplied with the autonomous cooling system with emitter-source of the activity of 30 mCi (iThemba LABS production) and new positron transfer channel are presented in report.

DESIGN AND CONSTRUCTION OF THE TRANSFER CHANNEL

The new positron transfer channel (Fig. 1, 2) has been assembled at the LEPTA facility. It allows us to develop the advanced PAS method — so called «Positron Annihilation Life-time Spectroscopy» (PALS).

Positron lifetime spectroscopy measures the elapsed time between the implantation of the positron into the material and the emission of annihilation radiation. When positrons are trapped in open-volume defects, such as in vacancies and their agglomerates, the positron lifetime increases with respect to the defect-free sample. This is due to the locally reduced electron density of the defect. This method allow to determine defect concentration and its type.

#meshkov@jinr.ru

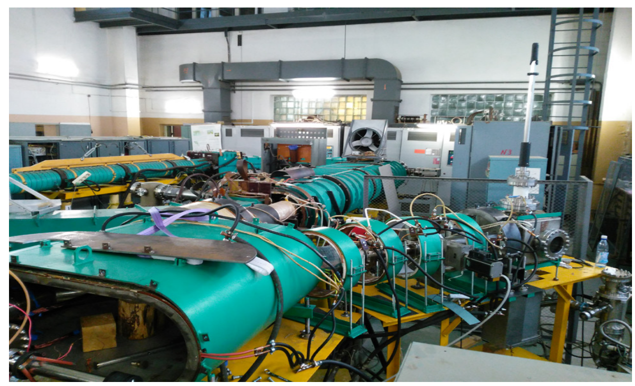

Figure 1: Positron transfer channel.

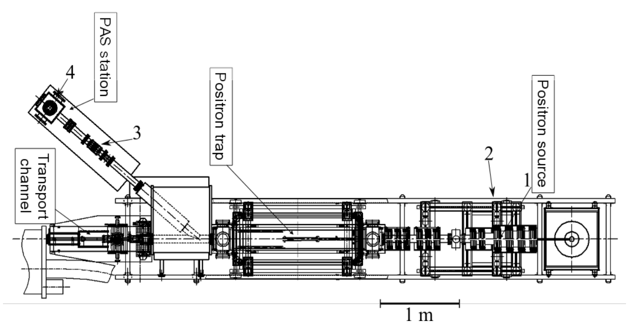

Figure 2: Scheme of the positron transfer channel.

The channel comprises four parts: cryogenic positron source equipped with closed loop LHe supply system (Fig. 3, pos. 1), pulsed voltage gap (Fig. 3, pos. 2), electrostatic acceleration gap (Fig 3, pos. 3), and the target box (Fig 3, pos. 4) containing samples to be studied by PALS method.

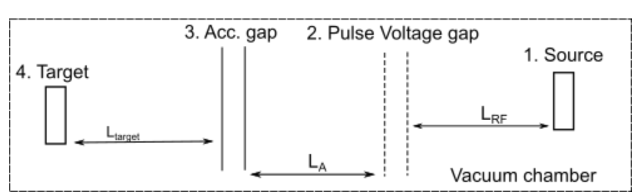

Figure 3: Scheme of the PALS method, with formation of the ordered positron flux: 1. Cryogenic positron source (Fig. 3); 2. Pulsed voltage gap; 3. Acceleration gap (electrostatic field); 4. Target — a sample for PAS studies.

ISBN 978-3-95450-181-6

NEUTRON GENERATORS OF THE NG-10 SERIES FOR METROLOGY

D.A. Solnyshkov, G.G. Voronin, A.V. Kozlov, A.N. Kuzhlev, N.P. Mikulinas, A.V. Morozov
JSC "NIIEFA", St. Petersburg, Russia

Abstract

Neutron generators NG-10 and NG-10M with a neutron yield of $1\cdot10^{10}$ n/s and $2\cdot10^{11}$ n/s respectively have been designed in the JSC "NIIEFA". The generators are high-voltage accelerators with target devices, in which Ti-T/Ti-D targets of different diameters are used. A duoplasmotron allowing a beam current up to 5 mA to be obtained is used in the NG-10 generator, and the NG-10M employs a microwave ion source providing the beam current up to 10 mA. The power supplies, which are under a high voltage, are controlled via fiber-optic communication lines. A beam of ions produced in the ion source is accelerated up to 150 keV in a sectionalized accelerating tube, separated in mass with an electromagnetic mass-separator and focused onto a target with a doublet of electromagnetic quadrupole lenses.

The generators are equipped with several lines to transport the beam to target devices, which can be placed in separate rooms. In addition to a high and stable yield of neutrons when operating continuously, the generators can provide the pulsed mode with a time from 2 µs up to 100 µs and pulse repetition rate from 1 Hz up to 20 kHz.

INTRODUCTION

Neutron generators NG-10 [1] and NG-10M designed in NIIEFA are intended for application in metrological laboratories as apparatus generating reference neutron fluxes and can be also used for neutron-activation analysis in different fields of science and engineering. The machines are designed for neutron yields up to 10^{11} n/s in the continuous operating mode. The generators consist of a deuterium ion accelerator with an accelerating voltage continuously adjustable in the range of 120-150 keV, beam current of atomic deuterium ions on a target up to 2 mA and a series of target devices, in which Ti-T and Ti-TD targets of different diameters are used. In addition to a high and stable in time neutron yield in the continuous mode, such generators provide pulse neutron fluxes with pulse durations and pulse repetition rates varying over a broad range [2, 3].

The ion beam produced by the ion source is accelerated up to 150 keV in a sectionalized accelerating tube, separated in mass with an electromagnetic mass-separator and then focused to a target by a doublet of quadrupole electromagnetic lenses. The generators can be equipped with lines to transport beams to target devices placed in separate rooms.

VERSIONS OF ION SOURSE

A duoplasmatron-type source is used in the NG-10 generator. Duoplasmatron is the most widely used ion source applied in neutron generators. However, poisoning of the used heated cathode as a consequence of a micro leakage appeared in the discharge chamber or gas-supply system of the source makes necessary its cleaning or replacement, which requires opening of the vacuum volume and results in long-term shutdowns of the generator. The general view of the NG-10M generator is shown in Fig. 1.

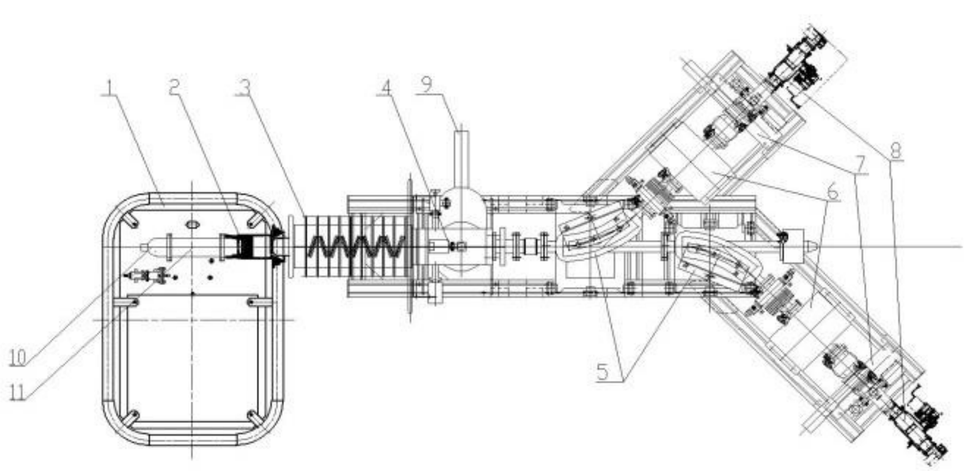

Figure 1: The NG-10M ion accelerator. General View. 1 - high-voltage terminal, 2 - ion source, 3 - accelerating tube, 4 - vacuum chamber, 5 - electromagnetic mass-separator, 6 - quadrupole lens, 7 - gate valve, 8 - target device, 9 - gate valve, 10 - magnetron, 11 - circulator.

ISBN 978-3-95450-181-6

MODIFICATIONS OF ELECTRON LINEAR ACCELERATORS PRODUCED IN NIIEFA FOR STERILIZATION

Yu.V. Zuev, A.P. Klinov, A.S. Krestianinov,O.L. Maslennikov, V.V. Terentyev
JSC NIIEFA, St. Petersburg, Russia

Abstract

The paper analyses modifications of electron linear accelerators equipped with one and the same accelerating structure produced in NIIEFA. The structure operates in the standing-wave mode at a frequency of 2856 MHz. The accelerators are designed for electron beam processing and provide beam energies in the range of 8-11 MeV and beam average powers up to 10-12 kW.

INTRODUCTION

A variety of facilities for radiation sterilization with a beam of accelerated electrons was designed and manufactured in NIIEFA [1,2].The paper outlines features of UELR-10-10S [2,6], UELR-10-10T [3], UELR-10-15S [4], LAE10/15 [5] accelerators, in which one and the same accelerating structure is used. The accelerators differ in microwave power sources, electron guns, beam scanning and extraction devices, composition and arrangement of auxiliary systems, consequently, in operational parameters and cost.

ACCELERATING STRUCTURE

All the listed above accelerators employ a biperiodic electrodynamic structure, which consisting of forty five cells placed on one axis, Fig. 1. The first ten cells form a 5-gap buncher, which provides high capture of beam in the acceleration (up to 85% of the continuous beam) and implements the beam focusing with the RF field.

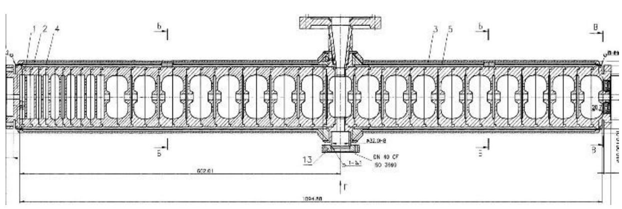

Figure 1: Layout of the accelerating structure.

Cells of the bunching part are cylindrical and U-shaped with a 3.5 mm-thick separating wall. The diameter of beam apertures in the first 4 cells of the buncher is 8 mm, and that in all the rest cells of the structure is 10 mm.

A regular part of the structure consists of Ω-shaped accelerating cells alternating with short (4 mm long) cylindrical coupling cells. Calculated values of the Q-factor and shunt-impedance of the accelerating cells are 14800 and 2.9 MΩ, respectively.

RF coupling of the cells is carried out by pairs of azimuthal slots. The working, π/2, mode of the accelerating field oscillations is excited at a frequency of fo=2856 MHz. The RF power is input to the structure through cell # 27, matching iris aperture and wave transformer. The accelerating structure length is 1.1m.

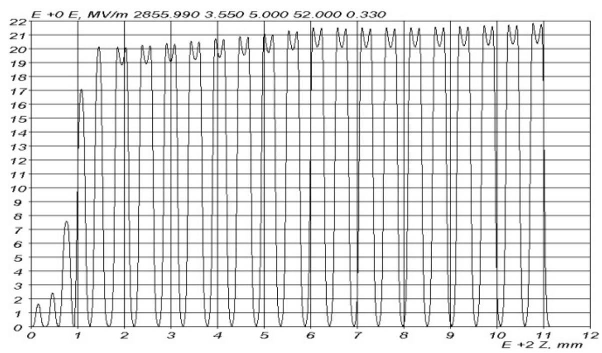

Figure 2: Field distribution on the structure axis.

The nominal distribution of the electric field in the structure is shown in Fig. 2, the energy spectrum corresponding to this field is given in Fig. 3. The electron spectrum width is not more than ±3%. The designed beam injection energy is 50 keV.

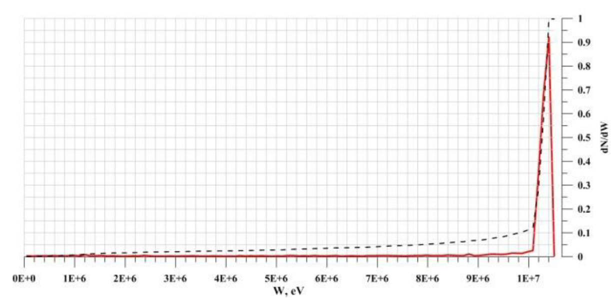

Figure 3: Energy distribution of electrons at the structure output (red solid line) and its integral (black dashed line).

THERMAL LOAD OF THE STRUCTURE

Thermal stability of the structure is maintained by a cooling jacket made of non-stainless steel and welded to the structure. To compensate the temperature non-uniformity along the structure, the cooling jacket is made double with oppositely directed water flows.

Table 1 demonstrates results of thermal and structural analysis of the structure for 2 values of the average RF power, P_W^{avr}, dissipated on the walls. Data in the table were calculated for water input temperature of 20°C and are designated as follows: Q_W is the cooling water flow rate, ΔT_W is the water heating, ΔP_W is the pressure drop, T_{MAX} is the maximum temperature and ΔL_{MAX} is the maximum displacement (strain).

ISBN 978-3-95450-181-6

DEVELOPMENT OF THE BEAM DIAGNOSTIC SYSTEM FOR THE RADIOBIOLOGICAL RESEARCH AT THE PROTON LINEAR ACCELERATOR I-2*

A.V. Bakhmutova, N.V. Markov, A.V. Kantsyrev, A.A. Golubev,
Institute for Theoretical and Experimental Physics NRC «KI», Moscow, Russia

Abstract

At the present time at ITEP there is a possibility to investigate the biological mechanisms of the low energy protons on living systems on linear accelerator I2. The unique high current linear accelerator allows to obtain 20 MeV intense proton beams. They could be used for the radiobiological research in a wide range of absorbed doses and for different cell types. Currently some preliminary experiments were made to specify diagnostic equipment required for further investigations. This work presents the main results on the proton beam parameters measurements such as beam current, beam cross section dimension as well as the measurements of the absorbed dose and depth dose distribution using different types of detectors.

INTRODUCTION

For the last few years the distant radiation therapy with 70-230 MeV proton beam are on the rise in the world. According to PTCOG report 13 centers for proton radiation therapy are put into operation for last two years. Besides the general number of centers where the patients are irradiated, do not exceed 60 [1]. Though the amount of information has been collected for more than a half-century' history of the radiation therapy there are a set of questions needed further radiobiological investigations [2]. Now besides medical application the radiobiological research with low energy proton and ion beam of micron and submicron size develop worldwide (so-called microbeam) [3]. The main goal of this research is the biological effect investigation of charged particles on the level of single cell. It allows developing a deeper understanding of the ionizing radiation biological effect. Now at ITEP it is possible to provide the above-mentioned radiobiological research on proton linear accelerator I-2. The accelerator parameters allow to obtain high intensity proton beam with the energy approximately 20 MeV thus radiobiological investigations in the wide range of absorbed doses for different types of cells could be carried out. In this article, the made experimental setup for further radiobiological research and diagnostics system is described. Also the main results on the proton beam parameters measurements such as beam current, beam cross section dimension using different types of detectors and the measurements of the absorbed dose and depth dose distribution.

*Work supported by by the Russian Foundation for Basic Research, project no. 16-32-00393.

EXPERIMENTAL SETUP

For the experiment the proton beam with the energy of 24.6 MeV was used. Figure 1 gives the overview of the experimental scheme.

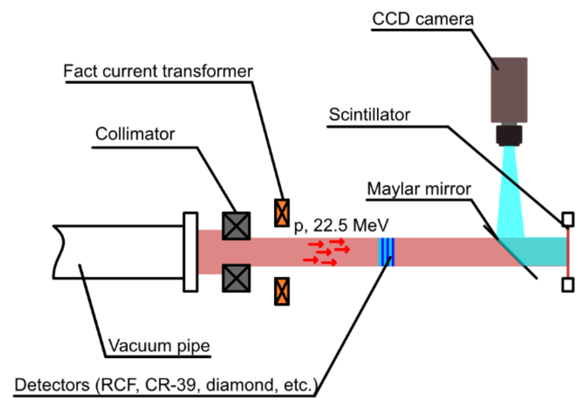

Figure 1. The view of the experimental setup.

The lateral size of the beam field in the area of measuring equipment is given by collimating system consisting of different sizes of brass collimator. The fast current transformer FCT-082 (Bergoz, France) was used as the main monitor to measure the number of particles. This detector is a broadband transformer of AC current with bandwidth of 700 MHz. The signal of current transformer is read off by oscilloscope DPO-3034 Tektronix (USA). The view is shown in Fig.2. The digitized signal send to software PTEK and the number of particles was calculated [4].

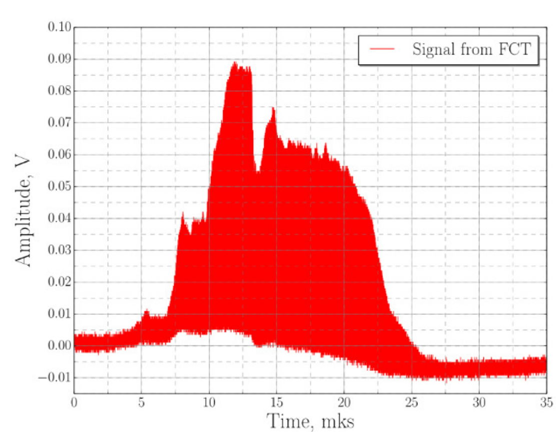

Figure 2. The output signal of FCT.

ISBN 978-3-95450-181-6

MODELING OF ADSR DYNAMICS WITH PROTON LINAC IN MULTI-POINT APPROXIMATION

A. G. Golovkina*, Saint Petersburg State University, St. Petersburg, Russia

Abstract

The mathematical model of multi-point kinetics is proposed in the paper. The transients in subcritical reactor driven by proton linac taking into account the fuel and coolant temperature feedbacks are analyzed using this model. In contrast to the widely used point kinetics model, the proposed model makes it possible to more accurately take into account the heterogeneity of the material composition in the core. That is the one of the main features of transmutation systems with accelerator-driver.

INTRODUCTION

Accelerator Driven System (ADS) is a combination of high-power electronuclear neutron source with subcritical reactor [1]. In such systems external neutrons comes from the interaction of high energy proton beam with a heavy atom nucleus (spallation). ADS is of interest nowadays due to its prospects in long-living radionuclides transmutation [2], also subcritical condition in ADS provides advantages from safety standpoint in comparison with regular critical nuclear reactors.

Due to development of subcritical reactor technology for transmutation of long-living radionuclear waste, reactor cores with significant fuel spacial inhomogeneity are widely considered. Cascade system consisting of fast neutron section (plutonium fuel) and thermal neutron section (uranium fuel) can be treated as an example of such core [3, 4]. During dynamical processes analysis in the reactor with fuel inhomogeneity it is necessary to calculate kinetics characteristics (prompt mean lifetime, delayed-neutron fraction) correctly [5]. These parameters depend on fission nuclides and neutron spectrum in the reactor core [6]. In this paper multi-point kinetics model is proposed. This model allows to estimate the influence of fuel inhomogeneity in the reactor core on the kinetics characteristics better, than the well-known point kinetics model [7]. It is compared with well-known point kinetics model in dynamics analysis of subcritical reactor with homogeneous and heterogeneous fuel composition driven by proton linac.

MULTI-POINTS KINETICS EQUATIONS DERIVATION

In the general case nonstationary neutron distribution in the reactor core is described by the following set of integro-differential equations [8]

$$
\begin{aligned}
\frac{1}{v}\frac{\partial F(\mathbf{r},E,\mathbf{n},t)}{\partial t} &= -\mathbf{n}\nabla F(\mathbf{r},E,\mathbf{n},t)+ \\
&\int_0^{E_0} dE' \int (1-\beta)\nu_{E'}(\mathbf{r})\Sigma_f(\mathbf{r},E')\frac{\chi(E)}{4\pi}F(\mathbf{r},E,\mathbf{n},t)d\Omega' - \\
&\Sigma_{ais}(\mathbf{r},E)F(\mathbf{r},E,\mathbf{n},t)+\sum_{i=1}^{6}\lambda_i C_i(\mathbf{r},t)\frac{\chi_{di}(E)}{4\pi}+ \\
&\int_0^{E_0} dE' \int \omega(E,E',\mathbf{n}\cdot\mathbf{n}',\mathbf{r})F(\mathbf{r},E,\mathbf{n},t)d\Omega' + q(\mathbf{r},E,\mathbf{n},t), \\
\frac{\partial C_i(\mathbf{r},t)}{\partial t} &= \int_0^{E_0} dE' \int \beta_i\Sigma_f(\mathbf{r},E')F(\mathbf{r},E,\mathbf{n},t)\nu_{E'}(\mathbf{r})d\Omega' - \\
&\lambda_i C_i(\mathbf{r},t).
\end{aligned} \tag{1}
$$

Here $F(\mathbf{r},E,\mathbf{n},t)$ — neutron flux, $C_i(\mathbf{r},t)$ — concentration of the i-th energy group delayed neutron precursors, $q(\mathbf{r},E,\mathbf{n},t)$ — external source, λ_i — decay constant of i-th energy group delayed neutrons, β_i — i-th energy group delayed neutron fraction, $\beta=\sum_{i=1}^{6}\beta_i$, $\Sigma_{ais}(\mathbf{r},E)$ — macroscopic loss cross-section, $\Sigma_f(\mathbf{r},E)$ — macroscopic fission cross-section, $\nu_{E'}(\mathbf{r})$ — average number of neutrons produced per fission under the interaction of neutrons with energy E', $\omega(E,E',\mathbf{n}\cdot\mathbf{n}',\mathbf{r})$ — probability of neutrons of state $(E',\mathbf{n}')$ to move to state $(E,\mathbf{n})$ in elastic and inelastic scattering. Functions $\chi(E)$ and $\chi_i(E)$ describe normed delayed and prompt neutrons energy respectively.

Function $F(\mathbf{r},E,\mathbf{n},t)$ and $C_i(\mathbf{r},t)$ satisfy the following initial and boundary conditions

$$
\begin{aligned}
F(\mathbf{r}_b,E,\mathbf{n}_{in},t)=0, \quad C_i(\mathbf{r}_b,t)=0, \\
F(\mathbf{r},E,\mathbf{n},0)=\tilde{F}_0(\mathbf{r},E,\mathbf{n}), \quad C_i(\mathbf{r},0)=c_{i0}(\mathbf{r}).
\end{aligned} \tag{2}
$$

Widespread point kinetics method supposes separation of spatial and temporal variables:

$$F(\mathbf{r},E,\mathbf{n},t)\approx\tilde{F}(\mathbf{r},E,\mathbf{n})\phi(t),$$

where $\tilde{F}(\mathbf{r},E,\mathbf{n})$ is a solution of corresponding stationary equation with boundary condition like Eq. (2).

Point kinetics equations are the following:

$$
\begin{aligned}
\frac{d\phi(t)}{dt} &= \frac{\phi}{l}\left(\frac{k_{\text{eff}}-1}{k_{\text{eff}}}-\beta_{\text{eff}}\right)+\sum_{i=1}^{6}\lambda_i C_{\text{eff}i}(t)+q_{\text{eff}}(t), \\
\frac{dC_{\text{eff}i}(t)}{dt} &= \frac{\beta_{\text{eff}i}\phi(t)}{l}-\lambda_i C_{\text{eff}i}(t),
\end{aligned} \tag{3}
$$

where l — prompt average lifetime, β_{eff} — effective delayed neutron fraction, $C_{\text{eff}i}(t)$ — effective concentration of the i-th group delayed neutron precursors, $q_{\text{eff}}(t)$ — effective external neutron source intensity [9].

* a.golovkina@spbu.ru

ISBN 978-3-95450-181-6

RADIATION FROM OPEN-ENDED FLANGED WAVEGUIDE WITH DIELECTRIC LOADING *

V.V. Vorobev, S.N. Galyamin†, A.A. Grigoreva, A.V. Tyukhtin
St. Petersburg State University, 7/9 Universitetskaya nab., St. Petersburg, 199034 Russia

Abstract

Terahertz radiation is considered as a promising tool for a number of applications. One of the possible ways to emit THz waves is to pass short electron bunch through a waveguide structure loaded with dielectric [1]. Previously we considered the extraction of radiation from the open end of the waveguide with dielectric loading in both approximate and rigorous formulation [2]. We also developed a rigorous approach based on mode-matching technique and modified residue-calculus technique for the case when the waveguide with dielectric is co-axial with infinite waveguide with greater radius [3]. The study presented here is devoted to the case when the waveguide with open end has a flange and enclosed into another waveguide with a greater radius. The case of the flanged waveguide in the unbounded vacuum space can be described as the limiting case of the problem under consideration. We perform analytical calculation (based on mode-matching technique and modified residue-calculus technique) for the case of vacuum waveguide with a flange (dielectric with very high permittivity instead of flange is also considered), direct numerical simulation for this case and compare results. The case of inner waveguide with flange and dielectric filling is investigated numerically.

ANALYTICAL RESULTS

In this report, we consider 3 problems (Fig. 1). In problem (a), a semi-infinite ideally conducting ($\sigma = \infty$) cylindrical waveguide with radius b enclosed into a concentric infinite waveguide with radius $a > b$. Coaxial domain (2) is filled with a homogeneous dielectric ($\varepsilon_0 > 1$). In problem (b), coaxial part is terminated by ideally conducting flange. Problem (c) differs from (b) by filling the inner waveguide with dielectric ($\varepsilon > 1$). All structures are excited by a single TM_{0l} mode propagating from the inner waveguide. Below we present rigorous theory for the problem (a), which can be easily modified for problem (b). Problem (c) is investigated numerically. Incident field in cylindrical frame ρ, ϕ, z is

$$H^{(i)}_{\omega\phi} = J_1(\rho j_{0l}/b)e^{-\gamma^{(1)}_{zl} z}, \quad (1)$$

where $J_0(j_{0l}) = 0$, $\gamma^{(1)}_{zl} = \sqrt{j^2_{0l}b^{-2} - k^2_0}$, $\mathrm{Re}\gamma^{(1)}_{zl} > 0$, $k_0 = \omega/c$. The reflected field in the domain (1) is

$$H^{(1)}_{\omega\phi} = \sum\nolimits_{m=1}^{\infty} B_m J_0(\rho j_{0m}/b)e^{\gamma^{(1)}_{zm} z}. \quad (2)$$

* Work supported by Russian Foundation for Basic Research (grant No. 15-02-03913) and Government of Saint Petersburg.
† s.galyamin@spbu.ru

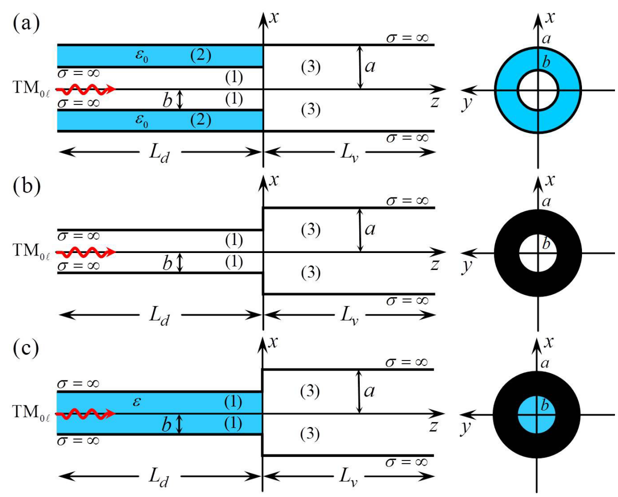

Figure 1: Geometry of the problems.

Fields generated in domains (2) and (3) are:

$$H^{(3)}_{\omega\phi} = \sum\nolimits_{m=1}^{\infty} A_m J_0(\rho j_{0m}/a)e^{-\gamma^{(3)}_{zm} z}, \quad (3)$$

$$H^{(2)}_{\omega\phi} = C_0\rho^{-1}e^{\kappa^{(2)}_{z0} z} + \sum\nolimits_{m=1}^{\infty} C_m Z_m(\rho\chi_m)e^{\kappa^{(2)}_{zm} z}, \quad (4)$$

where $\gamma^{(3)}_{zm} = \sqrt{j^2_{0m}a^{-2} - k^2_0}$, $\kappa^{(2)}_{z0} = -ik_0\sqrt{\varepsilon_0}$, $\kappa^{(2)}_{zm} = \sqrt{\chi^2_m - k^2_0\varepsilon_0}$, $\mathrm{Re}\gamma^{(3)}_{zm} > 0$, $\mathrm{Re}\kappa^{(2)}_{zm} > 0$,

$$Z_m(\xi) = J_1(\xi) - N_1(\xi)J_0(a\chi_m)N_0^{-1}(a\chi_m), \quad (5)$$

χ_m is solution of dispersion relation for domain (2),

$$J_0(b\chi_m)N_0(a\chi_m) - J_0(a\chi_m)N_0(b\chi_m) = 0. \quad (6)$$

Performing matching of $H_{\omega\phi}$ and $E_{\omega\rho} = c(i\omega\varepsilon)^{-1}\partial H_{\omega\phi}/\partial z$ for $z = 0$, and integrating separately over $0 < \rho < b$ and $b < \rho < a$ with eigenfunction of domains (1) and (2) correspondingly, we can obtain the following infinite systems for unknown coefficients:

$$\sum_{m=1}^{\infty}\left(\frac{\tilde{A}_m}{\gamma^{(3)}_{zm} - \gamma^{(2)}_{zn}} + \frac{\tilde{A}_m q_n}{\gamma^{(3)}_{zm} + \gamma^{(2)}_{zn}}\right) = 0, \quad (7)$$

$$\sum_{m=1}^{\infty}\left(\frac{\tilde{A}_m q_n}{\gamma^{(3)}_{zm} - \gamma^{(2)}_{zn}} + \frac{\tilde{A}_m}{\gamma^{(3)}_{zm} + \gamma^{(2)}_{zn}}\right) = \frac{-4\tilde{C}_n\gamma^{(2)}_{zn}\kappa^{(2)}_{zn}}{\kappa^{(2)}_{zn} + \varepsilon_0\gamma^{(1)}_{zn}}, \quad (8)$$

$$\sum_{m=1}^{\infty}\frac{\tilde{A}_m}{\gamma^{(3)}_{zm} - \gamma^{(1)}_{zp}} = -\delta_{lp}bJ_1(j_{0p})\gamma^{(1)}_{zl}, \quad (9)$$

ISBN 978-3-95450-181-6

RADIATION OF A BUNCH FLYING FROM THE OPEN END OF A WAVEGUIDE WITH A DIELECTRIC LOADING*

S.N. Galyamin†, A.V. Tyukhtin, Saint Petersburg State University, St. Petersburg, Russia
A.M. Altmark, S.S. Baturin, Saint Petersburg Electrotechnical University "LETI", St. Petersburg, Russia

Abstract

In this paper we proceed with our investigation of Terahertz emission from beam moving in waveguide structures with dielectric layer [1]. Recently we have considered an open-ended waveguide (with uniform dielectric filling) placed inside regular vacuum waveguide of a larger radius and excited by a single incident waveguide mode [2]. Here we present analytical results for the case where the structure is excited by a moving charge. We also perform simulations using CST® PS code and compare results.

THEORY

Analytical methods for investigation of various waveguide discontinuities have been developed several decades ago [3, 4]. However, the number of problems analysed by rigorous methods is quite limited; as a rule, they belong to the situation where the structure is excited by a specified waveguide mode.

Here we apply the modified residue-calculus technique to investigation of radiation from a charge (or Gaussian bunch) moving along the axis of a semi-infinite cylindrical waveguide with uniform dielectric filling and having an open end. We consider this waveguide to be placed inside coaxial infinite vacuum waveguide. This problem is of interest in the context of development of Terahertz radiation source based on waveguide structures loaded with dielectric and excited by short electron bunch [5].

Geometry of the problem under consideration is shown in Fig. 1. A semi-infinite ideally conducting ($\sigma=\infty$) cylindrical waveguide with radius b filled with a homogeneous dielectric ($\varepsilon>1$) is put into a concentric infinite waveguide with radius $a>b$. A point charge q moves along the axis with constant velocity $\vec{V}=\beta c\vec{e}_z$. Fourier harmonic of the magnetic component of the incident field has the following form (cylindrical frame r,φ,z is used):

$$H_{\omega\varphi}^{(i)}=\frac{iq\tilde{s}}{2c}\left[H_1^{(1)}(r\tilde{s})-\frac{H_0^{(1)}(\tilde{r}\tilde{s})}{J_0(\tilde{r}\tilde{s})}J_1(r\tilde{s})\right]e^{i\omega z/V}, \qquad (1)$$

where $\tilde{r}=b$, $\tilde{s}=s=\sqrt{\omega^2V^{-2}(\varepsilon\beta^2-1)}$ for $z<0$, and $\tilde{r}=a$, $\tilde{s}=s_0=\sqrt{\omega^2V^{-2}(\beta^2-1)}$ for $z>0$ ($\operatorname{Im}\tilde{s}>0$). The reflected field in the domain (1) is

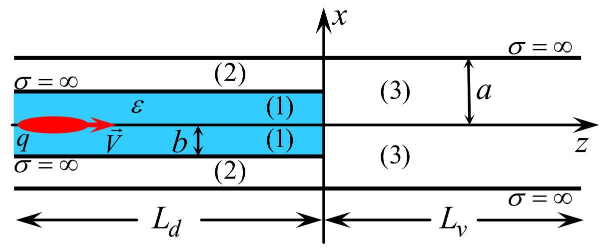

Figure 1: Geometry of the problem.

$$H_{\omega\varphi}^{(1)}=\sum\nolimits_{m=1}^{\infty}B_mJ_0(rj_{0m}/b)e^{\kappa_{zm}^{(1)}z}, \qquad (2)$$

where $J_0(j_{0m})=0$, $\kappa_{zm}^{(1)}=\sqrt{j_{0m}^2b^{-2}-k_0^2\varepsilon}$, $\operatorname{Re}\kappa_{zm}^{(1)}>0$, $k_0=\omega/c$. The fields generated in domains (2) and (3) can be presented by the following series:

$$H_{\omega\varphi}^{(3)}=\sum\nolimits_{m=1}^{\infty}A_mJ_0(rj_{0m}/a)e^{-\gamma_{zm}^{(3)}z}, \qquad (3)$$

$$H_{\omega\varphi}^{(2)}=C_0r^{-1}e^{\gamma_{z0}^{(2)}z}+\sum\nolimits_{m=1}^{\infty}C_mZ_m(r\chi_m)e^{\gamma_{zm}^{(2)}z}, \qquad (4)$$

where $\gamma_{zm}^{(3)}=\sqrt{j_{0m}^2a^{-2}-k_0^2}$, $\gamma_{z0}^{(2)}=-ik_0$, $\gamma_{zm}^{(2)}=\sqrt{\chi_m^2-k_0^2}$, $\operatorname{Re}\gamma_{zm}^{(2,3)}>0$,

$$Z_m(\xi)=J_1(\xi)-N_1(\xi)J_0(a\chi_m)N_0^{-1}(a\chi_m), \qquad (5)$$

χ_m is the solution of the dispersion relation for the domain (2),

$$J_0(b\chi_m)N_0(a\chi_m)-J_0(a\chi_m)N_0(b\chi_m)=0. \qquad (6)$$

Performing the matching of the components $H_{\omega\varphi}$ and $E_{\omega r}=c(i\omega\varepsilon)^{-1}\partial H_{\omega\varphi}/\partial z$ for $z=0$, and integrating these relations separately over $0<r<b$ with $J_0(rj_{0m}/a)$ and over $b<r<a$ with $Z_m(r\chi_m)$, after cumbersome calculations we obtain the following infinite systems for unknown coefficients:

$$\sum_{m=1}^{\infty}\left(\frac{\tilde{A}_m}{\gamma_{zm}^{(3)}-\gamma_{zp}^{(1)}}+\frac{\tilde{A}_m\rho_p}{\gamma_{zm}^{(3)}+\gamma_{zp}^{(1)}}\right)+\frac{q}{4j_{0p}cJ_1(j_{0p})}\times$$
$$\times\left[\left(\pi bs_0^2J_1(j_{0p})h_0-2ij_{0p}b^{-1}\right)\left(F_{vp}^-+\rho_pF_{vp}^+\right)+\right. \qquad (7)$$
$$\left.+F_{dp}^++\rho_pF_{dp}^-\right]=0,$$

*Work supported by the Grant of the President of Russian Federation (No. 6765.2015.2) and the Grants from Russian Foundation for Basic Research (No. 15-32-20985).
† s.galyamin@spbu.ru

ISBN 978-3-95450-181-6

CHARGED BEAMS OPTICAL PROPERTIES OF SCATTERING MEDIA

V.G.Kurakin, P.V.Kurakin, Lebedev Physical Istitute, Moscow, Russia

Abstract

Distribution function for scattering angle and transverse displacement is used to derive the phase-plane portrait transformation in scattering medium for incoming charged particle beam. The phase-plane portrait of scattered beam depends strongly on incoming beam ellipse proportions and orientation, and simple matching conditions and expression has been derived. It is shown as well that in heterogeneous medium incident beam experiences trajectory refraction and reflection at the out coming medium border. Reflection criterion had been derived. This feature of scattering media may be used for beam control in accelerator based application.

INTRODUCTION

Metallic foil and dielectric films on charged particle beam path are quit natural elements of accelerators, storage rings and beam lines. These used for example for vacuum volumes separation, may serve as beam targets for various functions, as extraction window. Together with desired functionality, beam emittance growth is usually undesired consequent of beam-target interaction. For some application detail beam characteristic after its interaction with target are quit necessary. For example, this is true in the case when extracted beam is directed to experiment area and has to be matched with beam line optics. Another example is a target in tagged photons experiment in ecologically clean energy recovery accelerator [1]. Here electrons directed to accelerator after target and precise tuning of scattered beam is necessary to avoid particle losses. Charge exchanged injection into ion accelerator or storage ring is accompanied by multiple interaction of stored bunches with stripping target and bunch phase portrait evolution is desired for adequate storage process description.

Multiple Coulomb scattering of moving charges is the main process in media that results in emittance growth. We use classical distribution function for charged particle being scattered in media to explore particle dynamics, phase space concept being used. The concept of beam matching with scattering media is introduced and formula for beam emittance growth for matched beam has been derived. Distribution function for scattering in homogeneous infinite media is used to explore off normal incidence of a charge on a scattering plate. Formula connecting critical angle and media and particle parameters for the reflection phenomena is derived.

PHASE PORTRAIT OF SCATTERED BEAM

Let us imaging needle-shaped charged particle beam that moves in x direction and traverses a plate (target) from homogeneous material, placed perpendicular to x axis. Beam particles interact with target nuclei and change there impulses. We neglect energy lost and concentrating ourselves on transverse motion. One may consider particle motion the same for any transverse coordinate for homogeneous infinite scattering media. In such assumptions a probability to find a charge at depth x with any transverse coordinate y moving at angle θ relative direction of motion of incident needle-shaped beam in plane (x,y) is described by the formula [2,3]

$$P(x,y,\theta)dyd\theta = \frac{2\sqrt{3}}{\pi}\frac{1}{\Theta_s^2 x^2}\exp\left[-\frac{4}{\Theta_s^2 x}\left(\theta^2 - \frac{3y\theta}{x} + \frac{3y^2}{x^2}\right)\right]dyd\theta \quad (1)$$

Here Θ_s is physical quantity integrating scattering media and moving charge properties:

$$\Theta_s^2 = \left(\frac{E_s}{\beta cp}\right)^2 \frac{1}{X_0}, \quad (2)$$

where β, p, c are relative particle velocity $\beta = v/c$, particle impulse and light velocity respectively, v is particle velocity, X_0 - radiation length, E_0 is the constant with energy dimension:

$$E_s = \left(\frac{4\pi}{\alpha}\right)^{1/2} m_e c^2 = 21 \text{ MeV} \quad (3)$$

Here $\alpha = e^2/\hbar c = 1/137$ - is fine structure constant, e, m_e are electron charge and its mass respectively, $\hbar$ is Planck constant.

According to relation (1) scattered beam is described by Gaussian low in coordinate system $y/x;\theta$. The lines of equal probabilities are similar ellipses tilted at angle $\approx 1.08 \cong 62$ degrees to axis $\eta = y/x$. The tilted ellipse reflects those evident fact that transverse displacement of scattered particle and its direction of motion are not statistically independent. The relative number of particles enveloped by ellipse

$$3\eta^2 - 3\eta\theta + \theta^2 = F = const \quad (4)$$

depends on F value. Its average value is

$$\langle F\rangle = \frac{2\sqrt{3}}{\pi}\frac{1}{\Theta_s^2 x}\int \begin{matrix}(3\eta^2 - 3\eta\theta + \theta^2)\times \\ \exp\left[-\frac{4}{\Theta_s^2 x}(3\eta^2 - 3\eta\theta + \theta^2)\right]\end{matrix} d\eta d\theta = \frac{1}{4}\Theta_s^2 x \quad (5)$$

Let us call the ellipse of equal probability (4) with $F = \langle F\rangle$ by “elementary scattering ellipse” while the area ε_s enveloped by this ellipse by “elementary scattering emittance”. Taking into account that ellipse area described by equation (4) (emittance normalized by target thickness) is equal to $S = 2\pi F/\sqrt{3}$ we arrive at relation

$$\varepsilon_s = \frac{\pi}{2\sqrt{3}}\Theta_s^2 x^2 \quad (6)$$

One has to keep in mind that the emittance defined over average value encloses definite part of scattered particle

ISBN 978-3-95450-181-6

DESIGN STUDY OF THE PROTON LINAC FOR RADIOPHARMACEUTICALS PRODUCTION

G. Kropachev, A. Balabin, D. Seleznev, and A. Sitnikov, T. Kulevoy, ITEP, Moscow, Russia

Abstract

The 8 MeV 200 MHz linac for acceleration of quasi cw 0.2 mA proton beam is under development at ITEP. The linac is designed for radiopharmaceuticals production which will be used in the Positron-Emission Tomography. The linac includes RFQ and DTL sections with 6D-beam matching between them. The DTL section has modular structure and consists of separated individually phased IH-cavities with beam focusing by permanent magnet quadrupoles located between the cavities. This DTL structure provides linac compactness and enables its tuning and commissioning cavity by cavity. Results of beam dynamic simulation and electrodynamics characteristics of linac cavities are presented.

INTRODUCTION

The 8 MeV 200 MHz linac for acceleration of 20 mA/pulse (0.2 mA average current at duty cycle 1%) proton beam is under development at ITEP. The linac is designed for radiopharmaceuticals production which will be used in the Positron-Emission Tomography. Such beam parameters provides generation of ^{18}F production and they should be obtained without activation of linac materials.

The linac consists of RFQ and DTL with 6D-beam matching between them. We proposed the modular DTL structure consisting of a number of separate individually phased accelerating cavities with beam focusing by permanent magnet quadrupoles (PMQs) located between them. The cavities are placed in the separate vacuum tanks with the identical length. PMQs can have the modular construction with constant gradient which greatly simplifies the manufacturing [9]. The linac basic parameters are shown in Table 1.

Table 1: The Linac Basic Parameters

Ions	H^+
Operating frequency	200 MHz
Beam energy	0.07÷8 MeV
Injection current	20 mA
Normalized beam emittance	0.2 π cm mrad
Normalized acceptance	0.5 π cm mrad
Transmission	> 90 %
Pulse power losses	< 1 MW
Maximum field strength	1.8 Kp
Length	~5 m

We proposed to use duoplasmatron as ion source for the linac. This ion source can provide the required beam current of 20 mA with normalized emittance lower than 0.2 π cm mrad (see Table 1).

The operating frequency equal to 200 MHz is determined by following factors:

- required acceptance (which should be higher than the beam emittance at least in 2.5 times [1]);
- accelerator compactness (the linac has to be located both in standard hospital office and in the transport unit [8]
- soft requirements to the RF structure manufacturing and adjustment.

The maximum strength of the electric field on the surface is limited by E_{smax} = 1.8* Kp = 270 kV/cm, where Kp is the Kilpatrick limit.

LINAC MAIN PARAMETRS

The layout of the medical linac and some of its parameters are given in Fig. 1. Below these parameters will be discussed.

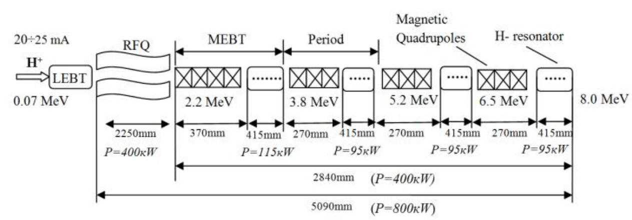

Figure 1: Layout of the medical linac.

RFQ Parameters

The RFQ consists of the matching, bunching, and regular acceleration sections. The 6D-beam matching is realized in the initial matching section. The adiabatic beam bunching is carrying out at quasi-stationary bunch mode [1]. In the regular acceleration section the protons are accelerated at constant synchronous phase of -35 degrees which achieved at intervane voltage of 147.5 kV.

To choose the injection voltage U_{inj} the following features should be taking into account. From one side to decrease the bunching section length U_{inj} should be decreased. From other side, increase of U_{inj} simplifies the vane manufacturing. The increase U_{inj} also reduces the space charge effects in the LEBT. Taking into account all these features the injection voltage U_{inj} was chosen equal to 70 kV (Fig. 1). The main RFQ parameters are presented in Table 2.

Transverse matching of continuous beam from the duoplasmatron with RFQ is realized in LEBT (Fig. 1) by two electrostatic einzel lenses with voltage ≤ 50 kV.

ISBN 978-3-95450-181-6

HIGH-CURRENT PULSING DEUTERON ACCELERATOR WITH ENERGY OF 500 KeV

K.I. Kozlovskij, E.D. Vovchenko, A.A. Isaev, M.I. Lisovskij, A.E. Shikanov, National Research Nuclear University "MEPhI" (Moscow Engineering Physics Institute), Moscow, Russia

Abstract

In this work it is reported about development of compact prototype of fast ions and deuterons accelerator with next parameters: energy is up to 400 keV, electric current is more than 1 kA and current density is more than 20 A/sm^2 in pulses with duration up to 0,5 µs and repetition frequency is equal to 1 Hz. Method of electron magnetic insulation in accelerating gap was applied and optimized in the accelerator; intensive laser-plasma ion source was used.

INTRODUCTION

Researches in the area of magnetic insulation applied to compact diode systems for neutrons generation initially are introduced in the work [1]. Two possible schemes of electronic conductivity dampening exist. In the first case, the field of constant magnets with azimuthal symmetry is used [2,3]. In the second case pulsing helix magnetic field is applied [2,4]. However, it is experimentally established, that electronic conductivity dampening by the field of constant magnets [3] has a series of significant shortcomings. These shortcomings are connected with complex configuration of magnetic field and its inhomogeneity.

It was established by authors, that similar shortcomings to a lesser extent appears in diodes with pulsing magnetic insulation. In this work results of experimental investigation of similar diodes were set out.

EXPERIMENT

For the plasma production, YAG laser, activated by neodymium, generating pulses of infrared rays in modular Q mode with wave length of 1.06 µm, energy ≤ 0.85 J and duration is about 10 ns. was used.

Magnetic field in the diode configured with the help of helix, which forming surface had a frustaconical shape. Critical distinction between this experiment and experiment, conducted earlier is in the use of more powerful laser, high-stable PVG with characteristics, mentioned above and original scheme of start on the basis of laser controllable arrester (LCA).

An important aspect is the use of high-voltage pulse generator according to the scheme of Arkadyev-Marx, generating at idling conditions with amplitude of 400 kV and first half wave duration of 1 µs, in which original scheme of its start, based on LCA, is applied.

A laser target in the form of a tablet made of TiD was placed on the anode. Deuterons are extracted from the laser plasma in an electric field formed by a positive high-voltage pulse on the anode.

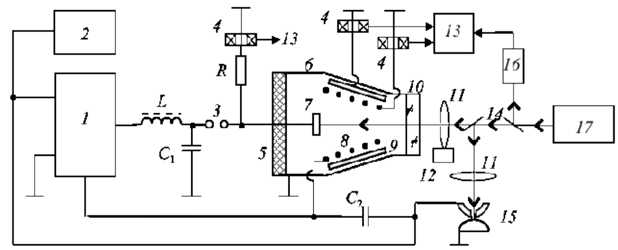

Figure 1: Scheme of experiment “Formation of deuteron flux”: 1 – PVG (2–30 cascades); 2 – PVG charging unit; 3 – arrester-peaker; 4 – Rogowski coils; 5 – insulator; 6 – vacuum chamber; 7 – plasma forming target; 8 – helix; 9 – ion collector (cathode); 10 – optical window; 11 – focusing lens; 12 – scanning device; 13 – oscillograph; 14 – partially transparent mirror; 15 – LCA; 16 – Photoelectronic coaxial converter PCC; 17 – laser.

We applied a pulsed magnetic isolation for suppression of parasitic electron current due to secondary electron emission at the cathode. Conical spiral is placed in the diode gap in front of the cathode, which also had a conical shape (Fig. 1). In addition, conical surface of the cathode and conical spiral are parallel. Diode system placed in a vacuum chamber pumped to a pressure of 10^{-2} Pa.

A laser plasma emission is accompanied by its expansion in the radial direction. The flow of deuterons reaches the conical spiral with a delay $\tau_P \approx 250 - 300$ ns.

Estimation of the efficiency of generating the magnetic field showed that current in the conical spiral achieved 60% from its maximum value after 300 ns from the beginning of the expansion of a laser plasma (i.e. when the flow of deuterons reaches the conical spiral).

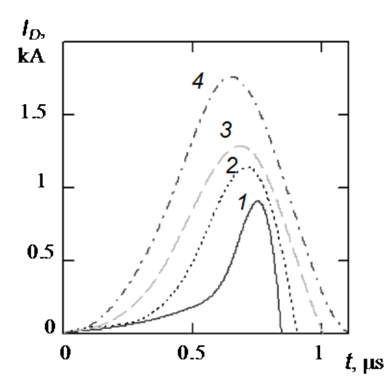

Figure 2: Diode current $I_D(t)$ at laser energies: *1* – 80 mJ, *2* – 200 mJ, *3* – 380 mJ, *4* – 750 mJ.

ISBN 978-3-95450-181-6

BEAM INJECTOR FOR VACUUM INSULATED TANDEM ACCELERATOR*

A. Kuznetsov#, A. Gmyrya†, A. Ivanov, A. Koshkarev‡, A. Sanin, D. Kasatov, K. Blokhina†,
BINP SB RAS, Novosibirsk, Russia

Abstract

The Vacuum Insulated Tandem Accelerator (VITA) is built at the Budker Institute of Nuclear Physics. The accelerator is designed for development of the concept of accelerator-based boron neutron capture therapy of malignant tumours in a clinic [1]. In the accelerator the negative hydrogen ions are accelerated by the high voltage electrode potential to the half of required energy, and after conversion of the ions into protons by means of a gas stripping target the protons are accelerated again by the same potential to the full beam energy. The epithermal neutrons generation reaction is $^7Li(p,n)^7Be$, and the estimated proton current for minimal therapeutic neutron flux should be higher than 3 mA @ 2.5 MeV energy [2] meanwhile about 10 mA required for comfortable BNCT treatment. During the facility development, the proton beam was obtained with 5 mA current and 2 MeV energy [3]. To ensure the beam parameters and reliability of the facility operation required for clinical applications, the new injector was designed based on the ion source with a current up to 15 mA [4], providing the possibility of preliminary beam acceleration up to 120-200 keV. The paper presents the status of the injector construction and testing.

INTRODUCTION

The VITA facility design is shown at Fig. 1. The first stage of acceleration – acceleration of ions – takes place in the area between the entrance volume of the accelerator and the high voltage electrode and the second stage – acceleration of protons – between the high voltage electrode and the beginning of high energy beam line. The gas stripping target is located inside the high voltage electrode and inflates up to 0.23 l×Torr/s into the accelerator volume to provide up to 99% conversion of ions into protons. Several innovative ideas were realized in the accelerator design to allow stable acceleration of intense beam in a compact facility.

The initial ion beam is produced by the injector composed of the ion source, low energy beam line and magnetic elements providing focusing and correction of the beam. Series of investigations have revealed the limitations of injecting current. The main problems are the ions loss due to high residual gas concentration and the ability of the stripping gas to rich the injector and corrupt the stability of the ion source [4]. To provide a reliable H- beam for clinical application of the facility the new injector is designed.

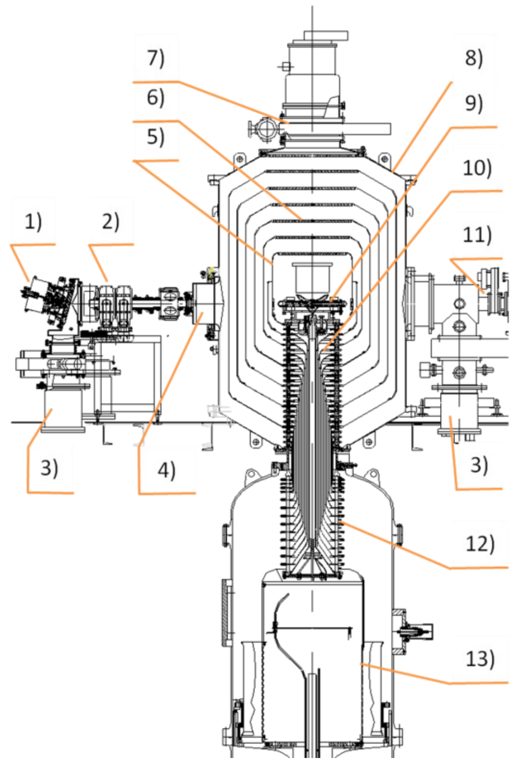

Figure 1. Scheme of the VITA facility: 1 – H ion source; 2 – low energy beam line; 3 - turbomolecular pump; 4 – entrance volume of the accelerator; 5 – high voltage electrode; 6 – electrode shutters; 7 – cryo pump; 8 – accelerator vacuum volume; 9 – stripping target; 10 – feedthrough insulator (vacuum part); 11 – high energy beam line; 12 – feedthrough insulator (gas part); 13– high voltage source.

INJECTOR DESIGN

The new injector proposed for the VITA facility [5] is under construction at BINP. The final design scheme of the injector is presented at Fig. 2. The surface-plasma ion source with Penning discharge and with hollow cathode (1) is used to generate the 15 mA H^- beam with energy up to 32 keV. The generated beam is bent by the magnet (4) and directed into the pre-accelerating tube. The usage of this magnet allows solving several tasks: splitting the beam from the gas and caesium flux, additional beam focusing to ensure axially symmetric parallel beam with round profile in the output, protect the ion source from the back streaming particles from the accelerator channel. The diaphragm with the beam diagnostics is located between the magnet and the accelerator tube. Measuring

* Applied research is carrying out with the financial support of the Russian Federation represented by the Ministry of Education and Science of Russia (unique identifier RFMEFI60414X0066)
#A.S.Kuznetsov@inp.nsk.su
† Second affiliation: NSTU, Novosibirsk, Russia
‡ Second affiliation: NSU, Novosibirsk, Russia

ISBN 978-3-95450-181-6

HIGH SPEED CRYOGENIC MONODISPERSE TARGETS FOR HIGH INTENSITY CYCLIC AND LINEAR ACCELERATORS

A.Boukharov, E.Vishnevkii, NRU MPEI, Moscow, Russia

Abstract

The basic possibility of creation of high speed cryogenic monodisperse targets is shown. According to calculations at input of thin liquid cryogenic jets with a velocity of bigger 100 m/s in vacuum the jets don't manage to freeze at distance to 1 mm and can be broken into monodisperse drops. Drops due to evaporation are cooled and become granules. High speed cryogenic monodisperse targets have the following advantages: direct input in vacuum (there is no need for a chamber of a triple point chamber and sluices), it is possible to use the equipment of a cluster target, it is possible to receive targets with a diameter of $D < 20$ µk from various cryogenic liquids (H_2, D_2, N_2, Ar) with dispersion less than 1%, the high velocity of monodisperse granules(> 100m/s), exact synchronization of the target hitting moment in a beam with the moment of sensors turning on

Development of accelerating technique made possible receiving the high-energy beams of elementary particles. Interaction between such beams and cryogenic monodisperse targets will allow to solve fundamental problems of nuclear physics.

The cryogenic monodisperse target is the most perspective target for future experiment of "PANDA" [1-3]. "PANDA" is a unique experiment within the project of the new European accelerator FAIR in Darmstadt (Germany). The physical program of the experiment is research of fundamental problems of nuclear physics, finding of new extremal matter forms.

Cryogenic monodisperse targets have the following unique properties:

1. The small size of monodisperse targets – diameter is from 20 micron to 100 microns. Targets can be received from hydrogen or its isotopes, nitrogen, argon, neon, krypton and xenon.
2. High luminosity of targets and a possibility of registration of particles dispersion at angle of 4π.
3. Renewability – targets pass through a beam during small time.

Cryogenic monodisperse targets represent the flow of solid monodisperse granules of the small sizes received from liquefied gas. The liquid cryogenic jet follows from the generator of monodisperse drops in the vacuum chamber. Under the influence of special perturbation the jet breaks up to drops .Because pressure in the vacuum chamber is smaller than pressure about drops surface, there is intensive evaporation of liquid. As a result drops are cooled, freeze and become solid granules. Passing through system of sluices the granules accelerate and come to the working camera where there is an interaction to an accelerating beam or laser ray. For reduction of leaking and increase of granules speed it is possible to use two and more vacuum chambers divided by sluices. After interaction with high-energy beam the granules get to the cooled trap and deposit on its walls.

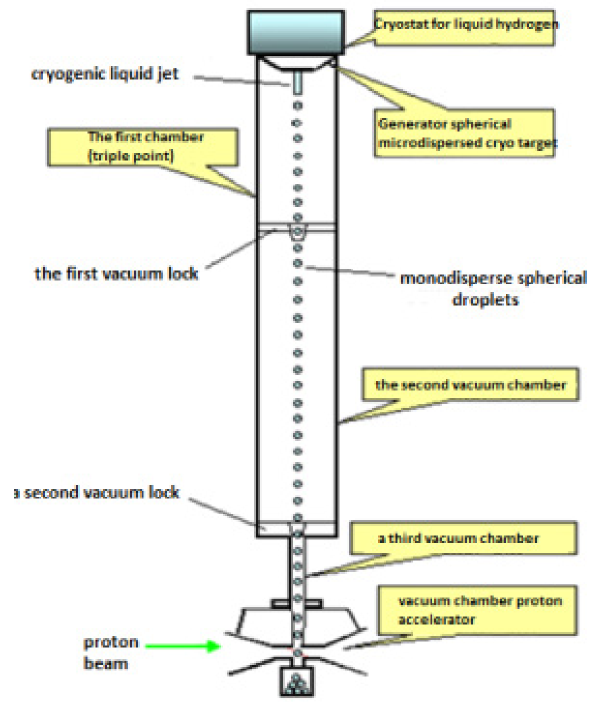

Figure 1: The detailed description cryogenic corpuscular targets.

The detailed description of the operation of installations on receiving cryogenic corpuscular targets is provided in [4-5] and fig. 1.

The important effect on stability of targets flow have sluices and especially the first sluice connecting the triple point camera to other vacuum chambers. If to remove the first sluice, not to allow to a liquid cryogenic jet to freeze and directly to send drops to the second vacuum chamber, then it is possible to simplify construction of installation and to reduce its sizes.

Operation purpose: to prove the possibility of application without sluice method of receiving monodisperse cryogenic targets.

For realization of purpose the model of the expiration of a jet to the low pressure area was created in the software PHOENICS and distribution of temperature to jet surfaces is investigated by the numerical method.

ISBN 978-3-95450-181-6

THE MULTIPOLE LENS MATHEMATICAL MODELING

E.M. Vinogradova*, A.V. Starikova,
Saint Petersburg State University,
7/9 Universitetskaya nab., St. Petersburg, 199034 Russia

Abstract

In the present work the mathematical model of the multipole system is presented. The multipole system is composed of arbitrary even number of the uniform electrodes. Each of the electrodes is a part of the plane. The potentials of the electrodes are the same modulus and opposite sign for neighboring electrodes. The variable separation method is used to solve the electrostatic problem. The potential distribution is represented as the eigen functions expansions. The boundary conditions and the normal derivative continuity conditions lead to the linear algebraic equations system relative to the series coefficients.

INTRODUCTION

Electrostatic multipole systems are widely used in the accelerator technology for the charged particle beams transport [1]– [3]. In this paper the mathematical modeling of the electrostatic multipole system is presented. The multipole system consist of the even number uniform plate electrodes of the same shape and size. Fig. 1 shows a schematic representation of the multipole system. The similar system was investigated in [4]. A quadrature expression was obtained for the field potential and the constraints imposed on the electrode potentials, under which such a solution is possible, were determined. In our work a system with an arbitrary even number $2N$ of electrodes is modeled. The variable separation method [5]– [7] is used in plane polar coordinates (r, α) to solve the boundary-value problem for the Laplace equation [8].

The multipole potential distribution has the planes of symmetry $\alpha = (\pi k)/N$ and planes of antisymmetry $\alpha = \pi/(2N) + (\pi k)/N$, $k = \overline{0, N-1}$. An additional plane $r = R_2$ can be introduce to limit the area of the problem under consideration without loss of generality. Thus it suffices to consider sector $0 \le \alpha \le \pi/2N$, $0 \le r \le R_2$ to find the electrostatic field. Schematic diagram of the multipole system sector is presented on Fig. 2 ($\alpha_1 = \pi/2N$).

The problem parameters are:

$(R_1, 0)$ — the coordinate position of the multipole electrode's edge,

R_2 — the radius of the area,

$\alpha_1 = \pi/2N$ — the boundary of the area (the plane of antisymmetry),

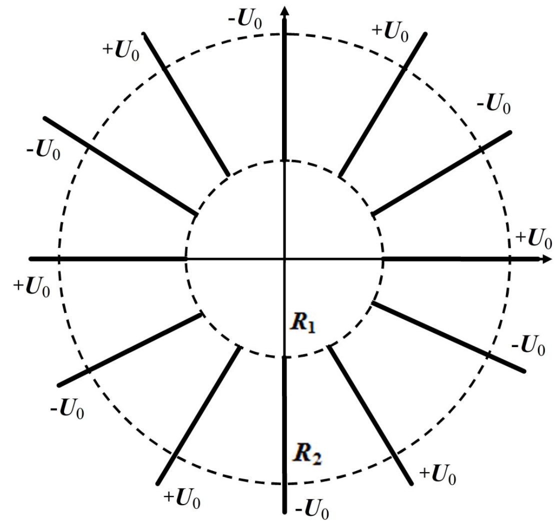

Figure 1: Schematic representation of the multipole system.

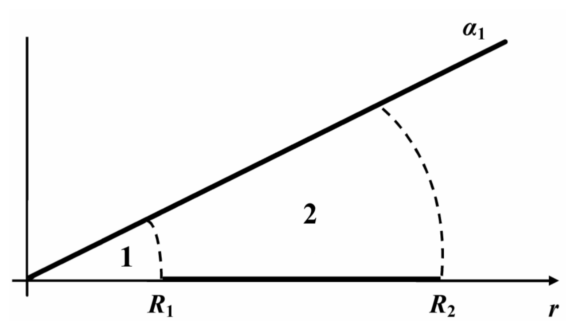

Figure 2: Schematic representation of the multipole system sector.

U_0 — the multipole electrode potential ($\alpha = 0$, $R_1 \le r \le R_2$).

MATHEMATICAL MODEL

The electrostatic potential distribution $U(r, \alpha)$ in the area $(0 \le r \le R_2, 0 \le \alpha \le \alpha_1)$ satisfies the Laplace equation and the boundary conditions

* e.m.vinogradova@spbu.ru

ISBN 978-3-95450-181-6

USE OF STRUCTURAL-VARIATIONAL METHOD OF R-FUNCTIONS IN MATHEMATICAL MODELING OF MAGNETIC SYSTEMS

O.I. Zaverukha, M.V. Sidorov
Kharkiv National University of Radioelectronics, Ukraine

Abstract

Magnetic systems are widespread in nature and technics. It is atoms in crystal grid of ferromagnetic, magnets of accelerating installations, space satellites stabilization systems etc. Due to high cost of full-scale study of such systems during last decades mathematical modeling and numerical analysis with computer started to come to the fore. The methods of finite differences, finite element, boundary integral elements and others are mainly used for the numerical analysis of the magnetic systems. Each of mentioned methods has its own advantages and disadvantages [1]. The main shortcoming of all listed methods is necessity in generation and adjustment new computational grid according to characteristics of each area. The structural-variational method of R-functions [5,6,8], proposed by Rvachev V.L., academician of National Academy of Sciences of Ukraine, is an alternative to all existing methods of numerical calculation of magnetic particles. In the context of solving mathematical physical problems the *R*-function method allows to create the structures for solving the boundary value problems – the bundles of functions that exactly meet the boundary conditions of the problem. With this approach the geometry of the area is accurately taken into account. So, the development of existing methods of numerical analysis of magnetic systems with *R*-function methods is the scientific problem of current interest.

PROBLEM DEFINITION

Consider a magnetic system (figure 1), consisting of ferromagnetic Ω_f and vacuum Ω_v with closed current windings Ω_c. Magnetostatic problem is stated – find the magnetic field distribution, that created by steady currents and magnetization of isotropic ferromagnetics [2,3]. Let's assume that lengthwise cut is substantially larger than the transverse. Then vector potential of magnetic induction vector will have only one nonzero coordinate $u = u(x, y)$ and we can proceed from Maxwell's system of equations for stationary magnetic field to scalar equation

$$\frac{\partial}{\partial x}\left(\frac{1}{\mu}\frac{\partial u}{\partial x}\right)+\frac{\partial}{\partial y}\left(\frac{1}{\mu}\frac{\partial u}{\partial y}\right)=-\mu_0 J_z(x, y)\,,\ (x, y)\in\mathbb{R}^2. \quad (1)$$

Here μ is function of the permeability of a ferromagnetic, which is known in Ω_f nonlinear function from magnetic field intensity vector (for nonmagnetic environment $\mu = 1$), μ_0 is vacuum magnetic permeability, $J_z(x, y)$ is z component of volumetric current density vector, that is different from 0 only in Ω_c and satisfies the equation $\iint_{\Omega_c} J_z(x, y)dxdy = 0$,

$$u(x, y) = \begin{cases} u_f(x, y), & (x, y)\in\Omega_f\,, \\ u_v(x, y), & (x, y)\in\Omega_v\,. \end{cases}$$

Equation (1) should be supplemented with conjugation conditions at the border $\partial\Omega_{fv}$ that separates ferromagnetic and vacuum

$$u_f\big|_{\partial\Omega_{fv}} = u_v\big|_{\partial\Omega_{fv}}\,,\quad \frac{1}{\mu}\frac{\partial u_f}{\partial \mathbf{n}}\bigg|_{\partial\Omega_{fv}} = \frac{\partial u_v}{\partial \mathbf{n}}\bigg|_{\partial\Omega_{fv}}\,, \quad (2)$$

where $\mathbf{n}$ is the unit vector normal to $\partial\Omega_{fv}$, and with conditions on infinity:

$$\lim_{x^2+y^2\to+\infty} u = 0\,. \quad (3)$$

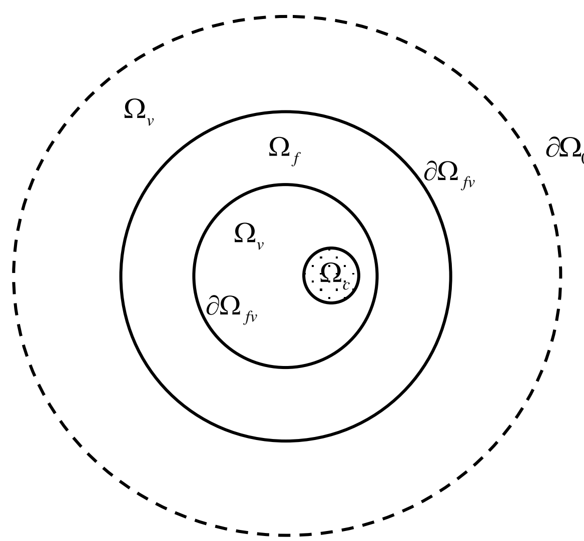

Figure 1: Magnetic system.

BUILDING OF SOLVING STRUCTURE

Let's replace condition on infinity (3) with other condition

ISBN 978-3-95450-181-6

THE DESIGN OF PERMANENT MAGNET SPREAD SYSTEM FOR 0.5 MeV IRRADIATION ACCELERATOR

J. Huang†, M.W. Fan, L.G. Zhang, C. Zuo, Y.Q. Xiong, T.Q. Yu, J. Yang, K.J. Fan, W. Qi,
School of Electrical and Electronic Engineering, Huazhong University of Science and Technology, Wuhan,430074, P. R. China

Abstract

The traditional electron beam scanning magnet has many disadvantages, for example, the regulatory of excitation current is very complex and the irradiation uniformity as well as the irradiation area is very difficult to improve and expand. Thus, the author of the paper proposes an innovative technology of a permanent magnet spread system for 0.5MeV irradiation accelerator which uses a special configuration of the magnetic field to spread electron beam bunch directly and would remarkably improve the spread uniformity, simplify the accelerator and would be helpful to protect the titanium window and expand the irradiation area. Also, the technology could as well be used on the electron beam irradiation of those irregular structured objects of large size.

INTRODUCTION

Irradiation processing has been widely applied in industries of manufacture, agriculture, bio-medicine and environmental protection because of its energy saving and environmentally friendly advantages [1, 2]. An electron irradiation accelerator, with its benefits of controllable energy, operational efficiency, no radioactive pollution source, and no energy consumption when the machine is cut off, etc, has been widely adapted in the irradiation processing industry [3, 4].

A high voltage electron accelerator mainly consists of an electron gun and an accelerator tube that is followed by a scanning magnet system, which usually uses a dipole electromagnet with a saw tooth wave energy supply [5], as shown in Fig. 1. When the electron beam passes through this system, the dipole electromagnet scans the beam in the transversal direction like the row scanning of a TV set [6].

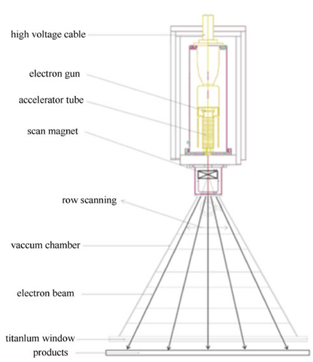

Figure 1: High voltage electron accelerator with a beam scanning device**.**

However, its shortcomings are as follows:

1. When the electron beam moves along a linear line, it tends to become overheated in some areas and burn the titanium film [7].
2. It also causes "Tail sweep" phenomenon and uneven irradiation.
3. The excessive use of electricity is liable to lead malfunction in the power system [8].
4. the speed of the conveyer belt has negative effects on the even distribution of irradiation.

The lab's invention to directly spread the electron beam with multi-pole magnetic field of specially constructed permanent magnets has perfectly addressed the inherent shortcomings of the conventional electromagnet scanning method.

THEORETICAL PRINCIPLE

Considering the relativistic effect, an electron's mass is decided by Eq. (1).

$$m = \frac{m_0}{\sqrt{1-\beta^2}} = m_0\gamma \tag{1}$$

According to the charged particle dynamics,

$$\frac{d(m\vec{V})}{dt} = e\vec{B} \times \vec{V} \tag{2}$$

Where B refers to the density of magnetic induction, e refers to the electron charge and, V refers to the electron velocity. If a Cartesian coordinate is used, Eq. (2) will be written as

$$\begin{cases} d(mv_x)/dt = qv_yB_z - qv_zB_y \\ d(mv_y)/dt = qv_zB_x - qv_xB_z \\ d(mv_z)/dt = qv_xB_y - qv_yB_x \end{cases} \tag{3}$$

In Eq. (3), the subscript refers to x, y and z components. By applying four order Ruge-Kutta's numerical integration, the equation can be solved numerically.

The deflecting distance S of electrons will be calculated by Eq. (4),

$$\begin{aligned} \vec{F} &= m\vec{a} \\ S &= \int_{t1}^{t2} atdt \\ t &= \frac{L}{V_z} \end{aligned} \tag{4}$$

In this equation, a is the acceleration of electron, L the height of scanning box, and V the velocity along the z-axis direction. The velocity changes in a limited region, which means the distance of the electron deflection is limited in a small region. This theoretically justifies that a permanent magnet combination may satisfy the requirements of different energies. To prove the com-

ISBN 978-3-95450-181-6

MEASURING SYSTEM FOR FLNR CYCLOTRONS MAGNETIC FIELD FORMATION

I.A. Ivanenko, G.N. Ivanov, V.V. Aleinikov, V.V. Konstantinov, FLNR, JINR, Dubna, 141980, Russia

Abstract

Since beginning of millennium, three new heavy-ion isochronous cyclotrons, DC72, DC60 and DC110, were created in FLNR, JINR. At the present time the activities on creation of the new cyclotron DC280 for Super Heavy Facility are carried out. The one of the main problem of cyclotron creation is a formation of the isochronous magnetic field. The FLNR measuring system bases on Hall probes and provide the measuring accuracy 10^{-4}. The paper presents the features, measuring and exploitation results of FLNR cyclotrons magnetic field formation.

INTRODUCTION

During the last twenty years the series of magnetic field measurements for FLNR new and operated cyclotrons were carried out. The purpose of these measurements were the increasing of the efficiency of operated cyclotrons U400, MC400 and IC100 and magnetic field formation for new cyclotrons DC72, DC60 and DC110 [1, 2]. This experience formed a general approach to mapping system creation and measurement philosophy. The common feature is a measuring in a polar coordinate system with the several, 8 or 14, Hall probes. The probes number depends on the cyclotron pole radius and extremely decreases the measuring time. The another feature is a usage of a toothed belt around the pole for azimuthal moving. For radial and azimuthal stepping motion of the magnetometer bar the pneumatic engines are used. Because presented cyclotrons have different parameters of the magnetic structures, such as pole diameter, sectors and pole gaps, the magnetometer bar is created separately for each cyclotron. The magnetometer electronics and pneumatic system of bar stepping motion are unificated and stay the same with minimal changing.

MECHANICAL SYSTEM

For magnetic field measurements at FLNR cyclotrons the polar coordinate mapping system was chosen. The mechanical part of magnetometers consists of the bar for radial motion of Hall probes and the system of bar azimuthal motion. Hall probes are placed at the plank that is moved radially along bar with a step 10mm. The usage of several probes decreases the number of radial steps of the plank and, as a result, a time of mapping. At the table 1 the number of probes - Nh, number of plank steps - Ns, the radiuses of mapping Rb and pole Rpole for FLNR new cyclotrons are presented. To control the coherence of the measuring data between the probes, the additional radial step is used. Then the total plank steps equal Ns+1. At the additional step the previous probe at its last position stands at the first position of the next probe. As a rule this difference is very small, some gausses, and can be corrected numerically in the processing program.

Figure 1: DC72 magnetometer with gear wheel.

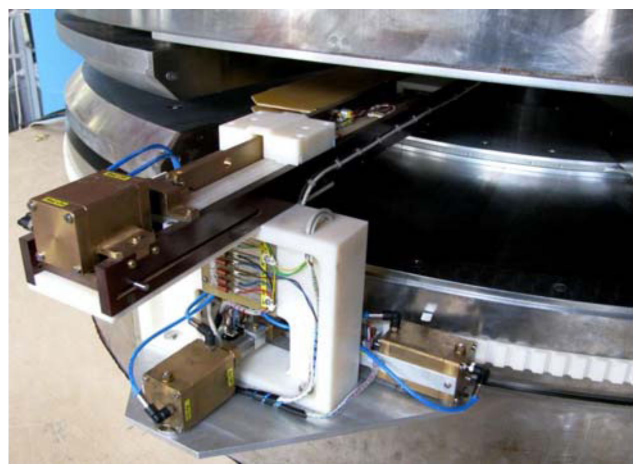

Figure 2: DC110 magnetometer with toothed belt.

The earlier versions of FLNR magnetometers used gear wheel for azimuthal motion, figure 1. The problem was that for each cyclotron the individual gear wheel must be created. It increase the price of magnetometer manufacturing dramatically. For DC110 and DC280 cyclotrons we refused to use the wheel and replaced it by a toothed belt, figure 2.

Table 1: Mapping System Radial Parameters

cyclotron	Nh	Ns	Rb	Rpole
DC280	14	16	2240mm	2000mm
DC110	8	16	1280mm	1000mm
DC60	8	14	1120mm	810mm
DC72	8	20	1600mm	1300mm

ISBN 978-3-95450-181-6

MAGNETIC MEASUREMENT SYSTEM FOR THE NICA COLLIDER DUAL DIPOLES

M. Shandov, V. Borisov, A Bychkov, O. Golubitsky, H. G. Khodzibagiyan, S. Kostromin, M. Omelyanenko, A. Schemchuk, Veksler and Baldin Laboratory of High Energy Physics, Joint Institute for Nuclear Research, Dubna, Russia.

Abstract

NICA collider magnetic system consists of 80 dual-aperture dipole superconducting magnets. Measurement of magnetic field parameters is assumed for each collider's magnet. This paper describes magnetic measurements methods and developing of dedicated system.

INTRODUCTION

NICA (Nuclotron-based Ion Collider fAcility) is a new accelerator complex presently under construction at the Joint Institute for Nuclear Research (JINR) in Dubna, Russia to study properties of dense baryonic matter. NICA booster and collider composed more than 250 superconducting (SC) magnets [1]. These magnets will be assembled and tested at a new test facility in the Veksler and Baldin Laboratory of High Energy Physics (VBLHEP) JINR. The program for magnets testing includes warm and cold magnetic measurements (MM). The some of the details for measuring system for carrying out MM of a twin-aperture dipole magnet of collider is made and tested. Full-scale prototype of measurement shaft and plain bearing with teflon liner were tested in cold MM of quadrupole lens of NICA and sextupole lens SIS100. The basis of design laid down to magnetic measurement system for dipole magnets of NICA booster [2].

TWIN-APERTURE (DUAL) DIPOLE MAGNET FOR THE NICA COLLIDER

The Nuclotron-type design based on a cold (4.5K) window frame iron yoke and a saddle-shaped SC winding cooled with a two-phase helium flow has been chosen for the NICA booster and collider magnets. Main characteristic of the NICA twin-aperture dipole collider magnets are given in [1]. The twin-aperture dipole collider magnets with installed magnetic measuring system (MMS) is shown in Fig. 1. The general view of magnet is shown in Fig. 2.

Reference Magnet Field

Each magnet has an additional winding (see Fig. 1 Pos. 6) consisting of 4 conductors located in the corners of magnet yoke. This winding generate the reference magnetic field, directed parallel to the magnet poles, which used for positioning of measuring coils of separate sections relatively each other and magnet median plane.

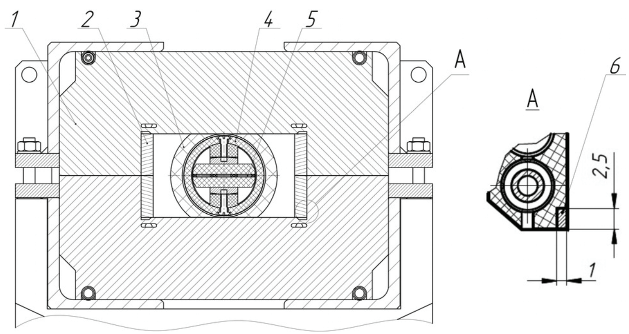

Figure 1: Cross-section view of dipole magnet for the NICA collider with MMS: 1. Yoke, 2. Main coil, 3. Plain bearing of measurement shaft, 4. Measurement shaft, 5. PCB with harmonic coils, 6. Reference coil.

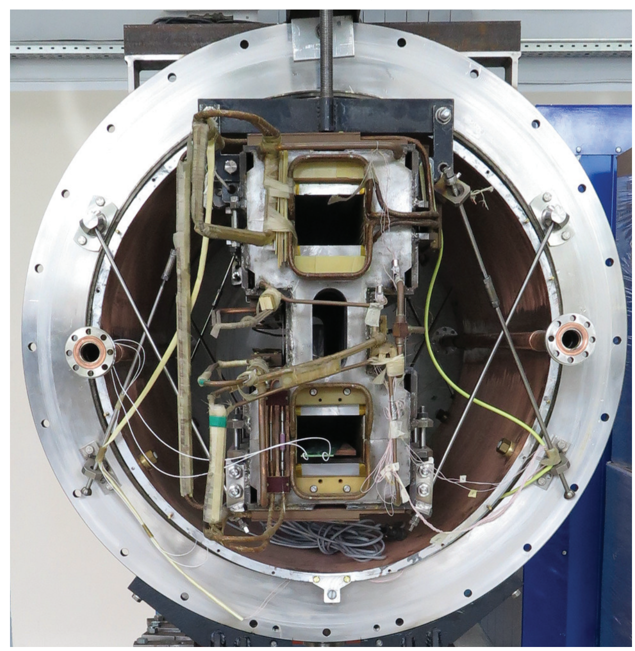

Figure 2: The twin-aperture dipole magnet mounted in a cryostat.

THE MAGNETIC MEASUREMENT SYSTEM

According to the technical specification the following parameters of dipole collider magnet have been measured:

- field at the center of magnet;
- magnetic field integral;
- effective length;

ISBN 978-3-95450-181-6

SIMULATION OF PRECISION MAGNETIC SHIELDING SYSTEM FOR BEAM INJECTORS IN TOKAMAKS

A. Bazarov, V. Amoskov, E. Gapionok, V. Kukhtin, E. Lamzin, D.V. Efremov Scientific Research Institute of Electrophysical Apparatus, 3 Doroga na Metallostroy, St.Petersburg, 196641, Russian Federation
V. Belyakov, S. Sytchevsky, St.Petersburg State University, 7/9 Universitetskaya embankment, St.Petersburg, 199034, Russian Federation
Yu. Gribov, ITER Organization, Route de Vinon-sur-Verdon, CS 90 046, 13067 St Paul Lez Durance Cedex, France

Abstract

Beam injectors in tokamaks are utilized for plasma heating and diagnostics. Due to the relatively large distance between the injectors and plasma, the tokamak stray magnetic field inside injectors during the operation should be very low (down to the tenths of Gauss) to avoid the deflection of the ion beams. The Magnetic Field Reduction System (MFRS) should be used to reduce the stray magnetic field produced by the tokamak EM systems and plasma to an acceptable level inside the injectors. In total, the complex MFRS can consist of a passive magnetic shield and active coils to provide the strict design criteria during a plasma scenario.

To provide precise computations, detailed numerical models of MFRS should have the dimensions up to several tens of millions of degrees of freedom. Such problem could be solved only with the use of high-efficiency vector algorithms and parallel computations.

The paper is dedicated to simulation of MFRS for beam injectors in tokamaks.

INTRODUCTION

High-energy neutral beams (NB) are used in present-day tokamaks for additional heating to provide plasma burn and current drive [1]. The heating is the most effective when the NBs are injected into plasma in the direction of the plasma current.

NB injection is also one of the basic techniques of plasma diagnostics. It allows detection of plasma particles and measurement of local plasma parameters from the plasma response to the injected beams.

The NBs are produced by neutralization of accelerated ions. The main components of an NB injector are a beam source, a gap where the beams are extracted, formed and accelerated, a neutralizer, commonly with a gas target, and a residual ion dump.

The paper describes the model and computational results for the Diagnostic Neutral Beam Injector (DNBI) of ITER tokamak.

The residual field inside ITER DNBI during operation should be as low as 0.2 Gs in the Neutralizer region and 0.5 Gs in the Gap region to avoid the deflection of the ion beams. The Magnetic Field Reduction System (MFRS) should be used to reduce the stray field produced by the tokamak EM systems and plasma [2, 3, 4], reaching 150-500 Gs at the injector location, to an acceptable level inside the injectors. The DNBI MFRS consists of a passive magnetic shield (PMS) and active correction and compensation coils (ACCC) to provide the strict design criteria during a plasma scenario. A CATIA model of ITER DNBI PMS is shown in Fig. 1.

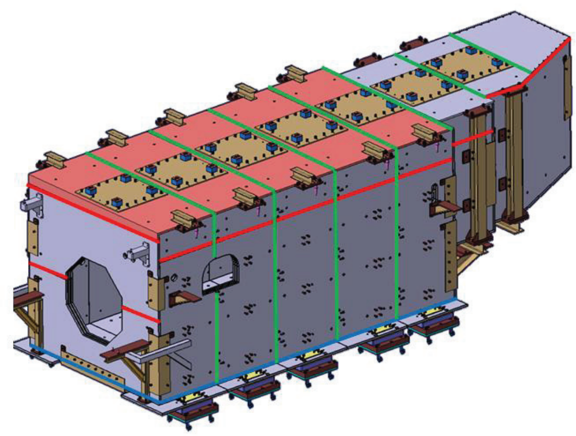

Figure 1: CATIA model of ITER DNBI PMS. Colored lines show 1 mm construction air gaps locations.

MAGNETIC MODEL

The tokamak is modeled as a set of PF coils, central solenoid (CS) and plasma, presented with a circular moveable current filament. The stray field of the tokamak is calculated with the code KLONDIKE [5] that implements integral volume elements and the Biot-Savart integration.

The FE approach is used for modeling the PMS. PMS is a bolted assembly of panels composed of three 50 mm thick low carbon steel (S235) plates with a 25 mm air gap between the plates. Also, the model includes the Neutralizer case made of 35 mm thick soft iron sheets to provide an additional shield for stray field reduction in the Neutralizer as the most magnetically crucial component. Circular holes in PMS are modeled as rectangular ones with the same area. The FE model and the computations were performed with the code KOMPOT [6].

ISBN 978-3-95450-181-6

MODELING MAGNETIC EFFECTS OF STEEL REBAR OF CONCRETE SURROUNDINGS FOR ELECTROPHYSICAL APPARATUS

V. Amoskov#, A. Bazarov, M. Kaparkova, V. Kukhtin, E. Lamzin, B. Lyublin, JSC «NIIEFA», St.Petersburg, Russia
V. Belyakov, S. Sytchevsky, St.-Petersburg State University, Russia
Y. Gribov, ITER IO, France

Abstract

The article describes an advanced approach to modelling magnetic properties of reinforced concrete structures taking into account the anisotropic effect due to rod layers orientations. The equivalent model has been validated in the computation of a test problem. For comparison, simulations have been carried out with a detailed 3D FE model that describes each of the steel rods. The equivalent model has required a few times less finite elements than the detailed model. A comparison of the fields obtained has demonstrated a very good match, even for the distances comparable with the rebar rod gaps.

INTRODUCTION

Buildings for large electrophysical apparatus, such as accelerators, experimental fusion devices, customs examination equipment, industrial and medical tomography systems etc, are typically constructed of reinforced concrete with steel rebar. Particularly, the ITER Tokamak Complex has steel rebar with a complex pattern [1, 2]. The rebar is arranged as a stack of criss-cross layers of steel bars filling from 1.5% to 12% of the structures [1]. Some of the reinforced structures are located as close as 5 – 10 m to the tokamak. The steel rebar in concrete are magnetized by the stray fields generated by the plasma and tokamak magnets (EMS ITER) up to saturation.

Previous studies have revealed a noticeable effect of the magnetized rebar on a field distribution in the plasma region [3] and outside the tokamak [4], thus making concern for performance, electromagnetic compatibility and safety. Strict design criteria are adopted for the acceptable level of field perturbations and efficiency of shielding the tokamak components, primarily injectors and analyzers.

Voluminous ferromagnetic structures may reduce the natural level of Earth's magnetic field (EMF) in the buildings. Russian safety standards for construction specify the acceptable EMF reduction as a half of the natural level [5]. For assessment of the interior EMF, mathematical modelling is applied with the use of simplified models for reinforced structures.

HOMOGENEOUS ISOTROPIC MODEL

Large electrophysical devices produce stray fields that are much higher than EMF, while massive ferromagnetic structures of the building affect the field distribution noticeably. This makes correct information about the stray field essential for the medical and safety engineering provisions as well as to ensure the normal operations of equipment sensitive to magnetic fields. The effect of the magnetized ferromagnetic structures can be evaluated with the use of solid steel models, models with effective volumetric steel fractions, or isotropic models for reinforced concrete. In particular, the authors have developed the Magnetic Model of the ITER Tokamak Complex, ver.1 (MMTC1) [6] that includes the bioshield with its lid, basemat, ceiling, walls, and seismic pit.

A challenging issue in modeling reinforced structures is to adequately describe the steel rebar arrangement. The layered pattern of the rebar produces a complicated field map inside the structures and near the tokamak building. However, at a distance comparable with a typical step of the rebar, contributions of separate steel bars are smoothed, and the reinforced concrete structure acts as a solid body with averaged magnetic properties. These properties are dictated by a magnetization curve of the steel and the layered pattern of the rebar.

In the MMTC1 each reinforced concrete structure was represented via a spatially homogeneous equivalent with isotropic magnetic properties [6]. The B-H characteristic of the equivalent was given as $B = 0.5 \cdot k \cdot f(H)$, where $B = f(H)$ is the magnetization curve of the steel rebar [7], k is the filling factor, 0.5 is the correction coefficient for the layered pattern. The correction coefficient is taken from the assumption that only 50% of bars which are co-directed with the magnetic field can effectively conduct the flux. $\eta = 0.5$ is applicable for any direction of the external field coplanar with the rebar layers. If the external field has a component normal to the rebar layers, the equivalent permeability and magnetization should be significantly lower as the bars are oriented normally to the field. The results obtained with the MMTC1 suggest that the normal field would have a weak effect on the rebar magnetization. However, more reliable modeling seems desirable.

ADVANCED LAYERED MODEL

Papers [1, 2] describe an advanced isotropic model for concrete structures with steel rebar that that takes into account anisotropic effects due to the rebar pattern. As compared to the homogeneous isotropic model, the proposed model provides more accurate assessment of the magnetic effect of the rebar with the same computational cost. For a detailed model describing every steel bar individually the computational cost is extremely high.

#sytch@sintez.niiefa.spb.su

ISBN 978-3-95450-181-6

MAGNETIC SYSTEMS FOR BEAM TRANSPORT AT EXTRACTION CHANNELS OF ILU ACCELERATORS

V. Bezuglov, A. Bryazgin, B. Faktorovich, E. Kokin, V. Nekhaev, A. Panfilov, V. Radchenko, E. Shtarklev, V. Tkachenko, A. Vlasov, L. Voronin, BINP SB RAS, Novosibirsk

ABSTRACT

This paper is devoted to magnetic systems for beam transport at extraction channels of electron industrial accelerators of the ILU type. The extraction systems meant for energy of the accelerated electrons up to 10 MeV and beam power up to 100 kW are described. Special attention is paid to forming of the dose field in a radiation zone. In paper the magnetic system for bending of the nonmonochromatic beams is offered to application. The essence of the described device consists in application of two identical magnetic mirrors in which distribution of magnetic field on depth is formed so that natural rise of magnetic field intensity on an entrance to a mirror is followed by decrease of this field under a certain law [1]. In the issue of impact on charged particles of forces arising in cylindrical lenses of each mirror is possible to compensate angular divergence of strongly nonmonochromatic beams in gaps of magnetic mirrors and to receive after bending a beam with parameters close to phase characteristics of an input beam.

BEAM EXTRACTION SYSTEMS

Radiation technologies reached now such wide application in the industry that became its separate branch. And improvement of generators of electron beams occurs at the same time to high-quality improvements of extraction devices. Rigid modern requirements to uniformity of dose fields of electronic accelerators demand detailed consideration of the questions connected with operation of extraction devices. The extraction systems of ILU accelerators are meant for energy of the accelerated electrons up to 10 MeV and beam power up to 100 kW. The received nonuniformity of the dose field in radiation zone is up to ±5%. The most optimal for application in radiation technologies are ILU-10 accelerator (5 MEV, 50 kW) and ILU-14 accelerator (10 MEV, 100 kW).

The accelerated beam at ILU is scanned on the required sizes of the irradiated object in the triangular metal vacuum chamber (bell), the scanning electromagnet is located in triangle peak, and an extraction window from a titanic foil 50 microns thick on the opposite side. The power supply system of the scanning electromagnet forms a current pulse, in a form reminding piece of a sinusoid with duration of 0.5 ms and adjustable amplitude. The current density at edges of a foil increases, and for achievement of the dose uniformity the speed of beam scanning to edges should be raised. Necessary uniformity of output current density is reached by installation before a scanning electromagnet of the system for scanning magnetic field correction. The additional correcting field leads to equalizing of beam scanning speeds along the output bell (see figure 1).

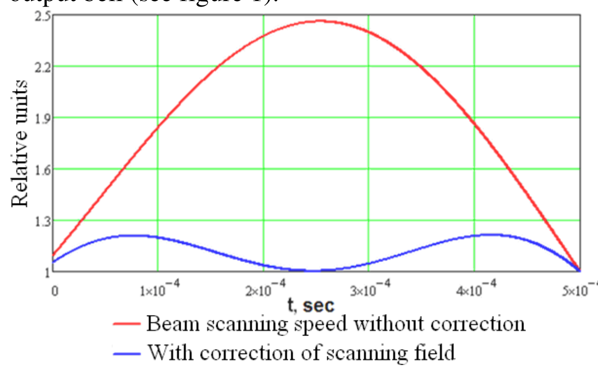

Figure 1: Beam scanning speed along the extraction window during the pulse.

The correction system of the scanning field was tested on the ILU-10 accelerator. For the distribution received without scanning correction, nonuniformity of a dose was ±13%. The optimum form of correction of the scanning magnetic field providing nonuniformity of distribution of a beam current density of ±5% was selected (figure 2).

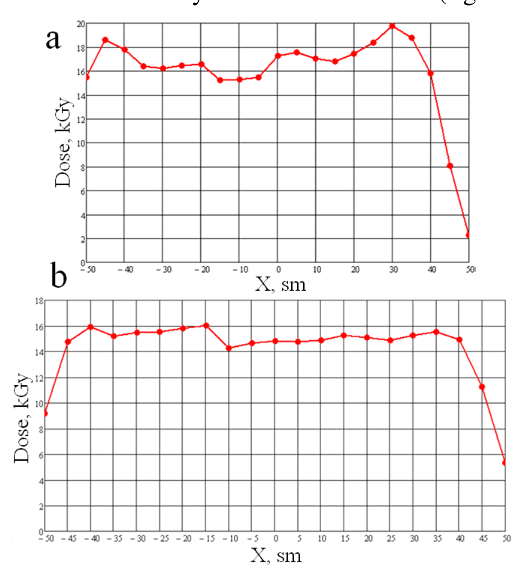

Figure 2: Dose field distribution along extraction window without correction of scanning (a) and with correction (b).

To provide the maximum penetration depth of electrons in material the beam should pass to atmosphere perpendicular to the irradiated production on all length of the accelerator extraction window. For this purpose near extraction window are set two bending electromagnets (Panofsky's lenses). In figure 3 electron trajectories at the extraction channel using the bending electromagnets and without them are given.

ISBN 978-3-95450-181-6

MAGNETIC MEASUREMENT SYSTEM FOR THE NICA QUADRUPOLE MAGNETS

A. Shemchuk, V. Borisov, A. Donyagin, O. Golubitsky, H.G. Khodzhibagiyan, M. Shandov, LHEP, JINR, 141980, Dubna, Moscow Region, Russia

Abstract

NICA is a new accelerator collider Nuclear Research (JINR) in Dubna. More than 250 superconducting magnets need for the NICA booster and collider. These magnets will be assembled and tested at the new test facility in the Laboratory of High Energy Physics JINR. A method of measuring of the quality of the magnetic field in the aperture of the quadrupole magnet for the booster synchrotron is described. Commissioning of equipment for magnetic measurements in the aperture of the doublet of quadrupole lenses is described.

INTRODUCTION

At the Laboratory of High Energy Physics (LHEP) creation of the first stage of technical complex [1] for assembly and testing of SC magnets for the NICA and FAIR project is finished. The program of testing of magnets includes «warm» and «cold» magnetic measurements. It is necessary to assemble and test 48 quadrupole magnets for NICA booster synchrotron. For measurement of characteristics of the quadrupole magnets two main sensors are used.

QUADRUPLE MAGNET FOR THE NICA BOOSTER

The quadrupole magnet consists of the focusing and defocusing lenses which are rigidly connected among themselves. The parameters of the quadrupole magnet are presented in [2] and Table 1. 3D view of the magnet shown in Figure 1.

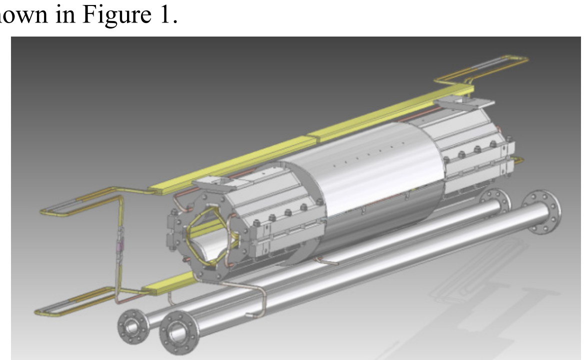

Figure 1: 3D view of the quadrupole magnet.

REQUIREMENTS FOR COMPOSITION OF MAGNETIC MEASUREMENTS

Requirements

- ✓ For all quadrupole lenses before the magnetic test in a superconducting mode, it is necessary to make measurements at normal (room) temperature. Thus, there is no need for magnetic measurements in the lenses with obviously unacceptable characteristics at 4.5 K temperature.
- ✓ The parameters of the harmonic coils must provide measurement accuracy according to specifications (see Table 1) during tests at 4.5 K.
- ✓ Both cold and warm serial measurements of the magnets are carried out without the vacuum chamber of the beam.
- ✓ For the 3-5 quadrupole lenses serial measurements should be supplemented by studies not included in a standard set of procedures:
  - The study of the effects (both static and dynamic) distortion values of the harmonics of the magnetic field associated with the presence of the vacuum chamber
  - Study of hysteresis effects
  - To study the influence of Assembly/disassembly of the lens on the measured parameters
  - The study of the dependence of field harmonics from the current. In particular, the necessary measurement of harmonics with a maximum field installation, field injection and 5-7 intermediate values. This task necessarily involves the need to accurately determine the values of the current in the main windings corresponding to three values of the fields.

Values which are Necessary to Measure

Based on the requirements for the creation of the measuring bench formulated the table 1. It contains both relative and absolute error.

It is necessary to measure the next parameter, quadrupole magnet:

- The gradient in the center of the magnet
- Integral gradient
- The effective length
- The offsets of the magnetic axis of the magnet, with respect to the geometric axis.
- The angle of rotation of the magnetic field relative to the yoke
- The relative Central and integral harmonics, to 6 inclusive

METHODS AND IMPLEMENTATION OF MEASUREMENTS

In accordance with the requirements specified in Table 1 was chosen 2 methods of measurement. The first method of harmonic coils [4], the second method of tangential coils.

ISBN 978-3-95450-181-6

FIRST EXPERIENCE OF THE HTS-II DIPOLE TYPE MAGNETS DEVELOPMENT AT NIIEFA

I. Rodin#, E. Andreev, V. Amoskov, V. Glukhich, A. Dyomina, V. Kukhtin, E. Lamzin, E. Zapretilina, JSC «NIIEFA», St.Petersburg, Russia
V. Belyakov, S. Sytchevsky, St.-Petersburg State University, Russia
S. Samoilenkov, JSC "SuperOx", Moscow, Russia

Abstract

The possibility to design, manufacture and test the dipole type magnets from the second generation high-temperature superconductors (HTS-II like YBCO and ReBCO) was demonstrated at the Efremov Institute. The paper describes available computation techniques, design approaches and manufacturing equipment, which could be used to meet the modern requirements for the magnets of accelerators, research equipment, magnet levitation systems etc. The manufacturing equipment comprises the winding lines and insulating devices to provide different configurations and insulating schemes of coils. Additionally, an equipment to produce the Roebel-cable for high current applications was procured and put in operation. As an example, the results of development of the HTC-II dipole type magnets for the different kind dummies of maglev systems are presented. The ReBCO tapes produced by JSC "SuperOx" (Moscow) were used. Up to 0.5 T magnets cooled by liquid nitrogen were designed as a part of levitation system consisting of permanent, HTS-II and normal conductive magnets. Comprehensive tests verified the computation results and demonstrated the readiness to develop HTS-II dipole magnets under the customer requirements.

INTRODUCTION

Over the last fifty years the Efremov Institute holding leading position in design and production of large-scale superconducting magnets was successfully developing low temperature superconductor technology (LTS). However, progress in high temperature superconductivity (HTS) urged the Efremov magnet department to apply considerable efforts to that new area. Starting with measurements of YBCO monocrystals [1], and testing HTS-I current leads it gradually turned to HTS-II tapes, cables and windings. When looking at the critical characteristic of the ReBCO tape (Fig. 1), three specific regions of HTS application could be distinguished:

- Low temperature and high or extra high field – magnets for NMR spectrometry.
- When operating temperature ranges from 20 to 40 K, the HTS can replace LTS in their traditional 5 to 15 T applications – dipoles, magnetic lens etc.
- Low field and LN temperature (the most attractive region from cryogenic point of view) – current leads, power cables, small coils (<0.5 T), bias coils for electromagnets etc.

Some aspects of the work, which seem prospective for accelerator magnets, research equipment, levitation systems and other applications, are reported below.

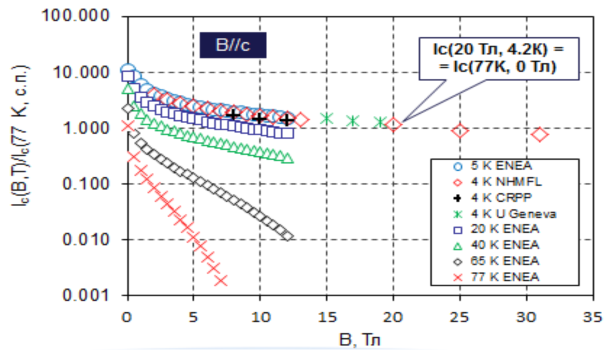

Figure 1: Critical characteristic of ReBCO tape.

WINDING AND INSULATING EQUIPMENT

The HTS-II conductors suitable for coil winding are thin multilayer tapes. Typical dimensions of the tape are - width from 4 to 40 mm and thickness for 40 to 600 µm. A special insulating and winding equipment is needed to handle such a delicate conductor. The necessary equipment has been designed, manufactured, procured and put in operation in the Efremof Institute. The equipment allows winding of round, racetrack and saddle-shape coils up to 1.5 diameters. It can work with tapes, flat cables (Roeble or Rutherford type) and round wires with thickness ranges from 10 µm to 1.5 mm. The winding machine can get wire supply form nine delivery spools, so it can perform winding following "n-in-hand" technique. The optimal n in this scheme is two or three "elements", where an "element" is a composition of two or three tapes, for example, HTS tape, hastelloy tape and insulation tape. The machine can produce a pulling force up to 12 kg per spool. When performing racetrack or saddle winding the pulling force should vary with angle of the spin-table rotation. A special system controls the machine operation and the pulling force variation can be pre-programmed. Main parameters of the winding process are set form the touch panel and displayed at the monitor of the control console. The winding machine is shown in Fig. 2. At the rotating table in Fig. 3 is a coil in process of winding and assembly. The coil is 400 mm round section of the SMES model. It is designed to operate at

#rodin@sintez.niiefa.spb.su

ISBN 978-3-95450-181-6

THE NONSYMMETRICAL VARIANT OF THE NONFERROMAGNETIC EXTRACTION KICKER MAGNET OF THE NICA BOOSTER

V. S. Aleksandrov†, A.V.Tuzikov, A. A. Fateev, Joint Institute for Nuclear Research, Dubna, Moscow Region, Russian Federation

Abstract

Development and creation of the NICA acceleration complex are continued at JINR (Dubna). One of the main facilities of the complex is the Booster in which preliminary acceleration and cooling of an ion beam is performed. Further acceleration is fulfilled in the circular accelerator NUCLOTRON. The beam transfer from the Booster into the NUCLOTRON is provided by means of the fast extraction system and one of its central elements is the kicker magnet. For the beam deflecting into the extraction septum-magnet it is supposed to use the nonferrous kicker magnet consisting of two couples of conductors. Recent changes made in configuration of the Booster extraction section demand decrease of the kicker magnet length that leads to change of the beam extraction scheme. This report is devoted to the choice of the alternative design of the magnet (the nonsymmetrical variant).

INTRODUCTION

Within the NICA [1] project creation and development not only traditional, but also new transition systems of a beam is supposed. In article [2] the kicker magnet consisting of two couples of conductors in which the ferromagnetic yoke is not used is offered.

According to [3] extraction of ions from the Booster it is supposed to carry out in 2 stages. At the first stage the circulating beam is brought to a septum-magnet knife by means of a bump subsystem of a closed orbit. At the second stage an extraction of ions from the Booster is carried out actually. The kicker magnet represents two couples of conductors established inside vacuum box parallel to an axis of driving of a beam. Maximal magnetic field – 0.13 T, the corresponding current in conductors of a magnet – 15 kA. Inhomogeneity of a magnetic field in the area occupied by a bunch does not exceed ±1 %.

THE EXPECTED BEAM PARAMETERS

Calculated parameters of a beam in the location of a kicker magnet on energy of injection and the maximal energy are given in Table 1. The option of an extraction called in Table 1 "initial" was assumed at the time of the publication of article [2].

Table 1: Beam Parameters

	injection	extraction options	
		initial [2]	new [3]
ε_x, π mm · mrad	150	15	3
ε_y, π mm · mrad	10	2	1.5
Max β_x, mm / mrad	12	12	12
Max β_y, mm / mrad	12	12	6.5
D_x, m	1	1	0.1
Δp/p	$\pm5\cdot10^{-4}$	$\pm3.6\cdot10^{-3}$	$\pm5\cdot10^{-4}$
Max A_x, mm	43	17	6
Max A_y, mm	11	5	3.3

NONSYMMETRICAL VARIANT OF THE KICKER MAGNET

New parameters of a bunch at the maximal energy, in particular, considerably smaller cross sectional dimensions, and also pulse character of a magnetic field, give the possibility to offer a kicker magnet consisting of one couple of conductors and the copper screen replacing the second couple of conductors with an opposite direction of current (Fig. 1).

As a current pulse length in a kicker magnet is about one microsecond, the strong skin effect takes place, and numerical simulation of magnetic fields can be carried out in the following approach. The magnetic field in conductors is absent, current is distributed on a surface of conductors. In model of an infinitely long magnet a current is directed along a longitudinal axis. Respectively the vector potential of a magnetic field has only a longitudinal component. In such approaching the problem of calculation of a pulse magnetic field is equivalent to an electrostatic task. It allows to carry out calculations for the choice of a configuration of couple of conductors and the screen by means of a POISSON [4] package in twodimensional model, trying to obtain the required distribution of a horizontal component of an electric field.

In calculations the following main variants of a magnet were considered: variant with the flat screen and variants with screens arched in the vertical plane with various radii of curvature. For expansion of area of uniformity of the field the distances between main elements were increased from 40 to 50 mm.

In Fig. 2 corresponding distributions of the field are shown.

† aleks@jinr.ru

ISBN 978-3-95450-181-6

FAST KICKER FOR HIGH CURRENT ELECTRON BEAM MANIPULATION IN LARGE APERTURE

V. Gambaryan, A. Starostenko, BINP SB RAS, Novosibirsk, Russia

Abstract

Pulsed deflecting magnet (kicker) project was worked out in BINP (Budker Institute of Nuclear Physics). The kicker design task is: impulsive force value is 1 mT*m, pulse edge is 5 ns, and impulse duration is about 200 ns. The unconventional approach is for plates to be substituted by a set of cylinders. Obtained magnet construction allows controlling field homogeneity by changing currents magnitudes in cylinders. Furthermore we demonstrated the method of field optimization. In addition the harmonic components measurement technique was considered and the possibility to control harmonic components value was shown.

THE KICKER CONCEPT DESIGN

The kicker design should accept several requirements. The first one is vacuum chamber and kicker symmetry axis coincidences. The second one is that central angel should be about 90˚. The optimisation parameter is magnetic field homogeneity in centrally located square area (2 cm x 2 cm).

THE KICKER ACTUAL DESIGN

Taking into account the kicker design optimization results described in [1], the BINP designers developed a kicker prototype. The kicker dimensions were selected based on measurements. The magnet cross section is shown in Fig. 1. The physical magnet length is about 650 mm. The magnet aperture is 100 mm. The vacuum chamber diameter is 164 mm. The cylinder diameter is 28 mm. The cylinders are made of steel, as well as the body of the magnet. The ceramic feedthrough also was developed in BINP.

For the simulation of dynamics of charged particles beams the CST Studio is used. These simulations are in the initial stage. Only preliminary calculations have been held. One of the first results is shown in Fig. 2.

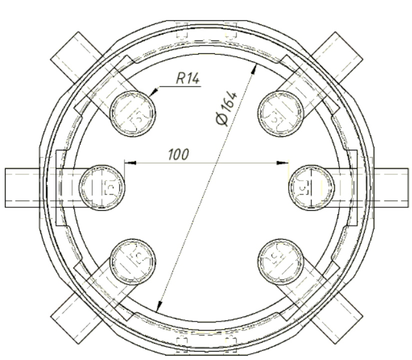

Figure 1: The kicker actual design (all dims are in mm).

MAGNETIC FIELD MEASUREMENTS

To control magnetic field quality the experimental measurements was carried out.

Experimental Stand Description

Experimental stand shown in Fig. 3 consists of the following parts:

1. Kicker
2. Pulse generator
3. The induction coil magnetometer
4. VSDC2 - Precision digital signal integrators with an accurate synchronization [2]
5. Hand caliper
6. Step motors with controllers
7. PC with a special software

The kicker is fixed on a metal frame. Step motors provide the movement in the horizontal plane. The vertical displacement of step motors is realized only by screws turning by hand. For both step motors we have to control vertical position using hand caliper. All of the stand components were precisely aligned with the help of BINP geodesy group.

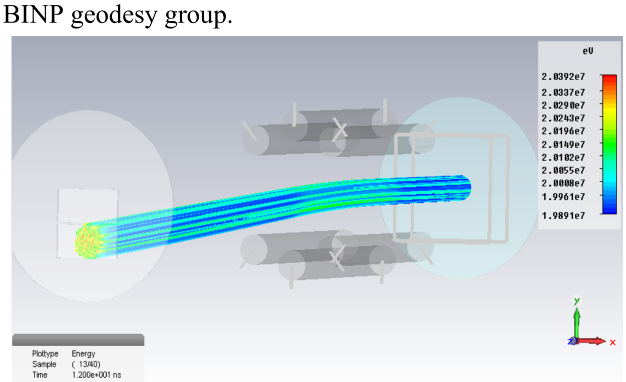

Figure 2: Beam dynamics simulation in CST.

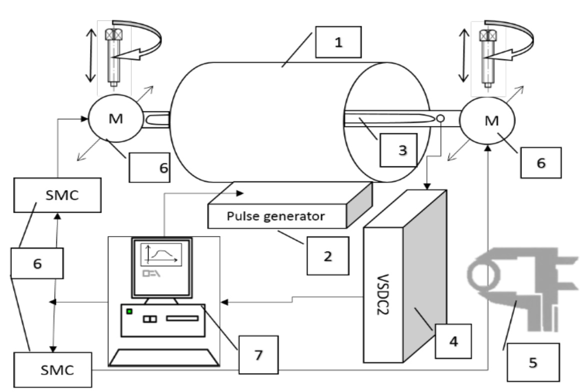

Figure 3: The principal scheme of magnetic field measurement stand: 1) kicker, 2) pulse generator, 3) the induction coil magnetometer, 4) VSDC2, 5) hand caliper, 6) step motors with controllers, 7) PC with special software.

ISBN 978-3-95450-181-6

A SYNCHROTRON RADIATION BEAMLINE INSTALLED AT BINP TO STUDY THE HIGH LUMINOSITY LHC VACUUM SYSTEM

A. Krasnov[1*], V. Anashin, A. Semenov[2], D. Shwartz[1], BINP SB RAS, Novosibirsk, Russia
V. Baglin, P. Chiggiato, B. Henrist, CERN, Geneva, Switzerland
[1] also at NSU, Novosibirsk, Russia
[2] also at NSTU, Novosibirsk, Russia

Abstract

In the framework of the HL-LHC project, the vacuum performance of new surface material needs to be studied. In particular, a-C coating is proposed as an anti-multipactor surface for the HL-LHC superconducting final focusing system. Since the protons will generate synchrotron radiation (SR) with ~ 10 eV critical energy and ~10^{16} ph/m/s flux, it is therefore of great importance to study the impact of such photons on a-C coating held at room and cryogenic temperature and compares the results against present LHC material. This paper describes the construction and the parameters of the experimental set-up based on a new Synchrotron Radiation beamline of the BINP booster synchrotron, BEP. The experimental program done in collaboration between CERN and BINP, to perform measurements of photon stimulated gas desorption, photon distribution and photo-electron emission provoked by synchrotron radiation is also presented.

INTRODUCTION

The CERN Large Hadron Collider (LHC) is currently operating at nominal luminosity with proton-proton collisions at 13 TeV in the center of mass. Its upgrade, the High Luminosity LHC (HL-LHC), is designed to provide about 10 times more integrated luminosity with the aim to achieve ~3000 fb^{-1} by the mid-2030ies [1]. To do so, the circulating current is doubled, the beam size and the crossing angle at the collision point are further reduced to achieve a desired levelled luminosity five times larger than the LHC nominal luminosity.

In these storage rings, the vacuum system is subjected to synchrotron radiation (SR) and electron bombardment due to the build-up of an electron cloud. In particular, the vacuum level in the vicinity of the experimental areas should be kept to a minimum in order to maintain the beam induced background to acceptable values. In HL-LHC, the final focusing system consists of three superconducting quadrupoles, so called “Inner Triplets”. The vacuum system houses a shielded beam screen, operating in the ~60 K range, which intercepts the debris produced at the interaction point, thereby protecting the 1.9 K cold mass from radiation damage.

In the context of the HL-LHC project, the vacuum performance of new surface material needs to be studied in details. In particular, amorphous carbon (a-C) coating [2,3] is proposed as an anti-multipactor surface with the objective to minimize the heat load induced by the electron cloud on the shielded beam screen and the background to the experiment due to proton scattering onto the residual gas. Since the protons in the HL-LHC Inner Triplets generates SR with ~ 10 eV critical energy and ~ 10^{16} ph/m/s flux, it is therefore of great importance to study the impact of such photons on a-C coating held at room and cryogenic temperature and compare the results against present LHC material.

The new beam line facility, presently under construction at BEP, BINP, provides SR irradiation at ~10 mrad grazing angle with 10-1300 eV critical energy and ~$5\cdot10^{16}$ ph/m/s flux. It is designed to study photon stimulated molecular gas desorption, photo-electron emission and photon reflectivity of candidate HL-LHC materials held at room and cryogenic temperature.

*a.a.krasnov@inp.nsk.su

SR BEAM LINE

BEP is the booster synchrotron of the collider VEPP-2000. The machine is part of the new injection complex at BINP. BEP was re-designed and reconstructed to operate with electron or positron at energies in the range 50 ÷ 1000 MeV, with a nominal operation at 300 MeV. Nevertheless, a continuous operation is possible up to 900 MeV. The main SR parameters of a BEP dipole magnet at electron energies 200, 300 and 900 MeV are shown in Table 1. They cover the range of parameters for LHC and HL-LHC.

Table 1. SR Parameters at Different Particles Energy in BEP

Parameter	min	nominal	max
E [MeV]	200	300	900
Beam current [A]	0.5	0.5	0.5
Bending magnet radii [mm]	1280		
SR critical energy [eV]	14	47	1260
SR flux [ph/mrad/s]	1.1E15	1.8E16	5.6E16
SR power [W/mrad]	0.009	0.045	3.6
SR vertical divergence [mrad] at Ec	2.5	1.7	0.56

EXPERIMENTAL INSTALLATION

A schematic diagram of the experimental set-up on the BEP SR Beam Line is shown in Figure 1. The main elements are: “P” – a pivot point to allow a precise tuning

ACHIEVEMENT OF NECESSARY VACUUM CONDITIONS IN THE NICA ACCELERATOR COMPLEX

A.V. Smirnov#, A.M. Bazanov, A.V. Butenko, A.R. Galimov, H.G. Khodzhibagiyan, A.V. Nesterov, A.N. Svidetelev, A.M. Tikhomirov, JINR, Dubna, 141980, Russia

Abstract

NICA is the accelerator collider complex under construction at the Joint Institute for Nuclear Research in Dubna. The facility is aimed at providing collider experiments with heavy ions up to Gold in a center of mass energy range from 4 to 11 GeV/u and an average luminosity up to 10^{27} cm^{-2} s^{-1}. The collisions of polarized deuterons are also foreseen. The facility includes two injector chains, a new superconducting booster synchrotron, the existing superconducting synchrotron Nuclotron, and a new superconducting collider consisting of two rings, each of about 500 m in circumference [1].

Vacuum volumes of the accelerator booster and Nuclotron and the superconducting collider are divided into volumes of superconducting elements thermal enclosure and beam chambers. The beam chambers consist regular cold periods, which are at a temperature of 4.2K to 80K, and warm irregular gaps at room temperature. Operating pressure in thermal enclosure vacuum volumes have to maintained in the range of 1×10^{-7} to 1×10^{-4} mbar, in the beam chamber cold and warm areas – not more than 2×10^{-11} mbar. The description of way to achievement and maintenance of the working vacuum in the NICA project are presented.

GAS COMPOSITION OF THE VACUUM VOLUMES

Gas composition in vacuum volumes depending on many factors: choice of material, purity, heating of vacuum system, type of pumps, temperature mode, photon, electron or ion bombardment of the surface, etc.

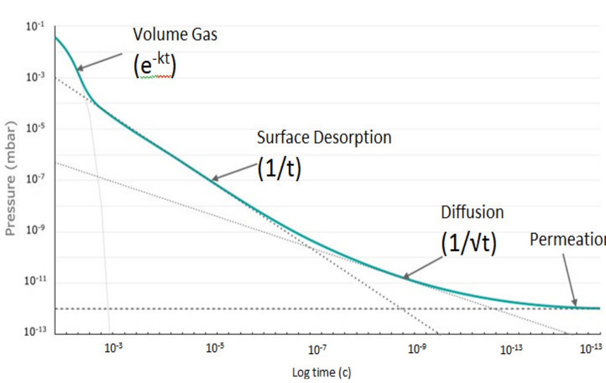

Figure 1 : Pump-down diagram.

The main gas constituents of the atmosphere are nitrogen and oxygen. Other gases, such as argon, carbon dioxide and water steam are less than 1% of the total volume of air.

Water is the main component in the unheated metal vacuum chambers. Degassing of water is not significantly dependent on the nature of the metal, surface treatment, and temperature conditions (at temperatures less than 110°C). Currently there are practically no methods other than baking to remove water from the metal surfaces. Diagram of achieving extreme-high vacuum is shown in Figure 1.

Hydrogen is the main residual gas, which is desorbed from the metal surface, when obtaining an ultra-high vacuum. The process of hydrogen degassing depends on the properties of the metal and capacity of the surface at a constant temperature. Heating at a high temperature (up to 900°C) reduces the content of hydrogen on the surface by more than two orders of magnitude [2].

VACUUM VOLUMES OF THE NICA

NICA complex consists of two warm linear injectors, two superconducting synchrotron (Nuclotron and booster), one superconducting collider and warm transport beam channels.

All vacuum volumes can be divided on three different types. The first type is volumes without beam, for example the thermal enclosure vacuum volumes. The second type is the volumes, through which beam passes one time. It is the vacuum chambers of linear accelerators and transport channels between accelerators and areas of experiment. The third type is the volumes, through which beam passes many times. It is the volumes of booster, Nuclotron and collider.

The linear accelerators' volumes of LU-20 and LUTI (Linear accelerator of heavy ions) are required vacuum not worth then 1×10^{-7} mbar. Such value is more determined by resistance to high-voltage breakdown and less by accelerating particles.

The vacuum degree in transport channels depends on adjacent vacuum volumes. For example, the vacuum value for transport channel of the beam transfer from LUTI to booster needs to be not more than 1×10^{-7} mbar from the one side and not less than 1×10^{-11} mbar from the another side. And the channel must have high resistance to residual gas migration from LUTI to booster. For the transfer beam channel from Nuclotron to experimental building is enough roughing vacuum (1×10^{-2} mbar).

Requirements for vacuum in booster, Nuclotron and collider are the highest. At the same time the booster requirements are higher than in collider at the expense of low beam energy – 1×10^{-11} mbar. Vacuum in collider must be better than 1×10^{-10} mbar because of prolonged being of particles inside the vacuum chamber – about one

#smirnov@jinr.ru

ISBN 978-3-95450-181-6

HARDWARE FOR INCREASING RELIABILITY OF THE POWER SUPPLY SYSTEM FOR CORRECTOR MAGNETS OF THE EUROPEAN XFEL

O. Belikov, V. Kozak, E. Kuper, A. Medvedko, BINP, Novosibirsk, Russia
H.-J. Eckoldt, N. Heidbrook, DESY, Hamburg, Germany

Abstract

The modern linear accelerators, which are quite long, need a lot of electromagnets to correct the position of beam of charged particles. Typically, each corrector electromagnet shall be powered by a separate high-precision current source. Using a large number of high-precision power supplies reduces the reliability of the power supply system. To avoid this we have developed a system of "hot" replacement of power supply, which enables remote replacement of a faulty power supply with a backup one.

INTRODUCTION

The total length of the European XFEL is 3.4 km. 296 corrector electromagnets correct the electron beam position, each magnet powered by an individual high-precision current source [1]. Main parameters of the sources are listed in Table 1.

Table 1: Parameters of power supplies for corrector magnets.

Parameter	Specified Value	Units
Output current, max.	± 5 / 10	A
Output voltage, max.	± 70 / 60	V
Short-term current deviations (up to 1 sec)	< 10	ppm
Long-term current deviation (1 sec to several years)	< 100	ppm
Mean time between failures (MTBF)	≥ 100 000	hrs

A failure even in a single power supply for the corrector magnets significantly affects the electron beam quality. In continuous operation of the XFEL, the estimated amount of faults will be 1 failure per 14 days. The power supplies are distributed along the length of the complex, and it takes quite a time to replace a faulty crate. Given the estimated time for troubleshooting, these time losses are considered as inadmissible.

STRUCTURE OF POWER SUPPLY MODULE

To minimize the downtime at the European XFEL, it was decided to use a redundancy system, i.e. to complement the power supply group with a backup source module, which may be switched on instead of any other. The structure of such a module is shown in Fig. 1. In normal operation, seven power supplies feed the corrector magnets. The eighth power supply (the backup one) is switched to an equivalent load, which enables monitoring of its operability. If one of the normal sources fails, the control system can switch the respective correction magnet to the backup power supply, and the power supply system will continue normal operation.

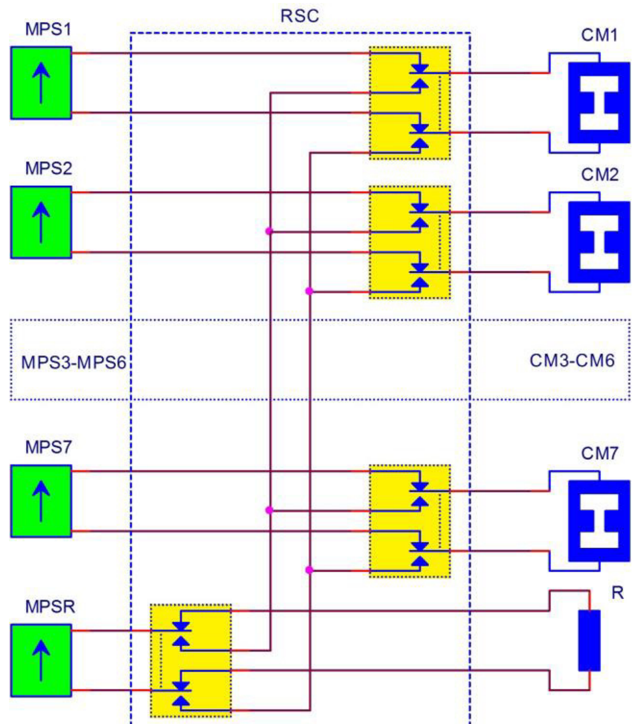

Figure 1: Function chart of power supply module. MPS – Magnet power supply; RSC – Redundancy system crate; CM – Corrector magnet; R – Dummy load.

INCREASING POWER SUPPLY SYSTEM RELIABILITY

48 power modules feed the corrector magnets of the European XFEL, each module having a backup power source. Increase in the number of the power supplies will result in a bigger estimated number of failures. With the redundancy system, a power supply failure that requires operating personnel intervention may occur only in the case of breakage of two or more sources from one module. If maintenance works to replace faulty power supplies are carried out once a month, one can calculate the probability of failure of the power supply system per year by the following formula:

$$P = \frac{N \cdot (n-1) \cdot P_i^2}{12},$$

ISBN 978-3-95450-181-6

ELECTROMAGNETIC COMPATIBILITY OF THE POWER SUPPLY SYSTEM FOR CORRECTOR MAGNETS OF THE EUROPEAN XFEL

O. Belikov, V. Kozak, BINP, Novosibirsk, Russia
H.-J. Eckoldt, N. Heidbrook, B. Moelck, DESY, Hamburg, Germany

Abstract

The power supply system for the corrector electromagnets of the European XFEL includes over 300 precision current sources with an output power of up to 600 W. BINP developed, manufactured and supplied the power sources for the corrector magnets. For reliable operation of the physical installation, at the design stage it was necessary to ensure electromagnetic compatibility of the power supplies with other electronic equipment of the European XFEL.

INTRODUCTION

During the development of high-precision power supplies for electromagnets, it is necessary to ensure compliance of the precision and stability of the power supply parameters. This is a challenge on large physical installations because the power supplies shall work in contact with a variety of other electronic devices. It is therefore necessary to make the power supplies capable to work in a specific electromagnetic environment, while maintaining the stability of their parameters and without creating intolerable electromagnetic disturbances to other electronic devices.

BINP members developed MPS-10-60, a prototype of the power supplies for the corrector magnets [1]. This prototype was verified in relation to compliance with certain directives of the EMC international standard: EN 61000-4, EN 61000-6, EN 55011, and EN 61326-1. The tests were conducted at the EMC Laboratory "TÜV NORD" (Hamburg). Upon successful completion of all the tests, the production of 400 power supplies for the corrector electromagnets of the European XFEL started.

GENERIC EMISSION OF THE POWER SUPPLIES

For the sake of convenience of arrangement and maintenance of the power supply system, all the sources were made with natural air cooling. The cases of the power supplies are heated during operation, which results in output current instability caused by temperature drift. Therefore, high-precision power supplies should have high efficiency. Reducing the dynamic losses in switching elements often leads to an increase in the radiated power of electromagnetic interference. Electromagnetic shielding of the units of the power supply inverter would not be effective in this case since the screens hinder cooling. The largest emission amplitudes were in the frequency ranges of 30 ÷ 60 MHz (interference from the rise/fall of the fast switches mosfet of the inverter) and 100 ÷ 200 MHz (interference from the CAN line). Additional low-pass filters turned out to be helpful in both cases. A graph of the radiated emission of power supply for the corrector magnets in the frequency range from 30 MHz to 1 GHz is shown in Fig. 1.

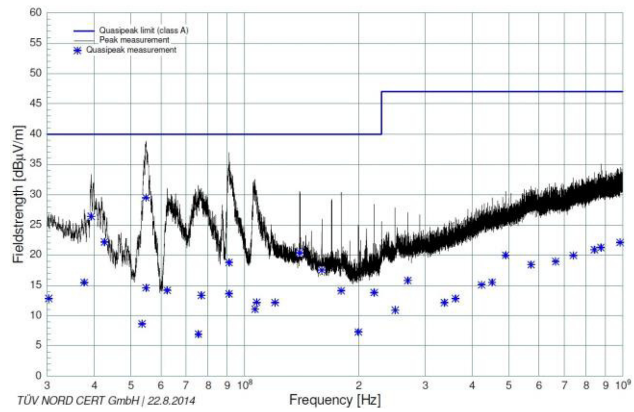

Figure 1: Radiated emission. Vertical antenna polarization.

In addition to the radiated emission, we measured the amplitude of the conducted emission of power supply to a 230 VAC mains in the frequency range from 150 kHz to 30 MHz. The maximum amplitudes of the emission were observed at the switching frequencies of the power switches. The emission decreased after addition of a CM/DM power line filter. A graph of the conducted emission is shown in Fig. 2.

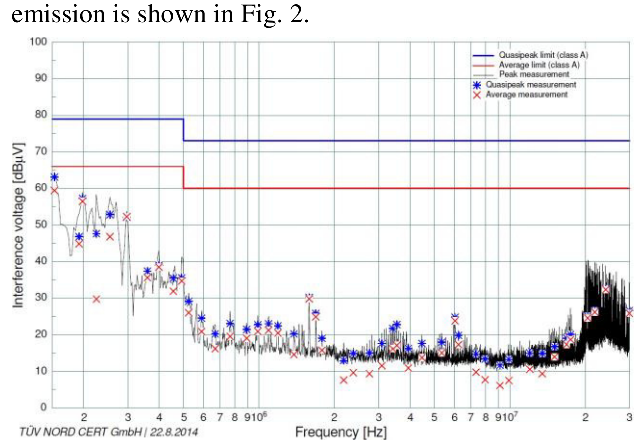

Figure 2: Conducted emission. Disturbing voltage on conductor L.

IMMUNITY TO INDUCED DISTURBANCE

Below are described tests that were carried out for verification of the immunity of the power supply output parameters to the effects of conducted and inducted interference. During the tests, external devices were controlling the stability of the power supply parameters.

ISBN 978-3-95450-181-6

CORRECTOR MAGNET POWER SUPPLIES OF THE EUROPEAN XFEL

O. Belikov, V. Kozak, A. Medvedko, D. Skorobogatov, R. Vahrushev, BINP, Novosibirsk, Russia.
H.-J. Eckoldt, N. Heidbrook, DESY, Hamburg, Germany.

Abstract

The total length of the European XFEL is 3.4 km. The electron beam parameters are corrected by about 300 corrector magnets, each powered by an individual power supply. BINP performed the development, production and delivery of the power supply system for the corrector magnets. For the powering of the corrector magnets, seven types of precision power supplies with output currents of up to 10 A and output voltages of up to 70 V were developed.

INTRODUCTION

The European X-ray Free-Electron Laser (XFEL) is designed for generation of synchrotron radiation with an intensity of 27 000 bunches per second, a wavelength of 0.05 to 4.7 nm, and a peak brightness of $5 \cdot 10^{33}$ ph/(s·mm^2·mrad^2·0.1% bandwidth). To attain the above parameters it is necessary to have an electron beam of extreme quality [1]. The XFEL structure comprises a linear superconducting accelerator with a maximum electron energy of 17.5 GeV, several photon tunnels with undulators, and experiments halls. The total length of the tunnels is 5.77 km (Fig. 1). The XFEL magnetic system structure includes 296 corrector electromagnets:

- Injector tunnel (XTIN) – 13 pcs.
- Entrance shaft (XSE) – 12 pcs.
- Linac tunnel (XTL) – 122 pcs.
- Shaft 1 (XS1) – 35 pcs.
- Distribution tunnel 1 (XTD1) – 32 pcs.
- Distribution tunnel 2 (XTD2) – 44 pcs.
- Distribution tunnel 3 (XTD3) – 22 pcs.
- Distribution tunnel 4 (XTD4) – 7 pcs.
- Distribution tunnel 5 (XTD5) – 9 pcs.

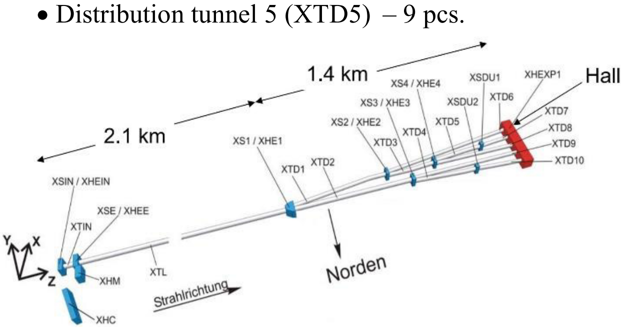

Figure 1: XFEL nomenclature.

In accordance with the requirements to the magnetic system, each corrector electromagnet shall be powered by a separate precision current source (magnet power supply, MPS). The MPS required parameters are given in Table 1.

Table 1: Requirements to Corrector Power Supplies

Parameter	Specified Value	Unit
Output current, max.	± 5 / 10	A
Output voltage, max.	± 70 / 60	V
Minimum current setting step	< 4	ppm
Short-term current deviations (up to 1 sec)	< 10	ppm
Long-term current deviation (1 sec to several years)	< 100	ppm
Temperature coefficient of output current drift	< 6	ppm/K
Output current non-linearity	< 20	ppm
Efficiency of power part	> 90	%
Mean time between failures (MTBF)	> 100 000	hrs

STRUCTURE OF POWER SUPPLIES

The power supplies for the XFEL corrector magnets are divided into two groups, with maximum output currents of 5 A and 10 A. Since the corrector electromagnets have different resistances, power supplies with different maximum output voltages were required. The result is seven types of the power supplies, the maximum values of their output parameters shown in Table 2.

Table 2: Maximum output currents and voltages of power supplies.

Power supply	Maximum output current, A	Maximum output voltage, V
MPS-5-24	5	24
MPS-5-48	5	48
MPS-5-72	5	72
MPS-10-15	10	15
MPS-10-30	10	30
MPS-10-45	10	45

The circuitry design relies on double pulse conversion (Fig. 2).

ISBN 978-3-95450-181-6

HIGH-VOLTAGE POWER SUPPLY FOR GOG-1001

V. Dokutovich†, D. Senkov, A. Chernyakin,
Budker Institute of Nuclear phisics SB RAS, Novosibirsk, Russia

Abstract

The submitted report contains the description of the high-current high-voltage quasipulse four-channel laser pumping power supply. Channels are the completely identical. It is possible to feed up to 10 kJ on each channel with up to 5 kA of output current. Source controller is developed with PLM, Atmega MCU and ARM type CPU which allows to optimize operations of device, and also to make a number of calculations. The controllers are connected by internal control network for more flexibility and efficiency. The description of the source and the test results are presented.

INTRODUCTION

At the present stage of development of systems of deduction of high-temperature plasma the question of stability of walls of a vacuum chamber remains very urgent. One of the key problems is firmness of diverter plates during the pulse. The particle fluxes influence on them and energy leading to formation of serious defects, melting and intensive evaporation of material. The studying of these processes demands carrying out dynamic measurements directly during intensive radiation of material. It is for this purpose offered to use the measuring technique of scattering of synchrotron radiation, and for model operation of thermal influence to use a laser radiation [1]. The laser impulse with energy of 1000 J is formed by GOG 1001. This is the optically-excited laser. There are four flashlight gas-discharge valves are used for laser pumping.

The high-voltage quasipulse source which would perform not only function of supply, but also monitoring of lamps status during the pulse. It is necessary for a delivery of system of pump excitation. The source offered below which has the following parameters was developed for these purposes:

- An opportunity to feed at the same time up to four lamps
- Peak energy to 10 kJ on one lamp
- Amplitude of output current to 5 kA.

DESCRIPTION

The block diagram of a source is shown on Fig.1. The source consists of the discharge circuit giving to lamps energy from accumulative capacity and the parallel scheme of ignition of an arch in a lamp [2]. In total 4 channels are executed equally and are started synchronously. Charging of capacity of a discharge circuit is carried out by the linear charger. The power supply controller allows both manual control from the forward panel of a source and removed from the workstation. The management of charging, with start-up and monitoring of work of a source is also provided.

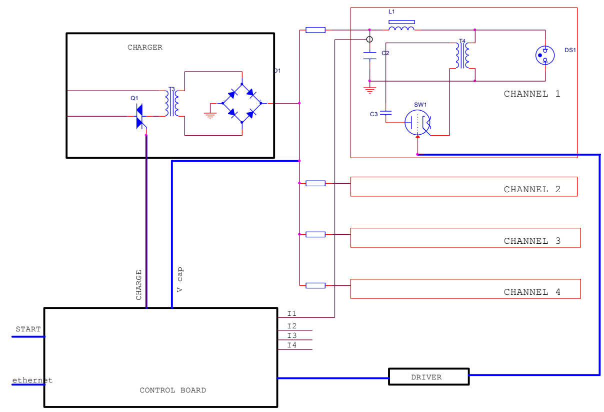

Figure 1: Block diagram of a source.

Charger

The charger represents a step-up transformer with the bridge rectifier and the current-limiting resistor at the output. At achievement by tension on the storage capacitance bank voltage of the assigned level the charging source is disconnected by a TRIAC switch. For compensation of an electrostatic leakage when maintaining the given tension on capacity the switch carries out short-term (on 50 ms) ON-state of the charging source.

Discharge Circuit

The bank of k75-100 750 µF type capacitors everyone with an operating voltage up to 6 kV are used as the store of energy. Each capacitors connected through the throttle to the load. Switching is carried out by a path of ignition of the electrical discharge in the lamp. The discharge caused by voltage pulse produced with the parallel contour representing a step-up transformer with 3 µF capacity switching to the primary winding with the thyratron-based switch. The capacitance charged up to the voltage of 3 kV. The low-current small-size high-voltage converter is used for charging of this capacity. Application of the described scheme of start allows changing the energy of flash in very wide limits: beginning from 1% of rated power that favourably distinguishes the described source created for the same purposes before.

ISBN 978-3-95450-181-6

AUTOMATED SYSTEM FOR PRECISION CURRENT SOURCES TESTING

E. Bykov, O. Belikov, A. Batrakov, E. Gusev, V. Kozak, BINP, Novosibirsk, Russia

Abstract

The beam correction system for European XFEL includes about 400 precise current sources. The every current source must tested and verified in concordance with specifications before including in XFEL equipment. For this purpose there was developed the automated system that allowed to test up to 7 current sources simultaneously. The system consists hardware stand and software that written for Linux OS. The stand was equipped emulated real load test loads, with precise DCCT and by precise analog-to-digital converters with CANbus interface. During testing the current in each current source was changed and digitized in concordance with different algorithms. The duration of typical session was 25 hours. The specific software was developed for this stand. It provides testing process, collecting and storing the primary information and displaying the first information. There are addition utilities which allows to make different analyzes in off-line mode using data accumulated during tests. The article provides a detailed description of the stand and main results.

INTRODUCTION

In 2009 at the DESY (Deutsches Elektronen-Synchrotron) research center, construction of the world's largest free-electron laser was started. The project was called XFEL (X-ray free-electron laser).

The realization of this international project will make it possible to observe molecules in dynamics while they are involved in chemical reactions.

The XFEL has a total length of 3.4 km and consists of a linear accelerator and a complicated magnetic focusing system. The XFEL beam correction system consists of almost 400 corrective dipole magnets. To ensure the power supply for these magnets, the BINP has been contracted to design and provide four hundred precision current sources. The sources have to meet a number of requirements, some of which are listed below:

- The RMS noise of output current in the frequency range from 0 Hz to 1 kHz should not exceed 10 ppm.
- The deviation of the absolute value during long-term use should be not more than 100 ppm.
- To control a number of parameters, each precision source must be tested during 25 hours with a gain of statistical data.

Considering the above requirements, it is reasonable to create an automated system that would be able to perform the real time test for several precision current sources simultaneously.

Physically, the automated system consists of a stand, to which seven precision current sources can be connected, and the software that automatically controls the stand.

BLOCK DIAGRAM OF THE STAND

Figure 1 shows a block diagram of the stand. The stand has seven independent channels, which provide a non-contact method of measuring current in a range of ± 10 amps. The channel has a power input for connecting a precision power source and output for connecting an equivalent load. In the figure, the precision sources are indicated as MPS, and the equivalent load is shown as a series connection of resistance and inductance. Furthermore, each channel has two additional analog outputs: **C** (Current) for indicating the measured current equivalent (in volts) and **T** (Temperature) for indicating the temperature equivalent (in volts) from the temperature sensor in the channel. Current and temperature values are measured by six-channel ADC of CPS01 controller. CPS01 controllers and MPS precision sources are controlled via CANbus.

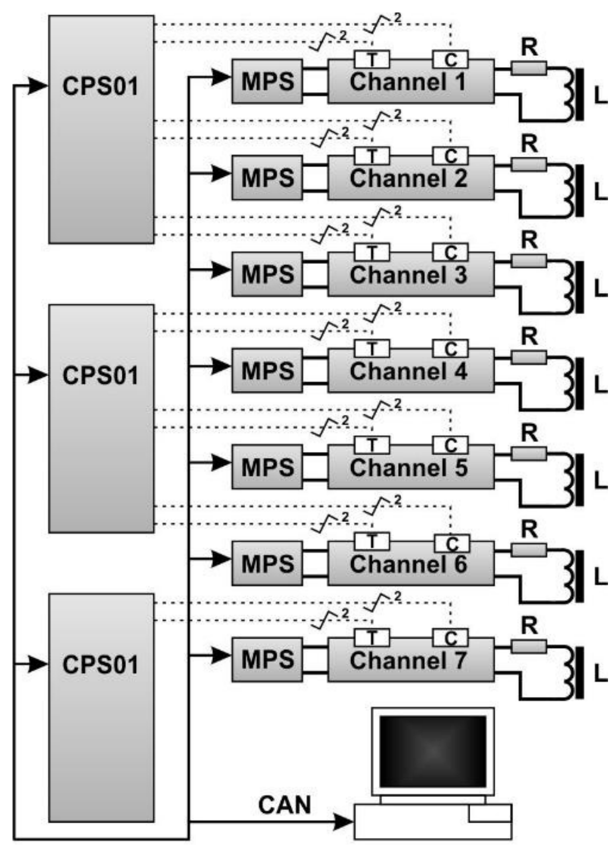

Figure 1: Block diagram of the stand.

ISBN 978-3-95450-181-6

THE PULSED HIGH VOLTAGE POWER SUPPLY FOR THE NICA BOOSTER INJECTION SYSTEM

V.A.Bulanov, A.A. Fateev†, E.V. Gorbachev, H.P. Nazlev, Joint Institute for Nuclear Research, Dubna, 141980, Russia

Abstract

Three pairs of electrostatic deflecting plates will be used in the injection system of booster ring. The electric circuit and design of the power supply system for one plate are presented in the report. The experimental results of testing are also presented.

INTRODUCTION

The NICA ion collider [1] is currently under construction at Joint Institute for Nuclear Research. The booster of the main accelerator NUCLOTRON is used for initial acceleration and cooling of ion beams.

Electrostatic septum and three deflecting devices will be used in the booster injection system [2]. Electric plates are used as actuating elements. Hydrogen thyratrons are used as switches.

PARAMETERS OF ELECTRIC PULSES

The number of supplied plates and amplitude of applied voltages depend on type of injection [2]. All electrical plates are supplied with identical pulses that differ in amplitude of the applied voltage. Main parameters of electric pulse with maximum amplitude are shown in Table 1.

Table 1: Main Characteristics of Electric Pulse

Maximum electrical potential on the plate	60 kV
Duration of pulse plateau at least	30 us
Nonuniformity of voltage on the plateau	≤ 1%
The discharge time	≤ 0,1 us
Residual voltage	≤ 0,5 kV

The parameter values given in Table 1 are generally achieved without major difficulties except for residual voltage value.

To reduce residual voltage and improve reliability of high voltage components, it was decided to use a pulse charging.

The conceptual version of such scheme was tested and results were published [3]. Then the parameters of main elements were optimized and device was designed and manufactured.

THE POWER SUPPLY SCHEME AND DESIGN

PSPICE model of the power supply circuit is presented in Fig.1.

The initial pulse of the thyristor generator is applied to the primary winding of the step-up transformer. We use industrial measuring transformer GE-36. Thyratron is triggered near the top of the pulse when the current in the primary winding of the transformer crosses zero value.

The discharge chain C_1, R_2-R_3 maintains the discharge current through the thyratron in a few tens of microseconds, thereby preventing fast afterpulses. Slow processes are suppressed by leakage of charges through the secondary winding of transformer. Besides that the reversal magnetization of the transformer produces negative potential of several tens of volts at the diode set.

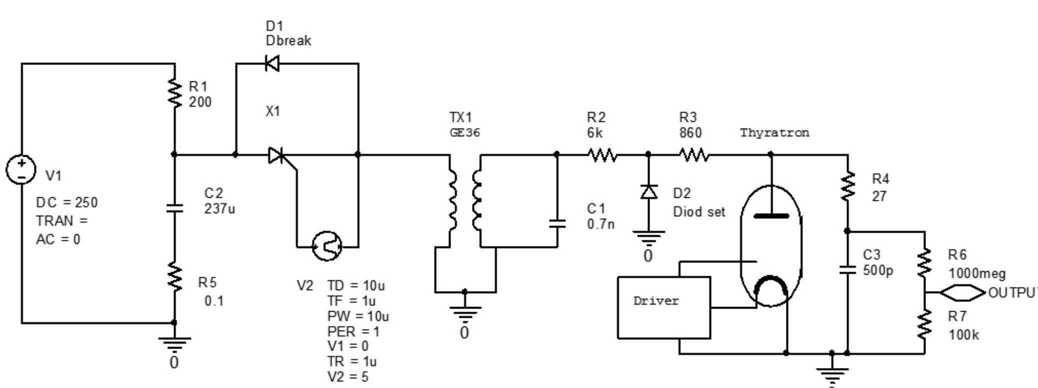

Figure1: PSPICE model of the power supply circuit. C_3-equivalent load, R_6-R_7 – divider VD-60

† fateev@sunse.jinr.ru

ISBN 978-3-95450-181-6

GENERATOR OF HIGH-VOLTAGE PULSE FOR HIGH-CURRENT ACCELERATOR OF DEUTERON WITH LASER STARTS

A.A. Isaev, E.D. Vovchenko, K.I. Kozlovskij, A.E. Shikanov, National Research Nuclear University "MEPhI" (Moscow Engineering Physics Institute), Moscow, Russia

Abstract

The report deals with the source of pulsed high voltage, and simultaneously, source of the pulsed current for the magnetic insulation of electrons near the cathode that was developed for a high-current accelerator of deuterons with laser-plasma anode. The accelerating voltage up to 400 kV and ion current about 1 kA have been achieved. The current in the spiral inductor has reached 5 kA and it excludes breakdown between the cathode and anode for 0.5 µs. For synchronization of physical processes in accelerator of deuterons with pulsed power, the laser control is applied.

INTRODUCTION

Currently for a number of applied problems of geophysics are used small-size pulse neutron generators [1]. The sources of neutrons with gas-filled or vacuum accelerating tubes are most developed and used in such researches. The alternative schemes of the neutron generator based on vacuum diode with coaxial electrode geometry and laser plasma as an efficient source of deuterons [2, 3] are developing in addition to these researches. In this diode is used the direct acceleration of deuterons to cathode and isolation of the electron current by using magnetic field. The laser plasma is generated by using of Nd: YAG laser with a wavelength of 1.06 µm and contains deuterons produced from TiD target placed at the anode. Diode system is placed in a vacuum chamber with a residual pressure of 10^{-2} Pa.

For diodes with coaxial geometry of electrodes, there are two possible schemes of suppression of electron current: a field of permanent magnets with azimuthal symmetry [4] and pulsed magnetic field of the spiral inductor [5]. Analysis of computer experiment showed that a permanent ring magnet does not provide the reliable insulation of electronic current near the poles. This leads to a rapid breakdown of the diode gap and decreasing the accelerating voltage.

In diodes with pulsed magnetic insulation, these problems occur to a lesser extent. In this case, for effective magnetic insulation it is necessary to synchronize three processes: expansion of a laser plasma, the formation of accelerating voltage and generation of the increasing magnetic field. To solve this problem the authors have developed the original scheme of the pulsed power supply, in which the laser-triggered gap runs Marx generator of the high voltage (U ≈ 400 kV) and the magnetic field generator with high current (I ≈ 10 kA). The features of the coordinated work of these generators with physical processes in the accelerator diode is considered in this article.

THE MARX GENERATOR

A high-voltage Marx generator is the main part of the pulsed power supply. The generator is made according to the scheme with unipolar charging and without change of the polarity of the output voltage. It consists of 30 stages (n = 30), each of them uses two capacitors K15-4 connected in parallel with a total capacitance of C_0 = 2 x 4700 = 9400 pF. In the charging circuits is used a high-voltage resistor with resistance R_0 = 16 kΩ. Each of stages stored 1.0 – 1.7 J of energy at a charging voltage of 15 –18 kV. Open circuit voltage is 400 kV, capacitance in peak is $C_{marx} = C_0 / n$ = 310 pF.

In the first stage of the Marx generator is applied the laser-triggered gap, the second stage uses the field distortion gap. In the rest stages of the Marx generator installed uncontrolled spark gaps. All gaps operate in air at atmospheric pressure.

Stable running of the laser-triggered gap (*LG*) with a time delay of not more than 50 ns is obtained at energies of laser are more W ≥ 80 mJ. In this case, the main energy of the laser pulse (85− 90%) is directed to the laser target. Note that the use of laser control greatly simplifies the synchronization of Marx generator with a laser plasma.

The field distortion gap (*FDG*) provides reliable switching of the second stage. To run this gap in the first stage of the Marx generator attached simple high-voltage generator. Its principle of operation is based on fast discharge of the capacitance (C = 470 pF) on the pulse transformer because of the switching of the laser-triggered gap (Fig. 1). Transformer is made on a rod core of ferrite M400HH. The number of turns in the primary and secondary windings of the transformer is equal to w_1 = 5 and w_2 = 25, respectively.

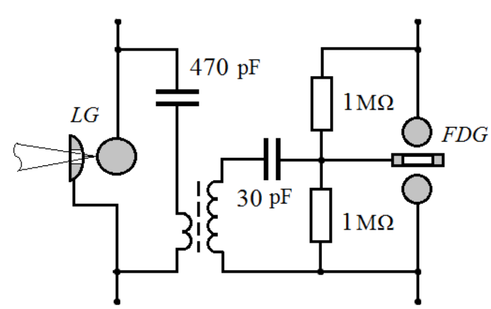

Figure 1: Electrical circuit of the simple high-voltage generator for switching field distortion gap (*FDG*).

In addition, more stable running was observed when the low-voltage electrode of gaps in the second, third and fourth stages of Marx generator was connected to the

ISBN 978-3-95450-181-6

THE AUTOMATION OF ENERGY RAMPING FOR THE MAIN STORAGE RING OF KSRS

Y. Krylov, E. Kaportsev, K. Moseev, N. Moseiko, A. Valentinov, NRC Kurchatov Institute, 1 Kurchatov sq., 123182 Moscow, Russia

Abstract

Kurchatov Synchrotron Radiation Source (KSRS) is the complex of electron synchrotrons specialized as a source of synchrotron radiation. The running cycle of KSRS main storage ring includes the energy ramping from 450 MeV up to 2.5 GeV. Fast and reliable energy ramping algorithm was developed and implemented at KSRS main storage ring. Using the hardware decisions on the basis of the NI units and CAN-bus interface, the control system is developed and launched for the power supplies of magnetic elements.

ENERGY RAMPING PROCESS

Magnetic system of KSRS main ring includes one family of bending magnets, 6 families of quadrupole lenses, two families of sextupole lenses for chromaticity correction [1]. The supply current of the bending magnets varies from 1270 A up to 7200 A, it determines the machine energy. The currents of the quadrupole power supplies vary from 80 A up to 760 A depending on the energy and number of the family. The currents of sextupole power supplies vary from 0.4 A up to 8 A. As a result saturation of iron exists at high energy, while residual magnetization manifests at low energies. Thus, a simple proportional increase of the currents will lead to the betatron tune shifts during energy ramping.

The process of energy ramping between injection energy 0.45 GeV and working energy 2.5 GeV consists in proportional change of magnetic field in bending magnets, field gradients in quadrupole and sextupole lenses. To facilitate the energy ramping process, 9 intermediate regimes were introduced at a distance of 10 - 20% in energy one from another. The regime means list of power supply settings. Magnetic measurements were conducted to determine right currents for all power supply families in each regime. Field in bending magnets was measured with an accuracy of 0.00001 using NMR sensor. For the quadrupole lenses measurements were carried out by Hall effect sensor with an accuracy of 0.001. Relative changes of the field gradients in each family in all intermediate regimes were measured [2].

Complicated algorithm with 9 intermediate regimes (collections of power supplies settings) was developed to produce fast and efficient energy ramping. The correction of closed orbit, betatron tunes and chromaticity is accomplished in each regime in static conditions. Special file is used to provide acceleration or deceleration of power supplies in dynamic conditions. This scheme allows to compensate betatron tune shifts during energy ramping. Power supplies are not stopped on intermediate regimes; speed of current changing is continuous function of time.

Fast and reliable energy ramping algorithm was developed and implemented at KSRS main storage ring [2]. Whole process takes 2 minutes and 40 seconds, beam losses doesn't exceed 2 – 3 %, betatron tune shifts are less than 0.015.

For more accurate reproduction of the results standard demagnetization cycle was introduced. After the work on the energy of 2.5 GeV currents of power supplies of the magnetic elements rise above the maximum working value, then gradually, over 80 seconds, fall below the minimum values of the injection energy, then regime of injection is restored. In every state a 30 seconds pause is maintained. The practice showed that after this demagnetization cycle betatron tunes returned to its initial values with a good accuracy of about 0.003.

KSRS MAIN RING CONTROL SYSTEM

KSRS control system (CS) is the multilayer and multiprocessor design consisting of three levels: executive, server and operator (see in Figure 1).

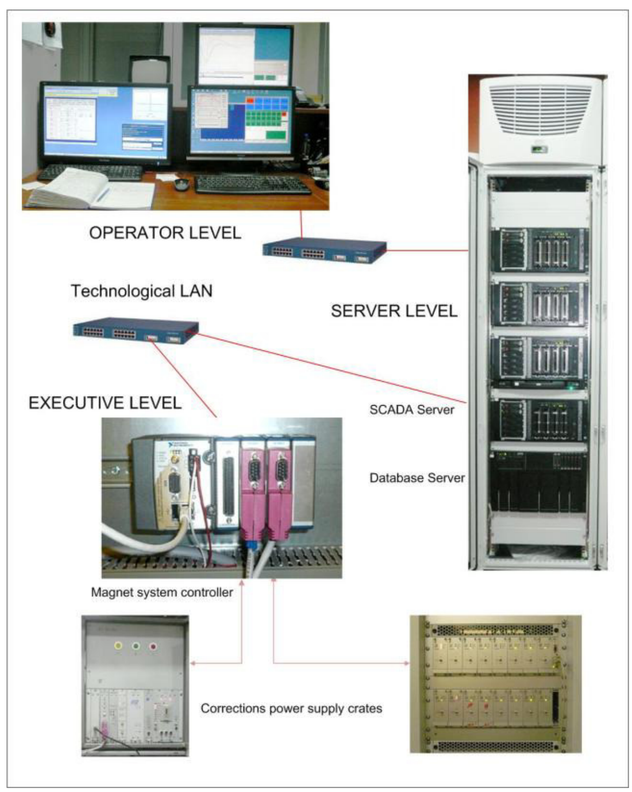

Figure 1: KSRS magnet system control.

ISBN 978-3-95450-181-6

SOLID-STATE MODULATORS FOR PARTICLE ACCELERATORS

A. A. Zavadtsev†, D. A. Zavadtsev, D. V. Churanov, D. A. Zybin,
Nano Invest, LLC, Moscow, Russia

Abstract

A series of the wide parameter range solid-state high-voltage modulators has been developed and built as a power supplies for the magnetrons and the klystrons in the particle accelerators. The series includes 60 kV/100 A/6 μsec modulator with pulse transformer for 3 MW magnetron, 60 kV/300 A/6 μsec direct switch modulator for 6 MW multi-beam klystron, 110 kV/80A/6 μsec direct switch modulator for 3 MW klystron, 130 kV/100 A/6 μsec modulator with pulse transformer for 5 MW klystron, 250 kV/250 A/6 μsec modulator with pulse transformer for 20 MW klystron. The last modulator is under construction. All other modulators have been supplied to customers in Russia as well as in Europe.

INTRODUCTION

The solid-state modulators are used to feed klystrons and magnetrons in the particle accelerators more and more often. These modulators include the semiconductor HV switch (IGBT or MOSFET) instead of the tube one in traditional modulators. The main advantages of the solid-state modulator are low voltage on each switch connected in series, long lifetime, and easy control.

Several schemes of the solid-state modulator are used at the modulator building.

The first modulator type is a series switch. It includes serial IGBT switches discharging the full-voltage capacitor to the load (klystron) [1, 2].

The second modulator type is a high-voltage pulse generator with parallel charging of the capacitors and discharging them to the load in serial circuit. V. K. Arkadiev and N. V. Baklin have built this generator with mechanical switch in 1904. E. O. Marx suggested the use of the discharger as a switch in this generator in 1924. IGBT is used as a switch in this generator now [3]. The voltage in the load is a sum of the capacitor voltages.

These modulator types can be used with the pulse transformer.

The next modulator type includes a number of modules, each of which includes the capacitor, the switch and the pulse transformer [2]. The secondary windings of these pulse transformers are connected in series, so the load voltage is a sum of module voltages.

Another approach is used in the modulator including one complex pulse transformer with several primary windings and one secondary one [4]. The modules are connected to the primary windings. The magnetic flows of the primary windings are added in the pulse transformer core. So the secondary voltage is a sum of primary voltages times transformer ratio.

MODULATOR WITH ADDING MAGNETIC FLOW

The modulator with adding magnetic flow in the pulse transformer has been built for HV feeding of 2.5-3 MW S-band magnetron in the electron linac [5].

Eleven 1 kV modules are connected to eleven primary windings of the pulse transformer. All equipment is located in the oil-tank as this is shown in Figure 1.

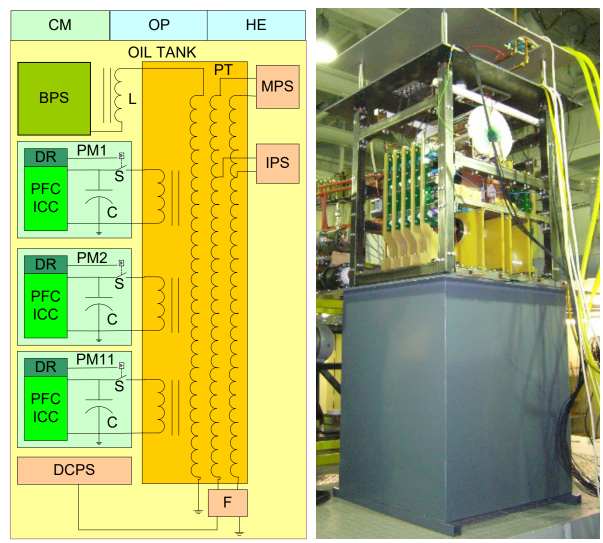

Figure 1: Modulator with adding magnetic flow.

Main modulator parameters are

- voltage 55 kV;
- current 100 A;
- pulse length 0-6 μsec;
- average power 4.5 kW;
- bifilar secondary winding for power supply of magnetron filament;
- terminals at secondary winding for reduced injector voltage.

DIRECT SWITCH 60 KV MODULATOR

The direct switch solid-state Arkadiev type modulator has been developed for 6 MW multi-beam klystron. Two modulators have been built for the 40 MeV electron linac [6]. Each modulator includes 6 modules with 10 levels of the Arkadiev generator. The modulator is shown in Figure 2, in the cabinet, where the klystron is located too.

Main parameters of the modulator are:

- voltage 60 kV;
- current 300 A;
- pulse length 0-6 μsec.

† azavadtsev@yandex.ru

ISBN 978-3-95450-181-6

SWITCHING NETWORK UNITS FOR HIGH CURRENTS AND VOLTAGES OR PLASMA APPLICATIONS

F. Burini, M. Pretelli, G. Taddia, S. Tenconi, OCEM Power Electronics, Bologna, Italy
A. Lampasi, P. Zito, National Agency for New Technologies, Energy and Sustainable Economic Development (ENEA), Frascati, Italy

Abstract

OCEM and ENEA gained a wide experience in the design and experimental characterization of fast and accurate switching systems for high DC currents, as required to control magnets and superconductors. The exploited idea consists in inserting an electronic switch in parallel to a fast electromechanical switch in air, to combine the benefits of both devices. The electronic switch is turned on and off to support the electromechanical commutations, reducing the jitter to tens microseconds and limiting the arcs that would reduce the system lifetime. During the performed tests, DC currents up to 20 kA were diverted in less than 100 µs with good repeatability. In case of emergency, the current can be interrupted in few tens of milliseconds. If necessary, a resistor can be inserted in parallel to the switch to dissipate the energy trapped in inductive loads or to produce desired overvoltages (a voltage up to 5 kV was reached in this configuration). Specific circuits were designed to preserve the components from transient voltage overshoots. This switching system is expected to work for 10000 operations without major maintenance. The developed solutions may be extended to many relevant applications as particle accelerators and HVDC networks.

INTRODUCTION

The poloidal field (PF) coils, as the central solenoid (CS), of a new Tokamak generally consist of a number of superconducting coils, each connected to a dedicated power supply (PS) circuit. To initiate the plasma breakdown, an abrupt current derivative shall be produced almost simultaneously in all the PF coils, to produce an adequate voltage transient across them [1], [2]. As the power and voltage ratings of the PSs are limited, to about 20÷30 MVA and ±1 kV dc, a Switching Network Unit (SNU) is put in series to each of the poloidal circuits. An interruption nominal voltage up to 5 kV, a DC current up to 20 kA and an opening/closing time lower than 1 ms are required. The simultaneous opening of the SNUs shall be synchronized within 0.5 ms. The coil inductance is normally very high (up to tens of mH), so the current must be diverted into resistor banks R1 (the R1 resistance value can be pre-adjusted by selectors, in order to match the maximum current to be interrupted). After plasma breakdown and current ramp-up, the SNU hybrid switch shall be reclosed and from this time on the PSs will control the current in the circuit. The basic circuit diagram of Hybrid Switching Unit is reported in Fig. 1.

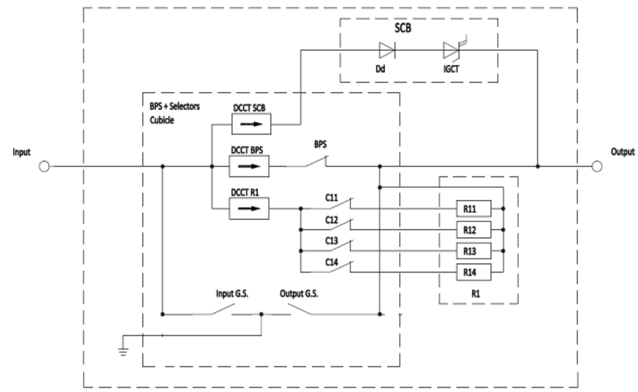

Figure 1: Functional Scheme of the hybrid SNU.

CHARACTERISTICS AND OPERATION OF THE HYBRID SWITCHING CIRCUIT

Operation and Ratings of the Switching Network Unit

Table 1 reports the main SNU parameters, whose detailed power circuit diagram is reported in Fig. 2. The opening and re-closing of the hybrid switch (hereafter referred to as SS) can be repeated every thirty minutes, generally for about ten hours per day; the SS structure improves and adapts the use of a solid state Static Circuit Breaker (SCB), in parallel with the main electromechanical By-Pass Switch (BPS). The use of a hybrid circuit breaker for DC applications is in principle not new and has been proposed and developed in the past for some Tokamak and Naval applications [3], [4].

When applied to Tokamaks, the reasons of the hybrid configuration come from the specific working cycle: the central solenoid current is ramped up for a maximum of 60 s and then, at a predefined time, the voltage across them is abruptly reversed. So, while the mechanical BPS carries the current for most of the operational time, the SCB “masks” the inadequate velocity and repeatability of the BPS in commutation, giving the hybrid switch the precision timing and velocity of solid state devices; moreover, the power dissipated in the arcing across the BPS contacts is greatly reduced and the operational life of mechanical contacts is correspondingly increased.

The Hybrid SNU detailed circuit diagram is reported in Fig. 2. It is worth pointing out that even though the Base Power Supplies are normally able of four-quadrant operation, the SCB are unidirectional devices, since they operate at the beginning of the tokamak current pulse; but

ISBN 978-3-95450-181-6

300 kV HIGH-VOLTAGE SOURCE WITH UP TO 15 kW OUTPUT POWER

D.V. Senkov, I.A. Gusev, A.Yu. Protopopov, D.N. Pureskin, M.A. Scheglov,
Budker INP, Novosibirsk, Russia

Abstract

The presented report contains the description of high-voltage source with output voltage up to 300 kV and output current up to 50 mA. The source consist of the chopper with IGBT switches working with a principle of pulse-width modulation and the full H-bridge converter with IGBT switches, both working on programmed from 15 to 25 kHz frequency, and the high voltage transformer powering the eight-stage multiplier with the additional capacity filter at output. The transformer and multiplier both are made in common volume separated on oil tank part with silicon oil for transformer and SF6 part for multiplier. The additional capacity filter provides low ripple and noise level in working range of output currents. The source can operate in normal mode with series of high-voltage breakdown in output voltage. In the high-voltage breakdown the released in load and matching circuit energy is less than 40 J at maximum operating voltage 300 kV. The efficiency of system is more than 80% at the nominally output power 15 kW. The description of the source and the test results are presented.

DESCRIPTION

The presented source was designed for accelerator electron gun of Siberian Synchrotron and Terahertz Radiation Centre. That was reason for some specific terms like: strong reliability to high-voltage breakdown, low energy dissipated in high voltage breakdown, low voltage ripple for maximal power operation. The energy is dissipated in components of source and in the load during the high voltage breakdown less than 30 J for 260 kV operations. The basic characteristics of high-voltage source are shown in Table 1.

OVERVIEW

The circuit diagram of power part of high-voltage source is shown in Fig.1. The high-voltage source consists of the 20 kHz power converter with insulated gate bipolar transistors (IGBT) as switches (part A) and high-voltage transformer with the four-stage multiplier (part B). The power converter consists of 3-phase rectifier VD1, electromagnetic (EMI) filter F1, switch SW1, rectifier's filter capacitors C1-C2, 20 kHz chopper with IGBT switch Q1, 20 kHz inverter with IGBT switches Q3-Q6, output filter circuit L2 C5 C6, and isolation transformer T1.

Input Rectifier

EMI filter is used to eliminate high-frequency noise to the power line from the source. 3-phase rectifier and filter C1-C2 is used to convert input AC 3-phase voltage 380 V 50 Hz to DC-link 550-600 V voltage. Contactor SW1 consists of 2 groups of contact: the first is used for soft start of converter and another is used for normal operations.

Table 1. Basic Characteristics of High-Voltage Source

Parameter	**Unit**			
		Min	**Nom**	**Max**
Output voltage	kV	10	260	300
Output current	mA		15	50
Output power	kW			15
Voltage ripple (full load)	%			0.2
Long term stability	%			0.1
Transient time	ms		50	
Converter frequency	kHz	15	20	25

Chopper

The chopper switch Q1 is operated with principle of pulse-width modulation on programmed from 15 kHz to 25 kHz frequency synchronously with inverter. The output voltage of chopper is changed from 10 to 450 volts DC by control circuit to obtain the required output high voltage of source.

Inverter

Full-bridge inverter Q3-Q6 converts DC voltage from chopper's capacitors C3-C4 to AC voltage with programmed from 15 to 25 kHz frequency.

Filter Circuit

The matching circuit consists of elements C5 and L2 and low pass filter L2 C6 are used for minimizing transient process and for improving efficiently of design. The matching circuit is used for protection reasons. When there is a high voltage breakdown or over current the matching circuit limits the rate of current rise in the inverter. Magnetising inductance of high voltage transformer, its capacitance calculated to primary side in parallel with C6 and the matching circuit organize low-pass filter for all high harmonics of inverters rectangular waveform voltage. That way, sinusoidal voltage is feed in the high-voltage transformer, because all high harmonics are filtered. In other case, the presence of high harmonics causes power dissipation in the coils because of skin-effect. Also this harmonics can induce the singing in the winding of high-voltage transformer and this effect increases the output zero load voltage and complicates the reduction transient over voltage.

ISBN 978-3-95450-181-6

HIGH-PRECISION RAMPED HIGH-VOLTAGE SOURCE WITH UP TO 50 kV OUTPUT VOLTAGE

D.V. Senkov, I.A. Gusev, A.A. Zharikov, A.M. Batrakov, A.Yu. Protopopov,
Budker INP, Novosibirsk, Russia

Abstract

This report describes the precision high-voltage ramped high-voltage power system. The output voltage up to 50 kV with 10 ppm precision. The power system consists of the 3 kW high-voltage source based on multiplier, precision high-voltage divider with digital interface and high-voltage discharge switch to provide low ramp-down time for output voltage. The power system is planned to use in the NIKA booster electron cooler project. The description and test results are presented.

DESCRIPTION

The presented source was designed as part of electron cooler for booster ring of NIKA project (JINR, Dubna). The booster operating circle scenario is shown on Fig. 1. The electron cooling is planned to use at the injection plato and at the extraction plato. That was reason for some specific terms like: low transient process time after voltage increase, high voltage stability (10 ppm) in the full range of output voltage. The high-voltage terminal (see cooler electrical diagram Fig. 2) is the sourse of 2-3 mA current ripples at 150 and 300 Hz. So the high-voltage source have to suppress load voltage variation generated by this ripples to the 10ppm level. The basic characteristics of high-voltage source are shown in Table1.

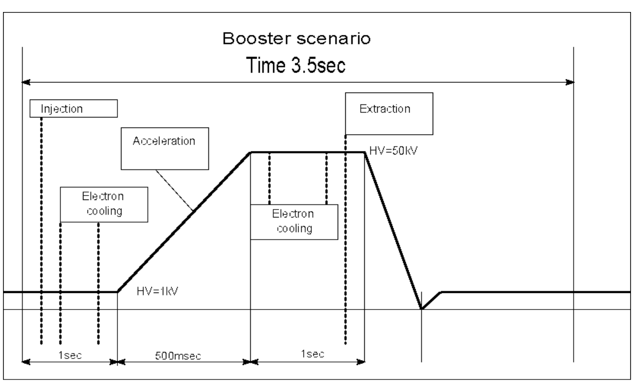

Figure 1: Booster operating cycle scenario.

Overview

The high-voltage source consists of the 20 kHz power converter, high-voltage transformer with the two-stage multiplier (part B) the separate precision high-voltage divider with digital output (Part C) and the ripple suppressor (Part D). The power converter with high-voltage multiplier generates 0-50 kV output voltage. The precision high-voltage divider is used for feedback loop. The analogue ripple suppressor is used to decrease output voltage variations at 150 and 300 Hz caused by the external (from load) current ripples. The suppressor increase effective gain of feedback system at these frequencies.

Table 1. Basic Characteristics of High-Voltage Source

Parameter	**Unit**			
		Min	**Nom**	**Max**
Output voltage	kV	0.5	50	55
Output current	mA		0.2	10
Output power	kW			3
Voltage ripples(nom load)	ppm			10
Long term stability	ppm			10
Transient time	ms		100	
Converter frequency	kHz		20	

Power Converter

The power converter uses two DC-link stage to decrease voltage ripples. First AC-DC converter supply its output with stabilized 50 VDC voltage. The boost stage can increase this voltage to level 50-250 V in depends on specified power source output voltage. This boost stare feeds the 20 kHz full-bridge inverter operates with PWM modulation to precision regulate the output voltage.

High-Voltage Transformer and Multiplier

Sectioned high-voltage transformer consists of two high voltage sections, joined in series. The nominal output voltage of transformer is 30 kV. The multiplier has two parallel connected brunches. Each brunch is the same.

The multiplier brunch is complete design and it includes multiplier, output filter capacitors, output current sensor and protection system voltage divider resistors. Output filter capacity is chosen to decrease output voltage 40 kHz ripples less than ±0.01% for full load operation, and 10ppm ripples at nominal output current. The silicon oil [1] is used as insulator the high voltage volume.

High-Voltage Divider

The separate precision high voltage divider is used for feedback system. This divider is located is separate oil tank heated to 40 °C. Its consists of two independent divider with and precision ADC board. The fiber link is used for output voltage data transmit to power source feedback system. In addition, the voltage information

ISBN 978-3-95450-181-6

POWER SUPPLIES FOR IHEP NEGATIVE HYDROGEN IONS SOURCE

B.A. Frolov, National Research Centre “Kurchatov Institute” State Research Center of Russian Federation – Institute for High Energy Physics, Protvino, Moscow Region, Russia
V.S. Klenov, V.N. Zubets, Institute for Nuclear Research, Russian Academy of Science, Moscow, Russia

Abstract

The source of negative hydrogen ions is constructed at IHEP for the implementation of multiturn charge-exchange injection to increase the intensity of IHEP buster. Surface-plasma ion source (SPS) with Penning discharge is selected as source of H-minus ions. A set of power supplies for SPS which includes the extraction voltage power supply, the discharge power supplies, the hydrogen gas pulse valve power supply, cesium oven and cesium storage device temperature controllers was designed, constructed and tested on the equivalent loads. This set of power supplies will allow to commission and test the ion source with the beam extraction energy up to 25 keV and repetition rate of 25 Hz.

INTRODUCTION

For injection into IHEP LU-30 RFQ the source of H-minus ions should generate the beam with current not less than 50 mA, pulse duration up to 200 mks, repetition rate - 25 Hz, normalized rms emittance no more then 0,25 mm*mrad, e/H^- ratio < 5 providing a long-term stability and reproducibility of the parameters [1]. To provide these requirements surface-plasma ion source based on the Penning discharge cell with an axially symmetric emission aperture the two-stage system of cesium supply and pulsed gas valve is developed.

A power supply system which includes the extraction voltage power supply, the Penning gas discharge power supplies, the hydrogen gas pulse valve power supply, cesium oven and cesium storage device temperature controllers should provide the operation of the ion source.

GAS DISCHARGE POWER SUPPLIES

Gas discharge power supplies must provide the ignition of discharge, burning high-current pulsed glow discharge with a current up to 150 A in the conditions when the internal resistance of the discharge is less than 1 ohm with pulse durations of 25 up to 200 microseconds and pulse repetition rate of 25 Hz.

Gas discharge power supply consists of the following components: a thyristor unit, transistor unit, power supply, isolation transformer. The external view of the front panel is shown in Fig. 1.

Thyristor unit generates pulses with fixed amplitude of 800 V. These pulses are applied through the 30 ohms limiting resistance to the primary winding of the output isolation transformer for “ignition” of the high-current discharge which afterwards is picked up by the stabilized current of the transistor block.

Transistor unit generates amplitude-adjustable powerful current pulses with the stabilization on pulses top in the primary winding of output isolation transformer. The regulating element is the transistor MG400H1FK1.

Power supply unit is the power source for the transistor unit with the ability to turn off on the "alarm" signal received from the transistor unit. The power supply unit provides also the voltage for ± 12 V transistor and thyristor units.

Thyristor unit, transistor unit and power supply unit are designed in the same construction design «Vishnya»

Figure 1: General view of the gas discharge power supplies.

Discharging current generator prototype tests on the equivalent load were carried out. The 0.5 Ohm, 1 Ohm, 3 Ohms resistances of appropriate power were used as equivalent load. Tests were conducted at the pulses repetition rate of 25 Hz. The waveform of the output current on resistance of 1 Ohm is shown in Fig.2.

Tests of the gas discharge power supplies prototype were also conducted when working with the H-minus ion source of injector INR RAS linac. The waveforms of the ion source operating parameters are shown in Fig.3. The top beam (blue) is the voltage at the discharge, the lower beam (yellow) is the discharge current.

These tests demonstrated the ability of gas discharge power supply to provide the required parameters in various modes of source operation including the discharge ignition, the transition to a low-voltage (cesium) regime and work in conditions of intensive breakdowns in the 15 kV extraction gap.

ISBN 978-3-95450-181-6

THE STUDY OF THE ELECTRICAL STRENGTH OF SELECTED INSULATORS WITH A DIFFERENT SHAPE OF THE SURFACE

Ya.A. Kolesnikov#, A.A. Gmyrya, D.A. Kasatov, A.M. Koshkarev, A.S. Kuznetsov, A.N. Makarov, E.O. Sokolova, I.N. Sorokin, I.M. Shchudlo, S.Yu. Taskaev, Budker Institute of Nuclear Physics, SB RAS, Novosibirsk, 630090 Russia

Abstract

In the BINP SB RAS was proposed and created a source of epithermal neutrons for BNCT. The proton beam obtained on a tandem accelerator with vacuum insulation. Sectionalized demountable feed through insulator is an integral part of the accelerator. Voltage from the high voltage source distributed to the electrodes via resistive divider. Because of the small amount of current (hundreds of microamperes) flowing through the divider, dark currents that occur in the accelerating gaps, can significantly affect the uniform distribution of the potential along the accelerating channel, and, consequently, on the beam transportation. Therefore there is a need to change the design of the feed through insulator which will allow to set potentials at the electrodes directly from the high voltage rectifier sections.

To study the feasibility of such changes has been designed and built an experimental stand, in which a single insulator with double height subjected to the same conditions as in accelerator. On the experimental stand was studied electrical strength of ceramic and polycarbonate insulators with a different shape of the surface. The paper presents the results of experimental studies of insulators. Their application will get rid of the voltage divider inside the feed through insulator and realize the scheme which allows to set potential on the electrode gaps directly from the rectifier section. This will increase the operating voltage of the accelerator and its reliability.

INTRODUCTION

In 1998, for high-current proton beams BINP proposed a new type of accelerator - tandem accelerator with vacuum insulation. At present, on the accelerator neutron source there were conducted various experiments for the development of Boron Neutron Capture Therapy (BNCT) [1]. The principle of BNCT technique is simple and elegant: a boron-containing agent is injected in patient's blood, and then part of the body with tumor is irradiated with neutrons. During the nuclear reaction $n(^{10}B, ^{7}Li)\alpha + \gamma$ most of the energy (84%) is allocated within $3 \div 10$ µm, which matches with the size of the mammalian cells. Illustration of BNCT idea is presented in Figure 1.

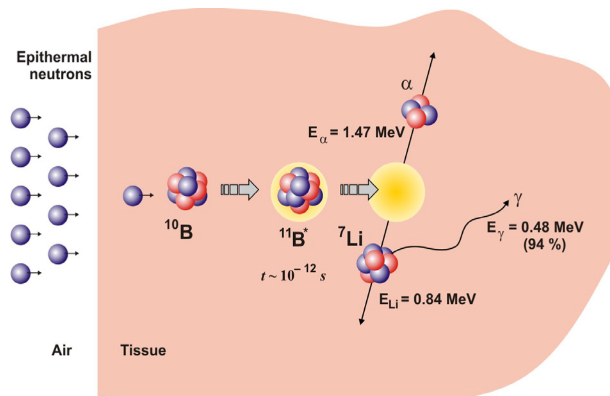

Figure 1: Principle of BNCT.

DESIGN OF THE ACCELERATOR

Figure 2 presents the scheme of the tandem accelerator with vacuum insulation. The outgoing beam from the source of negative hydrogen ions *1* with 23 keV energy and 5 mA current is rotated by 15° in a magnetic field , focused by a pair of magnetic lenses *2*, injected into the accelerator and accelerated up to 1 MeV. In the argon stripping target *7*, mounted inside the high voltage electrode *5*, negative hydrogen ions are converted into protons. Then protons are accelerated by the same potential 1 MV up to 2 MeV. The potential at the high voltage electrode *5* and five intermediate electrodes *6* of accelerator supplied from the high voltage source *10* using a feedthrough insulator *9*, wherein the ohmic divider is installed. Pumping of the gas is maintaining by turbo-molecular pumps *8* installed on the ion source chamber and at the exit of the accelerator, and a cryogenic pump *4* via jalousies [2].

Accelerator produces a stationary proton beam with 2 MeV energy and 5 mA maximum current with 0.1% high energy monochromaticity and 0.5% current stability [3]. On the accelerator the generation of neutrons is achieved and the effect of neutron radiation on cell cultures is studied [4]. For the therapy it is necessary to increase the voltage up to 1.15 MV and is desirably to increase proton beam current to the value 10 mA.

Figure 3 shows one of the main elements of the accelerator – sectioned assembled feedthrough insulator using which voltage from the high voltage rectifier is applied to the central electrode and the intermediate electrodes.

#i.kolesnikov@g.nsu.ru

ISBN 978-3-95450-181-6

OBTAINMENT OF 5 mA 2 MeV PROTON BEAM IN THE VACUUM INSULATION TANDEM ACCELERATOR*

I. Shchudlo#, D. Kasatov, A. Koshkarev, A. Makarov, Yu. Ostreinov, I. Sorokin, S. Taskaev,
BINP and Novosibirsk State University, Novosibirsk, Russia

Abstract

In BINP the neutron source for BNCT based on proton accelerator was designed and built. It is necessary for the therapy to ensure a stable proton beam current of not less than 3 mA with energy 2 MeV. During the injection of negative hydrogen ion beam into the accelerator the unwanted charged particles are produced, affecting the stability of beam parameters. The article describes methods of suppression of undesirable charged particles and the results of experiments.

INTRODUCTION

Boron-neutron capture therapy (BNCT) [1] is a promising method of malignant tumours treatment. For implementation the technique in clinical practice the accelerator based compact epithermal neutron sources with energy of protons from 2 to 3 MeV and a current at least of 3 mA are required. To solve this problem in BINP a new type of particle accelerator was proposed and developed – vacuum insulation tandem accelerator. In the accelerator construction the high rate of acceleration of ions and the insulator placed remote from acceleration channel are implemented [2]. After reducing of dark current to an acceptable level [3], optimizing of injection of negative hydrogen ion beam into the accelerator [4] and optimizing of stripping gas target [5], the proton beam current increased from initial values of approximately 140 μA [6] to a value 1.6 mA [7], stable over time more than hour. While explaining the causes of the current limitation in the acceleration channel a significant flow of electrons and the counter-flow of positive ions generated in the accelerating channel and in the stripping target were detected and measured [8]. The paper describes details of further modernization of the accelerator and presents experimental results on the suppression of unwanted fluxes of charged particles and increasing proton beam current.

EXPERIMENTAL RESULTS

Scheme of the vacuum insulation tandem accelerator is shown at Fig. 1. Negative hydrogen ion beam with an energy of 23 keV and current of 6 mA leaves the source *1*, after that it is rotated in magnetic field at an angle of 15°, focused by a pair of magnetic lenses *2*, injected into the accelerator and accelerated to an energy of 1 MeV. In the gas (argon) stripping target *7* mounted inside the high-voltage electrode *6*, negative hydrogen ions are converted into protons, which are accelerated to an energy of 2 MeV by the same potential. To the high-voltage *6* and five intermediate electrodes *5* the potential is supplied from a high voltage power supply (sectional rectifier) *9* (most of the source is not shown) through the insulator with resistive divider *8*. Turbo molecular pumps *10* installed in the ion source chamber and in the output of the accelerator, and a cryogenic pump *4* through the blinds in high-voltage electrodes provide vacuum pumping.

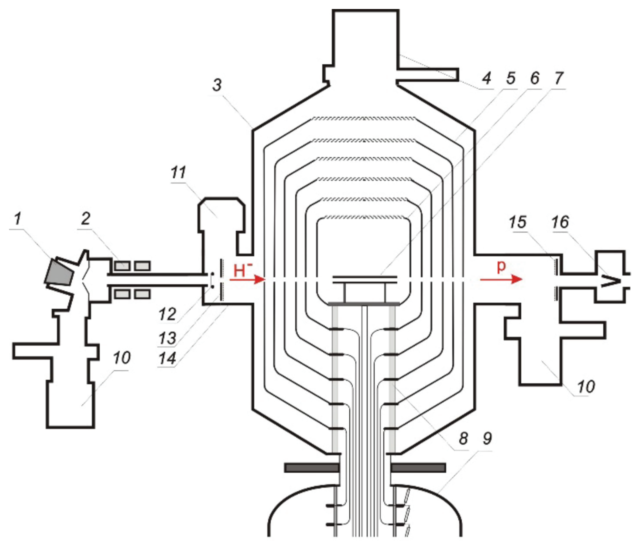

Figure 1: Vacuum insulation tandem accelerator. *1* - negative hydrogen ion source, *2* - magnetic lenses, *3* - accelerator, *4* - cryogenic pump, *5* - intermediate electrodes, *6* - high-voltage electrode, *7* - gas stripping target, *8* – insulator, *9* - high voltage power supply, *10* - turbo molecular pump, *11* - cryogenic pump, *12* – ring, *13* - metal cooled aperture and detector with a grid, *14* - input vacuum volume, *15* - detector with a grid, *16* - Faraday cup. The arrows indicate the direction of the negative hydrogen ion beam (H^-) and protons (p).

Modernization of the accelerator was as follows. The water-cooled metal diaphragm *13* with a 20 mm hole with possibility of centring along the beam axis was installed in the vacuum chamber *14* at the accelerator input. That aperture is considered to reduce the flow of gas and ultraviolet from the source of negative hydrogen ions in the accelerating channel. At the upper flange of input vacuum volume through the slide valve DN 250 the cryopump On-Board 250F (CTI-Cryogenics, USA) *11* was installed. This should improve the vacuum conditions in the beam-transporting channel and in the accelerating channel. In front of the cooled diaphragm a metal ring *12* was installed. Negative potential applied on this ring should suppress the flow of electrons that accompany the beam of negative

* The study was funded by the grant from the Russian Science Foundation (Project No.14-32-00006) with support from the Budker Institute of Nuclear Physics and Novosibirsk State University.
#Cshudlo.i.m@gmail.com

ISBN 978-3-95450-181-6

LOSS ANALYSIS OF INSULATED CORE TRANSFORMER HIGH VOLTAGE POWER SUPPLY*

Y.F. Zhang, M.K. Li, H. Liang, T.Q. Yu, J. Yang#, J. Huang, Y.Q. Xiong, W. Qi, C. Zuo, L.G. Zhang, T. Liu
School of Electrical and Electronic Engineering, Huazhong University of Science and Technology, Wuhan, 430074, P. R. China

Abstract

Insulated core transformer (ICT) electron accelerator is an ideal prototype in low energy radiation processing industry, and ICT high voltage power supply is the essential apparatus. Conventional ICT high voltage power supply uses laminated silicon steel sheets as magnetic cores and works at 50 Hz. In a novel design of the ICT high voltage power supply, the magnetic cores made of ferrite material are adopted to increase the frequency and improve the performance. Focusing on the new scheme, the loss calculation of the high voltage power supply was carried out. The loss of ferrite magnetic cores and the windings was analysed and simulated.

INTORDUCTION

Insulated core transformers (ICT) are widely used in electron accelerators in irradiation processing industry [1]. Conventional ICT high voltage power supply uses laminated silicon steel sheets as magnetic cores and works at 50Hz. At present, the rapid developments of the fields of power electronics, electrical materials and high voltage technology make it possible to adopt new technologies and designs in ICT high voltage power supply, and a novel design of high frequency ICT high voltage power supply was proposed (see Fig. 1): ferrite magnetic cores, 4-phase structure and 5 kHz square wave as the excitation source are adopted [2]. As the frequency of the ICT is raised, the volume and the weight of the ICT high voltage power supply will be improved, and the output voltage will be more stable.

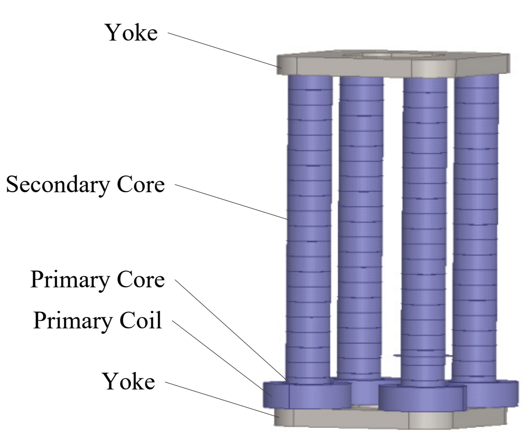

Figure 1: The 3D model of the 4 phase high frequency ICT.

*Work supported by National Natural Science Foundation of China (11305068)
#jyang@mail.hust.edu.cn

The high frequency ICT consists of 4 phases and each phase has a primary core and 20 secondary cores. There are insulated sheets to isolate the potential of the magnetic cores. Each secondary core has a rectifier circuit, and all rectifier circuits are connected in series to get the high DC voltage. With the existence of the insulated sheets, the leakage magnetic flux cannot be ignored. The induced voltage will be lower in the coils, which are further from the primary coil. The total number of the cores is 84 and there are also two yokes. The loss of magnetic cores cannot be neglected. The eddy current loss of the coils should also be considered with the high frequency of the excitation source and the leakage magnetic flux acts on the coils. These two kinds of loss need to be calculated when analyzing high frequency ICT efficiency.

FERRITE MAGNETIC COER LOSS

The magnetic core loss includes eddy current loss, hysteresis loss and excess loss. The rapidly changing magnetic flux density *dB/dt* will cause the induced voltage E(r, t), where r is the radius of the magnetic core. Because of the resistance of the ferrite core, the eddy current exists, which causes the eddy current loss per unit volume:

$$P_{\mathrm{e}} = \frac{1}{V}\cdot\frac{1}{T}\int_0^T\int_0^{r_0} dP_e drdt \tag{1}$$

Where V is the volume of the ferrite core, T is the time period, r_0 is the radius of the ferrite core, and dP_e is the instantaneous power which given by

$$dP_{\mathrm{e}} = \frac{E(r,t)^2}{R} \tag{2}$$

R is the equivalent resistance of the instantaneous induced current.

Using (1) and (2), we can obtain:

$$P_{\mathrm{e}} = \frac{1}{2\rho r_0 T}\int_0^T\int_0^{r_0} r^3\cdot\left(\frac{dB}{dt}\right)drdt \tag{3}$$

Transform the formula (3), the eddy current loss per unit volume is obtained finally by:

$$P_{\mathrm{e}} = \frac{U_1{}^2}{8\pi\rho N^2 A} \tag{4}$$

Where U_1 is the input excitation voltage, ρ is the resistivity of the ferrite core, A is the area of the cross section of the magnetic core, N is the number of turns. For the high frequency ICT, the waveform of the input excitation voltage is square, so the eddy current loss can be presented by [3]:

ISBN 978-3-95450-181-6

A NOVEL DESIGN OF INSULATED CORE TRANSFORMER HIGH VOLTAGE POWER SUPPLY*

M.K. Li, M.W. Fan, Y.F. Zhang, H. Liang, L. Yang, T.Q. Yu, J. Yang#, J. Huang, K.J. Fan, Y.Q. Xiong, W. Qi, C. Zuo, L.G. Zhang, T. Liu
School of Electrical and Electronic Engineering, Huazhong University of Science and Technology, Wuhan, 430074, P. R. China

Abstract

Insulated core transformer (ICT) high voltage power supply is an ideal model for industrial radiation accelerator at energy below 1MeV. Compared to the traditional scheme, a novel ICT high voltage power supply was put forward. Conventional silicon steel sheets were replaced with manganese zinc ferrites, raising working frequency from 50Hz to thousand hertz. Magnetic structure was changed from three-phase structure to four-phase structure. Accordingly, excitation voltage was changed from three-phase sinusoidal wave to square wave. Polyimide was chosen as insulation material instead of teflon or mica. A prototype of 400kV/50mA was designed, simulated and verified with the aid of finite element analysis software. To optimize the voltage distribution, corresponding flux compensation methods were raised to solve the problem of flux leakages.

INTRODUCTION

ICT high voltage power supply has been widely used in electron accelerator [1][2]. ICT is the kernel component of the accelerator, and its conventional magnetic core structure is shown in Fig.1. There are three groups of cores between the top yoke and the bottom yoke. Each group consists of a primary core and a plurality of segmented secondary cores. Each primary core is wound with primary coil. Each secondary core is wound with secondary coil and then connected to corresponding voltage doubler rectifier circuit, which converts AC voltage to DC voltage. Finally, all rectified voltages are connected in series to obtain the desired high voltage. Between all neighbouring cores are gaps filled with insulation materials of high dielectric strength. For the purpose of clarity, coils and circuits are not shown in Fig.1.

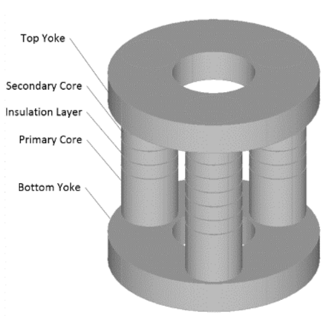

Figure 1: Structure of conventional ICT.

*Work supported by National Natural Science Foundation of China (11305068)
#jyang@mail.hust.edu.cn

The conventional design is as follows [3][4]: silicon steel sheets are selected as magnetic materials; three-phase sinusoidal wave with the working frequency of 50Hz is selected as excitation voltage; teflon or mica sheets with a thickness of several millimeters are selected as insulation material. When in operation, three-phase AC voltage (380V) is connected to delta-connected primary coils through a three-phase column type variable transformer, which controls the output voltage.

With the rapid development of power electronics, magnetic materials and insulation materials, new materials and technology can be introduced to improve the performance of ICT high voltage power supply, and the new design was proposed. Compared to the traditional scheme, it can effectively improve the efficiency of energy transfer, and reduce the volume of power supply and the requirement of rectified capacitance. It can finally achieve fast and precise control of the high-voltage output, and it's also stable and easy to maintain.

GENERAL DESIGN

Magnetic Material

Raising working frequency is an effective method to reduce the volume of ICT. As frequency increases, however, eddy-current loss of the silicon-steel sheet increases sharply, resulting in severe Joule heat and low efficiency. To solve this problem, manganese zinc ferrite is introduced. Compared to silicon steel, although the relative permeability and saturation magnetic flux density of manganese zinc ferrite fall, its electrical resistivity increases greatly, which effectively restrain the eddy-current loss and enable it to function well at high frequency.

Magnetic Structure

The magnetic structure of designed ICT is shown in Fig.2. To increase the breakdown voltage, the whole power supply is enclosed in an airtight steel barrel, fulfilled with sulfur hexafluoride at certain pressure. The working frequency can reach thousand hertz as manganese zinc ferrite is introduced. Consequently, the size of magnetic cores and the capacity of the rectifier capacitors decrease greatly. As magnetic structure is changed from three-phase structure to four-phase structure, excitation voltage is changed from three-phase sinusoidal wave to square wave consequently. This kind of structure improves the utilization of space and further reduces the volume of ICT.

ISBN 978-3-95450-181-6

NEW SUPERCONDUCTING LINAC INJECTOR PROJECT FOR NUCLOTRON-NICA: CURRENT RESULTS

A.V. Butenko, A.O. Sidorin[1], G.V. Trubnikov[1],
Joint Institute for Nuclear Research, Dubna, Moscow Region, Russia,
M.A. Gusarova, T.V. Kulevoy[2], M.V. Lalayan, S.M. Polozov[2], A.V. Samoshin, S.E. Toporkov,
V.L. Zvyagintsev[3], National Research Nuclear University – Moscow Engineering Physics Institute, Moscow, Russia
M.A. Batouritski, S.A. Maksimenko, Institute for Nuclear Problems, Belarusian State University, Minsk,
A.A. Marysheva, V.S. Petrakovsky, I.L. Pobol, A.I. Pokrovsky, D.A. Shparla, S.V Yurevich,
Physical-Technical Institute, National Academy of Sciences of Belarus, Minsk,
[1]also at Saint-Petersburg State University, Saint-Petersburg, Russia
[2]also at Institute of Theoretical and Experimental Physics of NRC "Kurchatov Institute", Moscow, Russia
[3] also at TRIUMF, Vancouver, Canada

Abstract

The joint collaboration of JINR, NRNU MEPhI, INP BSU, PTI NASB, BSUIR and SPMRC NASB started in 2015 a new project on the development of superconducting cavities production and test technologies and new linac-injector design. This linac intend for the protons acceleration up to 25 MeV (up to 50 MeV after upgrade) and light ions acceleration up to ~7.5 MeV/u for Nuclotron-NICA injection. Current status of linac general design and results of the beam dynamics simulation and SRF technology development are presented in this report.

INTRODUCTION

Nuclotron-based Ion Collider fAcility (NICA) is new accelerator complex developing and constructing at JINR [1-4]. The injection system of operating Nuclotron and new NICA is under upgrade now. It was consisted of old Alvarez-type DTL called LU-20. The pulse DC forinjector was replaced by new RFQ linac which was developed and constructed by joint team of JINR, ITEP and MEPhI [5] and commissioned on December, 2016. The first technical session was done on May-June, 2016, with new injector [6] and the first experimental session is under operation at present (November, 2016). The other heavy ion linac for beams with charge-to mass ration Z/A=1/8-1/6 was developed by joint team of JINR, Frankfurt University and BEVATECH and it is under installation and commissioning at present.

The possibility of LU-20 replacement by new superconducting (SC) linac of 25 MeV for protons [7, 8] and up to 7.5 MeV/nucleon for deuterium beam is discussed now. Project should also include upgrade option up to 50 MeV for the proton beam. Beam intensity and quality could be sufficiently increased in Nuclotron and NICA after new linac commissioning.

Technologies which are necessary for serial SC cavities manufacturing are now absent in Russia. JINR in cooperation with the INP BSU and the PTI NASB done the pilot project of elliptical cavities fabrication and testing [9-11]. Now a new collaboration of the JINR, the NRNU MEPhI, the ITEP NRC "Kurchatov Institute", the INP BSU, the PTI NASB, the Belarusian State University of Informatics and Radioelectronics and the Scientific and Practical Material Research Center of NAS of Belarus is established. The new collaboration declares two main aims of cooperation: development of technologies for SC cavities production and construction of the new linac – the injector for the Nuclotron-NICA complex. The first results of the linac general layout development and beam dynamics simulation are presented in the paper.

NEW SUPERCONDUCTING LINAC GENERAL SCHEME AND THE FIRST VERSIONS OF LAYOUT

Superconducting linac would to be consisting of a number of superconducting independently phased cavities and focusing solenoids. Low to mid-energy linear accelerator development is challenging because of serious limitations imposed on non-relativistic beam accelerating and focusing systems. This task could be solved using RF accelerator with identical short SC cavities with independent phase control for high energy gain and focusing solenoids. This design is economically allowable in the case of identical cavities, otherwise the total accelerator cost dramatically increases. Such linac design was called modular. It means that RF wave for all cavities will have the same phase velocity value. Wave and particle synchronous motion will be not observed here due to of particles reference phase slipping. The slipping value should not exceed some allowable limits otherwise the rate of the energy gain decreases, both transverse and longitudinal beam stability disturbs and current transmission decreases [12-13].

Starting 2014 two SC linac designs were proposed, discussed and simulated [7]. The first preliminary design was done with the following assumptions: the injection

ISBN 978-3-95450-181-6

SERIES MAGNETIC MEASUREMENTS OF NICA BOOSTER DIPOLES

V. Borisov, A. Bychkov, A. Donyagin, O. Golubitsky, H. Khodzhibagiyan,
S. Kostromin, M. Omelyanenko, M. Shandov, A. Shemchuk, Laboratory of High Energy Physics,
Joint Institute for Nuclear Research, Dubna, Russia

Abstract

NICA booster magnetic system consists of 40 dipole and 48 quadrupole superconducting (SC) magnets. Measurement of magnetic field parameters is assumed for each booster magnets. At the moment six series dipole magnets are assembled and have passed all tests. Booster dipole magnets are 2.14 m-long, 128 /65 mm (h/v) aperture magnets with design similar to Nuclotron dipole magnet but with curved (14.1 m radius) yoke. They will produce fields up to 1.8 T. The magnetic field parameters will be measured at "warm" (300 K) and "cold" (4.5 K) conditions. The obtained results of magnetic measurements of first five magnets are summarized here.

INTRODUCTION

At the Laboratory of High Energy Physics (LHEP) the technical complex [1] for assembly and testing of SC magnets for the NICA and FAIR project is lunched for pass whole cycle operating at assembling and series testing mode. Five magnets were done. The testing program of magnets includes “warm” and cold magnetic measurements (MM).

DIPOLE MAGNET FOR THE NICA BOOSTER

The Nuclotron-type design based on a window frame iron yoke and a saddle-shaped SC winding has been chosen for the NICA booster and collider magnetic system. A cross-section view of the booster dipole magnets with installed magnetic measuring system (MMS) is shown on Fig. 1.

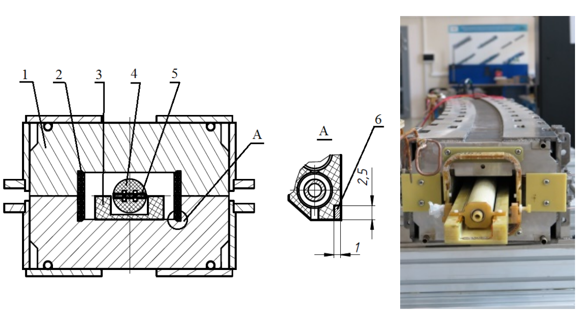

Figure 1: Cross-section view of the bent dipole magnet for the NICA booster with magnetic measurement system. 1. Yoke, 2. Main coil, 3. Base of MMS frame, 4. MMS frame, 5. PCB with harmonic coils, 6. Reference coil.

The NICA Booster operating cycle consists of stages of linear field ramping up and down with a ramp rate of 1.2 T/s and two stages with a constant field. Injection magnetic field is 0.11 T, at electron cooling is 0.56 T.

SPECIFICATION FOR MAGNETIC MEASUREMENTS

According to the specification following parameters of Booster dipole magnets have to be measured:

- Relative variation of effective lengths

$$L_{eff} = \frac{\int_{-\infty}^{\infty} B_y ds}{B_y(0)} \qquad \delta L_{eff} = \frac{\Delta L_{eff}}{< L_{eff} >} \le 5\cdot 10^{-4}$$

- Angle between the magnetic and mechanical median plane (Dipole angle)

$$\alpha_1 = -arctg(\frac{a_1}{b_1}) \quad \delta(\alpha_1) \le 0.1\,\text{mrad}$$

- Relative integrated harmonics up to the 5th

b_2^*	$5\cdot 10^{-4}$
a_2^*	$5\cdot 10^{-4}$
b_3^*	10^{-3}
b_n^* , a_n^* , $n>3$	10^{-4}

THE MAGNETIC MEASUREMENT SYSTEM

Magnetic measurements were carried out by means of the rotating harmonic coils probes. Detailed description of magnetic measurement system and methods was done in papers [2], [3].

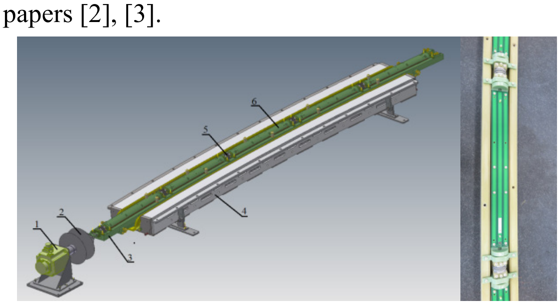

Figure 2: Layout of bottom part of magnets yoke with installed MMS: 1. Servomotor, 2. Bobbin for the cable, 3. Base of frame, 4. Bottom part of yoke, 5. Flexible coupling, 6. Measuring section.

ISBN 978-3-95450-181-6

HIGH-POWER HIGH-TEMPERATURE GRAPHITE BEAM DUMP FOR E-BEAM IRRADIATION TEST OF PROTOTYPE IF TARGET IN RISP

K.V. Gubin, ILP SB RAS, Novosibirsk, Russia
Yu.I. Maltseva, P.V. Martyshkin, BINP, Novosibirsk, Russia
J.-W. Kim, J.Y. Kim, Y.-H. Park, IBS, Daejeon, Korea

Abstract

Nowadays project RISP is developed in IBS, Daejeon [1,2]. One of the main project device is graphite target system meant for production of rare isotopes by means of the in-flight fragmentation (IF) technique. The power inside the target system deposited by the primary beam with energy of 200 MeV/u is estimated to be around 100 kW [3]. The target represents rotating multi-slice graphite disc cooled by thermal radiation [4]. Necessary step of target development is integrated test of target prototype under high power electron beam modelling real energy deposit into target. This test is planned to be held in BINP, Novosibirsk, with the use of ELV-6 accelerator [5-7]. Heavy-ion beam will be modelled by the e^- beam of ELV-6 accelerator with diameter down to ~1 mm and energy 800 keV (minimum possible).

IF target is not full stopping target for an electron beam with energy 800 keV. Considerable part of beam energy will be not absorbed by a target material and must be deposited into special beam dump. In this paper the design of beam dump of the graphite cone geometry cooled by thermal irradiation is described.

BEAM DUMP PURPOSE AND LAYOUT

Beam dump is mainly purposed for utilization of electrons passed through the rotating target and removing the excess energy from experimental area. Beam dump is insulated from installation body. Simultaneously it means prevention the direct passing of high-energy electrons into metal surfaces. Moreover, it is specified using of current signal from beam dump for fast interlock unit. These tasks cause general layout of beam dump devise is shown in Fig. 1.

- Graphite conical beam dump with thickness 2 mm absorbs most part passed electrons and removes its energy by the thermal irradiation. The thickness of graphite is enough for electron beam full stopping.
- Cylindrical graphite blanket protects the outlet metal devices from electrons scattered with high angles. This device also is cooled by thermal irradiation.
- Water beam dump and additive cooling panel removes heat by water cooling channels. Also this devices saves overheat of the different parts of installation against of direct graphite thermal irradiation.
- Ceramic insulator gives possibility to measure electron beam current through graphite cone.

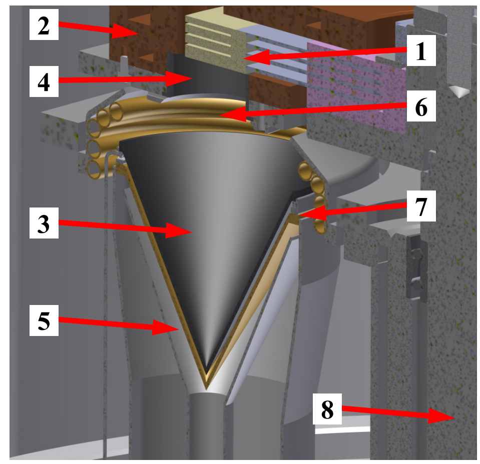

Figure 1: Layout of beam dump: 1 – multi-slice rotating target, 2 – cooling panel, 3- graphite cone beam dump, 4 – graphite blanket, 5 – water beam dump, additive cooling panel, 7 – ceramic insulator, 8 – target shaft.

Main problem of beam dump development is optimization of device size and placement. First of all, beam dump must have enough large size for providing high flow of thermal irradiation without overheat of graphite more than 1900-2000 °C. In other hand, a beam dump size is limited by maximum sizes of installation: distance between target shaft and electron beam axis is ~ 10 cm. Also, operational conditions of beam dump will determine maximum possible electron beam power during experiment

Principal subtasks of target development are next:

- simulation of electron beam scattering and passing through rotated target,
- estimation of beam dump heating, temperature and thermal stress distribution, ultimate parameters of electron beam,
- estimation of heat removal by external cooling channel,
- optimization of beam dump design and operational conditions,
- definition of ultimate experimental regime for the next prototype test [4, 7].

SIMULATION OF ELECTRON BEAM SCATTERING

Simulation of electron beam passing through the rotating target was performed by G4beamline code based on GEANT4 by means of Monte Carlo method. Main

ISBN 978-3-95450-181-6

A FARADAY CUP FOR A LOW CHARGE LWFA ELECTRON BEAM MEASUREMENT

K.V. Gubin, V.I. Trunov, ILP SB RAS, Novosibirsk, Russia
V.V. Gambaryan, A.E. Levichev, Yu.I. Maltseva, P.V. Martyshkin, A.A. Pachkov, S.N. Peshekhonov, BINP SB RAS, Novosibirsk, Russia

Abstract

Nowadays laser wakefield acceleration (LWFA) is considered as one a perspective method for GeV electron beam production. Combination of laser accelerated electrons and Compton backscattering of probe light beam opens possibility to create the table top source of femtosecond light beam in x-ray and gamma range. Project of laser-driven Compton light source started in ILP SB RAS in collaboration with BINP SB RAS. Production of 1-10 pC electron beams sub-ps time range duration with energies up to 100 MeV is expected as a result of the first stage of the project. Since energy of electrons does not exceed of 100 MeV, it allows using Faraday cup (FC) with reasonable dimensions, instead of commonly used integrating current transformer (ICT). Geometry of the FC was optimized taking into account of beam stopping simulation as well as low capacity requirement. RF properties, simulation of the system operation were carried out. System has been tested at the VEPP-5 electron linac. Results of development and testing of this FC are presented.

INTRODUCTION

At the present time, the impressive progress in laser wakefield acceleration (LWFA) of charged particles gives grounds to consider LWFA as a perspective method of electron beam production in the GeV energy range [1,2].

LWFA experiments are currently prepared at the Institute of Laser Physics (ILP) in collaboration with Budker INP. The experiments are based on the two-channel multi-terawatt femtosecond high contrast, high angle stability laser system with the pulse repetition rate of 10 Hz, which is developed at ILP [3].

To pursue further studies of laser-based acceleration techniques, a specialized experimental facility was designed. A sketch of the experimental stand is shown in Fig. 1. Scenario and design of stand are traditional for LWFA devices: sub-PW high-contrast femtosecond laser pulse will be responsible for gas ionization and formation of the plasma channel inside the supersonic gas jet, wakefield excitation, and trapping of plasma electrons by the wave.

General parameters of the LWFA stand are [4]:

- laser system: repetition rate is 10 Hz, pulse energy is 100÷300 mJ, pulse duration is ~20 fs, central wavelength is 810 nm;
- acceleration area: diameter is ~ 10÷15 μm, length is ~ 0.5 mm;
- supersonic He jet: diameter is ~1.2 mm, gas density is $10^{18}÷10^{19}$ cm^{-3}, Mach number is 3.5÷4, gas backpressure is 5÷10 atm;
- expected parameters of the electron beam are: up to 50-100 MeV of energy, 1-10 pC of charge, 1-10 mrad of angular divergence, ≤ 0.1 ps of beam duration.

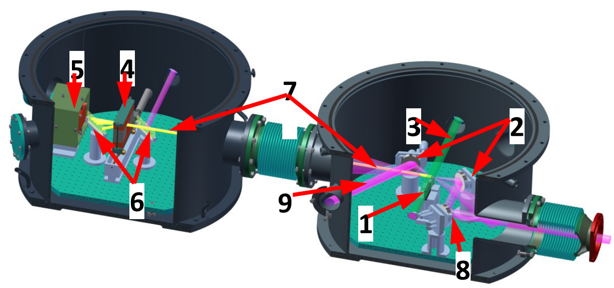

Figure 1: Two experimental chambers (without the compressor chamber): 1 – supersonic gas jet, 2 – focusing mirrors, 3 – laser beam for diagnosing the jet density, 4 – electron spectrometer magnet, 5 – Faraday cup, 6 – luminophor screens, 7 – electron beam, 8 – driving laser beam, 9 – scattered laser beam.

FC PURPOSE AND REQUIREMENTS

Beam current measurement is a necessary constituent of any accelerator facility. Usually the ICT (Integrating Current Transformer) device is used as a detector of charge in LWFA electron bunch [2,5-7]. This method has the principal difficulties:

- ICT is indirect diagnostic;
- ICT demands periodic recalibration of complicated equipment set;
- ICT system is expensive (tens of thousands euro).

However, in our case of intermediate energy range (10÷100 MeV) we can use alternative variant of diagnostic. It is Faraday cup (FC). FC gives us a possibility to have direct current measurements with high accuracy and reliability without any additional complicated electronics and does not need special recalibration procedures. Moreover, FC can be used for calibration of more complicated systems in future.

The FC development is constrained by the conflicting demands:

- Compact size (boundary dimensions 20-25 cm). Device must be placed inside limited volume of experimental vacuum chamber.
- Small capacity, not more than 10-30 pF (several tens pF including output circuit). It is caused by small

ISBN 978-3-95450-181-6

MEASUREMENT OF GAMMA BEAMS PROFILE BY CHERENKOV RADIATION IN FIBERS*

A.V. Vukolov†, A.I. Novokshonov, A.P. Potylitsyn, S.R. Uglov, E.N. Shuvalov
National Research Tomsk Polytechnic University, Tomsk, Russia

Abstract

Results of γ-beam profile experimental investigations measuring of Cherenkov radiation [1] generated in an optical fiber with 0.6 mm and 5 mm diameter are presented. These experiments were carried out on γ beams of the linac "Philips SL-75" and the betatron, both with 6 MeV energy. In works [2, 3] authors have showed feasibility of Cherenkov radiation applying for high energy beam diagnostics. In our work the Cherenkov radiation yield dependence on the fiber orientation with respect to the beam axis was investigated and showed that the maximal light yield corresponds to the angle between fiber and beam axes closed to the Cherenkov angle [1]. Proposed technique for measurements of γ and electron [4] beam profiles is insensitive to low energy part of the bremsstrahlung spectrum and to undesirable background in contrast with well-known technique based on ionization chambers. Using such a technique it is possible to construct compact and noise insensitive device. It is also possible to reach submillimeter spatial resolution.

INTRODUCTION

A wide application of γ beams in different fields requires beam profile measurement with a good accuracy. The most wide-spread technique of beam profile measuring is based on its detection by ionization chamber or by scintillator. But these techniques have spatial resolution exceeding 1 mm. One can also use X-ray films [5] to reach submillimeter resolution, but such a technique is an off-line one. All these disadvantages indicate a necessity of new, alternative device development.

In works [1–3] a feasibility of Cherenkov radiation applications for high-energy beams diagnostics is shown. In this work a diagnostic technique for γ-beams with MeV energies and mm sizes is suggested. This technique is based on detection of Cherenkov radiation, generated by γ or electron beams, passing through the optical fiber.

Cherenkov radiation is emitted in cone with the opening angle [1]:

$$\cos\theta_{ch}(\lambda) = \frac{1}{\beta n(\lambda)} \tag{1}$$

where $\beta = v/c$, λ - wavelength, n - refractive index.

Number of photons, emitted by an electron, can be estimated from [1]:

$$\frac{d^2N}{dx d\lambda} = 2\pi\alpha\left(1 - \frac{1}{\beta^2 n^2}\right)\frac{1}{\lambda^2} \tag{2}$$

where x - passed by a particle distance, α - thin structure constant, z - particle charge. The estimation of Cherenkov photons yield in glass for the λ = 400÷700 nm gives result about 20 photons per 1 mm. The outgoing angle for photons in glass (n = 1.47) is $\theta_{ch} \approx 46^o$.

MEASUREMENTS OF THE LINAC GAMMA BEAM

Experimental setup

A schematic of experimental setup is shown in Fig. 1. The γ-beam generated by the linear accelerator "Philips SL-75" was registered by the optical fiber with 0.6 mm diameter, which was connected to the silicon photomultiplier (PMT). The fiber length was about few meters, this allowed the locate PMT far from the beam. The accelerator has 6 MeV energy, 1 GHz frequency and 4 μs duration. The dose rate at 0.5 m distance from collimator was 4 Gr/min. The fiber was located at 20 cm distance from the collimator. An orientation dependence of intensity on angle θ between a beam axis and fiber was measured for angular range $0^o \div 180^o$.

The PMT has 6×6 mm^2 active area, 300÷800 nm spectral range, 47% photon registration efficiency at 420 nm wavelength, 10^6 gain coefficient and low supply voltage - 24.5 V. Additional advantages of the PMT are its compact size, insensibility to influence of magnetic fields, mechanical reliability, weak reaction on ionization radiation and possibility of operation in vacuum.

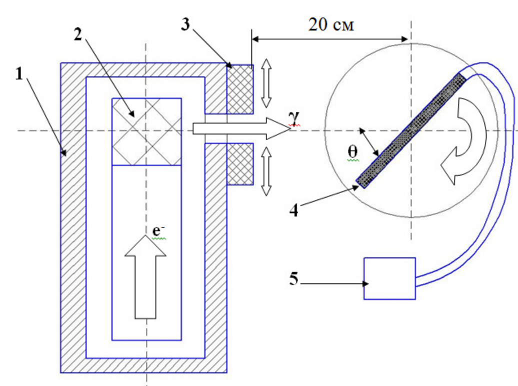

Figure 1: Schematic of experimental setup. 1 - radiation shielding, 2 - linear accelerator, 3 - collimator, 4 - optical fiber, 5 - silicon PMT.

Results

In Fig. 2 the orientation curves for different collimator sizes are shown. These curves were measured by the fiber

* This work was partially supported by the Russian Ministry of Education and Science within the program "Nauka" Grant # 3.709.2014/K
† vukolov@tpu.ru

ISBN 978-3-95450-181-6

DIELECTRIC CHART AS A TOOL FOR DIAGNOSIS OF DIELECTRIC MATERIALS

V.A.Klemeshev*, A.G.Karpov†, Saint-Petersburg State University,
7/9 Universitetskaya emb., St. Petersburg, 199034, Russia

Abstract

One of the most informative diagnostic methods dielectric materials is the analysis of the complex permittivity depending on the frequency of the electric field [1]. Dielectric chart is the dependence of the imaginary part of the complex permittivity of its real part. Thus, difference between the real dielectric chart from the reference or change it during the operation can be a means of diagnostics of dielectric materials. Dielectric chart in the classical theory of Debye is a semicircle with its center lying on the real axis. For solid dielectric the dielectric chart deviation from the semicircle can be quite large, but it still remains a circular arc. This deviation is characterized by parameter α (in the case of the Debye $\alpha = 0$). To clarify the physical meaning of the deviations of the experimental data on the Debye theory, expressed in the value of α, several possible causes have been considered: the effect hindered reorientation of dipoles, the effect of the non-sphericity of the molecules, the complex nature of viscosity. However, the main cause of deviations, in our opinion, is the availability of the distribution of relaxation times around a central relaxation time, in particular, due to defects in the sample. Gaussian distribution width increases rapidly with increasing α. In this paper we propose an algorithm for calculating α, allowing you to quickly determine the condition of the sample on a single parameter.

INTRODUCTION

One of the most informative diagnostic methods for dielectric materials is the analysis of the complex permittivity ε^* depending on the frequency of the electric field [1, 2]. But the presentation in the form of frequency dependency does not allow to easily analyze data and assess the significance of the deviation from the expected relationship. A more appropriate presentation is a dielectric diagram (Argand diagram) in the complex plane when built dependence of the imaginary part of the complex permittivity ε'' of the real part of it ε', and each point is characterized by individual frequency (Fig. 1). Difference between the real dielectric chart from the reference or change it during the operation can be a means of diagnostics of dielectric materials.

DIELECTRIC DIAGRAM

Dielectric diagram according to the classical equations of Debye is a semicircle with its center lying on the real axis (ε'), and crosses the real axis at the points ε_0 and ε_∞ (see Fig. 1). We introduce the notation

$$\begin{aligned} u &= \varepsilon^* - \varepsilon_\infty, \\ v &= (\varepsilon^* - \varepsilon_\infty) i\omega\tau_0, \\ u + v &= \varepsilon_0 - \varepsilon_\infty, \end{aligned}$$

where τ_0 — relaxation time, ε_0 — the value of the real part of the dielectric permittivity at a frequency $\omega = 0$, ε_∞ — the value of the real part of the dielectric permittivity at a frequency $\omega \to \infty$, the difference between ε_0 and ε_∞ attributed to dipole.

The values v and u may be considered as vectors in the complex plane, and in Debye case they are perpendicular, and their sum is constant and equal to the real value of $\varepsilon_0 - \varepsilon_\infty$.

The deviation from the semicircle can be very large for solid dielectrics. Nevertheless, depending on ε' ε'' still represent circular arcs.

In equivalent circuit for the experimental dependence the impedance is $Z = \tau_0(i\omega\tau_0)^{-\alpha}/(\varepsilon_0 - \varepsilon_\infty)$, and the phase angle between the active and reactive components does not depend on the frequency and is equal to $\alpha\pi/2$. Since the angle between the axis ε' and the radius vector to the point ε_∞ on diagram arc circle in the complex plane is also equal to $\alpha\pi/2$, it is reasonable to assume that the properties of the dielectric are determined by the value α. Angle $(1-\alpha)\pi/2$ (between the vectors v and u in the complex plane) does not depend on the frequency and is equal to half of the arc angle. Consequently,

$$u + v = u[1 + f(\omega)e^{i(1-\alpha)\pi/2}] = \varepsilon_0 - \varepsilon_\infty,$$

where $f(\omega)$ — real function of frequency and other parameters. Since $e^{i(1-\alpha)\pi/2} = i^{(1-\alpha)}$, then

$$\varepsilon^* - \varepsilon_\infty = (\varepsilon_0 - \varepsilon_\infty)/[1 + i^{(1-\alpha)} f(\omega)].$$

From general considerations, it can be assumed that this relationship will look $\omega^{(1-\alpha)}$, when the complex form ε^* is the result of the initial hypothesis that the applied field is given by $E = E_0 e^{i\omega t}$. If ω is the result of linear operations over the exponent, the dependence on ω is identical to depending on the imaginary unit i, so that

$$\varepsilon^* - \varepsilon_\infty = (\varepsilon_0 - \varepsilon_\infty)/[1 + (i\omega\tau_0)^{1-\alpha}].$$

for $0 < \alpha < 1$.

The dependence of $\ln|u/v|$ on $\ln\omega$:

$$\ln|u/v| = (1-\alpha)\ln\omega\tau_0 = (1-\alpha)\ln\omega + (1-\alpha)\ln\tau_0,$$

* v.klemeshev@spbu.ru
† a.g.karpov@spbu.ru

ISBN 978-3-95450-181-6

POSSIBILITIES OF DIFFRACTION RADIATION NON-DESTRUCTIVE DIAGNOSTICS FOR NON- AND MODERATELY RELATIVISTIC BEAMS*

D. A. Shkitov#, A. P. Potylitsyn, Tomsk Polytechnic University, Tomsk, Russia

Abstract

In this report the estimations of diffraction radiation yield from a slit target for European Spallation Source proton beam parameters is given. The possibilities of the non-destructive bunch length diagnostics using the diffraction radiation for non- and moderately relativistic beams of this accelerator are investigated.

INTRODUCTION

Diffraction radiation (DR) in mm wavelength region from relativistic electrons was first observed in 1995 [1]. Since then, the development of new approaches using the DR for charged particle beam diagnostics is continued. The DR is a radiation which occurs when charged particle moves near the media and only the electromagnetic field of particle interacts with the media. One significant advantage of DR diagnostics in contrast with transition radiation (TR) is its non-destructive character.

For instance, a rather well-known in scientific accelerator community the non-destructive diagnostic method of transversal bunch size determination is to use a slit target with optical diffraction radiation (ODR) [2]. Another examples are to use the radiation interference in order to determine such parameters as a bunch emittance based on system of two slit target [3] and a bunch length based on double DR target (where one plate is movable) [4].

However, all of these approaches were tested on the electron accelerators. For proton accelerators the studies of TR/DR application for diagnostics were conducted much less than for electron accelerators. There are a few articles which dedicated to the transverse beam shape measurements of relativistic proton beams using optical transition radiation (OTR) [5-7]. The possibilities of DR transverse size diagnostics for relativistic proton beams were discussed in [8] in optical wavelength range as well.

In this report we present the estimations and simulation results characterizing the DR applicability for non-destructive diagnostics of non- and moderately relativistic proton beams with the parameters of European Spallation Source (ESS) [9].

THEORY BACKGROUND

For the DR simulation we have used the generalized surface current method [10]. This method can be applied for the transition radiation and diffraction radiation calculations from different surfaces and for arbitrary particle energy. However, the only ideal conductivity of the target may be considered.

In our geometry a charged particle moves in the center between two semi-infinite plates through the slit. Using the formula obtained in Ref. [11], we may calculate the spectral-angular distributions in the single particle approximation from the slit target. In Fig. 1 the scheme of DR generation from this target is shown.

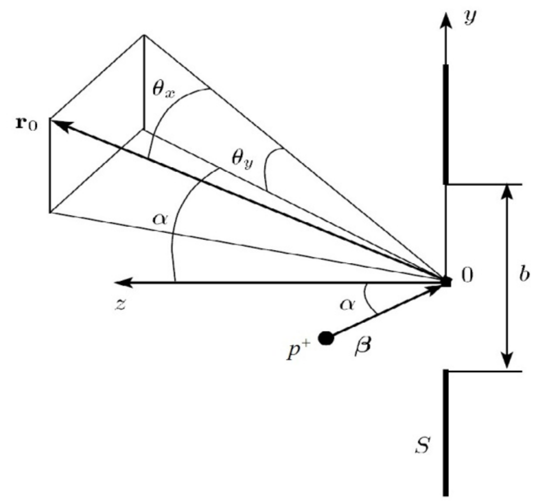

Figure 1: The scheme of DR generation by charged particle [11].

Here β is a particle velocity (in units of the light speed c), α is incidence angle, b is the slit width, S is an area of target surface, r_0 is a distance to observation point, θ_x and θ_y are the observation angles and γ is the Lorentz factor. Hereinafter in our calculations, we will assume that the angle $\alpha = 0°$.

DR YIELD ESTIMATIONS

The ESS is a multi-disciplinary research facility based on the world's most powerful neutron source [9]. The facility includes the most powerful linear proton accelerator ever built. The construction of the facility began in the summer of 2014. In Table 1 the main parameters of ESS proton beam are listed. In this facility the accelerator up to 90 MeV (γ = 1.1) of protons is normal and up to 2 GeV (γ = 3.1) is superconductive.

Table 1: Simulation Parameters

Name	Value
Proton energy, E_e	up to 90 MeV "warm" up to 2000 MeV "cold"
Bunch length, σ_z (r.m.s.)	~1 – 4 mm
Bunch size, σ_t (r.m.s.)	~0.5 – 4.5 mm
Bunch population, N_e	~$1.83{\cdot}10^8$
Bunches in macro-pulse, N_b	~$6.13{\cdot}10^6$
Repetition rate, f	14 Hz
Macro-pulse duration	2.86 ms

* Work was partially supported by the RFBR grant No 15-52-50028.
# shkitovda@tpu.ru

ISBN 978-3-95450-181-6

THE MAGNETIC ENERGY ANALYZER FOR ELECTRON BEAM OF LUE-200 LINAC OF IREN FACILITY

A.P. Sumbaev, N.I. Tarantin, V.I. Shokin, JINR, Dubna, Moscow region, 141980 Russia

Abstract

Theses for a base substantiation, results of the calculation for the electron optical parameters and design features of the magnetic energy analyzer for the beam of the LUE-200 electron linac are presented. The static dipole magnet with homogeneous transverse field and with a combined function (the function of a spectrometer and of a spectrograph) established after the second accelerating section, allows to spend measurements in a wide energy range of the analyzed particles up to 224 MeV with the instrumentation resolution not worse ±7 %.

INTRODUCTION

IREN Facility [1,2] of the Joint Institute for nuclear research as a particle energy analyzer uses the static analyzer with magnetic spectrometer and functions as a spectrograph. Feature LUE-200 is the vertical axis of the accelerator and beam transport channel to the target, so convenient for hosting and maintenance analyzer configuration is in the form of a dipole magnet with rotation sector beam at an angle of close to $\Phi = \pi/2$, set so that the longitudinal axis of the accelerator tract passes through the magnet median plane. The energy of the accelerated electrons can vary from 15 to 100 MeV, with the one accelerating sections, and up to 100 - 200 MeV when accelerator is operating in full. When you select the main axis provide turning radius analysing magnet R_0 = 0.5 m its magnetic rigidity BR [Tm] = E [MeV]/300 should vary within 0.05 – 0.66 Tm.

ANALYZER DESIGN

The analyzer consists of an electromagnet, the vacuum chamber and the detector - registrar. The principle circuit of the analyzer is presented at Fig. 1. The analyzer electromagnet is made in the “Ш” shape. The yoke of the magnet is mounted on one of the "racks", "beams" of the yoke form the side walls and the median plane of the poles is aligned with the axis of the accelerator. The analyzer is installed in the channel of beam transportation between the second accelerating section and a target (Fig. 2). The magnet is mounted on the rails on which the magnet can be rolled horizontally away from the accelerator (Fig. 3). When the beam is transported to the target, the analyzer is disabled, and the residual magnetization of the yoke is removed by the powering of the magnet from the low current power supply. The current value is selected by the absence of deflection of the beam passing through the analyzer.

To control the position of the beam at the input and output of the vacuum chamber of the analyzer using a “beamviewers”. The analyzer can operate in two modes. When changing beam energy analyzer mode of the spectrometer, the changing of the level of the magnetic field is adjusted for accepting of particles with energies E_0 from 10 MeV to 200 MeV. In the mode of the spectrograph at a fixed level of the field corresponding to the electron energy E_0, the analyzer has ability to simultaneously register particles in the energy range $E_0 \pm 0.5E_0$.

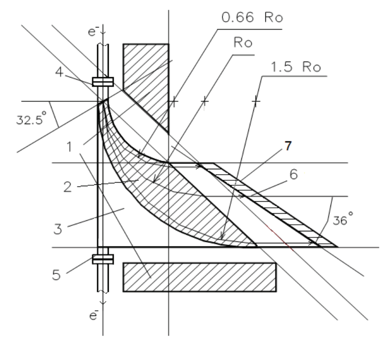

Figure 1: The principle circuit of the analyzer - axial section on median magnet plane. 1 – yoke of the electromagnet, 2 - electromagnet pole, 3 - the vacuum chamber, 4 and 5 - entrance and target branch pipes, 6 - detector window, 7 - the detector - registrar.

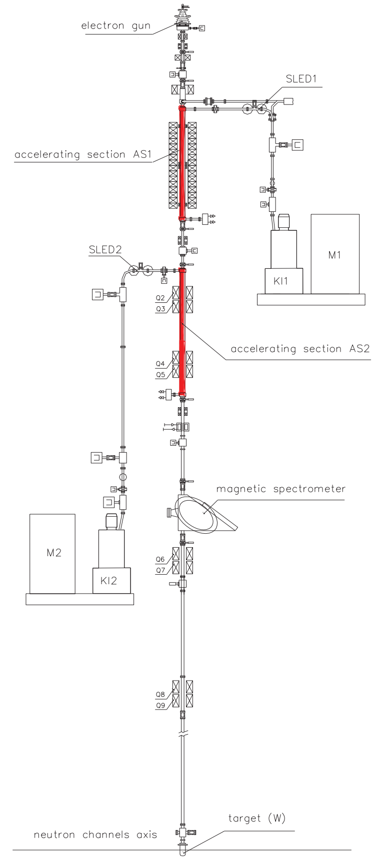

Figure 2: Scheme of the accelerator.

ISBN 978-3-95450-181-6

THE LONGITUDINAL BROADBAND IMPEDANCE AND ENERGY SPREAD MEASUREMENTS AT VEPP-4M

V. M. Borin[1], V. L. Dorokhov, V. A. Kiselev, G. Ya. Kurkin, O. I. Meshkov[1], S. A. Nikitin, M. A. Skamarokha, Budker Institute of Nuclear Physics, Novosibirsk, Russia
[1]also at Novosibirsk State University, Novosibirsk, Russia

Abstract

The paper presents studies of the longitudinal broadband impedance of VEPP-4M and measurements of its bunch energy spread at different energies in range of 1.45 – 3.5 GeV. In order to measure the longitudinal bunch size at different currents we used “PS-1/S1” streak camera with picosecond temporal resolution. Considering that influence of collective effects is negligible at low currents we determined bunch energy spread from its length at low currents. Collected bunch length data demonstrate microwave instability thresholds and potential well distortion lengthening. Potential well distortion was studied at 3 GeV and 3.5 GeV. Measured potential well distortion lengthening was used to estimate a value of the reactive part of the longitudinal impedance. Observed microwave instability thresholds was used to measure the value of broadband impedance. Measured value of the VEPP-4M is 7.9 ± 1.5 Ω.

ELECTRON BUNCH LENGTH

Natural Length

A length of the electron bunch is determined by synchrotron oscillations and has no current dependence if collective effects are negligible [1]. While the energy spread is determined by the balance between quantum excitation and synchrotron damping, so longitudinal bunch size σ_S and its relative energy spread σ_E / E are:

$$\sigma_S = \frac{\sigma_E}{E}\frac{\alpha c}{\omega_S}, \tag{1}$$

where α is the momentum compaction factor, c is the speed of light, ω_s is the synchrotron oscillation frequency.

Intrabeam Scattering

With the increasing of electrons density in the bunch the effects of the intrabeam scattering (or multiple Touscheck effect) becomes significant. The effect is based on transferring of momentum from transverse plane of motion to the longitudinal that leads to growth of bunch energy spread and bunch lengthening [2]. Growth of energy spread can be obtained as a solution of (2-4):

$$\left(\frac{\sigma_{ET}}{E}\right)^6 = \frac{N r_0^2 \beta_x \tau_E \omega_S f(x_m)}{2^5 \pi \gamma^3 \left(\beta_x U_x + \eta^2\right)\sqrt{k\beta_z U_x \alpha}}; \tag{2}$$

$$\chi_m = \frac{N^{1/3} r_0 \beta_x^2 Q_s^{1/3} \left(\sigma_{ET}/E\right)^{-3}}{2\sqrt{\pi}\gamma^2\left(\beta_x U_x + \eta^2\right)^{7/6}\left(k\beta_z U_x\right)^{1/6}\left(\alpha R\right)^{1/3}}; \tag{3}$$

$$f(\chi_m) = \int_{\chi_m}^{\infty} \frac{1}{\chi}\ln\left(\frac{\chi}{\chi_m}\right) e^{-\chi} d\chi . \tag{4}$$

Where N is a number of particles in the bunch, βx, βz is a horizontal and vertical beta functions, τ_E is a synchrotron damping time, γ is the Lorentz factor, η is a dispersion function, k is a betatron coupling, r_0 is the classical electron radius, Q_s is a synchrotron tune, σ_{ET} is the energy spread induced by intrabeam scattering, U_x is determined by (5).

$$U_x = \frac{\tau_x}{\tau_E} < \frac{1}{\beta_x}\left[\eta^2 + \left(\beta_x \eta' - \frac{1}{2}\beta_x' \eta\right)^2\right] > \tag{5}$$

Where τ_x is horizontal betatron damping time and the averaging is made in bending magnets only. Since these effects are independent then the total bunch length is quadratic sum of lengths.

Wake Field Interactions

There are two effects appearing due to interaction of the bunch with induced wake fields. First is the effect of potential well distortion that leads to bunch lengthening or shortening depending on the value of impedance. The synchrotron frequency shifts due to this effect also. The effect can be observed even at low bunch currents. Lengthening caused by this effect is expressed by (6).

$$\left(\frac{\sigma_s}{\sigma_{s_0}}\right)^3 - \left(\frac{\sigma_s}{\sigma_{s_0}}\right) + I_b \frac{\alpha Im\left[\left(z_{\parallel}/n\right)_{eff}\right]}{\sqrt{2\pi} E Q_{s_0}^2}\left(\frac{R}{\sigma_{s_0}}\right)^3 = 0 \tag{6}$$

Where I_b is the bunch current, E is a bunch energy, R is an average radius of accelerator, $Im\left[\left(z_{\parallel}/n\right)_{eff}\right]$ is an imaginary part of the longitudinal effective impedance and subscript 0 stands for values at low currents where the effect is negligible.

As bunch current increase, as we can observe a threshold of the microwave instability. The effect leads to a growth of a length and energy spread of the bunch but the synchrotron frequency of the bunch remains undisturbed [3]. Microwave instability threshold is determined by (7).

$$I_{th} = \frac{\sqrt{2\pi}\alpha E \sigma_s}{R\left|z_{\parallel}/n\right|_{BB}}\left(\frac{\sigma_E}{E}\right)^2 \tag{7}$$

Where I_{th} is the threshold current and $\left|z_{\parallel}/n\right|_{BB}$ is an absolute value of the longitudinal broadband impedance.

ISBN 978-3-95450-181-6

THE PEPPER-POT EMITTANCE MEASURING DEVICE AT THE 400 keV H-MINUS LEBT CHANNEL

V.S. Klenov, S.E. Bragin, O.T. Frolov, S.E. Golubovski, O.V. Grekhov, O.M. Volodkevich, V.N. Zubets, Institute for Nuclear Research Russian Academy of Sciences, Moscow, Russia

Abstract

The emittance measuring device has been developed for operational control of INR RAS linac 400 keV H-minus injector beam parameters. It includes the "pepper-pot", the quartz screen, the CCD camera, PC, the software for camera data processing and beam phase portrait formation. The device has been mounted at the first straight section extension of H-minus LEBT after 45 degree bending magnet. When the bending magnet is switched off the device is possible to measure and to represent single shot beam phase portrait. The results of the H-minus beam emittance measurements and the device performance have been discussed.

INTRODUCTION

Registration of light, received on the scintillator after passing the ion beam through mask with a set of holes ("pepper-pot"), allows, in principle, to measure the emittance of the ion beam in a single shot beam pulse.This method of measuring the emittance associated with the interception of the beam, and is usually implemented by inputting the emittance measuring device into the beamline [1-2]. The H-minus LEBT of INR RAS linac contains 45 degree bending magnet, this allowed to mount an emittance measuring device at the straight extension after bending magnet (Fig. 1). Aiming beam at device is possible to produce by switching off the bending magnet, and the parameters of beam emittance at the entrance to the bending magnet can be calculated from the experimentally obtained values by the reverse linear transformation for a drift length through the magnet.

EQUIPMENT, CALIBRATION AND EXPOSURE REDUCING

For testing of this emittance measuring device in the H-minus LEBT channel of INR RAS linac was assembled the system, which included "pepper-pot", the quartz screen and the CCD-camera type "VIDEOSCAN-415-USB".

Diagram of this emittance measuring device is shown in Fig.2 The camera uses CCD-matrix SONY ICX415AL with 780*582 pixels image format and 12-bit digitization. "Pepper-pot" had a set of holes with a diameter of 0.2 mm, arranged with a pitch of 3 mm for a field of approximately 100x100 mm^2. Distance from "pepper-pot" to the screen was 200 mm.

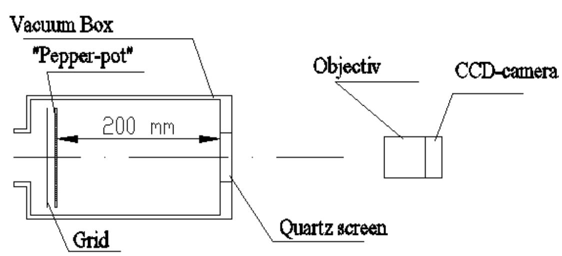

Figure 2: Diagram of emittance measuring device.

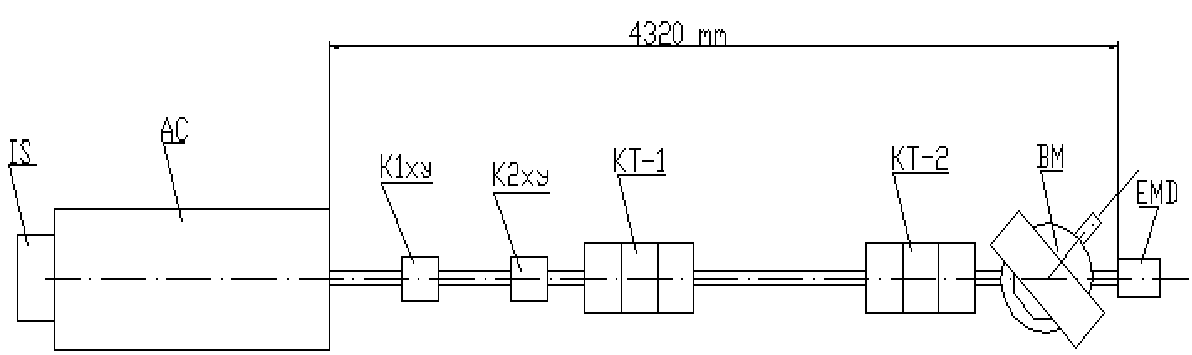

Figure 1: Scheme of the beam line channel with the emittance measuring device. IS – H-minus ion source, AC – 400 keV acceleration column, K1xy, K2xy – steering magnets, KT-1, KT-2 - quadrupole triplets, BM – bending magnet, EMD - emittance measuring device.

ISBN 978-3-95450-181-6

MODERNIZATION OF THE ELECTRON BEAM STABILIZATION SYSTEM IN THE KSRS

K. Moseev#, E. Kaportsev, Y. Krylov, A.Valentinov,
NRC Kurchatov Institute, Moscow, Russia

Abstract

The stabilization system is designed to prevent drift of the spot SR at the experimental stations by local changes of the orbit. This system was developed and implemented about twelve years ago as an element of the ACS and worked well. Produced by modernization has led to the need of adaptation of the system of stabilization not only in hardware but also in software. Work on updating of the stabilization system and will be shown next.

The running cycle of Kurchatov Synchrotron Radiation Source (KSRS) includes the injection of electrons with energy 80 MeV from the linear accelerator in the booster storage ring Siberia-1, the accumulation of a electron current up to 400 mA and, then, electron energy ramping up to 450 MeV with the subsequent extraction of electrons in the main ring, storage ring Siberia-2, and accumulation there up to 300 mA, and at last the energy ramping up to 2.5 GeV. [1] This mode is the basic mode for obtaining SR by users of the experimental stations. The high stability of the x-ray beam at the entrance of the experimental station is one of the most important conditions for the successful functioning of the SR source. (Fig.1)

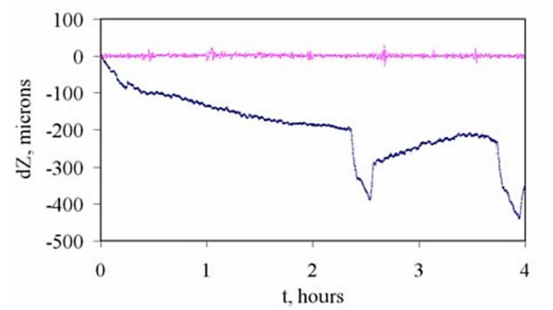

Figure 1: SR beam position at an entrance of experimental station. Bottom line – feedback system is switched off, top line – feedback is switched on. Standard deviation from initial position in last case was 4.5 microns.

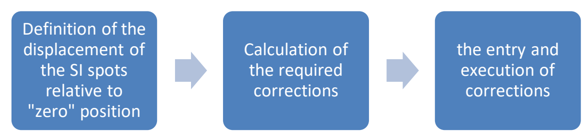

Figure 2: The principle of the stabilization system.

LOCAL FEEDBACK SYSTEM TO CORRECT SYNCHROTRON RADIATION BEAM POSITION AT SIBERIA-2 STORAGE RING

Stabilization system (SS) is part of a control system of accelerator complex and is designed to prevent drift of the spot SR at the experimental stations by local changes of the orbit [2].

Stabilization system provides feedback spot position SR at the experimental stations and the current in the correctors. Information about the position of the spot SR is obtained from the video camera, then it is calculated the deviation from the nominal position and the value of the required correction. Needed position of the beam in the area of the controlled channel is provided specific for this channel set, containing 3 or 4 corrector, so that the changes don't affect the orbit outside the correction area (Fig.2).

LOCAL FEEDBACK SYSTEM. REALIZATION AND MODERNIZATION

SR beam position monitor is a stripe of phosphor using side part of SR beam. A few dozen frames of digital image exposure is processed to determine the center of the spot of SR. The output of the program is the value of deviation of the beam from the nominal position. This value is written to the database table. Further there is a similar process the next channel. The operator at any time has the ability not only to enable or disable the stabilization, but also to adjust the position of the SR spots. In addition, there is the ability to accurately define the area of illumination to reduce the impact of probable defects of the camera and the phosphor (Fig.3).

The program calculate the necessary correction values, referring to the database, receives the position deviation of the beam from the nominal position and the set of coefficients for the calculation, selected in advance. The result of this program is the set of values of the currents of the correctors are also recorded in the database table. Further, similarly calculated for other stations (Fig.4).

#kirit@yandex.ru

ELECTRODYNAMIC CHARACTERISTICS OF RF-DEFLECTOR FOR BUNCH SHAPE MONITOR

D. Chermoshentsev†[1], A. Feschenko, S. Gavrilov, Institute for Nuclear Research of the Russian Academy of Sciences, Moscow, Russia and Moscow Institute of Physics and Technology, Moscow, Russia
[1] also at Skolkovo Institute of Science and Technology, Skolkovo, Russia

Abstract

Bunch shape monitors, based on a transverse RF-scanning of secondary electrons, are used for measurements of particles longitudinal distribution in bunches at different linear ion accelerators. The phase resolution of such monitors depends crucially on accuracy of fabrication and tuning of RF-deflector, thus preliminary simulations of its electrodynamic characteristics are of importance for subsequent commissioning of the monitor. Simulations of basic operational electrodynamic parameters and some experimental results are presented.

INTRODUCTION

Bunch shape monitor (BSM) [1] uses the technique of coherent transformation of a temporal bunch structure into a spatial charge distribution of low energy secondary electrons through RF-modulation [2]. The main part of BSM is RF-deflector. The deflector is combined with electrostatic lens, thus enabling simultaneous focusing and RF-scanning of the electrons. Typically, BSM deflectors are RF-cavities based on parallel wire lines with capacitive plates. Electrical length of the deflectors is usually λ/4 or λ/2 (Fig. 1). The electrodes with deflecting plates 1 are supported by ceramic insulators. Focusing potentials are supplied at a zero electrical field points via ceramic resistors 4, which are used to diminish the influence of external connections.

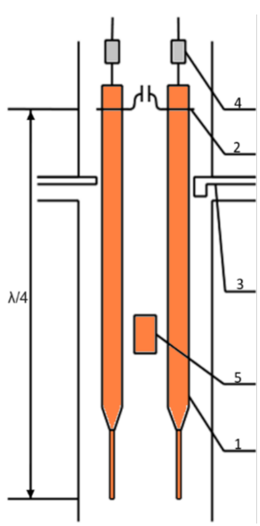

Figure 1: Scheme of λ/4 (left) and λ/2 (right) RF-deflectors.

In λ/4-type deflector resonant frequency is adjusted by moving jumper 2. The jumper consists of two collets connected by ceramic capacitors. Coupling loops 3 are used to drive the cavity and to pick up the RF-signal.

In λ/2-type deflector resonant frequency is adjusted by changing the length of the electrodes with screws 2. Capacitive couplers 3 are used for driving and control.

Tuners 5 with different geometries are intended for fine frequency tuning of both cavity types from outside vacuum. Tuning of RF-deflectors includes adjustment of resonant frequency and input matching of RF-couplers to minimize reflections.

For proper operation, a deflector development should begin from preliminary calculations of its electrodynamic parameters, such as: resonant frequency, quality factor and equivalent impedance as well as S-parameters.

RESONANT FREQUENCY

Development process of BSM is based on COMSOL Multiphysics, that provides comprehensive simulations of all characteristics, including RF-parameters [3].

A frequency of RF-deflecting field should be equal or multiple to the RF-field frequency in the accelerator. Geometry of the RF-cavity can be simply calculated via Eigenfrequency solver. However these simulations should take into account positions of ceramic insulators (electrode holders), which change the resonance frequency crucially, because of rather high relative permittivity (about 10).

If the deflector is tuned in the air, it needs extra tuning from outside vacuum after pumping, due to the shift of resonance frequency. The exact values depend on the temperature and humidity of the air, but the difference is rather small (less than 100 kHz for operational frequencies) and can be easily compensated (Fig. 2) by fine tuner, which geometry and stroke can be simulated preliminarily.

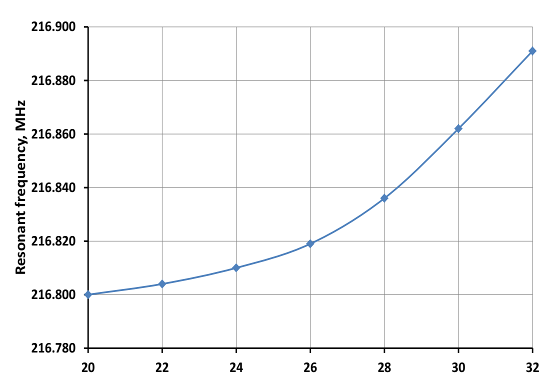

Figure 2: Example of experimental dependence between resonant frequency and tuner position in the λ/4-type deflector with operational frequency 216.816 MHz.

† dmitriy.chermoshentsev@phystech.edu

ISBN 978-3-95450-181-6

PROPOSAL TO SYMMETRIC QUENCH DETECTION AT SUPERCONDUCTING ELEMENTS BY BRIDGE SCHEME USAGE

E.V. Ivanov, A.O. Sidorin, A.L. Svetov, JINR, Dubna, Moscow Region

Abstract

In the frame of the NICA project [1] two new superconducting accelerators will be constructed – the Booster and the NICA collider. Specialized facility for manufacturing and testing of the SC magnets for the NICA and FAIR projects is under development at JINR [2]. Proposal to quench detection system for these and similar facilities is described in this paper.

INTRODUCTION

Currently to detect the active phase on the superconducting elements of modern accelerator complexes widely used method of active phase voltage selection out of the total voltage drop at the controlled element and further analysis to meet the criteria of the quench.

The voltage on the inductive superconducting element is described by the formula:

$Vm = Lm\frac{dI}{dt}$, where Vm – voltage at inductance element, Lm – inductance of a magnet. Voltage at the beginning of quench is Vsm=Rq*I+$Lm\frac{dI}{dt}$ =Rq*I+Vm, where Rq- is resistance of a region with active phase.

Selected quench voltage is Vq=Vsm-Vm is analyzed by the detector logic to meet the criteria of exceeding the voltage threshold Vth by amplitude during predefined time Tv. Exceeding of these thresholds is a condition to turn protective systems on and start energy evacuation from the magnetic system of the accelerator.

It should be noted that the quench voltage Vq is typically ≈100÷200 mV, and voltage Vsm and Vm change dynamically during acceleration cycle in the range from –10V to +10V depending on the rate of change of the magnetic field and of the element inductance.

Thus, the detection scheme must reliably identify the voltage Vq over a wide dynamic range regardless of the instantaneous voltage on the element at each moment of time [3].

Basically bridge scheme is used to select quench signal Vq. This method of detection is widely used due to its undeniable advantages that are missed in other solutions. So, the bridge is completely passive element, so it can detect the signal of any dynamic range in amplitude. The signals from the magnetic elements in the bridge scheme are differential, thus making the bridge scheme insensitive to induced noise. And moreover the bridge scheme is pretty simple, cheap in realization and very robust.

While using the bridge scheme, it is very important that arms of the bridge – that is controlled inductance - have a minimum length. Otherwise due to phase shifts to obtain the bridge scheme being balanced is possible only at one fixed frequency. Herewith any change of the voltage (rise and/or decline) will result in short-term dynamic disbalancing.

So the optimal usage of the bridge scheme to protect quench of a superconducting accelerator elements is to use it in schemes with mid-point connection. In such a solution the scheme logic compares signals from two halves of a magnet. Such a bridge scheme should use the minimum possible inductance, and the shortest linear connections.

Some publications (TEVATRON [4], LHC [5], and the latest SIS 100 documents) indicate the possibility of the so-called "symmetric quench" to occur while using the protection system with mid-point connection scheme. That is the appearance of the active area at the mid-point connection and its symmetric uniform propagation resulting in the bridge scheme disbalancing not happened. Earlier to exclude this situation the sensors with group of magnets bridging were mostly used. Recently some attempts are made to measure the quench by non-bridge sensors.

Unfortunately, the comparison of signals without using the bridge scheme implies necessity to use a very accurate differential amplifier with large dynamic ranges of input voltage and low drift in both measurement channels. Today such devices appear in catalogues of some manufacturers, although usage of these amplifiers in real accelerators is still very difficult to be widely used. In addition, for comparison of the real and reference signals you need to have the reference signal exactly copying the controlled signal and having no phase shift and noise. This fact is the main difficulty to implement such methodology. Realization of such a reference signal is quite difficult structurally.

As an alternative, at the LHC obtaining the derivative is implemented by measuring the current in the circuit before and after the controlled magnet with the subsequent differentiation and averaging. This method is very complex and expensive, and is used in circuits with currents less than 700A and very large (~1V) threshold.

SIS 100 proposes to use one supplementary superconducting filament as a reference winding. The method is also very complex and difficult in design.

In this paper we propose a solution for a problem of the symmetric quench detection while using a bridge detector for the magnetic elements of the NICA accelerator complex, LHEP, and the like [3].

ISBN 978-3-95450-181-6

APPLICATION OF MODEL INDEPENDENT TECHNIQUES AT VEPP-2000 AND SIS100

D. Rabusov, Yu. Rogovsky, BINP, Novosibirsk, Russia

Abstract

In order to exploit an accelerator successfully all parameters should be set correctly. To check and fix errors in the accelerator lattice measurements of parameters of the betatron motion and measurements of optical functions of the accelerator lattice are used. Due to Model Independent Analysis it is possible to carry out measurements of the beta-function and the phase advance fast. Using NAFF technique lets us compute betatron tune with good precision. Limiting capabilities of the MIA at SIS100 project are discussed, implementation of the MIA and the NAFF techniques at booster VEPP-5 and at collider VEPP-2000 are shown.

INTRODUCTION

In order to receive the information about settings of an accelerator we can use MIA (Model Independent Analysis) [1] and NAFF (Numerical Analysis of Fundamental Frequencies) [2]. These techniques demand beam histories — arrays of data from BPMs (Beam Position Monitors), which have the information about the betatron motion of the beam. We don't have enough possibilities to describe these methods, but full specification you can find in the references.

SIS100. THE RESULTS OF SIMULATIONS

SIS100 is a future synchrotron for acceleration of high intensity and high energy ion beams with primary significance in the FAIR project. In its design the synchrotron has six equivalent sectors and is served by 84 BPMs.

To examine the limiting capabilities of the future diagnostic system of SIS100 and the MIA technique, numerical simulations were applied. At first, particle tracking with MADX [3] was used, then simulated "beam histories" were filtered and analyzed with MIA. Received results (shown on Figure 1 and 2) were compared with the beta-function and the phase advance, that are calculated using MADX. For all these calculations parameters were applied: $n = 200$ turns, the level of the noise $\Delta x = 100$ μm; amplitudes of the simulated betatron oscillations were ≈ 1 mm. The error of MIA calculations is determined as:

$$\delta = 100\% \cdot \frac{1}{m}\sum_{i=1}^{m} \left|\frac{f_i^{MADX} - f_i^{MIA}}{f_i^{MADX}}\right| \quad (1)$$

where f is β or ϕ, $\phi_i = \Psi_i - \Psi_{i-1}$. The difference between the model beta-function in positions of BPMs and measured by MIA is less than 2 %. For the phase advance precision is better than 1 %. Also the relative error of calculations raises almost linearly in the observed range of noise-amplitude ratio. Furthermore the MIA error decreases when n raises. These results are shown on the Figure 3.

Finally, we tested limiting capabilities of MIA using the "beta-beating" task. We applied the unrealistically big gradient error at the level equal to 5%. Results are shown on the Figure 4. Green triangles are the distorted beta functions at the BPMs, blue points are the ideal beta-functions at the BPMs, red crosses are β calculated by MIA. Here we found that calculations of the β-function are very sensitive for varying scaling factor (J^{-1}).

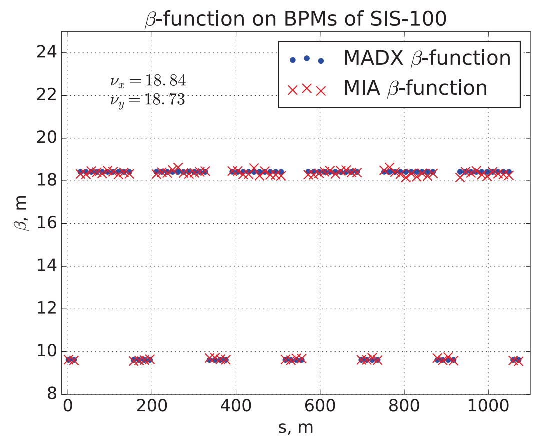

Figure 1: Values of β-function at BPMs for SIS100.

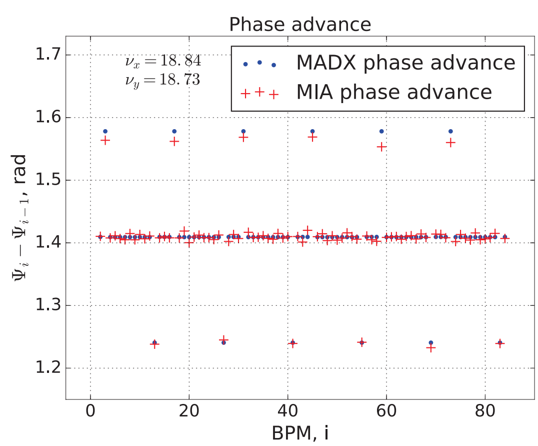

Figure 2: The phase advance between neighboring BPMs.

ISBN 978-3-95450-181-6

BEAM DIAGNOSTICS AND INSTRUMENTATION UPGRADE FOR MULTIPURPOSE RESEARCH COMPLEX OF INR RAS

S. Gavrilov†, V. Gaydash, V. Gorbunov, Y. Kalinin, Y. Kiselev, P. Reinhardt-Nickoulin, I. Vasilyev
Institute for Nuclear Research of the Russian Academy of Sciences, Moscow, Russia

Abstract

Accelerated proton beam of INR linac is used for various facilities in multipurpose research complex of INR RAS, including experiments of neutron investigations and medical physics laboratories. In recent years beam instrumentation for transport channels of the complex has been upgraded and supplemented. Electrostatic pick-ups, beam current transformers, ionization chambers, multiwire SEM-grids, as well as its front-end and processing electronics were developed and combined to improve beam diagnostics. Some technical details and available results of beam measurements are presented in the paper.

INTRODUCTION

Multipurpose research complex (MRC) [1] of INR RAS includes four beam outlets (Fig. 1): three neutron facilities of neutron investigations laboratory (time-of-flight RADiation Experiment, pulse neutron source IN-06, lead neutron slowing-down spectrometer LNS-100) and research Complex of Proton Therapy, which is a part of medical physics laboratory.

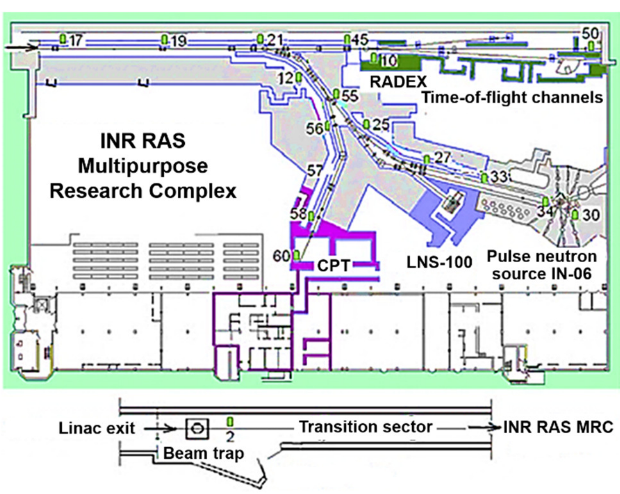

Figure 1: Layout of INR RAS MRC.

Depending on beam user requirements INR RAS linac has to provide beam parameters in a wide range of values: beam energy 100÷209 MeV, pulse current 0.01÷15 mA, pulse repetition rate 1÷50 Hz, pulse duration 0.3÷180 µs. Moreover, these parameters can be changed several times during a shift for different research groups, that needs not only reliable operation of the linac in different duty cycles, but also a universal beam instrumentation available for routine beam control in the whole range of parameters.

† s.gavrilov@gmail.com

DIAGNOSTICS AT THE LINAC EXIT

Beam emittance and position measurements at the linac exit are of importance for proper matching with the linac-MRC transition sector. In-flight beam diagnostics before a beam trap is provided by Beam Cross Section Monitor (BCSM) [2]. The monitor, utilizing a residual gas ionization, enables to observe 2D beam cross section, beam position and profiles, as well as transverse emittance ellipses (Fig. 2), which can be reconstructed [3] from beam profiles data during linear transformations in phase space by variation of fields in upstream quads.

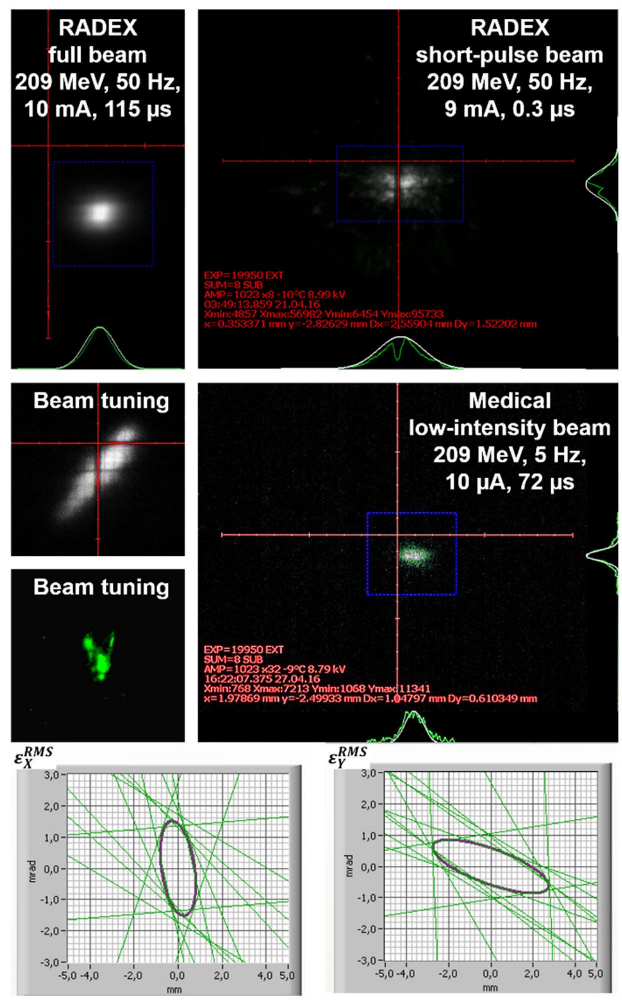

Figure 2: BCSM results for different beam parameters.

Now BCSM is a reliable tool for efficient beam tuning and an accurate non-destructive diagnostics at the linac exit in the whole required range of beam parameters.

ISBN 978-3-95450-181-6

THERMAL LOADS OF WIRE-BASED BEAM INSTRUMENTATION AT ION LINACS

M. M. Churaev†[1], S. A. Gavrilov, Institute for Nuclear Research of the Russian Academy of Sciences, Moscow, Russia and Moscow Institute of Physics and Technology, Moscow, Russia
[1] also at Skolkovo Institute of Science and Technology, Skolkovo, Russia

Abstract

Wire-based beam instrumentation remains a reference for calibration of many other instruments, providing direct and accurate measurements with high resolution. However increasing of a beam power of existing and forthcoming ion linacs results in strict constraints on operation modes acceptable for control and diagnostics. Relevant simulations of wire thermal loads are necessary not only for a mode choice, but also for a preliminary design of such instrumentation. Simulations for different wire materials and various beam parameters are made. Features of the model are discussed. Numerical estimations and conclusions are presented in comparison with some experimental results.

INTRODUCTION

Beam ionization losses are the main target heating mechanism at ion linacs. In wire-based instrumentation excessive heating may cause different problems. Firstly, temperature increase results in rise of thermionic emission, that makes additional electric noise, and accuracy in case of secondary emission based measurements goes down. Secondly, overheating can change metal structure of wire or result in wire breakage. Moreover, thermal expansion affects accuracy.

MODEL

Calculations were done using finite elements analysis in COMSOL Multiphysics package. For the computing geometrical mesh with 1/10 of wire radius in cross-section and 1/50 of wire length in longitudinal direction was chosen.

Temperature dependences of thermal conductivity, heat capacity and total hemispherical emissivity of wire material are taken into account (Figs. 1-3).

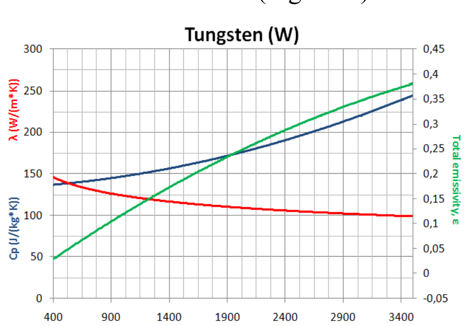

Figure 1: Thermal properties of tungsten.

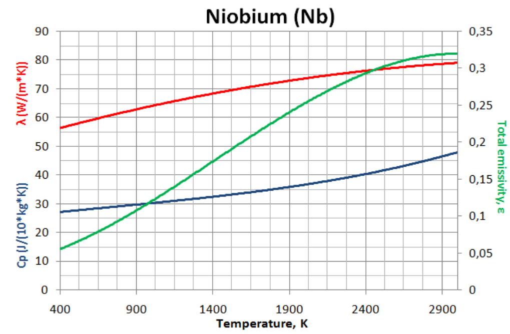

Figure 2: Thermal properties of niobium.

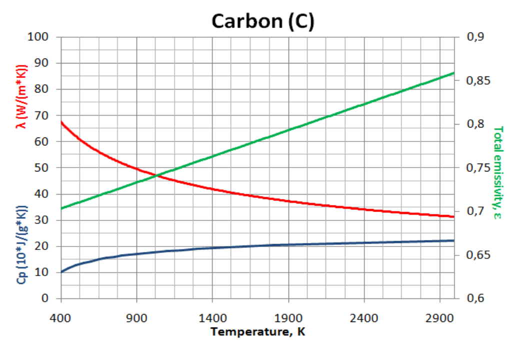

Figure 3: Thermal properties of carbon.

Ambient temperature and initial wire temperature assumed to be 293 K. Considering wire holder being well thermal conductive, boundary conditions can be set as constant temperature 293 K at the wire edges.

Beam is described by: ion parameters, energy, pulse current and duration, pulse repetition frequency, RMS transverse sizes. The wire center supposed to be in the beam center. Function of ionization losses of projectiles are taken from SRIM tables [1]. Volume density of ionization losses (Fig. 4) in the wire is used further as a heat source.

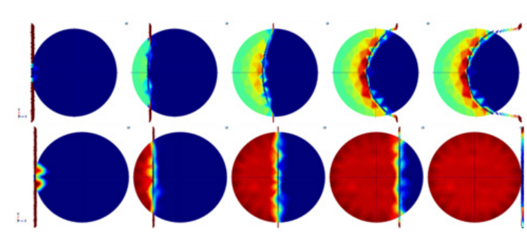

Figure 4: Density of ionization losses for low-energy and high-energy proton beam across the tungsten wire.

The most results are given for tungsten wire with diameter d=100 um in proton beam with RMS size 2x2 mm, unless otherwise specified.

† churaev@phystech.edu

THE LONGITUDINAL DISTRIBUTION AND BUNCH LENGTH MEASUREMENTS AT VEPP-2000 COLLIDER*

Yu. Rogovsky#, E. Perevedentsev, Yu. Zharinov, V. Volkov,
Budker Institute of Nuclear Physics, Novosibirsk, 630090, Russia
A. L. Romanov, Fermi National Laboratory, Batavia, IL 60510, USA

Abstract

The paper describes the bunch length measurement system for VEPP-2000 collider, equipped with optical analysers based on LI-602 dissector, which provides permanent measurements of the longitudinal beam profile. Potential well distortion lengthening was measured at different bunch currents for the energies below 500 MeV. First measurements reveals the presence of microwave instability with turbulent emittance growth. The thresholds of these processes was used to estimate the values of reactive part of the longitudinal impedance. Measured energy loss factors was compared with computer simulations for the RF cavity. All results will be discussed and further estimations will be given.

VEPP-2000 OVERVIEW

The VEPP-2000 collider [1] exploits the round beam concept (RBC) [2]. This approach, in addition to the geometrical factor gain, should yield the significant beam–beam limit enhancement.

Collider itself hosts two particle detectors [3], Spherical Neutral Detector (SND) and Cryogenic Magnetic Detector (CMD-3), placed into dispersion-free low-beta straights. The density of magnet system and detectors components is so high that it is impossible to arrange a beam separation in the arcs. As a result, only a one-by-one bunch collision mode is allowed at VEPP-2000.

Table 1: VEPP-2000 Main Parameters @ E = 1 GeV

Parameter	Value
Circumference (C)	24.3883 m
Energy range (E)	150÷1000 MeV
Number of bunches	1 × 1
Number of particles per bunch (N)	1×10^{11}
Betatron functions at IP ($\beta^*_{x,y}$)	8.5 cm
Betatron tunes ($\nu_{x,y}$)	4.1, 2.1
Beam emittance ($\varepsilon_{x,y}$)	1.36×10^{-7} m rad
Beam–beam parameters ($\xi_{x,y}$)	0.1
Luminosity (L)	1×10^{32} cm^{-2} s^{-1}

The layout of the VEPP-2000 collider as it worked until 2013 is presented in Figure 1. The main design collider parameters are listed in Table 1.

*Work supported by the Ministry of Education and Science of the Russian Federation, Nsh-4860.2014.2
#rogovsky@inp.nsk.su

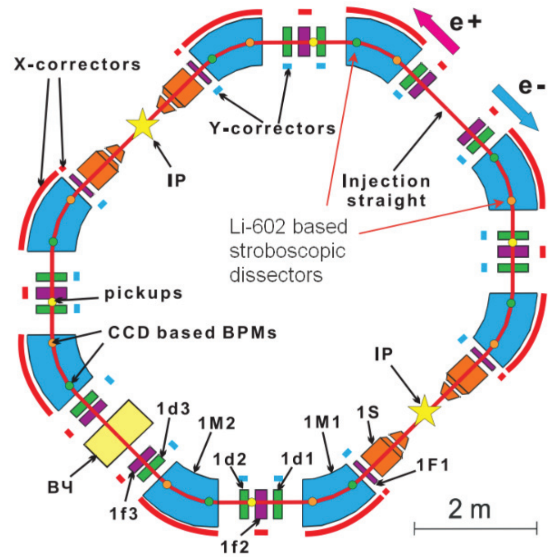

Figure 1: VEPP-2000 collider layout.

BEAM DIAGNOSTICS

Diagnostics is based on 16 optical CCD cameras that register the visible part of synchrotron light from either end of the bending magnets and give full information about beam positions, intensities and profiles. In addition to optical beam position monitors (BPM) there are also four electrostatic pickups installed in the technical straight sections, two photomultipliers for beam current measurements via the synchrotron light intensity, and one beam current transformer as an absolute current monitor.

In 2013 VEPP-2000 was equipped with two phi-dissectors [4] – stroboscopic image dissector with electrostatic focusing and deflection, that gives information about e+/e− longitudinal distribution of particles and bunch length.

In general, the instrumental temporal resolution of the dissector is determined by a set of different factors. The most important ones: energy and angular distribution of the photoelectrons emitted by a photocathode; quality of the electron image in the plane of the slit aperture; light image size at the photocathode; amplitude and frequency of sinusoidal sweep voltage; slit aperture size.

The contribution to the instrumental temporal resolution of the first factor is estimated as equal (or less) to 1.0 ps. value and contribution of other factors can be measured. For this purpose a point-like image of the continuous light source is projected onto photocathode and the signal

ISBN 978-3-95450-181-6

BEAM DIAGNOSTICS OVERVIEW FOR COLLECTOR RING AT FAIR*

Yu.A. Rogovsky†, D.B. Shwartz, Budker INP SB RAS, Novosibirsk, Russia and Novosibirsk State University, Novosibirsk, Russia and FSBI "SSC RF ITEP" of NRC "Kurchatov Institute", Moscow, Russia
E.A. Bekhtenev, O.I. Meshkov, Budker INP SB RAS, Novosibirsk, Russia and Novosibirsk State University, Novosibirsk, Russia
M.I. Bryzgunov, Budker INP SB RAS, Novosibirsk, Russia
O. Chorniy, GSI Helmholtzzentrum für Schwerionenforschung, Darmshtadt, Germany

Abstract

The Collector Ring (CR) [1] is an essential ring of the new international accelerator Facility of Antiproton and Ion Research (FAIR) [2] at Darmstadt, Germany. It will operate with antiproton energy of 3 GeV and has a complex operation scheme and several types of operational cycles. In this paper, we present an overview of all diagnostic systems, which are planned for commissioning and operations. Challenges and solutions for various diagnostic installations will be given.

INTRODUCTION

The main emphasis of the CR is laid on the effective stochastic precooling of intense Rare Isotope Beams (RIBs), secondary stable beams and/or antiproton as well. Special task – mass and half-life measurements of very short-lived nuclides (down to few tens μs) will be performed in the CR operated in isochronous mode [3].

Table 1: Main Parameters of the CR

Parameter	Value		
Circumference	221.45 m		
B ρ	13 Tm		
Mode	**p-bar**	**RIB**	**Isochronous**
Max. intensity	10^8	10^9	$1\text{-}10^8$
Particl. charge	1	40-100	40-100
Repetit. rate	1	1	—
Kinetic energy	3 GeV	740 MeV/u	400-790 MeV/u
Lorentz γ	4.20	1.79	1.43 – 1.84
Transition γ_{tr}	4.83	2.727	1.43 – 1.84
Slip factor |η|	0.014	0.1776	0
Acceptance	240	200	100
RF freq., MHz	1.315	1.124	0.968-1.137
RF harmonic	1	1	—
Betatron tunes	4.39/3.42	3.40/3.44	2.21/4.27
Bunch length	50 ns	50 ns	—

There are several types of operational cycles with beams in CR starting from injection and finishing with extraction, and beam parameters (see Table 1) change significantly during the cycles. The momentum spread is largest at injection, when very short bunches of several tens ns from the production targets (either RIBs or antiprotons) are injected. At this instant, the horizontal aperture of the ring is filled.

After a 1.5 ms bunch rotation and a 150 ms adiabatic debunching, the momentum spread is decreased, whereas this process leaves the transverse emittance unchanged in both directions. After these procedures the bunch fills all the perimeter of the CR. The reduced momentum spread is a necessary prerequisite for stochastic cooling. The cooling time for the antiprotons is 10 s and is estimated as 5 s after further CR upgrade. The cooling time for highly charged RIBs is much shorter (1.5 s). After the procedure of stochastic cooling, all phase subspaces are strongly reduced. The cooling is followed by the re-bunching procedure in 130 ms and further extraction of the beam.

Beam parameters changes significantly during the cycles as well as along the ring [4]. This demands an exceptional high dynamic range for the beam instrumentation and non-destructive methods are mandatory for high currents as well as for the low current secondary beams due to the low repetition rate. Precise measurements of all beam parameters and automatic steering with short response time are required due to the necessary exploitation of the full ring acceptances.

BEAM DIAGNOSTICS SUITE

The beam diagnostic systems are designed to provide a complete characterization of the beam properties including beam closed orbit, size, tune, circulating current, fill pattern, lifetime, chromaticity, beam loss pattern, beam density distribution, emittance, and bunch length. A large number of beam monitors and will be installed in the ring (see Table 2).

Electrostatic Pick-ups (18 combined and 1 vertical) measure the beam centre-of-charge transverse position in a non-interceptive way. In normal operation mode, the Pick-up signals are averaged for orbit corrections [5]. Alternatively, a subset of the monitors can be read out turn-by-turn, synchronized to the bunch passage for tune measurements, etc.

A Fast Current Transformer provides the longitudinal structure with turn-by-turn resolution during bunch rotation in longitudinal phase space. A DC Current provides the total number of ions circulating in the ring. Both Fast CT and DC Current Transformers will have calibration coils

* The work is carried out with the financial support of FAIR-Russia Research Center
† rogovsky@inp.nsk.su

ISBN 978-3-95450-181-6

SYSTEM OF THERMOMONITORING AND TERMOSTABILIZING OF KURCHATOV SYNHROTRON RADIATION SOURSE

N. Moseiko, E. Kaportsev, K. Moseev, Y. Krylov, A. Valentinov, Y. Efimov, National Research Centre Kurchatov Institute, Moscow, Russia

Abstract

The modern system of thermomonitoring and thermostabilizing of KSRS is described. The system provides: a monitoring of temperatures of the magnets and RFresonators of KSRS; informing operator on violations of the course of technological process; data protection from illegal access; archiving and displaying of archive data in a trend type. The system includes 480 temperature sensors of the AD592 type, providing the accuracy of measurements 0, 2 C^0. System of thermo stabilizing of the linear accelerator the proportional integral differentiating regulator for support of stability of temperatures at the level of 0, 05 C^0 .

INTRODUCTION

The National Research Centre Kurchatov Institute, completed work on the creation of a new automated control system (ACS) accelerator-storage complex (ASC) "Siberia" [1-5] on the basis of modern servers, network equipment, the VME hardware, National Instruments company modules and new power ASC equipment (with built-in controllers). It uses software tools: Citect SCADA 7.2 (full version), Lynx OS Runtime, LabVIEW-2013 development environment Thursday PK-166 software, OS ARTX166, PCAN-Evaluation, and others. As part of a new ACS was developed modern system of temperature control and temperature stabilization of ASC "Siberia".

APPLICATIONS

TERMOCS operator's application consists of a set of video imaging that are designed to display information about the temperature adjustment is-ditch, lenses and bending magnets ASC "SIBERIA" [1-5]. In this video frame (Fig. 1) shows designed to display the current temperature correctors, lenses and bending magnets of a linear accelerator, a small storage, the EOC-1 and the EOC-2.

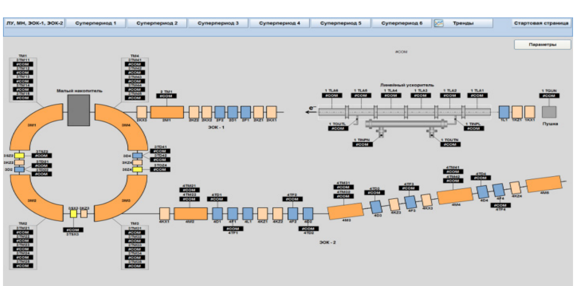

Figure 1: Video frame "LU, PL, EOC-1 and EOC-2".

In this video frame (Fig. 2) shows display the current temperature correctors, lenses and bending magnets in each superperiod Accumulate large-telja.

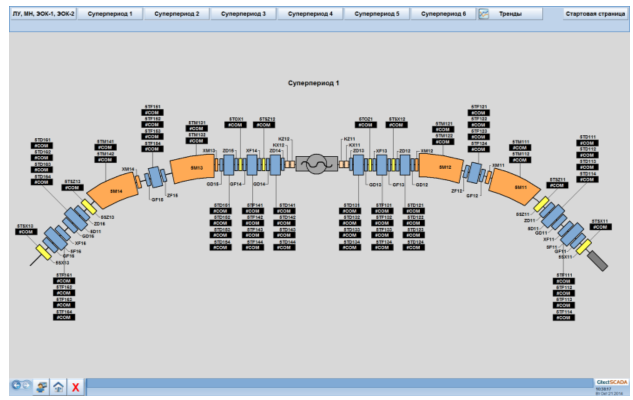

Figure 2: Video "Superperiod 1"- "Superperiod 6".

In this video frame (Fig. 3) shows intended to display archival temperatures in graphs.

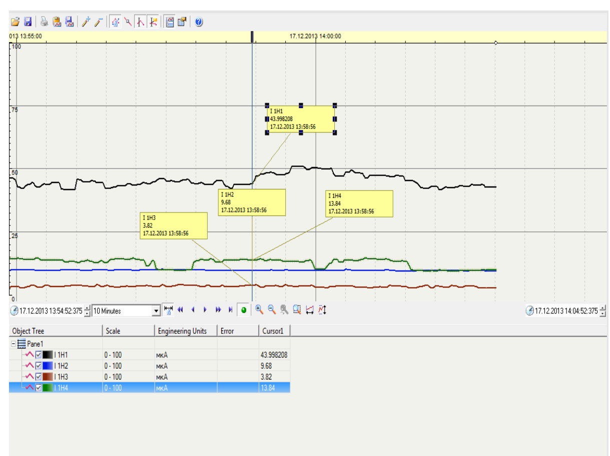

Figure 3: Video frame "Trends".

WORKING WITH TREND

To work with the current and historical trends using «Process Analyst» (Fig. 4). The horizontal axis of the graph is the time axis, which is equal to the selected interval, co-tory user-configurable. The vertical axis represents the values of technological parameters imposed on the chart. Setting trends and management is carried out by the following elements:

- Addition and removal of curves with the trend;

MONITORING OF LOW INTENSITY ION BEAMS AT FLNR ACCELERATOR COMPLEX

Yu.G. Teterev, S.V. Mitrofanov and A.I. Krylov, Flerov Laboratory of Nuclear Reactions, Joint Institute for Nuclear Research, Dubna, Moscow Region, Russia

Abstract

Detectors are developed to diagnose ion beams inside the accelerator, during beam transportation, and to control beam in the user area. The intensity of beam in the range from several ions per second up to pnA, the energy, the density distribution and the grade of the beam are monitored by the detectors. Depending on the operating conditions the ionization chambers, the proportional counters, the scintillation detectors and lamellar sensors with dual screen are used. The main criteria for the detector design are the reliability in long time operation under radiation, in magnetic fields and in rapidly changing vacuum conditions, and the possibility of quick repair or replacement. The diagnostic detectors are located in the channels to study the radiation resistance of electronics, and in the channel for the biological research.

INTRODUCTION

Beams of accelerated ions of low intensity are required for applied research, e.g., research of radiation resistance of electronics [1] or in biology. The intensity of these beams is less at three or more orders of magnitude than those used at the FLNR accelerator complex traditionally. There is a need to create a new set of diagnostic tools with greater sensitivity. A new set based on the detectors that are traditionally used in physical experiments. When choosing the detectors the conditions in which they will operate are taken into account. For example, detectors placed inside the cyclotron are exposed to a strong magnetic field, high radio frequency field and x-radiation. The detectors operate in high vacuum, which must not be spoiled. It is not always possible to remove the detector from the vacuum chamber. It can only be moved to the periphery, if the cyclotron works on the traditional beams. The detector should be reliable and resistant to radiation.

MEASUREMENT OF BEAM CURRENT INSIDE THE CYCLOTRON

Two different detectors operating in the current mode are designed and tested to work inside the cyclotron. First one is the detector based on secondary emission; the second one is the air filled ionization chamber with a thin metallic entrance window. Currents produced by these detectors are measured by means of amplifiers, the minimum value of the input current which is 1 pA.

The detector based on secondary emission consists of three lamellae, one of which is located in the center perpendicularly to the beam axis, the other two above and below, respectively. The width of each lamella is 8 mm, the thickness is 1 mm, and the distance between the centers of the lamellae is 11 mm. Each lamella is surrounded by a screen. The screen is open only from the side of the ion beam. Voltage +9 V from a battery is fed to the screen. The emission electrons arising from the bombardment of ion beam are collected by the screen. This screen is surrounded by second screen which is grounded. Dual screening reduces noise level to less than 1 pA. Current from each of the lamella is measured.

The described detector allows measuring the ion current only in arbitrary units. The output of the secondary electron emission depends on the type of ion, its energy and is proportional to the differential energy loss in the material of the lamella. The experiment on the calibration of the detector by the external beam of argon with energy of 32 MeV/nucleon shows that the detector can be used on the beam intensities higher than10^4 ions/s.

In the same calibration experiment it was shown that a detector with ionization chamber can be used on the beam intensities by three orders of magnitude lower. Special measures are adopted to prevent x-ray radiation from dees on the readings of the detector. Current from ionization chamber is measured on collector, in front of which there are two identical electrodes. The voltage on these two electrodes is supplied with the opposite polarity. Currents in the chamber compensate each other in the absence of the beam. The beam is passed only through space between the collector and one of the opposite electrodes. In spite of the high sensitivity, the camera has some disadvantages. One of them is the presence of the entrance window, which limits the application of the detector for measuring the intensity of ions having a small path length. Another disadvantage is the presence of gas in the volume of the ionization chamber inside a cyclotron that can create an emergency situation.

THE DETECTOR TO MEASURE THE BEAM CURRENT AFTER THE EXIT FROM THE CYCLOTRON

Gas-filled detector is mounted directly after the beam extraction from a cyclotron. The working gas of the detector is air. The input window of the detector with a diameter of 60 mm is closed by a foil of stainless steel with a thickness of 6 µm. The detector can operate in two modes: proportional counter and ionization chamber. The detector is a set of interleaved grids, the anodes and cathodes. The anodes are coiled from a wire thickness of 20 µm, and the cathodes from wire thickness of 100 µm. Voltage 1800-2100 V is supplied to the counter. Its efficiency is nearly 100% for all ions. Similar proportional counter filled with air is described in [2].

ISBN 978-3-95450-181-6

DIAGNOSTICS OF ACCELERATOR BEAMS BY THE DEPENDENCE OF THE VAVILOV-CHERENKOV RADIATION INTENSITY ON THE REFRACTIVE INDEX OF THE RADIATOR "*n*"

K. A. Trukhanov†, SSC RF Institute of Biomedical Problems, RAS, Moscow, Russia
A. I. Larkin, Moscow Engineering Physics Institute, Moscow, Russia
V. I. Shvedunov, Skobeltsyn Institute of Nuclear Physics Institute MSU, Moscow, Russia

Abstract

The report presents the methods for finding of the particle velocity (energy) distribution of accelerator beams. Velocity distribution is deduced from the Volterra integral equation of the first kind with the right part, which is defined by the dependence of Cherenkov radiation (CHR) intensity on *n*, experimentally obtained for the given beam. Velocity distribution is the second derivative of CHR intensity. The problem of stability of the second derivative is solved by attracting a priori information. Using of optical dispersion of radiator is discussed. It enables to find velocity distribution even for the single bunch of particles. The method also enables to find velocity distribution for beams with a noticeable transverse velocity of the particles. The method is virtually non-destructive in many cases.

INTRODUCTION

The development of the non-intercepting methods for finding a velocity (energy) distribution of particles in accelerator beams is of great importance for irradiation process control in industry, medicine and science.

Existing methods of charged particle beam diagnostics have well-known disadvantages especially in the case of high energy beams. The non-traditional method of accelerator beam diagnostics based on the use of the CHR is considered below.

CHR angular distribution is used for a long time for determination of the velocity or the energy spectra of the charged particles [1]. However application of this method for the accelerator beams and especially for the electron beams of the high intensity industrial accelerators is limited by an essential transverse velocity component of the particles in the beam "smearing" the angular distribution of the radiation. Addition difficulty consists in superimposing of a transition radiation at radiator boundaries on the CHR angular distribution.

We consider two methods for finding a velocity (energy) particle distribution of beams based on the dependence of the CHR intensity and its spectral distribution on the phase velocity of the electromagnetic waves in the optical ranges (Fig. 1). The methods are practically non-intercepting and may be convenient for the energy and the energy spectrum measurements of beams including high intensity electron beams.

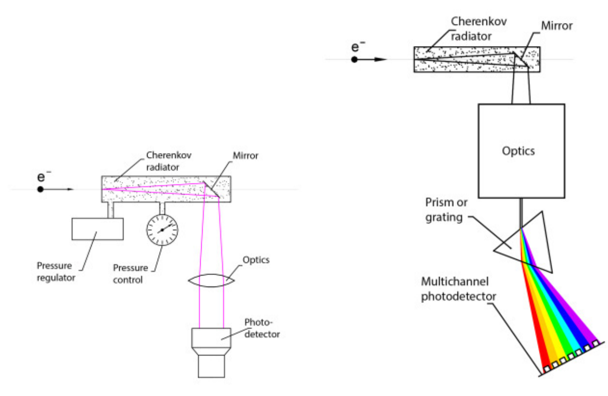

(a) (b)

Figure 1: Two methods for finding a velocity (energy) particle distribution with CHR. (a) The photons yield is registered by a photodetector depending on gas pressure. (b) The photons spectrum is recorded by the spectrum analyzer.

THEORETICAL BASES AND RESULTS

For the first time the possibility of determination of average electron velocity in the beam of the electron accelerator (the 4.5 MeV microtron) by the measurements of CHR intensity dependence on a radiator refraction index *n* in an optical range was demonstrated in [2, 3].

CO_2 was used as a radiator. The gases, which refraction index n varies with pressure p as $n(p) = 1 + kp$ at $kp<<1$, are natural choice of the CHR medium in this case. Once p passes the threshold of CHR for the maximum electron beam velocity in the detector ($1/\beta_{max} = 1+kp$) the CHR intensity I grows nonlinearly as more and more particles produce the CHR. Beginning from point where the minimal electron velocity β_{min} of beam particles becomes equal to the phase light velocity in the gas -radiator an intensity I of CHR in the detector is dependent on kp linearly. The intersection of the extrapolated CHR linear part with a background level corresponds to the average electron velocity in the beam [2, 3].

The same method was proposed in the work [4, 5] carried out 15 years later without reference to [2, 3]. No nonlinear part in *I(n)* dependence was noted.

In works of one of us (K.T.) [6] it was shown that nonlinear part of the intensity curve can be used for obtaining the velocity distribution and the energy distribution of the particles in the beam.

† trukhkt@com2com.ru

ISBN 978-3-95450-181-6

COAXIAL QUARTER WAVELENGTH IMPEDANCE CONVERTER FOR COUPLING CONTROL OF TRIODE CAVITY

K. Torgasin†, H. Zen, K.Morita, S.Suphakul, T. Kii, K. Nagasaki, K. Masuda and H. Ohgaki
Institute of Advanced Energy, Kyoto University, Kyoto, Japan

Abstract

In this work we describe the development of a coaxial quarter wavelength impedance transformer. The transformer is used for coupling control of a pre-bunching cavity for a triode type thermionic RF gun in Kyoto University Free Electron Laser (KU-FEL) facility. The application of prototype of impedance transformer could convert the coupling situation of the triode cavity from undercoupled to overcoupled state. The advantage of tested prototype is high power tolerance and out vacuum application. Further development of the prototype should ensure coupling control for beam loading compensation.

INTRODUCTION

The KU-FEL (Kyoto University Free Electron Laser) facility uses an S-band 4.5 cell thermionic RF gun as an electron source [1]. The gun is strongly suffering from back-bombardment effect, which causes decrease of beam energy during the macropulse. A promising cure for the electron back-bombardment problem is an introduction of triode configuration. In the triode structure a small pre-bunching cavity is set prior to the main accelerating body for controlling of injection timing. For the triode configuration the reduction of the back streaming electron energy for more than 80% is expected [2].

We have designed a small coaxial cavity as the pre-buncher of thermal emitted electrons. Figure 1 shows the longitudinal and cross sectional view on the triode cavity for the 4.5 cell triode type thermionic RF gun as designed for KU-FEL facility.

The cavity contains thermionic cathode for electron beam generation. For sake of compactness the cavity is coupled to RF power by longitudinal coaxial waveguide. The cathode was designed for overecoupled conditions. The overcoupling is intended to compensate for power absorption by the electron beam. For higher beam current higher overcoupling condition is required. The pre-bunching cavity was fabricated and cold tests at low and high power conditions were performed. However the fabricated cavity was revealed to be in underecoupled conditions [3].

In order to change the coupling conditions of the triode cavity we have developed an external quarter wavelength coaxial impedance transformer. We have applied a prototype of the impedance transformer with successful conversion of the undercoupled conditions to overcoupled. Further development could allow us selective adjustment of the coupling.

In this work we report about coupling conversion for triode cavity applying λ/4 impedance transformer.

† konstant@iae.kyoto-u.ac.jp

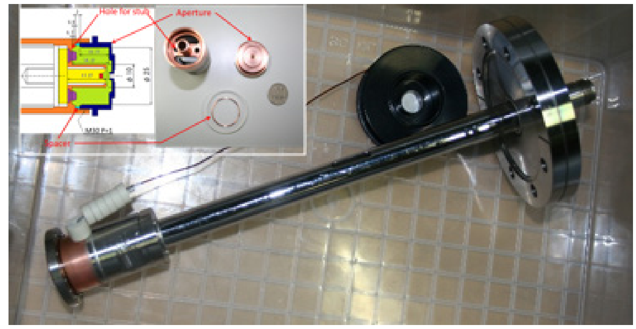

Figure 1: Pre-bunching triode cavity with longitudinal power coupling for a triode type thermionic RF gun.

CAVITY RF COUPLING

Coupler can be defined as a network that allows to transfer power from an RF source to the cavity. Due to impedance and frequency mismatch between the RF power generator and the cavity load some power might be reflected at the coupler. The impedance mismatch is characterized by reflection coefficient Γ. In steady-state case without frequency mismatch the Γ is determined by coupling coefficient κ.

$$\kappa = \frac{1+\alpha|\Gamma|}{1-\alpha|\Gamma|}\begin{cases}\alpha = +1\ overcoupled \\ \alpha = -1\ undercoupled\end{cases}$$

The coupling coefficient represents the ratio of the impedances from the transmission line and the cavity on resonance

$$\kappa = \frac{Z_L}{Z_0}\begin{cases}1 > overcoupling \\ 1 = critical\ coupling \\ 1 < undercoupling\end{cases}$$

In general the reflection coefficient is the ratio of complex amplitudes of inputted and reflected waves. Thus it can be determined from inputted and reflected power ratio at resonance $\Gamma=(P_{ref}/P_{in})^{1/2}$. The corresponded coupling conditions are evaluated from the power transient signal. Figure 2 shows the scheme of transient signals for different coupling conditions.

The triode cavity was evaluated by low power test, which has revealed the undercoupled conditions [3]. For high beam current generation overcoupling conditions are required in order to compensate for beam loading effect. Due to geometrical limitations the coupling change of the cavity is not possible [4]. In order to change the coupling condition we develop an external impedance transformer for the triode cavity.

ISBN 978-3-95450-181-6

INTEGRATED INSPECTION METHOD OF MOTOR TRANSPORTS BASED ON ACCELERATION TECHNOLOGY

A.M. Fialkovsky, T.R. Virkunen, P.O. Klinovsky, K.V. Kotenko, V.P. Malyshev,
NIIEFA, St. Petersburg, Russia

Abstract

Integrated inspection method of motor transports was suggested based on linear electron accelerator and neutron generator, which helps to detect substances forbidden for carrying, including explosives, narcotic drugs and fissionable materials. The linear high-frequency electron accelerator is a source of X-ray bremsstrahlung. The result of scanning is an introscopical image of a motor transport with color-selected suspicious substances. The neutron activation analysis of these substances with neutron generator as a neutron source lets detect elemental substance composition as well as identify explosives or narcotic drugs. This article contains accelerator specifications, which lets implement suggested method.

PURPOSE

The purpose of the inspection system (IS) is an examination of motor transports. IS lets detect and identify substances forbidden for carrying including explosives, narcotic drugs and fissionable materials. Integrated informational and technical system of the IS aims to let the operator make valid decision on the presence or absence of the transportation rules violation signs.

IS provides:

- Visualization of inspected object contents.
- Recognition of the different devices located therein, objects and substances.
- Determining load merchandise volume of the container and inspect the contents of the spatial location.
- Coordinate attachment of the detected items to their location.
- Ability to recognize items of different materials (metals, organic substances, including elemental analysis).
- Ability to view the structural cavities and spaces between walls, ceilings and container floors, car components.

Additional specialized process equipment of the IS allows inspection of the driver and the persons accompanying the vehicle.

All information contributes to the overall control of cargo, identifying caches and prohibited substances.

The complex information technology tools of the IS are placed in a one-story industrial building (customs examination hall) and in the control room unit. The walls of the inspection hall are made of reinforced concrete, weighing not less than 2350 kg / m^3. The IS contains all necessary systems to ensure efficient functioning and safety management system. The basis of the IS is the system of inspection of containers loaded and trucks using the accelerator, which is the source of the X-ray bremsstrahlung with 6 MeV energy in the normal mode and an additional method for the implementation of the dual energy – 9 MeV.

General view of the IS is shown in Fig. 1.

Figure 1: General view of the IS building.

INTEGRATED METHOD

To solve the problem of identification and detection of the prohibited items in the inspected vehicle there is provided an integrated method comprising applying the following techniques:

αβγ Channel

Detection system of radioactive and fissile materials monitors the vehicle for the presence of radioactive and fissile materials.

X-Ray Channel

Scans the vehicle and gets its picture at two radiation energies; displays images on the screen completely without loss of visual information with a quality that allows the detection of hidden places, objects and substances under control; identifies suspicious areas for the presence of hazardous (explosive) substances by dual-energy and transmits their coordinates to the neutron - sensing module for detailed substance identification.

n-Neutron Channel

Neutron - sensing system conducts the spectral analysis of the selected areas and performs identification of substances, including drugs and explosives.

ISBN 978-3-95450-181-6

MEASUREMENT OF THE ION BEAM PROFILE WITH THE D-PACE WIRE SCANNER*

E.O. Sokolova#, D.A. Kasatov, A.M. Koshkarev, A.N. Makarov, I.N. Sorokin, I.M. Shchudlo, S.Yu. Taskaev, BINP SB RAS, Novosibirsk, Novosibirsk State University, Russia
A.A. Gmyrya, Ya.A. Kolesnikov, A.S. Kuznetsov, BINP SB RAS, Novosibirsk, Russia

Abstract

In The Budker Institute of Nuclear Physics the accelerator-based source of epithermal neutrons was invented and now operates to be used in the Boron Neutron Capture Therapy (BNCT) [1]. For several reasons the real beam flow in the facility differs from the calculated one. To take into account this distinction it is necessary to provide continuous monitoring of the beam parameters. This paper describes the method of diagnostics of the ion beam with the D-pace wire scanner and the results, which were obtained, using this method.

INTRODUCTION

The principle of operation of the facility is as follows. The negatively charged ion beam is generated on the ion source, then it is injected in the tandem accelerator with vacuum insulation. After a recharge of negatively charged ions of hydrogen into positively charged protons in the gas stripper a proton beam is formed, which is accelerated to the doubled potential of the high voltage electrode. On the lithium target, as a result of a threshold reaction ^{7}Li(p,n)^{7}Be, the neutron flux is generated [2].

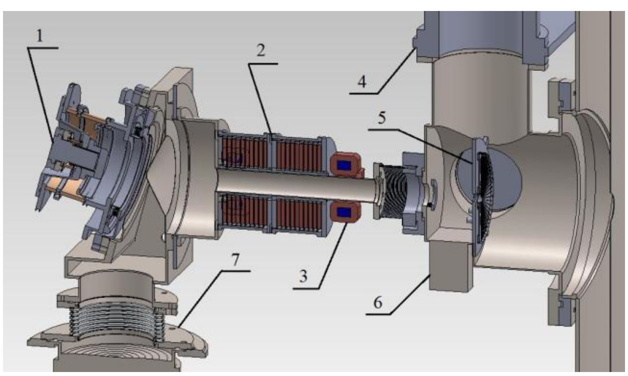

Figure 1: Low-energy part of accelerator. 1 – H^{-} ion source, 2 – magnetic lenses, 3 – corrector, 4 – cryosorption pump, 5 – cooled diaphragm, 6 – D-Pace wire scanner, 7 – differential pumping system.

Figure 1 shows the view of low-energy part of the facility, where the measurement of the beam profile was carried out. Between the diaphragm and the first electrode the beam is accelerated by the electromagnetic field. In the area of the diaphragm the powerful electrostatic lens is formed, also the accelerating field falls into the collimator of the diaphragm, as it could be seen in the figure 2. This phenomenon could lead up to the refocusing of the beam, in this way it could become strongly divergent and the emittance could increase significantly. Moreover, a huge part of the beam could be lost, as it wouldn't fall into the gap of electrodes, setting on their surface, which could lead up to redistribution of voltage and to electrical breakdown as a result [3].

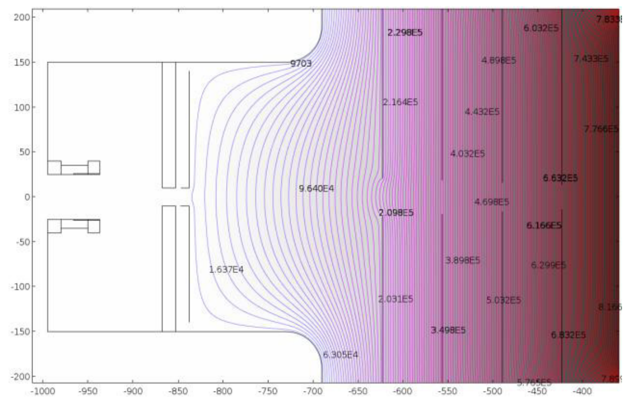

Figure 2: Calculated field distribution inside the vacuum chamber at the entrance to the accelerator.

In order to take into account the described phenomena it is necessary to monitor the beam thoroughly, since the beam should be led with minimal losses. In this way, it was proposed to install The D-Pace OWS-30 Oscillating Wire Scanner Probe (TRIUMF-Licenced) inside the vacuum chamber before the diaphragm. For this purpose the necessary changes of the design of the vacuum chamber were implemented, which allow to set the device with the possibility of adjustment of its position.

RESULTS OF EXPERIMENTS

The experiments were carried out under different conditions of focusing and current of the ion beam. In the standard mode the current is supplied to the lenses is 54 A, to the corrector 2.4 A.

* The study was supported by grants from the Russian Science Foundation (Project no. 14-32-00006), the Budker Institute of Nuclear Physics and the Novosibirsk State University.
#e-mail: buiya@bk.ru

ISBN 978-3-95450-181-6

MEASUREMENT OF THE PROTON BEAM PROFILE VIA AN ACTIVATION METHOD OF DIAGNOSTICS*

E.O. Sokolova#, D.A. Kasatov, A.N. Makarov, I.M. Shchudlo, S.Yu. Taskaev, BINP SB RAS, Novosibirsk, Russia and Novosibirsk State University, Russia
Ya.A. Kolesnikov, BINP SB RAS, Novosibirsk, Russia

Abstract

In The Budker Institute of Nuclear Physics the accelerator-based source of epithermal neutrons was invented and now operates to be used in the boron neutron capture therapy. Neutrons on the facility are generated during the threshold reaction ^{7}Li(p, n)^{7}Be which occurs when the proton beam is thrown on the lithium target. To control the neutron output it is necessary to monitor the parameters of the accelerated proton beam. The spatial distribution of the accelerated proton beam was measured exactly on the lithium target, using an activation method of diagnostics.

INTRODUCTION

The principle of operation of the facility is as follows. The negatively charged ion beam is generated on the ion source, then it is injected in the tandem accelerator with vacuum insulation. After a recharge of H^- beam into positively charged protons in the recharging gas target a proton beam is formed, which is accelerated to doubled potential of the high voltage electrode. On the lithium target as a result of a threshold reaction ^{7}Li(*p, n*)^{7}Be the neutron flux is generated [1]. General view of the accelerator is shown in fig. 1.

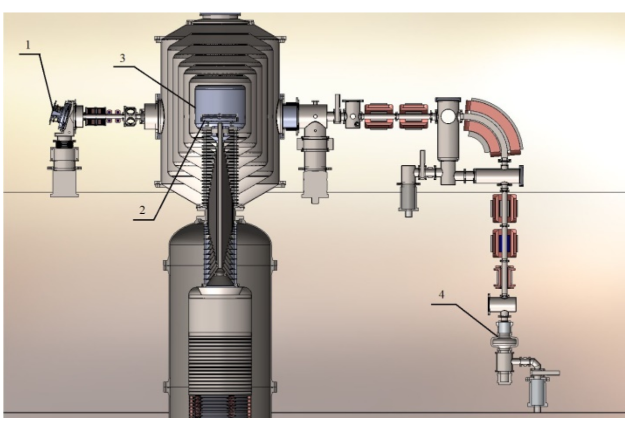

Figure 1: Vacuum insulation tandem accelerator. 1 – H⁻ ion source, 2 – gas recharging target, 3 – high voltage electrode, 4 – lithium neutron-generating target.

As a result of an interaction between protons and lithium on the neutron-generating target an accumulation of the radioactive isotope of beryllium takes place. It was proposed to track down an area of the beryllium storage in order to restore a profile of the proton beam.

THEORETICAL FOUNDATION

The neutrons are generated during an inelastic scattering of 2 MeV proton beam on the lithium nuclei according to the reactions [2]:

$$^7Li + p \rightarrow \ ^7Be + n - 1{,}646 \text{ MeV},$$
$$^7Li + p \rightarrow \ ^{7*}Be + n - 2{,}076 \text{ MeV } (\sim 10\%),$$
$$^{7*}Be = \ ^7Be + \gamma + 430 \text{ keV}.$$

The process of an inelastic scattering is characterized by the resonance energies: 1.05, 2.05, 2.25 MeV, which are close to the threshold reaction of the neutron generation 1.882 MeV. The flux of gamma-quants with the energy of 0.478 MeV is equal to the flux of neutrons. To decrease the gamma-quants flux the thin layer of lithium is sprayed to the copper substrate.

After an experiment there is a radioactive isotope ^7Be is accumulated, which has a half-life of 53.6 days. The tracking of gamma-quants with the energy of 478 keV, released during the beryllium decay, could serve an alternative way of the proton beam profile measurement in an accelerating part of the facility. To implement such a method the gamma-spectrometric complex was involved, that consists of the scintillation NaI-detector, which was pre-calibrated for energy, and the lead shielding with the collimation hole of 8 mm. The measurement of gamma-radiation is carried out after an experiment, remotely from the facility.

With the penetration of ionizing particles in the scintillator material the flash of luminescence occurs, then it is converted into a pulse of electrical current by the photomultiplier, finally the electronic system records it.

RESULTS OF EXPERIMENTS

For the restoring of the beam profile the neutron-generating target was imposed a proton beam influence during 25 minutes. The measurement of gamma-radiation was carried out one week later after an experiment, in order to exclude the short-lived gamma-quants.

The lithium target substrate is moved in increments of 1 cm before the collimation hole of the lead shielding (the center of the target is the point [0;0] in the figure 2), in this way the counting speed was determined in the line of a full absorption. The luminescence intensity distribution on the target surface, defined as the number of recorded events to the time of statistics collecting, is shown in fig.2.

* The study was supported by grants from the Russian Science Foundation (Project no. 14-32-00006) and the Budker Institute of Nuclear Physics and Novosibirsk State University.
#e-mail: buiya@bk.ru

ISBN 978-3-95450-181-6

DIGITAL-TO-ANALOG BEAM ENERGY AND CURRENT STABILIZATION OF ELV ELECTRON ACCELERATORS

D.S. Vorobev, E.V. Domarov, S.N. Fadeev, N.K. Kuksanov, A.V. Lavrukhin, P.I. Nemytov,
Budker Institute of Nuclear Physics, SB RAS, Lavrentyev av. 11, Novosibirsk, 630090, Russia

Abstract

The methods of links between technology line and ELV accelerator control system are described. accelerator control system are described. The problems of the fast control of the beam current are revised. The method of improving the rising of beam current and stability of electron energy is shown.

INTRODUCTION

ELV industrial electron beam accelerator is effective instrument for radiation treatment applications. Especially frequently it is used in cable and heat shrink tube manufacturing. Accelerator is only a part of technology line. There are underbeam transportation line, take-up and pay-off systems, safety system etc… All of them are controlled by signals from ELV control system, which are generated on base of the values as electron energy and beam current. There are 2 well-known methods of controlling the transportation line. The first: there ELV is master, line is slave (see Fig. 1). What things are the most important for this method?

For accelerator:

- stable parameters (better stability – less inhomogeneity of absorbed dose);
- smooth beam operation (except dose inhomogeneity, fast beam current changes can break treated cable or tube).

For technology line:

- quick response for incoming parameters changes;

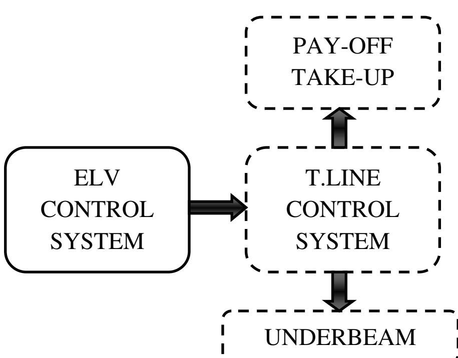

Figure 1: Accelerator is master.

Other method, where the accelerator is a slave, the technology line is a master, and accelerator parameters (beam current) follow production line velocity (see Fig. 2). Unlike the first method, here the most important things will be:

For accelerator:

- stable parameters (better stability – less inhomogeneity of absorbed dose);
- quick response for incoming parameters changes;

For technology line:

- smooth velocity;

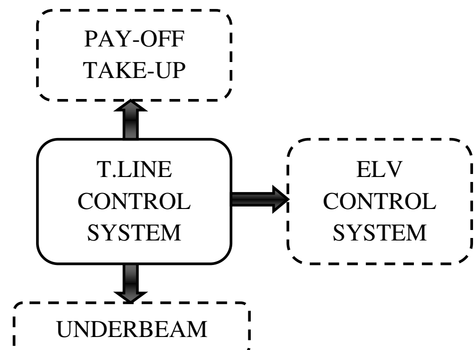

Figure 2: Technology line is master.

For second method the accelerator should provide enough performance and quick response.

New technologies of rubber component irradiation treatment are increasing the performance of technology lines, so they are using second method of links the accelerator to technology line. It led us to find possibility to increase the velocity of beam current control (speed of ascending/descending of beam current value).

STABILIZATION SYSTEMS

Systems of energy and current stabilization are based on analog PID-controllers. They provide good stability at sufficient speed-work. Energy stabilization system separated from current stabilization. It is enough fast (time constant is 0.5 sec) for 100 kW accelerator. Energy stabilizer output is directly connected to Pulse Width Modulator of power supply cabinet, and has feedback from energy sensor (it can be resistive divider or rotary voltmeter).

Current stabilizer is mix of analog PID and digital matrix. Current stabilizer is controlling heating of electron gun filament (heater of cathode), and has feedback from beam current sensor. Cathode heater has a big inertia, so time constant of analog PID should be about 3-5 sec. Low speed of PID is good for steady state, but seriously increases time of transient process. Digital matrix is software part of current stabilizer. Each matrix elements is delay, between present and next (or previous) moments of setting the beam current value to input of current stabilizer. Then during the beam ascend or

ISBN 978-3-95450-181-6

DEVELOPMENT OF THE HARDWARE-SOFTWARE COMPLEX PIRS-5 FOR FIELD MEASUREMENTS IN ACCELERATING STRUCTURES

G. Pomogaybo, S. Toporkov, M. Lalayan, National Research Nuclear University MEPhI, Moscow, Russia

Abstract

Hardware-software complex «PIRS-5» was developed to make measurements in warm accelerating structures. The idea was to create full-automatic measuring system, which can measure electrical field at the bead position with non-resonant and resonant pull techniques. PIRS-5 has postprocessor, which calculate electrical component from the frequency, reflection or transmission coefficient, shunt and effective shunt impedance. This work describes the construction of this complex, its mathematical part and possible future modifications.

PIRS-5 LAYOUT AND SCHEMATICS

Measurement setup PIRS-5 is software and hardware complex developed for electrodynamical characteristics measurements of accelerating structures. "PIRS" is acronym for Russian "facility for resonator parameters measurements" initially developed at MEPhI by Prof. A.Ponomarenko and his research team. After series of renovations and upgrades it became powerful tool for accelerating structures research nad development led by RF lab tem at MEPhI. Vector network analyzer being the key element of this setup is able to measure resonant frequencies and quality factors without any additional hardware or software involved. But field distribution inside accelerating structure and corresponding parameters like shunt impedance are not so easily acquired. In this paper new upgraded version is described. Algorithms and software part were substantionally altered and redesigned. Both resonant and non-resonant measurements of electromagnetic fields became possible using this implementation. New software allows computation of shunt impedance and effective shunt impedance computation based on electric field measured.

Measurement setup schematics is illustrated on Fig. 1. It is quite ordinary hardware for this kind of measurements based on small perturbation technique. It includes Vector network analyzer Agilent 8753ET (1), control PC (2), accelerating structure under test (3), coupling antenna (4), small dielectric or metal bead (5), bead moving and positioning system (6) actuated by step motor (7). Latter is powered and PC controlled via step motor controller (8).

It was already mentioned, that Agilent VNA is the main RF measuring device able to acquire accelerating structure parameters operated up to 6 GHz. Bidirectional GPIB interface connects it to PC and provides VNA control and data transfer. Accelerating structure under test is connected to VNA port by one or two coupling pickups chosen accordingly to particular measurement task. Small dielectric or metal perturbing bead attached to nylon string is travelling along cavity axis. Mechanical system allows precise

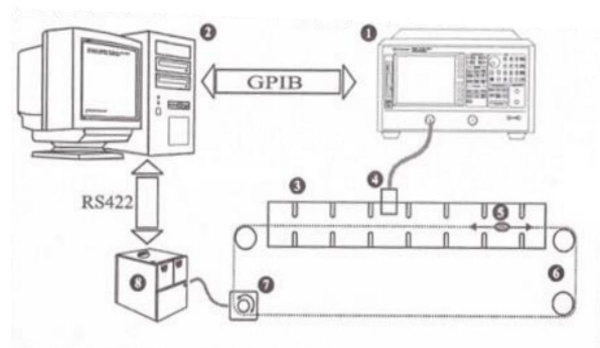

Figure 1: PIRS-5 layout.

string alignment and bead position determination. Computer controls all the hardware, provides data storage and user interface.

PIRS-5 SOFTWARE

Control software developed for PIRS-5 consists of two main algorithms (see Fig.2).

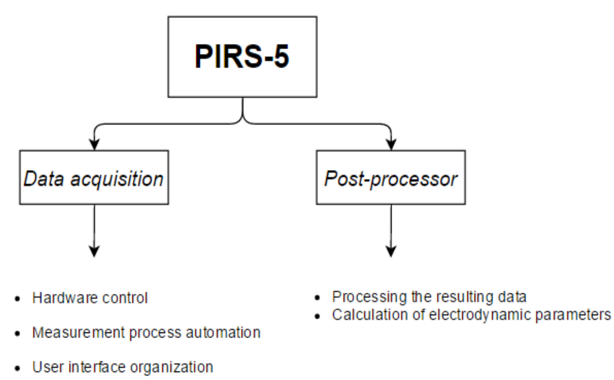

Figure 2: PIRS-5 software.

They are algorithm of data acquisition and post-processor. Let us consider algorithm features paying brief attention to the user interface implementation details. After user enters cavity length, measured quality factor and bead form-factor program starts measurement. This algorithm is illustrated on Fig. 3.

ISBN 978-3-95450-181-6

LONGITUDINAL BEAM DISTRIBUTION MEASUREMENTS IN DAMPING RING OF VEPP-5 INJECTION COMPLEX

V.V. Balakin†[1], D.E. Berkaev, O.V. Anchugov, O.I. Meshkov[1], V.L. Dorokhov, G.Ya. Kurkin, F.A. Emanov[1],
Budker Institute of Nuclear Physics, Novosibirsk, Russia
[1]also at Novosibirsk State University, Novosibirsk, Russia

Abstract

Injection Complex VEPP-5 was turned into operation in the end of 2015 in the Budker Institute of Nuclear Physics (Novosibirsk, Russia). The main task of the facility is production, acceleration and transportation of high intensity electron and positron beams for two BINP's colliders. Now, VEPP-5 successfully delivers electron and positron beams to VEPP-2000 and ready to start operation with VEPP-4M. Beam diagnostics issues are very important for VEPP-5 facility tuning during the operation. Longitudinal beam diagnostic based on synchrotron radiation in the VEPP-5 Damping Ring is presented in the article. Equipment operation principle, main measurement results and future prospects are presented in this paper.

IC VEPP-5 OVERVIEW

Injection complex (IC) VEPP-5 [1] was constructed for production, acceleration and transportation of high intensity electron and positron beams for two BINP's colliders – VEPP-4M [2] and VEPP-2000 [3]. IC [4] consists from thermionic electron gun, two linear accelerations, conversion system, damping ring (DR) and transporting channels (transfer line K-500).

DISSECTOR OPERATION PRINCIPLE

One of the main method of measurement of fast processes is electro-optical chronography. Stroboscope method is used in the circular accelerators, where dissector is used as converter (Figure 1).

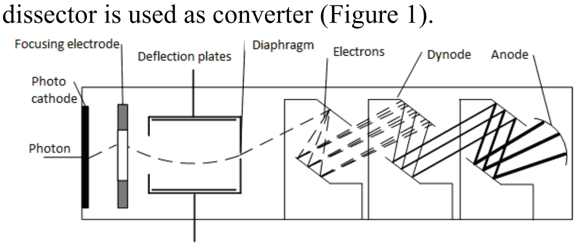

Figure 1: Dissector structure.

Let the light signal reached the dissector photocathode has time distribution $I(t)$. If high frequency sweep and incoming light impulses are synchronized, electron distribution $q(x)$ occurs in the plane of the diaphragm seal. Distribution $q(x)$ precisely imitates time distribution of light signal $I(t)$. Average anode current of photomultiplier $I_a(t)$ is proportional to light intensity falling onto photocathode. It is possible to shift different parts of distribution $q(x)$ on diaphragm seal changing voltage phase on dissector's deflection plates (see on Figure 2). Thus, photomultiplier's anode current will follow the shape of studied signal $I(t)$, if the parameters of incoming photocathode light signal be stable.

All temporal characteristics are true for distribution $q(x)$, but system applying dissector has some features:

- Researched object's information represented as electrical signal;
- Electrical signal precisely imitates temporary structure of light impulse, because there is no phosphor and microchannel decay;
- There is possibility to observe fast shape and duration changes of researched signal (the scale of hundreds synchrotron oscillations).

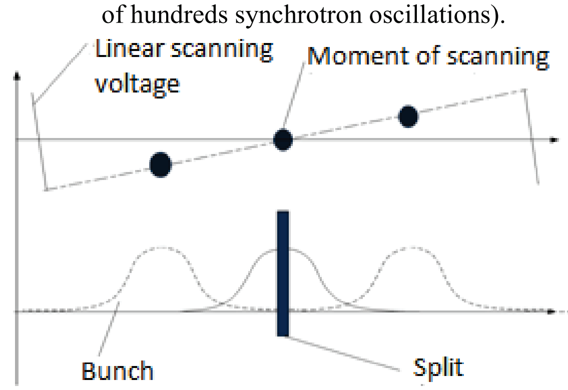

Figure 2: Scanning process.

Electron bunch length is far less than the perimeter of DR ($\sigma_z \ll \Pi$). Thus, it is necessary to scan distribution $q(x)$ with low frequency voltage applied to the deflection plates synchronously with high frequency voltage (see on Figure 3).

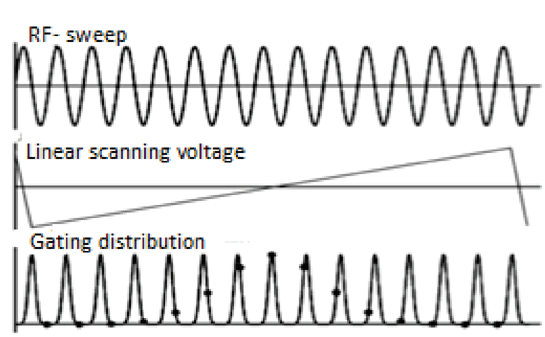

Figure 3: Synchronously scanning process.

† balakinvitalyv@gmail.com

ISBN 978-3-95450-181-6

HOST-BASED SYSTEM TO CONTROL THE ACCELERATOR

V.N. Zamriy, JINR, Dubna, Russia

Abstract

The report discusses development of the host-based system to control the accelerator. We consider modes of timing and allocation of operations of the system node. The time of any working cycle, rate of a data flow and an amount of serviced tasks are coordinated with characteristics of the node. Estimations of the readout rate of the data and the waiting time demonstrate the system efficiency. The data acquisition technique has been developed to provide checking of pulse parameters and control the linac LUE-200 of the neutron source IREN.

STATEMENTS OF A PROBLEM

Considered technique of synchronized data acquisition has been developed to control the linear accelerator of electrons LUE-200 of the neutron source IREN [1].

A multiplex system of timed data acquisition for monitoring parameters of the working cycle (at time period T, from one pulse of the electron beam up to another one, and cycle repetition rate – 1 / T ≤ 150 per second) has been offered and tested while the linac LIU-30 and full-scale test facility IREN were equipped with instruments [2].

Timed procedures of data acquisition are applied in the host-based solutions for a group of tasks to supervise process variables and control pulsed facilities [3].

The advanced system is aimed at carrying out several (up to N) tasks simultaneously. For this purpose it require to apply groups of N (an order 10) channels, one able to complete up to K (~100) measurements during the given time interval of the period T.

Some timed operations of the channels are assumed to be fulfilled by means of common nodes (with the timing controller) of the system. A link exchange of a node supports reading the data (at rate n) to feedback control.

Then procedure flowcharts of the engineering with the timed data interchange on the base of the system node allows one finding more efficient structural solutions.

Characteristics of operations of the channels and node should be coordinated and high enough to provide the minimum waiting time of service, taking into account the time period and rate of the data flow.

Key characteristics of channels and system node are coordinated to minimize a service time. Their idle time factors (P_1 and P_2) are examined, and also at possible queue of service requests.

The timing controller and link exchange of the node integrate the HB system, started at a working cycle. Diagnostics of process variables is complete for the cycle to feedback control.

Performance and number of serviced channels at chosen sync modes for such system are examined further.

The further analysis of operations forms requirements and approaches to develop system engineering.

THE PROCEDURE OF HOST-BASED DATA ACQUISITION

The host-based solutions of the type A, B and C for comparison are shown (Fig. 1).

The operations of the channels include groups of synchronized measuring and quantization of the process variables. Timed data acquisition and exchange of links (communication channels) for data processing provide the feedback control.

Levels of the main operations are applicable for the solutions based on the host with the link exchange. In the developed circuit (at first, type A, then B and C as the next step) the main operations of the channels are fulfilled simultaneously in the assemblies connected via the link exchange of the node.

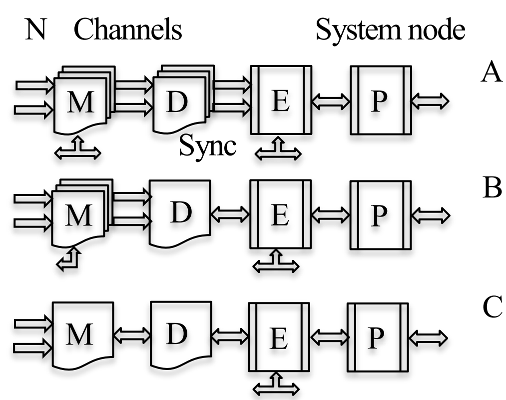

Figure 1: Procedure flowcharts of A, B and C type.

The operations M, D, E and P represent timed measuring of process variables, data acquisition and link exchange with interface to control.

The conditions of parallel operations lead to more sophisticated modes of the timing. Problems of the traffic of the data from all channels require coordination of the data readouts and of the data flow for the link exchange.

Estimations of the data readout rate and amount of data from the channels have been considered, first of all, under conditions of levels of A and advanced type B.

The procedures at the node levels cause timing problems to be solved and also put the requirements to the node. Development of the system on purpose to increase a data flow has led to higher requirements, especially when the data convenient for feedback control, are necessary.

Performance of operations at various timing modes of system is examined at complex requirements to pulsed facilities of the linac.

The amount and rate of the data gained during the accelerating cycle, attained number of channels which should be serviced, and also possible waiting time of operations, both for channels and node, will be considered

ISBN 978-3-95450-181-6

CONTROL SYSTEM FOR THE 1 MW NEUTRAL BEAM INJECTOR*

V.V.Oreshonok†[1], V.V.Kolmogorov, Budker INP, Novosibirsk, Russia
A.N.Karpushov, Swiss Plasma Center – EPFL, Lausanne, Switzerland
[1]also at Novosibirsk State University, Novosibirsk, Russia

Abstract

This paper presents general description of hardware and software of the neutral beam injector control system. The system is developed for control of the neutral beam injector which operates with 15-25 keV deuterium and hydrogen beams of 2 s maximum duration. It performs injection parameters calculation according to the desired beam power vs time curve, synchronizes and protects the injector subsystems and acquires its data during the shot. It also controls the injector operation between the shots.

The system is based on an industrial computer with National Instruments PCIe boards: two PCIe-7842R reconfigurable input-output modules and a PCIe-6323 data acquisition module. An in-house developed interfacing module (cross-box) as well as serial to fiber optic converters are used for galvanic isolation and electrical compatibility with the injector subsystems. User interface software and PCIe boards programmable logic firmware are implemented in LabVIEW. Injection calculations and results acquired are represented with MATLAB.

INTRODUCTION

An 1 MW neutral beam injector has been designed and built by the Budker Institute of Nuclear Physics (Novosibirsk, Russia) for the TCV tokamak of the Swiss Plasma Center (Lausanne, Switzerland) [1]. The injector parameters are shown in the Table 1. It operates in the pulsed mode and is aimed to produce deuterium and hydrogen neutral beams with an ability of the beam on/off modulation with millisecond resolution and of gradually varying the power injected into tokamak.

Table 1: Neutral Beam Injector Parameters

Parameter	Value
Max power injected in tokamak	1 MW
Beam power range	30 – 100 %
Beam power stability	± 5 %
Beam energy range	15 – 25 keV
Max injection pulse duration	2 sec.
Time delay between consecutive pulses	5 – 30 min.

The injector consists of an ion source connected to a vacuum tank where the gas neutralizer, bending magnet, residual ion dumps and moving calorimeter are mounted. The injector subsystems are located in two areas: gas system, ignition system, vacuum system, thermocouple modules of movable calorimeter and ion dumps and some parts of the RF supply are mounted near the injector in the tokamak zone. The rest parts including high-voltage supply system, power supplies for the ion source grids and bending magnet, RF supply electronics as well as control system equipment are located in the electronics zone being 50 meters away.

CONTROL SYSTEM

The system to control the injector was decided to be based on an industrial computer with a set of embeddable input-output modules. As injector operates in pulsed mode all its subsystems must be synchronized carefully during the injection pulse (shot). Also care should be taken of monitoring the subsystems status between the shots. Total number of channels required to control the injector operation is as follows:

- 24 analog input channels with the rate of 5 kSamp/s for monitoring the subsystems operation during the shot;
- 8 analog output channels with 10 kSamp/s rate to control subsystems parameters during the shot;
- 16 digital output channels with the maximum rate of 10 kSamp/s used for subsystems synchronization during the shot;
- 16 digital input channels with 10 kSamp/s maximum rate used as interlocks during the shot and between the shots as well;
- up to 40 digital input/output channels with the rate of less than 1 Samp/s to control and monitor the injector subsystems between the shots.

Since the control system equipment is distanced from the injector itself and partly from its subsystems, it was decided to isolate the system galvanically and connect with distant injector elements using optical lines and communication interfaces to avoid interference and cross-talks from injector and tokamak operation.

Hardware

Shown on the Fig. 1 is the injector control system block diagram. A SuperLogics industrial computer SL-3U-H77EB-GK with Windows 7 OS is chosen to run the control system software. It uses three PCI Express data acquisition modules by National Instruments as peripherals. Two of them are PCIe-7842R [2]: these reconfigurable input-output modules are based on a user-programmable Virtex-5 FPGA. Each module also has 16-bit resolution analog outputs with independent rate of up to 1 MSamp/s and analog inputs up to 200 kSamp/s. Another module used is PCIe-6323 data acquisition device [3] with 32 analog inputs of 16-bit resolution and 250 kSamp/s rate. Synchronization between PCIe modules is implemented by means of RTSI bus.

* This work supported in part by the Swiss National Science Foundation.
†V.V.Oreshonok@inp.nsk.su

ISBN 978-3-95450-181-6

CONTROLLER OF POWER SUPPLIES FOR CORRECTOR MAGNETS OF EUROPEAN XFEL

V. Kozak, O. Belikov, BINP, Novosibirsk, Russia

Abstract

The European XFEL is under construction now in Hamburg [1]. It is a big international project. Budker Institute of Nuclear Physics (BINP) developed, produced and delivered power supplies for corrector magnets of XFEL. A controller for these power supplies was developed. It provides an 18 bits resolution of digital-to-analog converter and 6 channels of precise analog-to-digital converter with high accuracy and resolution. A combination of the general-purpose functions with the specific function for power supplies allowed using the same controller for different equipment of corrector magnet subsystem. Here is described the controller, its properties and main applications.

INTRODUCTION

The European XFEL is 3.4-kilometre-long facility, which is located mainly in underground tunnels. It consists of a linear accelerator, undulators, electron and photon beam transport system. Eleven countries make the joint efforts for this international project. The Budker Institute of Nuclear Physics (BINP) takes participation in creating the European XFEL. BINP produces and delivers warm magnets, vacuum chambers, some cryogenic equipment and so on.

In frame of this works the BINP develops, builds and commissions the family of power supplies for corrector magnets. The family consists of models with output current 5 and 10 Amperes and with different output voltages. The quantity of power supplies to be 330 pieces [2]. Really the quantity should be above 400 pieces, it will be explained below. The Fig.1 shows the power supply.

Figure 1: The power supply for corrector magnets.

The requirements to power supplies includes high accuracy (less than 100 ppm), low output ripples (less than 10 ppm) and high reliability (MTBF >100000 hrs). The high reliability is required to reduce the pause in XFEL operation during replacing failed power supply by spare one. To reduce this time there is used the same trick like in most DESY installations- each rack with power supplies (up to 7) is equipped by spare power supply and controlled switch. When control software detects a failed power supply it tries to restart it and this attempt was not successful it replaces a failed power supply by spare one.

CONTROLLER OF POWER SUPPLIES

There was decided to use analog regulation for power supplies. That means we need a precise digital-to-analog (DAC) channel, a few of precise analog-to-digital (ADC) channels and discrete input/outputs. Using a modular approach in developing power supply we can implement the controller as a universal module (Fig.2.) which may be used in different applications.

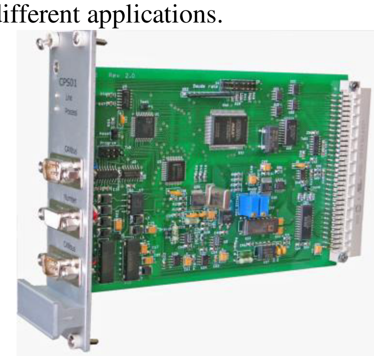

Figure 2: Controller CPS01.

The second possible application is providing an interface for the controlled switch. All power supplies for corrector magnets are located in 48 euro-racks. So, we have 48 controlled switches (one per rack). For this purpose is suited more simple device which have not ADC and DAC. But even the simple device should have network interface, microcontroller and something else. And more important we should have separate documentation, separate production order and separate certification for European standards. More cheap way is to increase total quantity of identical controllers.

Most power supplies for magnet system in XFEL use CANbus as lowest level network. So, it is the reason for our choice of the same interface.

The controller was implemented using typical structure for similar applications (Fig.3.).

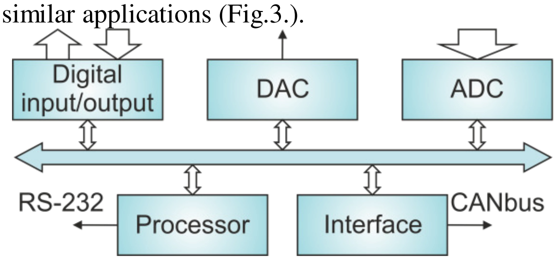

Figure 3: The structure of controller CPS01.

As for DAC, there is used chip AD5781- 18-bits DAC (Analog Devices). We use circuitry recommended by producer. The parameters of this chip satisfy the specification requirements. When we choose DAC chip

ISBN 978-3-95450-181-6

DATA PROCESSING AUTOMATIZATION FOR GAMMA-SPECTROMETRY DIAGNOSTICS OF NEUTRON ACCELERATOR BNCT*

T.A. Bykov, Novosibirsk State University, Novosibirsk, Russia
D.A. Kasatov, Budker Institute of Nuclear Physics, Novosibirsk, Russia

Abstract

There is the accelerator-tandem at the Nuclear physics institute in Novosibirsk which is suitable for malignancies treatment such as glioblastoma and melanoma using BNCT methods.

There are different gamma spectrometry diagnostics which apply under this project. One of these is used to determine the parameters of the neutron beam. The method is to irradiate a set of activation foils with neutrons. Then measure the gamma-spectrum of foils using gamma detector. Based on these data it can be calculated the activity of foil, as well as the amount and the energy of neutrons.

For data processing of these diagnostics there was developed software which is used for convenient display of gamma-spectrometer data and the activity of the foil. Software allows setting a canal calibration and the sensitivity calibration which is needed to calculate the foil activity.

INTROCUTION

One of the most important and still unsolved problems is dosimetry of BNCT on all the stages of treatment. [1] Experiments are carried out to determine the parameters of generated neutron flow, using activation methods, and accompanying gamma-radiation. In this experiments it was used the spectrometric complex with NaI scintillator which must have automatic and operative data processing. The data processing task include automatic calibration, noise reduction, determination of the energy of the peak and the substance activity.

For these tasks the software was developed which allows processing the data in semi-automatic mode.

SUBJECT AREA

Activation method is used for determination of the current and the spectrum of neutrons. The special set of foils is used for the experiments (Au, Co, Cu, Fe, In, 5.2% Lu-Al, 81.3% Mn-Cu, Mo, NaCl, Sc, W). These foils are irradiated with neutrons during the experiment. Then the gamma-spectrum of foils using gamma detector is measured. Output spectrum data and period of measurement are saved into special file with specified format. As a result of the experiment there is a set of files with the spectrum data for every foil. These files are the input data for developed program.

These data have the following features. The graph of the spectrum has a shape of decaying exponent with a peak in the Gaussian form for some energy, and also the noise which has about the same amplitude on the entire spectrum (see Fig. 1).

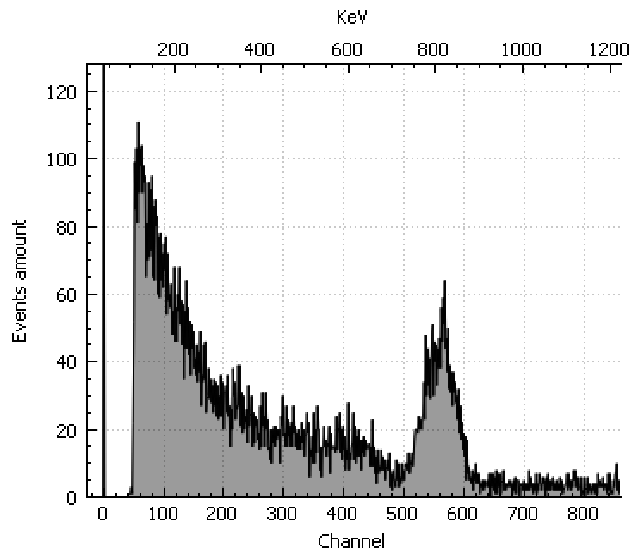

Figure 1: The graph of the spectrum of manganese isotope (^{56}Mn).

The noise amplitude in the spectrum is depends on the period of measurement and background during the measurement.

The number of peaks may be different and depends on the substance.

DATA PROCESSING

In the program the data processing consists of the following steps performed sequentially.

Noise Reduction

This module uses discrete wavelet transform.[2] The obtained spectrum data are represented as a mathematical function of amplitude by time i.e a signal with amplitude by time. The wavelet transform converts the signal from the time-amplitude representation to the time-frequency representation. In this subject area the useful information in the signal is a low-frequency component with large amplitude, i.e, trend, while noise is a high-frequency component and has a small amplitude.

The signal is decomposed into transform coefficients, then the coefficients with the amplitude below a user-specified values are reset to zero. and then performed the inverse wavelet transform. As a result, all of the useful low-frequency component of the signal remains, and small high-frequency noise is removed.

*Work supported by a grant from the Russian Science Foundation (Project No.14-32-00006) with support from the Budker Institute of Nuclear Physics and Novosibirsk State University.

ISBN 978-3-95450-181-6

VME BASED DIGITIZERS FOR WAVEFORM MONITORING SYSTEM OF LINEAR INDUCTION ACCELERATOR LIA-20

E.S. Kotov, A.M. Batrakov, G.A. Fatkin, A.V. Pavlenko, K.S. Shtro, M.Yu. Vasilyev,
Budker Institute of Nuclear Physics SB RAS, Novosibirsk, Russia

Abstract

The Linear Induction Accelerator LIA-20 is being created at the Budker Institute of Nuclear Physics. Waveform monitoring system (WMS) is an important part of LIA-20 control system. WMS includes "slow" and "fast" monitoring subsystems. Three kinds of digitizers have been developed for WMS.

"Slow" subsystem is based on ADCx32. This digitizer uses four 8-channel multiplexed SAR ADCs (8 µs conversion cycle) with 12 bit resolution. Main feature of this module is program configurable channel sequencing, which allows to measure signals with different timing characteristics.

Two types of digitizers are involved in "fast" subsystem. The first one, ADC4x250-4CH, is 4-channel 250 MSPS digitizer. The second one, ADC4x250-1CH, is single channel digitizer with sample rate of 1 GSPS. Resolution of both devices is 12 bit. "Fast" modules are based on the common hardware.

This paper describes hardware and software architecture of these modules.

INTRODUCTION

The linear induction accelerator with energy of 20 MeV (LIA-20) intended for pulsed X-ray radiography with high space resolution is under development in the BINP (Novosibirsk, Russia). In the total control system one of the most important is the waveform monitoring system. For linear induction accelerators which are high-power, high-voltage pulsed installations, waveform monitoring, i.e. registration of waveforms of signals received from a wide range of sensors in each operating cycle, is the most informative, although very expensive way to control the normal operation of equipment [1, 2].

It is assumed that in the final version the WMS will enable the registration of two thousand waveforms with different durations. Analysis of the data obtained immediately at the end of the operating cycle will make a conclusion about the current condition of the installation elements and their operation in the last cycle. At the same time, data archiving, performed for many operating cycles, and their appropriate processing will allow to identify and study in detail trends in the equipment, the evolution of their parameters and thus to predict possible failures.

Operating cycle of the LIA-20 can be divided into three phases: a preparatory, acceleration phase and an experimental phase. The typical duration of the processes in the preparatory phase are in the range of 0.2 – 20 ms, in the acceleration phase – 100 – 400 ns, and in the experimental phase, when the beam is directed into several routes, the signal durations are 20 – 50 ns. The signal bandwidth in the first phase does not exceed 10 – 20 kHz, in the second it is 30 – 40 MHz, and in the third – 200 MHz.

Thus, three types of modules are required for arranging the waveform monitoring. The first one is to have the sampling rate 50 – 100 kSPS and can be built based on the multiplexed ADC chips. The second one must provide the sampling rate of 3 – 5 ns/sample. The fastest module should have a speed not less than 1 ns/sample. Note that for a full-scale waveform monitoring is necessary to record signals for the first phase in 1563 channels, for the second – in 840 channels and for the third – in 18 channels.

The following describes structural schemes of modules used in the WMS, discusses the features of the chosen solutions, ways of errors minimizing. Some details of schemes and the resulting device parameters are presented.

SLOW WMS DIGITIZERS ADCX32

"Slow" WMS subsystem provides data acquisition of Pulsed HV System (PHVS) signals (see Fig. 1). PHVS includes 27 HV chargers, 480 pulse modulators with Pulse Forming Networks (PFN) for supplying accelerating inductors, 64 pulsed demagnetizer and 32 magnetic lens supply units. Such parameters as HV charger voltage, PFN voltage, demagnetizer current and magnetic lens current should be measured with an error not exceeding 0.1%. The durations of PHVS elements processes differ significantly as shown in timing diagram of PHVS operation (see Fig. 1). Thus, "slow" WMS should be able to digitize 1563 signals in time range 500 us – 20 ms.

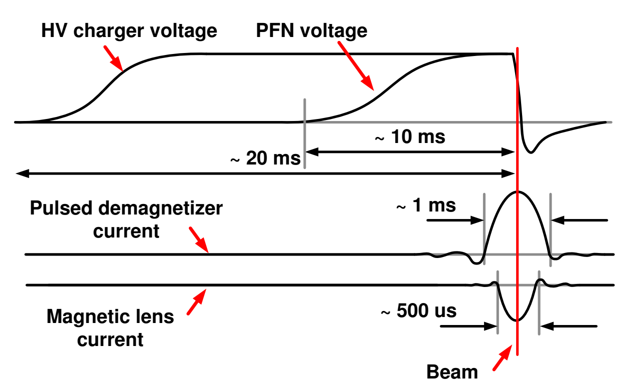

Figure 1: PHVS timing diagram.

The basic idea of "slow" WMS digitizer design is using four 8-channel multiplexed 1 MSPS SAR ADCs with

ISBN 978-3-95450-181-6

SYSTEM OF GEODETIC MEASUREMENTS FOR LIA-20.

A.G.Chupyra, E.A.Bekhtenev[1], G.V.Karpov,
Budker Institute of Nuclear Physics, Novosibirsk, Russia,
[1] also at Novosibirsk State University, Novosibirsk, Russia.

Abstract

The system of geodetic measurements for accelerator LIA-20 is presented in this paper. The system consists of two subsystems. The first one is hydrostatic level system and the second one is system with the stretched wire. The system of geodetic measurements controls vertical and horizontal shifts of the accelerating structures, and also their inclinations in the longitudinal and cross directions.

INTRODUCTION

LIA-20 is a new accelerator for radiography which is now under development and construction. It consists of the injector and a number of accelerating modules placed on girders. Total length of the accelerator is about 70 meters. The accelerator is designed to provide a electron beam with energy up to 20 MeV, current 2 kA and lateral size of beam less than 1 mm. The last condition requires a careful alignment of the accelerator's elements and further monitoring of their positions. It is necessary to control change of the accelerating module's position less than 0,1 mm on height and less than 1 milliradian on angle. System for geodetic measurements is developed for this purpose.

The system consists of two subsystems. The first one is hydrostatic level system and the second one is system with the stretched wire. The system of geodetic measurements controls vertical and horizontal shifts of the accelerating structures, their inclinations in the cross directions and its rotation angle around the longitudinal axis (Fig.1).

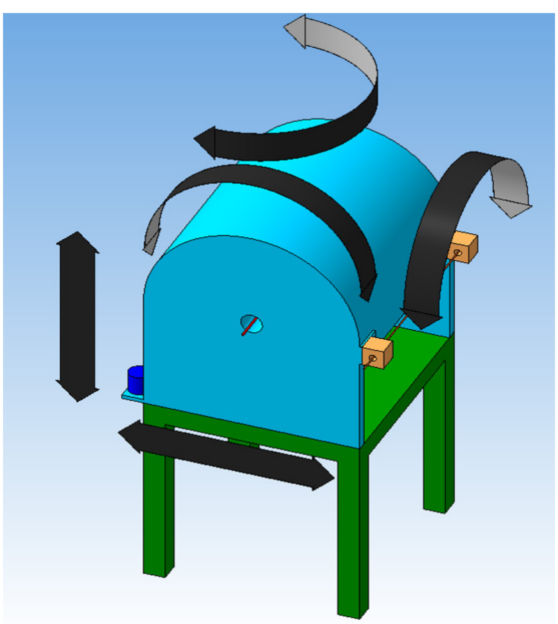

Figure 1: Movement types measured by the system.

HYDROSTATIC LEVEL SYSTEM

General Description

Hydrostatic level system is based on principle of communicating vessels. All water level measuring sensors are linked to its neighbours by a system of tubes. So the principle is based on the equilibrium of the pressure of liquid in communicating vessels (see Fig. 2).

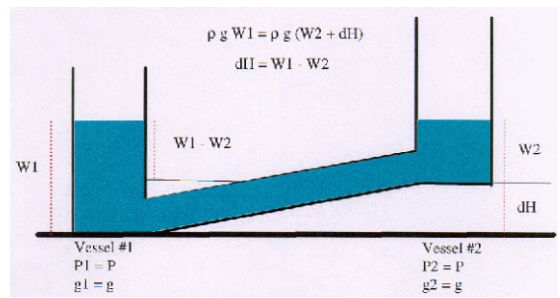

Figure 2: The principle of communicating vessels.

Ultrasonic level sensor

Ultrasonic Level Sensor (ULS) is designed to work into the hydrostatic level system for monitoring of vertical position of the accelerating modules. The resolution of the ULS is 0.2 µm and the accuracy is 5 µm in measurement range of 5 mm.

A pulse-echo method is used in ULS for water level measurements. The ultrasonic hydro-location is well known and widely distributed method of distance measurements for many applications. One of precise methods was described by Markus Schlösser and Andreas Herty [1]. Their idea is to locate not only the water surface in a vessel, but also two addition surfaces with calibrated distance between them (D1) and at the calibrated distance to alignment reference target (D2), see Fig. 3.

The pulse-echo ultrasonic measurements can determine the location of free water surface in a vessel or location of reflective surface into water by accurately measuring the time required for a short ultrasonic pulse generated by a transducer to travel through a thickness of water, reflect from the free water surface or from the reflective surface, and be returned to the transducer. The two-way transit time measured is divided by two to account for the down-and-back travel path and multiplied by the velocity of sound in the test material.

$$d = v \cdot t / 2 \quad (1)$$

Here ***d*** is the distance from the surface of transducer to the reflective surface or to free water surface, ***v*** is the

ISBN 978-3-95450-181-6

THE NEW CONTROL FOR MAGNET SYSTEM OF KSRS

E. Kaportsev, A. Valentinov, Yu. Krylov, K. Moseev, N. Moseiko, RRC Kurchatov Institute, Moscow, Russia

Abstract

The running cycle of Kurchatov Synchrotron Radiation Source (KSRS) includes the injection of electrons with energy 80 MeV from the linear accelerator in the booster storage ring Siberia-1, the accumulation of a electron current up to 400 mA and, then, electron energy ramping up to 450 MeV with the subsequent extraction of electrons in the main ring, storage ring Siberia-2, and accumulation there up to 300 mA, and at last the energy ramping up to 2.5 GeV. [1]

Several years ago, a modernization of the current system of automated control systems (ACS) has started. Modernization has affected the most important parts of the system - the system of data collection and monitoring system. Used advanced solutions based on CAN and VME and modular complexes National Instruments.

This article describes some of the features of the most important part of the control system - the controller of the magnetic system and software management environment.

APPOINTMENT OF ACS

The existing automated control system (ACS) accelerator-storage complex (UNK) "Siberia" - synchrotron radiation source and center of collective use NRC "Kurchatov Institute" was established over 20 years ago on the basis of the control equipment in the CAMAC standard. Currently, there is an active modernization and replacement of outdated equipment with new, modern and more productive. [2]

The control apparatus of the new ACS with integrated processors, as well as acquired powerful servers, the operator's computer and network equipment has developed software (software) at all levels of the ACS.

The control system of the magnetic system is one of the most important parts of the ACS. So far, the management system used obsolete equipment in the CAMAC standard, as well as outdated transformer type current sources controlled by the analogue signal.

We have improved the management of the magnetic system, setting a new high-performance controller, and using a new, more accurate current sources, controlled by a digital signal on the CANOpen standard.

CONTROL OF THE MAGNETIC SYSTEM

The magnetic system is controlled by a controller NI cRIO-9081 (Figure 1). In the chassis of the controller is installed one discrete I/O module NI 9425 and two double-channel CAN module NI 9853. To control the high-current and the low-current magnets control module uses two CAN network. One CAN network connected to smart crate-controller K167 [3] and CAN-DAC power supply units of the quadrupole lens and bending magnets of the accelerator. The second network, connect the power supply control units of the correction magnets of the accelerator.

Smart crate-controller K167 used to translate commands transmitted from magnetic controller via the CAN bus system into CAMAC commands. Management of the high-current sources of bending magnets and quadrupole lenses is performed by using a 20-bit DAC-20. Measurement of currents on the buses is performed by means of 20-bit ADC 20. All these units are installed in the CAMAC crate. For transmitting diagnostic signals (interlocks, errors) used CEDAC20 units installed in the power supply cabinet.

To control the current sources of the electron beam orbit correction system uses specialized correction control units (CCU). These blocks have been specifically designed by our employees. CCU provides translation of commands transmitted from the controller of the magnetic system via the CAN bus into CANOpen command. Each CCU manages the 16 th power supplies developed by a third party specifically for the needs of Kurchatov Institute.

DAC and ADC management teams made directly via the CAN bus, ie, values of DAC and ADC values are transmitted via the CAN bus. The mechanism works as follows: during the execution mode (magnetization reversal, injection, energy recovery) is carried out pre-entry table the estimated current values in the controller's memory. Then, on command from the old system, a magnetic system controller begins to record currents in the DAC current sources corresponding channels. Recording is carried out simultaneously with the record values RF parameters of the system, connected to the old control system.

SYNCRONIZATION WITH OLD ACS.

To synchronize the operation of the controller of the magnetic system with the old control system, we using one channel of the controlled registers in the crate CAMAC, and one channel of discrete input NI9425. The operator selects the desired mode of operation using the appropriate snap-in of the CitectSCADA system [4]. This command is transmitted to the RF generator control system, as well as the program for calculating of currents table. After all preliminary calculations have been made, the controller of the magnetic system is commanded to start through the channel of the register, and the process entering the into the synchronous mode.

ISBN 978-3-95450-181-6

PRESENT STATUS OF VEPP-5 INJECTION COMPLEX CONTROL SYSTEM

F. Emanov*, D. Berkaev, D. Bolkhovityanov, P. Cheblakov , BINP, Novosibirsk, Russia

Abstract

VEPP-5 injection complex is being put into operation as beam source of VEPP-2000 and VEPP-4 colliders at the end of 2016. Its control system is being upgraded in order to reliably work with beam users and increase its manageability computer infrastructure was reconsidered to provide high availability and flexibility through virtualization of control servers. The paper presents architecture and implementation of complex computer infrastructure. A control software set based on CXv4, EPICS and VCAS frameworks under operating system Linux deals with a set of CAN, CAMAC and Ethernet specialized hardware. The software and hardware architecture and implementation is described.

INTRODUCTION

VEPP-5 injection complex [1] (IC) is linear accelerator based e+/e- beam source with a damping ring and transfer lines. IC is now being put into operation to provide beams for VEPP-2000 and VEPP-4 colliders. This requires continuous functioning of control system infrastructure and development of software for joint operation with colliders.

In order to ensure reliability of control system infrastructure and hence on the whole injection complex it is proposed to deploy separated network infrastructure and high availability cluster of control servers based on modern virtualization techniques.

Software structure principles for joint operation with beam users was proposed earlier [2] and then corrected according to development and operation experience.

CONTROL SYSTEM INFRASTRUCTURE INITIAL STATE

There is the following set of control system hardware at the beginning of work:

- 126 CAN DAC/ADC and other devices developed in BINP [4, 5, 6] connected via CANGW [3] embedded computers or dedicated desktop PC,
- 17 CAMAC crates with specialized electronic modules and fast ADCs, 1 cPCI crate with ADC200me [7]
- 8 Ethernet photo-cameras
- 15 Ethernet BPM processors [8]
- 5 RS-485 controllers connected via Moxa UC-7112-lx plus embedded computer
- 2 former control room workstations working as control system servers, 3 main control room workstations and 6 old PCs as control system terminals

* F.A.Emanov@inp.nsk.su

All the Ethernet controllers are connected to dedicated controllers network, which is also connected to control system servers. PCs are connected to BINP network, which is currently used for communication between IC and colliders control systems. Hardware related issues are the following: lack of CANGW performance for some tasks, no reliability assurance for mission-critical devices and network connections (control servers, vacuum control, communications with beam users), complexity of infrastructure service and deployment of new devices. Historically injection complex computers were bare metal with Linux OS installed, and there were no network infrastructure services. Therefore, additional difficulty was to work around maintenance or failure of institution network infrastructure services.

INFRASTRUCTURE UPGRADE

The project

In order to solve the described above problems control system infrastructure upgrade was proposed with following outline:

- Replace network switches with managed ones and build VLANs for BINP network, controllers, computers and IPMI.
- Add direct optical links from IC network to beam users networks for operation data exchange.
- Deploy infrastructure servers for internal networks: 2 servers as hosts for general services, network boot servers and remote storage for operating systems, 2 Firewall servers.
- Create high-availability cluster of 4 control servers based on virtualization platform. 2 CAN servers (with 5 PCI/PCIe slots for CAN adapters) connected to the same CAN lines for reliability assurance, 2 Main control system servers directly connected to high volume shared storage for operation history data or other big data volume applications.
- Replace CAMAC-based stepper motor controllers with CAN ones. This is required due to incompatibility of old CAMAC controllers with managed switches.
- Replace old PC terminals with thin clients in order to reduce maintenance requirements.

The resulting sketch of control system infrastructure is shown on Fig. 1.

The implementation

In order to reduce the range of equipment we decided to use close Supermicro platforms for servers and control room workstations. Since some of servers have 10G

ISBN 978-3-95450-181-6

DEVELOPMENT AND IMPLEMENTATION OF THE AUTOMATION SYSTEM OF THE ION SOURCE FOR BNCT*

A.M. Koshkarev#, S.Yu. Taskaev, Budker Institute of Nuclear Physics, Novosibirsk, Russia and Novosibirsk State University, Novosibirsk, Russia
A.S. Kuznetsov, A.L. Sanin, V.Ya. Savkin, P.V. Zubarev, Budker Institute of Nuclear Physics, Novosibirsk, Russia

Abstract

To operate a source of negative hydrogen ions an automatic distributing control system was developed. This system consists of master controller (Slab C8051F120) and a set of peripheral local controllers (PLC) based on microcontroller Slab C8051F350. Using an optical link between PLC and master controller there was created a system resistant to high-voltage breakdown of the ion source.

To control the system, a special programming language has been created. It includes procedures for checking the necessary parameters, setting the value of the physical quantities to simplify the experiment, verifying the lock status and protection. This system provides two programmable timers, as well as procedures in emergency situations, such as: lack of water, poor vacuum. It can be operated in semi-automatic mode, if the script asks operator about preferable actions and then continues the script depending on the response. All scripts are performed in master controller, and this makes system very rapid (for example system response time is 1 ms).

INTRODUCTION

One of the most important stages in the development of new facilities is to automate and connect all control units together. To achieve this goal, the automation of power supply units in the new ion source injector was carried out. The ion source injector is located in a research facility BNCT [1]. This method of treatment is very effective against a number of currently incurable radioresistant tumors, such as glioblastoma multiforme and metastatic melanoma [2, 3]. Frequent changes of control commands and their parameters during experiments cause serious problems. Therefore, the scripting language consisting of control commands was developed. It allows operator to implement all sorts of automatic control algorithms and conduct experiments with minimal outer control. Automation, conducted within the framework of this work, simplifies significantly the operation of the facility.

SUBJECT AREA

The ion injector comprises several high-voltage power sources, temperature and vacuum level nodes, requiring remote control and data capture.

Power sources are controlled by identical and interchangeable modules of programmable logic controller (PLC), receiving commands from a personal computer through a switch. Each PLC has a microcontroller and several analog and digital channels, which are connected via serial interfaces SPI & I2C with the PLC microcontroller. The microcontroller allows operator to test devices on the board if they are connected with each other. In conditions of high electromagnetic noise the distributed control system with sufficient independence of modules increases the reliability of the entire control system.

The structure of the control system is shown in Fig. 1.

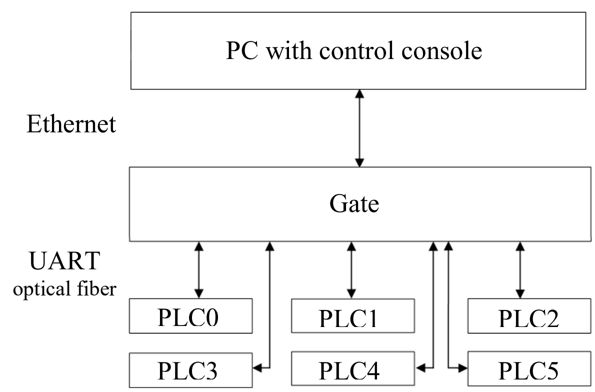

Figure 1: Structure of the control system.

ALGORITHMS

Commands are usually repeated during the experiment and for convenience to operator algorithm scenarios have been developed. Operator can create a certain set of commands once and then these commands can be repeatedly applied. Command can be as unconditional execution of some action, and also it can be a check of channel status. After checking it is possible to jump to another line in the scenario.

The switch algorithms allows user to apply two modes: manual and automatic. In manual mode, the operator can change the values of PLC. On the other hand, automatic mode allows user to run the script, which will perform the control over the experiment without operator. A block diagram of the basic algorithm is presented in Fig. 2.

The developed switch algorithms allow user to control automatically the ion source. Link between the management console and the switch is not required. Accordingly, if the operator console suddenly loses contact with the switch, the experiment will not stop, and the switch will continue to capture the critical parameters

*Work supported by part by the Russian Science foundation (project no. 14-32-00006), the Budker Institute of Nuclear Physics and Novosibirsk State University.
#koshkarev_al@mail.ru

ISBN 978-3-95450-181-6

STABILIZATION OF THE EQUILIBRIUM POSITION OF A MAGNETIC CONTROL SYSTEM WITH DELAY*

A.Yu. Aleksandrov†, A.P. Zhabko, I.A. Zhabko, Saint Petersburg State University, Saint Petersburg, Russia
A.A. Kosov, Matrosov Institute for System Dynamics and Control Theory of Siberian Branch of Russian Academy of Sciences, Irkutsk, Russia

Abstract

A model of magnetic suspension control system of a gyro rotor is studied. A delay in the feedback control scheme and dissipative forces occurring due to energy losses at the interaction of the magnetic field with currents in the control loops are taken into account. Two approaches to the synthesis of controls stabilizing the equilibrium position of the considered system are proposed. The results of a computer simulation are presented to demonstrate effectiveness of the approaches.

INTRODUCTION

Nonlinear oscillatory systems are widely used for the modeling charge particles motions in cyclotrons in neighborhoods of equilibrium orbits [1–3]. They are also applied for the analysis and synthesis of magnetic control devices [4, 5]. In particular, magnetic systems of retention of power gyro rotors are used in modern control systems of spacecraft orientation with long periods of autonomous operation. An actual problem for such systems is stabilization of their operating modes.

It is worth mentioning that realistic models of numerous control systems should incorporate delay in feedback law [6]. It is well-known that delay may seriously affect on system's dynamics. Therefore, it is important to obtain restrictions for delay values under which stability can be guaranteed.

In this paper, analytical and numerical investigations of stability of the equilibrium position for a nonlinear oscillatory system are presented. The system can be treated as a mathematical model of magnetic suspension control system of a gyro rotor [5]. A delay in the feedback control scheme and dissipative forces occurring due to energy losses at the interaction of the magnetic field with currents in the control loops are taken into account.

Two approaches to the synthesis of stabilizing controls are proposed. With the aid of a computer simulation of dynamics of closed-loop systems, a comparison of these approaches is fulfilled, and their features and conditions of applicability are determined.

* The research was partially supported by the Saint Petersburg State University (project No. 9.37.157.2014), and by the Russian Foundation for Basic Research (grant Nos. 15-08-06680-a and 16-01-00587-a).

† a.u.aleksandrov@spbu.ru

STATEMENT OF THE PROBLEM

Consider the control system

$$\begin{cases} \ddot{x}(t) - p(x(t), y(t))y(t) = u_x, \\ \ddot{y}(t) + p(x(t), y(t))x(t) = u_y. \end{cases} \tag{1}$$

Here $(x(t), y(t))^T$ is the state vector, u_x and u_y are control variables, and function $p(x, y)$ is defined by the formula

$$p(x, y) = \alpha + \beta(x^2 + y^2),$$

where α and β are constant parameters. Thus, the considered system is affected by non-conservative forces and control ones. Equations of the form (1) are used, for instance, for modeling rotor dynamics in magnetic suspension system [5].

In the present paper, we will assume that $\alpha = 0$, and non-conservative forces are generated in the electromechanical system with a certain delay $\tau \geq 0$. The reason for arising the delay is an inertia in response of the magnetic suspension control system on rotor deviations from the equilibrium position. It should be noted that the value of delay might be unknown. In addition, we will assume that the system is affected by a dissipative force $(F_x, F_y)^T$ depending only on the velocities.

Thus, the rotor dynamics is described by the equations

$$\begin{cases} \ddot{x}(t) - \beta\left(x^2(t-\tau) + y^2(t-\tau)\right) y(t-\tau) \\ \qquad + F_x(\dot{x}(t), \dot{y}(t)) = u_x, \\ \ddot{y}(t) + \beta\left(x^2(t-\tau) + y^2(t-\tau)\right) x(t-\tau) \\ \qquad + F_y(\dot{x}(t), \dot{y}(t)) = u_y. \end{cases} \tag{2}$$

We assume that initial functions for solutions of (2) belong to the space $C^1([-\tau, 0], R^2)$ of continuously differentiable functions $\varphi(\theta) = (\varphi_x(\theta), \varphi_y(\theta))^T : [-\tau, 0] \to R^2$ with the uniform norm

$$\|\varphi\|_\tau = \max_{\theta\in[-\tau,0]} \left(\|\varphi(\theta)\| + \|\dot{\varphi}(\theta)\|\right),$$

and $\|\cdot\|$ denotes the Euclidean norm of a vector.

For the desired position of the rotor axis we have $x = y = 0$. It is known, see [7], that if $\tau = 0$ and $u_x = u_y = 0$, then the equilibrium position

$$x = y = \dot{x} = \dot{y} = 0 \tag{3}$$

of system (2) is unstable. Therefore, we should to design a feedback control law stabilizing the equilibrium position.

ISBN 978-3-95450-181-6

SOFTWARE AND COMPUTATIONAL INFRASTRUCTURE OF LIA-20 CONTROL SYSTEM

A. Senchenko#, G. Fatkin, S. Serednyakov, BINP SB RAS and Novosibirsk State University, Novosibirsk, Russia
P. Selivanov, BINP SB RAS, Novosibirsk, Russia

Abstract

The linear induction accelerator LIA-20 for radiography is currently under construction at Budker Institute of Nuclear Physics.

This paper presents software architecture and computational infrastructure for the accelerator controls. System and application software are described. Linux operating system is used on PC and embedded controllers. Application software is based on TANGO. Overall data transfer rate estimations are provided.

LIA-20 PROJECT

Linear Inductor Accelerator LIA-20 is designed to provide three electron bunches with energy up to 20 MeV, current up to 2 kA and lateral size after focusing on the target less than 1 mm. It is planned to provide three consecutive bunches, with one of them divided into 9 angles. The accelerator will be used for the flash X-Ray radiography.

LIA-20 consists of the injector, 30 “short” accelerating modules (SAM) and 12 “long” ones (LAM). Injector generates beam with the energy up to 2 MeV. SAM increases the energy by 0.33 MeV and LAM increases the energy by 0.66 MeV. The total length is about 75 meters. Structure is described in detail in [1].

Control units are placed along the installation. All units are based on uniform VME crate and connected via Ethernet.

DATA RATES

All channels could be divided into following groups:

Fast. All measurements faster than 10 us: voltage on inductor, currents on lenses and beam position monitor.

Slow. This group includes measurements with duration up to several milliseconds (charging device, degaussing current).

Timing. These channels provide all devices with proper start pulse.

Interlock. These channels belong to subsystem that prohibit experiment in case of component malfunction or failure.

Technological controls. This group incorporates vacuum controls, optical system alignment [4], control of power supplies.

First four groups are bound to machine cycles, while the last one is continuous.

Tables 1 present the summary of channels and data rates. Estimations are provided for one-bunch cycle.

COMPUTATIONAL INFRASTRUCTURE

Computational infrastructure components are distribute across two areas: control room and experimental hall (see Fig.1). Control rack and operators PC are located in control room. Control rack is equipped with two server, UPS and 24 port switch. The switch provides connectivity between server, UPS, operator's PC and experimental hall switch. All VME crates are located in experimental hall and connected via two switches. Description of components are provided below.

Server:
- CPU 2.0 GHz, Cores 4
- Intel x86-64
- RAM 32GB
- Gigabit Ethernet
- 4TB SCSI
- RAID 5

VME Crate Controller:
- PowerPC - based
- Diskless network boot

Operator's PC:
- CPU 2.2, Cores 4
- Intel x86-64
- RAM 4GB
- Up to 4 monitors

Table 1: Data Rates Estimation

Channel type	Number of channels		Data rate	
	whole system	per VME crate	whole system	per VME crate
Fast	594	22	5.7 MB/cycle	214 KB/cycle
Slow	1485	55	13.5 MB/cycle	0.5 MB/cycle
Timing	1485	55	13.5 KB/cycle	0.5 KB/cycle
Interlock	1485	55	13.5 KB/cycle	0.5 KB/cycle
Technological control	1000	~40	513 KB/min	19 KB/min
	6000	~280	19.3 MB/cycle + 540 KB/min	3.5 MB/cycle + 19.5 KB/min

#a.i.senchenko@inp.nsk.su

ISBN 978-3-95450-181-6

THE STOCHASTIC CHARACTERISTICS STABILITY IN THE PROBLEM OF OBSERVATION AND ESTIMATE OF THE CHARGED PARTICLES MOVEMENT

M. Chashnikov, Saint Petersburg State University, Saint-Petersburg, Russia

Abstract

The charged beam moving in the accelerator is modelled by particle-in-cell method. The control with delay in the connection canal is simulated by the after-effect. Thus, the model is described by system of the differential equations with delay. We observe and estimate changes of particles coordinates in the cross-section of the accelerator. It is supposed that initial conditions are the set with random error and we have chance of updating the solution in periodic timepoints with the same error. The dependence between the estimate dispersion and the measuring error dispersion is recieved.

INTRODUCTION

Consider a beam of charged particles, moving in the accelerator. We research them by particle-in-sell method. Suppose that the problem is to calculate the coordinates in the transverse section of the accelerator.

We'll linearize the equations, describing one of the large particles movement. Herewith we add a delay in the system. In such way we'll simulate the control with delay in the connection canal [1].

Thus the dynamic of the beam coordinates will be described by the linear equations system with delay:

$$\dot{z}(t) = Az(t) + Bz(t-h), \tag{1}$$

where A, B nonsingular 2x2 constant matrices,

$$z(t) = \begin{pmatrix} x_1(t) \\ x_2(t) \end{pmatrix}$$

is the vector of the beam coordinates in the cross-section of the accelerator. The solution of the equation is uniquely determined by the initial function $\varphi(t)$, defined on the interval $[-h; 0]$.

Suppose we can measure the initial position of the beam with some error. We'll designate by $\hat{z}(t)$ the solution with measured initial values $\hat{\varphi}(t)$, $t \in [-h; 0]$, and consider its difference with the exact solution.

$$\bar{z}(t) = z(t) - \hat{z}(t)$$

The value of the error is obviously depending on the measuring error of the initial value, which is equal

$$\bar{\varphi}(t) = \varphi(t) - \hat{\varphi}(t)$$

We suppose that the measuring error is a centered random variable and that the errors of the components measuring aren't depending on each other. Thus, $\bar{\varphi}(t)$ on $[-h; 0]$ is a centered random vector with the covariation matrix $\sigma^2 I$.

Now we'll build the upper limit of the covariation matrix $D(\bar{z}(t))$ as a function of t for $t > 0$. We note, that for each A, B, z there is

$$\left\|\sqrt{AA^{\mathrm{T}}}z\right\| \geq \|Az\|, \left\|\sqrt{BB^{\mathrm{T}}}z\right\| \geq \|Bz\|.$$

Because of the positive definiteness of the matrices $\sqrt{AA^{\mathrm{T}}}$ and $\sqrt{BB^{\mathrm{T}}}$, if we put them into (1) instead of A, B, then each component $\dot{z}(t)$ will have the same sign as the corresponding component $z(t)$, and it means that the module of each component is monotonicaly increasing on $t > 0$, and $\|z(t)\|$ is increasing too. Thus, if we change the equation (1) with

$$\dot{w}(t) = \left(\sqrt{AA^{\mathrm{T}}} + \sqrt{BB^{\mathrm{T}}}\right)w(t), \tag{2}$$

we get the function, which is the upper limit of the solution of the system (1). At each moment it will be a random vector, and its covariation matrix norm will be larger than the covariation matrix norm of the system (1) solution.

OBSERVATION WITH CORRECTION

Consider the set of the moments $n\tau$, then the solution of (2) at these moments is given by the formula $w(n\tau) = \Phi_n w(0)$, where $\Phi_n = e^{\left(\sqrt{AA^{\mathrm{T}}}+\sqrt{BB^{\mathrm{T}}}\right)n\tau}$.

The covariation matrix of $w(n\tau)$ is:

$$D\big(w(n\tau)\big) = \Phi_n \sigma^2 I \Phi_n^{\mathrm{T}} = \sigma^2 \Phi_n \Phi_n^{\mathrm{T}} = \sigma^2 \Phi_n^2$$

because of the symmetry of the matrix Φ_n. Because of the positive definiteness of the matrix Φ_n^2 matrix its spectral norm is equal its largest eigenvalue $e^{2\lambda n\tau}$, where λ is the largest eigenvalue of the matrix $\sqrt{AA^{\mathrm{T}}} + \sqrt{BB^{\mathrm{T}}}$. If we want to bound the error dispersion of $\bar{z}(t)$, we can bound the function $M(t) = \big\|D\big(w(t)\big)\big\|$.

Suppose on each segment $[n\tau - h, n\tau]$, $\tau = const$, $\tau > h$, $n = 1,2, \ldots$, we can measure the values of $z(t)$ with the error dispersion σ^2. Then we have 2-dimensional case of the dynamic filtration, described in [2].

Suppose this correction will be made not surely, but with the probability, which means that $M(t)$ will be a stochastic function. At each moment $n\tau$ we can calculate its expectation value $E\big(M(n\tau)\big)$ and the dispersion $D\big(M(n\tau)\big)$. Thus, the function $M(t)$ is left-continuous function and it increases on each segment $(n\tau, (n+1)\tau]$, and then it begin to increase from the value σ^2.

Let p is chance of correction response at any moment $n\tau$, $n = 1,2, \ldots$ Denote $q = 1 - p$, $E_n = E\big(M(n\tau)\big)$, $D_n = D\big(M(n\tau)\big)$, $Y_n = \sigma^2 e^{2\lambda n\tau}$. It is obvious that the set of possible values E_n is $\{Y_i\}_{i=1}^n$.

STOCHASTIC CHARACTERISTECS STABILITY

Lemma 1

E_n is monotonically increasing by n.

ISBN 978-3-95450-181-6